



UNIVERSIDAD DE  
MURCIA

DEPARTAMENTO DE  
BIOQUÍMICA Y  
BIOLOGÍA MOLECULAR (A)

---

# **ESTUDIO DE LA FUNCIÓN DE LA FAMILIA DE PROTEÍNAS QUINASAS C EN EL CÁNCER DE MAMA**

RUBÉN LÓPEZ NICOLAS

MEMORIA

Presentada para optar al grado de Doctor con Mención Europea

2011





**UNIVERSITY OF  
MURCIA**

DEPARTMENT OF  
BIOCHEMISTRY AND  
MOLECULAR BIOLOGY (A)

---

# **ROLE OF PROTEIN KINASE C IN BREAST CANCER CELLS**

RUBÉN LÓPEZ NICOLAS

2011



## ÍNDICE



---

<b>PRÓLOGO (RESUMEN EN CASTELLANO)</b>	<b>1</b>
<b>I. INTRODUCCIÓN Y OBJETIVOS.</b>	<b>3</b>
I.1. PROTEÍNAS QUINASAS C: Estructura y clasificación.	3
I.2. Proteínas Quinasas C y cáncer.	5
I.3. Objetivos.	6
<b>II. MATERIALES Y MÉTODOS.</b>	<b>7</b>
II.1. Construcciones de ADN plasmídico.	7
II.2. Cultivos celulares y transfecciones.	8
II.3. Microscopía confocal.	8
II.4. Purificación y medidas de actividad quinasas.	9
II.5. Microarrays.	9
II.6. Análisis estadístico.	10
<b>III. LOCALIZACIÓN DE PKC<math>\alpha</math> DEPENDIENTE DE ÁCIDO ARAQUIDÓNICO.</b>	<b>11</b>
<b>IV. EFECTO DEL ÁCIDO OLEICO EN CÉLULAS MODELO DE CÁNCER DE MAMA A TRAVÉS DE PKC<math>\alpha</math>.</b>	<b>12</b>
<b>V. EFECTO DE LOS ÁCIDOS GRASOS OMEGA-3 Y LA INHIBICIÓN DE LA EXPRESIÓN DE PKC<math>\alpha</math> EN CÉLULAS MODELO DE CÁNCER DE MAMA.</b>	<b>13</b>
<b>VI. CARACTERIZACIÓN BIOLÓGICA DE DAG-LACTONAS A TRAVÉS DE PKCs.</b>	<b>14</b>
<b>VII. PERFIL DE EXPRESIÓN GÉNICA EN CÉLULAS MODELO DE CÁNCER DE MAMA EN AUSENCIA DE PKC<math>\alpha</math>.</b>	<b>15</b>
<b>VIII. EL TRATAMIENTO DE CÉLULAS MODELO DE CÁNCER DE MAMA CON SALINOMICINA POTENCIA EL EFECTO DE LA INHIBICIÓN DE LA PKC<math>\alpha</math>.</b>	<b>16</b>
<b>IX. CONCLUSIONES.</b>	<b>17</b>

---

<b>ABBREVIATIONS</b>	<b>19</b>
<b>CHAPTER I: INTRODUCTION AND OBJECTIVES.</b>	<b>21</b>
<b>1. Introduction to PROTEIN KINASE C. Structure and classification.</b>	<b>23</b>
<b>2. Conserved regions in PKC.</b>	<b>25</b>
2.1. Pseudosubstrate domain.	25
2.2. C1 domain. Structure, function and regulation.	25
2.3. C2 domain. Structure, function and regulation.	28
2.4. Catalytic domain. Structure and regulation.	35
<b>3. Variable regions.</b>	<b>38</b>
<b>4. PKC activation mechanism.</b>	<b>39</b>
4.1. Activation model of classical and novel PKCs.	40
<b>5. Pathways where PKC is involved.</b>	<b>43</b>
<b>6. Other bioactive lipids able to activate PKC.</b>	<b>45</b>
6.1. Fatty acids.	45
6.2. DAG-lactones.	47
<b>7. Introduction to PKC and cancer.</b>	<b>49</b>
<b>8. PKC isoforms in Breast Cancer.</b>	<b>54</b>
<b>9. PKC isoforms as target in cancer therapy.</b>	<b>57</b>
<b>10. Objectives.</b>	<b>60</b>
<b>CHAPTER II: MATERIALS AND METHODS.</b>	<b>61</b>
<b>1. Construction of expression plasmids.</b>	<b>63</b>
1.1. Construction in plasmid pEGFP-N3.	64
1.2. Construction in plasmid pECFP-N3.	65
1.3. Construction in plasmid pCGN.	66
1.4. Site-directed Mutagenesis.	67
1.5. Amplification and purification plasmid DNA.	68

---

<b>2. Cell culture.</b>	73
2.1. MCF-7 cells.	73
2.2. BT-474 cells.	75
2.3. MDA-MB-231 cells.	76
2.4. Inhibition of PKC $\alpha$ expression using small interference RNA.	77
2.5. Migration assays.	78
2.6. Invasion assays.	79
2.7. Proliferation assays.	80
2.8. Apoptosis assays.	81
<b>3. Confocal microscopy.</b>	83
3.1. Introduction to confocal imaging.	83
3.2. Microscope used.	85
3.3. Fluorescent substances used.	87
3.4. Media used in stimulation of living cells in confocal microscope.	89
3.5. Image processing and analysis.	89
3.6. Immunofluorescence.	97
<b>4. Electrophoresis techniques.</b>	98
4.1. Agarose gel preparation.	98
4.2. Acrylamide gel preparation.	99
<b>5. Western Blot.</b>	99
<b>6. Fluorescence Resonance of Energy Transfer (FRET).</b>	109
<b>7. PKC<math>\alpha</math> purification.</b>	103
<b>8. Kinase activity assays.</b>	104
<b>9. Microarrays.</b>	105
9.1. Introduction of microarrays.	105
9.2. Overview of preparation for gene expression array.	106
9.3. Sample preparation.	110
<b>10. Statistical analysis.</b>	113

---

<b>CHAPTER III: MOLECULAR MECHANISM OF PKC<math>\alpha</math> LOCALIZATION BY ARACHIDONIC ACID. THE C2 DOMAIN ALSO PLAYS A ROLE.</b>	<b>115</b>
<b>1. Introduction.</b>	117
<b>2. Results.</b>	118
2.1. Arachidonic acid induces the PKC $\alpha$ translocation to the plasma membrane in a Ca <sup>2+</sup> -dependent manner.	118
2.2. The C2 domain of PKC $\alpha$ plays an important role in the AA-dependent membrane localization of the enzyme.	125
2.3. Role of the C1 domain of PKC $\alpha$ in the AA-dependent membrane localization.	128
<b>CHAPTER IV: EFECT OF OLEIC ACID ON BREAST CANCER CELLS THROUGH PKC<math>\alpha</math>.</b>	<b>131</b>
<b>1. Introduction.</b>	133
<b>2. Results.</b>	135
2.1. Oleic acid induces PKC $\alpha$ plasma membrane translocation and co-localization with actin filaments in breast cancer cells.	135
2.2. Characterization of the activation mechanism of PKC $\alpha$ by oleic acid.	139
2.3. Oleic acid induces the PKC $\alpha$ translocation to plasma membrane in a Ca <sup>2+</sup> -dependent manner.	140
2.4. Inhibition of PKC $\alpha$ expression reduces the proliferation rate in breast cancer cell lines and synergizes with oleic acid.	145
2.5. Effect of oleic acid addition and inhibition of PKC $\alpha$ expression on the migration and invasion capacities of MCF-7 and MDA-MB-231 cell lines.	148
2.6. Oleic acid and inhibition of PKC $\alpha$ induce apoptosis in breast cancer cell lines.	151

---

**CHAPTER V: STUDY OF THE ROLE OF OMEGA-3 FATTY ACIDS AND PKC $\alpha$  DEPLETION IN BREAST CANCER CELLS. 153**

- 1. Introduction.** 155
- 2. Results.** 157
  - 2.1. Omega-3 fatty acids induce PKC $\alpha$  plasma membrane translocation and co-localization with actin filaments in breast cancer cells. 157
  - 2.2. Characterization of the activation mechanism of PKC $\alpha$  by DHA and EPA. 161
  - 2.3. Effect of omega-3 fatty acids and inhibition of PKC $\alpha$  expression on the migration and invasion capacities of MCF-7 and MDA-MB-231 cell lines. 164
  - 2.4. Omega-3 fatty acids and inhibition of PKC $\alpha$  induce apoptosis in breast cancer cell lines. 169

**CHAPTER VI: CHARACTERIZATION OF BIOLOGICAL ACTIVITY OF DIACYLGLYCEROL-LACTONES AND ITS EFFECT ON PKCs. 173**

- 1. Introduction.** 175
- 2. Results.** 180
  - 2.1. Translocation of EGFP-tagged PKC isoenzymes in response to DAG-lactone derivatives. 180
    - 2.1.1. Effect of PMA and 153C-022 on PKC localization. 181
    - 2.1.2. Effect of 153B-143 on PKC localization. 186
  - 2.2. Tightness of the plasma membrane binding interactions measured by FRAP. 189
    - 2.2.1. Effect of PMA and 153C-022 on fluorescence recovery after photobleach PKC $\alpha$ . 189
    - 2.2.2. Effect of PMA, 153C-022 and 153B-143 on fluorescence recovery after photobleach PKC $\epsilon$ . 190
    - 2.2.3. Effect of PMA, 153C-022 and 153B-143 on fluorescence recovery after photobleach PKC $\delta$ . 191

<b>CHAPTER VII: GENE EXPRESSION PROFILE OF BREAST CANCER CELLS IN ABSENCE OF PKC<math>\alpha</math>.</b>	<b>193</b>
<b>1. Introduction.</b>	195
<b>2. Results.</b>	196
2.1. Inhibition of PKC $\alpha$ expression in MCF-7 cells.	196
2.1.1. Genes down-regulated after PKC $\alpha$ inhibition.	197
2.1.2. Genes up-regulated after PKC $\alpha$ inhibition.	199
2.1.3. Validation of arrays data.	201
2.2. Inhibition of PKC $\alpha$ expression in MDA-MB-231 cells.	208
2.2.1. Genes down-regulated after PKC $\alpha$ inhibition.	208
2.2.2. Genes up-regulated after PKC $\alpha$ inhibition.	210
2.2.3. Validation of arrays data.	212
<b>CHAPTER VIII: CHARACTERIZATION OF SALINOMYCIN EFFECT ON BREAST CANCER CELLS THROUGH PKC<math>\alpha</math>.</b>	<b>219</b>
<b>1. Introduction.</b>	221
<b>2. Results.</b>	223
2.1. Effect of salinomycin on the migration and invasion capacities of breast cancer cell lines with down-regulated PKC $\alpha$ .	223
2.2. Salinomycin induces apoptosis in breast cancer cell lines with down-regulated PKC $\alpha$ .	227
<b>CHAPTER IX: DISCUSSION AND CONCLUSIONS.</b>	<b>231</b>
<b>1. Discussion.</b>	233
1.1. Role of the C2 domain in the arachidonic acid-dependent localization and activation of PKC $\alpha$ .	233
1.2. Role of the C1 domain in the arachidonic acid-dependent localization and activation of PKC $\alpha$ .	235
1.3. Role of C1 and C2 domains in the localization and activation of PKC $\alpha$ induced by oleic acid.	237
1.4. Effect of PKC $\alpha$ depletion and oleic acid on breast cancer cell lines.	239
1.5. Localization and activation mechanism of PKC $\alpha$ induced by omega-3 fatty acids.	241

---

1.6. Omega-3 fatty acids reduce the malignancy of breast cancer cell lines through PKC $\alpha$ .	243
1.7. Synthetic charged DAG-lactones induce localization of several PKC isoform to the plasma membrane.	244
1.8. DAG-lactones anchorage PKC isoform to the plasma membrane in a more subtle manner than phorbol ester.	247
1.9. Studies on gene expression arrays reveal that PKC $\alpha$ depletion decreases the malignancy of MCF-7 and MDA-MB-231 breast cancer cells.	248
1.10. The effects of salinomycin on breast cancer cells are enhanced by PKC $\alpha$ depletion.	249
<b>2. Conclusions.</b>	<b>251</b>
<b>ANNEX I (MCF-7 DEREGULATED GENES)</b>	<b>255</b>
<b>ANNEX II (MDA-MB-231 DEREGULATED GENES)</b>	<b>263</b>
<b>BIBLIOGRAPHY</b>	<b>269</b>



PRÓLOGO

RESUMEN EN CASTELLANO



# I. INTRODUCCIÓN.

## I.1. PROTEÍNAS QUINASAS C: Estructura y clasificación.

Las Proteínas Quinasas C (PKC) constituyen un grupo de enzimas con actividad fosfotransferasa que fosforilan específicamente residuos de Ser y Thr de sus proteínas sustrato. Están involucradas en diversas vías de transducción de señales en las células, participando en multitud de funciones fisiológicas, así como procesos patológicos como el cáncer y determinadas cardiopatías entre otros (Nishizuka, 1995; Newton, 2001; Ohno y Nishizuka, 2002; Corbalán-García y Gómez-Fernández, 2006). Su ubicuidad y diversidad funcional, las hacen una familia muy importante de proteínas, cuyo objeto de estudio es de gran relevancia.

Esta familia de enzimas se compone de 10 isoenzimas, que están codificados por 9 genes en mamíferos. Cada isoenzima se expresa en una amplia variedad de células y además cada célula expresa un gran número de estas proteínas, siendo así una familia muy ubicua, además del gran número de funciones celulares que desempeña.

Las isoenzimas de la PKC se han clasificado en tres subfamilias en base a su estructura primaria y dependencia de distintos cofactores para obtener un incremento de su actividad enzimática (Figura I.1):

**a) PKC clásicas o convencionales:** incluye las isoenzimas PKC $\alpha$ ,  $\beta$ I,  $\beta$ II y  $\gamma$  (Inoue y col., 1977; Coussens y col., 1986). Presentan un dominio pseudosustrato, el dominio C1 capaz de interaccionar con DAG y ésteres de forbol, y un dominio C2 capaz de unir Ca<sup>2+</sup> y fosfolípidos aniónicos.

**b) PKC nuevas:** en esta subfamilia se agrupan las isoenzimas  $\epsilon$ ,  $\delta$  (Ono y col., 1987a),  $\eta$  (Osada y col., 1990) y  $\theta$  (Osada y col., 1992). Este grupo posee los mismos dominios reguladores que las PKC clásicas, pero el dominio C2 es insensible a Ca<sup>2+</sup>, por eso este grupo de enzimas solo necesita de fosfolípidos aniónicos y DAG o ésteres de forbol para activarse totalmente.

**c) PKC atípicas:** es una subfamilia compuesta por dos miembros, la PKC $\zeta$  y la PKC  $\iota/\lambda$  [PKC $\iota$  (isoforma en humanos) (Selbie y col., 1993)/ PKC $\lambda$  (isoforma en ratón) (Akimoto y col., 1994)]. Este grupo solo posee el dominio pseudosustrato, un dominio C1 incapaz de interaccionar con DAG o ésteres de forbol y otro llamado PB1 encargado de interaccionar con otras proteínas.

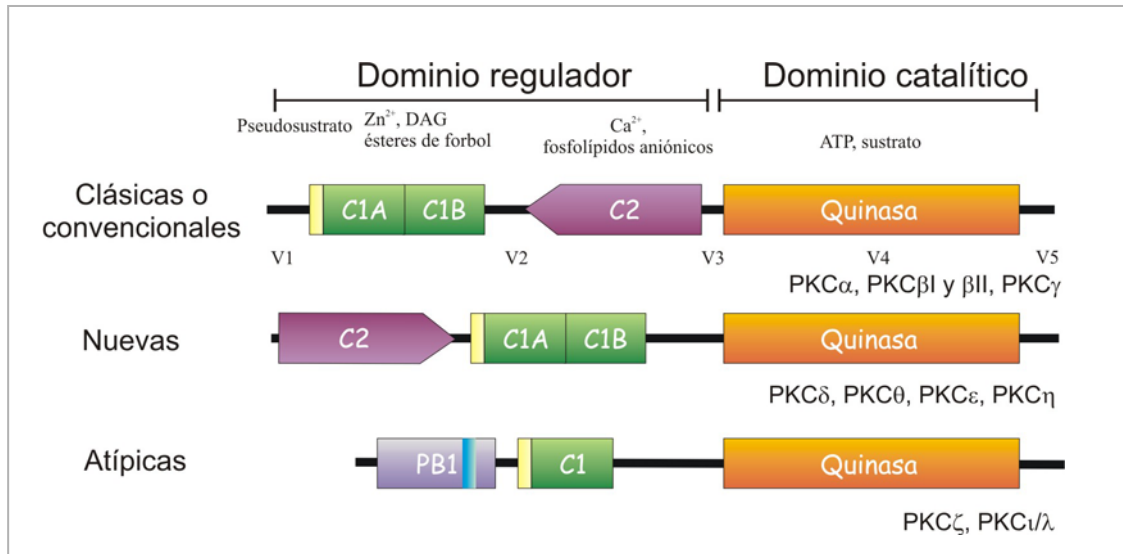


**Figura I.1. Representación esquemática de la estructura primaria de los isoenzimas de la PKC.** Se muestran los distintos dominios que lo forman, así como los requerimientos de cofactores para su regulación. En el extremo amino terminal se encuentra la región reguladora, con el dominio pseudosustrato, y los dominios C1 y C2, que unen diferentes cofactores según el tipo de isoenzima. El extremo carboxilo terminal, contiene la región catalítica del enzima con el dominio quinasa de unión al ATP y al sustrato. Las regiones variables se muestran nombradas como V1, V2, V3, V4 y V5. La región en azul presente en el dominio PB1 de las atípicas. (Tomado de Corbalán García y Gómez Fernández, 2006).

El dominio C1 suele presentarse en *tandem* formando 2 subdominios, cada uno de los que posee una secuencia consenso del tipo **HX<sub>12</sub>CX<sub>2</sub>CX<sub>13/14</sub>CX<sub>2</sub>CX<sub>4</sub>H X<sub>2</sub>CX<sub>2</sub>CX<sub>7</sub>C** siendo imprescindible para la coordinación de dos iones de zinc. Presentan una estructura globular, donde los aminoácidos se agrupan en una distribución polarizada; en la parte superior, por donde se unen al DAG o ésteres de forbol, se encuentran residuos aromáticos, mientras que en la parte media se encuentran aminoácidos catiónicos.

El otro dominio de la región reguladora es el dominio C2, cuya estructura es un  $\beta$ -sandwich compuesto por ocho cadenas  $\beta$  dispuestas de forma antiparalela y que están conectadas por medio de lazos de estructura flexible tanto en la parte alta como baja del dominio (Figura I.2) (Cho y Stahelin, 2006). En las PKCs clásicas el principal papel de este dominio es actuar como motivo de anclaje a la membrana activado por  $\text{Ca}^{2+}$  (Corbalán-García y Gómez-Fernández, 2006; Cho y Stahelin, 2006).

El dominio presenta dos regiones funcionales importantes; la primera es la *región de unión a calcio* localizada en la parte superior y encargada de unir dos o tres iones  $\text{Ca}^{2+}$  dependiendo de la isoenzima, además de PtdSer (Conesa-Zamora y col., 2000; Ochoa y col., 2002). La otra región importante es la *región polibásica o rica en lisinas*, la cuál ha sido sugerida como la que une específicamente PtdIns(4,5)P<sub>2</sub> (Sánchez-Bautista y col., 2006).

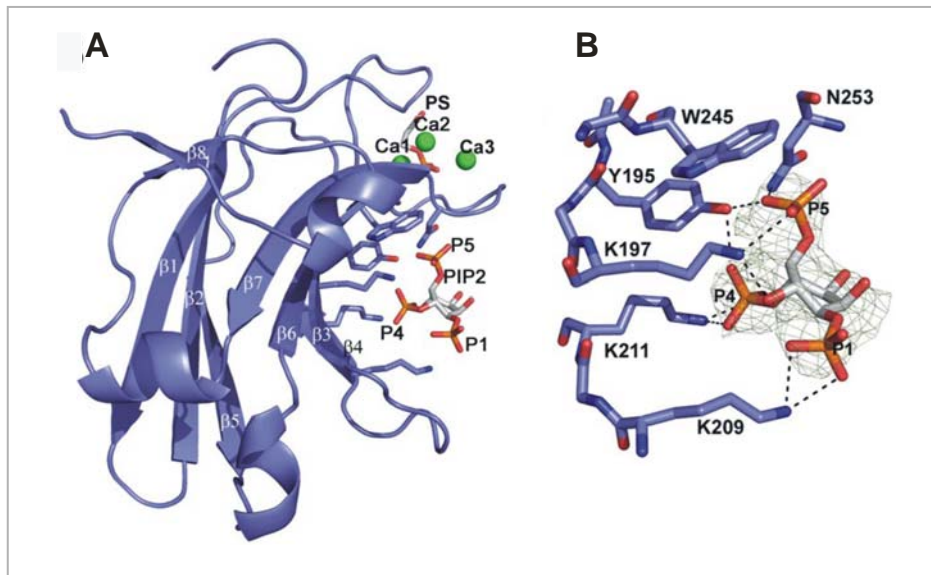


**Figura 1.2. Representación del dominio C2.** (A) Se observa la unión a la PtdSer por la *región de unión de Ca<sup>2+</sup>* en la parte superior del esquema, y a una molécula de PtdIns(4,5)P<sub>2</sub> (o PIP2) por la *región polibásica* en el centro del esquema. (B) Se representa amplificado un detalle de la *región polibásica* del dominio C2, concretamente los residuos de las cadenas β3 y β4 encargados de la interacción con el PtdIns(4,5)P<sub>2</sub> (Tomado de Guerrero-Valero y col., 2009).

Para la activación de la PKC, antes debe localizarse en membranas biológicas donde se encuentren sus cofactores. En el caso de las PKCs clásicas, la translocación es mediada por los dominios C1 y C2 siendo primeramente la interacción del dominio C2 con la PtdSer de la membrana a través de Ca<sup>2+</sup>, lo que favorece que el dominio C1 interactúe con DAG, permitiendo un mejor anclaje de la PKC a la membrana (Corbalán-García y Gómez Fernández, 2006). La PtdSer y el DAG son los cofactores clásicos, pero hoy en día se ha visto que otros lípidos también son capaces de activar diferentes isoenzimas de PKC (López-Andreo y col., 2005).

## I.2. Proteínas Quinasas C y cáncer.

La familia de PKC, además de participar en multitud de funciones biológicas, fue involucrada en el cáncer inicialmente por ser el receptor celular de los ésteres de forbol. Más tarde se vio su relación con otros oncogenes, confirmando el papel de la PKC en el cáncer.

A diferencia de otras proteínas, su influencia en el desarrollo de cáncer no es por mutación, sino por una desregulación de sus niveles en células tumorales, pudiendo estar más o menos sobre- o sub-expresada en función de la isoenzima y tipo de cáncer. En el caso concreto del cáncer de mama, se ha visto una sobre-expresión de la PKCα siendo la causante de la generación de resistencia frente a diversos agentes terapéuticos (Gill y col., 2001).

Por todo ello las diferentes isoenzimas de PKC han sido elegidas como posibles dianas en el tratamiento de varios tipos de cáncer. Hoy en día se han rechazado muchos de los compuestos propuestos, principalmente por la falta de especificidad contra una determinada isoenzima de PKC. Dado que el cáncer es una afección multifactorial donde están implicadas un gran número de proteínas, la estrategia seguida en la actualidad se basa en el tratamiento con varios compuestos simultáneamente con el fin de inhibir al máximo número de rutas posibles (entre ellas las conducidas por PKC), mejorando así la eficacia del tratamiento.

### **I.3. OBJETIVOS.**

Los objetivos concretos de esta Tesis Doctoral son los siguientes:

- Caracterización del mecanismo molecular por el cuál el ácido araquidónico induce la localización y posterior activación de PKC $\alpha$ .
- Determinación de la función de los dominios reguladores C1 y C2 de la PKC $\alpha$  en la localización celular y activación provocada por el ácido araquidónico, oleico, eicosapentaenoico y docosahexaenoico.
- Determinación de los efectos que tienen el ácido oleico y algunos ácidos grasos omega-3 como el EPA y DHA en cultivos celulares provenientes de cáncer de mama.
- Caracterización de las funciones desempeñadas por la PKC $\alpha$  en células MCF-7 y MDA-MB-231 estimuladas con ácido oleico, eicosapentaenoico y docosahexaenoico.
- Caracterización de los efectos que tienen las DAG-lactonas con carga positiva en la localización de diferentes isoformas de PKC en células MCF-7.
- Determinación del grado de anclaje de diferentes isoformas de PKC en la membrana plasmática de células MCF-7 en presencia de DAG-lactonas con carga positiva.
- Determinación de las funciones de PKC $\alpha$  en líneas celulares invasivas (MDA-MB-231) y no invasivas (MCF-7).
- Caracterización de los efectos de la salinomicina en líneas celulares de cáncer de mama y la función que PKC $\alpha$  desempeña en este proceso.

## II. Materiales y Métodos.

### II.1. Construcciones de ADN plasmídico.

Los ADN correspondientes a diferentes isoenzimas de PKC fueron cedidos por los Drs. Y Nishizuka y S Ono. Éstos fueron amplificados mediante PCR y expresados en *Escherichia coli* siguiendo el protocolo propuesto por Cohen y col., 1973, con el fin de producir grandes cantidades de plásmidos. Las construcciones que se generaron fueron las siguientes:

CONSTRUCCIONES	OLIGONUCLEOTIDOS USADOS	ENZIMAS RESTRICCIÓN
PKC $\alpha$ -WT-EGFP (PKC $\alpha$ -EGFP)	5' ATTCTCGAGCTATGGCTGACGT 3' CCGCCTACCTACGCACTTTGCAAGAT	KpnI/XhoI
PKC $\alpha$ D246N/D248N-EGFP	5' ATTCTCGAGCTATGGCTGACGT 3' CCGCCTACCTACGCACTTTGCAAGAT	KpnI/XhoI
PKC $\alpha$ K197A/199A-EGFP	5' ATTCTCGAGCTATGGCTGACGT 3' CCGCCTACCTACGCACTTTGCAAGAT	KpnI/XhoI
PKC $\alpha$ K209A/K211A-EGFP	5' ATTCTCGAGCTATGGCTGACGT 3' CCGCCTACCTACGCACTTTGCAAGAT	KpnI/XhoI
PKC $\alpha$ W58G-EGFP	5' ATTCTCGAGCTATGGCTGACGT 3' CCGCCTACCTACGCACTTTGCAAGAT	KpnI/XhoI
PKC $\alpha$ F60G-EGFP	5' ATTCTCGAGCTATGGCTGACGT 3' CCGCCTACCTACGCACTTTGCAAGAT	KpnI/XhoI
PKC $\alpha$ Y123G-EGFP	5' ATTCTCGAGCTATGGCTGACGT 3' CCGCCTACCTACGCACTTTGCAAGAT	KpnI/XhoI
PKC $\alpha$ L125G-EGFP	5' ATTCTCGAGCTATGGCTGACGT 3' CCGCCTACCTACGCACTTTGCAAGAT	KpnI/XhoI
PKC $\delta$ -WT-ECFP (PKC $\delta$ -ECFP)	5' AAGGTACCGGGCGGCGCACCGTTCCTGCGCATC 3' CGGGATCCTCACTATTCAGGAATTGCTCATA	BamHI/KpnI
PKC $\alpha$ -WT-HA (PKC $\alpha$ -HA)	5' ATTCTCGAGCTATGGCTGACGT 3' CCGCCTACCTACGCACTTTGCAAGAT	XbaI/KpnI
PKC $\alpha$ D246N/D248N-HA	5' ATTCTCGAGCTATGGCTGACGT 3' CCGCCTACCTACGCACTTTGCAAGAT	XbaI/KpnI
PKC $\alpha$ K197A/199A-HA	5' ATTCTCGAGCTATGGCTGACGT 3' CCGCCTACCTACGCACTTTGCAAGAT	XbaI/KpnI
PKC $\alpha$ K209A/K211A-HA	5' ATTCTCGAGCTATGGCTGACGT 3' CCGCCTACCTACGCACTTTGCAAGAT	XbaI/KpnI
PKC $\alpha$ W58G-HA	5' ATTCTCGAGCTATGGCTGACGT 3' CCGCCTACCTACGCACTTTGCAAGAT	XbaI/KpnI

## **II.2. Cultivos celulares y transfecciones.**

Para esta Tesis Doctoral se usaron tres líneas celulares provenientes de cáncer de mama, concretamente BT-474, MCF-7 y MDA-MB-231. Todas se crecieron en medio de cultivo DMEM 4,5 g/l glucosa suplementado con 10% suero bovino fetal, antibiótico, glutamina y piruvato; además de ello la línea MDA-MB-231 también se suplementó con aminoácidos no esenciales.

Las transfecciones con ADN plasmídico se realizaron de forma distinta según la línea celular, para MCF-7 se utilizó Lipofectamina 2000 siguiendo las recomendaciones del fabricante, mientras que para BT-474 se usó la electroporación con los siguientes parámetros:

Protocolo Square wave: 2 pulsos de 200 V de 8 ms cada uno, con descanso de 5 s entre ambos.

Para la inhibición de la expresión de PKC $\alpha$  se utilizaron diferentes oligos de ARN de interferencia según la línea celular y se electroporó siguiendo las condiciones siguientes para las tres líneas celulares:

Protocolo Square wave: 2 pulsos de 800 V de 0,2 ms cada uno, con descanso de 5 s entre ambos.

## **II.3. Microscopía confocal.**

Se usó el microscopio confocal Laica TCS SP2 AOBS (Leica, Heidelberg, Germany) con el objetivo Nikon PLAN APO-CS 63x 1.4 NA (aceite de inmersión) para visualizar las células que expresan las construcciones fluorescentes y que han incorporado el indicador de Ca<sup>2+</sup> Fluo-3.

Las células cargadas con Fluo-3 o transfectadas con construcciones de EGFP, fueron excitadas con el láser Ar/ArKr a 488 nm y la emisión se recogió entre 500-520 nm. En el caso de construcciones ECFP se utilizó el láser diodo azul a 405 nm para la excitación y 470-490 nm para la detección.

Se recogieron series de imágenes respecto al tiempo y los datos de localización y flujos de Ca<sup>2+</sup> se analizaron con el programa Imagen NIH (<http://rsb.info.nih.gov/ij/> 1997-2010).

## II.4. Purificación y medidas de actividad quinasa.

Para la obtención de proteínas parcialmente purificadas (concretamente los dos mutantes de la PKC $\alpha$  de la *región polibásica* y un mutante del dominio C1A) se transfectaron células HEK-293 mediante la técnica de fosfato de calcio. Después de expresar la proteína de interés, se lisaron las células y se introducía el sobrenadante en una columna de DEAE-Sephacel. Para la elución de la proteína de interés se utilizó el sistema EconoSystem por medio de un gradiente salino.

Con estas enzimas parcialmente purificadas se llevaron a cabo experimentos de actividad enzimática utilizando el isótopo radiactivo  $^{32}\text{P}$ . El proceso consiste en simular las condiciones óptimas para la activación de la enzima, es decir, presencia de vesículas lipídicas,  $\text{Ca}^{2+}$ , ATP (una parte marcado con radiactividad) y como sustrato se utilizó la histona III-S. Tras 10 minutos de actuación de la PKC, se para la reacción con BSA y tricloroacético para finalmente medir, mediante un contador de centelleo, el grado de marcaje de la histona con el isótopo radiactivo.

## II.5. Microarrays.

Después de crecer las células en las condiciones adecuadas, se les extrae el ARN total utilizando el RNeasy Plus kit para posteriormente marcarlo con biotina. Este proceso de marcaje conlleva una serie de pasos como la transcripción reversa, purificación del cADN obtenido para después llevar a cabo la transcripción *in vitro* donde el nuevo ARN sintetizado es marcado con biotina. Para todo esto se utilizó el MessageAmp™ II-Biotin *Enhanced* Kit siguiendo las condiciones del fabricante.

A continuación ese ARN marcado se fragmenta para hibridarlo con el GeneChip® Probe Array (Affymetrix) durante 16 horas a 45°C. Por último se introduce el chip en las “Fluidics Stations” antes de escanearlo en el Affymetrix® GeneChip® Scanner 3000.

Los resultados obtenidos tras el escaneo, se analizan usando el programa R con el fin de extraer una lista con los genes expresados con diferencias significativas entre las células control y aquellas donde se ha inhibido la expresión de PKC $\alpha$ .

Por último esa lista de genes se introduce en la base de datos “GENECODIS” para hacer una clasificación según Gene Ontology y KEGG pathways.

## **II.6. Análisis estadístico.**

Los análisis estadísticos se realizaron por medio de los test de la chi-cuadrado, Kruskal-Wallis, Man-Whitney y de la varianza según cada caso. Se utilizó el paquete estadístico SPSS y se consideró una diferencia significativa cuando  $p < 0.05$ .

### III. Localización de PKC $\alpha$ dependiente de ácido araquidónico.

El ácido araquidónico es un ácido graso del tipo omega-6 muy frecuente en la grasa animal, así como en las membranas biológicas. Hay evidencias que sugieren que estos tipos de lípidos poseen capacidad tumoral y de metástasis (*Rose y Connolly, 2000*), de ahí el interés de estudiar el efecto de este ácido graso en células de cáncer de mama a través de la localización y posterior activación de la PKC $\alpha$ .

Los resultados nos confirman la capacidad del ácido araquidónico de localizar la PKC $\alpha$ , llevándolo a cabo de una forma dependiente de Ca $^{2+}$ . Además se observó que aunque el propio ácido graso no producía el aumento de calcio citosólico, cooperaba con la ionomicina (un ionóforo para el Ca $^{2+}$ ) a la hora de incrementar la concentración de dicho ión en el citoplasma.

Estudios posteriores han determinado que el dominio C2, principalmente la *región de unión a calcio*, de la PKC $\alpha$  es muy importante en el proceso de localización. En relación al dominio C1 se observó que el realmente importante es el subdominio C1A, mientras que el C1B no juega un papel tan importante en el proceso de localización de la PKC $\alpha$  mediado por ácido araquidónico.

De los resultados obtenidos se pudo concluir el mecanismo molecular por el que el ácido araquidónico induce la localización y posterior activación de la PKC $\alpha$ . Básicamente consiste en que tras una elevación en los niveles de Ca $^{2+}$  en el citoplasma la PKC $\alpha$  interacciona inicialmente con el ácido araquidónico a través de la *región de unión a Ca $^{2+}$*  del dominio C2 utilizando dicho ión como puente. Esta inicial interacción favorece que el subdominio C1A se una al ácido araquidónico disponible en la membrana plasmática, anclando así más firmemente la PKC $\alpha$  y permitiendo su posterior activación.

## **IV. Efecto del ácido oleico en células modelo de cáncer de mama a través de PKC $\alpha$ .**

Desde la antigüedad hasta nuestros días se le ha asignado un efecto protector del aceite de oliva frente al cáncer (y concretamente al de mama) y otras enfermedades cardiovasculares. Básicamente ese efecto es debido al ácido oleico y otras sustancias minoritarias como los compuestos fenólicos.

El ácido oleico, al igual que el araquidónico, es capaz de localizar la PKC $\alpha$  de una manera dependiente de Ca<sup>2+</sup>, interaccionando a través del la *región de unión a Ca<sup>2+</sup>* del dominio C2, jugando está un papel esencial en la localización y posterior activación de PKC $\alpha$ . En dichos procesos, tanto la *región rica en lisinas* como el dominio C1 no muestran un papel muy relevante aunque también son necesarios para una localización total y estable en la membrana plasmática para una posterior activación enzimática.

En relación a las funciones celulares estudiadas en los distintos modelos de cáncer de mama, se observó que el ácido oleico es capaz de inhibir levemente la capacidad proliferativa, migrativa e invasiva de las células estudiadas, así como activar la apoptosis también de una forma leve. Los mayores efectos en estos aspectos se encontraron cuando la expresión de la PKC $\alpha$  fue inhibida.

El mayor efecto mostrado por el ácido oleico en las células de cáncer de mama fue la desorganización del citoesqueleto provocando que las células se agranden y no lleguen a dividirse (de ahí la inhibición de la proliferación celular). Este efecto se vio potenciado con la inhibición de la expresión de PKC $\alpha$  en dichas células mediante el uso de ARN de interferencia.

## **V. Efecto de los ácidos grasos omega-3 y la inhibición de la expresión de PKC $\alpha$ en células modelo de cáncer de mama.**

A lo largo de la historia se ha considerado una relación entre la mayor ingesta de grasa en la dieta y una mayor incidencia en cáncer, pero estudios recientes revelan que es más importante el tipo de grasas ingeridas y no tanto la cantidad. De estos estudios se deduce que los ácidos grasos poli-insaturados, entre los que se incluyen los omega-3, ejercen un efecto protector y también mejoran el tratamiento con otros compuestos quimioterápicos.

En este estudio se valoró el efecto de dos omega-3 (EPA y DHA), así como la inhibición de la expresión de PKC $\alpha$ , en distintos aspectos del metabolismo en diversas líneas celulares provenientes de cáncer de mama.

Ambos ácidos grasos fueron capaces de localizar la PKC $\alpha$  en la membrana plasmática de las células estudiadas aunque solo el DHA fue capaz de conseguir la activación de la enzima estudiada. En este proceso se observó el papel esencial de *la región de unión de Ca<sup>2+</sup>* y *la región rica en lisinas*, ambas presentes en el dominio C2 de la proteína, mientras que el dominio C1 no era tan importante.

Después de estudiar la capacidad migratoria e invasiva de las células de cáncer de mama, observamos que ambos lípidos las inhiben, siendo más efectivo el DHA. Además, en función de la línea estudiada, se aprecia o no una gran sinergia en estos efectos cuando además se inhibe la expresión de la PKC $\alpha$ , llegando incluso a abolir la migración en células MCF-7.

Respecto a la apoptosis, ambos ácidos grasos aumentan la muerte celular programada, siendo mayor el efecto del DHA. Además, se ha diferenciado entre apoptosis temprana y tardía, poniéndose de manifiesto que estos ácidos grasos poli-insaturados actúan de una forma moderadamente rápida, ya que en tan solo 4 días de tratamiento, ya existe apoptosis temprana. En este aspecto, también existe una sinergia entre el tratamiento con estos omega-3 y la inhibición de la expresión de PKC $\alpha$ , pero esta vez en las células MDA-MB-231, induciéndoles un 70% de apoptosis cuando inhibimos la PKC $\alpha$  y tratamos con DHA al mismo tiempo.

## **VI. Caracterización biológica de DAG-lactonas a través de PKCs.**

Las DAG-lactonas son compuestos sintetizados químicamente y formadas por un anillo de cinco miembros al que se le unen diferentes cadenas pudiendo tener cientos de compuestos. Estas sustancias surgieron en un pasado reciente con el fin de modular específicamente la actividad de distintas enzimas que posean dominios C1 (entre ellas, la familia de PKC) ya que es dicho dominio la diana de estos compuestos.

De todas las DAG-lactonas probadas en este estudio, solo dos (153C-022 y 153B-143) mostraron efecto sobre alguna isoforma de PKC. Además también se demostró que ambos compuestos producían una más rápida localización que el éster de forbol en todos los casos.

El compuesto 153C-022 consiguió localizar tanto a isoenzimas clásicas (PKC $\alpha$ ) como nuevas (PKC $\epsilon$  y PKC $\delta$ ) a la membrana plasmática de células MCF-7, mientras que la otra DAG-lactona solo consiguió dicho efecto en las isoenzimas nuevas, sugiriendo que la estructura ramificada de 153B-143 muestra especificidad por los dominios C1 de esas PKCs.

También se estudió el grado de anclaje que ejercían las DAG-lactonas en las diferentes isoenzimas de PKC en la membrana plasmática tras su localización. Se observó que la DAG-lactona 153C-022 ancla de una manera más ligera la PKC $\alpha$  a la membrana que la PKC $\epsilon$ , permitiendo una mayor movilidad lateral por la membrana plasmática a la PKC clásica que a la nueva. Además se comprobó que esta mayor movilidad de la PKC $\alpha$  unida a la DAG-lactona también es significativamente mayor que la producida por dicha isoenzima unida a ésteres de forbol, lo que explicaría el efecto beneficioso del tratamiento con 153C-022 ya que la PKC $\alpha$  activaría una gran cantidad de rutas de señalización (tanto de proliferación como apoptosis), mientras que con ésteres de forbol se activaría pocas rutas (principalmente de crecimiento y proliferación) provocando el efecto tumorigénico típico de este compuesto.

## **VII. Perfil de expresión génica en células modelo de cáncer de mama en ausencia de PKC $\alpha$ .**

Una vez comprobados los efectos en la disminución de la capacidad proliferativa, migrativa e invasiva, así como la inducción de la apoptosis en diferentes modelos de cáncer de mama después de eliminar la PKC $\alpha$  en dichas líneas celulares, decidimos estudiar los genes que se veían afectados en estos eventos. Para ello, se inhibió la expresión de PKC $\alpha$  en una línea celular invasiva (MDA-MB-231) y otra no invasiva, se les extrajo el ARNm y se realizaron unos microarrays de expresión diferencial de genes de la plataforma Affymetrix.

Después de obtener la lista de genes con diferente expresión significativa, se clasificaron según el criterio de KEGG pathways presente en la base de datos GeneCodis disponible en la web. En ambas líneas celulares los grupos generados sugerían la hipótesis de que tras inhibir una enzima implicada en el desarrollo de cáncer (como es la PKC $\alpha$ ), muchos otros genes de supervivencia y multiplicación celular también se verían con una expresión reducida, mientras que aquellos genes implicados en apoptosis y parada del ciclo celular estarían sobre-expresados. Esto nos sugiere que la PKC $\alpha$  controla diversas rutas para la estimulación del crecimiento y la inhibición de apoptosis.

Los genes significativamente sobre- y sub-expresados en ambas líneas celulares son diferentes, aunque globalmente las rutas de señalización afectadas son similares y proponen efectos fenotípicos parecidos.

Los resultados nos sugerían la hipótesis de que tras inhibir la expresión de PKC $\alpha$ , las células tumorales tratan de suplir esa ausencia sobre-expresando otros genes, por eso decidimos hacer tratamientos conjuntos con la inhibición de la expresión de PKC $\alpha$  a la vez que inhibíamos específicamente las proteínas cuyos genes tenían una mayor expresión.

En el caso de MCF-7, las proteínas inhibidas fueron PLC, PKA, HER y PDGF, obteniendo resultados satisfactorios en la inhibición de la migración, llegando en algunos casos a la eliminación de la capacidad migratoria celular, así como en la estimulación de la apoptosis. Sin embargo en el caso de las MDA-MB-231, apenas se observó efecto en la migración, invasión y apoptosis tras inhibir específicamente las proteínas GGTaseI, FTase y MMP a la vez que se inhibía la expresión de PKC $\alpha$ .

## **VIII. El tratamiento de las células modelo de cáncer de mama con salinomicina potencia el efecto de la inhibición de PKC $\alpha$ .**

La salinomicina es un antibiótico que fue muy utilizado en el pasado para el tratamiento de coccidiosis en aves de corral, así como para un mayor engorde del ganado. Sin embargo hoy en día se ha visto el efecto beneficioso en el tratamiento del cáncer ya que es capaz de neutralizar las múltiples resistencias que generan las células cancerosas frente a numerosos compuestos, así como inducirles apoptosis.

En nuestro trabajo se planteó el estudio del mecanismo, a través de PKC $\alpha$ , por el cuál este antibiótico ejerce su acción en dos líneas celulares de cáncer de mama.

En MCF-7 observamos una gran inhibición de la migración, incluso fue eliminada cuando tratamos conjuntamente las células con este antibiótico e inhibimos la expresión de PKC $\alpha$ . También se obtuvieron resultados satisfactorios en apoptosis, ya que cuadruplicaba el porcentaje de células apoptóticas respecto a las células sin tratar. Estos resultados nos sugerían que la inhibición de la migración ejercida por la salinomicina la hacía implicando a la PKC $\alpha$ , mientras que la inducción de la apoptosis es independiente de esta enzima.

En el caso de MDA-MB-231, se obtuvieron resultados similares resultados en cuanto a la inhibición de la migración e invasión, a la vez que estimulaba la apoptosis. Sin embargo en esta línea celular las rutas implicadas en estos aspectos celulares fueron distintas ya que la PKC $\alpha$  no intervenía en la inhibición de la migración inducida por la salinomicina, mientras que sí juega un papel importante en la inhibición de la invasión y la estimulación de la apoptosis en dicha línea celular.

## IX. CONCLUSIONES.

Las conclusiones más importantes de esta Tesis Doctoral son:

- 1) La localización de PKC $\alpha$  en la membrana plasmática de células MCF-7 inducida por ácido araquidónico es un proceso dependiente de Ca<sup>2+</sup>. Este proceso empieza con la interacción del dominio C2 con el ácido araquidónico para finalizar con el anclaje estable a través del dominio C1A.
- 2) En la localización y activación de la PKC $\alpha$  por ácido oleico la *región de unión a calcio* juega un papel esencial, mientras que la *región rica en lisinas* y el dominio C1 tienen un papel menos relevante.
- 3) Los ácidos grasos omega-3 eicosapentaenoico y docosahexaenoico reducen la migración e invasión de células MDA-MB-231 de forma independiente a PKC $\alpha$ , mientras que en células MCF-7 solo el docosahexaenoico muestra efecto en la inhibición de la migración, aunque lo hace de una forma dependiente de PKC $\alpha$ . En la apoptosis, ambos omega-3 aumentan la muerte celular programada en ambas líneas celulares. Lo hacen de una forma dependiente de PKC $\alpha$  en el caso de MDA-MB-231, e independientemente en MCF-7.
- 4) La DAG-lactona 153B-143 interacciona específicamente con las isoenzimas de PKC nuevas.
- 5) Las diferentes isoenzimas de PKC muestran más afinidad por las DAG-lactonas que por el PMA, localizándose más rápido las nuevas que las clásicas.
- 6) La inhibición de la PKC $\alpha$  usando ARN de interferencia reduce la agresividad de las líneas celulares de cáncer de mama, frenándoles la tasa de crecimiento, migración e invasión, así como aumentando el nivel de apoptosis.
- 7) Tanto las células MCF-7 como MDA-MB-231 muestran un perfil de expresión génica tras inhibirles la expresión de PKC $\alpha$ , donde la mayoría de genes se expresan menos que en las células control. Esto indica el papel que tiene la PKC $\alpha$  en dichas líneas celulares.
- 8) La salinomicina inhibe la migración en MCF-7 de un modo dependiente de PKC $\alpha$ , mientras que la inducción de apoptosis lo hace independientemente de dicha enzima. En el caso de las células MDA-MB-231, la salinomicina inhibe la invasión y estimula la apoptosis involucrando la PKC $\alpha$ , mientras que la inhibición de la migración en dicha línea celular lo hace independientemente de la mencionada isoenzima.



## COMMON ABBREVIATIONS USED

AA	Arachidonic acid
ADP	Adenosine diphosphate
ALA	Alpha linolenic acid
AOBS	Acousto optical beam splitter
AOTF	Acousto optical tunable filter
ATP	Adenosine-5'-triphosphate
BME	Basement membrane extract
BSA	Bovine serum albumin
CDK	Cyclin-dependent kinase
CBR	Calcium Binding Region
CFP	Cyan fluorescent protein
CMV	Cytomegalovirus promoter
CSC	Cancer stem cells
DAG	Diacylglycerol
DAPS	1,2-diacetyl- <i>sn</i> -phosphatidyl-L-serine
DGK	Diacylglycerol kinase
DHA	Docosahexaenoic acid
DMBA	7,12-dimethylbenz(a)anthracene
DMEM	Dulbecco's modified Eagle's medium
PH domain	Pleckstrin homology domain
dsDNA	Double strand DNA
DTT	Dithiothreitol
ECFP	Enhanced cyan fluorescent protein
EDTA	Ethylenediaminetetraacetic acid
EGFP	Enhanced green fluorescent protein
EGFR	Epidermal growth factor receptor
EGTA	Ethylene glycol tetraacetic acid
EPA	Eicosapentaenoic acid
ER	Estrogen receptor
ERK	Extracellular signal-regulated kinase
FCS	Fetal calf serum
FRAP	Fluorescence recovery after photobleaching
FRET	Fluorescence resonance energy transfer
FTase	Farnesyltransferase
GAP43	Growth associated protein 43
GGTase I	Geranylgeranyltransferase I
GLA	Gamma linolenic acid
GTPase	Guanosine triphosphate hydrolase
HA-tag	Hemagglutinin-tag
HBS	Hepes buffer salinum
HSP90	Heat shock protein-90
IGFBPs	Like-insulin growth factor binding proteins
Ins(1,4,5)P <sub>3</sub>	Inositol-1,4,5-trisphosphate
IVT	<i>In vitro</i> transcription
JNK	c-Jun N-terminal kinase
Kan <sup>r</sup>	Kanamycin resistance

LA	Linoleic acid
LB	Lysogeny broth or Luria Bertani
MAPK	Mitogen-activated protein kinase
MARCKS	Myristoylated alanine-rich C-kinase substrate
MCS	Multiple cloning site
MDR	Multidrug resistance
MMP	Matrix metalloproteinase
MUFA	Monounsaturated fatty acid
NSCLC	Non-small cell lung cancer
OA	Oleic acid
PC-PLC	Phosphatidylcholine-dependent phospholipase C
PCR	Polymerase chain reaction
PDK-1	Phosphoinositide-dependent protein kinase-
PI	Propidium iodide
PIP kinases	Phosphatidylinositol phosphate kinases
PI3K	Phosphoinositide 3-kinase
PKA	Protein kinase A
PKB	Protein kinase B
PKC	Protein Kinase C
PKD	Protein Kinase D
PLC	Phospholipase C
PLC-PI	Phosphoinositide phospholipase C
PLD	Phospholipase D
PMA	phorbol 12-myristate 13-acetate
PSA	Ammonium persulfate
PtdCho	Phosphatidylcholine
PtdIns(4,5)P <sub>2</sub>	Phosphatidylinositol-4,5-bisphosphate
PtdSer	Phosphatidylserine
PUFA	Polyunsaturated fatty acid
rasGRP	Ras guanyl-releasing protein
RACK	Receptor for activated C-kinase
RB	Retinoblastoma protein
RNA	Ribonucleic acid
ROS	Reactive oxygen species
RT	Room temperature
RTK	Receptor tyrosine kinase
SDS-PAGE	Sodium dodecyl sulphate-polyacrylamide gel electrophoresis
SFA	Saturated fatty acid
siRNA	Small interference RNA
siRNA $\alpha$	Small interference RNA to inhibited PKC $\alpha$ expression
STAT	Signal transducer and activator of transcription
STICKs	Substrate that interact with C-kinases
TCA	Trichloroacetic
TEMED	Tetramethylethylenediamine
TGF $\alpha$ R	Transforming growth factor $\alpha$ receptor
TNF- $\alpha$	Tumour necrosis factor $\alpha$
VEGF	Vascular endothelial growth factor

## CHAPTER I

### INTRODUCTION AND OBJECTIVES



## 1. Introduction to PROTEIN KINASE C. Structure and classification.

There are many signalling enzymes in living cells which function by transmitting information from the plasma membrane to the nucleus. Protein kinases C (PKCs) are included in a group of enzymes with phosphotransferase activity. They specifically phosphorylate Ser/Thr in their target protein and they have a crucial role in signalling transmission since they are involved in several pathways, taking part in an enormous variety of physiological functions, including mitogenesis and cell proliferation, metabolism regulation, apoptosis, platelet activation, reorganization of actin cytoskeleton, ion channel modulation, secretion and neural differentiation, and also in many illnesses like cancer, lung and heart diseases (*Nishizuka, 1986; Nishizuka, 1992; Coleman and Wooten, 1994; Mangoura et al., 1995; Dekker and Parker, 1997; Mellor and Parker, 1998; Ron and Kazanietz, 1999; Dempsey et al., 2000; Griner and Kazanietz, 2007*).

There are several isoenzymes, which are expressed in a large variety of tissues, and every cell expresses a large number of these proteins which are activated in response to different metabolites. Bearing all this in mind, PKC is seen to be an ubiquitous enzyme and to possess wide functional diversity, which underlines the enormous importance of their study (*Bell et al., 1986; Nishizuka, 1992; Newton, 1995; Mellor and Parker, 1998*).

Classification of the ten PKC isoenzymes that exist is based on their primary structure and their dependence on different cofactors to attain the maximum enzymatic activity. These ten isoenzymes can be distributed in three groups:

- Classical or conventional PKCs (cPKC): these include PKC $\alpha$ ,  $\beta$ I,  $\beta$ II and  $\gamma$ . Two isoforms of PKC $\beta$  result from differential RNA processing. The difference lies in their carboxyl-terminal region, more specifically the V5 region, varying the localization in the active or inactive state (*Ono et al., 1986; Ono et al., 1987a; Disatnik et al., 1994; Luria et al., 2000*). Isoenzymes included in this family need DAG or phorbol ester, anionic phospholipid and Ca<sup>2+</sup> ions to reach their maximum activity.
- Novel PKCs (nPKC): this sub-family brings together isoenzymes  $\epsilon$ ,  $\delta$  (*Ono et al., 1987a*),  $\eta$  (*Osada et al., 1990*) and  $\theta$  (*Osada et al., 1992*). These isoforms require anionic phospholipids and DAG or phorbol esters to attain the highest activity, and they are Ca<sup>2+</sup>-independent.
- Atypical PKCs (aPKC): this sub-family is composed by only two members, PKC $\zeta$  and PKC  $\iota/\lambda$  [PKC $\iota$  for human (*Selbie et al., 1993*)/ PKC  $\lambda$  for mouse (*Akimoto et al., 1994*)]. Enzymes in this group only require acidic

phospholipids to be activated, although they can be regulated by ceramides and protein-protein interactions.

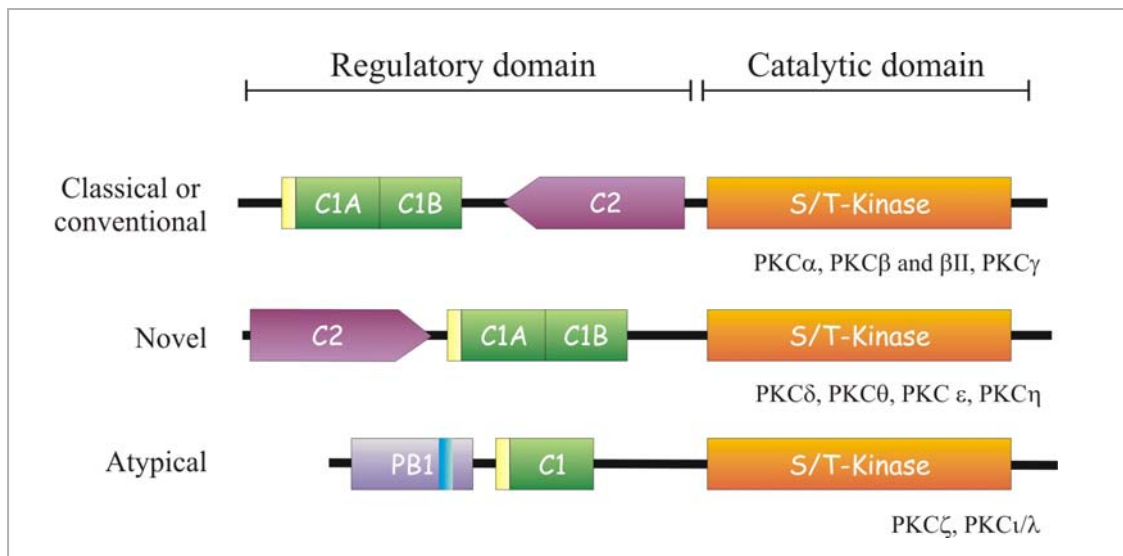


**Figure I.1. Scheme of primary structures of the members of Protein Kinase C family showing domain composition.** The regulatory domain is located in the amino terminal region containing different domains, depending on the isoenzyme. Pseudosubstrate (yellow); the C1 domain (green); the C2 domain (purple). The PB1 domain (violet), present in atypical PKC, is represented by a blue box [OPCA (Octicosapeptide repeat domain) is the motif where aPKC interact] (Taken from *Corbalán García and Gómez Fernández, 2006*).

As regards the primary structure of these mammalian kinases, it is possible to differentiate between a regulatory domain in the amino-terminal and a catalytic domain in the carboxyl-terminal region (*Coussens et al., 1986*). Of the five variable regions, the most important is V3, which separates both domains. The main differences between sub-families concern the regulatory region, while the catalytic domain is well preserved (Fig I.1).

Three domains can be distinguished in the regulatory region of cPKCs: a pseudosubstrate sequence, and the C1 and C2 domains. The pseudosubstrate sequence is able to block the catalytic centre and so inhibit enzymatic activity (*House and Kemp, 1987*). The C1 domain has a cysteine-rich region, appears in tandem (C1A and C1B) and it is responsible for binding diacylglycerol (DAG) and phorbol esters (*Bell and Burns, 1991*). The C1 domain is followed by the C2 domain, which is of type I and has binding sites for acidic phospholipids,  $\text{Ca}^{2+}$  and also for  $\text{PtdIns}(4,5)\text{P}_2$  (*Medkova and Cho, 1998; Corbalán-García et al., 1999; Verdaguer et al., 1999; Conesa-Zamora et al., 2000; Sánchez-Bautista et al., 2006; Marín-Vicente et al., 2007*).

Structurally, the nPKC group is very similar to cPKC, since novel isoforms have two C1 domains in tandem, but the C2 domain is type II and is nearer the amino-terminal region than the C1 domain (*Nalesfki and Falke,*

1996); it does not present a  $Ca^{2+}$  binding site and interacts with anionic phospholipids (García-García *et al.*, 2001; Ochoa *et al.*, 2001).

The regulatory region in the aPKC group is totally different from the others because they do not have a C2 domain, but only contain one C1 domain and a specific domain called PB1, which is located in amino-terminal region.

The catalytic domain, which is conserved in all subfamilies, contains the ATP binding site and the place where target proteins susceptible to be phosphorylated by PKC, are bound (Hanks *et al.*, 1988; Kemp and Pearson, 1990).

## **2. Conserved regions in PKC.**

### **2.1 Pseudosubstrate domain.**

Every PKC isoform has an auto-inhibitory pseudosubstrate domain, which is a small polybasic sequence formed by 20 amino acids and which maintains PKC in an inactive state by sterically blocking the active site of the kinase (House and Kemp, 1987; Makowske and Rosen, 1989; Soderling, 1990; Orr *et al.*, 1992).

The sequence of this domain is highly conserved in all isoforms, the only difference being the location along the PKC primary structure. It is also very similar to target sequences in proteins that are susceptible to phosphorylation by PKC. In this case, the difference is the substitution of one amino acid: while the target proteins contain a Ser/Thr residue, the pseudosubstrate contains an alanine (House and Kemp, 1987; Nishikawa *et al.*, 1997).

Several hypotheses have been proposed to explain the mechanism of PKC activation, and in all of them the pseudosubstrate domain must be released from the active site.

### **2.2. C1 domain. Structure, function and regulation.**

The C1 domain is in the regulatory region of each PKC isoform and is a member of a superfamily of Cys-rich domains that it is composed by approximately 50 amino acids.

In general, these domains are classified in two groups, depending on their capacity to bind DAG or phorbol esters.

- Typical C1 domains can bind effectors and are present in cPKC and nPKC (Fig I.2) (Ono *et al.*, 1989a; Burns and Bell, 1991; Quest *et al.*, 1994; Kazanietz *et al.*, 1994; Wender *et al.*, 1995; Bittova *et al.*, 2001). The C1 domain is also found in other proteins like Protein Kinase D (PKD), Diacylglycerol Kinase (DGK) (isoforms  $\beta$  and  $\gamma$ ), Chimerins, RasGRP and Munc 13, among others (Yang and Kazanietz, 2003).
- Atypical C1 domains can not bind DAG or phorbol esters. They are present in aPKC (Mellor and Parker, 1998; Newton and Johnson, 1998). Proteins other than PKC also possess this kind of C1 domain, for example DGK (isoforms  $\alpha$ ,  $\delta$ ,  $\eta$ ,  $\kappa$ ,  $\epsilon$ ,  $\zeta$ ,  $\iota$  and  $\theta$ ), Raf proteins, Vav proteins, Ras suppressor kinase and Rho kinase (Van Blitterswijk and Houssa, 2000; Kanoh *et al.*, 2002; Zhou *et al.*, 2002).

In cPKC and nPKC, the C1 domain is composed of a tandem of two subdomains, called C1A and C1B according to their position in amino-terminal end (Hurley *et al.*, 1997). Each of these subdomains shows a conserved sequence (HX<sub>12</sub>CX<sub>2</sub>CX<sub>13/14</sub>CX<sub>2</sub>CX<sub>4</sub>H X<sub>2</sub>CX<sub>2</sub>CX<sub>7</sub>C, where “H” is His, “X” is any amino acid and “C” is Cys) which is essential to coordinate two Zn<sup>2+</sup> ions (Ahmed *et al.*, 1991; Burns and Bell, 1991; Quest *et al.*, 1992). Both of these subdomains can bind DAG or phorbol esters, although some studies have demonstrated that each subdomain does so with a different affinity (Ananthamarayanan *et al.*, 2003), while the presence of only one is sufficient to ensure the smooth running of this part of the protein (Burns and Bell, 1991; Quest *et al.*, 1994; Kazanietz *et al.*, 1994; Wender *et al.*, 1995; Bittova *et al.*, 2001).

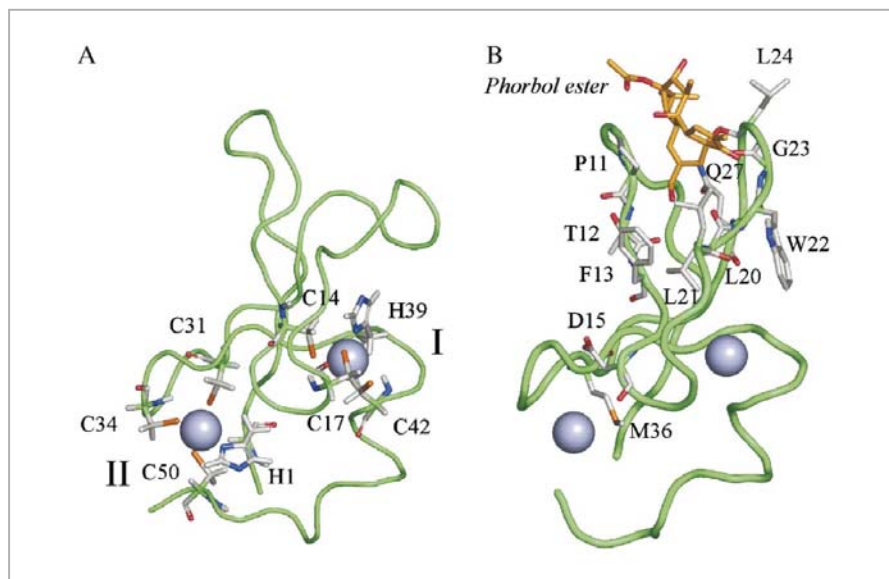


**Figure I.2. Overall structure of the C1B domains of PKC $\gamma$  and PKC $\delta$ .** (A) Overall structure of the C1B domain of PKC $\gamma$ . The zinc atoms are represented by big purple balls and the residues involved in coordinating these two zinc ions are represented by stick models with carbon in grey, nitrogen in blue and sulphur in yellow. (B) Overall structure of the C1B domain of PKC $\delta$  in complex with phorbol 13-acetate. The phorbol ester is represented as a stick model with carbon in yellow and oxygen in red (Taken from Corbalán-García and Gómez-Fernández, 2006).

Both C1 subdomains of this cPKC present a polarized distribution of hydrophobic and ionic amino acids. The top part of the molecule, where effectors like DAG/phorbol esters are bound, contains aromatic and aliphatic residues, whereas the middle part contains cationic residues (Fig I.3).

The results of many studies in which the role of most important C1 domain amino acids has been resolved, suggest that typical C1 domains present a polarized amino acid distribution, being hydrophobic at the top and bottom, and containing mainly cationic residues in the middle. The hydrophilic groove in the top is the site where ligands like DAG/phorbol esters bind and lead the penetration of this part of the domain into the membrane because of the hydrophobic amino acids in this part and the cationic residues in the middle part (Zhang *et al.*, 1995; Xu *et al.*, 1997; Pak *et al.*, 2001; Hurley and Meyer, 2001).

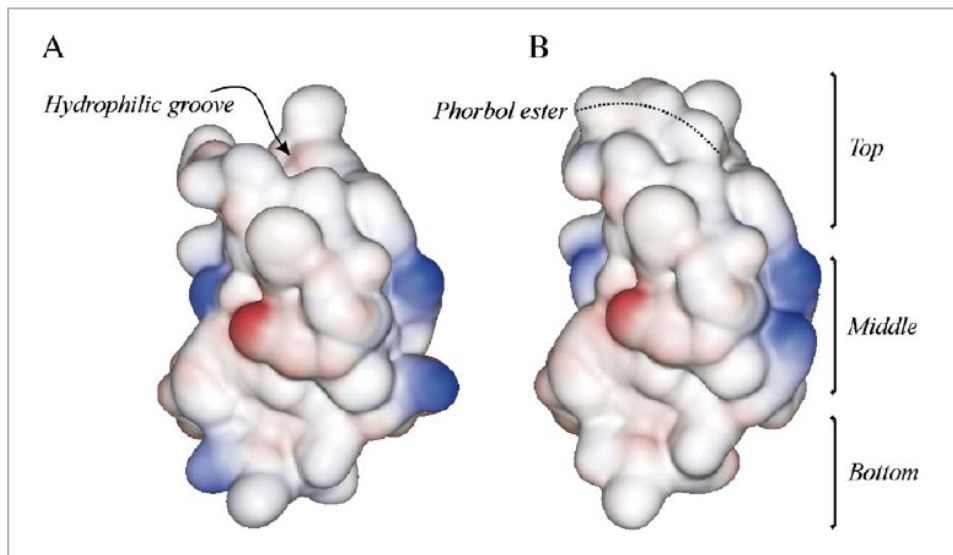


**Figure I.3. Molecular surface drawing of the C1B domain of PKC $\delta$  in the absence (A) or presence (B) of phorbol ester.** Positively and negatively charged regions are shown in blue and red, respectively, while the hydrophobic surface is depicted in grey. Note how the surface of the top third of the molecule is highly hydrophobic when the phorbol ester fits into the hydrophilic groove, facilitating membrane insertion of the domain under these conditions. The area occupied by the phorbol ester has been marked with a dotted line to facilitate interpretation of the figure (Taken from Corbalán García and Gómez Fernández, 2006).

The C1 domain plays a role in PKC binding to different membranes along the cell. As mentioned above, this domain is found in a large number of proteins which have several functions, and it is regulated by DAG/phorbol ester interactions (Yang and Kazanietz, 2003).

A common characteristic of classical and novel PKC is that both subfamilies have two C1 domains in tandem. Several studies have demonstrated that C1 subdomains, whether inside the same or in different

isoenzymes, are not equivalent and have different affinities for DAG and phorbol esters.

Based on our knowledge to date, it can be concluded that C1A and C1B subdomains of PKC respond in different ways to DAG and phorbol esters, so that the physiological results obtained using phorbol esters are not extrapolatable to those using DAG. Likewise, different isoenzymes show different responses, so that the results for one isoenzyme will not necessarily be the same for another even if they are from the same family (*Corbalán-García and Gómez-Fernández, 2006*). Biologically, these differences reflect the huge variety of situations in which different PKC isoenzymes may participate.

Besides DAG and phorbol esters, C1 domains can bind other lipids, such as phospholipids, ceramides and fatty acids. This part of the protein shows different affinities for these compounds, since during the interaction between them, PKC is translocated to different subcellular compartments for subsequent activation (*Kashiwagi et al., 2002; Becker and Hannun, 2003; Yagi et al., 2004; Sánchez-Bautista et al., 2009*).

One example is the case of C1B, but not C1A domain, of PKC $\epsilon$  which binds ceramides and arachidonic acid, although every ligand leads to a different location pattern due to the different binding mechanisms involved (*Kashiwagi et al., 2002*).

### **2.3. C2 domain. Structure, function and regulation.**

The whole structure of several C2 domains from several proteins, including Synaptotagmins and PKC, has been elucidated. In PKCs, the C2 domains were initially discovered as a Ca<sup>2+</sup> binding site of cPKC (*Coussens et al., 1986; Knopf et al., 1986; Ono et al., 1986*).

C2 domain is present in numerous proteins involved in cellular signalling, small GTPase regulation or vessel transport (*Nalefski and Falke, 1996; Rizo and Südhof, 1998*), for example phospholipase C (PLC) (*Rebecchi and Pentylala, 2000*) or phosphoinositide 3-kinases (PI3Ks) (*Walker et al., 1999*). It contains approximately 130 amino acids and it, together with C1 domain, takes charge of binding PKC to membrane in a correct position.

The structure of all C2-domains has a common overall fold: a single compact Greek-key motif organized as an eight-stranded anti-parallel  $\beta$ -sandwich consisting of a pair of four-stranded  $\beta$ -sheets (*Shao et al., 1996; Rizo and Südhof, 1998; Sutton and Sprang, 1998*).

Unlike C1 domain, C2 domains have a high degree of variability among themselves (*Nalefski and Falke, 1996; Rizo and Südhof, 1998*). The sequence of

amino acids is much conserved in  $\beta$ -strands and in some residues that have an essential role in this domain, like the amino acids involved in the coordination of  $\text{Ca}^{2+}$  ions (in cPKCs), in particular five aspartates (Fig I.4). There is great variability in the binding regions between  $\beta$ -strands, where residues like Pro and His are very common in these zones, which confer flexibility to them. As a result, a structural role is attributed to  $\beta$ -strands, while the binding regions reflect the specific function of the domain (Nalefski and Falke, 1996; Rizo and Südhof, 1998).

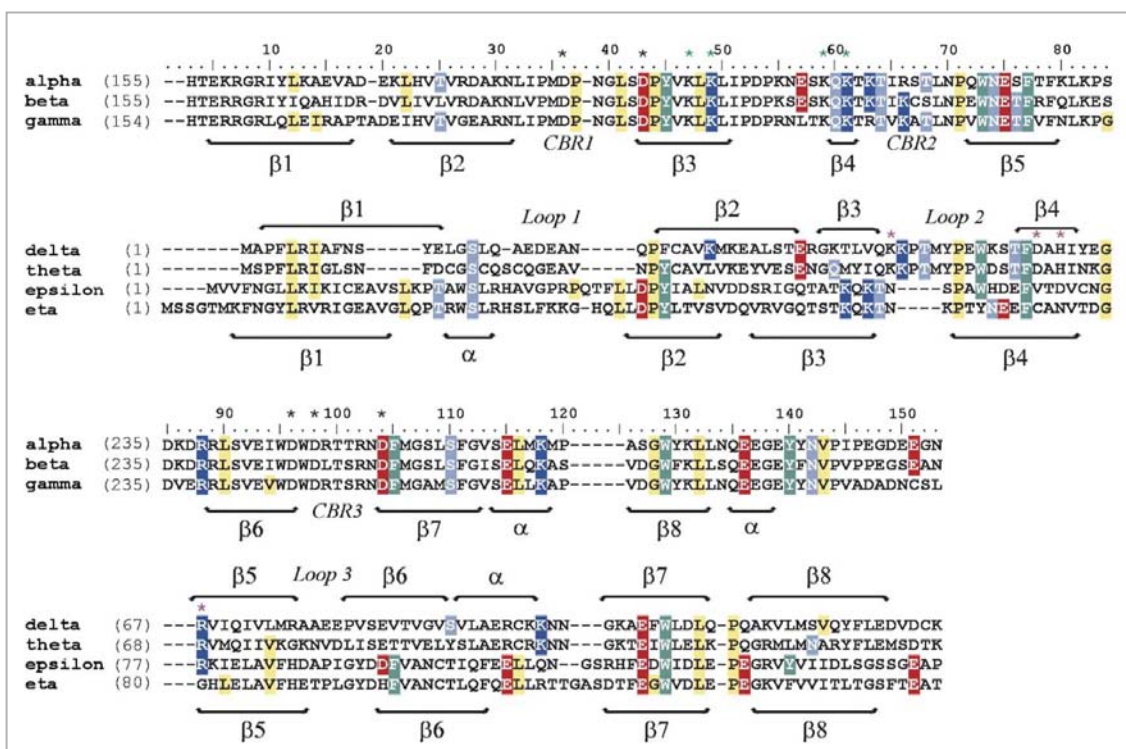


**Figure I.4. Sequence alignment of the seven C2 domains of conventional and novel PKCs.** Dashes indicate gaps. The coloured residues represent those exhibiting more than 50% homology. Aromatic residues are labelled in green, hydrophobic residues are labelled in yellow, positively charged residues are labelled in dark blue, negatively charged residues are labelled in red and charged residues in light blue. Black stars indicate the critical Asp residues involved in  $\text{Ca}^{2+}$  coordination and green stars indicate the Lys residues located in the Lys-rich cluster in cPKCs. Purple stars indicate the residues involved in the pTyr binding domain of PKC $\delta$ . C2 domains with topology I are grouped in the top part of the alignment (PKC $\alpha$ ,  $\beta$  and  $\gamma$ ) and C2 domains with topology II are grouped in the bottom part. Note that alignment of C2 domains with topology II contains two subgroups that have been denoted due to the important structural differences observed between PKC $\epsilon$  and PKC $\delta$  (Taken from Corbalán García and Gómez Fernández, 2006).

C2 domains can be classified in two groups (Pappa *et al.*, 1998; Sutton and Sprang, 1998; Verdaguer *et al.*, 1999; Ochoa *et al.*, 2001):

- The synaptotagmin-like variants, also referred to as the S-family or type I topology, which include the C2 domains of conventional PKCs.

- The PLC-like variants, also known as the P-family or type II topology, which include the C2 domains of novel PKCs.

The main difference between both topologies is that the first strand in the C2 domain with topology I occupies the structural position of the eighth  $\beta$ -strand in the C2-domain with topology II (Fig I.5). As a result, domains with topology II represent a circular permutation of those with topology I, and both are inter-convertible, since topology I becomes II when its amino- and carboxyl-terminal are linked and new termini are generated, cutting the connection between  $\beta 1$  and  $\beta 2$ -strands (Nalefski and Falke, 1996; Rizo and Südhof, 1998).

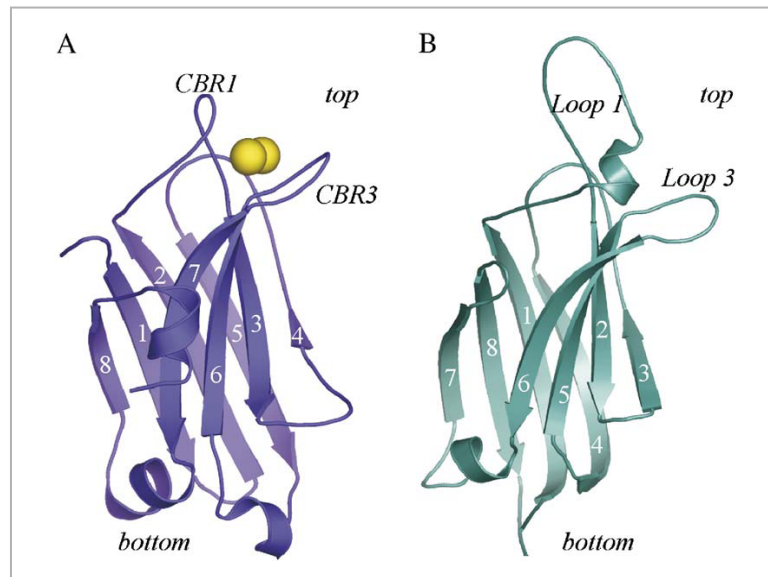


**Figure I.5. Ribbon diagrams of the C2 domain structures of PKC $\alpha$  (A) and PKC $\epsilon$  (B) as representative members of topology I and II, respectively.** The two different topologies result from a circular permutation of the  $\beta$ -strands that leaves the N- and C-termini either at the top or at the bottom of the  $\beta$ -sandwich, respectively. It is important to note that the membrane interaction area (CBR1 to 3 in topology I, and loops 1 to 3 in topology II) is located at the top of each domain independent of the topology exhibited (Taken from Corbalán García and Gómez Fernández, 2006).

C2 domains in classical and novel PKCs play an essential role in the activation of their proteins, since, together with C1 domain, they anchor the enzyme to the membrane due to their interaction with phospholipids. Besides anchoring PKC to the membrane, this domain has other functions, including protein-protein interactions.

The classical ligands to C2 domains are  $\text{Ca}^{2+}$  and anionic phospholipids like PtdSer (Newton and Johnson, 1998; Verdaguer et al., 1999). Besides PtdSer, other anionic phospholipids can activate PKC in the presence of  $\text{Ca}^{2+}$ ,

such as phosphatidylglycerol, phosphatidic acid and phosphatidylinositol-4,5-bisphosphate (PtdIns(4,5)P<sub>2</sub>) (Lee and Bell, 1991; Newton, 1993; Marín-Vicente, et al., 2008). Others lipids also intervene in the regulation of PKC: for instance, ceramides (Kashiwagi et al., 2002; Yakushiji et al., 2003), unsaturated fatty acids like arachidonic acid (O'Flaherty et al., 2001; López-Nicolás et al., 2006) and retinoid compounds (Randominska-Pandya et al., 2000; Boskovic et al., 2002; López-Andreo et al., 2005).

In PKC $\alpha$ , a classical PKC isoform, the exact binding site for different lipids has been identified; for example, PtdSer interacts in the so-called *Ca<sup>2+</sup> binding site* and PtdIns(4,5)P<sub>2</sub> binds in the so-called *lysine rich cluster* (García-García et al., 2001; Ochoa et al., 2002; Corbalán-García et al., 2003; Guerrero-Valero et al., 2009).

The C2 domain is responsible for binding Ca<sup>2+</sup>, and three different binding sites have been characterized (Ca1, Ca2 and Ca3) within the *Ca<sup>2+</sup> Binding Region*. All of them are located at the top of the  $\beta$ -sandwich where Ca<sup>2+</sup> ions coordination occurs, specifically in the connection loops between  $\beta$ -strands (Verdaguer et al., 1999; Ochoa et al., 2001). For this reason, the loops located in this part of the C2 domain are called CBR1 (Calcium binding region 1), CBR2 and CBR3, in order of the amino-terminal of the protein (Fig I.5).

CBRs provide all the necessary residues involved in Ca<sup>2+</sup> coordination: five aspartates (Asp187, 193, 246, 248 and 254), which are highly conserved among all classical PKCs (Fig I.4). Asp187 and Asp193 are located in the CBR1 (loop between  $\beta$ 2- and  $\beta$ 3-strands), where one of the calcium ions (Ca1) is lodged, whereas CBR3 (loop between  $\beta$ 6- and  $\beta$ 7-strands) includes Asp246, Asp248 and Asp254, and it is the site where Ca2 is lodged (Sutton and Sprang, 1998; Verdaguer et al., 1999) (Fig I.6).

Further mutagenesis studies at the *Ca<sup>2+</sup>-binding site* have demonstrated that individual Ca<sup>2+</sup> ions and their ligands play different roles in membrane binding and PKC $\alpha$  activation. The model suggested that Ca1 is involved in initial membrane anchoring, whereas Ca2 and Ca3 are involved in conformational changes (Edwards and Newton, 1997; Medkova and Cho, 1998; Corbalán-García et al., 1999; García-García et al., 1999; Conesa-Zamora et al., 2000; Bolsover et al., 2003).

The results of all biochemical and cellular studies carry out to date suggest a sequential model for classical PKCs membrane binding and activation. In the first step, an increase in intracellular Ca<sup>2+</sup> would result in binding of Ca1 and Ca2 when the protein is still in the cytosol, leading to membrane targeting of the enzyme through the C2 domain. There, PKC penetrates the membrane for a longer period of time, allowing the C1 domain to find the diacylglycerol generated upon receptor stimulation, finally leading

to complete activation of the enzyme (Feng *et al.*, 2000; Conesa-Zamora *et al.*, 2001; Nalefski and Newton, 2001; Bolsover *et al.*, 2003).

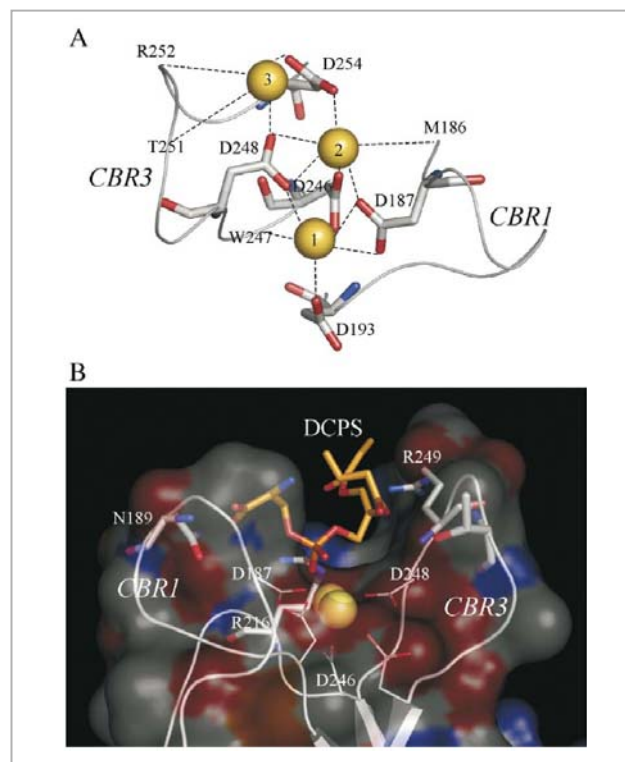


**Figure I.6.  $\text{Ca}^{2+}$  and phosphatidylserine-binding region of the  $\text{PKC}\alpha$ -C2 domain. (A)** Coordination scheme of the calcium ions in the structure determined for  $\text{PKC}\alpha$  in complex with  $\text{Ca}^{2+}$  and DCPS. Dotted lines represent the coordination established between the different carboxylate and oxygen groups, and Ca1, Ca2 and Ca3. **(B)** Lateral view of the surface model of the  $\text{Ca}^{2+}$  binding-region, the Asp residues involved in  $\text{Ca}^{2+}$  coordination have been represented as thin-stick models with carbon in grey and oxygen in red. Calcium ions are represented as yellow balls. The residues of the C2 domain directly involved in phosphatidylserine binding are shown as thick-stick models with carbon in grey, nitrogen in blue and oxygen in red. Additionally, DCPS is represented as a stick model and carbons have been colored in yellow. Note how the residues coordinating  $\text{Ca}^{2+}$  occupy the bottom of the crevice formed by CBR1, 2 and 3. The DCPS molecule is located on top of this area contributing to coordinate Ca1 through its phosphate moiety and acts as a cap held by residues of the C2 domain that directly interact with it (N189, R216, R249 and T251) (Taken from Corbalán García and Gómez Fernández, 2006).

Further crystallization of the C2 domain of  $\text{PKC}\alpha$  in complex with  $\text{Ca}^{2+}$  and 1,2-diacetyl-*sn*-phosphatidyl-L-serine (DAPS) demonstrated the presence of an additional binding site for anionic phospholipids in the vicinity of the conserved *lysine-rich cluster* in cPKCs (Ochoa *et al.*, 2002).

More specifically, it was found that Lys197 and Lys199, located in  $\beta 3$  strand, and Lys209 and Lys211, in  $\beta 4$  strand, establish a series of electrostatic interactions with a second DAPS molecule, suggesting that this site participates in the interaction of the C2 domain with the membrane (Fig

I.7). Other studies demonstrated that this area could bind other negatively charged molecules such as phosphate (Verdaguer *et al.*, 1999), phosphatidic acid (Ochoa *et al.*, 2002), all-*trans*-retinoic acid (Ochoa *et al.*, 2003; López-Andreo *et al.*, 2005) or phosphoinositides like PtdIns(4,5)P<sub>2</sub> (Marín-Vicente *et al.*, 2008).

A more extensive biochemical study using different acidic phospholipids demonstrated that the C2 domain of PKC $\alpha$  bind PtdIns(4,5)P<sub>2</sub>, preferentially through the  $\beta$ 4 strand of the *lysine-rich cluster* (Lys209/Lys211) (Fig I.7) (Corbalán-García *et al.*, 2003), leading to PKC $\alpha$  activation by means of a mechanism other than the classical one.

Recent studies have demonstrated that the C2 domains of three classical PKCs exhibit different affinity for the PtdIns(4,5)P<sub>2</sub>, which is bound through the *lysine-rich cluster* (Sánchez-Bautista *et al.*, 2006; Guerrero-Valero *et al.*, 2007). PKC $\gamma$ -C2 domain shows the lowest affinity for this lipid, while PKC $\alpha$ -C2 domain needs a lower amount of this lipid to localize in membranes (Guerrero-Valero *et al.*, 2007). Furthermore, two aromatic amino acids (Tyr195 and Trp245) have been implicated in the specific interaction between PKC $\alpha$ -C2 domain and the phosphate of the inositol ring from PtdIns(4,5)P<sub>2</sub>. These residues, similar to other cationic amino acids, like Lys197, Lys209, Lys 211 and Asn253, are highly conserved among all C2 domains with topology I, while the C2 domains of topology II do not preserve most of the residues responsible for the PtdIns(4,5)P<sub>2</sub> interaction (Guerrero-Valero *et al.*, 2009).

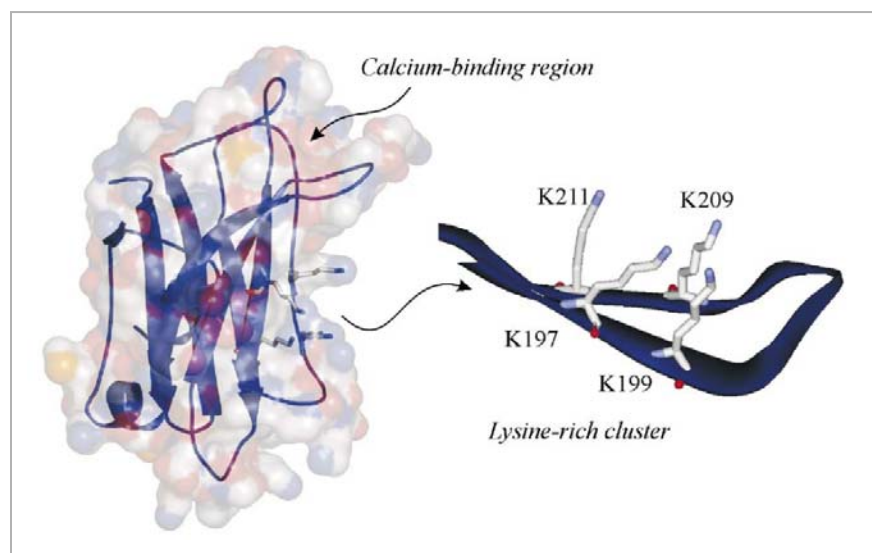


**Figure I.7. Localization of the *Lysine-rich cluster* in the C2 domain of PKC $\alpha$ .** Overall structure of the C2 domain of PKC $\alpha$  represented as a cartoon scheme over its molecular surface. The lysine residues involved in the cluster, which are located in  $\beta$ 3 and  $\beta$ 4 strands, are represented as stick models with carbon in grey and nitrogen in blue. Acidic surfaces are represented in red and basic in blue. Note how the  $Ca^{2+}$ -binding region is an area rich in negatively charged amino acids, while the *lysine-rich cluster* forms a basic surface. The inset shows an amplification of  $\beta$ 3 and  $\beta$ 4 strands of PKC $\alpha$  with the Lys residues forming the cluster represented by stick models (Taken from Corbalán García and Gómez Fernández, 2006).

Besides anchoring PKC in membranes, C2 domain seems to be involved in protein-protein interactions, mainly through the *lysine-rich cluster* (Mochly-Rosen et al., 1992; Ron et al., 1995).

It can be concluded that both PtdSer and PtdIns(4,5)P<sub>2</sub> are very important for regulating the localization and activation of classical PKCs through C2 domain interaction, specifically through the *Ca<sup>2+</sup>-binding site* and the *lysine-rich cluster* (Bolsover et al., 2003; Landgraf et al., 2008; Marin-Vicente et al., 2008).

In novel PKCs, the C2 domain shows some differences from classical isoforms; for example, it is the first conserved domain of amino-terminal; it presents a type II topology and it anchors to membranes in a *Ca<sup>2+</sup>-independent manner* (García-García et al., 2001; Corbalán-García et al., 2003).

This subfamily also contains an important region at the top of  $\beta$ -sandwich, although now, the connection chains between  $\beta$ -strands are called *loops* and no *Calcium Binding Regions* since these isoforms do not bind  $Ca^{2+}$  ions. *Loop 1* and *loop 3* are located in this region and are formed by  $\beta$ -1 and  $\beta$ -2, and  $\beta$ -5 and  $\beta$ -6 connections, respectively. Unlike the *Calcium Binding Region* (in cPKC), this region exhibits significant differences among novel isoforms (Fig I.4).

The binding mechanisms of nPKCs differ from those of cPKCs, not only due to the absence of appropriate residues to form the *Ca<sup>2+</sup> Binding Region*, but also due to the structure of the lipid docking motif formed by *loops 1 and 3* (Corbalán-García et al, 2003) (Fig I.8).

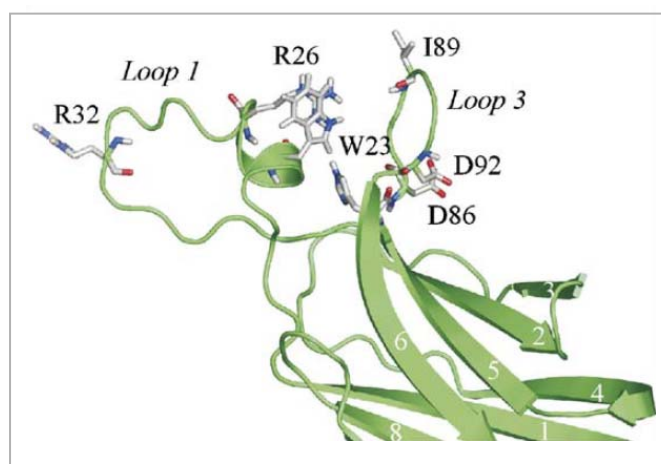


**Figure I.8. Residues involved in lipid binding of PKC $\epsilon$ -C2 domain.** The cartoon shows the 3D structure of PKC $\epsilon$ . The critical residues involved in phospholipid binding have been represented as stick models with carbon in grey, nitrogen in blue and oxygen in red (Trp23, Arg26 and Arg32 in loop1 and Ile89 in loop 3). Additional residues not involved in lipid binding are also shown: side chains of Asp86 and Asp92 are represented as stick models; observe how these chains point to the surface of the molecule, in the opposite direction to the side chains of the residues involved in phospholipid binding (Taken from Corbalán García and Gómez Fernández, 2006).

## 2.4. Catalytic domain. Structure and regulation.

The members of the ABC kinases family, PKA, PKB/Akt and PKC, show 40% sequence homology in their catalytic domain. Among PKC this percentage increases to 60% (Fig I.9) (Newton, 2003; Corbalán-García and Gómez-Fernández, 2006).

PKC	Activation loop	Turn motif	Hydrophobic motif
βI	484 DFGMCKENIWDG-VTTK T FCGTPDYIAPEII	628 NFDKFFTRHPPVL T PP-DQEVIRNIDQS---EFEGF S FVNSEFLKPEVKS	
α	481 DFGMCKEHMDG-VTTR T FCGTPDYIAPEII	625 NFDKFFTRGQFVL T PP-DQLVIANIDQS---DFEGF S YVNPQFVHPILQSAV	
βII	484 DFGMCKENIWDG-VTTK T FCGTPDYIAPEII	629 NFDKFFTRQFVEL T PT-DKLFIMNLDQN---EFAGF S YTNPEFVINV	
γ	498 DFGMCKENVFPG-STTR T FCGTPDYIAPEII	642 NFDKFFTRAAPAL T PP-DRLVLASIDQA---DFQGF T YVNPDFVHPDARSPTSPPVPVPM	
δ	489 DFGMCKENIF-GENRAS T FCGTPDYIAPEII	630 NFDPEFLNEKPOL S FS-DKNLIDSMDQT---AFKGF S FVNPKYEQFLE	
ε	550 DFGMCKEGLNG-VTTT T FCGTPDYIAPEII	697 NFDQDFTREEPVL T LV-DEAIVKINQE---EFKGF S YFGEDLMP	
ζ	394 DYGCKEGLPGD-TTS T FCGTPNYIAPEII	547 NFDQFTSEPVQL T PD-DEDAIKRIDQS---EFEGF E YINPLLLSTEESV	
η/L	496 DFGMCKEGICNG-VTTA T FCGTPDYIAPEII	632 NFDPDFIKKEPVQL T PI-DEGHLPMINQD---EFRNF S YVSPQLQP	
θ	522 DFGMCKENML-GDAKTN T FCGTPDYIAPEII	663 NFDKREFLNEKPRI S FA-DRALINSMDQN---MFRNF S FMNPGWGG	
ι/λ	387 DYGCKEGLRPGD-TTS T FCGTPNYIAPEII	542 NFDQFTNEPVQL T PD-DDDIVRKIDQS---EFEGF E YINPLLSAEECV	
PKBα/Akt1	304 ATMK T FCGTPEYLAPE	437 YFDEEFTAQMITI T PP-DQDDSMCEVDSERRPHFPQF S YSASGTA	
p70S6K	225 TVTH T FCGTIEYMAPE	358 QFDSKFTPTQTPVD S PD-DSTLSESANQV---FLGF T VVAP...	
PRK2	812 DRTS T FCGTPEFLAPE	945 NFDDEFTSEAPIL T PPREPRILSEEEQE---MFRDF D YIADWC	
PKA	193 GRTW T LCGTPEYLAPE	326 NFDYEEEEEIRV- S IN-EKCGK-----EFTEF	

**Figure I.9. Alignment of the activation loop, turn motif and hydrophobic motif phosphorylation sequences for the PKC isoenzymes, PKBα/Akt1, p70S6 kinase, PRK2 and PKAα.** Sequences shown are for human PKC isoenzymes α, ε, ζ, η/L θ and ι/λ and rat PKC γ and δ, rat PKC βI and βII, murine PKB α/Akt1, rat p70S6 kinase and murine PKA α. Amino acid residue numbers are indicated to the left of the sequences (Taken from Newton, 2003).

To date, the 3D structures of catalytic domain of some PKC have been solved: novel PKCθ (Xu *et al.*, 2004), atypical PKCι (Messersschmidt *et al.*, 2005; Takimura *et al.*, 2010), classical PKCβII (Grodsky *et al.*, 2006) and PKCα (Wagner *et al.*, 2009).

The catalytic domain of PKCs contains both the ATP binding and the consensus phosphorylation sites; it interacts with substrates and is responsible for phosphotransfer activity.

The kinase domains of PKC isoenzymes are closely related, as illustrated in the dendrogram (Fig I.10). Protein kinase fold is separated into two subdomains or lobes. The smaller N-terminal lobe, or N lobe, is composed of a five-stranded β sheet and one prominent α helix, called helix αC. The larger lobe is called the C lobe and is predominantly helical (Fig I.10) (Taylor and Radzio-Andzelm, 1994; Johnson and Lewis, 2001). Between them, there is a cleft where the ATP- and substrate-binding sites are located.

N lobe has a preserved region in all kinases, called the *glycine-rich loop*, whose consensus sequence is XGXXGX<sub>2</sub>GX<sub>16</sub>KX, where X is any amino acid and G is glycine. This region is located between β1 and β2 strands and it is

included in the ATP binding site. Its function consists of orienting the ATP  $\gamma$ -phosphate correctly for transferring to the target protein.

The C lobe includes *Activation loop*, *Turn motif* and *Hydrophobic motif*, and is responsible for target peptide union and the beginning of phosphate transfer. The *Activation loop* is located near the active site entrance and includes the region where the target proteins are phosphorylated. This zone, together with C1 domain, the ATP binding region and variable region 5 (V5), is involved in the specific recognition of substrates (Pears *et al.*, 1991).

In the zone where substrate phosphorylation occurs, two highly preserved regions can be differentiated in the kinase domain. One of them is the TDP region (Thr-Pro-Asp) and the other the DFG region (Asp-Phe-Gly/Tyr), which is also called the *central element of phosphate transfer* and which is preserved among every human PKC isoenzyme and other kinases (Kemp and Pearson, 1990; Taylor *et al.*, 1990). Only PKC $\alpha$  and  $\zeta$  present a slight difference since Phe is replaced by Tyr in the consensus sequence (Ono *et al.*, 1989b). Only one amino acid, an Asp residue which is present in all isoforms, is responsible for phosphate transfer in DFG (Fig I.9).

The *Turn motif* possesses a Pro rich sequence which includes the phosphorylatable residue (Thr for cPKCs and nPKCs; Ser for aPKCs). Structural models suggest this sequence correspond to a turn in the molecule, which is why it is called the *turn motif* (Figs I.9 and I.10) (Cenni *et al.*, 2002).

The *Hydrophobic motif* is so-named because the Ser/Thr phosphorylatable residues are surrounded by hydrophobic amino acids (Cenni *et al.*, 2002). This region is less preserved than the other two. Its consensus sequence is FXXFS/T/E, where X is any amino acid, and the end represents, depending on isoenzyme, a residue of Ser, Thr or Glu. Classical and novel PKCs possess a preserved residue of Ser or Thr which is phosphorylatable, whereas atypical isoforms possess a Glu that mimics, although not perfectly, the phosphorylation site (Messerschmidt *et al.*, 2005) (Fig I.9).

PKC isoenzymes are subject to precise structural and spatial regulation: their phosphorylate state, conformation and subcellular localization must be defined in a very precise way to preserve their correct physiological function. These kinases must be phosphorylated, the pseudosubstrate released from the active site and the enzyme must be in the correct intracellular compartment in order to carry on their catalytic role. If any of these requirements is not fulfilled, the cell signalling pathways through this enzyme will be interrupted (Newton, 2001), presenting diseases, like cancer.

PKC phosphorylation is the first step towards correct catalytic activity and towards correct intracellular localization. This phenomenon occurs in

three sequential steps, more specifically in three preserved Ser/Thr residues located in the catalytic domain (*Ron and Kazanietz, 1999; Cenni et al., 2002*). The first phosphorylation step takes place in the *activation loop*, and this is followed by two auto-phosphorylations happen, one in the *turn motif* and the other in *the hydrophobic motif* (Fig I.10). These phosphorylations are very well preserved among PKC isoenzymes, with the exception of atypical PKCs, where the third phosphorylation step does not occur.

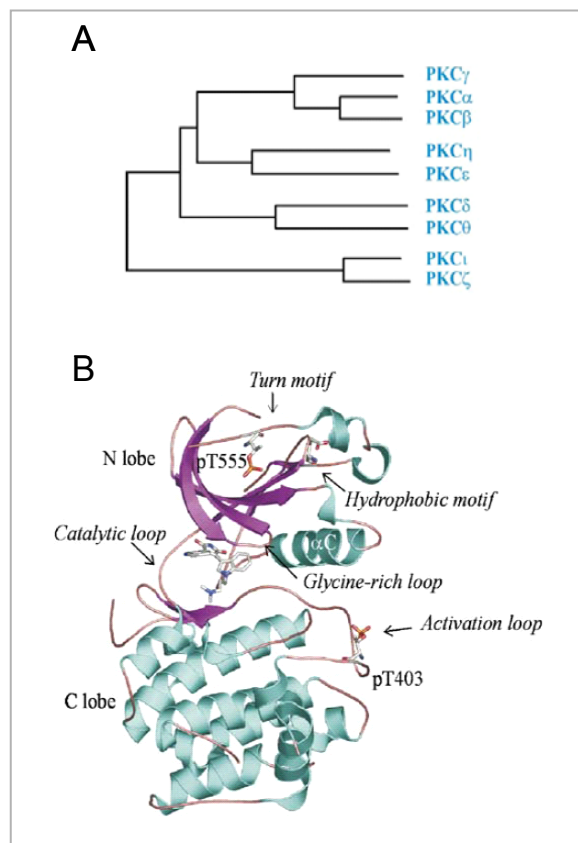


**Figure I.10. (A) Dendrogram of the protein kinase C family. (B) Overall structure of the catalytic domain of PKC $\iota$  in complex with the inhibitor bis(indolyl)maleimide.** The N-lobe is purple and the C-lobe is blue. PhosphoThr403 is represented as sticks, and the catalytic, activation and glycine rich loops are shown with arrows. PhosphoThr555 in the *turn motif* and the phosphorylation mimic Glu574 in the *hydrophobic motif* are also represented by sticks (Taken from *Corbalán García and Gómez Fernández, 2006*).

Phosphorylation of the *activation loop* occurs in a Thr whose position depends on the enzyme. Correct alignment of the catalytic site and subsequent steps in the activation process are essential (*Keranen et al., 1995; Tsutakawa et al., 1995*) (Fig I.9). This phosphorylation is carried out by phosphoinositide-dependent kinase-1 (PDK-1) and represents an important regulatory mechanism in PKC and other members of the ABC family (*Johnson and Lewis, 2001*). It seems that after Thr residue is phosphorylated, it interacts with two

amino acids (Arg and Lys) located in the *activation loop* very near the Asp residue, which has been proposed as the amino acid responsible for transferring phosphate to target proteins (Orr and Newton, 1994b). These ionic interactions provide the correct alignment of the *activation loop* to permit substrate binding (Xu et al., 2004; Messerschmidt et al., 2005).

The first phosphorylation in the *activation loop* is followed by auto-phosphorylation in the *turn motif*, specifically in a preserved Ser/Thr (the position changes with the enzyme) (Fig I.9) surrounded by a proline-rich sequence. This phosphorylation step produces a catalytically competent, thermo-stable and phosphatase-resistant enzyme (Bormancin and Parker, 1996; Edwards et al., 1999). When PKC has reached its mature state, the phosphate on the *turn motif* is the only one necessary to confer activity to the enzyme. Other studies have suggested that this motif, besides playing a role in PKC maturity and stability, could be an important place for protein-protein interactions (Yaffe et al., 1997; Newton, 2001).

After the *turn motif* is phosphorylated, the *hydrophobic motif* suffers another auto-phosphorylation, which is the only phosphorylation that is not essential to kinase activity (Newton, 2001). This motif is the least conserved among the three important regions of the catalytic domain, and even atypical PKCs show a Glu residue, which simulates the phosphate, where a Ser/Thr should appear (Fig I.9). Besides the phosphorylation of conserved residues, there are some amino acids (for example Ser, Thr or Tyr) that can be phosphorylated, influencing the function of mature PKC (Konishi et al., 1997; Nakhost et al., 1999). It is known that these amino acids near the carboxyl-terminal vary with individual isoforms and participate in substrate specificity of every PKC.

### 3. Variable regions.

In PKC isoforms several variable regions exist along the amino acids chain; a particular isoenzyme may contain up to five of such regions. They are called V1, V2, V3, V4 and V5 from amino to carboxyl-terminal and the function of which is very important for regulating PKC functions and interactions with other proteins.

V1 is located at the N-terminal end and is present in all PKC isoforms, although it differs slightly in each one, which has been related to substrate specificity of the isoenzymes (Schaap et al., 1990; Pears et al., 1991; Zidovetzki and Lester, 1992).

V2 is only present in classical and novel PKCs, where connects C1 and C2 domains, while V3, also called a hinge region, is very flexible (*Flint et al., 1990*) and appears in every PKC, connecting the regulatory and catalytic regions. This motif is essential for proper protein functioning, since it possesses a sequence sensitive to some proteases like trypsin and calpain, which may release the regulatory from the catalytic domain, generating a constitutive active enzyme (*Newton, 2001*).

The V4 region is located at the centre of the catalytic domain, while at the C-terminal we find the V5 region which consists of a 50 amino acid sequence. V5 has a regulatory function due to its proximity to the catalytic centre (*Bornancin and Parker, 1997; Edwards and Newton, 1997b*) and its inclusion of two auto-phosphorylation sites involved in PKC phosphoregulation (*Parekh et al., 2000*).

#### **4. PKC activation mechanism.**

A variety of stimuli may reach the plasma membrane, where they activate PKC along several pathways. Phospholipase C (PLC) is involved in the main pathway for classical and novel PKCs. This enzyme hydrolyzes PtdIns(4,5)P<sub>2</sub> to generate DAG and Ins(1,4,5)P<sub>3</sub>, (*Parker, 1999; Swannie and Kaye, 2002*) which activate PKC binding through the C1 domain and increase the level of cytoplasmic [Ca<sup>2+</sup>], respectively.

There are other secondary activation pathways in which DAG is produced constantly and where phosphatidylcholine (PtdCho) plays an important role, since it may act as a precursor of DAG in three different pathways (Fig I.11): the first following PLD (phospholipase D) activation, the second one due to ceramide cholinephosphotransferase activation, which synthesizes ceramides, and the third one catalyzed by PC-dependent phospholipase C (PC-PLC), although this pathway is unusual in mammals.

Besides classical cofactors like DAG and PtdSer, other compounds generated by these enzymatic activities may activate PKC, for example arachidonic acid (*López-Nicolás et al., 2006*), ceramides (*Kashiwagi et al., 2002*) and PtdIns(4,5)P<sub>2</sub> (*Guerrero-Valero et al., 2009*) among others (Fig I.11).

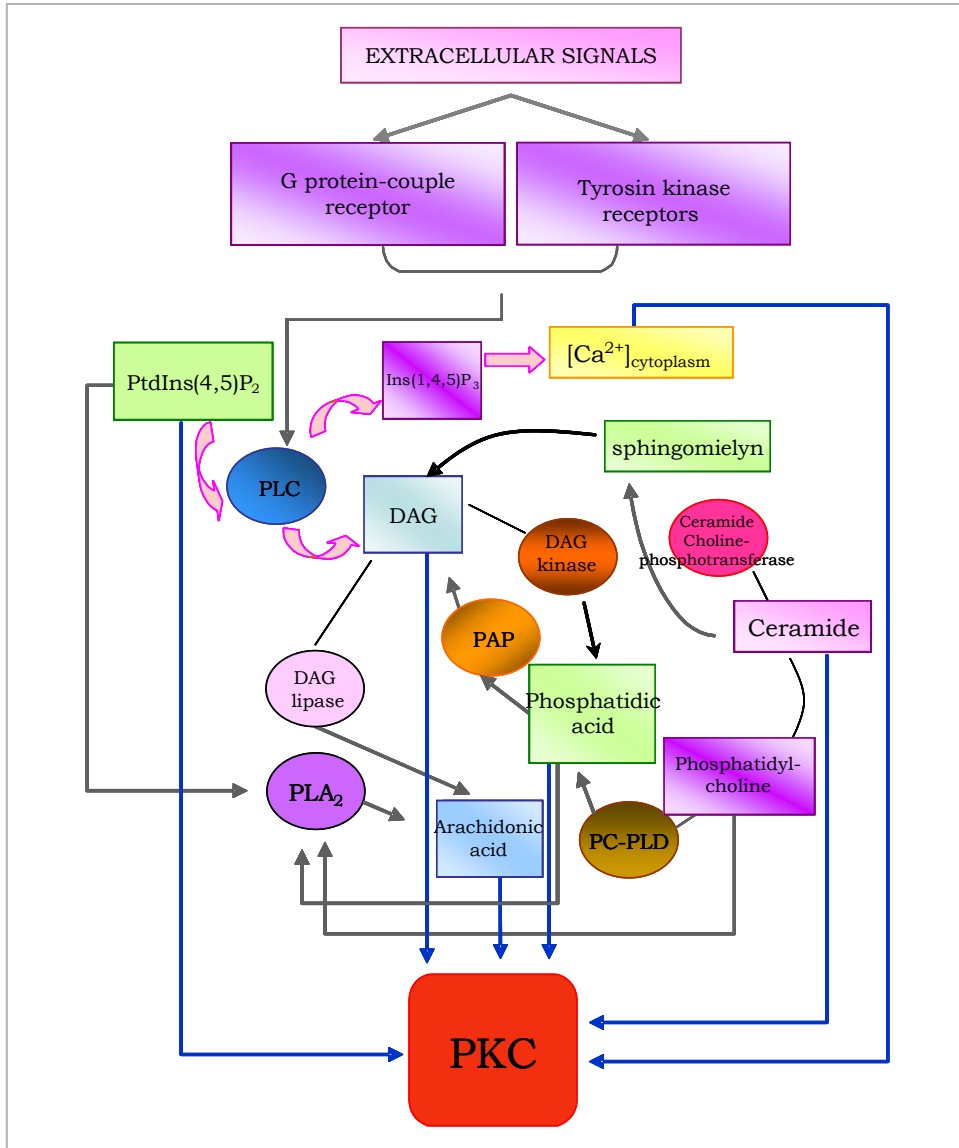


**Figure I.11. Schematic draw of PKC activation pathways.** Main pathway of PKC activation is mediated by PLC, marked with rose arrows. In the diagram is also represented enzymatic reaction that synthesizes PKC activators. All PKC activators represented in this diagram are joined with indicative box through blue arrows.

#### 4.1 Activation model of classical and novel PKCs.

PKC isoenzymes are matured by a series of ordered, tightly coupled, and constitutive phosphorylations that are essential for the stability and catalytic competence of the enzyme (*Parker and Parkinson, 2001; Newton, 2003; Rodríguez-Alfaro et al., 2004*) (Fig I.12).

As Newton exposes in her last review (*Newton, 2010*), recent studies have identified two new players in the novel and classical PKCs maturation process: heat shock protein-90 (HSP90), whose interaction with a specific motif on PKC is essential to allow phosphorylation to occur (*Gould et al.,*

2008), and the mammalian target of rapamycin (mTOR) complex 2 (mTORC2), a structure comprised of the kinase mTOR, Sin1, Rictor, and mLST8, whose integrity is required to allow the priming phosphorylations (Guertin *et al.*, 2006; Ikenoue *et al.*, 2008).

Regulation by HSP90: The first step in the maturation process is the binding of the chaperone HSP90 and the co-chaperone Cdc37 to a molecular clamp in the kinase domain composed by a conserved PXXP motif, which is essential for the HSP90 binding. Mutation in this protein or in the conserved motif of PKC, prevent the correct maturation of the kinase, which is degraded (Newton, 2010).

Regulation by priming phosphorylations: Three constitutively phosphorylated sites have been identified in the catalytic domain of PKC, which are conserved not only among all the PKC isoenzymes but among most of the AGC kinases, including PKB (Keranen *et al.*, 1995). These phosphorylations occur on 1) the *activation loop* at the entrance to the active site and 2) the *turn* and *hydrophobic* motifs that are located at the carboxyl-terminal region (Newton, 2001). It is important to mention that atypical PKCs possess a phospho-mimetic, Glu, occupying the phosphoacceptor position of the *hydrophobic motif* (Newton, 2010). The phosphorylations occur as follow:

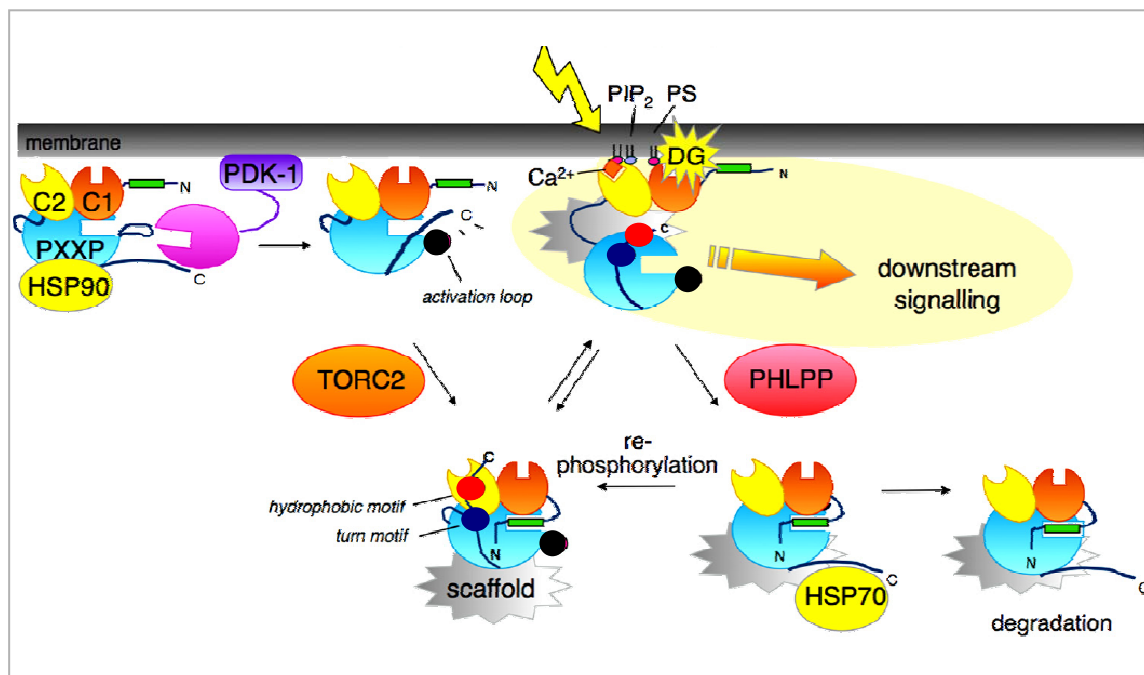
PDK-1 phosphorylates the *activation loop* of all PKC isoenzymes, an event that is essential for generating a catalytically competent enzyme (Dutil *et al.*, 1998; Le Good *et al.*, 1998). Phosphorylation is controlled by the conformation of PKC: newly synthesized PKC is in an open conformation (the pseudosubstrate is removed from the catalytic active centre) along the cytosol, thus unmasking the *activation loop* to allow phosphorylation by PDK-1 (Dutil and Newton, 2000) (Fig I.12).

After *activation loop* phosphorylation, two more phosphorylations take place, specifically in the *turn motif* (Hauge *et al.*, 2007) and in the *hydrophobic motif* (Behn-Krappa and Newton, 1999), the structure of mature PKC stabilizing.

It has recently been shown that phosphorylation of the *turn motif* depends on the mTORC2 complex (Facchinetti *et al.*, 2008; Ikenoue *et al.*, 2008). However, an auto-phosphorylation through an intramolecular reaction at the *hydrophobic motif* occurs (Behn-Krappa and Newton, 1999), which is also controlled by the interaction of HSP90 with the PXXP clamp described above.

In that moment PKC is in a catalytically competent but inactive. Classical PKCs become in active enzymes when some extracellular stimuli arrive to cellular surface and they induce generation of DAG and increasing level of  $[Ca^{2+}]$  cytoplasmic. After that cPKC localizes in membranes, starting with interaction between calcium ions and  $Ca^{2+}$  binding region of C2 domain, what make possible the interaction with PtdSer through this region. The *lysine-rich cluster* interacts with PtdIns(4,5)P<sub>2</sub>, which produces a correct orientation of cPKC in membrane, favouring C1 domain interaction with DAG and anchoring enzyme into membrane, what releases pseudosubstrate domain from active centre, generating a PKC catalytically competent and active (Corbalán García et al, 2003;Rodríguez Alfaro et al, 2004 ).

This activation model demonstrates that PKC is meticulously regulated, and that both phosphorylations and cofactor are needed for the catalytic function. However, other proteins and membrane properties intervene in PKC regulation. It is also important to mention that every mutation or mistake in any PKC maturation step entails kinase degradation (Guertin et al., 2006; Ikenoue et al., 2008).



## 5. Pathways where PKC is involved.

When activated, PKC is involved in a huge variety of intracellular pathways depending on which protein is phosphorylated, for instance transcriptional regulation, immune response and permeability modifications (Yang and Kazanietz, 2003).

As already mentioned, PKC can be activated by many compounds (Fig I.11) and this is reflected in its numerous and varied biological functions, which include mitogenesis and cell differentiation among others (Fig I.13). PKC is involved in contrasting biological functions like cell survival and apoptosis, which is due to the existence of different isoforms because, although all of them possess a well preserved catalytic region, every subfamily and isoform shows its own substrate preference, so that not all substrates can be phosphorylated by the same PKC.

Some studies have demonstrated that C1 domain and variable region V5 are involved in this specific substrate recognition (Pears *et al.*, 1991), while the interaction between PKC and other proteins involved in the correct presentation of the enzyme to phosphorylate specific substrates also seems important (Jacken and Parker, 2000).

---

**Figure I.12. Activation model of classical PKCs.** In this cartoon is shown the sequential activation of cPKCs. In resting conditions, PKC is inactive in cytoplasm next to membranes (top-left-species), where it suffers three phosphorylation. First, PDK-1 phosphorylates the *activation loop* (black circle), what allows to mTORC2 phosphorylates the *turn motif* (dark blue circle) and after that the third phosphorylation takes place in the *hydrophobic motif* (red circle). In that moment the pseudosubstrate domain (green rectangle) occupies the active centre of the catalytic domain, PKC keeping catalytically competent but inactive (bottom-left species). Some extracellular stimuli activate PLC, causing an increase in  $[Ca^{2+}]$  cytoplasmic and DAG in plasma membrane.  $Ca^{2+}$  ions allow the binding between C2 domain and PtdSer (PS) through the *calcium binding region*, thanks this ions act like a bridge. Besides C2 domain interacts with PtdIns(4,5) $P_2$  through its *lysine-rich cluster*. After this interaction, pseudosubstrate domain is released from active centre, favouring interaction of C1 domain with DAG generated in plasma membrane (top-right species). Now, PKC obtains an active conformation ready to phosphorylate its substrates, triggering downstream signalling (Corbalán García *et al.*, 2003; Rodríguez-Alfaro *et al.*, 2004). Note that this open conformation is sensitive to phosphatase PHLPP (PH domain leucine-rich repeat protein phosphatase) action, PKC being degraded (bottom-right species). In this point chaperone HSP70 can interact with the dephosphorylated *turn motif*, which promotes the PKC re-phosphorylation and re-entry into the pool of catalytically competent, but inactive kinases (Taken from Newton, 2010).

As shown in Figure I.13, PKC is involved in many biological functions, one of its most important roles being the regulation of gene expression. The two best known pathways in which PKC is involved are the activation of MAP kinases (MAPK) and NF- $\kappa$ B (Schonwasser *et al.*, 1998). While the first one enhances the transcription of genes involved in cell the cycle, the second one transcribes more specific genes and, together with AP-1, is essential in the regulation of the inflammatory response, cell survival and tumorigenesis processes.

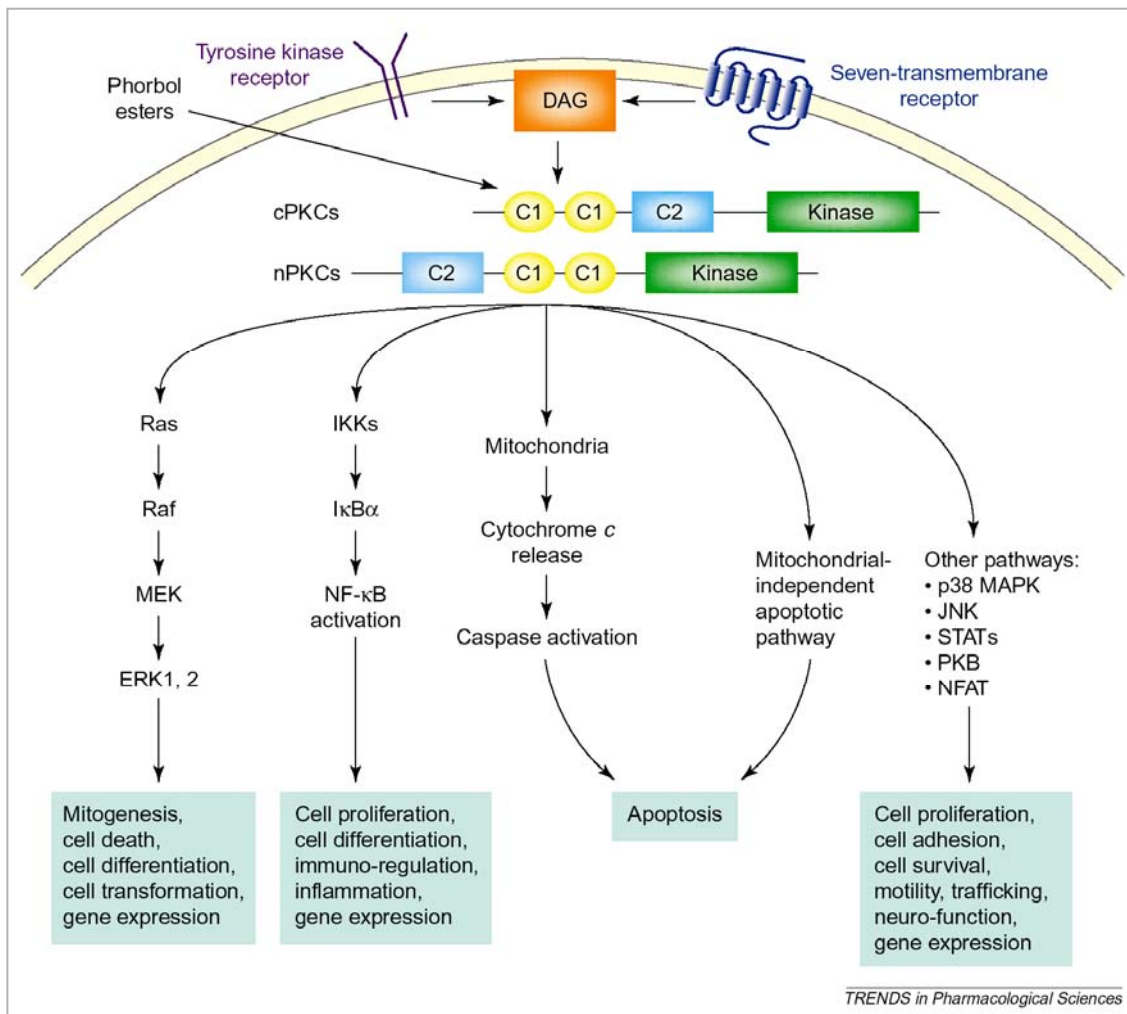


**Figure I.13. Schematic representation of different cellular functions where PKC is involved.** Different stimuli entail generation of PKC activators what produces a correct localization and activation of the enzyme, acquiring a perfect disposition to phosphorylate its substrates and participate in several signalling pathways, affecting biological function like mitogenesis, apoptosis or vessel traffic among others (Taken from Yang and Kazanietz, 2003).

## 6. Other bioactive lipids able to activate PKC.

As mentioned above, PKC isoforms can be activated by a variety of compounds, but only some fatty acids and DAG-lactones are briefly explained here, since they are studied in this Doctoral Thesis, for their relation with some diseases like cancer.

### 6.1. Fatty acids.

Cancer is the main cause of mortality worldwide, but the geographical differences in its incidence suggest an important role for environmental factors in the etiology of this disease, as well as genetic factors. Among environmental factors, nutrition is the most relevant; and among the large number of dietary compounds that have been related with cancer, dietary lipids are significant (*Bartsch et al., 1999; Kushi and Giovannucci, 2002*).

Lipid intake is a major determinant of the overall lipid composition of storage lipids and of membrane lipids, as assessed during dietary intervention studies carried out in animals and human (*Brown et al., 1991; Senkal et al., 2005; Kobayashi et al., 2006*). Due to the close relationship between the fatty acid composition of cell membrane phospholipids and cellular functions (*Hulbert et al., 2005*), interest in identifying the health-related effects of dietary changes in fatty acid intake is growing.

International variations in the incidence of breast and colon cancer are positively related with total fat intake (*Zusman et al., 1997; Bartsch et al., 1999; Kushi and Giovannucci, 2002*). However, total fat consists of different fatty acid families; for example, saturated fatty acids (SFAs), monounsaturated fatty acids (MUFAs), and  $\omega$ -3 and  $\omega$ -6 polyunsaturated fatty acids (PUFAs) (Fig I.14). Among MUFAs, oleic acid (OA, 18:1n-9) is the major fatty acid in olive oil. The  $\omega$ -6 series are widely consumed in Northern Europe and these include a precursor, linoleic acid (LA, 18:2n-6), which is abundant in food of animal origin, in vegetables and in oils such as sunflower, soy bean and grape seed. The  $\omega$ -6 series also contains the arachidonic acid (AA, 20:4n-6), which is a substrate of specific lipid oxygenases that form bioactive inflammatory mediators, and the gamma-linolenic acid (GLA, 18:3n-6) found in several vegetable sources. The  $\omega$ -3 series includes an essential fatty acid, alpha-linolenic acid (ALA, 18:3n-3) found in green vegetables and in several oils (rape, soybean); and highly unsaturated derivatives such as eicosapentaenoic acid (EPA, 20:5n-3) and docosahexaenoic acid (DHA, 22:6n-3), which are ubiquitous in mammals and abundant in oily fish, fish oils, seafood and marine products.

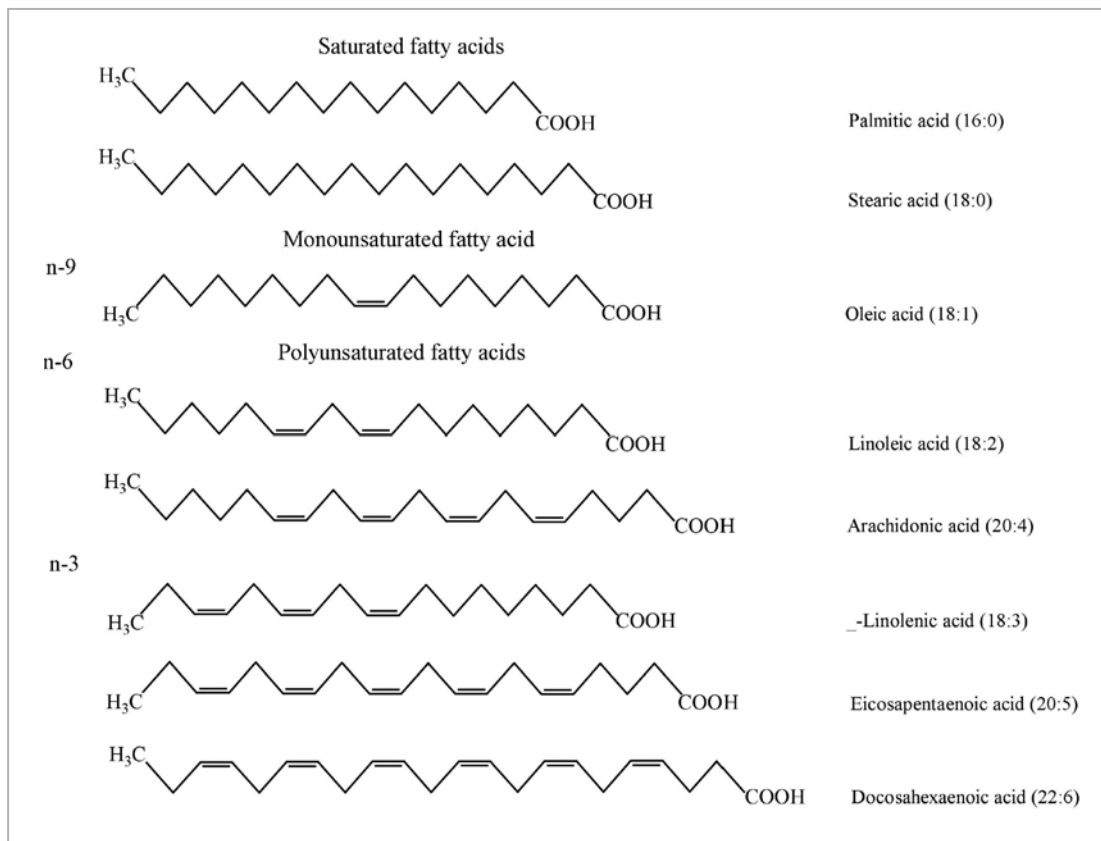


**Figure I.14. Chemical structures of major saturated, monounsaturated, and polyunsaturated fatty acids.** The number before the colon indicates the number of carbon atoms in the fatty acid chain, and the number after the colon indicates the number of double bonds. The conformation of the double bond is cis in configuration, and the first double bond located at 3rd, 6th, or 9<sup>th</sup> carbon from the terminal methyl group of a fatty acid is called n-3, n-6 and n-9 series fatty acids, respectively (Taken from *Tsubura et al., 2009*).

N-6 PUFAs, especially LA, have been shown to have a stimulating effect on breast, colorectal and prostate cancers in animal models (*Rose, 1997*). On the other hand, high levels of n-3 PUFA, especially EPA and DHA, inhibit breast and colon tumour growth and metastasis (*Ip, 1997*). As n-3 and n-6 PUFAs show opposite effects against breast and colon carcinogenesis, the balance between n-3 and n-6 intake may be more important than the overall intake of n-3 or n-6 PUFAs (*Bougnoux et al., 2005*). In general, the n-3/n-6 ratio is inversely related to breast cancer risk (*Zhu et al., 1995; Maillard et al., 2002*).

Olive oil and oleic acid intake have been related with an apparent protective effect against cardiovascular diseases and cancer. Although there is a degree of inconsistency between studies (*Takeshita et al., 1997; Solanas et al., 2002*), it can be concluded that this fatty acid possesses a potential protective effect against breast cancer. It is worth noting that olive oil is composed of oleic acid and other minor compounds whose relative content differs between types and varieties of olive oil, which may explain the inconsistency of the results obtained in studies (*Ip, 1997*). Along with oleic

acid, these minor compounds are responsible for beneficial effects on human health.

Considerable progress has been made in understanding the specific mechanisms by which dietary fat in general and olive oil in particular may exert their modulatory effects on cancer. The most noteworthy mechanisms are: the influence exerted on the stages of the carcinogenesis process (*Owen et al., 2005; Gill et al., 2005*), alteration of the hormonal status (*Larsson et al., 2004*), modification of the structure and function of cell membranes (*Hulbert et al., 2005; Yang et al., 2005*), modulation of cell signalling transduction pathways (*Bartoli et al., 2000; Yamaki et al., 2002*), the regulation of gene expression (*Moral et al., 2003; Menendez et al., 2005*) and influence on the immune system (*Miles et al., 2005*).

Besides having their own effects, some fatty acids show synergy with other substances. Long chain n-3 PUFA, such as DHA or EPA, improve the cytotoxic effects of several anti-cancer drugs belonging to different classes, for example anthracyclines (*Pardini, 2006; Calviello et al., 2009*). Several putative mechanisms accounting for DHA-induced tumour chemosensitization have been explored to explain the role of DHA in breast cancer cell lines. DHA-induced changes in drug uptake and the oxidative status of tumour cells are among the main mechanisms involved.

To summarize, many studies into fatty acids and health have been carried out and, although it is difficult to establish firm conclusions on the effect of each particular fatty acid in human epidemiological studies. Experimental studies in animals and cultured cells suggest that n-6 PUFAs (LA and AA) have a tumour-promoting effect (*Rose, 1997*), while n-3 PUFAs (EPA, DHA and ALA) exert an inhibitory effect on tumour growth (*Ip, 1997*). SFAs such as palmitic acid and stearic acid show a similar effect to n-6 PUFAs (*Carrol, 1991; Kushi and Giovannucci, 2002; Gonzalez, 2006*), while results concerning the action of oleic acid, a MUFA, are inconclusive (*Escrich et al., 2007*).

## **6.2. DAG-lactones.**

Since PKC was seen to be involved in cancer (these kinases are receptors for phorbol esters) (*Nishizuka, 1986*), there has been a search for substances able to inhibit it. A first approach targeted the catalytic domain, but as this domain is similar in all kinases this possibility was rejected. Nowadays, modulators specifically targeted against the C1 domain are being explored, since the number of C1 domains containing proteins is much lower than the number of kinases and also, there are potent natural products that can be directed against this domain like DAG and phorbol esters.

The most successful approach involved DAG-lactone, a conformationally constrained DAG analogue, whose synthesis is conceptually simple (*Nacro et al., 2000*), involving the joining of the *sn*-2-*O*-acyl moiety of DAG to the glycerol backbone with an additional carbon atom to complete a five-member ring (Fig I.15) (*Marquez and Blumberg, 2003*).

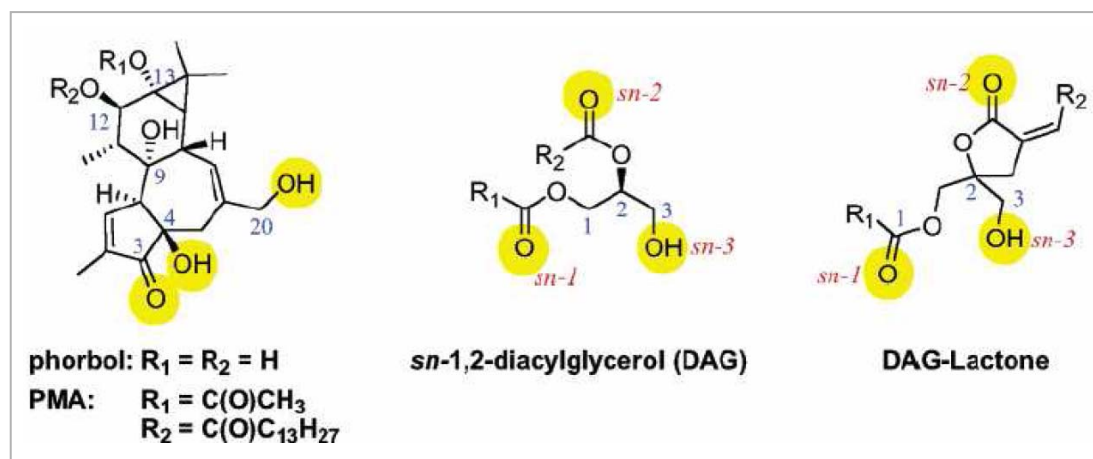


**Figure I.15. Structural comparison among phorbol ester, DAG and DAG-lactones.** These molecules share three bioequivalent groups (yellow) since they intervene in the interaction between C1 domain and membrane. Carbon positions are marked in blue, and in red (DAG and DAG-lactone) are marked carbonyl or OH groups which arise from carbon 1, 2 or 3. R1 and R2 are variable chains (Taken from *Tamamura et al., 2004*).

This lactone nucleus decreases the flexibility of the ligand conformation, favouring a stable union with the receptor due to a decrease in entropy in that interaction (*Marquez et al., 1999*). Moreover, the presence of variable acyl chains imparts substrate specificity to DAG-lactones and an increased affinity for PKC in a nanomolar range (*Marquez et al., 1999; Marquez and Blumberg, 2003*). These acyl chains favour specific interactions (with C1 domains) and unspecific ones (with phospholipids in membranes), which stabilize the union (*Colon-Gonzalez and Kazanietz, 2006*).

This basic DAG-lactone structure can be enhanced by a pharmacophore-guided approach. In this way, it has been demonstrated that specific hydrophobic substitutions generate DAG-lactones able to induce a PKC isoform-selectivity translocation to different subcellular compartments (*Pu et al., 2005*).

## 7. Introduction to PKC and cancer.

As Griner and Kazanietz discuss in a recent review (*Griner and Kazanietz, 2007*), protein kinase C (PKC) burst into the cancer research field in the early 1980s with its identification as a phorbol ester receptor. Phorbol esters, which are natural substances with tumour-promoting activity, had long been of interest in the cancer research field, since the prolonged topical application of these substances to mice promoted the formation of skin tumours (*Blumberg, 1988*). Seminal investigations established that PKC was one of the intracellular receptors, being that the first solid evidence for the involvement of a protein kinase in carcinogenesis (*Kikkawa et al., 1983*). Along these years a wide variety of proteins containing C1 domains have been demonstrated to be also phorbol esters receptors, making a more complex picture (*Colón-González and Kazanietz, 2006*).

Since then until now, many kinases, mainly receptor tyrosine kinases (RTK), have been associated with tumour development and progression. The activation of RTK causes autophosphorylation of the tyrosine kinase within its intracellular domain, which triggers a cascade of intracellular signals that ultimately promote malignant transformation and tumour progression (*Marmor et al., 2004*). Signalling cascades of particular interest include the PI3K pathway that leads to the activation of PDK-1 (3-phosphoinositide-dependent protein kinase-1) and AKT (also known as protein kinase B); and Ras/MAPK pathway that leads to the activation of Raf-1, MEK and MAPK. The JAK/STAT pathway is another important component of signal transduction following RTK activation, and PKC also plays important roles. Cancer-related processes, such as cell proliferation, enhanced survival/decreased apoptosis and metastasis (cell migration, adhesion and invasion), are promoted through these cascades (Fig I.16).

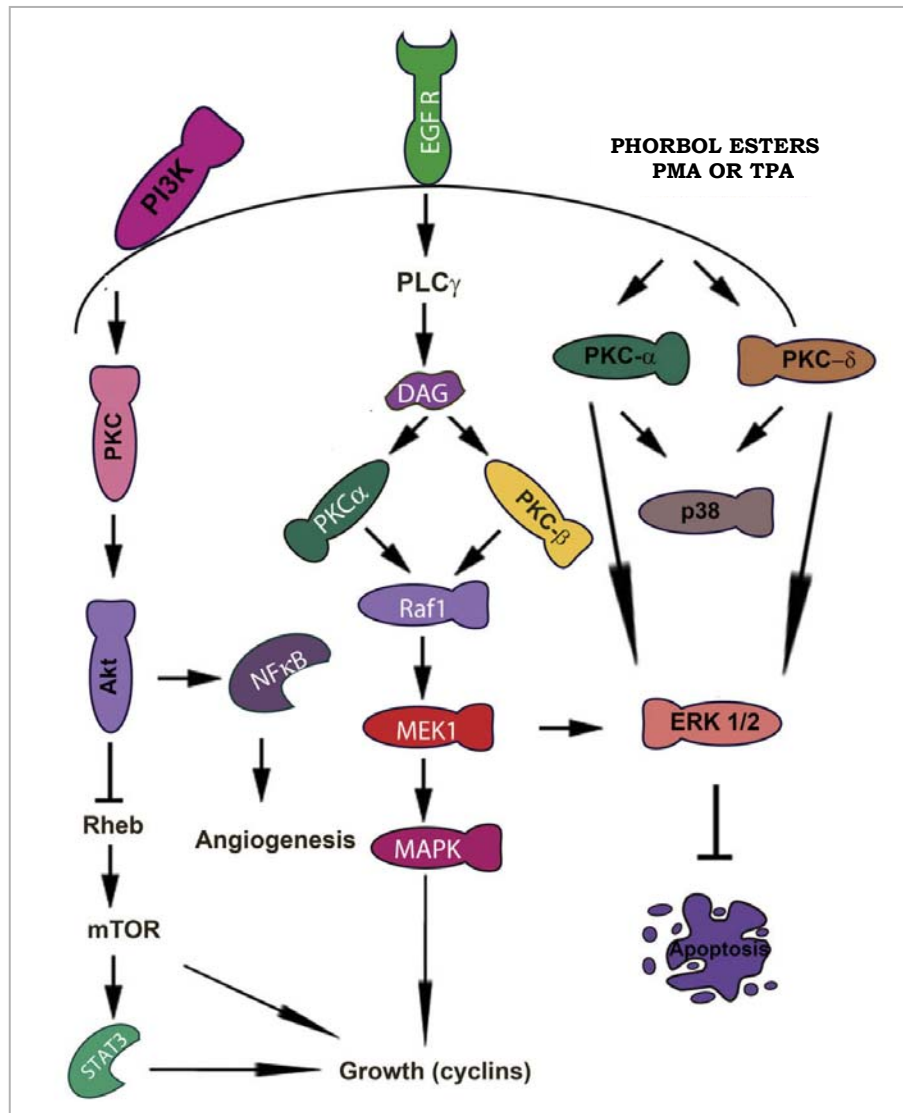


**Figure I.16. Schematic diagram of a comprehensive overview of PKC signalling.** The cartoon depicts the activation of PKC $\alpha$ , PKC $\delta$ , PLC-DAG and the subsequent downstream events include activation of the MEK-ERK and PI3K-Akt pathways (Taken from Ashhar S. Ali *et al.*, 2009).

Initial research on mouse skin carcinogenesis related PKC and cancer, but later studies in normal and tumour cells confirmed the involvement of PKC isoenzymes in mitogenesis, survival and malignant transformation (Griner and Kazanietz, 2007). Phorbol esters also cooperate with the Ras oncogenes in transformation, and it has been observed that in Ras-transformed cells exists a deregulated production of DAG, indicating that Ras and PKC might cooperate during transformation (Lacal *et al.*, 1987; Hsiao *et al.*, 1989). Functional links between PKC and several oncogenes, such as *fos* and *myc*, were identified later (Barr *et al.*, 1991; Han *et al.*, 1995), indicating that PKC might has an important role in many of the cancer signalling pathways.

The role of PKC in cancers is apparently not due to mutations in PKC genes unlike in the majority of genes involved in carcinogenesis, such as oncogenes and tumour suppressors. Mutations in genes encoding PKCs are found very rarely in human diseases; the reason in the case of PKCs is usually that some isoforms possess altered expression in different types of cancer (Roffey *et al.*, 2009). Of particular interest is the fact that PKC $\epsilon$  has been shown to be up-regulated in various types of cancer (Varga *et al.*, 2004; Pan *et al.*, 2005; Grossoni *et al.*, 2009), whereas PKC $\delta$  are down-regulated (Mandil *et al.*, 2001; D'Costa *et al.*, 2006). In some cancers there is a striking correlation between changes in expression and progression of the disease, suggesting their potential use as prognostic markers (Varga *et al.*, 2004).

The role of PKCs in cancer seems to result from their action as receptors for tumour promoting agents or from their action as downstream targets of growth factor receptors (Reyland, 2009). Furthermore, mutations in other cancer-related genes may change the original isoenzyme profile of a tissue and lead to carcinogenesis through the activation of specific isoenzymes (Sivaprasad *et al.*, 2006).

Although PKC isoenzymes have a clear role in tumorigenesis, it has been practically impossible to establish the relative contribution of every isoenzyme in this process, owing to the large different roles that PKC isoenzymes have and the fact that they vary according to the tissues and the cell type (Yang and Kazanietz, 2003).

The activation of different PKC isoenzymes has been shown to result in distinct cellular responses. Moreover, there is extensive cross-talk with different isoenzymes, and the overall response seems to depend on the presence or activity of the other isoenzymes in a particular cell type (Koivunen *et al.*, 2006).

The complexity of the different PKC isoforms on the level of differential expression under physiological conditions as well as on the level of physiological substrates complicates a clear assignment of a particular role to a given isoform or substrate. Thus, it is not surprising that in cancer a complex pattern of PKC over-expression and down-regulation has also been described, making it difficult to assign particular roles to PKC isoforms in cancer formation and progression (Reyland, 2009). However, many different tools have been developed to define isoform-specific functions of PKC: dominant inhibitory kinases, mouse models in which specific PKC isoforms are disrupted, and specific PKC isoform antisense/siRNA. Thanks to these tools, it has been provided evidence that PKC isoforms regulate a variety of essential biological processes, such as cell migration, contraction, immunity, neural plasticity, proliferation, differentiation, apoptosis and metabolism (Dempsey *et al.*, 2000). Importantly, the function of a specific PKC isoform can

vary between different cell types, implying that the specific responses may rely on the interaction of PKC isoforms with others proteins involved in regulatory pathways in the cell.

Alterations in PKC isoenzymes during cancer progression vary and depend on the cancer cell type, and no general conclusions can be made of the expression pattern with respect to carcinogenesis in general. However, the PKC isoforms most commonly associated with increased proliferation and/or survival, PKC $\alpha$  and PKC $\epsilon$ , are those most commonly over-expressed in human cancer, and represent potential oncogenes (*O'Brian et al., 2006*). The atypical isoforms PKC $\iota$  and PKC $\zeta$  should be added to this group, as their increased expression has recently been shown to correlate with tumour stages in non-small cell lung cancer, and their depletion was shown to reverse the transformed phenotype of these cells (*Hizli et al., 2006*). Most of the effects of these atypical PKC isoforms can be attributed to activation of the pro-survival NF- $\kappa$ B signalling pathway and the suppression of apoptosis (*Moscat et al., 2006*).

The vast majority of studies have demonstrated that increased PKC $\alpha$  activity is associated with the increased motility, invasion and metastasis of cancer cells, while inhibition of the enzyme effectively reverses the phenotype (*Masur et al., 2001; Tan et al., 2006*). These studies reveal the role of PKC $\alpha$  as inducer of proliferation and suppressor of apoptosis.

PKC $\epsilon$  also promotes cell survival in many cell types through increased activation of the Akt pathway and the up-regulation of pro-survival factors. This novel PKC isoform has been shown to be a transforming oncogene both in epithelial cells and fibroblasts, since its over-expression provides a proliferative advantage in various cell lines (*Cacae et al., 1996*). Moreover, there is growing evidence to support a role for PKC $\epsilon$  in promoting an invasive metastatic tumour-cell phenotype (*Pan et al., 2006*). PKC $\epsilon$  also protects against apoptosis and has been implicated in the resistance of tumour cells to anti-cancer drugs (*Ding et al., 2002*).

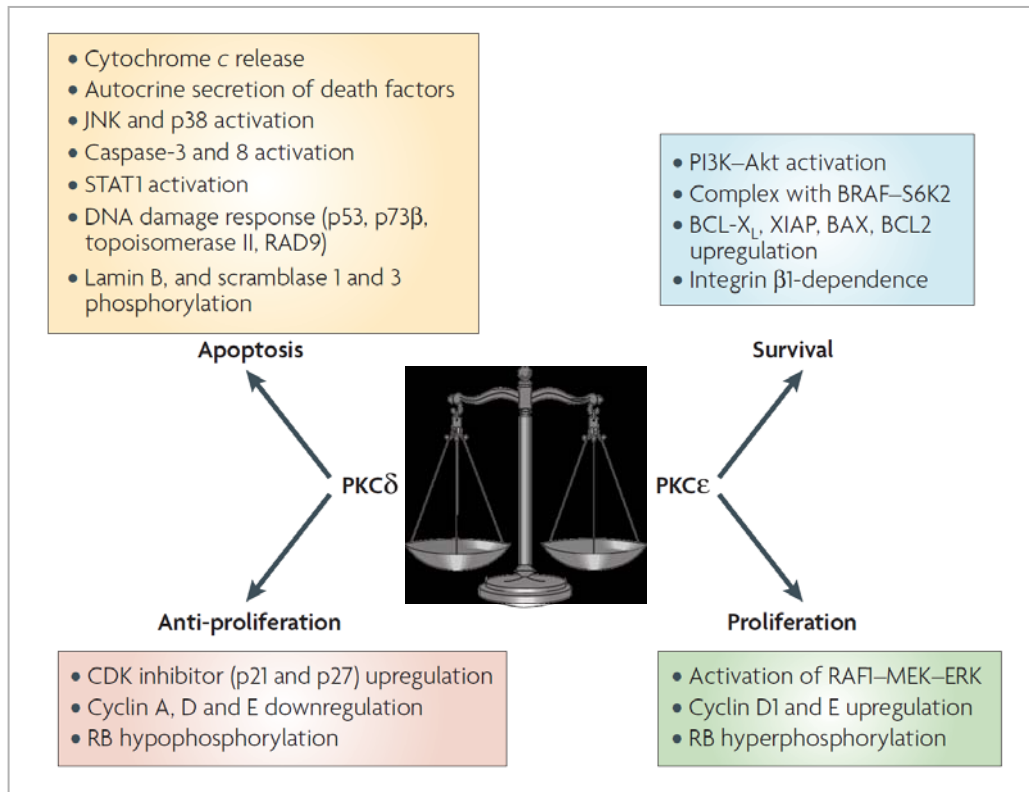


**Figure I.17. Opposing roles of PKCδ and PKCε.** According to PKC, the phenotype of tumour or normal cells depends on the ratio of pro-apoptical and negative proliferation regulators isoenzymes (PKCδ) and pro-mitogenic and pro-survival isoenzymes (PKCε). In this figure is represented the opposing roles of these two PKC isoforms in apoptosis, survival and proliferation (Taken from Griner and Kazanietz, 2007).

In contrast to PKCα and PKCε, it has been suggested that PKCδ is a tumour suppressor, since the loss of this novel PKC isoform is associated with cell transformation in some cases (Heit *et al.*, 2001). In addition, most studies with PKCδ suggest a pro-apoptotic and anti-proliferative role for this isoenzyme, which suppresses cell cycle progression (Lu *et al.*, 1997; Jackson and Foster, 2004; Santiago-Walker *et al.*, 2005). The mechanism by which PKCδ induces apoptosis seems to be well defined (Reyland 2009) (Fig I.18): it is known that this novel PKC is activated by numerous apoptotic stimuli and is required for apoptosis induced by genotoxins (Matassa *et al.*, 2001), oxidative stress (Majumder *et al.*, 2001) and death receptors. Treatment with the PKCδ selective inhibitor (rottlerin), expression of inactive kinase (PKCδ KD) (Matassa *et al.*, 2001) or the introduction of a PKCδ-specific RACK inhibitory peptide (Schechtman and Mochly-Rosen, 2002) have all been shown to inhibit apoptosis. All these studies point to an essential role for this isoform as a regulator of early events in the apoptotic pathway (Reyland, 2007).

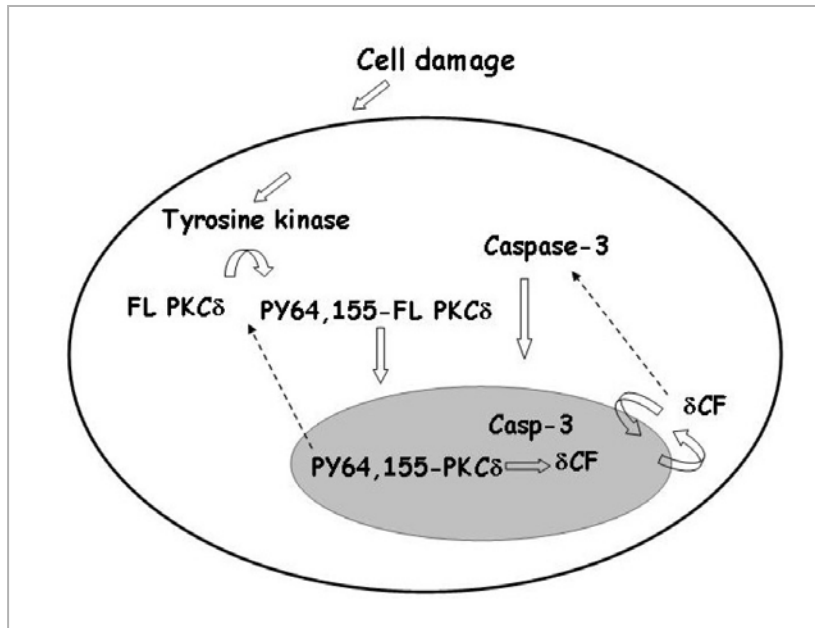


**Figure I.18. Regulation of the proapoptotic function of PKC $\delta$ .** In resting condition, PKC $\delta$  regulatory domain is responsible for the kinase inhibition, but when apoptotic signals arrive to the plasma membrane, some tyrosine kinases are activated, which phosphorylate PKC $\delta$  regulatory domain, allowing nuclear accumulation of active PKC $\delta$ . In that state, it may regulate proteins involved in the cell damage response and apoptosis induction (Taken from *Reyland 2009*).

Besides these alterations in PKC activity levels, some abnormal expression of other isoenzymes may also take place in different steps of cancer development, for instance, angiogenesis.

Griner and Kazanietz exhibited in their review in 2007 that PKC is involved in mediating vascular endothelial growth factor (VEGF)-induced angiogenesis. Most of the evidence points to PKC $\beta$  as being highly relevant in angiogenesis, not only in cell culture models but also in an *in vivo* setting. This isoenzyme, among others, is activated in response to VEGF receptor activation, and is an important mediator of VEGF-induced proliferation of endothelial cells (*Xia et al., 1996*) through ERK activation and retinoblastoma protein (RB) hyperphosphorylation (*Suzuma et al., 2002*).

## 8. PKC isoforms in Breast Cancer.

In 2000, over 1 million cases of breast cancer were diagnosed worldwide killing over 370,000 women (*Ferlay et al., 2001*). It is not surprising, therefore, that many projects are directed at understanding the specific role of several proteins involved in cancer, PKC family among them, and are looking for successful treatments against them.

As in other types of cancers, the role of PKC in breast cancer is not entirely known, but in general it is thought that PKC activity is increased in malignant breast tissue and in most aggressive breast cancer cell lines, suggesting that PKC plays a role in breast carcinogenesis and tumour progression. PKC activity has been reported to be high in surgical specimens of human breast tumours, compared with the expression of PKC activity in normal breast tissue obtained from the same patients (*Blobe et al., 1994; Gordge et al., 1996*). PKC expression has therefore been proposed as a potential marker for human breast cancer.

Although most studies on PKC and breast cancer have focused on classical isoform PKC $\alpha$ , it has been shown that other isoenzymes like PKC $\delta$ ,  $\epsilon$  and  $\beta$  also affect the invasive and chemotactic potential of human breast cancer (*Koivunene et al., 2006*).

PKC $\delta$  is thought to play a major role in anti-estrogen resistance in breast cancer cells and has been linked with acquired resistance to tamoxifen (Tam) in breast cancer patients (*Nabha et al., 2005*). This novel isoform seems to play a fundamental role in the regulation of growth in two estrogen receptor (ER) positive breast cancer cell lines (*Shanmugam et al., 2001*). ER-positive breast cancer cell lines express a considerable amount of PKC $\delta$ , whereas ER-negative cell lines express very little PKC $\delta$  (*Assender et al., 2007*). Also, the downregulation of PKC $\delta$  in MCF-7 (ER+) breast cancer cells increased cell motility, accompanied by a corresponding increase in MMP9 secretion (*Jackson et al., 2005*).

PKC $\epsilon$  and the antiproliferative effect of tamoxifen have been related due to the interaction observed between them in MCF-7 cells (*Lavie et al., 1998*). PKC $\beta$  may be a promoter of cell growth because the treatment of some breast cancer cell lines with specific inhibitors of this isoform reduced tumour growth and tumour-induced angiogenesis (*Sliva et al., 2002*).

Another aspect that suggests that PKC is involved in this type of cancer is multi-drug resistance (MDR) (*Lahn et al., 2004*). This phenomenon involves broad spectrum resistance to chemotherapeutic agents and a pronounced defect in the intracellular accumulation of the drugs, associated with over-expression of the drug efflux pump P-glycoprotein. Several studies pointed to a role for PKC, especially PKC $\alpha$  over-expression, in the regulation of the MDR phenotype, because several PKC inhibitors are able to partially reverse this problem.

The molecular mechanism seems to involve the phosphorylation of the linker region of P-glycoprotein by PKC, which leads to alterations in the P-glycoprotein ATPase and drug-binding functions (*Gupta et al., 1996; Gill et al., 2001*).

As regards PKC $\alpha$ , it has been observed that, in general, it is over-expressed in breast cancer and may predict resistance to tamoxifen (*Tonetti et al., 2002*). This classical isoform has been associated with malignant transformation, tumour cell proliferation, MDR, alteration of ER status and apoptosis in breast cancer. Many of these findings are based on studies with breast cancer cell lines, such as MCF-7 (ER+) and MDA-MB-231 (ER-).

PKC $\alpha$  has been associated with malignant phenotype in breast cancer, among other reasons because MCF-7 breast cancer cells transfected with this isoenzyme showed a shortened doubling time, and these cells also exhibited a highly malignant and metastatic growth when they were implanted in athymic mice, compared to their parental control (*Lahn et al., 2004*). Another factor in tumour progression is the activation of the telomerase (a RNA directed DNA polymerase that is normally repressed in somatic tissue) (*Li et al., 1998*). Recent studies suggest that PKC $\alpha$  activation leads to the phosphorylation of human telomerase associated protein 1 (hTEP1) and the telomerase catalytic subunit, human telomerase reverse transcriptase (hTERT) (*Lahn et al., 2004*). The phosphorylation of these proteins seems to be a prerequisite for the increased activation of the telomerase complex resulting in tumour cell growth (*Li et al., 1998*).

ER status is an important prognostic marker in breast cancer, an ER-negative status being associated with poor outcome (*Li et al., 2003*). Thus, factors contributing to ER-negative status, including the role of PKC $\alpha$ , have been investigated. ER-positive breast cancer cell lines (e.g., MCF-7 and ZR75.1) have low PKC $\alpha$  levels, while ER-negative breast cancer cell lines (e.g., MDA-MB-231 and MDA-MB-435) have high PKC $\alpha$  levels. MCF-7 cells and others ER+ breast cancer cell lines transfected with PKC $\alpha$  developed an ER-negative phenotype and showed a decrease in ER-dependent gene expression (*Ways et al., 1995; Tonetti et al., 2000*). These observations suggest that PKC $\alpha$  plays an important role in the development of the ER-negative status and in the resistance to selective estrogen receptor mediators (SERMs).

The relation between PKC $\alpha$  and apoptosis is through heregulins (HRG), a group of growth factors involved in the signalling network of human epidermal growth factor receptor (EGF-R). In the HER-2/neu expressing breast cancer cell line, SKBr3, HRG induces apoptosis via caspase 7 and 9. When these cells were induced to express PKC $\alpha$ , the apoptotic signal of HRG is dramatically attenuated, suggesting that PKC $\alpha$  may inhibit the HRG-mediated apoptosis of breast cancer cells (*Le et al., 2001*).

All these studies suggest that members of the PKC family, especially PKC $\alpha$ , have a potential interest as targets in the treatment of breast cancer.

## 9. PKC isoforms as targets in cancer therapy.

The PKC family is undoubtedly an attractive target for therapeutic intervention given its role in tumorigenesis and the potential for enhancing the cytotoxicity of existing drugs (Mackay and Twelves, 2003). The existence of different isoenzymes provides an opportunity to develop pharmacological agents that target specific PKC functions. This presents some advantages and disadvantages; on the one hand, the lack of mutations in genes encoding PKCs makes the enzyme a suitable target for cancer therapies, with no expected failure of the therapy due to gene mutations, and on the other hand, few of the currently available pharmacological agents exhibit a high degree of selectivity for a specific PKC isoform, and the majority also act on other protein kinases.

In the past, some compounds, such as staurosporine and several analogues (midostaurin (PKC412), UCN01, Go6976, enzastaurin (or LY317615) and ruboxistaurin (also known as LY333531)), were used to inhibit PKC and improve cancer treatments, but most of them were unsuccessful due to their low selectivity (interacting with the ATP-binding site conserved in kinases). Enzastaurin and ruboxistaurin specifically inhibit PKC $\beta$  and they are currently being tested in clinical trials.

Bryostatins, which act *via* the effector-binding C1A/B binding domains, have also been tested, but results in phase II studies were disappointing (Zonder *et al.*, 2001). Aprinocarsen or ISIS3521 is a PKC $\alpha$  antisense oligodeoxynucleotide but this, too, was rejected for cancer treatment after phase II/III studies.

All these compounds have anti-neoplastic effects as estimated by decreased invasion, the inhibition of angiogenesis, or reduced growth of cancer cells both *in vitro* and *in vivo* (Table I.1).

**Table I.1. Main Protein Kinase C inhibitors** (Modified from Mackay and Twelves, 2007).

DRUG	CLASS	SPECIFICITY/SELECTIVITY
PMA (TPA)	Phorbol ester	Non-specific
Staurosporine	Indolocarbazole	Poor specificity, also inhibits other Ser/Thr kinases and tyrosines kinases
PKC412 (midostaurin)	Indolocarbazole	PKCs $\alpha$ , $\beta$ , $\gamma$ , $\delta$ , $\epsilon$ , $\eta$ ; also inhibits tyrosine kinases
UCN01	Indolocarbazole	cPKCs > nPKCs
Go6976	Indolocarbazole	cPKCs > nPKCs
Bryostatin 1	Macrocyclic lactone	Activator of cPKCs and nPKCs, in presence of activating ligands acts as an antagonist
Tamoxifen	Nonsteroidal anti-oestrogen	PKCs $\alpha$ , $\beta$ , $\gamma$ , non-selective
Bisindolymaleimide (LY333531)	Indolocarbazole	PKC $\beta$
Enzastaurin (LY317615)	Indolocarbazole	PKC $\beta$
Aprinocarsen (ISIS3521)	Antisense oligonucleotide; 19-mer	PKC $\alpha$
ISIS9606	Antisense oligonucleotide; 19-mer	PKC $\alpha$

In general, none of these compounds has significant positive effects when they are used singly in human tumours, but clinical trials are under way to use them in combination with classical chemo-therapeutic agents or ionic radiation (Table I.2). In this respect, the combination of midostaurin with imatinib mesylate (Reichardt *et al.*, 2005), enzastaurin with gemcitabine and cisplatin (Rademaker-Lakhai *et al.*, 2004) and aprinocarsen with gemcitabine and carboplatin (Ritch *et al.*, 2006) are of note for the promising results obtained.

We now know that cancer cells contain many proteins with deregulated expression, so it is easy to understand why current treatments of cancer are based in combinations of different compounds to inhibit the different proteins involved in cancer development (PKC isoform included) in an attempt to improve the results of treatment.

**Table I.2. Main combinations studies with standard cancer therapeutics and Protein Kinase C inhibitors.** (Modified from Mackay and Twelves, 2007).

COMBINATIONS	PHASE
Gemcitabine and cisplatin +/- aprinocarsem	Phase III (NSCLC)
Paclitaxel and carboplatin +/- aprinocarsen	Phase III (NSCLC)
Gemcitabin, carboplatin and aprinocarsen	Phase II (NSCLC)
Gemcitabine, enzastaurin and cisplatin	Phase I
Enzastaurin and capecitabine	Phase I
Enzastaurin and premetexed	Phase I
Safingol and cisplatin	Phase I
UCN01 and topotecan	Phase I and II (ovarian)
UCN-01 and 5FU	Phase I
Paclitaxel and bryostatin 1 (pancreatic caner)	Phase II (pancreatic and prostate cancer)
Bryostatin 1 and interleukin 2	Phase II (RCC)
Bryostatin 1 and gemcitabine	Phase I
CCI779 and bryostatin 1	Phase I
Midastaurin and imatinib	Phase I and II (gastro-intestinal stromal tumour)

5FU, 5-fluorouracil; NSCLC, Non-small-cell lung cancer; RCC, renal cell carcinoma.

## 10. OBJECTIVES.

Previous studies carried out in our laboratory revealed the localization and activation mechanisms of different PKC isoforms through their regulatory domains induced by classical cofactors like DAG and PtdSer (*Verdaguer et al., 1999; Bolsover et al., 2003*) and also others as PtdIns(4,5)P<sub>2</sub> (*Corbalán-García et al., 2003; Marin-Vicente et al., 2008; Guerrero-Valero et al., 2009*).

However, the localization and activation models of different PKC isoforms by other physiologically important lipids, like fatty acids, or synthetic compounds such as DAG-lactones remain unknown. In addition, we shall attempt to shed light on the role that some PKC isoforms play in breast cancer cell lines.

Therefore, the specific objectives established at the beginning of this Doctoral Thesis were:

- Characterization of the molecular mechanism by which arachidonic acid promotes the localization and activation of PKC $\alpha$ .
- Determination of the role of the C1 and C2 regulatory domains of PKC $\alpha$  in cellular localization and activation induced by arachidonic acid, oleic acid, eicosapentaenoic acid or docosahexaenoic acid.
- Determination of the role of oleic acid and omega-3 fatty acids in breast cancer cells.
- Characterization of the role that PKC $\alpha$  plays in breast cancer cells stimulated with oleic acid, eicosapentaenoic acid or docosahexaenoic acid.
- Characterization of the effect of positive charged DAG-lactones on different PKC isoform localization in the plasma membrane of MCF-7 cells.
- Determination of the tightness of the plasma membrane anchorage of different PKC isoforms in MCF-7 breast cancer cells stimulated with PMA or positive charged DAG-lactones.
- Determination of the role of PKC $\alpha$  in the invasive and non-invasive breast cancer cell lines, MCF-7 and MDA-MB-231, by means of the siRNA technique.
- Characterization of the effects of salinomycin and the role of PKC $\alpha$  on breast cancer cell lines.

## CHAPTER II

### MATERIALS AND METHODS



## 1. Construction of expression plasmids.

Rat PKC $\alpha$  cDNA was a gift from Drs Y. Nishizuka and S. Ono (Kobe University, Kobe, Japan).

Full-length PKC $\alpha$  mutants were generated using the Quikchange XL site-directed mutagenesis Kit (Stratagene, La Jolla, CA, USA) (see section 1.4).

The DNAs of PKC isoforms were amplified by PCR using specific primers. The cDNA obtained was digested with same restriction enzymes than the vector in order to ligate them, using the T4 ligase, obtaining a recombinant vector. Later DH10B *Escherichia coli* strain was transformed with the ligation vector by heat shock (Cohen *et al*, 1973). Then it was plated on LB plates containing the appropriate antibiotic to select the antibiotic-resistant clones. Finally, these clones were amplified and purified to confirm the positive clones by sequencing them (Fig II.1).

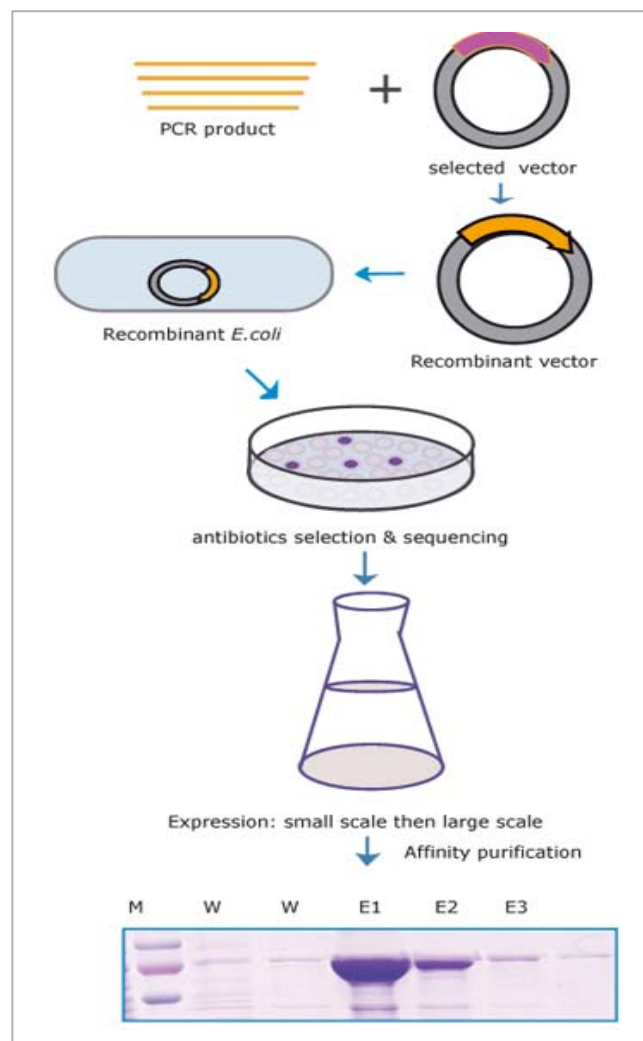


**Figure II.1. Schematic representation of expression vector construction.**

### 1.1. Constructions in plasmid pEGFP-N3.

The N-terminal fusions of rat PKC $\alpha$  and different mutants to EGFP were generated by inserting cDNAs into the multiple cloning site of the pEGFP-N3 (Clontech Laboratories, Inc. Palo Alto, CA, USA) mammalian expression vector which contains, besides EGFP sequence, a cytomegalovirus transcription promoter (P<sub>CMV</sub>), two replication origins (f1 and SV40), a kanamycin resistant gene and a multiple cloning site (MCS) (Fig II.2).

The mutants performed were as follow: PKC $\alpha$ D246N/D248N, PKC $\alpha$ K209A/K211A, PKC $\alpha$ K197A/K199A, PKC $\alpha$ W58G, PKC $\alpha$ F60G, PKC $\alpha$ Y123G and PKC $\alpha$ L125G.

The cDNAs were amplified by PCR using as a template the wild-type cDNA and the corresponding mutants with the following primers:

5' ATTCTCGAGCTATGGCTGACGTT  
3' CCGGGTACCTACTGCACTTTGCAAGAT

XhoI/Kpn-digested PKC $\alpha$  and mutated fragments were ligated with the XhoI/KpnI digested vector generating the different fusion constructs.

All constructs were confirmed by DNA sequencing, which was carried out in the Research and Development Support Center (CAID), University of Murcia (Spain).

Stability and viability of PKC $\alpha$  mutants were checked by measuring their specific kinase activity, that reached maximum values at oversaturating concentrations of the cofactors (*Conesa Zamora et al, 2000; Conesa Zamora et al, 2001; Rodríguez Alfaro et al, 2004*).

It has been also demonstrated that carboxi termini addition of the EGFP does not affect kinase activity or cofactor dependence of PKC $\alpha$  (*Almholt et al, 1999; Maasch et al, 2000; Vallentin et al, 2000*).

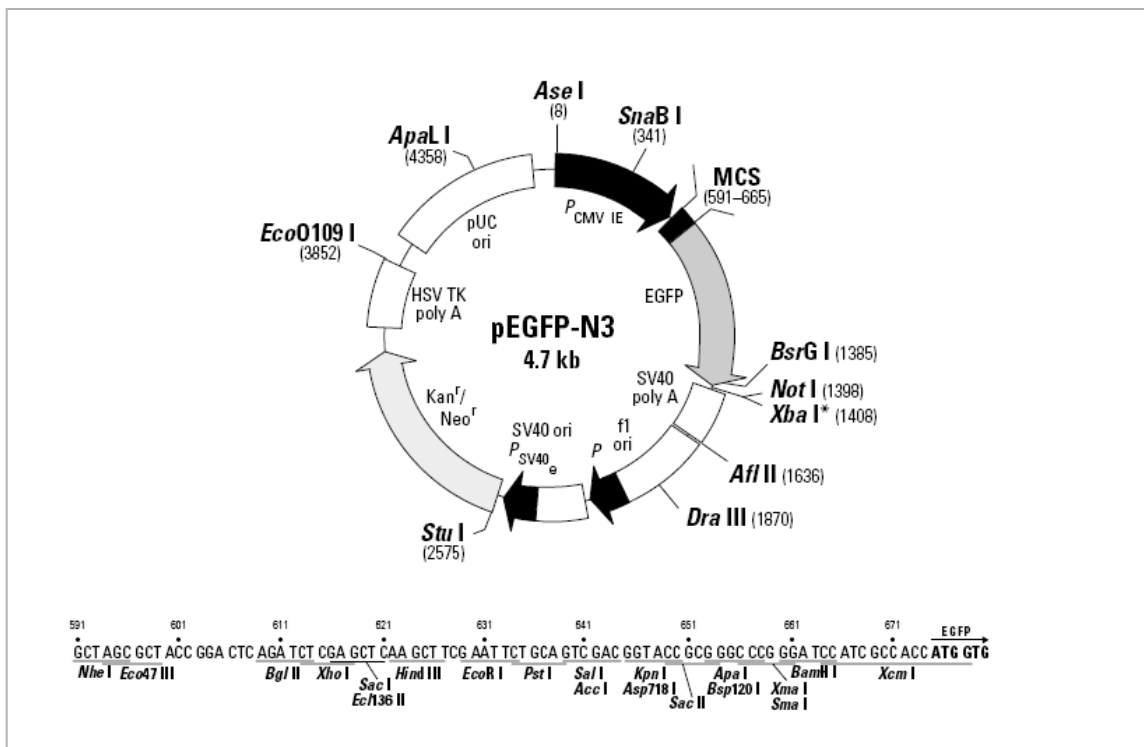


**Figure II.2. pEGFP-N3 mammalian expression vector and its multiple cloning site.** It is shown restriction sites along plasmid sequence and multiple cloning site. This plasmid also possesses a cytomegalovirus promoter ( $P_{CMV}$ ), two replication origins (f1 and SV40) and two genes of antibiotic resistance, kanamycin ( $Kan^r$ ) and neomycin ( $Neo^r$ ).

## 1.2 Constructions in plasmid pEGFP-N3.

This vector is similar to pEGFP, the difference is that pEGFP possesses a gene which codifies for Enhanced Cyan Fluorescent Protein (ECFP); instead of Enhanced Green Fluorescent Protein (EGFP).

This plasmid only was used for subcloning PKC $\delta$  isoenzyme. Steps were similar to pEGFP, but template and primers were different.

The cDNAs were amplified by PCR using as a template the wild-type cDNA and following primers:

5' AAGGTACCGGGCGGCGCACCGTTCCTGCGCATC  
3' CGGGATCCTCACTATTCCAGGAATTGCTCATA

BamHI/KpnI-digested PKC $\delta$  was ligated with the BamHI/KpnI digested vector generating the fusion construct.

Similar than before, the construct was confirmed by DNA sequencing, which was carried out in the Research and Development Support Center (CAID), University of Murcia (Spain).

### 1.3. Constructions in plasmid pCGN.

PKC $\alpha$  and some mutants were subcloned into the mammalian expression vector pCGN which contains the cytomegalovirus promoter and a multiple cloning site that allows expression of the genes fused 3' to the HA epitope, which is very useful for purification and immunoprecipitation assays (Tanaka and Herr, 1990; Rodríguez-Alfaro et al, 2004). The mutants performed were as follow: PKC $\alpha$ D246N/D248N, PKC $\alpha$ K209A/K211A, PKC $\alpha$ K197A/K199A and PKC $\alpha$ W58G.

In this case, template and primers were the same that were used in pEGFP PKC $\alpha$  constructs but now, restriction enzymes were XbaI/KpnI to digest PKC $\alpha$  wild type and mutated proteins, as well as vector.

**Table II.1. Plasmid constructions used along this Doctoral Thesis.**

CONSTRUCTION USED	OLIGONUCLEOTIDES USED	RESTRICTION ENZYMES
PKC $\alpha$ -WT-EGFP (PKC $\alpha$ -EGFP)	5' ATTCTCGAGCTATGGCTGACGT 3' CCGCCTACCTACGCACTTTGCAAGAT	KpnI/XhoI
PKC $\alpha$ D246N/D248N-EGFP	5' ATTCTCGAGCTATGGCTGACGT 3' CCGCCTACCTACGCACTTTGCAAGAT	KpnI/XhoI
PKC $\alpha$ K197A/199A-EGFP	5' ATTCTCGAGCTATGGCTGACGT 3' CCGCCTACCTACGCACTTTGCAAGAT	KpnI/XhoI
PKC $\alpha$ K209A/K211A-EGFP	5' ATTCTCGAGCTATGGCTGACGT 3' CCGCCTACCTACGCACTTTGCAAGAT	KpnI/XhoI
PKC $\alpha$ W58G-EGFP	5' ATTCTCGAGCTATGGCTGACGT 3' CCGCCTACCTACGCACTTTGCAAGAT	KpnI/XhoI
PKC $\alpha$ F60G-EGFP	5' ATTCTCGAGCTATGGCTGACGT 3' CCGCCTACCTACGCACTTTGCAAGAT	KpnI/XhoI
PKC $\alpha$ Y123G-EGFP	5' ATTCTCGAGCTATGGCTGACGT 3' CCGCCTACCTACGCACTTTGCAAGAT	KpnI/XhoI
PKC $\alpha$ L125G-EGFP	5' ATTCTCGAGCTATGGCTGACGT 3' CCGCCTACCTACGCACTTTGCAAGAT	KpnI/XhoI
PKC $\delta$ -WT-ECFP (PKC $\delta$ -ECFP)	5' AAGGTACCGGGCGGCGCACCGTTCCTGCGCATC 3' CGGGATCCTCACTATTCCAGGAATTGCTCATA	BamHI/KpnI
PKC $\alpha$ -WT-HA (PKC $\alpha$ -HA)	5' ATTCTCGAGCTATGGCTGACGT 3' CCGCCTACCTACGCACTTTGCAAGAT	XbaI/KpnI
PKC $\alpha$ D246N/D248N-HA	5' ATTCTCGAGCTATGGCTGACGT 3' CCGCCTACCTACGCACTTTGCAAGAT	XbaI/KpnI
PKC $\alpha$ K197A/199A-HA	5' ATTCTCGAGCTATGGCTGACGT 3' CCGCCTACCTACGCACTTTGCAAGAT	XbaI/KpnI
PKC $\alpha$ K209A/K211A-HA	5' ATTCTCGAGCTATGGCTGACGT 3' CCGCCTACCTACGCACTTTGCAAGAT	XbaI/KpnI
PKC $\alpha$ W58G-HA	5' ATTCTCGAGCTATGGCTGACGT 3' CCGCCTACCTACGCACTTTGCAAGAT	XbaI/KpnI

## 1.4. Site-directed Mutagenesis.

Site-directed mutagenesis was performed by using the Quikchange XL site-directed mutagenesis Kit (Stratagene, La Jolla, CA, USA). The basic procedure utilizes a supercoiled double-stranded DNA (dsDNA) vector with an insert of interest and two synthetic oligonucleotide primers, both containing the desired mutation (Fig II.3). The oligonucleotide primers, each complementary to opposite strands of the vector, are extended during temperature cycling by *Pfu Ultra* HF DNA polymerase, without primer displacement. Extension of the oligonucleotide primers generates a mutated plasmid containing staggered nicks. Following temperature cycling, the product is treated with *Dpn* I endonuclease (target sequence: 5'-GmATC-3') which is specific for methylated and hemimethylated DNA and is used to digest the parental DNA template and to select for mutation containing synthesized DNA. DNA isolated from almost all *E. coli* strains is *dam* methylated and therefore susceptible to *Dpn* I digestion. The nicked vector DNA incorporating the desired mutations is then transformed into XL10-Gold® ultracompetent cells.

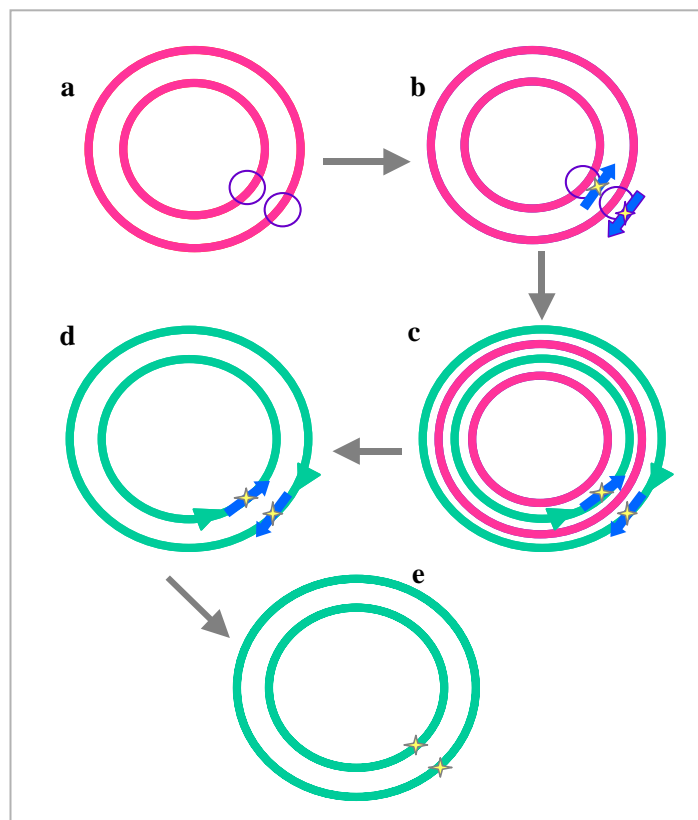


**Figure II.3. Schematic representation of clones construction with Stratagen mutagenesis system.** Beginning DNA (wild type) is drawn in pink, while new synthesized chains are green. Violet circles indicate the exact place where mutations are going to be included. Blue arrows represent synthetic oligonucleotides with mutations (yellow stars). (a) Double strand DNA which contains the target gene to be mutated. (b) Oligos with mutations are used in PCR reaction. (c) Template DNA is digested with *Dpn*I (a restriction enzyme). (e) Transforming ultracompetent cells with new synthesized DNA allow to obtain mutated DNA without nicks.

The specific protocol used was as follow:

#### 1.4.1. PCR reaction.

Prepare the sample reaction mixing buffer, plasmid dsDNA template, oligonucleotide primers, dNTP mix and QuikSolution; then add *Pfu Ultra* HF DNA polymerase. The cycling parameters were:

Segment	Cycles	Temperature	Time
1	1	95°C	3 minutes
2	30	95°C	1 minute
		60°C	1 minute
		68°C	5 minutes
3	1	68°C	7 minutes

Following temperature cycling, the reaction tubes were placed on ice for 2 minutes to cool them to  $\leq 37^{\circ}\text{C}$ .

#### 1.4.2. Dpn I Digestion of the Amplification Products.

DpnI restriction enzyme was added directly into each amplification reaction and then incubated at  $37^{\circ}\text{C}$  for 1 hour in order to digest the parental plasmid dsDNA.

#### 1.4.3. Transformation of XL10-Gold® Ultracompetent Cells.

2  $\mu\text{l}$  of DpnI-treated DNA were transferred to 45  $\mu\text{l}$  of pre-thawed XL10-Gold ultracompetent cells and after mixing gently, they were incubated on ice for 30 minutes. Following, tubes were put in a  $42^{\circ}\text{C}$  bath for 30 seconds to get a heat-pulse (this temperature and time is critical for obtaining highest transforming efficiencies). After that, samples were incubated again on ice for 2 minutes. Next, 0.5 ml of NZY+ broth were added to each tube and incubated at  $37^{\circ}\text{C}$  for 1 hour with shaking.

Finally the transforming results were plated on agar plates containing the appropriate antibiotic depending on the plasmid construction (ampicillin or kanamycin). After incubating them at  $37^{\circ}\text{C}$  for approximately 16 hours, 5 bacteria colonies were selected to amplify, purify and check the mutated DNA (see next section).

### 1.5. Amplification and purification plasmid DNA.

Firstly, *E. coli* DH10B was transformed with ligation results following heat-shock protocol described by *Cohen et al, 1973* (similar to XL10-Gold® ultracompetent cells mentioned before) in order to obtain colonies which possess the appropriate construction. Bacteria were plated on LB agar plates

with appropriate antibiotic to select only colonies with the right plasmid DNA inside. After approximately 16 hours at 37°C, ten bacteria colonies were selected and grown in 3 ml of LB media (again with the antibiotic) with orbital agitation for another 16 h to further extract and check the plasmid DNA. For this purification a commercial kit, called NucleoSpin® Plasmid QuickPure (Machery-Nagel, Düren, Germany), was used. This kit is based on a new specially treated silica membrane which allows speeding up the procedure by a combined washing and drying step.

With the NucleoSpin® Plasmid method, the pelleted bacteria were resuspended (Buffer A1) and plasmid DNA is liberated from the *E. coli* host cells by SDS/alkaline lysis (Buffer A2). Buffer A3 neutralizes the resulting lysate and creates appropriate conditions for binding of plasmid DNA to the silica membrane of the column. Precipitated protein, genomic DNA, and cell debris are then centrifuged. The supernatant was loaded onto a NucleoSpin® Plasmid QuickPure Column.

With the NucleoSpin® Plasmid QuickPure kit contaminations like salts, metabolites, nucleases, and soluble macromolecular cellular components are removed by only a single washing step with Buffer AQ. Pure plasmid DNA is finally eluted under low ionic strength conditions with slightly alkaline Buffer AE (5 mM Tris/HCl, pH 8.5).

The specific protocol is shown in the Figure II.4.

1 Cultivate and harvest bacterial cells		11,000 x g 30 s
2 Cell lysis		250 µl Buffer A1 250 µl Buffer A2 RT, 5 min 300 µl Buffer A3
3 Clarification of the lysate		11,000 x g 5 min
4 Bind DNA		Load supernatant  11,000 x g 1 min
5 Wash silica membrane		450 µl Buffer AQ  11,000 x g 3 min
6 Dry silica membrane	Drying is performed during centrifugation of the single washing step	
7 Elute DNA		50 µl Buffer AE RT, 1 min  11,000 x g 1 min

**Figure II.4. Plasmid DNA purification protocol at a glance using NucleoSpin® Plasmid QuickPure.**

To ensure the plasmid DNA was the correct one, without any mutation, all constructs were confirmed by DNA sequencing, which was carried out in the Research and Development Support Center (CAID), University of Murcia (Spain).

Once appropriate plasmid DNAs were obtained, we amplified them in a large-scale in order to get bigger amounts of it to transfect breast cancer cells.

Firstly, we transformed *E. coli* DH10B, in the same way than previous case. Next day, some of these resulting bacteria were inoculated in 500 ml of LB culture medium (plus appropriate antibiotic) and were incubated overnight at 37°C and orbital agitation. After this incubation, bacteria were centrifuged (7000 rpm for 15 minutes). Once the pellet is formed, we started the purification protocol using a commercial kit called NucleoBond® PC 2000 (Machery-Nagel, Düren, Germany). This kit is a patented silica-based anion-exchange resin for routine separation of different classes of nucleic acids.

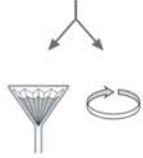
NucleoBond® PC kit employ a modified alkaline/SDS lysis procedure to prepare the bacterial cell pellet for plasmid purification. Both chromosomal and plasmid DNA are denatured under these alkaline conditions. Potassium acetate is then added to the denatured lysate, which causes the formation of a precipitate containing chromosomal DNA and other cellular compounds. The potassium acetate buffer also neutralizes the lysate. Plasmid DNA can revert to its native supercoiled structure and remains in solution. After equilibrating the appropriate NucleoBond® Column with equilibration buffer, plasmid DNA is bound to the anion-exchange resin and finally eluted after efficient washing of the column. After precipitation of the eluted DNA it can easily be dissolved in TE buffer for further use.

The specific protocol is shown in the Figure II.5.

DNA yield and quality of purify plasmid DNA, both small- and large-scale, can be measured using a UV spectroscopy:

- Quantity: 1 OD at 260 nm (1 cm path length) is equivalent to 50 µg plasmid DNA/ml.
- Quality: Absorbance ratio 260 nm/280 nm was used. A value of 1.8-1.9 is an indication for pure plasmid DNA.

Depending on further use of the purified plasmid, more sophisticated analytical methods may have to be applied for quantification or see the quality, for example nanodrop and bioanalyzer respectively.

<b>1</b>	<b>Cultivate and harvest bacterial cells</b>	4,500 - 6,000 x <i>g</i> 15 min at 4°C	
<b>2</b>	<b>Cell lysis</b>	High copy / low-copy	
	Buffer S1	45 ml / 90 ml	
	Buffer S2	45 ml / 90 ml RT, <5 min	
	Buffer S3	45 ml / 90 ml 0°C, 5 min	
<b>3</b>	<b>Equilibration of the column</b>	Buffer N2 20 ml	
<b>4</b>	<b>Clarification of the lysate</b>	Folded Filter or centrifugation	
		12,000 x <i>g</i> 50 min	
<b>5</b>	<b>Binding</b>	Load cleared lysate onto the column	
<b>6</b>	<b>Washing</b>	Buffer N3	
		High copy 2 x 35 ml	
		Low copy 2 x 50 ml	
<b>7</b>	<b>Elution</b>	Buffer N5 25 ml	
<b>8</b>	<b>Precipitation</b>	Isopropanol 18 ml	
		≥ 15,000 x <i>g</i> 30 min at 4°C	
<b>9</b>	<b>Wash and dry DNA pellet</b>	70% ethanol 7 ml	
		≥ 15,000 x <i>g</i> 10 min at RT	
		30 - 60 min	
<b>10</b>	<b>Reconstitute DNA</b>	Appropriate volume of TE	

**Figure II.5. Plasmid DNA purification protocol at a glance using NucleoBond® PC 2000.**

## 2. Cells culture.

### 2.1. MCF-7 cells.

MCF-7 has been one of the cell lines used along this work. This cell line comes from an adenocarcinoma (from pleural effusion) and it is a model cell line to study breast cancer.

These non-invasive epithelial stable cells keep some important characteristics of differentiated breast epithelium, like ability to group and also the ability to process estradiol through cytoplasmatic estrogen receptors (ER). MCF-7 cells present high amount of this receptor, what make them very useful to study the action mechanism of these hormones.

Other important characteristics of this cell line is that its growth can be inhibit by treatment them with Tumour Necrosis Factor  $\alpha$  (TNF $\alpha$ ); and they can secret like-insulin growth factor binding proteins (IGFBP's), whose process can be modulated with anti-estrogen treatment.

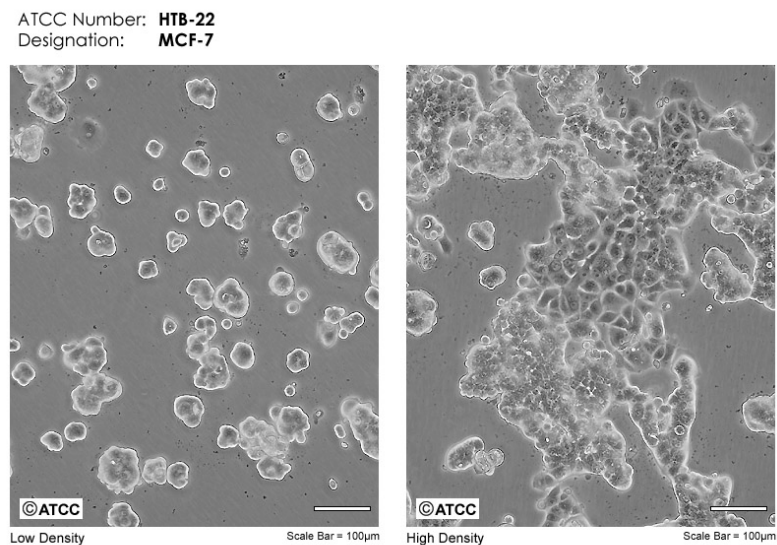


**Figure II.6. MCF-7 cells.** Left picture shows cells after a subculture (low density), whereas in the right one we can observe cells at high density.

#### 2.1.1. MCF-7 culture conditions.

MCF-7 cells were thawed in a 37°C water-bath from one vial kept in liquid nitrogen available in Experimental Sciences Support Service (SACE), at the University of Murcia (Spain), previously bought to ATCC (American Type Culture Collection). One vial, approximately 3 millions of cells, was grown in a 75 cm<sup>2</sup> ventilated flask with 10 ml of the appropriate growth medium.

The growth medium was DMEM (Dulbecco's modified Eagle's medium) without phenol red and with 4500 mg/L glucose. It was supplemented with 10% (v/v) fetal calf serum (FCS), antibiotic (penicillin 50 units/ml and streptomycin 50 µg/ml), sodium piruvate 110 mg/ml and glutamine 2 mM. This culture was kept at 37°C humidity heater with 7.5% CO<sub>2</sub>.

The medium was changed every two days for other 10 ml of fresh one until cells reached 80-85% confluency, approximately in 5 days. In this moment the culture was diluted in ratio 1:2 or 1:3.

To harvest the cells a 0.25% trypsin-0.25% EDTA solution was used during 3 minutes at 37°C. After that, trypsin was neutralized with growth medium and centrifuged at 250 g for 3 minutes. Finally, the supernatant was removed and the cells were resuspended in fresh growth medium in order to spread them in new ventilated flasks.

### **2.1.2. MCF-7 transfection.**

Before transfecting, cells were plated on glass coverslips inside 6 cm diameter plates, in a ratio of approximately 1 million of cells/plate. In this way, cells were 60-70% confluent after 16-24 hours.

Lipofectamine 2000 (Invitrogen, Carlsbad, CA, USA) was used to transfect cells. this is a lipidic solution, mainly consisting of cationic liposomes, which allows DNA entrance inside cells. The protocol used was as follow (for one 6 cm diameter plate):

Solution A: 0.1 ml DMEM without antibiotic nor FCS plus 2 µg DNA to transfect.

Solution B: 0.1 ml DMEM without antibiotic nor FCS plus 3 µl of lipofectamine 2000.

Both solutions were incubated separately for 5 minutes at room temperature and after that we mixed them and kept at 25°C during 20-30 minutes. Meanwhile, cells were washed twice with DMEM without antibiotic neither FCS and finally 0.2 ml of A+B mix was added to cells.

MCF-7 cells were incubated in a 37°C humidity heater with 7.5% CO<sub>2</sub> during 6-7 hours when this medium was changed for fresh growth medium. After 16-24 hours cells were examined in a confocal microscope.

## 2.2. BT-474 cells.

BT-474 has also been one of the cell lines used along this Doctoral Thesis. This cell line was isolated from a solid, invasive ductal carcinoma of the breast and it is worthy of note that do not metastasize to the bone (*Lasfargues et al, 1978*).

This epithelial cell line is reportedly tumorigenic in athymic nude mice and will form nodules in Amsterdam/IMR rats with regression in 10 days. BT-474 cells were found to be susceptible to mouse mammary tumour virus (RIII-MuMTV) and can support its replication (*Lasfargues et al, 1979*).

These epithelial stable cells keep some important characteristics of differentiated breast epithelium, like ability to group (desmosomes, tight and gap junctions were observed in transmission electron microscopy preparations). BT-474 cells express high amounts of EGF receptor, what make them very useful to study the action mechanism of this growth factor.

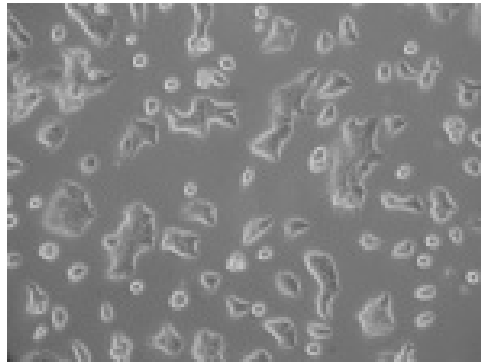


**Figure II.7. BT-474 cells.**

### 2.2.1. BT-474 culture conditions.

They were bought to ATCC and were cultured in the same conditions than MCF-7 cells, although in this case, BT-474 cells were harvested every 6-7 days in a ratio 1:3 or 1:5.

### 2.2.2. BT-474 transfection.

Cells were transfected at the same time that they were diluted, since electroporation technique was used.

After adding trypsin and neutralizing it, cells are counted in a Neubauer chamber and 10 millions of cells were separated to electroporate them.

After centrifuging, cells are resuspended in 400  $\mu$ l of electroporation buffer (composed by 20 mM Hepes pH 7.2, 120 mM NaCl, 5.5 mM KCl, 2.8mM MgCl<sub>2</sub> and 25 mM glucose). 30  $\mu$ g of plasmidic DNA, was added and the mix was incubated for 5 minutes in the electroporation cuvette (0.4 cm gap). After this time, electroporation shock in a BioRad electroporator (BioRad Laboratories, CA, USA) is carried out as explained below:

Square wave protocol was chosen and two 200 Volts electro-shocks were applied during 8 msec each, with 5 seconds between them. Quickly, cells were resuspended in fresh growth medium and aliquoted in 6 cm  $\varnothing$  plates with a sterile coverslip ( $2.5 \times 10^6$  cells / plate).

After 24-48 hours, cells were examined in a confocal microscope.

### 2.3. MDA-MB-231.

MDA-MB-231 is also a model breast cancer cell line which has been used along this work. This cell line comes from an adenocarcinoma (from pleural effusion) and it is a highly metastatic.

Their mainly characteristics are the epithelial morphology and monolayer growth, like both cell lines commented before. We have chosen this cell line due to its invasive capacity and the expression of some receptor like epidermal growth factor receptor (EGFR) and transforming growth factor alpha receptor (TGF alpha R).

This epithelial cell line is reportedly tumorigenic in nude mice and also in ALS treated BALB/c mice; forms poorly differentiated adenocarcinoma (grade III).

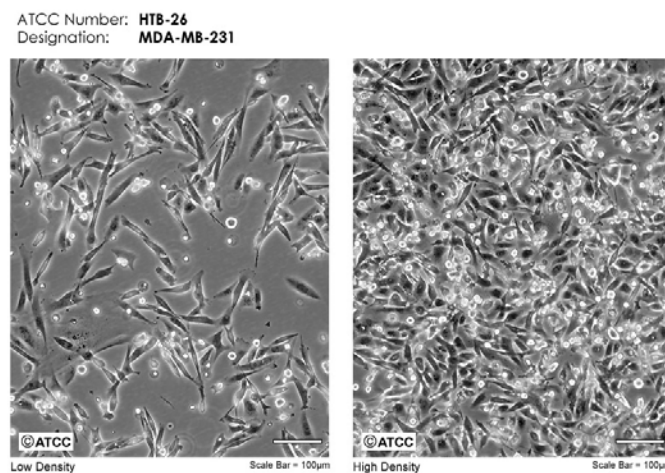


**Figure II.8. MDA-MB-231 cells.** Left picture shows cells after a subculture (low density), whereas in the right one we can observe cells in a high density.

### **2.3.1. MDA-MB-231 culture conditions.**

They were cultured in a similar way than MCF-7 and BT-474 cells, although existing several differences:

The growth medium was also supplemented with non essential aminoacids (besides 10% FCS, antibiotic, glutamine and pyruvate) and it is not changed directly every two days, since some life cells are floating in medium.

Cells were seeded in 75 cm<sup>2</sup> flask with 10 ml of growth medium, after 2-3 days, 5 ml of freshly medium were added without removing the existing one. 2 days later (4-5 days from subcultured time), cells had grown up to 85-90% confluency and another dilution was performed.

To harvest MDA-MB-231, similar to both cells lines explained before, trypsin is needed. In this occasion, medium is recollected from the flask (there are life cells in it) and cells are washed with PBS before adding 0.25% trypsin-0.53 mM EDTA for 3 minutes in a 37°C atmosphere. After that, we used the recollected medium to neutralize trypsin and next they were centrifuged at 200 g during 5 minutes.

Finally, the supernatant was removed and the pellet cells were resuspended in fresh growth medium in order to plant cells in new ventilated flasks, in a ratio 1:4 or 1:6.

## **2.4. Inhibition of PKC $\alpha$ expression using small interference RNA (siRNA).**

To inhibit PKC $\alpha$  on three cell lines used along this Doctoral Thesis, specific siRNA oligos were transfected by means of electroporation technique.

Both, electroporation buffer and siRNA oligos were commercial, specifically siPORT electroporation buffer (Ambion, Inc., Cambridge, USA) and stealth siRNA (Invitrogen, Oregon, USA) respectively. The oligos sequence was different among cells:

In MDA-MB-231, PKC $\alpha$  was inhibited using the following sequence:

5'- CCAUCGGAUUGUUCUUCUUCUCAA -3'

In MCF-7 and BT-474, PKC $\alpha$  were inhibited using the sequence:

5'- GCCUCCAUUUGAUGGUGAAGAUGAA -3'

Cells were harvested and once they were counted in Neubauer chamber, an aliquot of 3 millions of cells was taken and centrifuged separately. The

pellet was resuspended in 300  $\mu$ l of siPORT electroporation buffer and, together 1  $\mu$ M siRNA oligos, were put into an electroporation cuvette (0.4 cm) to carried out an electro-shock in a BioRad electroporator (BioRad Laboratories, CA, USA) as follows:

Square wave protocol was chosen and two 800 Volts electro-shocks were carried out during 0.2 msec each with 5 seconds between them. Quickly, cells were resuspended in fresh growth medium and aliquoted in appropriate number to run different assays (proliferation, migration, etc).

PKC $\alpha$  inhibition along time was analyzed by western blot, exactly after 24, 48, 72 and 96 hours after transfection. Cells were resuspended in 200  $\mu$ l of lysis buffer containing 50 mM Tris HCl pH 7.5, 150 mM NaCl, 1% Nonidet P-40 (Roche Diagnostic, GmbH, Germany), 10% glycerol, 5  $\mu$ l/ml protease inhibitor cocktail (Calbiochem, USA) and 2  $\mu$ l/ml both phosphatase inhibitor I and II (Sigma-Aldrich Chemistry, S.A., Madrid, Spain). After that, samples were passed through an insulin syringe on ice for 10 times, next they were centrifuged to 14000 rpm during 15 minutes at 4°C, and finally the supernatants were mixed with 5X sample buffer (200 mM Tris HCl pH 6.8 250 mM DTT, 5% SDS, 37.5% glycerol and 0.015% bromophenol blue) and were loaded into a polyacrylamide gel (SDS-PAGE).

## 2.5. Migration assays.

MCF-7 and MDA-MB-231 migration capacity under influence of fatty acids or some drugs were measured by using the wound healing method. It was also used to study different migration ability in cells mentioned before with and without PKC $\alpha$  ( $\Delta$ PKC $\alpha$ ).

To run these experiments 24-well plates were used. MCF-7 and MDA-MB-231 cells were plate in appropriate number in order to coincide high cell confluence (90-95%) and maximum inhibition of PKC $\alpha$  (72 hours in MCF-7 and 96 hours in the case of MDA-MB-231).

After electroporating cells (and starting inhibition of PKC $\alpha$  expression), as it has mentioned in previous section, cells were plated in 24-well plates (300000 MCF-7 cells/well; 240.000 MDA-MB-231 cells/well). During some days (2 in MCF-7 and 3 days in MDA-MB-231) they were growing with growth medium and after that, cells were serum starved (growth medium with only 0.5% FCS) for 16-24 hours.

After this incubation, a scratch wound was created in the monolayer using a sterile 10  $\mu$ l plastic pipette tip. Next, cells were washed twice with PBS and finally added the appropriate medium.

Photographs were taken immediately (0 hours) and several times later depending on cell line. For MCF-7 pictures were taken at 8, 24, 48 and 72 hours until the scratch was sealed; while MDA-MB-231 were at 4, 8, 12, 24 and 48 hours till monolayer is formed again.

## 2.6. Invasion assays.

Invasion is a fundamental function of cellular processes such as angiogenesis, embryonic development, immune response and metastasis of cancer cell. Due to that, along this work we decided to run some invasion assays to test some compounds like fatty acids and some specific inhibitors, as well as the PKC $\alpha$  inhibition. To carry out these experiments, we used MDA-MB-231 cells, since other cell lines are not able to invade, with BME Cell Invasion Assay kits (CULTREX, Trevigen Inc) following the protocol indicated by the manufacturer.

The protocol was as follow:

MDA-MB-231 cells were electroporated with siRNA, to inhibit PKC $\alpha$  expression, and plated with growth medium for approximately 24 hours, and after that, they were serum starved (medium with only 0.5% FCS) for another 16-24 hours. At this moment (16 hours prior beginning assay), top chamber of cell invasion device were coated with 50  $\mu$ l of 0.5X BME and incubated at 37°C in a CO<sub>2</sub> incubator.

After this time, cells were harvested and counted in order to suspend them in a ratio of 20.000 cells/50  $\mu$ l. Before planting cells, top chamber of cell invasion device were aspirated but not completely. Next 50  $\mu$ l of cells, with growth medium and appropriate compounds, were added to the top chamber and 150  $\mu$ l of growth medium to the bottom chamber. Finally, the chamber was assembled and incubated at 37°C and 7.5% CO<sub>2</sub> for 48 hours. In parallel, a plate of MDA-MB-231 cells were cultured to elaborate a standard curve.

To quantify the assay, we prepared the standard curve with known number of cells, specifically 20.000, 15.000, 10.000, 5.000, 2.000, 1.000 and 0, and added calcein-AM, for 1 hour at 37°C. Fluorescence was read in a fluorimeter (Fluostar Galaxy) with 485 nm excitation and 520 nm emission filters.

To measure the level of cell invasion in the different experiments, we aspirated the medium of the top chamber and every well was washed with 100  $\mu$ l of 1X wash buffer; next, bottom chambers were aspirated and washed with 200  $\mu$ l of 1X wash buffer each. Again, we aspirated the wash buffer and added calcein-AM to bottom chambers. We incubated them in a 37°C and 7.5% CO<sub>2</sub> heater for one hour and read the plate in the same condition as standard

curve (time and gain). Finally, we compared obtained data to standard curve, to calculate the number of cells that have invaded, as well as percentage of cell invasion in each condition. Every condition was repeated in three wells and three independent assays.

## **2.7. Proliferation assays.**

Proliferation experiments were also run in order to solve the effect of some fatty acids and the PKC $\alpha$  inhibition on this aspect, in three breast cancer cell lines.

To carry out that, we used the kit CyQUANT® NF Cell Proliferation Assay (Invitrogen, Oregon, USA). It is based on measurement of cellular DNA content via fluorescent dye binding, since cellular DNA content is highly regulated; it is closely proportional to cell number.

The assay does not require the use of radioisotopes, enzymes, or antibodies and is not dependent on physiological activities that may exhibit cell number-independent variability. The CyQUANT® NF protocol requires only aspiration of growth medium (for adherent cells), replacement with dye binding solution, incubation for 30–60 minutes, and then measurement of fluorescence in a microplate reader.

The experimental protocol was as follow:

Three cell lines were harvested and electroporated with siRNA (control or PKC $\alpha$  inhibition), as it has mentioned before. Cells were plated in nine 96-well microplates (one for each day) in a ratio of 9000 cells/well in the case of BT-474 cells, and 4500 cells/well for MCF-7 and MDA-MB-231 with growth medium. They were incubated at a 37°C and CO<sub>2</sub> atmosphere for 24 hours for cell adhesion.

After this incubation time, growth medium was removed from cells by gentle aspiration and 75  $\mu$ l of dye binding solution (a mixture of CyQUANT® NF reagent and dye delivery reagent) was added. A standard curve was elaborated to quantify the amount of DNA. The microplate was covered and incubated at 37°C during 30 minutes for equilibration of dye-DNA binding, resulting in a stable fluorescence endpoint. Finally, the fluorescence intensity of each sample (and standard curve) was measured in a fluorimeter (Fluostar Galaxy) with excitation at 480 nm and emission detection at 520 nm.

Every condition was tested in three wells and at least three independent assays.

## 2.8. Apoptosis assays.

Apoptosis is a carefully regulated process of cell death that occurs as a normal part of development. Inappropriately regulated apoptosis is implicated in disease states, such as Alzheimer's disease and cancer. Apoptosis is distinguished from necrosis, or accidental cell death, by characteristic morphological and biochemical changes, including compaction and fragmentation of the nuclear chromatin, shrinkage of the cytoplasm, and loss of membrane asymmetry (Lincz, 1998). In normal live cells, phosphatidylserine (PS) is located on the cytoplasmic surface of the cell membrane. However, in apoptotic cells, PS is translocated from the inner to the outer leaflet of the plasma membrane, thus exposing PS to the external cellular environment (Engeland *et al*, 1998). The human anticoagulant, annexin V, is a 35–36 kDa  $\text{Ca}^{2+}$ -dependent phospholipid-binding protein that has a high affinity for PS. Annexin V labeled with a fluorophore or biotin can identify apoptotic cells by binding to PS exposed on the outer leaflet (Engeland *et al*, 1998).

To carry out these experiments, we used the Vibrant® Apoptosis Assay kit (Invitrogen, Oregon, USA) with Alexa Fluor® 488 annexin V and PI for flow cytometry, since it allowed us to distinguish among live cells (no fluorescence), death cells (red fluorescence), apoptotic but not death cells (green fluorescence) and apoptotic-death cells (both, green and red fluorescence).

We followed the protocol indicated by the manufacturer, briefly:

Cell lines were harvested and electroporated with siRNA (control or PKC $\alpha$  inhibition), as it has mentioned before. Cells were plated, in a ratio of  $3 \times 10^5$  cells/35 mm Ø plate with growth medium. They were incubated at a 37°C and 7.5% of CO $_2$  for 24 hours for cell adhesion.

After this incubation time, medium was changed and the stimuli were added in the fresh medium. Besides stimulated cells with appropriate compounds, negative and positive controls were done (without any stimulant and 2  $\mu\text{M}$  of staurosporine for 24 hours, respectively).

Stimulated cells were growth for 4 days, in the case of MCF-7, or 5 days for MDA-MB-231. Following this time, the dying protocol started. Firstly, cells were harvested and counted to take an aliquot of  $2 \times 10^5$  cells, and then they were washed twice with PBS. In the last wash the supernatant was discarded and 100  $\mu\text{l}$  of 1X annexin-buffer were added to live cells; next 5  $\mu\text{L}$  Alexa Fluor® 488 annexin V and 1  $\mu\text{L}$  100  $\mu\text{g}/\text{mL}$  PI were added to every sample. All together were incubated at room temperature for 15 minutes and immediately after that, other 400  $\mu\text{l}$  of 1X annexin-buffer were added to every sample, to finally analyze them by flow cytometry measuring the fluorescence emission at

525 nm (FL1) and 575 nm (FL3).

### **2.8.1. Short introduction to flow cytometry.**

As its Latin name mean (cyto=cell; metry= measurement) it is a technique which measure properties of cells in a flowing system.

Principle of flow cytometry: a beam of light (usually laser light) of a single wavelength is directed onto a hydrodynamically-focused stream of fluid. A number of detectors are aimed at the point where the stream passes through the light beam: one in line with the light beam (Forward Scatter or FS) and several perpendicular to it (Side Scatter or SS and one or more fluorescent detectors).

Each suspended particle from 0.2 to 150 micrometers passing through the beam scatters in single-file; the light in some way and fluorescent chemical found in the particle or attached to it, may be excited into emitting light at a longer wavelength than the light source. This combination of scattered and fluorescent light is picked up by the detectors, and, by analyzing fluctuations in brightness at each detector (one for each fluorescent emission peak), it is then possible to derive various types of information about the physical and chemical structure of each individual particle, for example size and complexity or granularity.

This technique has numerous applications like measuring enzymatic activity, calcium fluxes, cytotoxicity of some drugs or antimicrobials substances, as well as cell cycle.

Some equipment, called cell sorter, also allows to separate cells with specific qualities (for instance, fluorescence intensity) in different subpopulations from a complex population.

The flow cytometer used to analyze apoptosis assays was the model Epics XL from Coulter (Fig II.9). It possesses a 15 mW at 488 nm line of an argon-ion laser for excitation and detectors for emission wavelength of 525, 575, 620 and 675 nm.



**Figure II.9. Epics XL-MCL (Multi-tube Carousel Loader) flow cytometer.**

## **3. Confocal Microscopy.**

### **3.1. Introduction to confocal imaging.**

Conceptualized in 1953, the Confocal Laser Scanning Microscopy has only in the past 15 years become a practical technique (*Boyde et al, 1983; Petran et al, 1986*). Today it is the technique of choice for biological research, chemical analysis, and materials testing (*Arribas et al, 2007*). An instrument of this kind represents a “fusion product” of contributions from many fields: microscopy, laser technology and optics for coherent light, video technology, electronics and computer technology.

Confocal microscopy detects structures by collecting light from a single focal plane of the sample, excluding light that is out of focus.

In a point scanning confocal system, the microscope lenses focus the laser light on one point in the specimen at a time (the *focal point*). The laser moves rapidly from point to point to produce the scanned image. Both fluorescent and reflected light from the sample pass back through the objective.

The microscope and the optics of the scanner module focus the light emitted from the *focal point* to a second point, called the *confocal point*. The pinhole aperture, located at the *confocal point*, allows light from the *focal point* to pass through the detector. Light emitted from outside the *focal point* is rejected by the aperture.

The confocal principle is illustrated schematically for the epi-illumination imaging mode (Fig II.10).

As in conventional epi-fluorescent microscopes, one lens is used as both condenser and objective. The advantage is eliminating the need for exact

matching and co-orientation of two lenses. A collimated, polarized laser beam from an aperture is reflected by a beam splitter (dichroic mirror or AOBS system) into the rear of the objective lens and is focused on the specimen. The reflected light returning from the specimen passes back through the same lens. The light beam is focused into a small pinhole (i.e., the confocal aperture) to eliminate all the out-of-focus light, i.e., all light coming from regions of the specimen above or below the plane of focus. The achieved optical section thickness depends on several parameters such as the variable pinhole diameter and the wavelength. The in-focus information of each specimen point is recorded by a light-sensitive detector (i.e., a photo-diode) positioned behind the confocal aperture, and the analogue output signal is digitized and fed into a computer.

The detector is a point detector and only receives light from one point in the specimen. Thus, the microscope sees only one point of the specimen at a time as opposed to the conventional microscope where an extended field of the specimen is visible at one moment.

The advantage of having a stack of serial optical sections through the specimen in digital form is that either a composite projection image can be computed, or a volume-rendered 3-D representation of the specimen can be generated on a graphics computer.

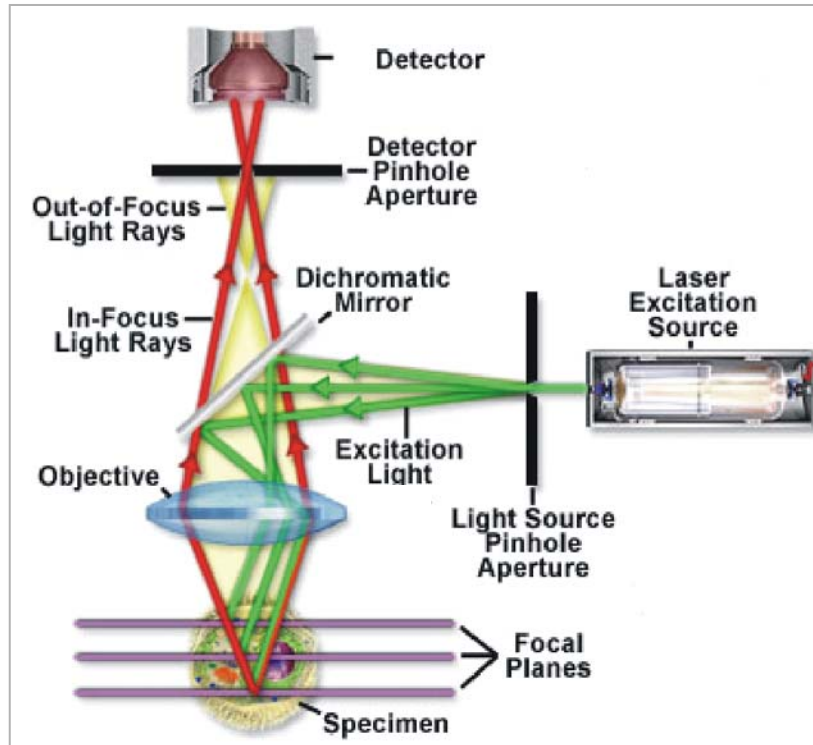


**Figure II.10. Representation of a confocal microscope.** It is shown the basic component of microscope. It is worthy of note that a dichroic mirror microscope is represented and not AOBS or AOTF systems which are present in the used confocal microscope along this Doctoral Thesis. Light from laser passes through a pinhole and excite the specimen after crossing dichroic mirrors (green arrows). The emitted light from specimen (red arrows), before arriving to detector, passes back through dichroic mirrors and a new pinhole in order to single focal plane information arrives to detector (Taken from [www.leica-microsystems.com](http://www.leica-microsystems.com)).

### 3.2. Microscope used.

Transfected cells with fluorescent constructs were examined under a confocal microscope type Leica TCS SP2 AOBS (Leica, Heidelberg, Germany) (Fig II.11), which has several lasers: ArKr (emits at 488 and 568 nm), GrHe (excites at 543 nm), HeNe (excites at 633 nm) and blue diode which excites at 405 nm. The objectives used were Nikon PLAN APO-CS 63X 1.2 NA (water) or 1.4 NA (immersion oil).

The LEICA TCS SP 2 system makes it possible to image a single, in-focus plane – horizontal or vertical – as well as a series of planes. A single vertical section, or xz-scan, allows you to see your sample as though from the side.

Besides, this confocal model was designed as an integrated system. Optical and mechanical elements work seamlessly with computer hardware and software. The integrated Leica Confocal Software package supports the complete imaging process, from optical sectioning, through image processing and analysis (which is the main application), to hard copy output.

In presence of EGFP, cells were excited with Ar/Arkr laser at 488 nm, while emission waves were captured to 500-525 nm. Cells transfected with ECFP constructs, excitation happened with diode blue laser at 405 nm, and emission waves between 470-490 nm.

In every assay, image series of 60-120 images were recorded in intervals of 5, 10 or 20 seconds depending on the experiment. This series were subsequently analyzed using ImageJ-NIH software ([http://rsb.info.nih.gov/ij/1997\\_2010](http://rsb.info.nih.gov/ij/1997_2010)).

In immunofluorescences the excitation of DAPI, Alexa Fluor 546 and Alexa Fluor 633 were carried out sequentially in order to not overlap emission spectra since Alexa 546 emits at 560-600nm, Alexa 633 at 620-680 nm and DAPI emits at 420-550.

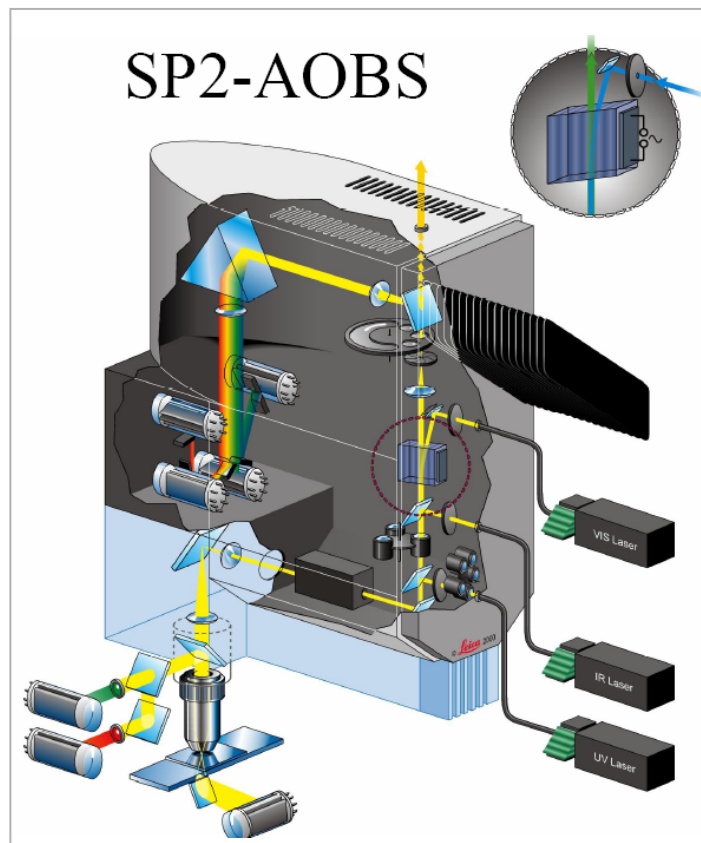


**Figure II.11. SP2 AOBS Leica Confocal Microscope.** Representation of optical circuit of confocal microscope used along this Doctoral Thesis. Note that it is represented a vertical microscope, while an inverted one has been used in this thesis, although light circuit is the same in both cases: the light from the excitant laser is polarized after passing through mirrors and later, when it go through a pinhole, is unified to excite the specimen. The emitted light go to detector and only the desired wavelength, selected by AOBS system, get it. In the detail picture is shown the AOBS system (Acousto Optical Beam Splitter). In this case, wavelength of excited or emitted light from specimen is controlled by this system independently of fluorophore used (Taken from [www.leica-microsystems.com](http://www.leica-microsystems.com)).

### 3.3. Fluorescent substances used.

Fluo-3 was used to measure cytoplasmic  $\text{Ca}^{2+}$ , since it increases its fluorescence intensity when it binds calcium. Particularly, acetoxy-methyl ester Fluo-3 (AM-ester Fluo-3) was used because this form is hydrophobic and can pass through plasma membrane easier. Once it is inside the cells, cellular esterases release hydrophilic Fluo-3 which can link  $\text{Ca}^{2+}$  (Novak and Rabinovitch, 1994; Tsien and col., 1995). Fluo-3 was excited at 488 nm while emission wavelength was detected at 510-580 nm (Table II.2).

In immunofluorescences several compound were used; DAPI to stain cells nucleus, Alexa Fluor 546 to mark cytoplasmic  $\text{PKC}\alpha$  and Phalloidin-Alexa Fluor 633 to dye actin fibres (Table II.2.).

For subcellular localization of PKC isoforms (wild type and mutants), some GFP variants were used, like EGFP and ECFP (Table II.2).

**Table II.2. Fluorescent substances used.**

Fluorescent substances	$\lambda$ excitation máx. (nm)	$\lambda$ emission máx. (nm)	Emission range (nm)
EGFP	488	520	500-540
ECFP	405	475	475-550
Fluo-3	488	525	510-580
DAPI	370	460	420-550
Alexa Fluor 546	535	575	560-600
Alexa Fluor 633	633	640	620-680

GFP, originally obtained from jellyfish called *Aequorea Victoria*, is known like Green Fluorescent Protein whose chromophore, called *aequorin*, is formed by 3 aminoacids (Ser-Tyr-Gly) located between residues 65-67 and it is able to absorb blue light and emit green one (Fig II.12.). GFP is incorporated in different plasmid in order to create, thanks to subclonation techniques, proteins fused to it.

Several GFP variants have been generated modifying initial chromophore. In this way, in EGFP (enhance-green fluorescent protein) Phe64 and Ser65 have been substituted by Leu and Thr respectively (Cormack et al, 1996) (Fig II.13). This variant emits 35 folds fluorescent intensity than no mutated GFP when it is excited to 488 nm.

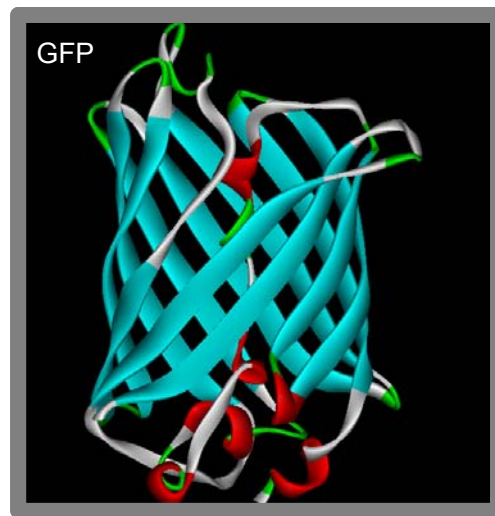


**Figure II.12. GFP tertiary structure.** The  $\beta$ -barrel of green fluorescent protein is shown, whose internal side possesses an  $\alpha$ -helix. The sequence of three aminoacids (Ser-Tyr-Gly) is essential to molecule fluorescence and it has been changed by means of site directed mutagenesis in order to enhance and obtain more excitation and emission ranges, what provides different applications in microscopy.

ECFP presents 6 changed aminoacids regards EGFP, mainly the substitution of Tyr66 by Trp is responsible to change the excitation and emission wavelength. Maximum light absorption of ECFP is 434 nm, and maximum emission is between 475-501 nm (Fig II.13).

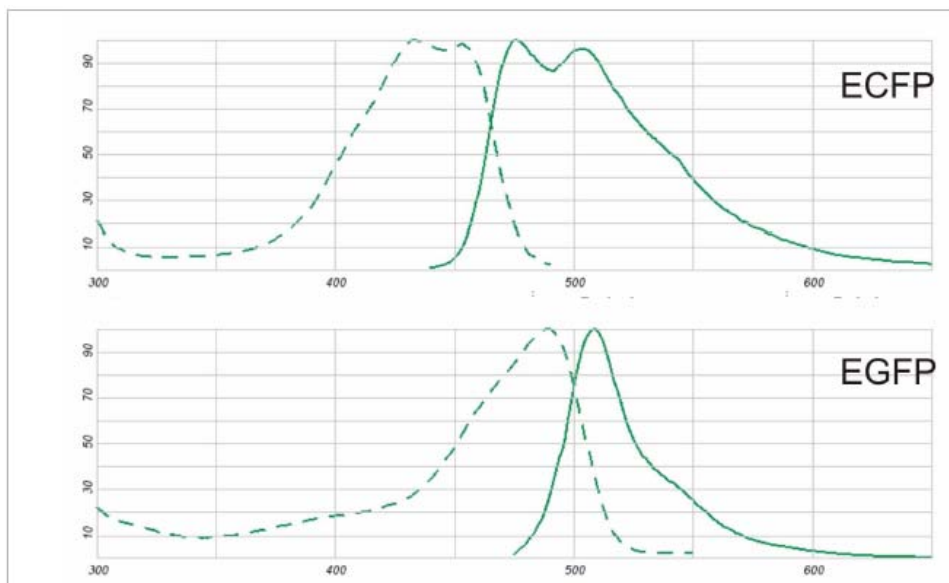


**Figure II.13. Emission spectra of derived fluorescent proteins from GFP.** It is shown excitation (dotted line) and emission (continue line) spectra of fluorescent proteins ECFP and EGFP.

### **3.4. Media used in stimulation of living cells in confocal microscope.**

To observe cells in confocal microscope, the coverslips were mounted in an special holder and washed with 3 ml Hepes Buffer Salinum (HBS) consisting of 120 mM NaCl, 2.5 mM glucose, 5.5 mM KCl, 3 mM CaCl<sub>2</sub>, 1 mM MgCl<sub>2</sub> and 20 mM HEPES pH 7.2.

All added substances were dissolved or diluted in 2 ml of HBS. Mostly compounds, like arachidonic acid, ionomycin, DAG-lactones, etc, were resuspended in DMSO and diluted to the final concentration with extracellular buffer, shortly before the experiment. During the experiment, the cells were not exposed to DMSO concentrations higher than 1%. Other substances, like fatty acids, were dissolved in ethanol or BSA/PBS and we worked in a similar way that explained before.

All the experiments were carried out at room temperature and, unless otherwise stated, on at least four different occasions. In each experiment, recordings were obtained for 2-6 cells.

Excitation and emission wavelengths were the same as they have been explained before.

In every assay, image series of 60-120 images were recorded in intervals of 5, 10 or 20 seconds depending on the experiment.

### **3.5. Image processing and analysis.**

In the first confocal microscopes, the detector was connected to an oscilloscope with long-persistence phosphor which would display an image as it was being scanned. In the instruments of today, the signal is digitized and recorded in a computer, what makes it possible to improve the image in a multitude of ways like contrast enhancement by thresholds, gamma correction (curvature of the image intensity value versus source intensity graph) or noise suppression among others.

Along this Doctoral Thesis, images were analyzed with two different softwares: ImageJ-NIH (<http://rsb.info.nih.gov/ij/>), 1997-2010, *Rasband, 1997*) and Leica software (Leica Confocal Software Lite). Both programs allow select interest area from every cell under study, and determined the average pixels intensity of it in every recorded time.

### 3.5.1. Analysis of intracellular $\text{Ca}^{2+}$ concentration.

The fluorescent  $\text{Ca}^{2+}$  indicator (AM-ester Fluo-3) used is not ratiometric, so some mathematics formulae have been used in order to calculate variation in cytoplasmic calcium level.

Stock solutions (2 mM) of AM-ester form of the fluorescent  $\text{Ca}^{2+}$  indicator were made using a solution of 2.5% (w/v) Pluronic F-127 in absolute DMSO. This stock was diluted 1000-fold in growth medium (without FCS) and applied to cells, previously washed with DMEM without FCS, for 30 minutes at 25°C in a 7.5%  $\text{CO}_2$  atmosphere.

Variations of intracellular calcium ( $[\text{Ca}^{2+}]_i$ ) were calculated by using the following expression:

$$\Delta F/F_0 = (F_t - F_0)/F_0 \quad (1)$$

where  $F_t$  is the fluorescence measured at each recorded time and  $F_0$  is the initial fluorescence. Both  $F_t$  and  $F_0$  were calculated as follow:

Using the Leica software, we drew small circles in cytoplasm of different cells in such a way that the software gives us the average intensity of fluorescence in every cell along the experimental time (Fig II.14). These raw data can be used to calculate variation in  $[\text{Ca}^{2+}]_i$  using the formula described above (1).

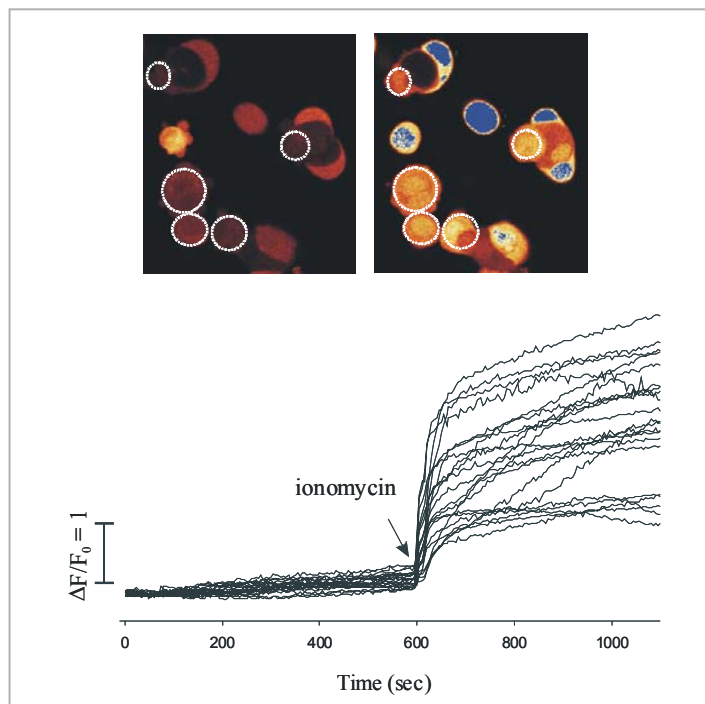


**Figure II.14. Representation of  $[\text{Ca}^{2+}]_i$  analysis in cells recorded in confocal microscope.** At the top of the picture it is shown cells loaded with Fluo-3. With the software we circle some cells cytoplasm (blue ones have saturated  $[\text{Ca}^{2+}]_i$  so not interest us) and we obtain raw data. At the bottom we can observe a final plot representing fold change in  $[\text{Ca}^{2+}]_i$  after adding ionomycin (calcium ionophore).

### 3.5.2. Analysis of PKC localization in the plasma membrane.

The time-series were analyzed using ImageJ-NIH software. An individual analysis of protein translocation for each cell was performed by tracing a line intensity profile across the cell (*Meyer and Oancea, 2000*). The relative increase in plasma membrane localization of the enzyme for each time-point was calculated by using the ratio:

$$R = \frac{I_{mp} - I_{cit}}{I_{mp}} \quad (2)$$

where R is the percentage of PKC in plasma membrane,  $I_{mb}$  is the fluorescence intensity at the plasma membrane and  $I_{cyt}$  is the average cytosolic fluorescence intensity (Fig II.15).

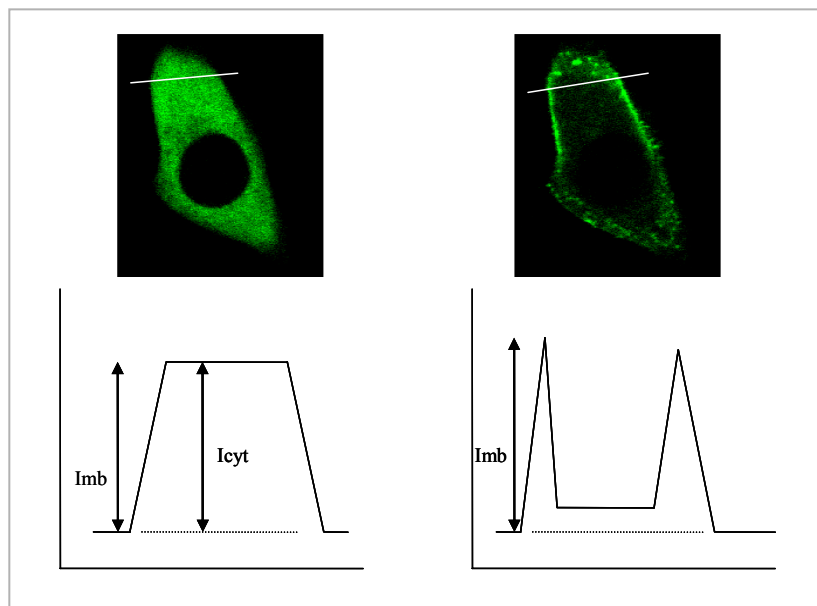


**Figure II.15. Representation of protein translocation analysis in cells recorded in the confocal microscope.** At the top of the picture it is shown transfected cells with PKC $\alpha$ -EGFP, at the beginning and final of a localization series. With the software we traced a line across the cell and we obtained the fluorescence intensity of every pixel along the line (it is shown at the bottom). After applying the formula  $R = (I_{mb} - I_{cyt}) / I_{mb}$ , we obtain  $R=0$  (on the left) and  $R=1$  (on the right).

After analyzing every frame of time-series cell by cell, R values and standard deviations were represented versus time showing the localization profiles of different isoenzymes and mutants. Directly from the chart we can calculate the localization half-time ( $t_{1/2}$ ) which means the necessary time to get 50% of maximum localization ( $R_{max}$ ).

### 3.5.3. Analysis of FRAP (Fluorescence Recovery After Photobleaching).

#### 3.5.3.1. FRAP introduction.

It is a technique that uses photobleaching of fluorescence compounds in living cells in order to measure some parameters related to molecules mobility.

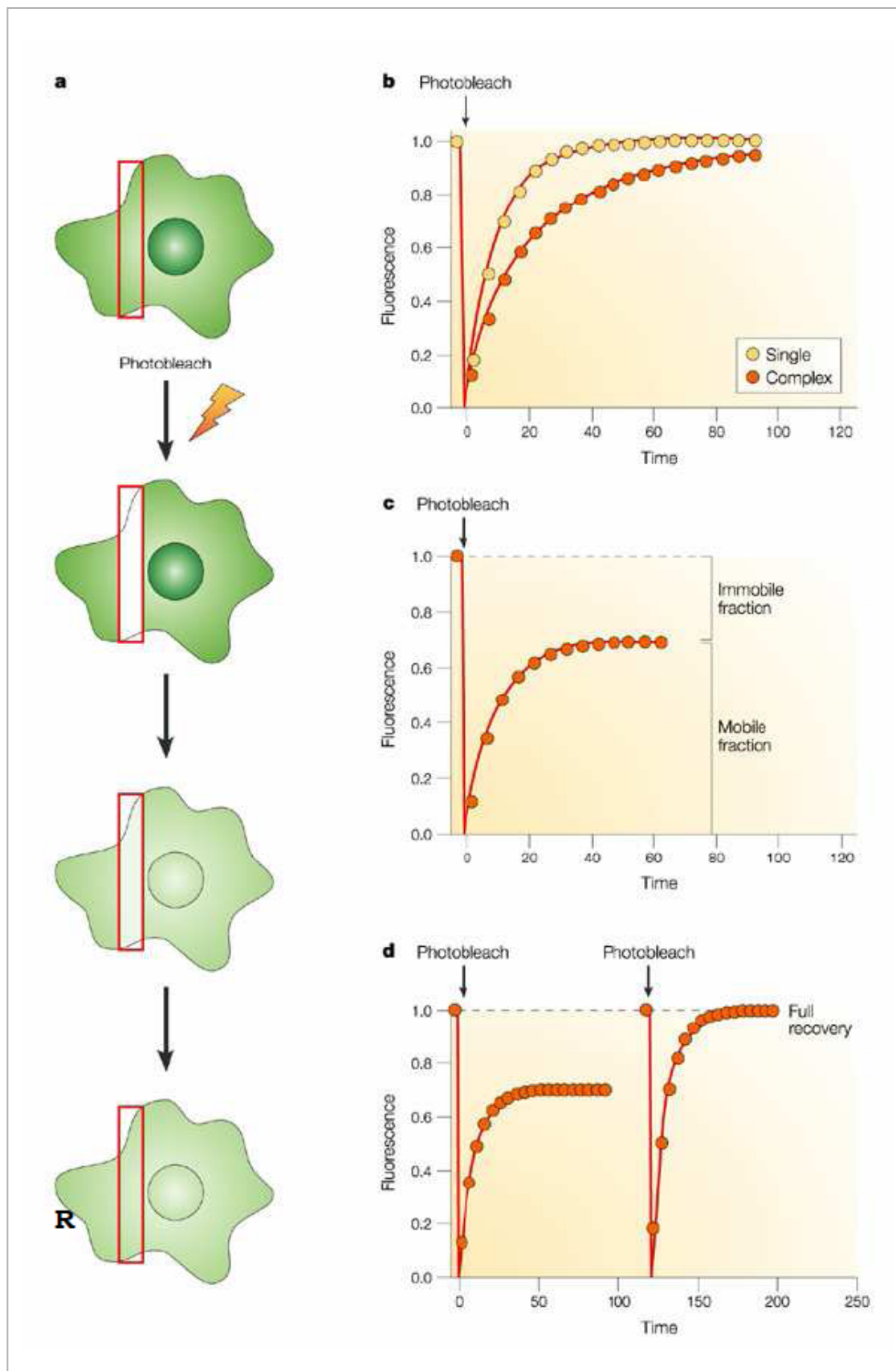
FRAP consists in photobleaching a small region with a maximum laser intensity and records immediately the fluorescence recovery in that part with a lower laser intensity (Fig II.16). Ideally, recovery kinetics only depends on mobility (effective diffusion coefficient and kinetics union to macromolecules structures) of the molecule under study. The time of fluorescence recovery in photobleached region depends on the number of mobile fluorescent particles that spread all over the bleached region. It is worthy to mention that 100% of fluorescence will never recover because we have removed some fluorescent molecules.

Besides, when recovery kinetics is measured, some properties of fluorescence molecule can be characterized; for instance: mobile/immobile ratio, lateral diffusion coefficient and time that protein is linked to macromolecular structures.

In the present work, photobleaching experiments were done by scanning a bleach region of 10  $\mu\text{m}$  width x 3.8  $\mu\text{m}$  height at maximum laser intensity with a high numerical aperture objective (Nikon HCX-PL-APO 63x/1.4-0.6 NA oil immersion). The pinhole was set at airy 2. During the recovery period, images from a single focal plane were recorded at lower laser intensity with time intervals of 2 s for 1 min, 5 s for 3.3 min and 10s for 3.3 min.

---

**Figure II.16. Fluorescence recovery after photobleaching.** **a)** A cell that expresses fluorescence molecules is recorded with low laser intensity before and after photobleaching (red square). Fluorescence recovery of bleached region is monitored along time. Analyses usually include compensation about fluorescence reduction in the whole cell. **b)** Fluorescence recovery can be analyzed in a FRAP curve. These graphics show recovery for one of the species (exponential curve with yellowish circles) or two equitative populations in two different ranges (double exponential curve shows in orange circles). **c)** Fluorescence recovery level in photobleached region reveals mobile and immobile fraction. **d)** A simple test to calculate photoinducible immobile fraction is to carry out a second FRAP in the region. In this example, mobile fraction of first FRAP is 70%. The recovery level can be determined normalizing the fluorescence signal in the region and repeating FRAP experiment. In absence of photo-damage, the recovery should be complete. (Taken from book *Nature Cell Biology*, 5<sup>th</sup> edition, 2003).



### 3.5.3.2. FRAP kinetics.

In a FRAP assay we can represent fluorescence intensity *versus* time, what allows us to calculate several parameters like mobile/immobile fractions, recovery half-time or basal fluorescence intensity (background) (Fig II.17).

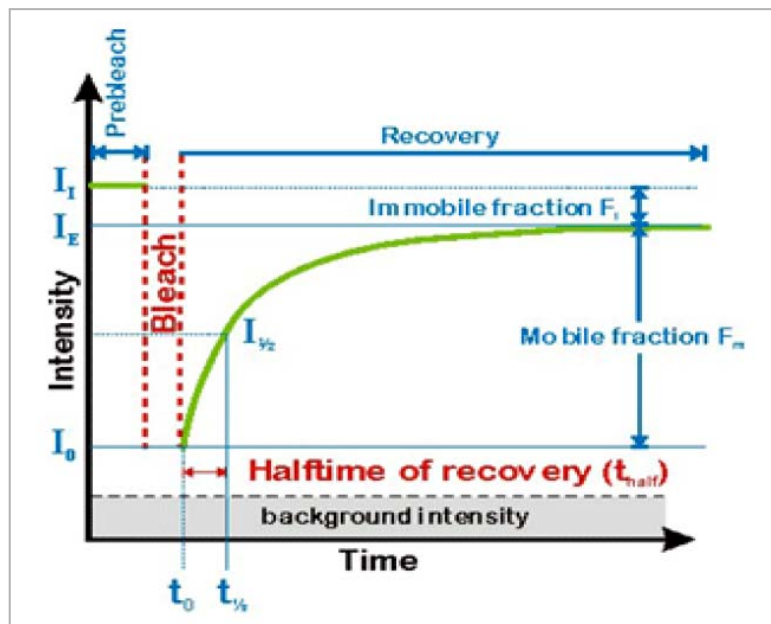


**Figure II.17. Graph obtained after FRAP experiment.** The main variables are shown: mobile/ and immobile fractions and recovery half-time. (Taken from EAMNE FRAP on-line teaching module, EMBL).

In pre-bleach period, the fluorescence intensity is maximum ( $I_i$ ). During bleaching, the fluorescence decreases up to a level slightly bigger than basal intensity (background) because molecules are constantly moving. During post-bleach the fluorescence of the bleach zone is recovered in variable speed depending on mobile fraction. The maximum fluorescence in this zone reaches a maximum value ( $I_E$ ), which is smaller than  $I_i$  due to immobile fraction. Besides, the number of bleached molecules decreases the amount of fluorescent molecules in the cell, so maximum intensity. The time in which is recovered the half-maximum fluorescence is called  $t_{1/2}$  and it is an important and characteristic parameter.

### 3.5.3.3. Data processing.

Data obtained directly from the graph (thanks to Leica confocal software) are raw data and they need three corrections: background subtraction, laser photobleaching and dilution of the probe after the photobleaching pulse (normalization) (Fig II.18).

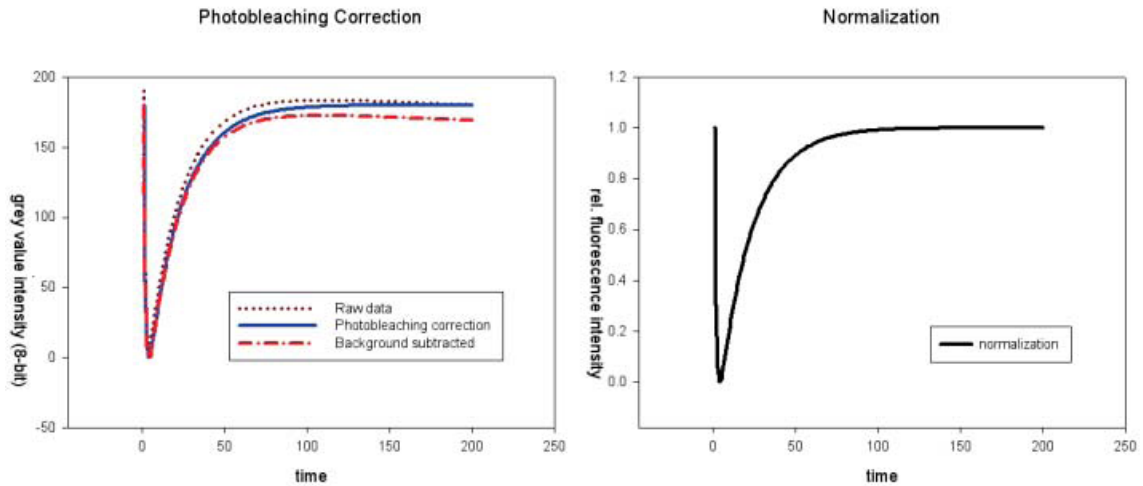


**Figure II.18. Representation of FRAP experiment raw data.** **Left image:** Raw data (dotted line), photobleaching correction (blue continue line) and data after background subtraction (red discontinue line). **Right image:** It is shown the final graph after data normalization regard 100% fluorescence (Taken from <http://www.dkfz.de/ibios/index.jsp> . Constantin Kappel et al.).

➤ Background subtraction.

We consider background as basal fluorescence of preparation (coverslips, medium, cells, etc) and we need subtract it in order to not fiddle results.

$$F_i = F(t) - F(bk) \quad (3)$$

$F_i$  means fluorescence after background subtraction.

$F_{(t)}$  means raw fluorescence (at every time).

$F_{(bk)}$  is background fluorescence.

➤ Laser photobleaching correction.

We can differentiate two kinds of photobleaching: one hand, laser photobleaching during bleach pulse, and the other hand, photobleaching during fluorescence recovery. To check this, we have to apply the following formula (after background subtraction):

$$F_{ii} = F_i(t) \cdot \frac{F_{precell}}{F_{postcell}} \quad (4)$$

$F_{ii}$  means corrected photobleaching fluorescence.

$F_{precell}$  is the average fluorescence during pre-bleach period in a cell that has not suffered FRAP, while  $F_{postcell}$  is during post-bleach time in the cell mentioned before.

- Normalization.

Normalization means remake a scale so that images represent 100% fluorescence and we can compare different FRAP experiments:

$$F_{iii} = \frac{F_{ii}(t)}{X_{prebleachFii}} \quad (5)$$

$F_{iii}$  is normalized fluorescence.

$X_{prebleachFii}$  means average fluorescence of images during pre-bleach period (they are the highest fluorescence values).

### 3.5.3.4. Estimation of different FRAP parameters.

Three parameters can be obtained for the FRAP experiments:

- Mobile fraction (Mf).

In *in vivo* experiments, mobile fraction is the percentage of molecules that shows diffusion around the cells. The interactions among molecules under study and others biomolecules (or proteins) can be fixed by preventing them from diffuse around the cell, so it is called immobile fraction.

$$Mf = 100 \times \frac{F_{precell}}{F_{postcell}} \times \frac{F_{iiixpostbleach(equil)} - F_0}{F_{iiixprebleach} - F_0} \quad (6)$$

$F_{precell}/F_{postcell}$  is a correction for fluorophore dilution around cell that suffers FRAP.

$F_0$  means the fluorescence intensity in the bleach region immediately after of photobleaching.

$F_{iiixpostbleach(equil)}$  is the average normalized fluorescence intensity in post-bleach equilibrium plateau.

$F_{iiixprebleach}$  is the average normalized fluorescence intensity before photobleach.

- Half-time fluorescence recovery ( $t_{1/2}$ ).

$T_{1/2}$  is the time in which 50% fluorescence, regards to maximum intensity, is recovered.

This parameter strongly depends on geometry of bleach region, so to compare different experiments it is essential that they have been recorded under the same size, geometry and relative position in the cells of bleach region.

$$t_{1/2} = \ln 2 \times \tau \quad (7)$$

where  $\tau$  is the recovery time constant.

- Lateral diffusion coefficient (D).

This parameter can be fitted to a single exponential function:

$$y = y_0 + a \cdot \left[ 1 - e^{\left(\frac{-t}{\tau}\right)} \right] \quad (8)$$

This simplified formula is very useful if the bleach region is a circle or rectangle and diffusion only happens in two dimensions (like happens in membranes), as we have supposed that occurs in our assays.

From the equation before (8),  $\tau$  can be calculated, so  $t_{1/2}$  can also be calculated and substituted in the next formula (Axelrod *et al.*, 1976) to obtain the D value:

$$D = 0.88 \times \frac{w^2}{4 \cdot t_{1/2}} \mu m^2 / s \quad (9)$$

where  $w$  is the radius of the bleach area

### 3.6. Immunofluorescence.

After preparing cells in appropriate conditions (suitable number of cells in coverslips) and incubate them during necessary time, immunofluorescence protocol starts fixing cells during 10 minutes with 2% formaldehyde-methanol free in phosphate-buffered saline (PBS, composed by 0.008 M sodium phosphate, 0.002 M potassium phosphate, 0.14 M NaCl, pH 7.4) followed by an incubation with 50 mM ammonium chloride for 5 min to neutralize fixation solution.

After that, cells were washed with PBS and permeabilized during 10 minutes with:

- 0.1% Triton-X100 in PBS for MCF-7
- 0.5% Triton-X100 in PBS for BT-474 and MDA-MB-231

Next cells were washed again and blocked with the product Image-iT-FX signal enhancer (Invitrogen, Oregon, USA) for 30 min at room temperature in dark humid chamber to avoid evaporation and drying of samples.

Afterwards, cells were incubated with the corresponding primary antibodies for 3 h at room temperature in the humidity chamber. PKC $\alpha$  was detected by using a primary polyclonal rabbit antibody (Abcam, Cambridge Science Park) with dilution 1:50 in 1% BSA/0.15% saponin/PBS.

After washing them, cells were blocked with 1% BSA in PBS for 20 minutes and immunoreactivity was detected with the suitable fluorophore-conjugated secondary antibody (Alexa fluor 546 goat  $\alpha$ -rabbit, Invitrogen, Oregon, USA), dilution 1:1000, during 1 hour in the dark and humidity chamber.

Again samples were washed with PBS and blocked with 1% BSA in PBS for 20 minutes to proceed to stain them with Phalloidin-Alexa Fluor 633 (Invitrogen, Oregon, USA) during 20 minutes at room temperature and dark and humidity chamber.

Finally, preparations were washed with PBS and mounted in slides with the product DAPI-Prolong Gold antifade reagent (Invitrogen, Oregon, USA).

## **4. Electrophoresis techniques.**

Two electrophoretic methods have been used in this Doctoral Thesis; one for separating fragments of nucleic acids (DNA and RNA) and another for proteins. In both cases the separation depends on the size of macromolecules.

### **4.1. Agarose gel preparation.**

The suitable amount of agarose is dissolved in TAE buffer, which contains 24.2% trizma base, 5.7% acetic glacial acid (v/v) and 50 mM EDTA pH 8.0.

Before agarose polymerizes, etidium bromide was added (2  $\mu$ g/ml) in order to visualize DNA fragments in the later steps. DNA is loaded in the gel with the help of loading buffer (0.25% brome-phenol blue (w/v), 30% glycerol (v/v) and Tris 0.5 mM pH 8.0).

After a suitable running time, the gel was exposed to ultraviolet (UV) light to visualize the DNA fragments.

## 4.2. Acrylamide gel preparation.

Polyacrylamide gels were elaborated under denaturalization conditions with SDS (SDS-PAGE), following *Laemmli (1979)* method. Mini-PROTEAN Tetra Cell (BioRad Laboratories, CA, USA) was used to run this kind of gels.

The running gel was composed by 10% acrylamide-bisacrylamide (w/v) dissolved in 0.375 M Tris-HCl buffer pH 8.8 and 0.1 % SDS (w/v). It was added 0.064% ammonium persulfate (PSA) (w/v) and 0.064% TEMED (w/v) to the mix in order to polymerize it.

Stacking gel was made above running gel. In this case, the mix contains 5% acrylamide-bisacrylamide (w/v) dissolved in 0.13 M Tris-HCl pH 6.8 and 0.1 % SDS (w/v). As before, PSA and TEMED were added to polymerize the mix, although in this occasion 0.1% (w/v). The function of this gel is to concentrate proteins in order for then to penetrate at the same time in running gel.

Samples were dissolved in Sample buffer (40 mM Tris-HCl pH6.8, 50 mM DTT (w/v), 1% SDS (w/v), 7.5% glycerol (w/v) and 0.003% bromophenol blue (w/v)) before loading them in stacking gel.

The running buffer used contained 25 mM Tris-HCl pH 8.3, 192 mM glycine and 0.1 % SDS (w/v).

The gel was stained with Coomassie Blue (0.1% Coomassie blue R-250 (w/v) dissolves in 40% methanol (v/v) and 10% acetic acid (v/v)) for 20 minutes and follow on destaining step with 40% methanol (v/v) and 10% acetic acid (v/v).

## 5. Western Blot.

After running a polyacrylamide gel with appropriate samples, proteins are transferred to 0.2  $\mu$ m pore nitrocellulose membrane. To do that, a semi-dry system from BioRad (BioRad Laboratories, CA, USA) was used with a continue potential of 20 V during one hour, and transfer buffer composed by 1X of NuPAGE commercial transfer buffer (v/v) and 10% methanol (v/v).

Non-specific interaction sites of the antibody were blocked with a solution of 2% BSA (w/v) in TBST (20 mM Tris-HCl pH 7.5, 150mM NaCl and 0.1% Tween-20 (v/v)) during one hour with gently agitation.

After that, membrane was incubated overnight with primary antibody in the appropriate dilution in blocking buffer (2% BSA in TBST) at 4°C. PKC $\alpha$  was detected by using a polyclonal rabbit antibody (dilution 1:500) (Abcam, Cambridge Science Park), while to detect GAPDH (dilution 1:1000) a monoclonal rabbit antibody was used (Abcam, Cambridge Science Park).

Next morning, membrane was rinsed for three times with TBST in agitation before a secondary blocking incubation (2% BSA in TBST) for 30 minutes.

Afterwards, the secondary antibody, which is marked with horse-radish peroxidase, (goat anti-rabbit) (Abcam, Cambridge Science Park) was applied to membrane in a dilution of 1:25000 (in blocking buffer). Next, the membrane was again washed for three times.

Finally, immunoblotting was detected with a fluorescence scanner (Thyphoon, Amersham Bioscience) after adding ECL plus substrate solution (Amersham biosciences) to the membrane for 5 minutes. To reveal the membrane, it was excited at 430 nm and detected at 503 nm. Captured images were analyzed in several ways thanks to software incorporated by Amersham.

## **6. Fluorescence Resonance of Energy Transfer (FRET).**

FRET is a very useful technique to detect interactions between biomolecules. Basically it consists in fluorescence energy transfer from a donor to an acceptor, so we excite a fluorescence donor and detect the emission fluorescence from the acceptor molecules whenever donor and acceptor are closer than 100 Å (*Lakowicz, 1983*).

The efficiency of energy transfer depends on spectra overlap of fluorescence emission donor and excitation acceptor (Fig II.19), relative orientation and distance between both molecules (0-100 Å).

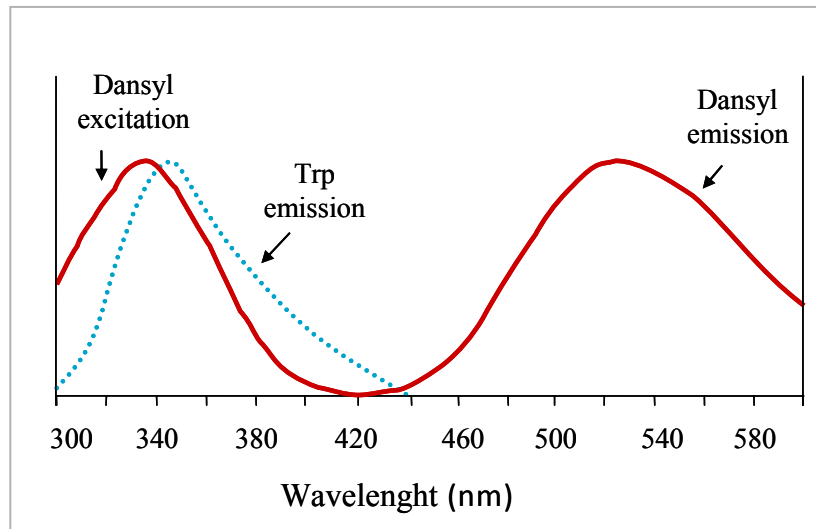


**Figure II.19. Overlap of emission and excitation spectra.** Emission spectra of the donor, Trp in this case, (blue dotted line) and excitation and emission spectra of the acceptor, dansyl derivated compound, (red continue line) are shown.

This efficiency of fluorescence energy transfer ( $E$ ) can be measured with next equation:

$$E = \frac{\tau_D - \tau}{\tau_D} \approx \frac{F_D - F}{F_D} \quad (10)$$

where  $F$  and  $F_D$  are the donor fluorescence emission in the presence and in the absence of acceptor.

The efficiency energy transfer allows us to calculate the distance between donor and acceptor ( $r$ ) as follows (Förster, 1996):

$$r = R_0 \left( \frac{1 - E}{E} \right)^{1/6} \quad (11)$$

being  $R_0$  a known parameter like *critical distance of Förster*, where the energy transfer is 50%.

Knowing the dependence of the distance between donor and acceptor to transfer energy, this technique has been widely used to measure lengths as well as to detect interactions between molecules (Corbalán-García *et al.*, 1994; Cubbit *et al.*, 1995; Hovius *et al.*, 2000; Singleton and Xiao, 2002). In this way, we can measure the union between a specific protein and model membranes in a huge variety of conditions, for instance the presence of different ligands in several concentrations. In these cases, Trp is used like donor and a fluorescent compound in membranes like an acceptor (normally, a dansyl derivated substance is used) (Fig II.20).

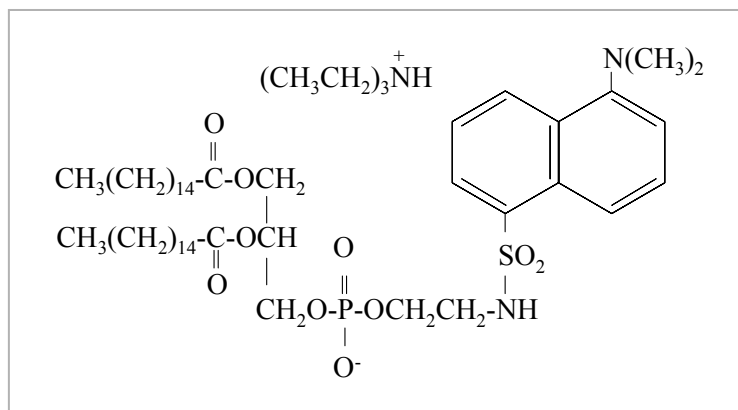


**Figure II.20. Molecular structure of dansyl-DHPE or d-PE** (*N*-(5-dimethylamino-naphthalene-1-sulfonyl)-1,2-dihexadecanoyl-*sn*-glycero-3-phosphoethanolamine).

To carry out FRET experiment in this Doctoral Thesis, PKC $\alpha$ -C2 domain was used as a donor and labelled liposomes as acceptor.

The lipids used for the reaction were dried under a stream of N<sub>2</sub> and the last traces of organic solvent were removed by keeping the samples under vacuum for 1 h. Lipids were suspended in 20 mM Hepes (pH 7.4), 0.05 mM EGTA and vortex mixed vigorously to form multilamellar vesicles. They were sonicated for 30 s for three times to form small unilamellar vesicles.

Equilibrium fluorescence experiments were carried out on a Fluoromax-3 fluorescence spectrometer at 25°C in a standard assay buffer composed of 20 mM Hepes (pH 7.4) and 100 mM NaCl. The excitation and emission slits widths were both 2 nm for all equilibrium fluorescence experiments.

The phospholipid dependence of PKC $\alpha$ -C2 domain (0.5 mM) docking on AA-containing vesicles was determined by using a mixture with 40 mol% AA, 55 mol% POPC and 5 mol% dDHPE. Sonicated lipids were titrated in, and the protein to-membrane FRET was monitored from, the intrinsic tryptophan (Trp) fluorescence emission at 340 nm and using an excitation of 284 nm.

Basically, experiments started with a mix composed by buffer, protein and EGTA (only in some control assays), where small unilamellar vesicles were added periodically. Control experiments to discard non-specific binding were performed using a mixture of vesicles containing 95 mol% POPC and 5 mol% dDHPE, and no FRET was detected.

All total lipid concentrations were divided by 2 to take into account the inaccessibility of one leaflet of the lipid vesicles to protein, due to the sealed nature of the bilamellar sonicated vesicles. FRET was analyzed by using the equations mentioned before (10 and 11).

## 7. PKC $\alpha$ purification.

PKC $\alpha$  wild type and some mutants (K209A/K211A, K197A/K199A and W58G) were partially purified from HEK-293 cells in order to run the kinase activity experiments (see next section).

HEK-293 cells were grown following ATCC recommendation (DMEM supplemented with 10% FCS, 2 mM L-glutamine and a mix of antibiotics, particularly 50 U/ml penicillin and 50  $\mu$ l/ml streptomycin). When cells reached 80% confluency, they were transfected with DNA constructs in pCGN plasmid following described protocol by *Wigler et al, 1977*. For each 9 cm  $\emptyset$  the mixtures were:

- Solution A: 0.54 ml Hepes 50 mM and 11  $\mu$ l of Na<sub>2</sub>HPO<sub>4</sub> 2 H<sub>2</sub>O 1,5 mM.
- Solution B: 0.48 ml TE buffer pH 8.0, 10  $\mu$ g of DNA and 66  $\mu$ l of CaCl<sub>2</sub> 2M.

Solution B was added to solution A, making a calcium phosphate precipitate. This mix was kept to RT for 10 minutes and then was added to cells. Plates were grown during 14 hours in a 5% CO<sub>2</sub> atmosphere, afterwards the medium was refreshed and cells were grown for another 48 hours in a 7.5% CO<sub>2</sub> atmosphere in order for them to express the maximum amount of protein as possible.

After this time, cells were washed twice with PBS and collected to start the purification protocol described by *Conesa-Zamora et al, 2001*. Cell pellets were resuspended in lysis buffer (composed by 20 mM Tris HCl pH 7.5, 10 mM EGTA, 2 mM EDTA, 0.25 mM sacarose, 1 mM PMSF, 10  $\mu$ g/ml leupeptin, 100 $\mu$ M Na<sub>3</sub>VO<sub>4</sub> and 50 mM NaF) with a ratio: 5 ml lysis buffer / g of cells. They were sonicated for 6 seconds 16 times controlling that pH keeps constant at 7.5.

The resultant lysate was centrifuged to 13000 rpm for 30 minutes and 4°C. The supernatant was collected and the pellet was resuspended again in the same volume of lysis buffer to sonicate and centrifuged it in the same way.

Both supernatant were mixed and it was ultra-centrifuged to 35000 xg during 30 minutes and 4°C. The sediment was discarded and the supernatant was added to a DEAE-Sephacel column (Sigma-Aldrich Chemistry, S.A., Madrid, Spain), previously equilibrated with Buffer E (20 mM Tris HCl pH 7.5, 0.5 mM EGTA, 0.5 mM EDTA and 10  $\mu$ M  $\beta$ -mercaptoethanol).

To elute proteins from the column, an EconoSystem (Bio-Rad Laboratories, Hercules, CA, USA) was used. Particularly, proteins were eluted from the column using a saline gradient from 0 to 1 M of NaCl dissolved in

buffer E; and they were collected in the fraction collector with a flux of 0.5 ml per minute.

Whole elution process was monitored with ultraviolet detector and later every fraction with PKC $\alpha$  wild type or mutants was checked using Western Blot. The fractions, which contained higher amount of proteins, were put together and were concentrated in a concentrator filter 30K (Ultrafree Millipore) and finally, they were aliquoted and frozen to  $-80^{\circ}\text{C}$  in the presence of 10% (v/v) glycerol and 0.05% (v/v) Triton X-100.

## 8. Kinase activity assays.

These assays were carried out using a partially purified PKC $\alpha$  wild type and several mutants (see previous section), specifically PKC $\alpha$ D246N/248N, PKC $\alpha$ K209A/K211A, PKC $\alpha$ K197A/K199A and PKC $\alpha$ W58G. It was used a technique described previously (López-Nicolás *et al*, 2006) in which it was measured the incorporation of radioactive phosphate [ $\gamma$ - $^{32}\text{P}$ ] to kinase substrate (histone III-S) in order to detect enzymatic activity.

The lipids used for the reaction were previously dried under a stream of  $\text{N}_2$  and the last traces of organic solvent were removed by keeping the samples under vacuum for one hour. Lipids were prepared in different percentages of fatty acids (FA) to solve the capacity of these compounds to activate PKC $\alpha$ . The POPC:FA ratios were:

100:0/ 98:2/94:6/92:8/90:10/88:12/84:20/80:20/75:25/70:30.

These lipids were resuspended immediately before using them in a buffer composed by 20 mM Tris-HCl (pH 7.5), 0.005 mM EGTA and vortex vigorously to form multilamellar vesicles. They were added to the reaction mixture, which contained 20 mM Tris-HCl (pH 7.5), 0.2 mg/ml of histone III-S, 20  $\mu\text{M}$  ATP, [ $\gamma$ - $^{32}\text{P}$ ] (300,000 cpm/nmol), 5 mM  $\text{MgCl}_2$  and 200  $\mu\text{M}$   $\text{CaCl}_2$ . The final concentration of lipids in the reaction mixture was 500  $\mu\text{M}$ .

The reaction was started by addition of 5  $\mu\text{l}$  of the PKC $\alpha$  (0.004  $\mu\text{g}/\text{ml}$ ) purified from transfected HEK293 cells. After 10 min, the reaction was stopped with 1 ml of ice-cold 25% (w/v) trichloroacetic acid (TCA) and 1 ml of ice-cold 0.05% (w/v) bovine serum albumin (BSA).

After precipitation on ice for 30 min, the protein precipitate was collected on a 2.5 cm glass filter (Sartorius, Göttingen, Germany) and washed with 10 ml of ice-cold 10% trichloroacetic acid. The amount of  $^{32}\text{P}$ i incorporated into histone was measured by liquid scintillation counting.

The linearity of the assay was confirmed from the time-course of histone phosphorylation during 30 min. Additional control experiments were performed with mock cell lysates to estimate the endogenous PKC $\alpha$  and non-specific activities, which represented less than 1% of the total enzyme activity measured.

Another control experiment was run without calcium in reaction mix was performed to measure basal kinase activity. Instead of Ca<sup>2+</sup>, 0.5 mM EGTA was added and the reaction time was 30 minutes.

Kinase activity assays were repeated at least for three times.

## **9. Microarrays.**

### **9.1. Introduction to microarrays.**

Microarrays have revolutionized basic scientific research and are constantly challenging our view of the genome and its complexity. They are finding their way from the research laboratory to the clinic, where they promise the same kind of revolution in patient care (*Apidianakis et al, 2005; Boerma et al, 2005*). Microarrays used in clinical research and clinical applications promise to help scientists develop more accurate diagnostics and create novel therapeutics. By standardizing microarray data and integrating it with a patient's existing medical records, physicians can offer more tailored and more successful therapies. The combination of a patient's genetic and clinical data will allow for personalized medicine, which is where GeneChip technology holds the greatest promise to improve health (*Schadt et al, 2004*).

GeneChip arrays are the result of the combination of a number of technologies, design criteria, and quality control processes. In addition to the arrays, the technology relies on standardized assays and reagents, instrumentation (fluidics system, hybridization oven and scanner), and data analysis tools that have been developed as a single platform (*Irizarry et al, 2003*).

Affymetrix platform, and gene expression array, was the chosen ones for run some microarrays experiment in this Doctoral Thesis, although there are more platforms and array models in the market. The affymetrix key assay steps are outlined in figure II.21.

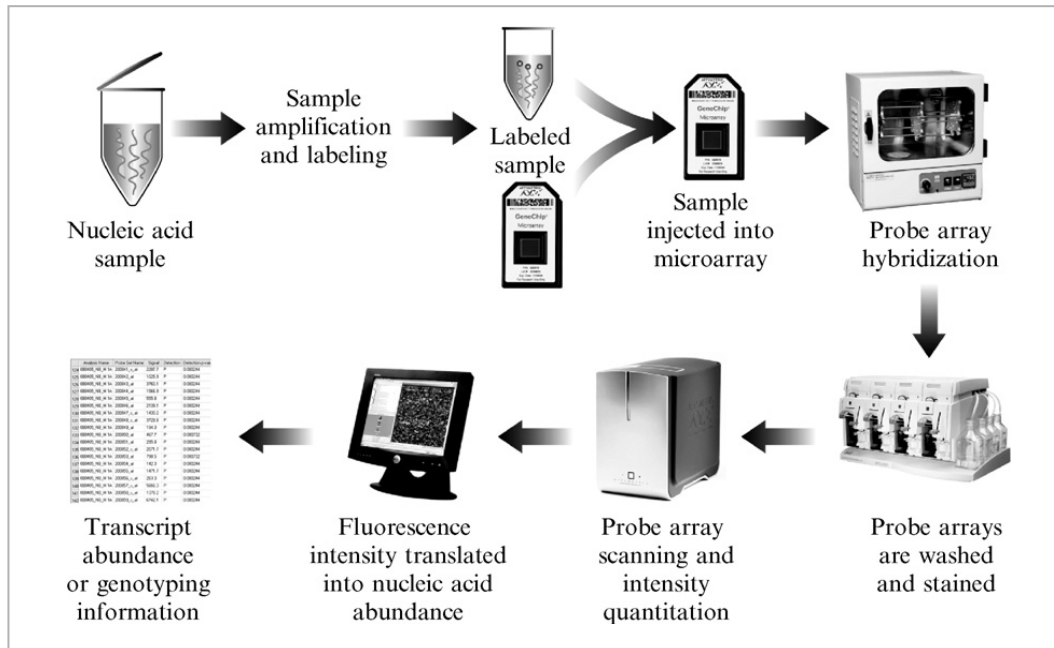


**Figure II.21. Flow-chart of a GeneChip System microarray experiment.** Once the nucleic acid sample has been obtained, target amplification and labelling result in a labelled sample. The labelled sample is then injected into the probe array and allowed to hybridize overnight in the hybridization oven. Probe array washing and staining occur on the fluidics station, which can handle four probe arrays simultaneously. The probe array is then ready to be scanned in the Affymetrix GeneChip scanner, where the fluorescence intensity of each feature is read. Data output includes an intensity measurement for each transcript or the detailed sequence or genotyping (SNP) information.

## 9.2. Overview of preparation for gene expression array.

### 9.2.1. Target Preparation.

Most target preparation protocols start with a purified nucleic acid sample that is usually amplified and then labelled and fragmented (Fig. II.22). RNA targets are prepared by *in vitro* transcription (IVT), which provides amplification of the target. Biotinylated nucleotides or analogues are incorporated into the target during the IVT process. The labeled RNA is then purified and fragmented by hydrolysis.

For gene expression assays, the most widely used sample preparation utilizes the IVT reaction as originally described by Eberwine and colleagues (*Van Gelder et al, 1990*). In this assay cDNA synthesis is initiated from an oligo(dT) primer that is also coupled to a T7 RNA polymerase primer. In this case cDNA synthesis starts adjacent to the poly(A) tail of the mRNA. After second strand synthesis, a double-stranded cDNA copy of each mRNA is created attached to the T7 RNA polymerase primer. An IVT reaction is then carried out to create a biotinylated RNA target (Fig II.22). A variation of this technique utilizes two rounds of IVT amplification and is used to create a target from very small amounts (100 ng or less) of starting material.

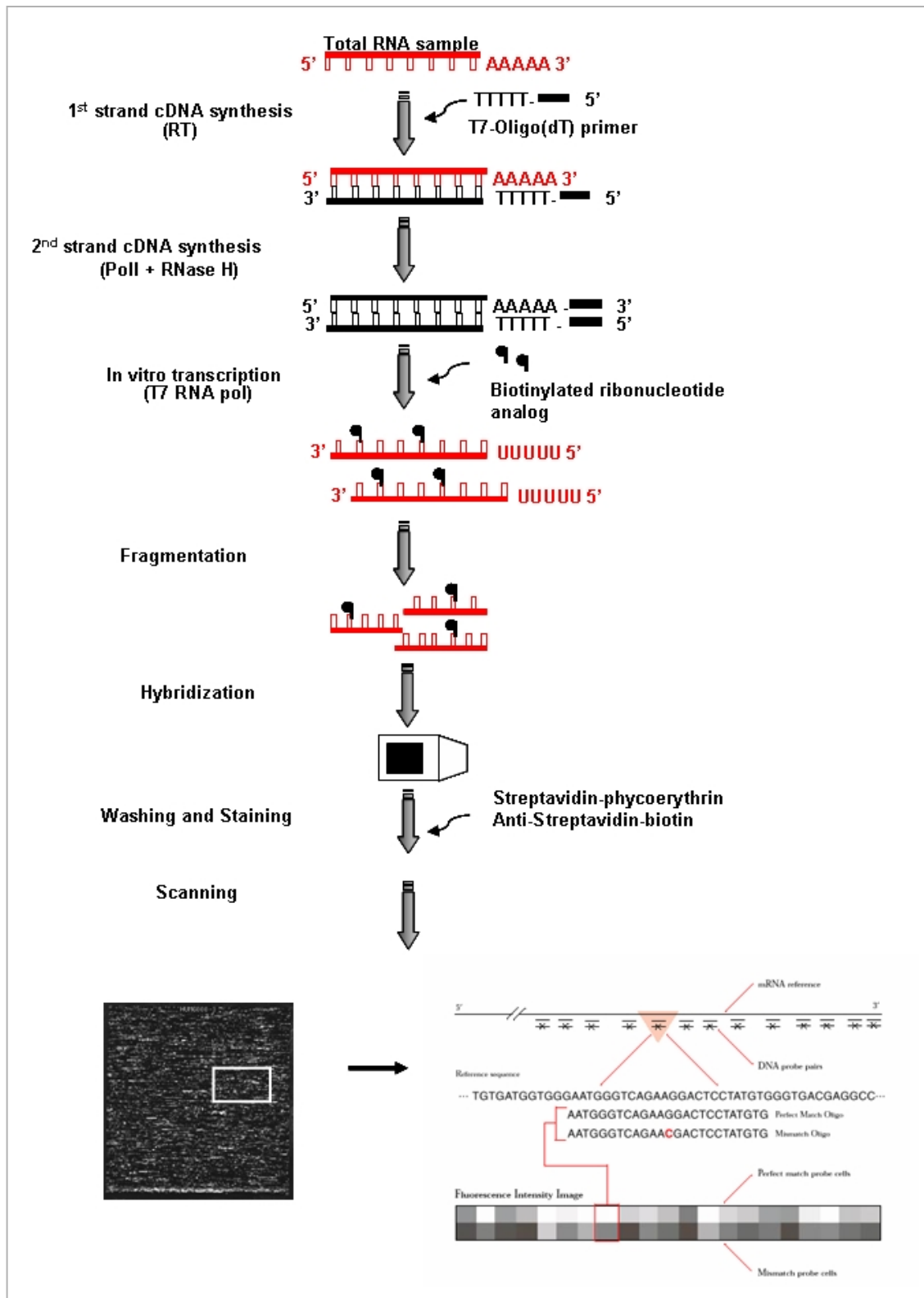


**Figure II.22. One-cycle sample preparation for gene expression profiling.** The flowchart depicts the steps by which eukaryotic samples are prepared for gene expression profiling. Briefly, total RNA or poly(A)-RNA is isolated. A primer that includes a poly(T) tail and a T7 polymerase binding site [T7-oligo (dT) primer] is used for reverse transcription, resulting in synthesis of the first strand complementary DNA (cDNA). The second cDNA strand is completed, resulting in a double-stranded cDNA. In the one-cycle method, the double-stranded cDNA is used as a template for *in vitro* transcription with biotinylated ribonucleotides, resulting in a biotin-labeled RNA sample. After cRNA fragmentation, the sample is ready to be hybridized to the array, washed and stained and finally scanned.

### **9.2.2. GeneChip Instrument Components and Associated Assay Steps.**

The GeneChip instrument components include a hybridization oven, the fluidics station, an optional autoloader, and a scanner (Fig. II.23). All of these instruments are designed to work together and, with the exception of the hybridization oven, are directed by the GeneChip operating software (GCOS). The hybridization oven can hold up to 64 probe arrays and provides continuous rotation and consistent temperatures over the 16 h that are typically required for hybridization. The temperature is tuneable to cover the different array applications and is usually selected between 40 and 50°.

After hybridization the arrays are transferred to the fluidics station. The fluidics station performs washing and staining operations for GeneChip microarrays, a crucial step in the assay that impacts data consistency and reproducibility. It washes and stains up to four probe arrays simultaneously. Unbound nucleic acid is washed away through a combination of low and high stringency washes. The stringency of the wash is determined by the salt concentration of the buffer and the temperature and duration of the wash, with the temperature and duration controlled by the fluidics station. The fluidics station contains inlets for two different buffers and heats buffers up to 50°, permitting temperature-controlled washes.

In the next step, bound target molecules are “stained” with a fluorescent streptavidin–phycoerythrin conjugate (SAPE), which binds to the biotins incorporated during target amplification. In the latest fluidics station, the 450 Model (the one which it was used in this Doctoral Thesis), wash and stain steps proceed in an automated fashion, ending with an array that is ready for scanning. The fluidics station is controlled by a computer workstation running GCOS.

The AutoLoader is a front-loading sample carousel that can be added to the latest generation scanners as an option. The AutoLoader increases throughput by permitting unattended scanning for up to 48 arrays. Arrays are maintained at 15°C prior to and after scanning. The instrument also includes a bar code reader that identifies the arrays, permits sample tracking, and aids in high-throughput analysis.

The current scanner is a wide-field, epifluorescent, confocal microscope that uses a solid-state laser to excite fluorophores bound to hybridized nucleic acids. The scanning mechanism incorporates a “flying objective,” which employs a large numerical aperture objective that eliminates the need for multiple array scans. The most recent version of the scanner has a pixel resolution of 0.7  $\mu\text{m}$  and is able to scan features with 5  $\mu\text{m}$  spacing. The scanner can resolve more than 65,000 different fluorescence intensities.

During the scan process a photomultiplier tube collects and converts fluorescence values into an electronic signal, which is then converted into the corresponding numerical values. These numerical values represent the fluorescence intensities, which are stored as pixel values that comprise the image data file (.dat file).

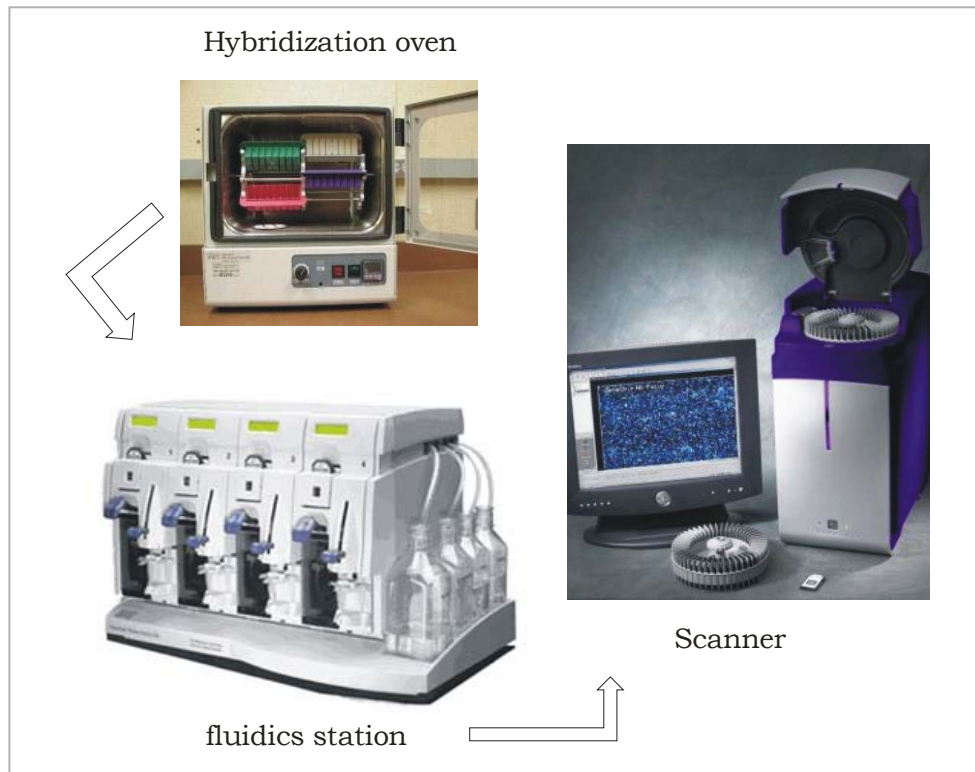


**Figure II.23. GeneChip instrument component from Affymetrix.** It is shown the hybridization oven, the fluidics station model 450 and the chip scanner with the AutoLoader.

### 9.2.3. Image and Data Analysis.

The next step in analysis is the assignment of pixels that make up the image (.dat) file to the appropriate feature. Previous methods have used a global gridding method in which the four corners of the array, defined by checkerboard patterns, serve as anchors for the grid. Features are then created by evenly dividing the area defined by the anchored corners into the known number of features for a given array. As the number of pixels per feature continued to decrease, an additional step called Feature Extraction was implemented to assign pixels to features in a more robust manner. In Feature Extraction the original pixels assigned to a feature are shifted as a block, a pixel at a time, and the coefficient of variation (CV) of pixel intensities for the shifted feature is computed. After allowing the feature pixels to shift up to a predetermined distance, the feature is defined where the pixel intensity CV is a minimum. Following Feature Extraction the intensity of each feature is calculated and stored in a .CEL file.

Regardless of application, the feature intensities found in .CEL files are used by analysis software to detect sequence variation or to differentiate gene expression levels of transcripts. During analysis, the use of multiple probes per genotype or gene is combined with standard statistical methods to provide a transparent and robust conversion of probe intensities to biological information.

For gene expression, a variety of algorithms exist to summarize multiple probe intensities (including perfect match (PM) or mismatch (MM) probes in a probe set) into an aggregate signal estimate that is correlated to the relative abundance of the transcript in the experimental sample. Detection calls are made by Affymetrix software through an arithmetic vote of probe pairs within a set designed to detect a specific transcript (GeneChip MAS5 and GCOS software). More widely used is an estimation of relative transcript abundance by a probe set signal and the trend has shifted away from median probe intensity based algorithms such as MAS5 to probe modelling algorithms such as dCHIP (Schadt *et al.*, 2004), RMA (Irizarry *et al.*, 2003), and PLIER Estimation (Affymetrix Technical Note, 2005). The probe modeling analysis software considers intrinsic probe behavior to account for systematic non-systematic biases, error, and allows for true replicate analysis.

It is still common for algorithms to use both PM and MM probes; however, PM-only algorithms are popular. Subtraction of MM probe intensity from the PM intensity or subtraction of modelled background estimates in PM-only analyses serves the same purpose, which is to estimate the true probe intensity by subtraction of background from the raw PM probe intensity. Raw probe intensity (PM or MM) is the sum of a true hybridization signal, specific cross-hybridization signal, non specific binding signal, and small amounts of signal generated by system noise. Background consists of everything but the true signal, and most would agree that, for an unbiased or true measurement of probe intensity, background must be subtracted from the raw perfect match probe intensity. For most Affymetrix expression measurements, subtraction of MM probe intensity is an accurate method to remove background. However, background can also be estimated in the absence of MM probes, for example, RMA. Continued discussion around this topic is indicative of the maturing thought in this area. Despite differences in precision, accuracy, and bias, most signal estimate-algorithms (PM, MM, or PM only) result in similar biological interpretations from the same data sets.

### **9.3. Sample preparation.**

MDA-MB-231 and MCF-7 cells lines were used to study gene expression profile after inhibition of classical isoform PKC $\alpha$ , so we can understand the role of this enzyme in these two models of breast cancer, invasive and non-invasive, respectively.

Cells were grown and electroporated with siRNA control and siRNA $\alpha$ , as it is mentioned before, to get cell with and without PKC $\alpha$  expression. After several days growing, specifically 5 for MCF-7 and 6 days for MDA-MB-231 cells, they were harvested, counted and washed with PBS to finally centrifuged them (approximately 5 millions of cells), aspirate supernatant and freeze the pellet with liquid nitrogen. The frozen cell pellets were kept in a -80°C freezer until further steps were done.

From now on, the work was carried out in the laboratory of the Center for Biological Sequence Analysis (CBS) at Technical University of Denmark (DTU) under the supervision of Professor Zoltan Szallasi.

The first step was the total RNA extraction, for what RNeasy® Plus kit (QIAGEN, GmbH, Germany) was used, following the manufactured protocol. Basically, the protocol is as follow: biological samples are first lysed and homogenized in a highly denaturing guanidine-isothiocyanate-containing buffer, which immediately inactivates RNases to ensure isolation of intact RNA. The lysate is then passed through a gDNA Eliminator spin column. This column, in combination with the optimized high-salt buffer, allows efficient removal of genomic DNA.

Ethanol is added to the flow-through to provide appropriate binding conditions for RNA, and the sample is then applied to an RNeasy spin column, where total RNA binds to the membrane and contaminants are efficiently washed away. High-quality RNA is then eluted in 30  $\mu$ l of water.

Next, total RNA is amplified and labelled with biotin (Fig II.22). To run that, we used the MessageAmp™ II-Biotin *Enhanced* Kit (Ambion, Inc., Cambridge, USA) following the manufacturer protocol. The steps included in this kit are (Fig II.24):

- **Reverse Transcription to Synthesize First Strand cDNA** is primed with the T7 Oligo(dT) Primer to synthesize cDNA containing a T7 promoter sequence.
- **Second Strand cDNA Synthesis** converts the single-stranded cDNA into a double-stranded DNA (dsDNA) template for transcription. The reaction employs DNA Polymerase and RNase H to simultaneously degrade the RNA and synthesize second-strand cDNA.
- **cDNA Purification** removes RNA, primers, enzymes, and salts that would inhibit in vitro transcription.
- **In Vitro Transcription to Synthesize aRNA** with Biotin-NTP-Mix generates multiple copies of biotin-modified aRNA from the double-stranded cDNA templates; this is the amplification step.
- **aRNA Purification** removes unincorporated NTPs, salts, enzymes, and inorganic phosphate to improve the stability of the biotin-modified aRNA.

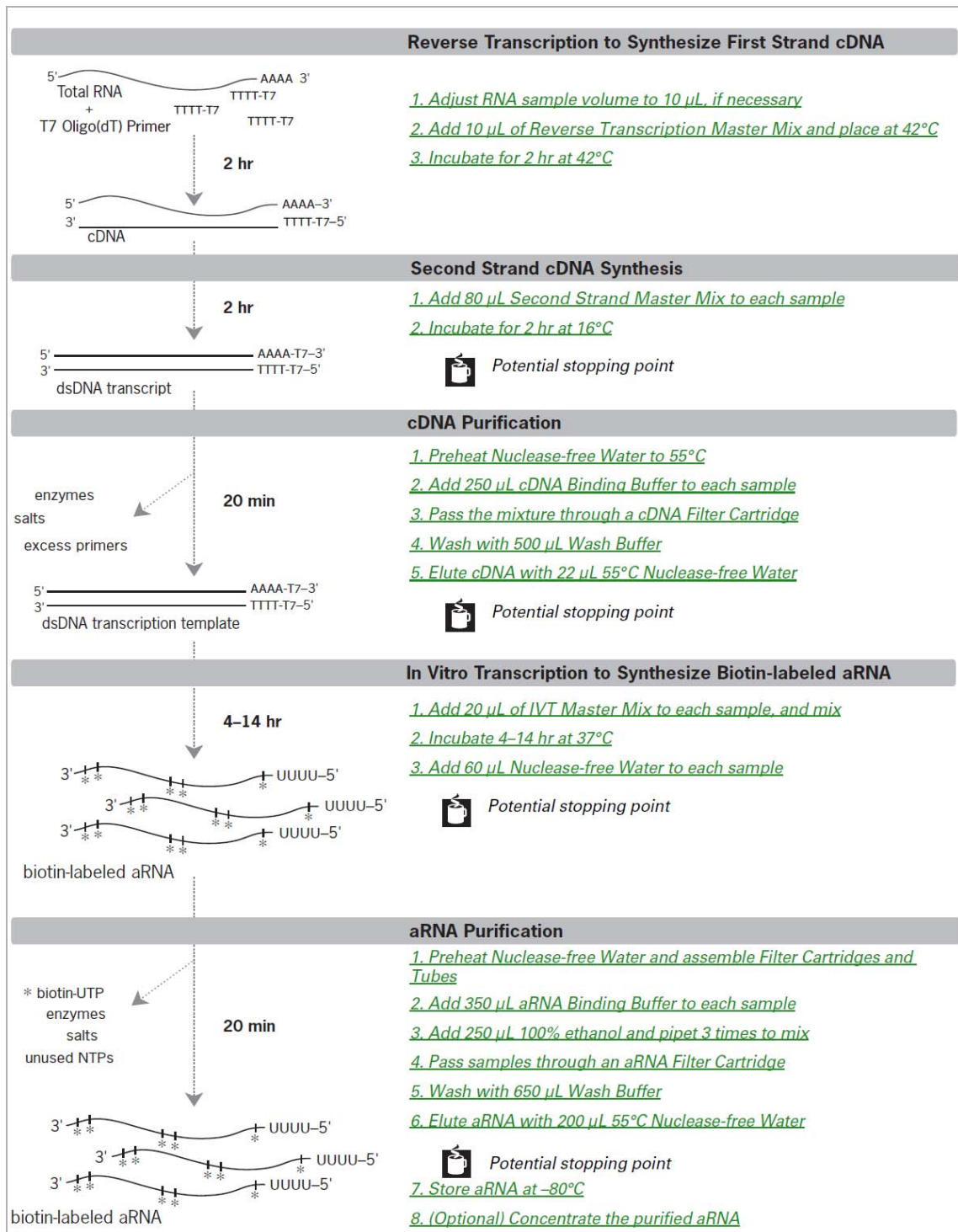


**Figure II.24. MessageAmp II-Biotin Enhanced aRNA Amplification Kit Procedure.**

Next step is the aRNA fragmentation to improve the hybridization kinetics and signal produced on oligonucleotide microarrays. Again, we used the MessageAmp™ II-Biotin Enhanced Kit (Ambion, Inc., Cambridge, USA) and follow the manufacturer protocol.

At this point, as well as after extracting total RNA, the quality and quantity of RNA were measured using Agilent 2100 bioanalyzer and nanodrop respectively.

After checking the purity and size distribution of aRNA, the hybridization was carried out. The appropriate cocktail (for a 100 Format (midi) array) was prepared, including the fragmented target, and probe array controls. After several centrifugations and incubations (see Affymetrix expression analysis technical manual for more details) the hybridization cocktail is injected in the GeneChip® Probe Array and it was incubated in the pre-heated hybridization oven at 45°C and 60 rpm agitation for 16 hours.

After this incubation, fluidics stations were set up to run the appropriate washing and staining steps before scanning the Probe Array in the pre-warmed Affymetrix® GeneChip® Scanner 3000.

Finally the obtained data were analysed with the program R to get a list of genes with significative expression level when control and mutant (without PKC $\alpha$  expression) are compared.

Once we had the gene list, it was introduced in the web database “GENECODIS” with level 4 of Gene Ontology (GO) to classify them depending on Biological Process (BP) and Molecular Function (MF) to get a better understanding of which signal transduction pathways are affected in cells when PKC $\alpha$  expression is suppressed.

Three control chips and three mutant samples of every cell line were run.

## 10. Statistical analysis.

Statistical significance was evaluated by chi-square, Kruskal-Wallis, Mann-Whitney tests and by analysis of the variance as applicable;  $p < 0.05$  was considered statistically significant. The statistical software program used was SPSS (Statistical Package for the Social Sciences, SPSS Inc., Chicago, 2008).



## CHAPTER III

### MOLECULAR MECHANISM OF PKC $\alpha$ LOCALIZATION BY ARACHIDONIC ACID. THE C2 DOMAIN ALSO PLAYS A ROLE



## 1. Introduction.

Arachidonic acid (AA) and its precursor, linolenic acid, are common dietary  $\omega$ -6 cis-polyunsaturated fatty acids that are sometimes found in the extracellular microenvironment (Larsson *et al.*, 2004). Although there is controversy concerning the effect of fat in the human diet on the development of breast cancer, there is substantial evidence supporting an effect of cis-polyunsaturated fatty acids in animal and cell models of mammary tumorigenesis and metastasis (Rose and Conolly, 1999; Cave, 1996). AA in an esterified form is present also in cell membrane phospholipids and is liberated by the action of several isoforms of phospholipase A2 (mainly the cytosolic PLA2) (Luo *et al.*, 2003) and from diacylglycerol by the action of diacylglycerol lipase (Chakraborti *et al.*, 2004). Besides the tumorigenic effect, AA is generated in a wide variety of cell types and participates, either directly or indirectly, in many cellular processes, including the inflammatory response, the contraction of cardiac myocytes, the regulation of ionic channels, cytokine synthesis, cell growth, eicosanoid metabolism, apoptosis, secretion and the regulation of gene expression (Liu *et al.*, 2001; Priante *et al.*, 2002; Bordin *et al.*, 2003; Patiño *et al.*, 2003; Moghaddami *et al.*, 2003).

A large variety of connections exists between PKC and AA in many different signalling pathways but, despite many studies, no clear picture has emerged concerning the molecular mechanisms involved in these processes. Despite of this ignorance, it is known that the action of AA on PKC is fine-tuning regulated; as an evidence of it, PKC regulates the AA synthesis and this fatty acid only affects some PKC isoforms depending on cell type (Mackay and Mochly-Rosen, 2001; Bordin *et al.*, 2003). Thus, it has been reported that PKC participates, either directly or through the phosphorylation of MAP Kinases, in the activation of phospholipase A2, which is one of the pathways leading to the production of arachidonic acid (Akiba *et al.*, 2002; Xu *et al.*, 2002).

In addition, it was long ago found that PKC could be activated by cis-unsaturated fatty acids (McPhail *et al.*, 1984), among them AA, which is released from the *sn*-2-position of phospholipids. Pioneering studies demonstrated that AA greatly enhanced the diacylglycerol (DAG) and phorbol ester-dependent activation of PKC in *in vitro* assays (Murakami and Routtenberg, 1985), suggesting that AA interacts with the C1 domain of PKC (Kashiwagi *et al.*, 2002). Since then, other authors have demonstrated either a competitive or a synergistic effect between the diacylglycerol and AA in influencing the membrane localization of PKC $\gamma$  when they were added directly to cell cultures (Shirai *et al.*, 1998). Furthermore, several *in vivo* studies have shown that PLA2 products, such as arachidonic acid and lysophosphatidylcholine, may activate the PKC signalling pathway, mainly by causing long-term responses.

Another important issue, and one that has caused great controversy, is the  $\text{Ca}^{2+}$ -dependence of the AA-dependent activation of PKC. Several studies point to a  $\text{Ca}^{2+}$ -independent mechanism (O'flaherty *et al.*, 2001), while other authors have suggested that PKC activation by AA is a  $\text{Ca}^{2+}$ -dependent process (Yagi *et al.*, 2004).

To shed light on all these questions, we have investigated the mechanism of activation of PKC $\alpha$  by AA in MCF-7 cells. We determined the functional domains involved in the localization of the enzyme in the plasma membrane and its subsequent activation. For this, we generated a wild-type PKC $\alpha$  fused to enhanced-green fluorescent protein (EGFP) and mutants of the *Ca<sup>2+</sup>-binding region*, the *lysine-rich cluster*, and the C1A and C1B subdomains. The results show PKC $\alpha$  localization into plasma membrane, where AA and ionomycin need to be added together. It was demonstrated also in this study that the *Ca<sup>2+</sup>-binding region* of the C2 domain is responsible for binding  $\text{Ca}^{2+}$  and for interacting with the AA incorporated into the membrane. Besides the C2 domain, it was demonstrated that only the C1A domain was important for the docking at the membrane of PKC $\alpha$ , with Trp58 being more important in the anchorage process.

## 2. Results.

### 2.1 Arachidonic acid induces the PKC $\alpha$ translocation to the plasma membrane in a $\text{Ca}^{2+}$ -dependent manner.

To investigate whether AA induces the localization of PKC $\alpha$  in the plasma membrane, MCF-7 cells were transfected with a fluorescent construct consisting of PKC $\alpha$  fused to EGFP (PKC $\alpha$ -EGFP). In steady-state conditions, the protein was distributed homogeneously through the cytosol. When the cells were stimulated with 50  $\mu\text{M}$  AA, no effect was observed on enzyme localization and the protein remained in the cytosol. However, the addition of 50  $\mu\text{M}$  AA and 5  $\mu\text{M}$  ionomycin resulted in maximal plasma membrane localization of PKC $\alpha$  60 s after such stimulation, where it remained for at least 200 s. It is important to mention that the protein translocated to the plasma membrane and was localized in patches throughout the cytosol in a pattern that is consistent with binding to the endoplasmic reticulum (Fig III.1).

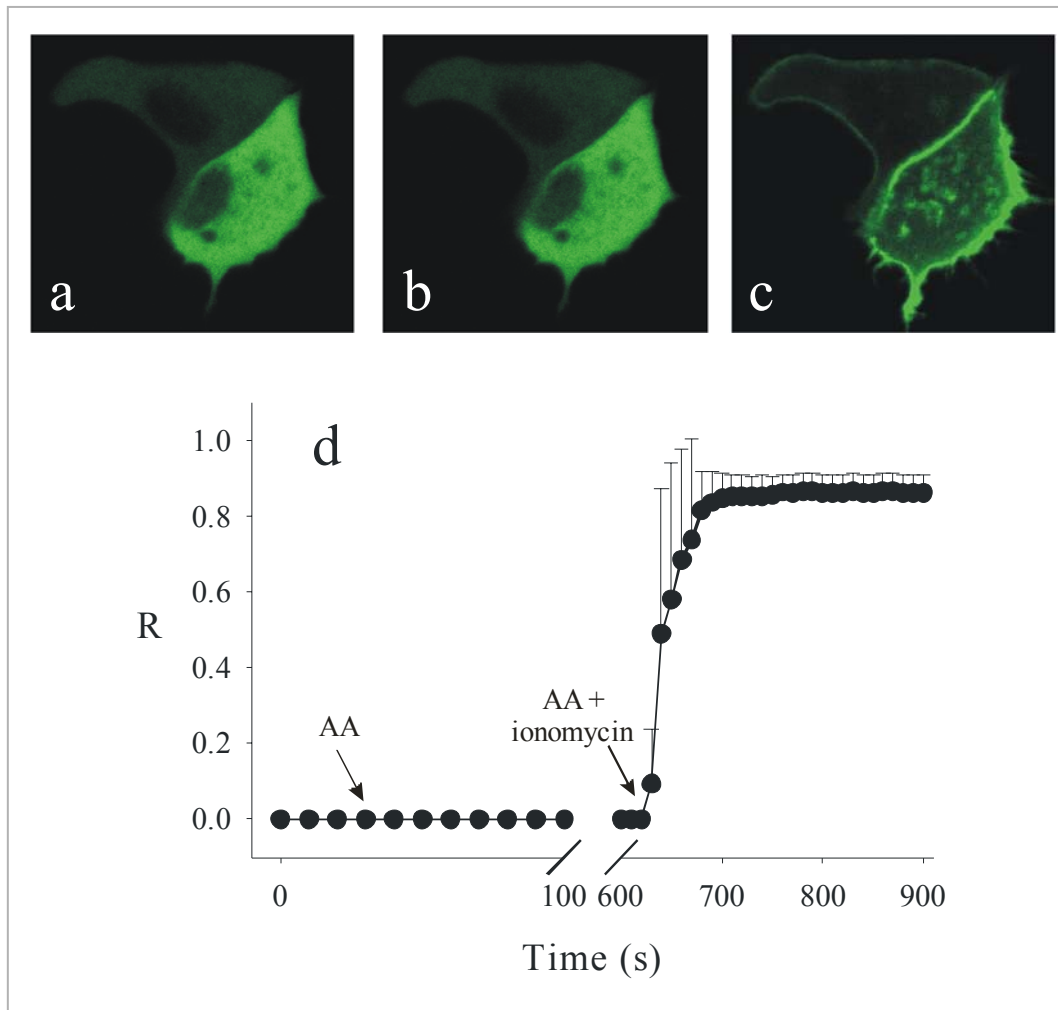


**Figure III.1. Arachidonic acid induces the PKC $\alpha$  translocation to the plasma membrane of MCF-7 cells in a Ca $^{2+}$ -dependent manner.** Confocal images of MCF-7 cells expressing PKC $\alpha$ -EGFP, incubated with 50  $\mu$ M AA for 10 min and with 50  $\mu$ M AA + 5  $\mu$ M ionomycin. The frames shown correspond to (a) time zero and (b) 500 s after AA stimulation, and (c) 100 s after the second addition of AA + ionomycin. (d) PKC $\alpha$ -EGFP fluorescence intensity was measured in the cytosol and in the plasma membrane in every frame of the time-series (one frame every 10 s). Protein localization was measured by a line profile (pixel density) traced in each frame as indicated in Materials and Methods and analyzed with the program ImageJ NIH. The resulting net change in PKC $\alpha$  localization is expressed as the  $(I_{mb} - I_{cyt})/I_{mb}$  ratio (R) and is represented versus time.

These results suggest that a combination of AA and intracytosolic Ca $^{2+}$  is needed to induce PKC $\alpha$  anchorage in membranes. To discard the possibility that only the increased level of Ca $^{2+}$  in the cytosol was responsible for this localization effect independently of AA, a control experiment was performed. In that, the MCF-7 cells transfected with PKC $\alpha$ -EGFP were stimulated with only 5  $\mu$ M ionomycin; no membrane localization was observed in this case, indicating that increases in both AA and intracytosolic Ca $^{2+}$  are essential for the localization mechanism of PKC $\alpha$  under these conditions.

Due to these unexpected results, we studied the intracellular concentrations of  $\text{Ca}^{2+}$  occurring in these cells when they were stimulated under the conditions indicated above. For this, MCF-7 cells were loaded with the  $\text{Ca}^{2+}$  indicator Fluo-3 AM and no  $[\text{Ca}^{2+}]_i$  elevation was observed in the cytosol when the cells were stimulated only with AA for 10 min. However, one- to three-fold increases in the basal  $[\text{Ca}^{2+}]_i$  were observed when the cells were stimulated with AA and ionomycin together. The  $[\text{Ca}^{2+}]_i$  was measured also when the cells were stimulated with 5  $\mu\text{M}$  ionomycin and only increments of 1.5-fold or below were observed under these conditions (Fig III.2), suggesting that this increase in  $[\text{Ca}^{2+}]_i$  was not sufficient to translocate  $\text{PKC}\alpha$  to the plasma membrane. Importantly, these data show that AA cooperates with ionomycin to increase the extent of the  $\text{Ca}^{2+}$  influx into the cytosol. Besides, the  $[\text{Ca}^{2+}]_i$  increase overlapped with the membrane localization profile of  $\text{PKC}\alpha$  (compare Figs III.1d and III.2a), suggesting that the increase in  $\text{Ca}^{2+}$  is the mechanism that triggers the targeting of the enzyme to the plasma membrane. However, whether AA participates directly or indirectly in this process is not clear.

To throw light on this question, we examined whether the pre-incubation with AA used in previous experiments (Fig III.1) was indispensable for inducing the membrane localization of  $\text{PKC}\alpha$ . Thus, transfected MCF-7 cells were stimulated directly with 50  $\mu\text{M}$  AA and 5  $\mu\text{M}$  ionomycin. Figure III.3 shows that  $\text{PKC}\alpha$ -EGFP translocated to the plasma membrane and vesicles to the same extent as that seen after pre-incubation with AA. However, when the plasma membrane localization profile was examined versus time (Fig III.3b), it was observed that maximal localization was more slowly attained and obtained at 150 s after stimulation. Importantly, when the intracytosolic concentration of  $\text{Ca}^{2+}$  was measured, increases of only 1.5-fold or less were detected (Fig III.3c). It is important to note that this concentration of  $\text{Ca}^{2+}$  itself was not compatible with protein localization in the plasma membrane (see Fig III.2b), indicating that the direct intervention of AA was necessary to anchor  $\text{PKC}\alpha$  in the plasma membrane and that AA and  $\text{Ca}^{2+}$  cooperate in this process.

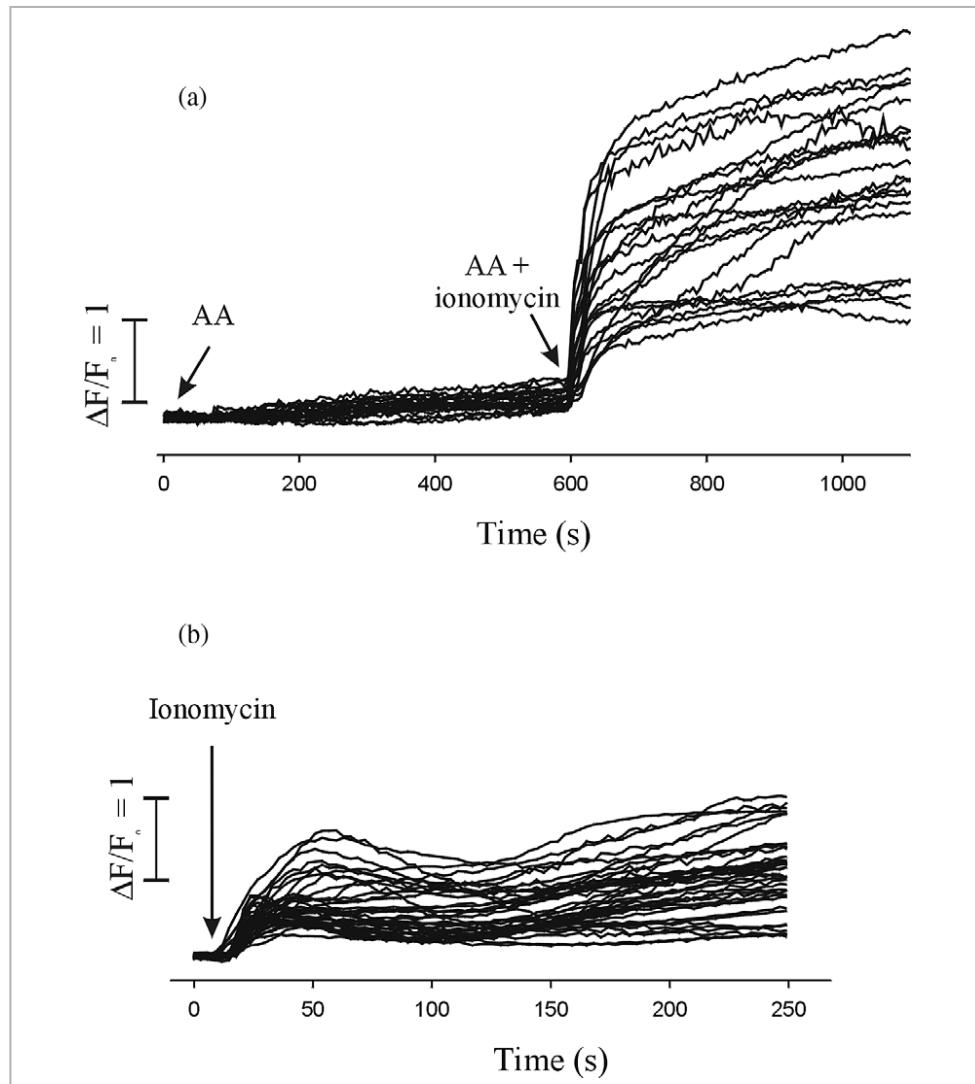


**Figure III.2. [Ca<sup>2+</sup>]<sub>i</sub> fluctuations during the different AA stimulations.** (a) Time-course of [Ca<sup>2+</sup>]<sub>i</sub> fluctuations were monitored with Fluo-3. The Figure shows different profiles representative of the wide range of the [Ca<sup>2+</sup>]<sub>i</sub> observed under the experimental conditions: pre-incubation with 50 μM AA for 10 min and a second stimulation with 50 μM AA + 5 μM ionomycin. (b) The time-course of [Ca<sup>2+</sup>]<sub>i</sub> fluctuations when the cells were loaded with Fluo-3 and stimulated with only 5 μM ionomycin. [Ca<sup>2+</sup>]<sub>i</sub> variations were expressed as  $\Delta F/F_0 = (F_t - F_0)/F_0$ , where  $F_t$  is the fluorescence measured at each recorded time  $t$  and  $F_0$  is the initial fluorescence. The profiles are representative of the variation observed in different cells and correspond to three independent experiments.

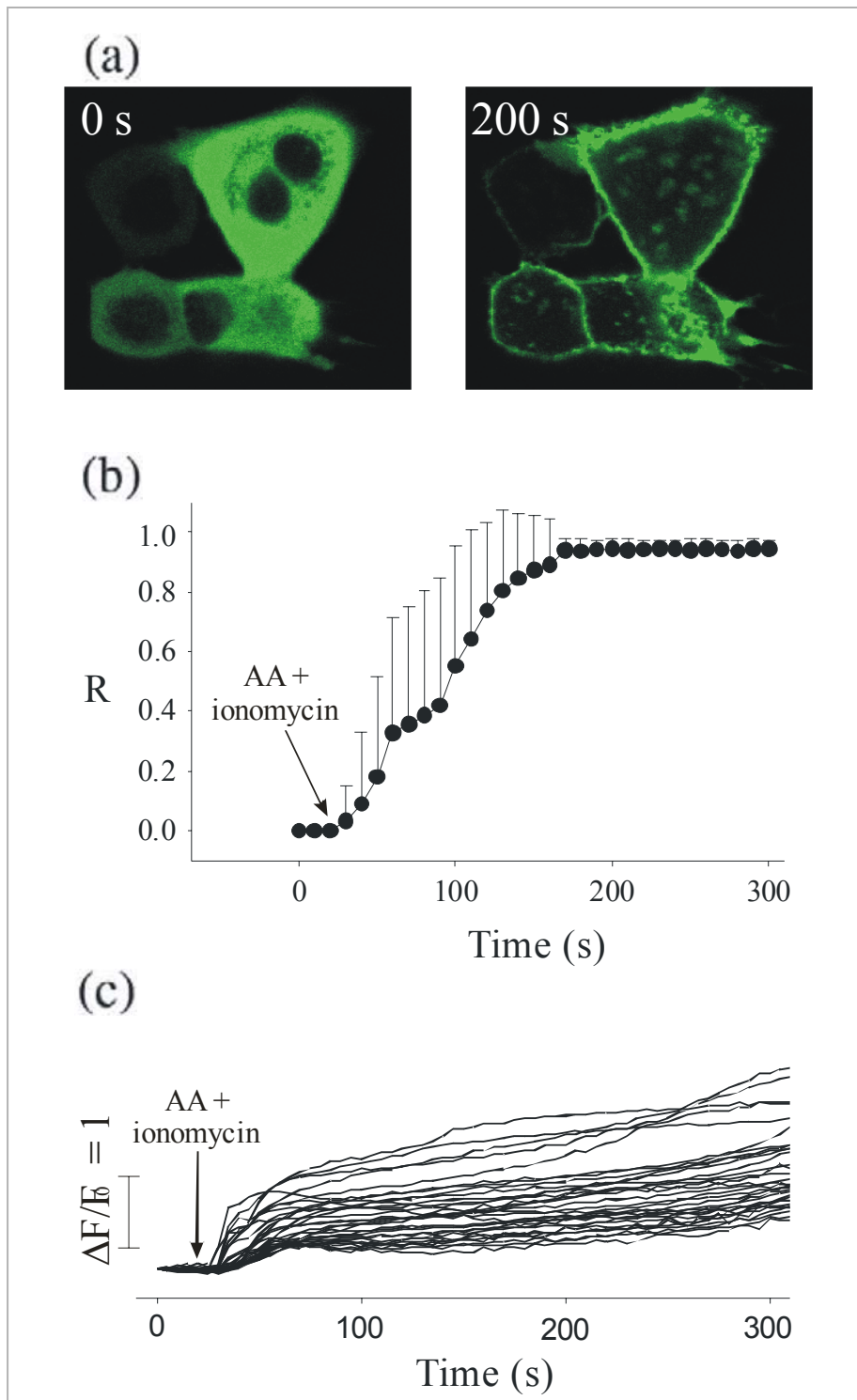


**Figure III.3. PKC $\alpha$  localizes in the plasma membrane of MCF-7 cells with direct stimulation by AA and ionomycin.** (a) Confocal images corresponding to MCF-7 cells treated with 50  $\mu$ M AA + 5  $\mu$ M ionomycin at time zero and 200 s after stimulation. (b) Time-course of the plasma membrane localization of PKC $\alpha$ -EGFP in MCF-7 cells (R). The profile shown is the average of the cells analyzed. Note that the translocation to the membrane profile is slower than in the case shown in Figure III.1, where the cells were pre-incubated with AA for 10 min. (c) Time-course of  $[Ca^{2+}]_i$  fluctuations when the cells were loaded with Fluo-3 and stimulated with only 50  $\mu$ M AA + 5  $\mu$ M ionomycin.  $[Ca^{2+}]_i$  variations are expressed as  $\Delta F/F$ . The profiles are representative of the variation observed in different cells and correspond to three independent experiments.

These results suggest that the pre-incubation with AA favoured both the effect of ionomycin on the Ca<sup>2+</sup> influx and the access of AA to its proper site in the inner leaflet of the plasma membrane. To confirm that, a control experiment was performed by stimulating the cells first with ionomycin for 160 seconds, followed by an addition of 50 $\mu$ M AA. Both the rate of plasma membrane localization and the [Ca<sup>2+</sup>]<sub>i</sub> were measured (Fig III.4). It was observed that the addition of AA after stimulation by ionomycin did not increase the [Ca<sup>2+</sup>]<sub>i</sub> beyond an increase about 1.5-fold, very similar to that observed when ionomycin and AA were added together, thus confirming that the pre-incubation with AA is preconditioning the cells to respond better to additions of ionomycin. When the protein localization in the plasma membrane was measured, it was observed that the translocation rate reached a maximum of only 50% after 440 s of stimulation with AA. It is important to note that under these conditions, AA was inducing a slower translocation rate than when AA and ionomycin were added together, suggesting that this treatment is less favourable to induce the protein localization in the membrane (compare Figs III.3b and III.4a). A more relevant finding is the confirmation that at low [Ca<sup>2+</sup>]<sub>i</sub>, AA is necessary to induce the anchoring of PKC $\alpha$  in the membrane, supporting the hypothesis that Ca<sup>2+</sup> and AA cooperate in this process.

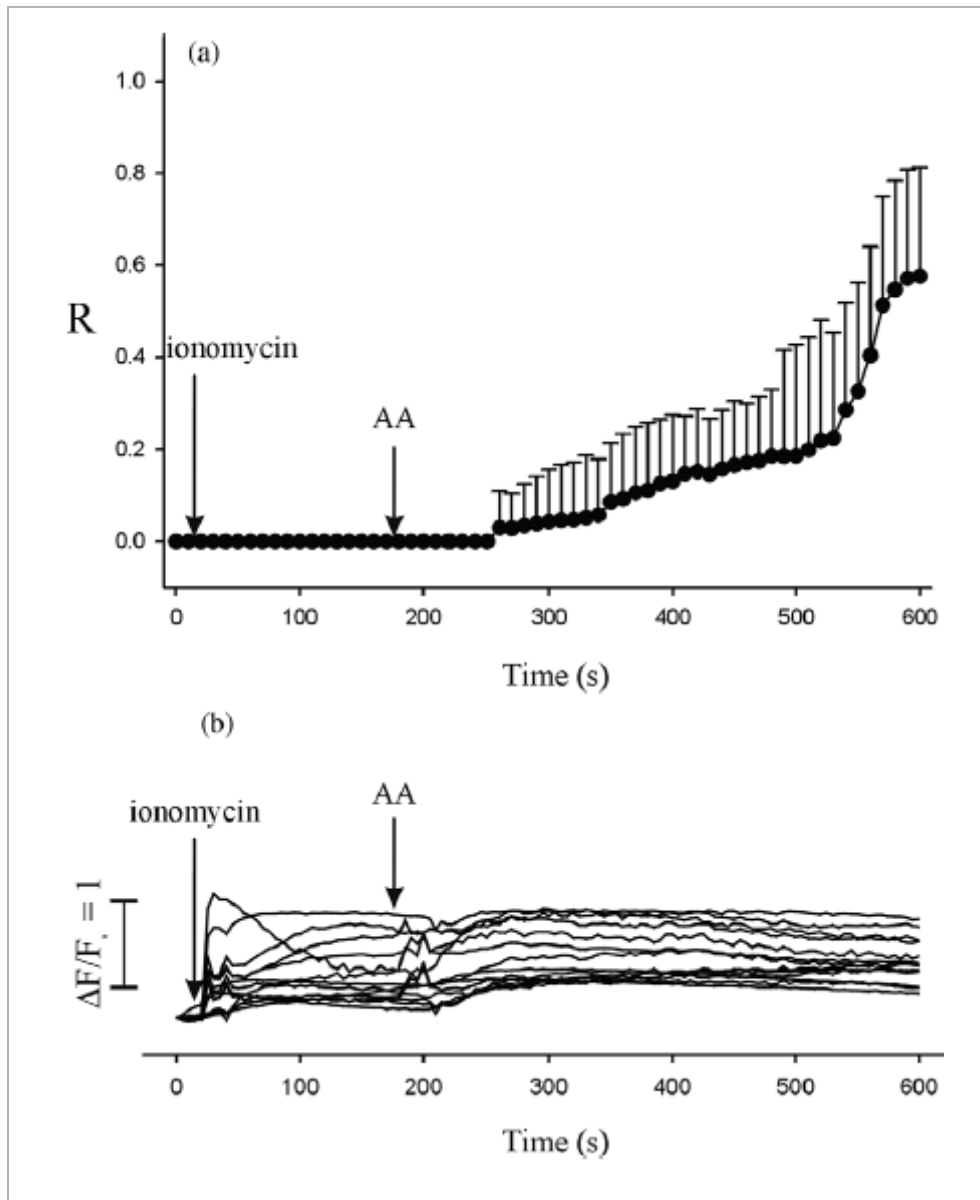


**Figure III.4. The addition of AA after ionomycin stimulation does not induce an increase in the  $\text{Ca}^{2+}$ -influx and slowly induces the AA dependent localization of PKC $\alpha$ .** (a) Time-course of the plasma membrane localization of PKC $\alpha$ -EGFP in MCF-7 cells (R). The cells were stimulated with 5  $\mu\text{M}$  ionomycin and after 160 s the cells were stimulated with 50  $\mu\text{M}$  AA. The profile shown is the average of the cells analyzed. Note that the profile of membrane translocation is slower than in the case shown in Figure III.3. In that case, the cells were stimulated simultaneously with 50  $\mu\text{M}$  AA and 5  $\mu\text{M}$  ionomycin. (b) Time-course of  $[\text{Ca}^{2+}]_i$  fluctuations when the cells were loaded with Fluo-3 and stimulated as stated above.  $[\text{Ca}^{2+}]_i$  variations are expressed as  $\Delta F/F_i$ . The profiles are representative of the variation observed in different cells and correspond to three independent experiments.

## **2.2 The C2 domain of PKC $\alpha$ plays an important role in the AA-dependent membrane localization of the enzyme.**

The complex activation mechanism of PKC $\alpha$  implies a conformational change induced by Ca<sup>2+</sup> that facilitates the accessibility of the C1 domain to its ligands (*Bolsover et al., 2003*). In addition, there is previous evidence suggesting that AA cooperates with DAG in this process (*Murakami and Routtenberg, 1985; Shinomura et al., 1991*), thus making it impossible to state categorically that the Ca<sup>2+</sup>-dependent membrane localization and activation of PKC $\alpha$  was due to a direct interaction between the C2 domain and AA.

To shed light on this possibility, we used two distinct mutants of the C2 domain: one inhibiting the *Ca<sup>2+</sup>-binding region* (PKC $\alpha$ D246N/D248N-EGFP) and the other inhibiting the *lysine-rich cluster* (PKC $\alpha$ K209A/K211A-EGFP). The mutants were expressed transiently in MCF-7 cells, which were stimulated under the same conditions as those expressing the wild-type PKC $\alpha$  (Fig III.5). It was observed that stimulation with AA alone did not induce membrane localization of the mutant proteins. When AA and ionomycin were added together, the mutant corresponding to the *Ca<sup>2+</sup>-binding region* did not localize in membranes. However, the mutant corresponding to the *lysine-rich cluster* localized both in the plasma membrane and vesicles 40 s after stimulation, suggesting that the substitution of these Lys residues by Ala does not affect the ability of the mutant to interact with membranes. On the contrary, it slightly increased the translocation rate into the plasma membrane.

Taken together, these results confirm the hypothesis that the C2 domain of PKC $\alpha$  plays an important role in the AA-dependent membrane localization and that the *Ca<sup>2+</sup>-binding region* is essential for this translocation to plasma membrane, while the *lysine-rich cluster* does not play a critical role in this process.

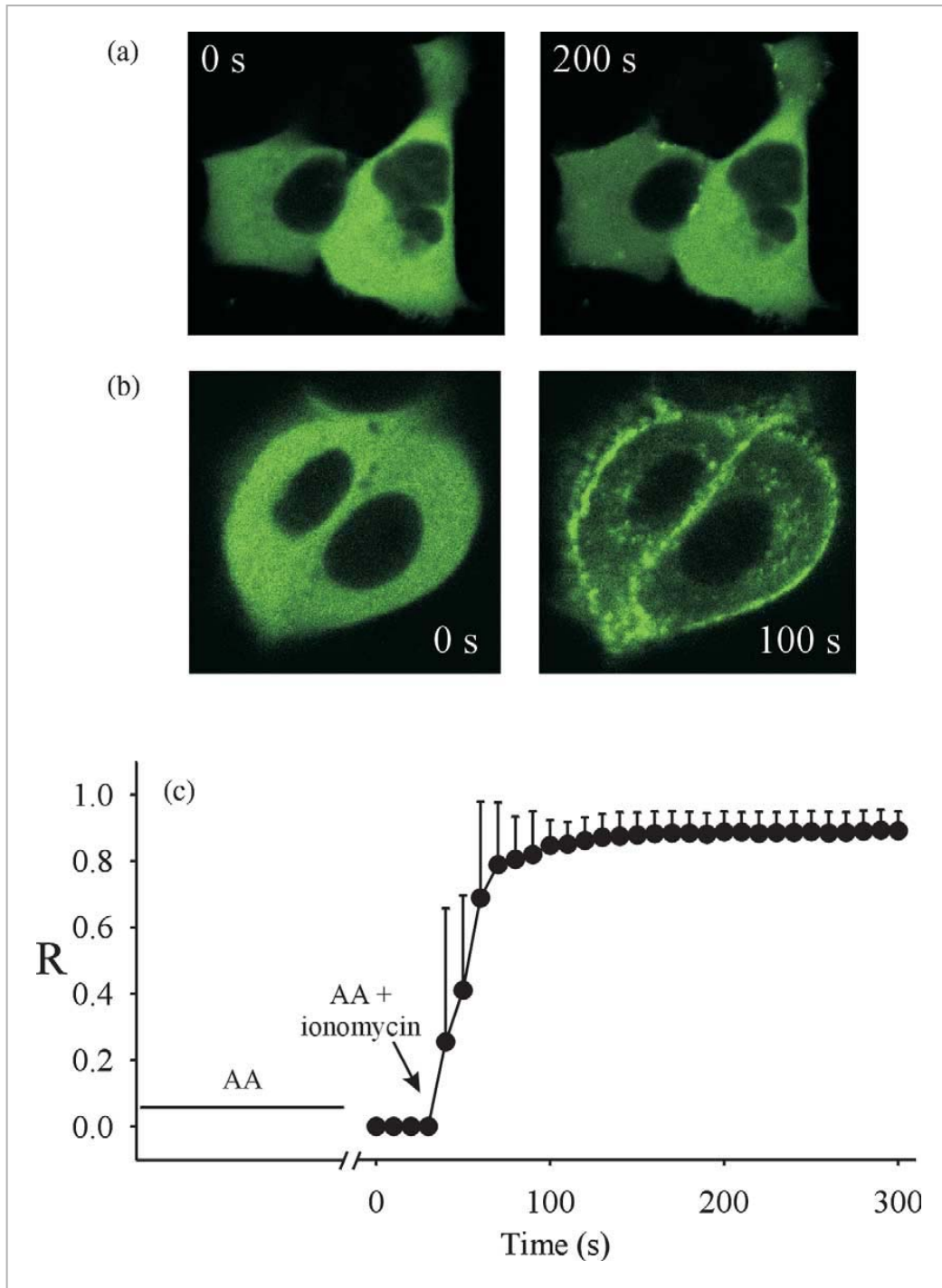


**Figure III.5. The  $Ca^{2+}$ -binding region in the C2 domain is a key motif for the AA-dependent localization of PKC $\alpha$ .** (a) Confocal images of MCF-7 cells expressing PKC $\alpha$ D246N/248N-EGFP and incubated with 50  $\mu$ M AA for 10 min and with 50  $\mu$ M AA + 5  $\mu$ M ionomycin afterwards. The frames shown correspond to time zero and 200 s after the second stimulation with AA + ionomycin. (b) Confocal images of MCF-7 cells expressing PKC $\alpha$ K209A/K211A-EGFP and treated under the conditions used for (a). (c) PKC $\alpha$ K209A/K211AEGFP fluorescence intensity was measured in the cytosol and in the plasma membrane in every frame of the time series (one frame every 10 s). The protein localization was measured by a line profile (pixel density) traced in each frame as indicated in Material and Methods. The resulting net change in the mutant PKC $\alpha$  localization is expressed as the  $(I_{mb} - I_{cyt})/I_{mb}$  ratio (R) and is represented versus time.

To further confirm the direct interaction of AA and the C2 domain, we employed the isolated C2 domain of PKC $\alpha$ , expressed in *Escherichia coli* and highly purified (García-García *et al.*, 1999), to monitor the protein-to-membrane fluorescence resonance of energy transfer (FRET) signal using lipid vesicles containing 40 mol% AA, 55 mol% POPC and 5 mol% N-(5-dimethylaminonaphthalene-1-sulfonyl)-1,2-dihexadecanoyl-sn-glycero-3-phosphoethanolamine (dansyl-DHPE). The binding ability of the C2 domain was tested by titrating increasing concentrations of the AA/POPC/DHPE mixture. As shown in Figure III.6, the FRET increased with the amount of lipid mixture added to the C2 domain in the presence of 200  $\mu$ M CaCl $_2$ , reaching a maximum of 0.5 with a  $K_D$  calculated at 6.52  $\mu$ M, and a Hill index of 1.66, suggesting a cooperative effect between Ca $^{2+}$  and the AA molecule. It is important to observe that when 0.5 mM EGTA was included in the assay, no FRET was observed between the C2 domain and the lipid vesicles, indicating that no interaction with the membranes occurs under these conditions.

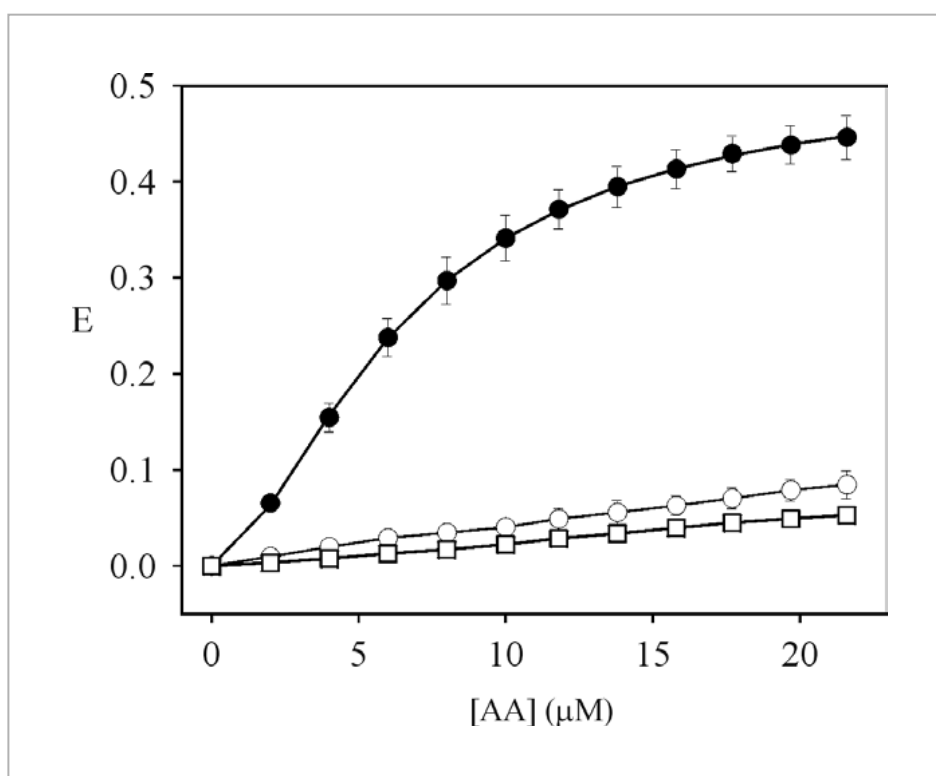


**Figure III.6. AA binds specifically to the PKC $\alpha$ -C2 domain.** A lipid mixture containing POPC/AA/DHPE (55:40:5 mol%) was titrated into a solution containing 0.5  $\mu$ M PKC $\alpha$ -C2 domain, 20 mM Hepes (pH 7.4), 100 mM NaCl, 0.1 mM CaCl $_2$  (●) or 0.5 mM EGTA (○). As a control, a lipid mixture containing POPC/DHPE (95:5 mol%) was titrated into a solution containing 0.5  $\mu$ M PKC $\alpha$ -C2 domain, 20 mM Hepes (pH 7.4), 100 mM NaCl, 0.1 mM CaCl $_2$  (□). Protein docking was assessed by protein-to-membrane FRET, using donor fluorescence to quantify the FRET. The continuous lines represent the best fit of the resulting FRET signal to the Hill equation.

### **2.3. Role of the C1 domain of PKC $\alpha$ in the AA-dependent membrane localization.**

To determine the role of individual C1 domains in the AA-dependent membrane localization of PKC $\alpha$ , we mutated prominent hydrophobic residues located along the rim of the diacylglycerol/phorbol ester-binding pocket that are exposed to the surface and oriented toward the membrane (*Zhang et al., 1995*) and have been demonstrated to be important for the membrane penetration and subsequent activation of PKC $\alpha$  (*Medkova and Cho, 1999*). Thus, we generated two mutants of the C1A domain, where the Trp58 and Phe60 were substituted by Gly (PKC $\alpha$ W58G-EGFP and PKC $\alpha$ F60G-EGFP) and two mutants of the C1B domain, in which Tyr123 and Leu125 were substituted by Gly (PKC $\alpha$ Y123G-EGFP and PKC $\alpha$ L125G-EGFP).

To understand how the C1 domain participates in the AA-dependent localization of PKC $\alpha$ , we monitored the membrane localization of the different C1 domain mutants fused to EGFP. Membrane translocation was induced by treating transiently transfected MCF-7 cells with 50  $\mu$ M AA and 10 min later with 50  $\mu$ M AA and 5  $\mu$ M ionomycin. Figure III.7 shows the plasma membrane localization profile obtained for each mutant. The PKC $\alpha$ W58G-EGFP mutant demonstrated the most damaging effect on membrane localization, since only about 70% of the protein was localized in the plasma membrane and, most importantly, the mutant protein became almost dissociated from the plasma membrane 200 s after stimulation, as shown in the time-lapse images (Fig III.7a). A smaller effect was observed in the case of the PKC $\alpha$ F60G-EGFP mutant, although this protein also exhibited a tendency to dissociate from membranes at a higher rate than the wild-type protein (Fig III.7b). Importantly, no effect was observed in the case of the PKC $\alpha$ L125G-EGFP mutant, where the protein was maximally localized in the plasma membrane 40 s after stimulation by 50  $\mu$ M AA and 5  $\mu$ M ionomycin (Fig III.7c). Similar results were observed for the PKC $\alpha$ Y123G-EGFP mutant (data not shown).

Taken together, these data suggest that the residues found on the edge of the ligand-binding pocket in the C1A domain, mainly Trp58, are important for the AA-induced membrane localization of PKC $\alpha$ , while the C1B domain does not seem to play a critical role in this localization mechanism.

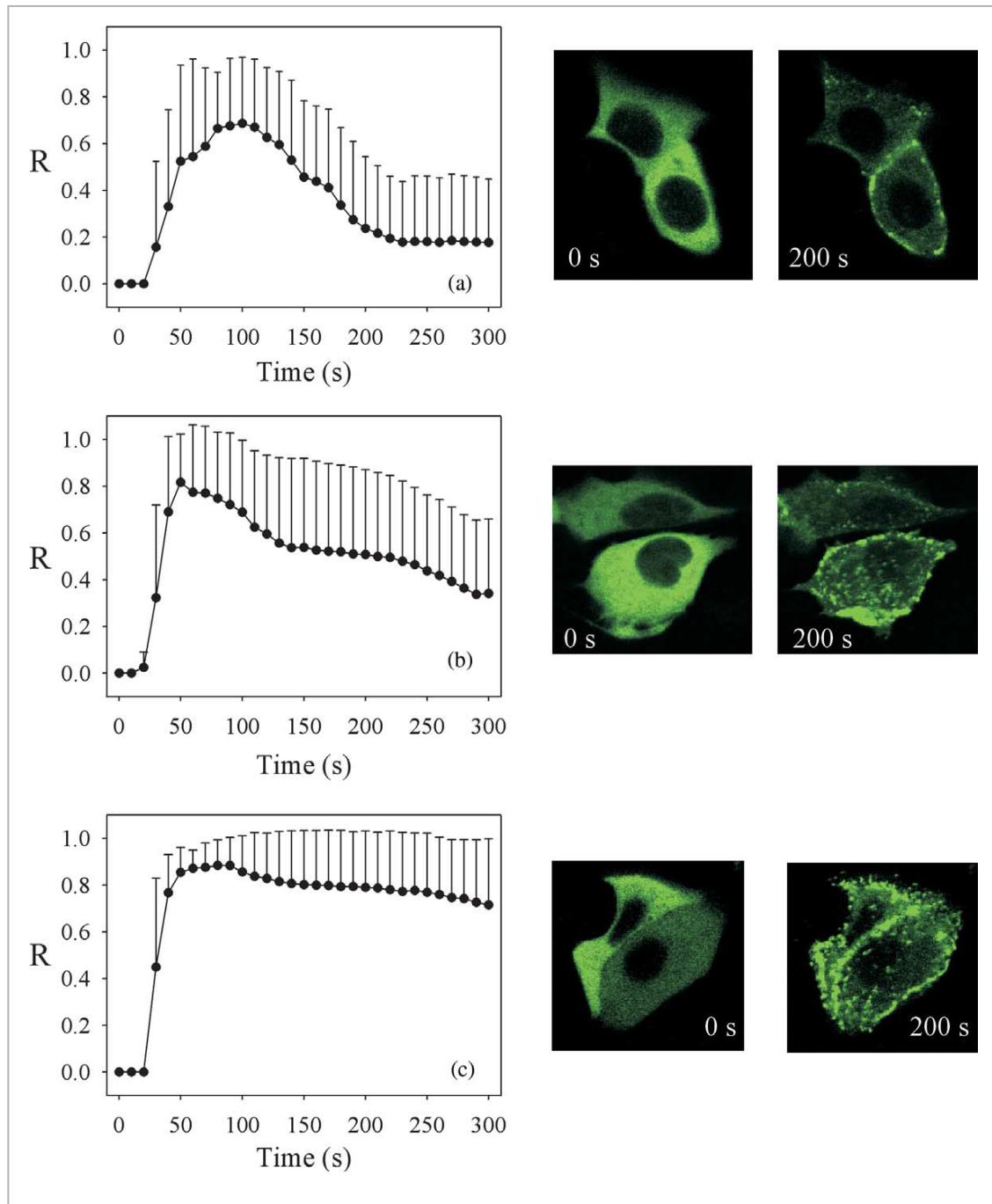


**Figure III.7. Role of the C1 subdomains in the AA-dependent localization of PKC $\alpha$ .** The mutants used in this assay were (a) PKC $\alpha$ W58G-EGFP, (b) PKC $\alpha$ F60G-EGFP and (c) PKC $\alpha$ L125G-EGFP. The activation was performed by pre-incubation of the cells with 50  $\mu$ M AA for 10 min followed by a second activation with 50  $\mu$ M AA + 5  $\mu$ M ionomycin. Protein localization was measured by a line profile (pixel density) traced in each frame as indicated in Material and Methods. The resulting net change in the mutant PKC $\alpha$  localization is expressed as the  $(I_{mb}-I_{cyt})/I_{mb}$  ratio ( $R$ ) and is represented versus time.



## CHAPTER IV

### EFFECT OF OLEIC ACID ON BREAST CANCER CELLS THROUGH PKC $\alpha$



## 1. Introduction.

It has long been thought that there might exist a positive relation between high fat diets and the high incidence of some types of cancer. However, it is now known that what is really important is the type of fat and not so much the quantity, which would explain the low incidence of breast, colon and skin cancer in Mediterranean countries where much olive oil is consumed. A similarly protective effect of olive oil is supposed in the case of cardiovascular diseases which also have a relatively low incidence in these countries. This effect is supposedly largely due to the fact that olive oil contains high quantities of oleic acid (OA), a monounsaturated fatty acid (18:1 n-9) (Trichopoulou *et al.*, 2000).

This 'dietary fat hypothesis' has been supported by a number of epidemiological and experimental data, which, taken together, providing evidence that dietary or exogenously derived fatty acids may play an important role in carcinogenesis and the evolution and/or progression of breast cancer (Pariza, 1987; Wynder *et al.*, 1997). However, more recent studies in laboratory animals and prospective epidemiological studies have generated results that do not support this strong association (Holmes *et al.*, 1999; Lee and Lin, 2000).

The results of studies with olive oil are of particular interest. On the one hand, the strongest evidence that monounsaturated fatty acids such as OA may influence the risk of developing breast cancer comes from studies in southern European populations, in whom intake of OA sources, particularly olive oil, might appear to be protective (Assman *et al.*, 1997; Lipworth *et al.*, 1997). On the other hand, research in cell lines and animal models have yielded inconsistent results ranging from non-promoting or low-promoting effects to be protective in the case of breast cancer (Zusman *et al.*, 1997; Bartsch *et al.*, 1999).

These conflicting results may be explained in part by the fact that olive oil was supplied to the animals or subjects rather than oleic acid alone. It is known that olive oil is composed of oleic acid and variable amounts of secondary compounds like squalene and phenolic constituents, which are present in different quantities in different types and varieties of the olives used to manufacture the oil, and contribute to antioxidant effect of olive oil (Hardy *et al.*, 1997; Martin-Moreno, 2000).

Moreover, our understanding of the specific molecular mechanisms by which fatty acids such as OA may exert an effect on breast cancer is relatively poor. At present, one hypothesis is that OA may protect against oxidative stress by being incorporated into the phospholipid membrane of breast tissue cells, resulting in a reduction in lipid peroxidation (Gill *et al.*, 2005). Besides

this preventive role, some reports have demonstrated that oleic acid cooperates with some standard drugs used in cancer treatment, promoting their anti-proliferative and/or pro-apoptotic effects (*Menendez et al., 2005*).

Neoplastic development is believed to be a multi-step process involving the expression of several oncogenes, like *fos* and *myc*, and the differential regulation of oncoproteins like Ras. PKC was initially seen to be involved in cancer when, in 1983, Kikkawa and co-workers and Leach and co-workers discovered that this kinase was a high-affinity intracellular receptor for the phorbol-ester tumour promoter. In later research, PKC was also related with onco-proteins (*Hsiao et al., 1989; Han et al., 1995*) placing this enzyme at the core of cancer signalling pathways. Nowadays, we know that the expression of PKC isoenzymes is deregulated in cancer, being over- or under-expressed, depending on isoform and type of cancer.

It has been observed that, in general, PKC $\alpha$  is over-expressed in breast cancer (*Tonetti et al., 2002*), in which it has been associated with malignant transformation, tumour cell proliferation, multi-drug resistance, the alteration of ER status and apoptosis.

In the recent past, olive oil intake was seen to act as a negative modulator of breast cancer in a 7,12-dimethylbenz(a)anthracene (DMBA)-induced mammary tumorigenesis model in rats, conferring a more benign clinical behaviour and a lower histopathological malignancy in the tumour (*Solanas et al., 2002*). Moreover, this effect was accompanied by a decrease in the mRNA coding for the oncogene *erbB-2* (*Moral et al., 2003*).

To shed light on the role of oleic acid in breast cancer, we investigated the effect of this monounsaturated fatty acid on several breast cancer cell lines in relation to PKC $\alpha$ . First, we ran some kinase activity assays and other assays on the plasma membrane localization of PKC induced by OA, using wild type and some mutants of functional domains. Moreover, we measured the proliferation, migration, invasion and apoptosis rate of culture cells incubated with this fatty acid. We also used cells in which PKC $\alpha$  expression was inhibited by siRNA and the effect on these cellular events was also measured.

## 2. Results.

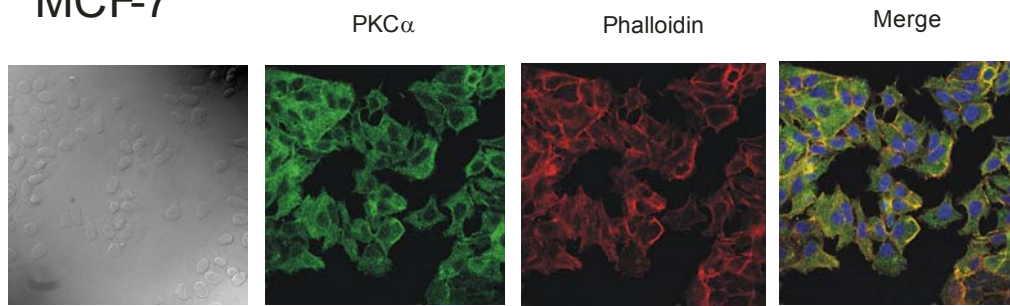
### 2.1. Oleic acid induces PKC $\alpha$ plasma membrane translocation and co-localization with actin filaments in breast cancer cells.

To investigate the effect of OA on PKC $\alpha$ -plasma membrane interaction, we studied the subcellular localization of the endogenous protein in MCF-7, BT-474 and MDA-MB-231 cells by immunofluorescence (PKC $\alpha$ -green-AlexaFluor 488) and F-actin polymerization by AlexaFluor 633-phalloidin labelling. Cells were treated for 48 h in growth medium in the presence and in the absence of 50  $\mu$ M OA (Fig IV.1).

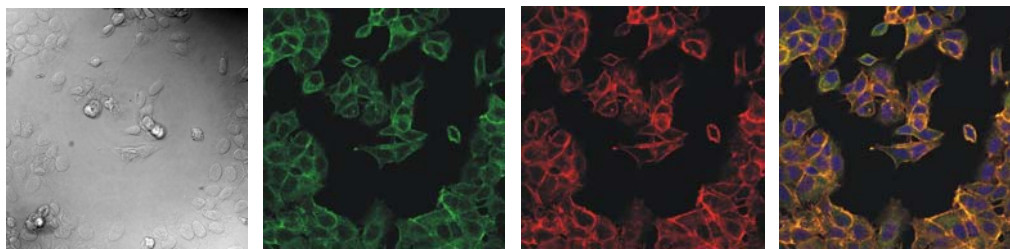
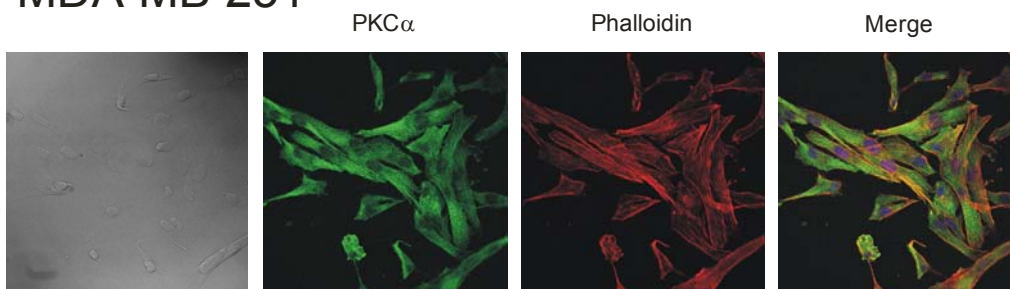
In resting conditions, the three cell lines tested showed PKC $\alpha$  distributed homogeneously throughout the cytosol with a very low percentage (approximately 9%) of cells exhibiting protein localized at the plasma membrane. After 48 hours in the presence of OA-BSA, the percentage of PKC $\alpha$  localized in the plasma membrane of the cells significantly increased to an extent that depended on the individual cell line. In MCF-7, approximately 3/4 of cells showed PKC $\alpha$  in the plasma membrane; in BT-474 half of the cells exhibited PKC $\alpha$  in the plasma membrane and in MDA-MB-231 hardly any cells were thus localized (Table IV.1). This suggests that OA may induce the translocation of PKC $\alpha$  from the cytosol to the plasma membrane and enhances its permanence in this compartment of breast cancer cells.

**Table IV.1. PKC $\alpha$  localization percentages upon OA stimulation**

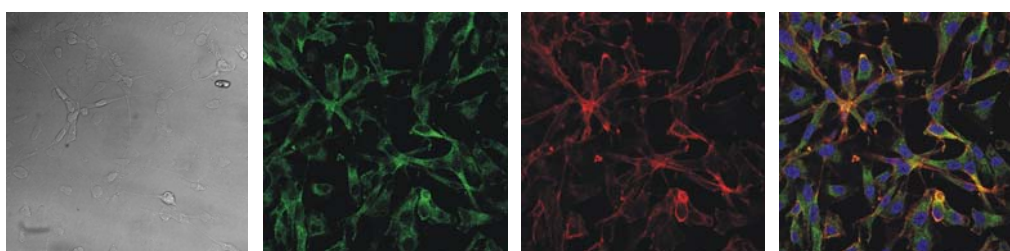
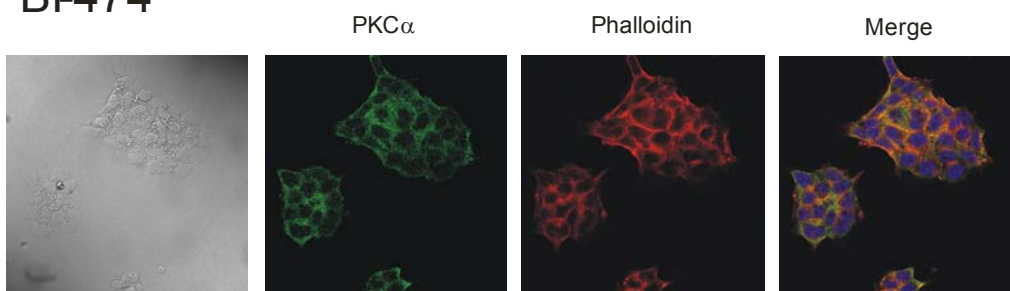
<b>CELL LINE</b>	<b>PKC<math>\alpha</math> LOCALIZATION PERCENTAGE IN RESTING CONDITIONS</b>	<b>PKC<math>\alpha</math> LOCALIZATION PERCENTAGE AFTER OA STIMULATION</b>
MCF-7	13.9 $\pm$ 6.9	73.0 $\pm$ 10.2
BT-474	5.0 $\pm$ 1.4	58.5 $\pm$ 6.7
MDA-MB-231	7.9 $\pm$ 4.8	28.4 $\pm$ 3.5

**MCF-7**

siRNAcontrol

siRNAcontrol + 50 $\mu$ M OA**MDA-MB-231**

siRNAcontrol

siRNAcontrol + 50 $\mu$ M OA**BT474**siRNAcontrol + 50 $\mu$ M OA

Since actin dynamics is correlated with cancer cell migration and invasion, we also studied the degree of actin polymerization after OA treatment. It was observed that OA induced the formation of F-actin rich structures at the edges of the cells that were co-localized with PKC $\alpha$  in the plasma membrane in MCF-7 and BT-474 cells (Fig IV.1).

Unlike in these two previous cell lines, stimulation with OA led to the almost total disappearance of actin fibres in MDA-MB-231 and the remaining cytoskeleton protein was spread homogeneously through the cytoplasm (Fig IV.1).

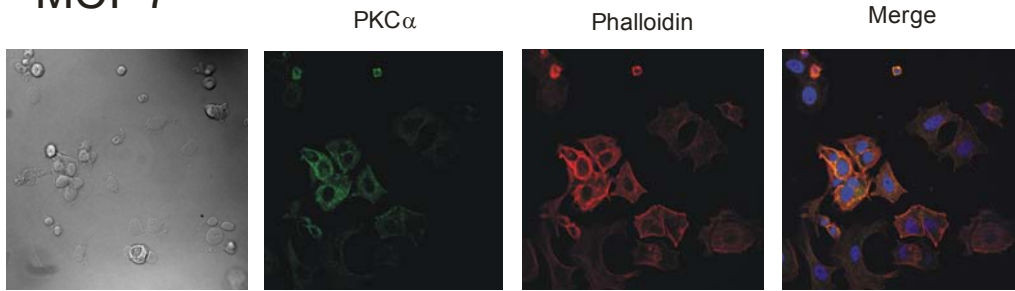
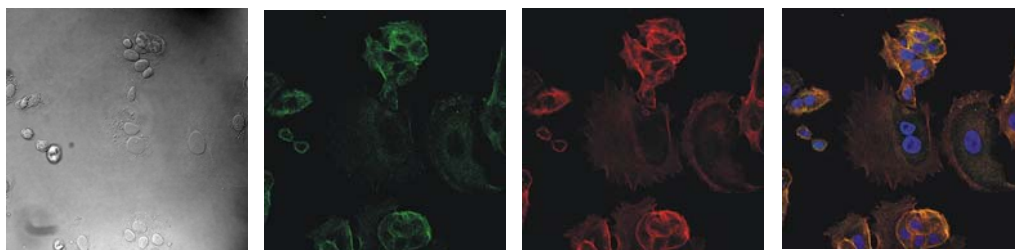
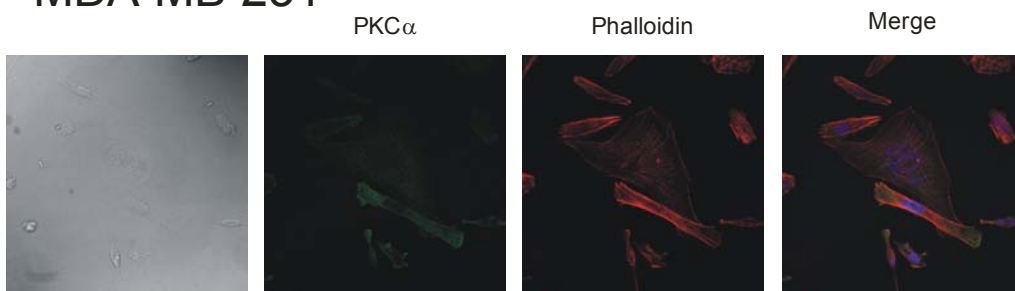
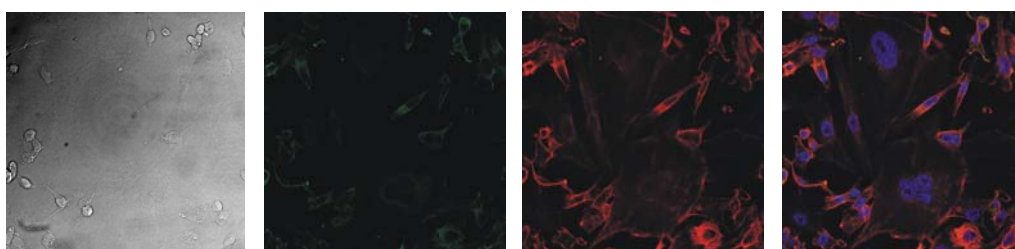
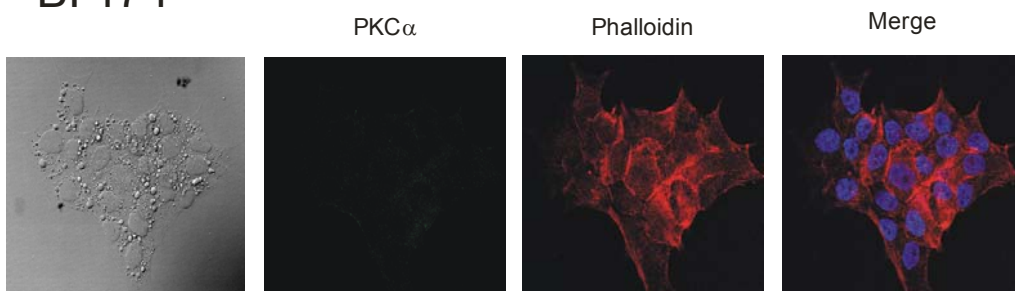
Moreover, we studied the role of PKC $\alpha$  in these cell lines by inhibiting its expression through specific siRNA $\alpha$ . In MCF-7 cells, the down-regulation of PKC $\alpha$  produced a slight increase in cell size and a lower degree of actin polymerization close to the plasma membrane, whereas the nuclei were not affected (Fig IV.2). These effects were even more evident when OA was added to MCF-7 cells without PKC $\alpha$ , when the cells increased in size and were more spread out (Fig IV.2).

In the case of BT-474 cells, the morphology and size hardly changed when PKC $\alpha$  was down-regulated, although it was observed that F-actin polymerization was disorganized, and only small zones in the plasma membrane showed real actin fibres. When we added OA to these mutant cells, the actin rich structures at the edge of the cells disappeared and the cytoplasm exhibited numerous large granules (Fig IV.2).

With regard to MDA-MB-231 cells, the typical fibroblast-like morphology of control cells was lost when PKC $\alpha$  expression was inhibited. The mutant cells were bigger, more rounded and more spread than control cells. In addition, the nuclei were fragmented, suggesting an apoptotic process (Fig IV.2). It was also found that the effect of OA on these cells without PKC $\alpha$  was somewhat similar to the effect seen in MCF-7 cells, that is, the effects on cell size and shape and cortical actin disorganization were even more pronounced (Fig IV.2).

---

**Figure IV.1. PKC $\alpha$  and F-actin co-localized in the plasma membrane of MCF-7, MDA-MB-231 and BT-474 breast cancer cell lines.** Cells were fed with growth medium (upper panels of each cell line) or 50  $\mu$ M OA-BSA during 48 hours (bottom panels), fixed with formaldehyde and processed for immunolabeling by using polyclonal Ab to PKC $\alpha$  (detected by using secondary Ab coupled to AlexaFluor 546), F-actin was determined by AlexaFluor633 labelled-phalloidin and DAPI staining was used to detect nuclei. RGB merged images including Alexa Fluor 546, Alexa Fluor 633 and DAPI are shown in the right panel (merge).

**MCF-7**siRNA $\alpha$ siRNA $\alpha$  + OA 50  $\mu$ M**MDA-MB-231**siRNA $\alpha$ siRNA $\alpha$  + OA 50  $\mu$ M**BT474**siRNA $\alpha$  + OA 50  $\mu$ M

## 2.2. Characterization of the activation mechanism of PKC $\alpha$ by oleic acid.

To study whether OA was involved directly in the activation of the enzyme, we measured the effect of increasing concentrations of this fatty acid on the catalytic activity of purified HA-PKC $\alpha$ . No activation of PKC $\alpha$  was detected in the presence of EGTA, and so the enzymatic activity was determined in the presence of saturating concentrations of Ca $^{2+}$  (0.2 mM). The results showed that the catalytic activity of the enzyme increased in parallel with the concentration of OA in the lipid vesicles, reaching maximal activity at 30 mol% OA, suggesting that this monounsaturated fatty acid itself is a potential activator of PKC $\alpha$  (Fig IV.3).

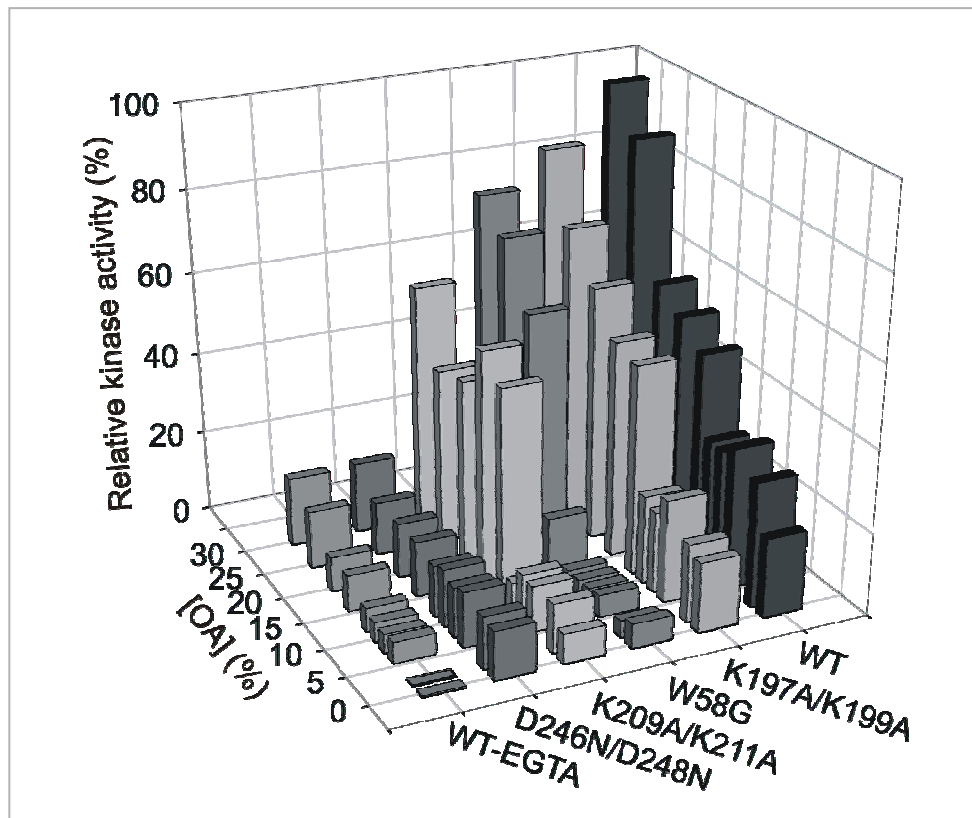


**Figure IV.3. Oleic acid-dependence of PKC $\alpha$  activities.** Proteins used in this study include wild-type PKC $\alpha$ , a mutant of *Calcium Binding Region* (PKC $\alpha$ D246N/D248N), two mutants of *Lysine Rich Cluster* (PKC $\alpha$ K197A/K199A and PKC $\alpha$ K209A/K211A) and a C1A subdomain mutant (PKC $\alpha$ W58G).

**Figure IV.2. Effect of down-regulating PKC $\alpha$  on morphology and subcellular localization of actin in MCF-7, MDA-MB-231 and BT-474 cells.** PKC $\alpha$  expression was inhibited with siRNA (see section II. Material and Methods). Cells were treated, fixed and fed as describe in figure IV.1.

Once it was demonstrated that OA can activate PKC $\alpha$  in a Ca<sup>2+</sup>-dependent manner, we studied the activation of several mutants in functional domains in order to identify the role of every domain in the activation mechanism of PKC $\alpha$  by oleic acid.

Three mutants of C2 domain were used, one of the *Calcium Binding Region* (PKC $\alpha$ D246N/D248N) and two of the *Lysine rich cluster* (PKC $\alpha$ K197A/K199A and PKC $\alpha$ K209A/K211A), and one mutant of the C1A subdomain. The kinase activity of each mutant was measured using increasing concentrations of OA in the lipid vesicles and the results were compared with those obtained for the wild type protein (Fig IV.3).

It was demonstrated that the ability of the HA-PKC $\alpha$ D246N/D248N mutant to be activated by OA was completely abolished, even at 30 mol% OA and saturating concentrations of Ca<sup>2+</sup>. As regards the *lysine rich cluster* mutants, differences in their kinase activity were found: while HA-PKC $\alpha$ K197A/K199A exhibited a similar degree of activation to the wild type, HA-PKC $\alpha$ K209A/K211A showed 40% inhibition at high concentration of OA.

The C1A subdomain mutant, HA-PKC $\alpha$ W58G, exhibited a slight inhibition of enzymatic activity at a low concentration of OA, but when the amount of fatty acid increased, the activation degree recovered and was similar to wild type protein.

Taken together, these results confirm the hypothesis that the C2 domain of PKC $\alpha$  plays an important role in the OA-dependent activation of the enzyme, and that the *Ca<sup>2+</sup>-Binding Region* is essential for the activation mechanism. On the other hand, the *lysine-rich cluster* does not play such a critical role in the activation of the enzyme, lysines 209 and 211 being the most important ones in this process. Moreover, it is suggested that the C1A subdomain might also participate in the OA-dependent activation of PKC $\alpha$ .

### **2.3. Oleic acid induces the PKC $\alpha$ translocation to plasma membrane in a Ca<sup>2+</sup>-dependent manner.**

To investigate whether OA induces the localization of PKC $\alpha$  in the plasma membrane, BT-474 cells were transfected with a fluorescent construct consisting of PKC $\alpha$  fused to EGFP (PKC $\alpha$ -EGFP). In steady-state conditions, the protein was distributed homogeneously through the cytosol. When the cells were stimulated with 50  $\mu$ M OA, no effect was observed on enzyme localization (Fig IV.2) and the protein remained in the cytosol. However, the addition of 5  $\mu$ M ionomycin resulted in maximal plasma membrane localization of PKC $\alpha$ , where it remained for at least 200 s (Fig IV.4).

These results suggest that a combination of OA and intracytosolic Ca<sup>2+</sup> is needed to induce PKC $\alpha$  anchorage in the plasma membrane. To discard the possibility that only the increased level of Ca<sup>2+</sup> in the cytosol was responsible for this localization effect independently of OA, a control experiment was performed, in which the BT-474 cells transfected with PKC $\alpha$ -EGFP were stimulated with only 5  $\mu$ M ionomycin. In this case no membrane localization was observed, indicating that increases in both OA and intracytosolic Ca<sup>2+</sup> are essential for the localization mechanism of PKC $\alpha$  under these conditions.

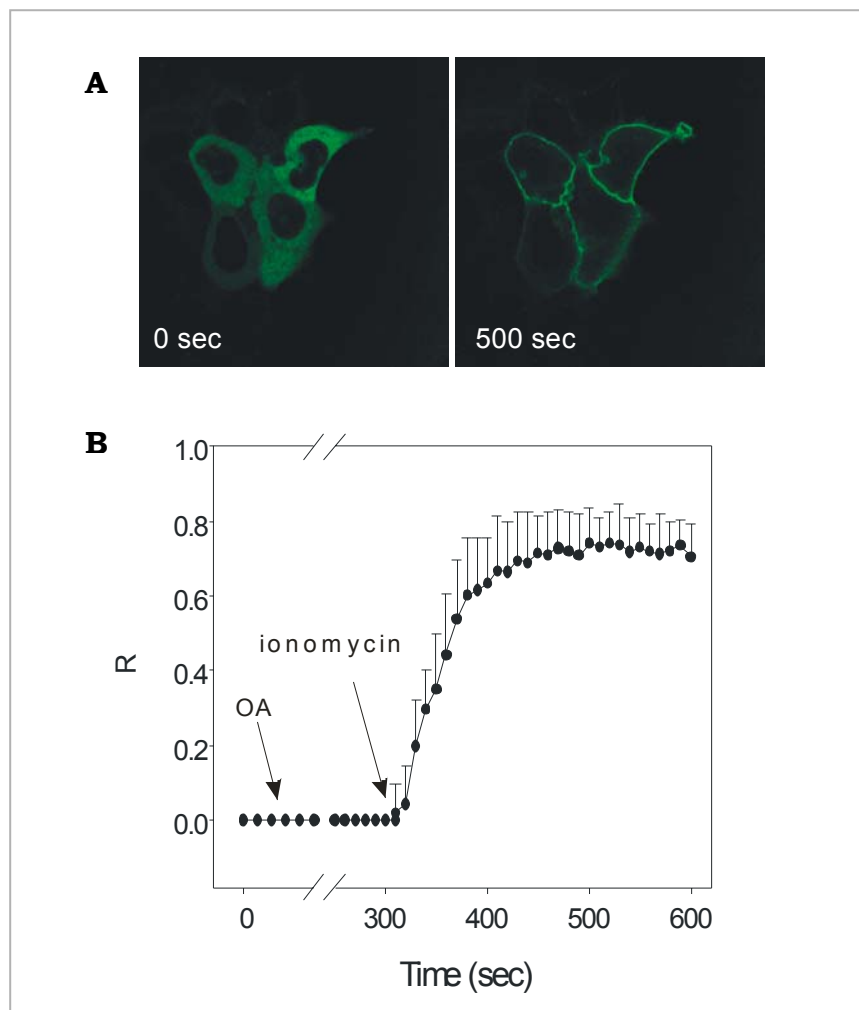


**Figure IV.4. Oleic acid induces the PKC $\alpha$  translocation to the plasma membrane of BT-474 cells in a Ca<sup>2+</sup>-dependent manner.** A) Confocal micrographs of BT-474 cells expressing PKC $\alpha$ -EGFP in resting conditions and 200 seconds after stimulation with 5  $\mu$ M ionomycin (500 sec after initial stimulation with 50  $\mu$ M OA). B) PKC $\alpha$ -EGFP fluorescence intensity was measured in the cytosol and in the plasma membrane in every frame of the time-series (one frame every 10 s). Protein localization was measured by a line profile (pixel density) traced in each frame as indicated in Materials and Methods. The resulting net change in PKC $\alpha$  localization is expressed as the  $I_{mb} - I_{cyt} / I_{mb}$  ratio (R) and is represented *versus* time.

Following these results, we studied the intracellular concentrations of  $\text{Ca}^{2+}$  occurring in these cells when they were stimulated under the conditions indicated above. For this, two breast cancer cell lines (BT-474 and MCF-7) and another cell line derived from non-tumorigenic breast tissue (MCF-10A) were loaded with the  $\text{Ca}^{2+}$  indicator Fluo-3 AM. Surprisingly, a transient approximately two-fold increase in the basal  $[\text{Ca}^{2+}]_i$  was observed in the cytosol when the tumorigenic cells were stimulated with 50  $\mu\text{M}$  OA (Fig IV.5), whereas no  $[\text{Ca}^{2+}]_i$  fluctuation was found in MCF-10A cells. However, the  $[\text{Ca}^{2+}]_i$  increase in BT-474 and MCF-7 was not sufficient to translocate  $\text{PKC}\alpha$  to the plasma membrane, as happens when 5  $\mu\text{M}$  ionomycin is added to cells.

These results suggest that the initial  $[\text{Ca}^{2+}]_i$  increase produced after OA stimulation is not sufficient to translocate  $\text{PKC}\alpha$  to the plasma membrane, perhaps because the fatty acid has not reached the inner leaflet of the plasma membrane.

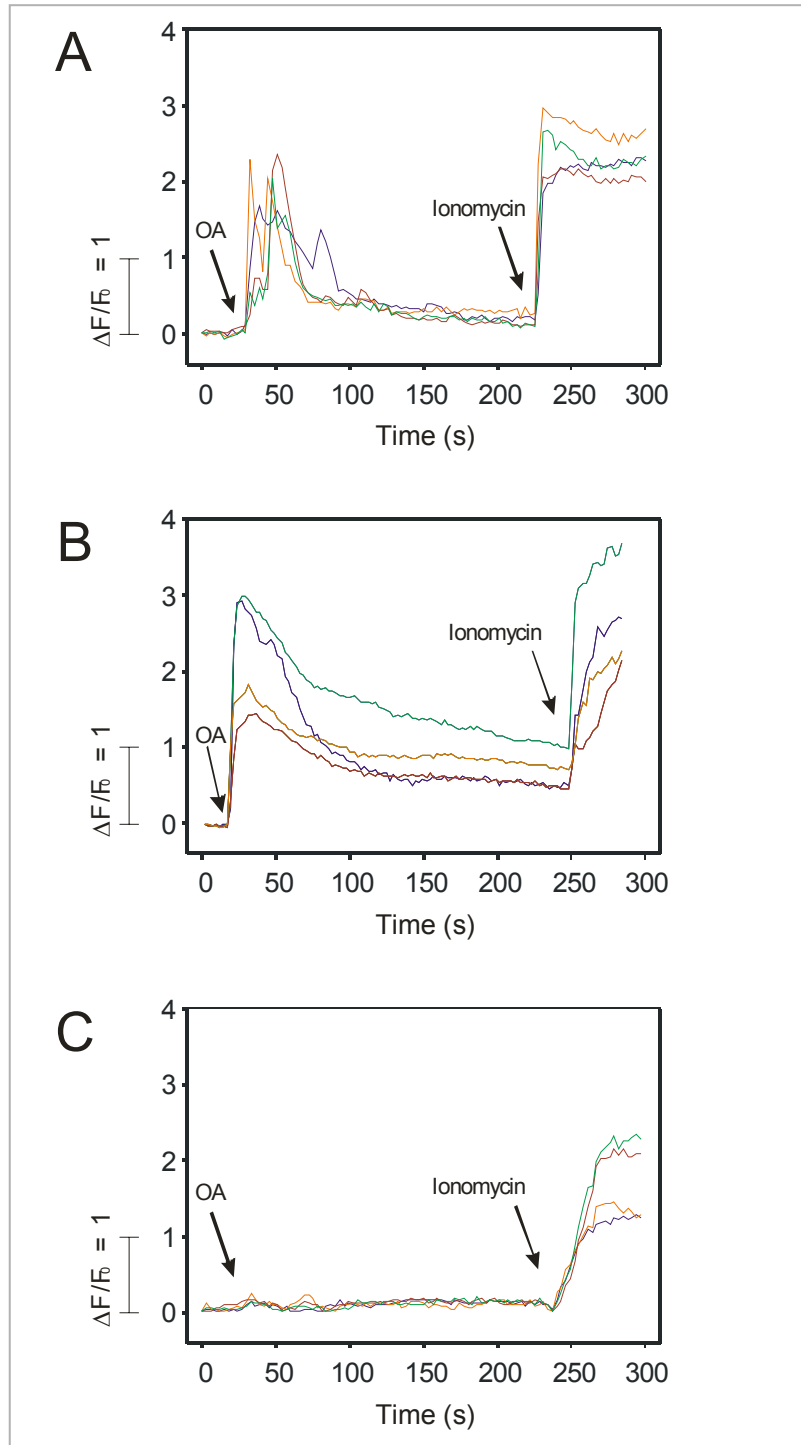


**Figure IV.5.  $[Ca^{2+}]_i$  fluctuations during the different stimulations in BT-474 (A), MCF-7 (B) and MCF-10A (C).** Time-course of  $[Ca^{2+}]_i$  fluctuations were monitored with Fluo-3. The Figure shows different profiles representative of the wide range of the  $[Ca^{2+}]_i$  observed under the experimental conditions: stimulation with 50  $\mu$ M OA and a second stimulation with 5  $\mu$ M ionomycin.  $[Ca^{2+}]_i$  variations were expressed as  $\Delta F/F_0 = (F_t - F_0)/F_0$ , where  $F_t$  is the fluorescence measured at each recorded time  $t$  and  $F_0$  is the initial fluorescence. The profiles are representative of the variation observed in different cells and correspond to three independent experiments.

Next, we studied the role of each domain in the translocation of PKC $\alpha$  to the plasma membrane using appropriate mutants fused to EGFP, more specifically PKC $\alpha$ D246N/D248N-EGFP, PKC $\alpha$ K209A/K211A-EGFP and PKC $\alpha$ W58G-EGFP. These mutants were expressed transiently in BT-474 cells, and stimulated under the same conditions as those expressing wild type PKC $\alpha$  (Fig IV.6).

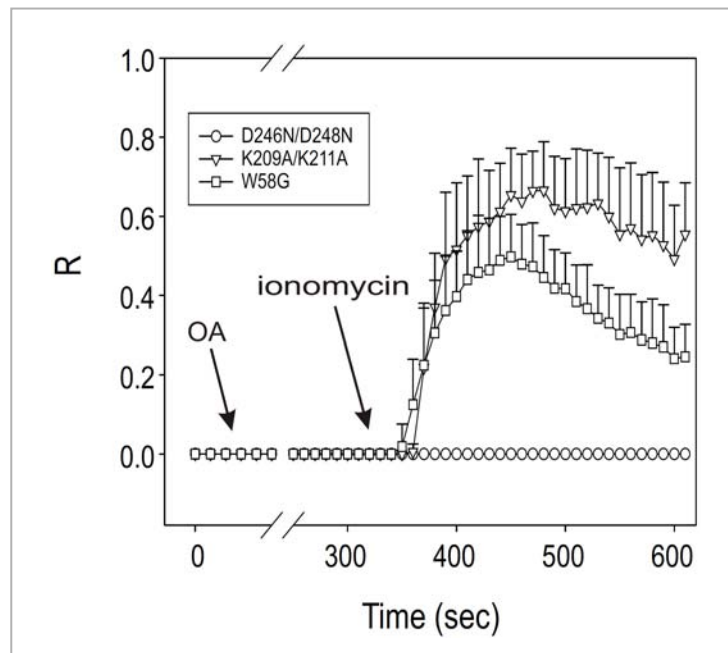


**Figure IV.6. Translocation profiles of PKC $\alpha$  mutants to plasma membrane.** PKC $\alpha$ D246N/D248N-EGFP ( $\circ$ ), PKC $\alpha$ K209A/K211A-EGFP ( $\diamond$ ) and PKC $\alpha$ W58G-EGFP ( $\square$ ) fluorescence intensities were measured in the cytosol and in the plasma membrane in every frame of the time-series (one frame every 10 s). Protein localization was measured by a line profile (pixel density) traced in each frame as indicated in Materials and Methods. The resulting net change in PKC $\alpha$  localization is expressed as the  $I_{mb}-I_{cyt}/I_{mb}$  ratio (R) and is represented *versus* time.

As expected, mutant proteins did not localize in the plasma membrane after OA stimulation, and only when ionomycin was added to cells, some mutants translocate. The *Calcium Binding Region* mutant did not localize in the plasma membrane, while the two other mutants interacted with the membrane but to different degrees. The *lysine rich cluster* mutant showed a slight decrease in the translocation rate compared with the wild type protein and returned slowly to cytosol. However, only 50% of the C1A subdomain mutant was localized in the plasma membrane and its tendency to dissociate from membranes was higher than that of the *lysine rich cluster* mutant.

These results coincide with those obtained in the kinase activity assays, suggesting that the *Ca<sup>2+</sup> binding region* is essential for the translocation and activation of PKC $\alpha$  induced by oleic acid, while other regions play a secondary role in this process, the C1A subdomain being more important than *lysine rich cluster*, especially Lys 209 and 211.

## **2.4. Inhibition of PKC $\alpha$ expression reduces the proliferation rate in breast cancer cell lines and synergizes with oleic acid.**

After demonstrating that OA can localize PKC $\alpha$  in the plasma membrane and activate it, we decided to study the effect of this fatty acid on the proliferation rate of several cell lines, specifically MCF-7, BT-474 and MDA-MB-231, in the presence and in the absence of PKC $\alpha$ .

Firstly we checked the expression level of PKC $\alpha$  by western blot during the nine days of the proliferation assays (Fig IV.7). Surprisingly, PKC $\alpha$  expression did not recover and reached maximum inhibition 3-4 days after siRNA $\alpha$  transfection, around 25-35% in MCF-7, 15-20% in BT-474 and 10-15% in MDA-MB-231 cells.

After checking the inhibition of PKC $\alpha$ , the proliferation assays were performed by measuring the DNA content of cell lines cultured in different conditions: cells transfected with siRNAcontrol or siRNA $\alpha$  in the presence or absence of oleic acid in the growth medium. To carry out this assay the commercial kit “CyQUANT® NF Cell Proliferation Assay Kit” (Invitrogen, Oregon, USA) was used, as described in Material and Methods section (Chapter II). The results were expressed as inhibition percentage of proliferation compared with the proliferation rate of control cells (cells transfected with siRNAcontrol and no OA in the medium).

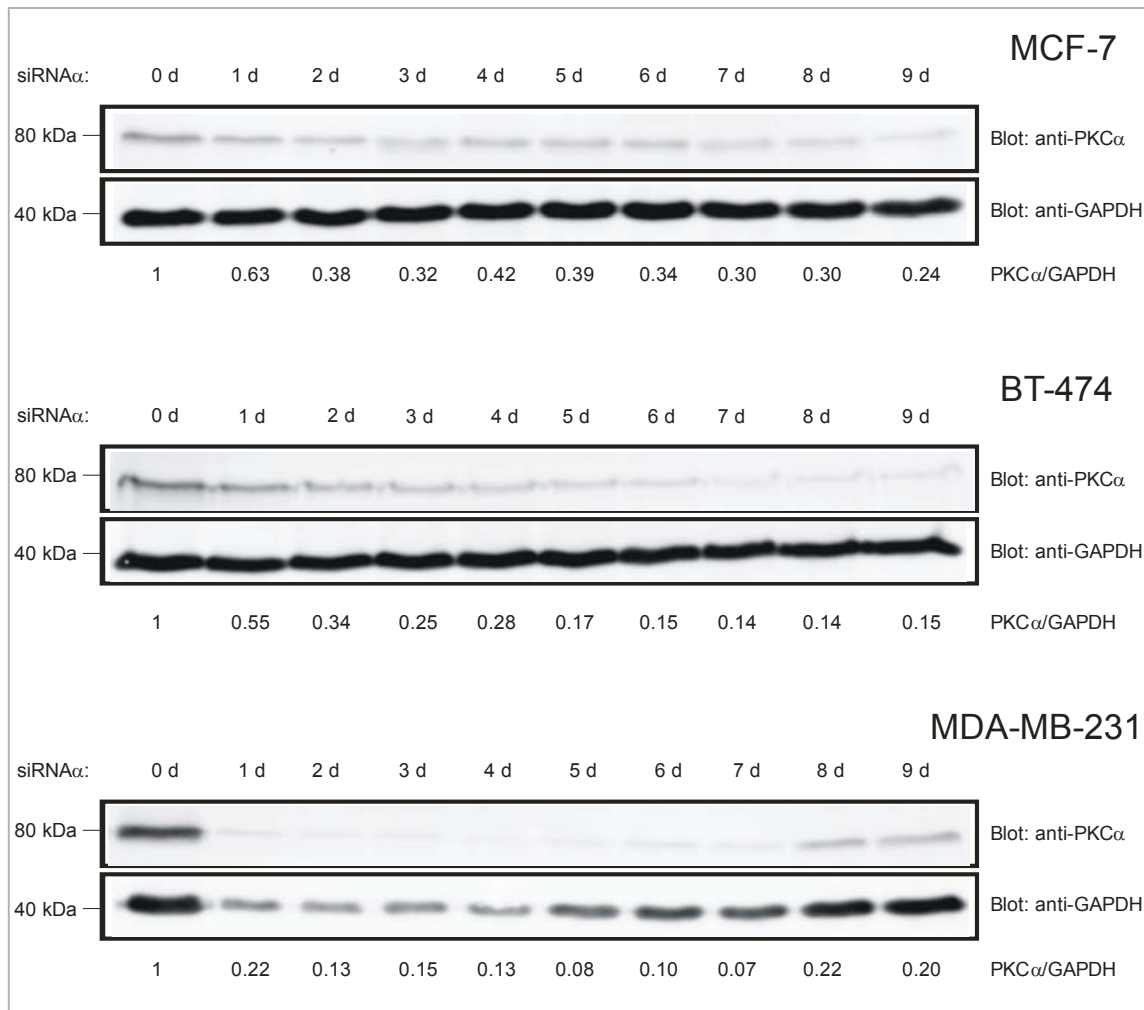


**Figure IV.7. PKC $\alpha$  expression inhibition by siRNA $\alpha$  in MCF-7, BT-474 and MDA-MB-231 cells.** The level of PKC $\alpha$  was checked by western blot and it was measured as a ratio PKC $\alpha$ /GAPDH, considering the basal level (100%) the ratio of day zero.

As can be observed in Figure IV.8, the addition of 50  $\mu$ M OA-BSA had a slight inhibiting effect on proliferation, which increased with time in MCF-7 and BT-474 cells, whereas in MDA-MB-231 the inhibition remained constant.

When we studied the effect of the inhibition of PKC $\alpha$  expression on the proliferation rate, a significant decrease in the cell growth of all the cell lines tested was observed. Maximum proliferation inhibition was reached on day five or six (depending on the cell line), after which the growth rate recovered to control levels, despite PKC $\alpha$  being down-regulated.

Moreover, when OA was added to these mutant cells, the inhibition of proliferation was slightly higher and the recovery was slower than in cells without PKC $\alpha$  growing in the absence of OA, suggesting that this fatty acid enhances the inhibiting effect of PKC $\alpha$  expression.

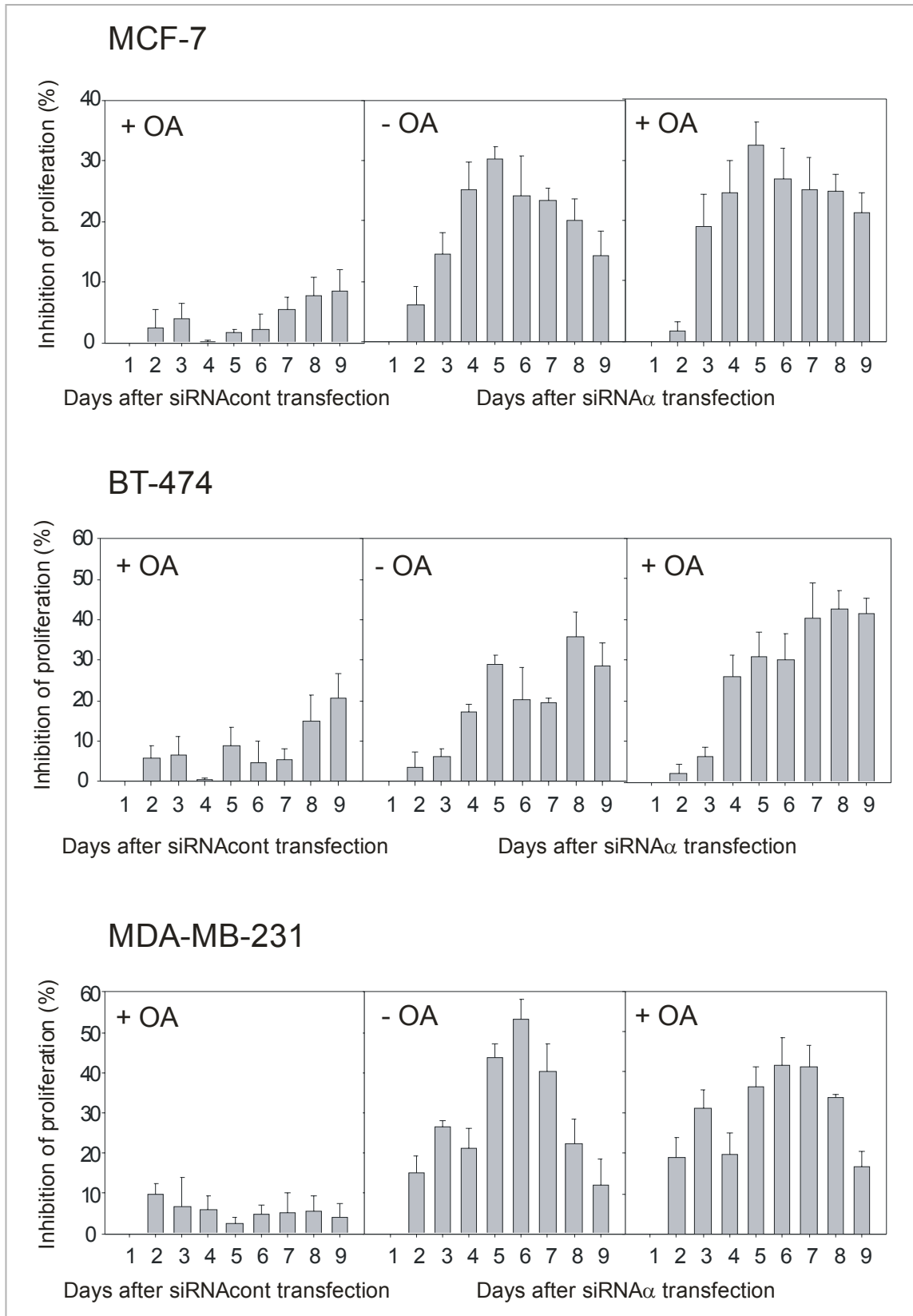


**Figure IV.8. Proliferation rates of MCF-7, BT-474 and MDA-MB-231 cells in presence or absence of oleic acid after inhibition of PKC $\alpha$  expression.** The inhibition of proliferation percentage was calculated comparing the DNA amount of every condition with control cells, every day. The profiles correspond to three independent experiments.

## **2.5. Effect of oleic acid addition and inhibition of PKC $\alpha$ expression on the migration and invasion capacities of MCF-7 and MDA-MB-231 cell lines.**

After proliferation, the effect of oleic acid and the inhibition of PKC $\alpha$  expression on the migration of tumour cells was studied.

For these assays, the wound healing technique was used as was described in Material and Methods. As expected, the two cell lines showed large differences in migration capacity: while MCF-7 control cells needed approximately 72 hours to seal the scratch wound, MDA-MB-231 control cells formed a monolayer in 24 hours (Fig IV.9).

MCF-7 cells growing in the presence of fetal calf serum (FCS) migrated faster than cells growing in serum-starved medium (0.5% FCS), although in this condition, cells also sealed the scratch wound, approximately one day later. The effect of OA was so subtle that it was decided to run wound healing assays in serum-starved medium to avoid masking the effect of the fatty acid on migration capacity with FCS. The presence of oleic acid did not result in any significant differences, although the inhibition of PKC $\alpha$  expression decreased the migration capacity of these cells by more than 60% in the absence or in the presence of OA (Fig IV.9). These results suggest that PKC $\alpha$ , but not OA, is involved in the migration of MCF-7 cells.

When MDA-MB-231 cells were studied, no differences were found with respect to OA treatment or to the inhibition of PKC $\alpha$  expression. These metastatic cells showed similar migration rates in the presence of growth medium (10% FCS) or serum starved medium (0.5% FCS), the presence or absence of OA and with or without PKC $\alpha$  (Fig IV.8C), suggesting that PKC $\alpha$  or OA are not involved in the migration process in these cells.

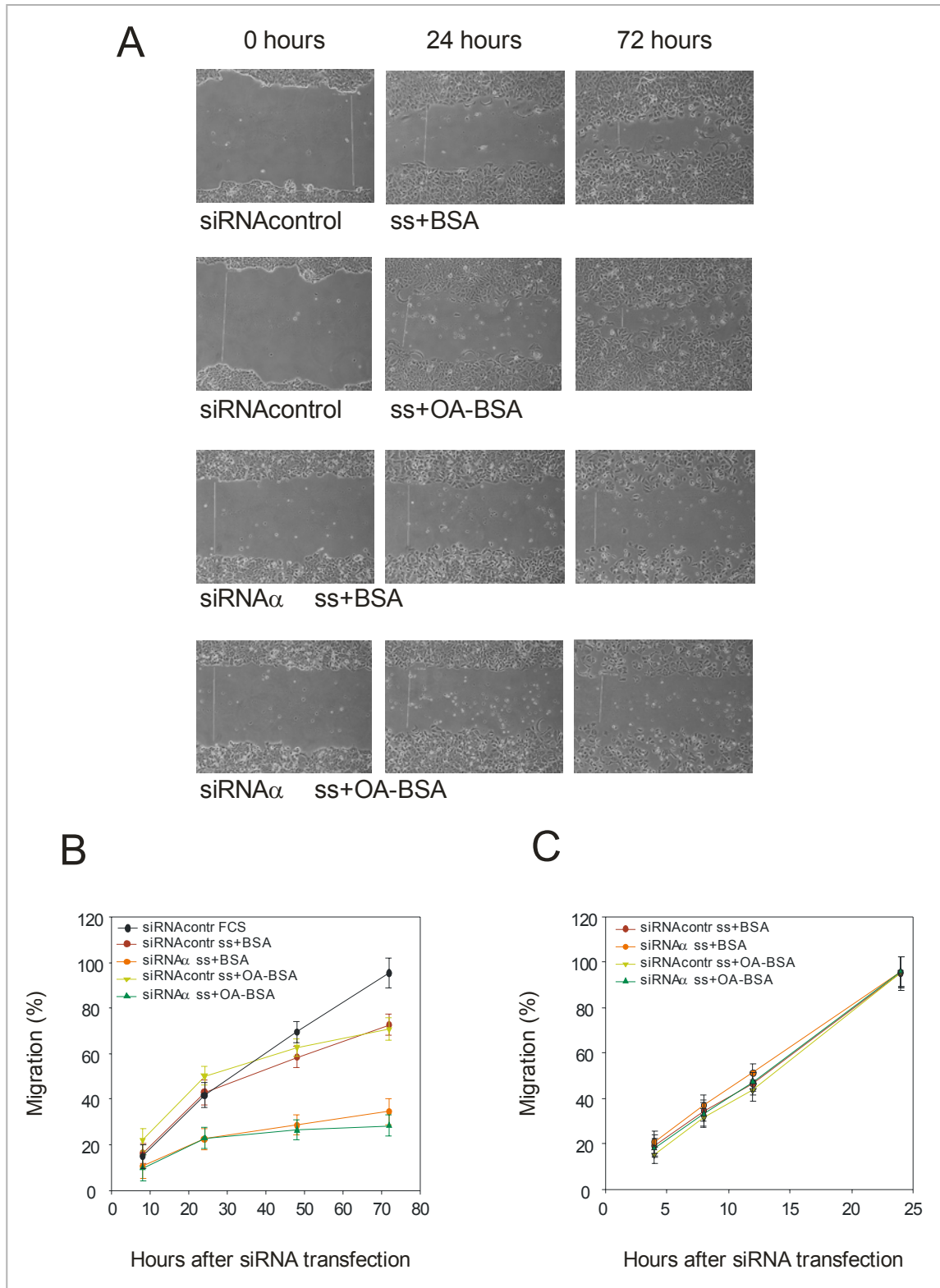


**Figure IV.9. Migration assays of MCF-7 and MDA-MB-231 cells stimulated with oleic acid.** A) Shows micrographs of MCF-7 cells immediately after making the scratch and 24 and 72 hours later. Two top rows represent cells transfected with siRNAcontrol and stimulated or not with oleic acid, while two bottom rows are the same but transfected with siRNA $\alpha$ . At the bottom the migration profiles of MCF-7 (B) and MDA-MB-231 (C) cells after different stimulations are shown. The migration profiles consist of measuring the width of scratch wound at every time, and the migration percentage was calculated regards to initial size of scratch. Results are representative of three independent experiments.

MDA-MB-231 cells also possess invasion capacity in BME (basement membrane extract) (Fig IV.10A). Control cells were transfected with siRNAcontrol and grown in the absence of oleic acid, exhibiting an invasion capacity of around 21% (Fig IV.10). When these cells were incubated with oleic acid for 48 hours, their invasiveness decreased slightly to 18%.

The most important effect as regards invasion capacity was found when siRNA $\alpha$  was transfected into cells; in this case, the results demonstrated that in the absence of PKC $\alpha$ , the invasion capacity decreased approximately 40%, with only 13.6% of cells being able to invade.

Besides, cells stimulated with oleic acid for 48 hours enhanced the effect of PKC $\alpha$  inhibition, decreasing the invasion ability of these cells to 12%. This combination was the best treatment for reducing the invasion capacity of MDA-MB-231.

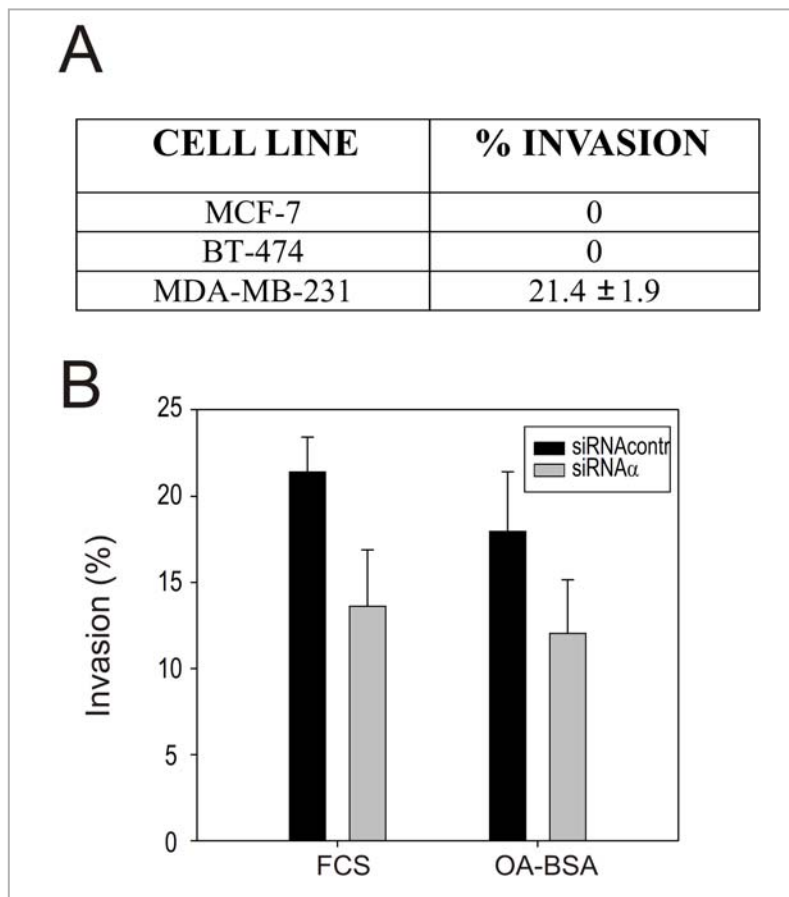


**Figure IV.10. Invasion capacity of MDA-MB-231 cells.** A) Shows the invasion percentage in 0.5X BME of three breast cancer cell lines tested. B) Represents the percentage of MDA-MB-231 cells transfected with siRNAcontrol or siRNA $\alpha$  in presence or not of oleic acid. Results are representative of three independent experiments.

## 2.6. Oleic acid and inhibition of PKC $\alpha$ induce apoptosis in breast cancer cell lines.

Another aspect studied in breast cancer cell lines upon stimulation with OA and after PKC $\alpha$  depletion was programmed cell death. Apoptosis percentages were measured using annexin V-Alexa Fluor® 488, allowing early and late apoptosis to be distinguished. The percentages of apoptosis in MCF-7 and MDA-MB-231 cells in several conditions are shown in Table IV.2.

MCF-7 cells transfected with siRNAcontrol and incubated with oleic acid for 4 days increased the apoptosis rate from 7 (control cells) to 10.7%. This value was even greater (almost twice the basal level) when cells possessing a low PKC $\alpha$  expression were used, in which case apoptosis reached almost 14%. However, when these cells were incubated with the monounsaturated fatty acid, no increase in apoptosis was found.

In the case of MDA-MB-231, the basal level of apoptosis was approximately 2.5%, which almost double when siRNA $\alpha$  was transfected into cells (4.5%). A slight increase was found when PKC $\alpha$  knockout cells were incubated with 50  $\mu$ M of oleic acid for 5 days (5.3%).

**Table IV.2. Apoptosis percentage of MCF-7 and MDA-MB-231 cells stimulated with oleic acid and transfected with siRNAcontrol and siRNA $\alpha$ .**

CELL LINE	CONDITIONS	% APOPTOSIS
	siRNAcontrol	7.0 $\pm$ 1.8
MCF-7	siRNAcontrol + OA-BSA	10.7 $\pm$ 2.6
	siRNA $\alpha$	13.7 $\pm$ 2.8
	siRNA $\alpha$ + OA-BSA	12.8 $\pm$ 5.0
	siRNAcontrol	2.5 $\pm$ 0.7
MDA-MB-231	siRNAcontrol + OA-BSA	3.7 $\pm$ 0.6
	siRNA $\alpha$	4.5 $\pm$ 1.7
	siRNA $\alpha$ + OA-BSA	5.3 $\pm$ 0.9

Data show the mean  $\pm$  standard deviation of 5-8 independent experiments.



## CHAPTER V

# STUDY OF THE ROLE OF OMEGA-3 FATTY ACIDS AND PKC $\alpha$ DEPLETION IN BREAST CANCER CELLS



## 1. Introduction.

Breast cancer remains a major public health problem with more than one million cases a year reported in the world, nearly half in North America and Europe (Parkin *et al.*, 2001). The prognosis of this disease relies on the characteristics of the tumour and on the quality of any treatment. Cancer treatment differs depending on the type of cancer but, in general, they consist of both loco-regional and systemic approaches, based on chemotherapy and then on hormonal manipulation, to prevent or delay the occurrence of metastases (Visvader and Lindeman, 2008; Polyak and Winberg, 2009).

Despite improved treatments and falling death rates, the rate of recurrence is still high and breast cancer remains the second cause of cancer-related death in women, with a yearly toll of more than 40,000 deaths in the United States, 11,000 in France and 9,000 in Spain, the EU country with lowest incidence of death caused by this type of cancer. This dramatically illustrates dramatically the failure of current treatments to prevent tumour re-growth from residual tumour cells, either locally or at distant sites. However, progress in systemic treatment has led to a reduced rate of metastases, principally in those breast cancers showing specific molecular alterations amenable to targeted therapies (Bougnoux *et al.*, 2010). In addition, Massagué's laboratory has developed new strategies for studying metastasis markers in mice, which should facilitate the development of new anti-metastatic agents (Bos *et al.*, 2010).

Beside approaches focused on tumour cells, many recent studies have stressed that the environment of the tumour (the microenvironment), as well as the environment of the host (the patient), are major determinants of tumour fate (Joyce and Pollard, 2009). A major goal for future breast cancer treatments remains the improvement of treatment efficacy, meaning increasing the toxicity to tumour tissue without any additional toxicity to healthy tissues. Therefore, further efforts should aim at identifying agents and/or developing original approaches with enhanced specificity toward tumour tissues (Bougnoux *et al.*, 2010).

Animal models addressing this issue rely on the evaluation of the effects of lipid components in the diet on either the inhibition of mammary tumour growth or the prevention of tumour appearance. The experimental models used include mice or rats treated with a diet containing polyunsaturated fatty acids (PUFAs) and either receiving transplanted tumours or subjected to chemical carcinogenesis. The lipids were generally provided as a mixture of several different fatty acids. Despite the controversial results obtained, it is generally admitted that omega-6 PUFAs tend to have a mammary tumour

enhancing effect and several animal studies have reported an antineoplastic role of omega-3 PUFAs (*Bougnoux et al., 1994; Bougnoux et al., 1999*).

In a seminal article, it was examined whether there is a relation between breast cancer evolution following treatment (with the occurrence of metastases as the endpoint) and dietary fatty acid intake (*Kohlmeier and Hohlmeier, 1995*). A protective effect of long chain omega-3 PUFAs, which include DHA and EPA, was observed. Thus, for the first time, a component of the host, the fatty acid profile of the adipose tissue, could be related to the prognosis of the disease.

These data relating the fatty acid profile of storage lipids to breast cancer survivorship indicate that diet, and not only the genomic alterations of the tumour, could influence the metastatic risk by preventing tumour re-growth (*Amaral et al., 2010*). Since tumour re-growth also depends on the efficacy of cancer treatments, a working hypothesis has been that identified dietary factors, such as PUFAs, may influence the efficacy of radio- or chemotherapy (*Calviello et al., 2009*).

The literature indicates that DHA sensitizes breast malignant tumours, but not healthy tissues, to chemotherapy and to radiotherapy through a variety of mechanisms, which are not well-known. Some of these proposed mechanisms are explained below.

A possible action mechanism resulting in increased apoptosis due to oxidative stress has been suggested (*Fite et al., 2007*). Studies carried out with the breast cancer cell line MDA-MB-231 showed that DHA enrichment of the culture medium increased the cytotoxic response to doxorubicin (a chemotherapeutic drug). This treatment effect was observed with most PUFAs, but its extent was proportional to their unsaturation degree. It has been hypothesized that DHA could weaken tumour cells while integrating into their membrane phospholipids because of its peroxidation following the oxidative stress induced by some type of chemical drugs like anthracyclines (*Vibet et al., 2008*). Normal cells and tissues are protected from the toxic effects of high concentrations of reactive oxygen species by antioxidant enzymes. Indeed, no increased toxicity of chemotherapy or radiation on normal tissues was found in rats fed with DHA (*Kato et al., 2002; Germain et al., 2003; Xue et al., 2007; Sun et al., 2009*). On the contrary, a reduction in antioxidant defences has been reported in cancer cells (*Oberley, 2002*).

Another mechanism proposed is that the incorporation of PUFAs, like DHA and EPA, into cell membrane phospholipids can modify the membrane's structure and permeability. In turn, this might alter the pharmacokinetic parameters of hydrophobic anti-cancer drugs diffusing across the membrane. In mammary tumour cell lines and in these experimental conditions, DHA-

induced chemosensitization altered intracellular drug concentration, depending on the anti-cancer agent tested (*Abulrob et al., 2000; Maheo et al., 2005*).

The third mechanism proposed hypothesizes that lipid rafts, and associated signal transduction, would be modified by the incorporation of DHA in the membranes. Lipid rafts are membrane microdomains rich in saturated fatty acids, sphingolipids, cholesterol and several signalling proteins, including the epidermal growth factor receptors (EGFR). Schley and co-workers have shown that EPA and DHA in cell cultures were incorporated into whole the membranes and lipid rafts of breast cancer cells (*Schley et al., 2007*). This was associated with reduced EGFR levels in the rafts and increased whole cell levels of phosphorylated EGFR (*Schley et al., 2007*). Although preliminary, such data on the ultrastructural alteration of lipid membrane microdomains by PUFAs suggests that such alterations might regulate several signalling pathways including EGFR, Akt, p38 MAPK or H-ras (*Biondo et al., 2008; Calviello et al., 2009*) and, in turn, potentially impact tumour cell response to chemotherapy.

In this chapter we shed light on the role of PKC $\alpha$  in the signalling pathways induced by omega-3 fatty acids, especially DHA and EPA, using several breast cancer cell lines as models.

## **2. Results.**

### **2.1. Omega-3 fatty acids induce PKC $\alpha$ plasma membrane translocation and co-localization with actin filaments in breast cancer cells.**

To study the effect of DHA and EPA on PKC $\alpha$ -plasma membrane interaction, we studied the subcellular localization of the endogenous protein in MCF-7 and MDA-MB-231 cells by immunofluorescence (PKC $\alpha$ -green-AlexaFluor 488) and F-actin polymerization by AlexaFluor 633-phalloidin labelling. Cells were treated for 48 h with growth medium in the presence and absence of 50  $\mu$ M EPA or DHA (Figs V.1 and V.2).

In the absence of omega-3 fatty acids, PKC $\alpha$  was distributed homogeneously throughout the cytosol with a very low percentage of cells exhibiting protein localized at the plasma membrane (14% and 8% in MCF-7 and MDA-MB-231, respectively). In the presence of DHA the percentage of PKC $\alpha$  localized in the plasma membrane of the cells increased to 42% and 53%, respectively. EPA only was tested in MCF-7 cells and the percentage of

cells with PKC $\alpha$  localized in the plasma membrane in this case was 64%. These results suggest that both polyunsaturated fatty acids induce the translocation of PKC $\alpha$  from the cytosol to the plasma membrane in the two cell lines tested, although to different degrees (Figs V.1 and V.2).

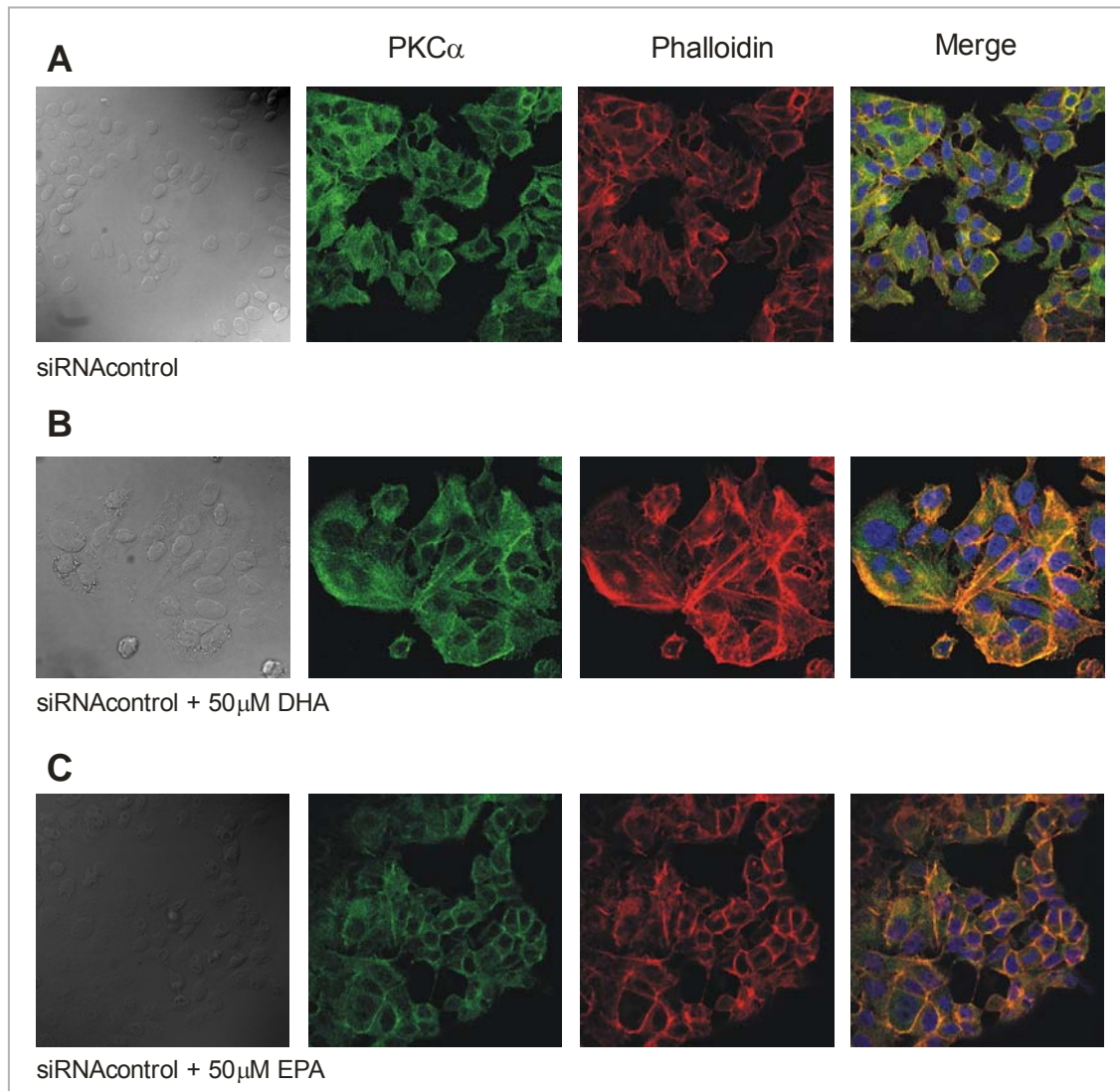


**Figure V.1. PKC $\alpha$  and F-actin co-localized in the plasma membrane of MCF-7 cells.** Cells were fed with growth medium (A), 50  $\mu$ M DHA-BSA (B) or 50  $\mu$ M EPA-BSA (C) during 48 hours, fixed with formaldehyde and processed for immunolabeling by using polyclonal Ab to PKC $\alpha$  (detected by using secondary Ab coupled to AlexaFluor 546), F-actin was determined by AlexaFluor633 labelled-phalloidin and DAPI staining was used to detect nuclei. RGB merged images including Alexa Fluor 546, Alexa Fluor 633 and DAPI are shown in the right panel (merge).

In addition, we studied the degree of actin polymerization after fatty acid treatments, since actin dynamics is correlated with the migration and invasion of cancer cells. In MCF-7 cells, it was observed that EPA and DHA

induced the formation of F-actin rich structures at the edges of the cells that were co-localizing with PKC $\alpha$  at the plasma membrane (Fig V.1). When we stimulated MDA-MB-231 cells with 50  $\mu$ M of DHA, it was observed that these cells showed a smaller and more granulose cytoplasm, and that actin polymerization was completely disorganized (no stress fibres were observed) (Fig V.2).

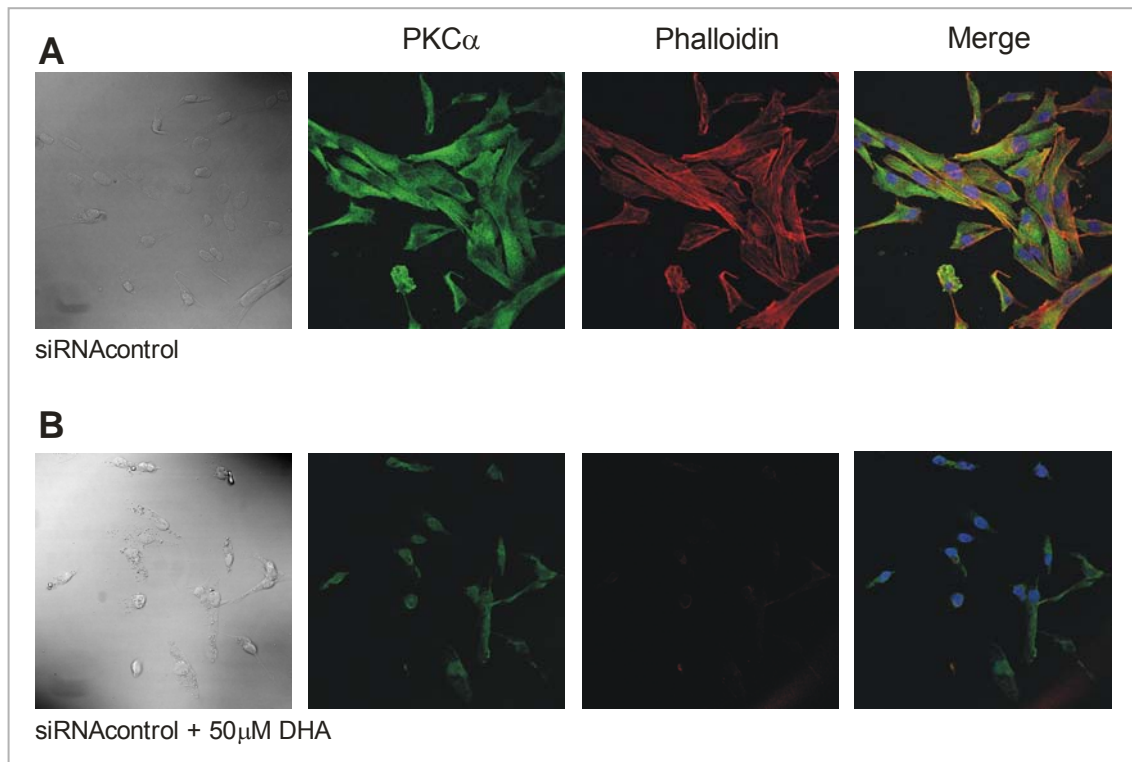


**Figure V.2. PKC $\alpha$  and F-actin co-localized in the plasma membrane of MDA-MB-231 cells.** Cells were fed with growth medium (A) or 50  $\mu$ M DHA-BSA (B) during 48 hours, fixed with formaldehyde and processed for immunolabeling by using polyclonal Ab to PKC $\alpha$  (detected by using secondary Ab coupled to AlexaFluor 546), F-actin was determined by AlexaFluor633 labelled-phalloidin and DAPI staining was used to detect nuclei. RGB merged images including Alexa Fluor 546, Alexa Fluor 633 and DAPI are shown in the right panel (merge).

We studied the role of PKC $\alpha$  in those cell lines inhibiting its expression by means of specific siRNA. In MCF-7 cells, the down-regulation of PKC $\alpha$  produced a slight increase in the cell size and a decrease in actin polymerization close to the plasma membrane, while the nuclei were not affected (Fig V.3).

In MCF-7 cells, the effect of both treatments together (suppression of PKC $\alpha$  and incubation with 50  $\mu$ M omega-3 fatty acids during 48 hours) was studied and the cells were observed to be larger. Besides, they were rounded and tended to spread; they also exhibited a high degree of disorganization of the cortical actin polymerization (Fig V.3).

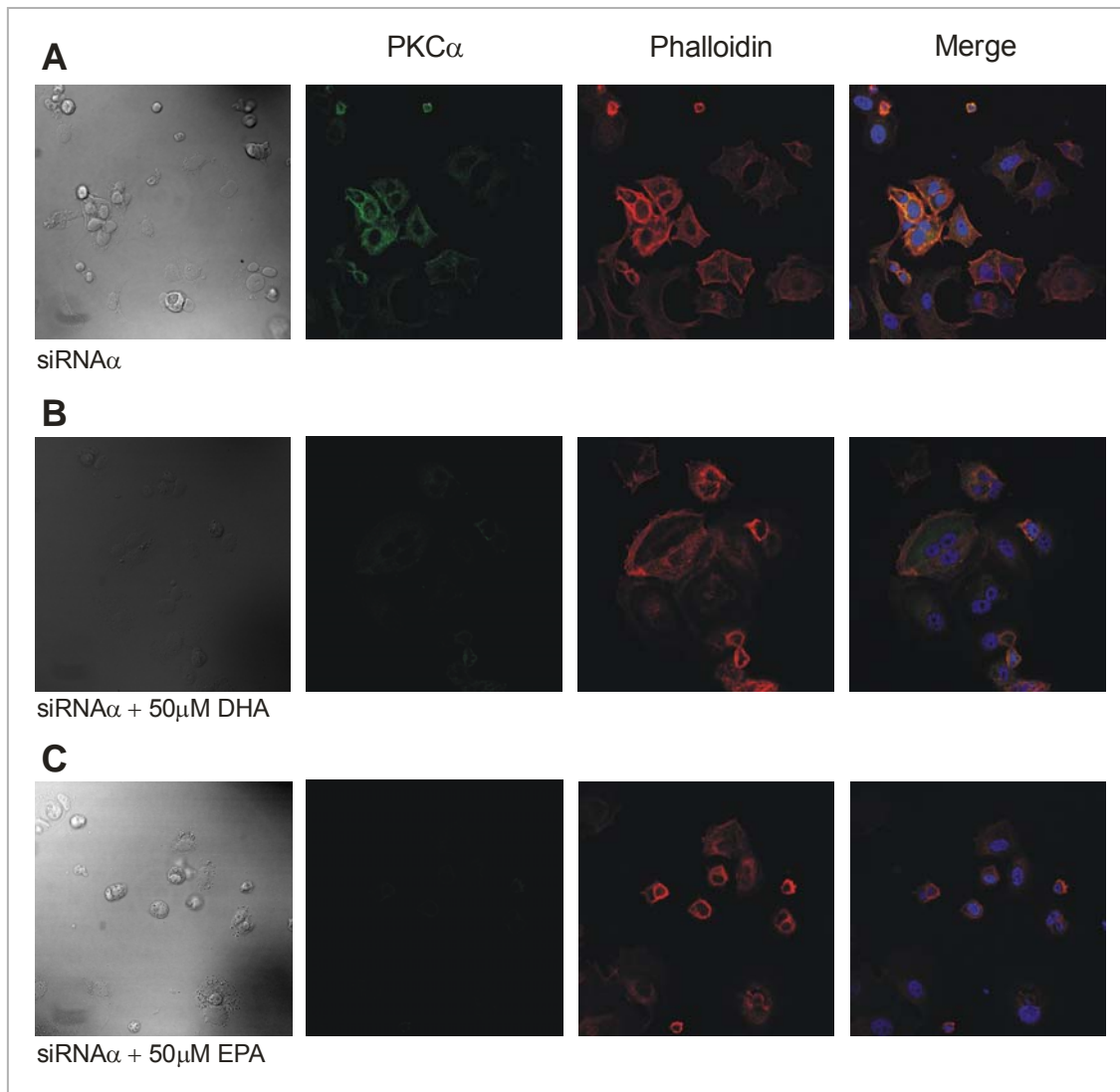


**Figure V.3. Down-regulated PKC $\alpha$  MCF-7 cells upon different treatments.** PKC $\alpha$  was down-regulated in MCF-7 cells by using electroporation and siRNA $\alpha$  and submitted to growth medium 72 hours (A), incubated during 48 hours with 50  $\mu$ M DHA-BSA (B) or 50  $\mu$ M EPA-BSA (C). Cells were fixed with formaldehyde and processed for immunolabeling by using polyclonal Ab to PKC $\alpha$  (detected by using secondary Ab coupled to AlexaFluor 546), F-actin was determined by AlexaFluor633 labelled-phalloidin and DAPI staining was used to detect nuclei (showing the integrity of the cells). RGB merged images including Alexa Fluor 546, Alexa Fluor 633 and DAPI are shown in the right panel (merge).

In the case of MDA-MB-231, cells expressing PKC $\alpha$  have a fibroblast-like morphology (Fig V.2), while those with down-regulated PKC $\alpha$  are larger, rounded and more spread. In these cells, the nuclei are fragmented, suggesting an apoptotic process (Fig V.4).

When the effect of DHA on cells with PKC $\alpha$  depletion was studied, we found a very low number of cells and with a striking morphology. Besides, the residual PKC $\alpha$  had penetrated the nucleus (Fig V.4).

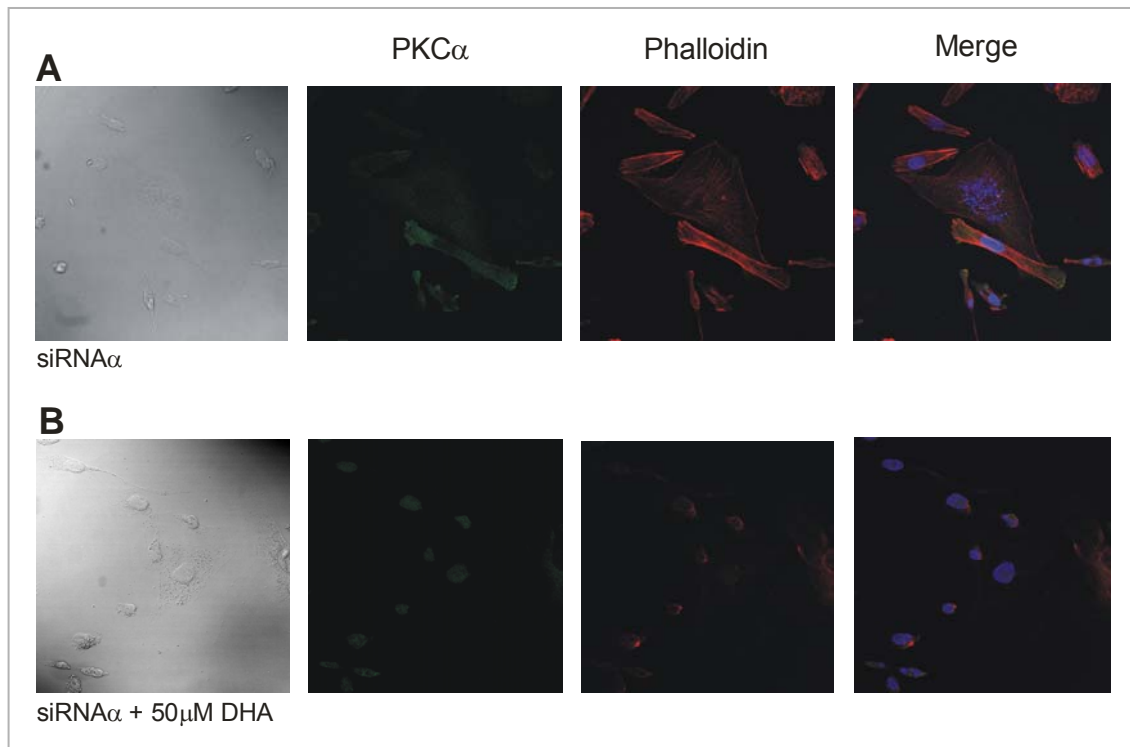


**Figure V.4. Down-regulated PKC $\alpha$  MDA-MB-231 cells upon different treatments.** PKC $\alpha$  was down-regulated in MDA-MB-231 cells by using electroporation and siRNA $\alpha$  and submitted to growth medium 72 hours (A), incubated during 48 hours with 50  $\mu$ M DHA-BSA (B) or 50  $\mu$ M EPA-BSA (C). Cells were fixed with formaldehyde and processed for immunolabeling by using polyclonal Ab to PKC $\alpha$  (detected by using secondary Ab coupled to AlexaFluor 546), F-actin was determined by AlexaFluor633 labelled-phalloidin and DAPI staining was used to detect nuclei (showing the integrity of the cells). RGB merged images including Alexa Fluor 546, Alexa Fluor 633 and DAPI are shown in the right panel (merge).

## 2.2. Characterization of the activation mechanism of PKC $\alpha$ by DHA and EPA.

After demonstrating that omega-3 fatty acids, more specifically DHA and EPA, localize PKC $\alpha$  in the plasma membrane (Figs V.1 and V.2), kinase activity assays were run to check whether these lipids were able to activate PKC $\alpha$  directly.

The experiments were carried out using model lipid vesicles with increasing concentrations of omega-3 fatty acids and purified HA-PKC $\alpha$ . In the case of EPA, no PKC $\alpha$  activity was found, even at high concentrations of this polyunsaturated fatty acid (80% of total lipids included in vesicles) (Fig V.5). To corroborate that the system works correctly, a further other experiment used a different fatty acid as a positive control, in this case oleic acid, which has been demonstrated to be able to activate PKC $\alpha$  (Chapter IV of this Doctoral Thesis) (Fig V.5).

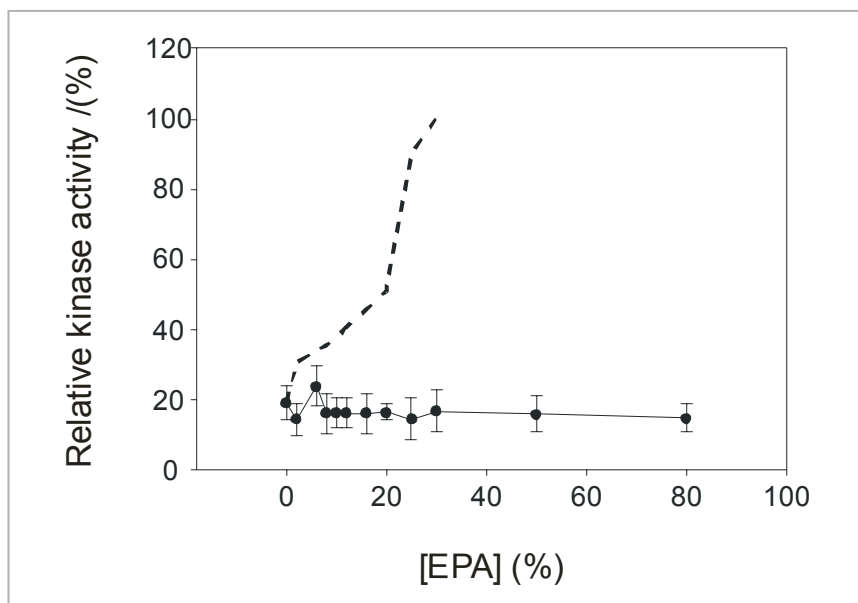


**Figure V.5. Eicosapentaenoic acid-dependence of PKC $\alpha$  activities.** It is shown the result of wild-type PKC $\alpha$  activity in the presence of calcium ion and lipid vesicles with increasing concentrations of EPA. In dotted line is represented the activation of wild-type PKC $\alpha$  by oleic acid as a positive control (vesicles containing 30% OA activate PKC $\alpha$  completely). Error bars indicate the S.D. for triplicate measurements.

However, DHA can activate PKC $\alpha$  in the presence of Ca $^{2+}$ , since in the presence of EGTA in the buffer, the isoform does not show any activity. The results demonstrate that the catalytic activity of the enzyme increased in parallel with the concentration of DHA in lipid vesicles, reaching a maximal activity at 30% DHA, which suggests that this polyunsaturated fatty acid is itself a potential activator of PKC $\alpha$  (Fig V.6).

Once it was demonstrated that DHA can activate PKC $\alpha$  in a Ca $^{2+}$ -dependent manner, we studied the activation of several mutants containing modifications of their aminoacidic residues located in the regulatory domains in order to ascertain the role of C1 and C2 domains in the activation of PKC $\alpha$  induced by this polyunsaturated fatty acid.

Three mutants of the C2 domain, one of the *Calcium Binding Region* (PKC $\alpha$ D246N/D248N) and two of the *Lysine rich cluster* (PKC $\alpha$ K197A/K199A and PKC $\alpha$ K209A/K211A), and one mutant of the C1A subdomain (PKC $\alpha$ W58G) were used. The kinase activity of each mutant was measured in the same conditions as the wild-type enzyme in order to compare them (Fig V.6).

The three C2 domain mutants showed residual catalytic activity, and only at high concentrations of DHA they recovered a little activity. At 30% DHA the activity of the three mutant proteins was similar but much lower than that of the wild-type, the inhibition reaching approximately 60%.

The C1A subdomain mutant, HA-PKC $\alpha$ W58G, showed inhibited of enzymatic activity at low concentration of DHA, but when the amount of fatty acid in the lipid vesicles reached 12%, the activation degree was recovered and was almost similar to that of wild type protein (only 20% inhibition).

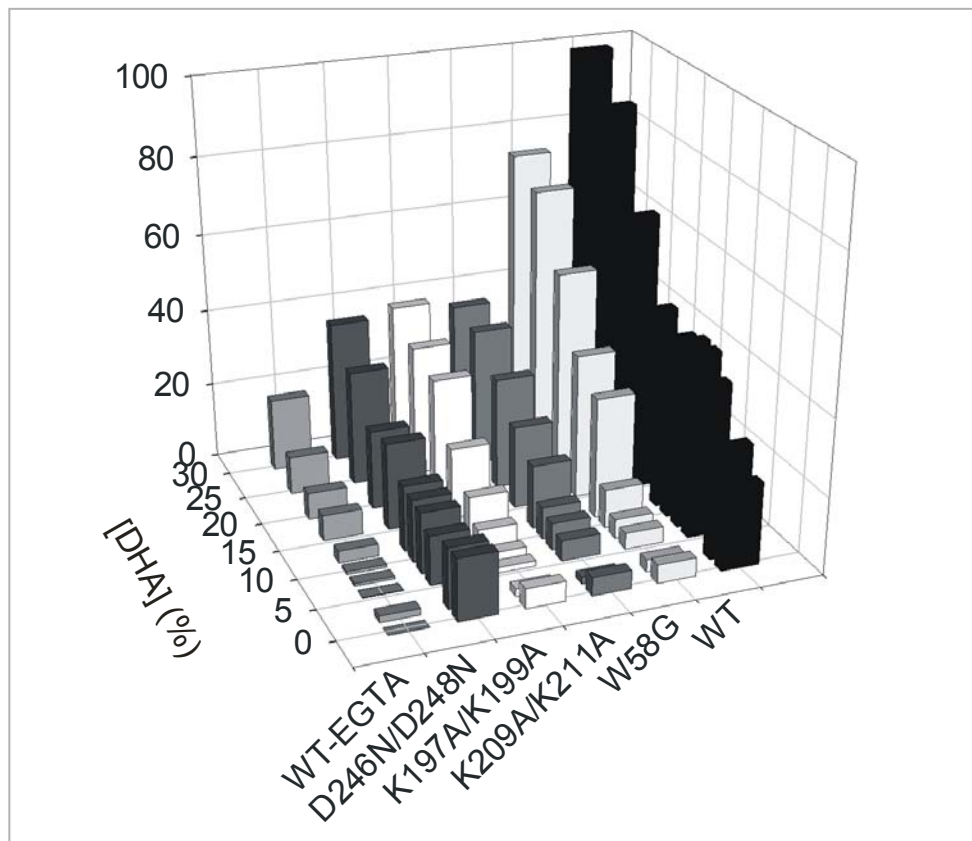


**Figure V.6. Docosahexaenoic acid-dependence of PKC $\alpha$  activities.** Proteins used in this study include wild-type PKC $\alpha$ , a mutant of the *Calcium Binding Region* (PKC $\alpha$ D246N/D248N), two mutants of the *Lysine Rich Cluster* (PKC $\alpha$ K197A/K199A and PKC $\alpha$ K209A/K211A) and a C1A subdomain mutant (PKC $\alpha$ W58G).

Taken together, these results confirm the hypothesis that the C2 domain of PKC $\alpha$  plays an important role in the DHA-dependent activation of the enzyme, both regions the *Ca<sup>2+</sup>-Binding Region* and the *lysine rich cluster* being essential for activation. Moreover, the results also suggest that the C1A subdomain plays a role in the activation although it is less crucial than that played by the C2 domain.

Taking into account all results obtained in the immunofluorescences and kinase activity assays, we can conclude that omega-3 fatty acids behave differently over PKC $\alpha$ . While EPA localizes the enzyme in the plasma membrane but is unable to activate it, DHA translocates the PKC $\alpha$  to the plasma membrane and also activates it in a Ca<sup>2+</sup>-dependent manner.

### **2.3. Effect of omega-3 fatty acids and inhibition of PKC $\alpha$ expression on the migration and invasion capacities of MCF-7 and MDA-MB-231 cell lines.**

Another aspect that we decided to study was the effect of EPA and DHA on the migration of both breast cancer cell lines in the presence and absence of PKC $\alpha$ .

To explore this, we used the wound healing assay as described in Materials and Methods (Chapter II). As expected, the two cell lines showed large differences in their migration capacity; while MCF-7 control cells needed approximately 72 hours to seal the scratch wound, MDA-MB-231 control cells form the monolayer in 24 hours (Figs V.7 and V.8).

50  $\mu$ M fatty acids cross-linked with bovine serum albumin (BSA) were added to cells growing in serum starved-medium (0.5% FCS) to detect any differences between treatments and to avoid the masking effect of fetal calf serum.

As mentioned in Chapter IV of this Doctoral Thesis, MCF-7 cells grow in the presence of 10% FCS and migrate faster than cells grown in serum-starved medium (0.5% FCS). Moreover, PKC $\alpha$  knockout MCF-7 cells inhibit their migration capacity by approximately 50% when compared with control cells.

MCF-7 cells growing in the presence of 50  $\mu$ M of DHA-BSA exhibited a 44% of migration capacity after 72 hours of treatment, compared with the 72% of control cells (serum starved+BSA). This inhibition was even greater when PKC $\alpha$  was down-regulated in the cells, when the migration capacity decreased to 15% when PKC $\alpha$  knockout MCF-7 cells were incubated with 50  $\mu$ M of DHA-BSA for 72 hours (Fig V.7B).

The micrographs of Figure V.7A depict the effect of DHA and PKC $\alpha$  depletion on migration, the disorganization of the cellular monolayer when we used both treatments were used together being evident.

These results suggest that PKC $\alpha$  and DHA are involved in the migration of MCF-7 cells, affecting the same signalling pathway, since they show synergism in this process.

When MCF-7 cells were incubated with 50  $\mu$ M of EPA-BSA, no effect was found in the migration capacity of MCF-7 cells (Fig V.7C).

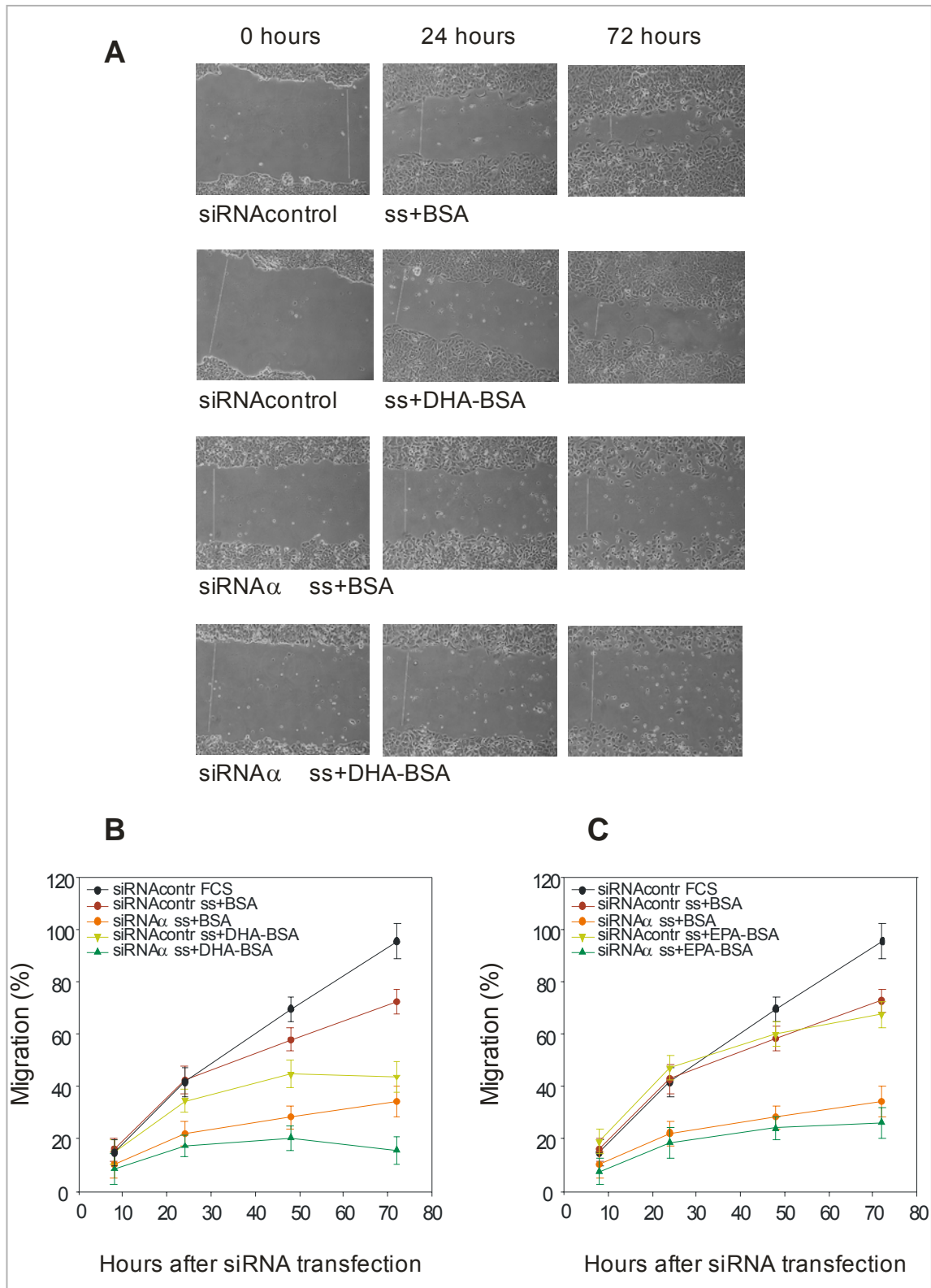


**Figure V.7. Migration assays of MCF-7 cells stimulate with omega-3 fatty acids.** A) Micrographs of MCF-7 cells immediately after making the scratch and 24 and 72 hours later. Two top rows represent cells transfected with siRNAcontrol and stimulated or not with DHA-BSA, while two bottom rows are the same but transfected with siRNA $\alpha$ . At the bottom, the migration profiles of MCF-7 cells treated with DHA-BSA (B) and EPA-BSA (C) are shown. The migration percentage was calculated with respect to initial width of the scratch. Results are representative of three independent experiments.

In the case of MDA-MB-231 cells, the migration rate was similar when they were grown in the presence or absence of fetal calf serum. Figures V.8B and V.8C only show the profiles measured in serum-starved medium. Both omega-3 fatty acids inhibited the migration of this cell line independently of PKC $\alpha$ , the effect of DHA being much higher than that of EPA. MDA-MB-231 cells reduced their migration capacity by approximately 65% when they were incubated with 50  $\mu$ M of DHA for 24 hours; while the addition of EPA to the medium inhibited migration by only 30% after 24 hours.

It is important to mention that DHA affected the morphology of MDA-MB-231 cells. After 24 hours of incubation, there were many spaces between the cells, which exhibited a granulose cytoplasm.

These results suggest that DHA and EPA, but not PKC $\alpha$ , are involved in the migration of MDA-MB-231 cells when they are incubated for at least 24 hours, since, after 12 hours in the presence of these fatty acids, cell migration was similar to that observed in control cells (ss+BSA).

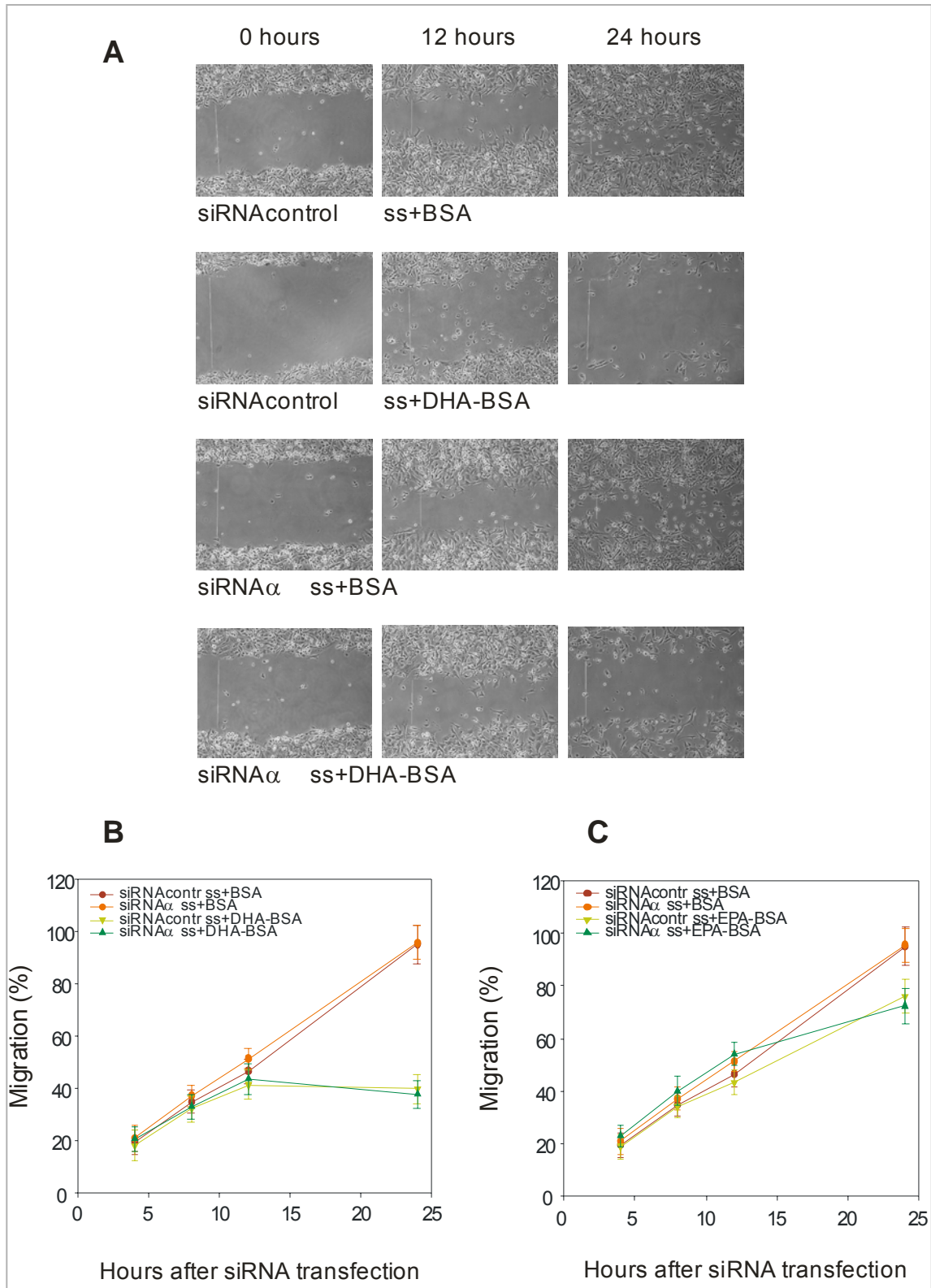


**Figure V.8. Migration assays of MDA-MB-231 cells stimulated with omega-3 fatty acids.** A) Shows micrographs of MDA-MB-231 cells immediately after making the scratch and 12 and 24 hours later. Two top rows represent cells transfected with siRNAcontrol and stimulated or not with DHA-BSA, while two bottom rows are the same but transfected with siRNA $\alpha$ . At the bottom it is shown the migration profiles of MDA-MB-231 cells treated with DHA-BSA (B) and EPA-BSA (C). The migration profiles consist of measuring the width of the scratch wound at every time, and the migration percentage was calculated with regards to the initial size of the scratch. Results are representative of three independent experiments.

Invasion assays were carried out in MDA-MB-231 cells, since they were the only cell line of the three tested that invaded BME (basement membrane extract) (Fig V.9A).

Both control and PKC $\alpha$  knockout cells showed a slightly lower invasion capacity when they were incubated with 50  $\mu$ M EPA-BSA for 48 hours (from 21.4% and 13.6% to 17.3% and 10.5%, respectively). When cells were incubated with DHA-BSA, inhibition was significantly stronger; in control cells invasion was reduced by approximately 50% (from 21.4% to 10.2%), while in mutant cells, invasion was inhibited by around 60% with respect to mutant cells growing without any fatty acids (from 13.6% to 5.3%).

Note that, as mentioned in the previous chapter of this work, the invasion capacity decreased by approximately 40% when the expression of PKC $\alpha$  in MDA-MB-231 cells was deleted (Fig V.9).

The best treatment to reduce the invasiveness of this cell line was to add 50  $\mu$ M DHA-BSA to PKC $\alpha$  knockout cells for 48 hours, in which case the invasion capacity fell to 5.3%, that is, the inhibition reached approximately 75% (Fig V.9).

These results illustrated the synergism that takes place between PKC $\alpha$  knockdown and DHA treatment in inhibiting such an important malignant characteristic of MDA-MB-231, that is invasiveness.

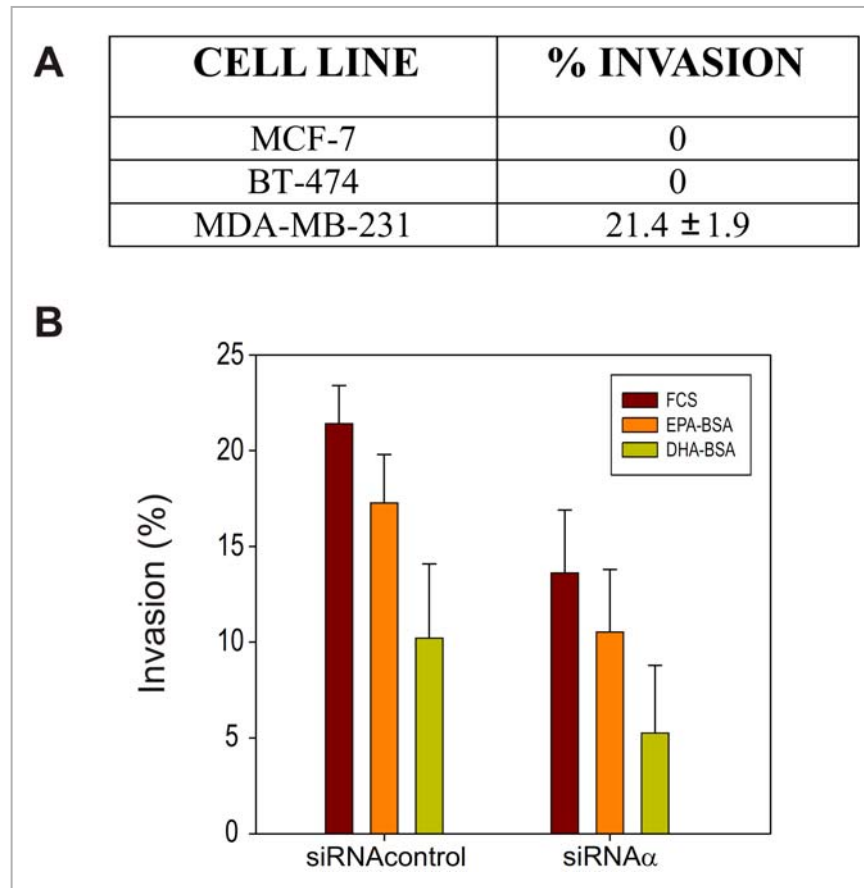


**Figure V.9. Invasion capacity of MDA-MB-231.** A) Shows the invasion percentage in 0.5X BME of the three breast cancer cell lines tested. B) Represents the percentage of invasion of MDA-MB-231 cells transfected with siRNAcontrol or siRNA $\alpha$  and stimulated with EPA, DHA or none of them. Results are representative of three independent experiments.

These results of migration and invasion assays are compatible with those obtained by Germain and co-workers, who proposed that the effects of omega-3 fatty acids on cell viability and hydroperoxide generation are proportional to the number of double bonds, the effects induced by DHA (6 double bonds) being more pronounced than those produced by EPA (5 double bonds) (Germain *et al.*, 1998).

#### **2.4. Omega-3 fatty acids and inhibition of PKC $\alpha$ induce apoptosis in breast cancer cell lines.**

Bearing in mind the above mentioned results, we decided to run some apoptosis assays to investigate the role of different omega-3 fatty acids in this aspect of breast cancer cell lines.

Table V.1 are represents all the apoptotic MCF-7 and MDA-MB-231 cells, including those which undergo early and late apoptosis in several conditions.

In MCF-7 cells, it was observed that both omega-3 fatty acids significantly increased (more than two fold) the percentage of apoptosis. In the case of cells without PKC $\alpha$  expression, the programmed cell death percentage rose to 13.7%, whereas in mutant cells incubated with 50  $\mu$ M DHA-BSA or EPA-BSA for 4 days the percentage of cells driven to apoptosis was similar to that of control cells, suggesting that there is no synergy between PKC $\alpha$  depletion and omega-3 fatty acid stimulation (Table V.1).

When MDA-MB-231 cells were tested, the percentage of apoptosis increased when 50  $\mu$ M of EPA-BSA or DHA-BSA were added to the growth medium. The first tripled programmed cell death, while the second one increased it more than 13 times with respect to control cells. When PKC $\alpha$  expression was inhibited in these cells and they were incubated with the fatty acids tested for 5 days, the increases were even bigger, reaching 18.6% and 70.3% of apoptosis in presence of EPA-BSA and DHA-BSA respectively.

These findings illustrate the enormous synergy between omega-3 fatty acids, mainly DHA, and PKC $\alpha$  depletion in MDA-MB-231 cells, since most of the cells undergo apoptosis.

<b>CELL LINE</b>	<b>CONDITIONS</b>	<b>% APOPTOSIS</b>
	siRNAcontrol	7.0 $\pm$ 1.8
	siRNAcontrol + DHA-BSA	16.1 $\pm$ 3.5
<b>MCF-7</b>	siRNAcontrol + EPA-BSA	15.5 $\pm$ 3.5
	siRNA $\alpha$	13.7 $\pm$ 2.8
	siRNA $\alpha$ + DHA-BSA	17.3 $\pm$ 4.2
	siRNA $\alpha$ + EPA-BSA	15.3 $\pm$ 2.7
	siRNAcontrol	2.5 $\pm$ 0.7
	siRNAcontrol + DHA-BSA	32.8 $\pm$ 9.3
<b>MDA-MB-231</b>	siRNAcontrol + EPA-BSA	8.6 $\pm$ 6.8
	siRNA $\alpha$	4.5 $\pm$ 1.7
	siRNA $\alpha$ + DHA-BSA	70.3 $\pm$ 5.2
	siRNA $\alpha$ + EPA-BSA	18.6 $\pm$ 3.2

**Table V.1. Apoptosis percentage of MCF-7 and MDA-MB-231 cells stimulated with omega-3 fatty acids and transfected with siRNAcontrol and siRNA $\alpha$ .** Data show the mean  $\pm$  standard deviation of 5-8 independent experiments.

The use of annexin V-Alexa Fluor<sup>®</sup> 488 to measure apoptotic cells allows us to distinguish between early and late apoptosis (Fig V.10). The apoptosis steps in MDA-MB-231 cells were analyzed and Figure V.10 shows

the corresponding Dot Blot graphs, in which cells were grouped into four populations, depending on their physiological state:

- Top left quadrant: cells stained with propidium iodide (PI), indicating dead cells.
- Bottom left quadrant: double negative cells, that is, cells not stained by PI or annexin V-Alexa Fluor® 488.
- Bottom right quadrant: cells only stained with annexin V-Alexa Fluor® 488, that is, cells in early apoptosis and not yet dead.
- Top right quadrant: double positive cells, that is, cells stained with annexin V-Alexa Fluor® 488 and PI, which indicates late apoptosis (apoptotic cells which have already died).

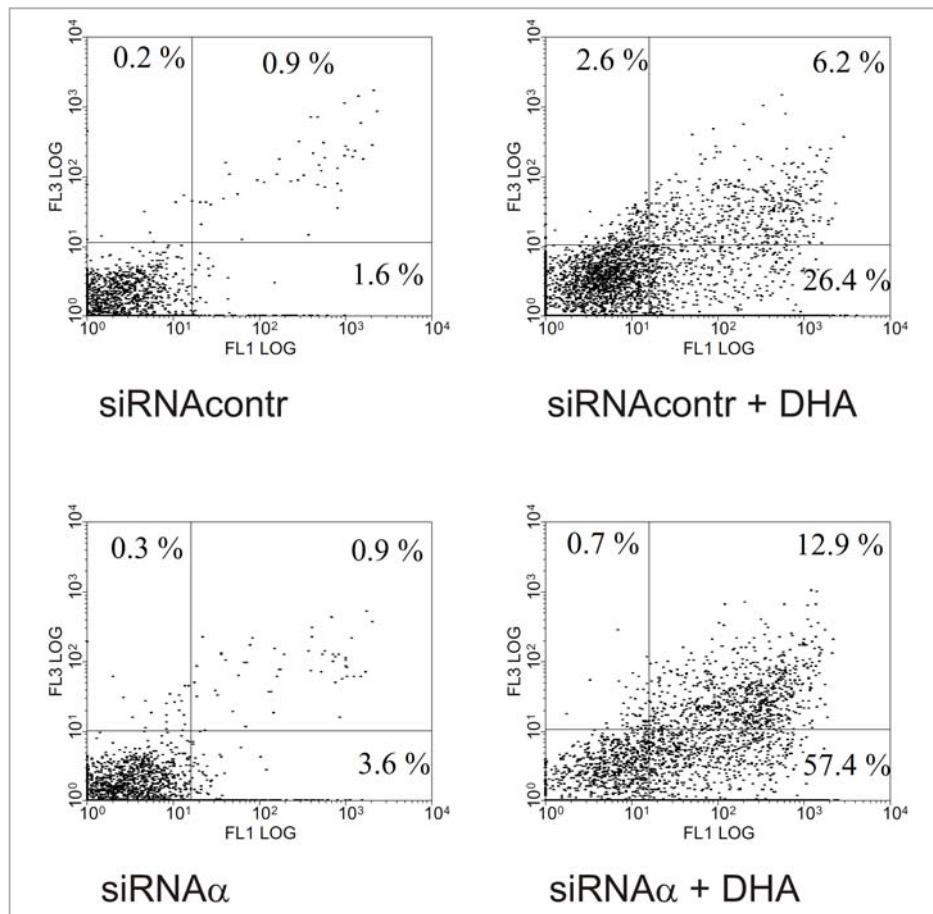


**Figure V.10. Apoptosis of MDA-MB-231 cells induced by docosahexaenoic acid.** Cells were stained with annexin V-Alexa Fluor 488 and PI, and detected by flow cytometry. The lower right quadrant (annexin-V<sup>+</sup> PI<sup>-</sup>) represents early apoptosis, whereas upper right quadrant (annexin-V<sup>+</sup> PI<sup>+</sup>) represents late apoptosis. All results are representative of five-eight independent experiment.

MDA-MB-231 cells showed an insignificant proportion of apoptosis in control conditions (0.9% and 1.6% in late and early apoptosis respectively), while cells incubated with 50  $\mu$ M of DHA-BSA for 5 days increased the apoptotic percentage to 32.8%, mainly early apoptosis (from 1.6% to 26.4%) (Fig V.10).

When we suppressed PKC $\alpha$  expression in MDA-MB-231 cells, apoptosis increased slightly, especially early apoptosis (3.6%), compared with control cells (1.6%). The biggest increase was seen when PKC $\alpha$  was suppressed and DHA-BSA was added to the growth medium, reaching 57.4% in early apoptosis and approximately 12.9% in apoptotic death cells (Fig V.10).

In general, the cell populations were not well-distinguished, although the cluster dots moved to the right, indicating an increase in the number of apoptotic cells.

## CHAPTER VI

### CHARACTERIZATION OF BIOLOGICAL ACTIVITY OF DIACYLGLYCEROL-LACTONES AND ITS EFFECT ON PKCs



## 1. Introduction.

PKC is a target for treating some diseases, for example breast cancer. Several compounds have been used, whose target is the catalytic domain, what implies low selectivity among kinases (*Takahashi et al, 1987; Meyer et al, 1989*). Nowadays, researches are looking for some drugs that modulate the regulatory domains of these kinases; one approach is the C1 domain of PKCs as a drug target. This provides some advantages like specificity among kinases, since few kinases possess this kind of domain, but however, is still an inconvenient to discern among the different PKC isoforms (*Marquez and Blumberg, 2003*).

As a second messenger, DAG mediates the action of numerous growth factors, hormones and cytokines by activating members of the protein kinase C (PKC) family, as well as several other families of signalling proteins, for instance RasGRPs and Chimaerins, that share with PKC the C1 domain as a DAG recognition motif. Many of these signalling pathways feature prominently in the development and properties of cancer cells (*Griner and Kazanitz, 2007*) and, in consequence, PKC isoenzymes are being actively pursued as therapeutic targets for cancer (*Mackay and Twelves, 2007*). The majority of C1 binding ligands that are utilized are structurally rigid and complex natural products, such as the prototypical phorbol esters and the bryostatins (*Choi et al, 2006*). These compounds bind to their C1 receptors with nanomolar affinities and are greater than 3 orders of magnitude more potent than the very flexible, natural DAG agonists.

During the past several years a family of conformationally constrained DAG analogues has been developed, known as DAG-lactones, which were designed to overcome this spread in potency between the natural product ligands and DAG (*Marquez and Blumberg, 2003*). The generation of the prototypical DAG-lactone template is conceptually simple (*Nacro et al, 2000*) and involves the joining of the *sn*-2-*O*-acyl moiety of DAG to the glycerol backbone with an additional carbon atom to complete a five-member ring (Fig VI.1). From this basic structure hundreds of combinations were chemically synthesized changing variable chains R1 and R2 (Fig VI.2), in order to increase affinity and specificity to PKC isoforms (*Pu et al, 2005*), for finally testing them biologically (*Duan et al, 2004; Duan et al, 2008*).

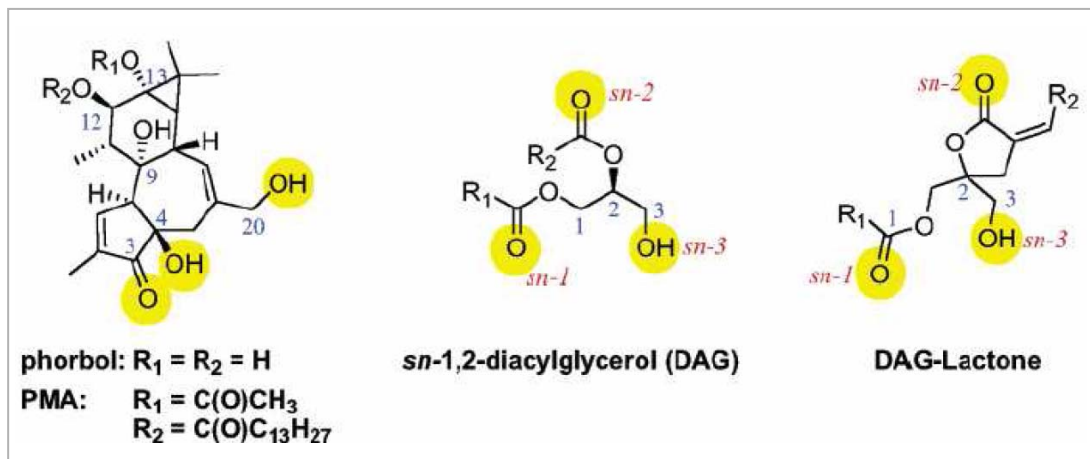


**Figure VI.1. Structural comparison among phorbol ester, DAG and DAG-lactones.** These molecules share three bioequivalent groups (yellow) since they intervene in the interaction between C1 domain and membrane. Carbon positions are marked in blue, and in red (DAG and DAG-lactone) are marked carbonyl or OH groups which arise from carbon 1, 2 or 3. R1 and R2 are variable chains (Taken from *Tamamura and col, 2004*).

Because electrostatic interactions are important for the initial membrane-binding process of PKC, particularly at the lipid bilayer interface, we decided to exploit the role of electrostatic attraction by adding a pyridine ring in R2 position. We reasoned that the pyridine ring could bear several alkyl groups of various sizes to generate a series of *N*-alkylpyridinium chains that could bind to negatively charged phospholipids or engage interactions with aromatic rings of certain amino acids in the C1 domain, such as Trp.

Besides electrostatic interactions, hydrophobic ones possess a huge importance in the biological response. In previous studies it was demonstrated the role of hydrophobicity of lateral chains in the kinetic and PKC $\delta$  localization patterns in the cells (*Wang et al, 2000*).

It is also worthy of note that PKC localization is also controlled by interactions with other proteins, forming multi-proteins complex what favours the signal transduction and confers PKC isoform-selectivity subcellular localization allowing the modulation of biological function in the cells (*Anikumar et al, 2003; Colon-Gonzalez and Kazanietz, 2006*). Other important factor in PKC localization is lipid-protein interactions, since membrane phospholipids can organize the signalling multi-proteins complex (*Duan et al, 2008*). In fact, it is demonstrated that lipid perturbations in plasma membrane modulate the PKC activity (*Goldberg and Zidovetzki, 1997*).

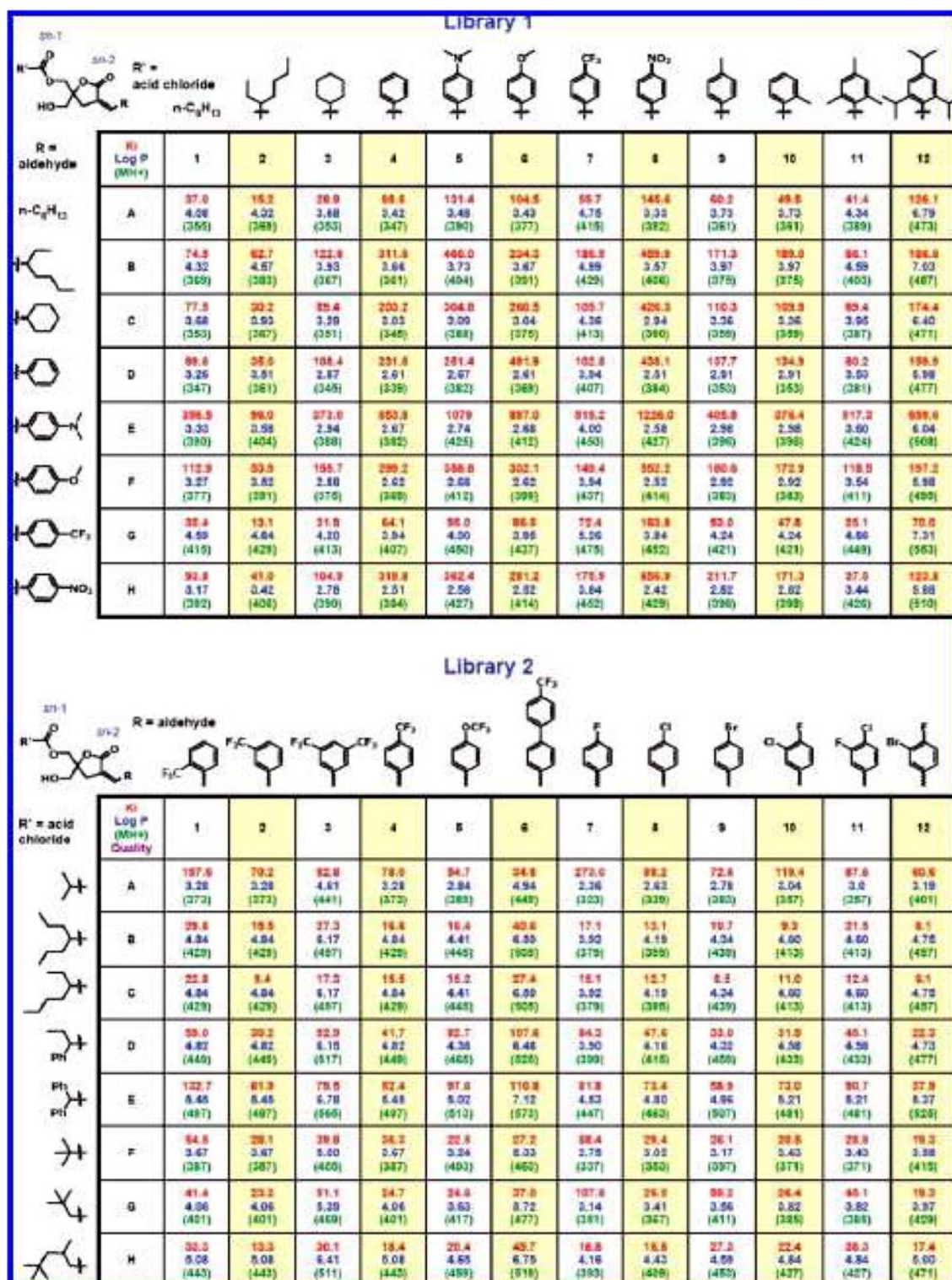


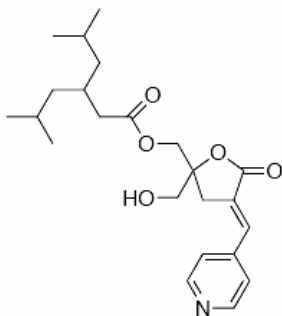
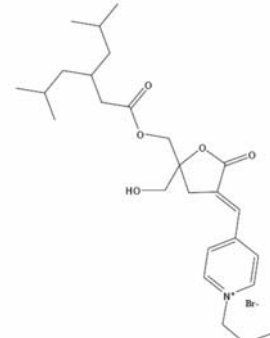
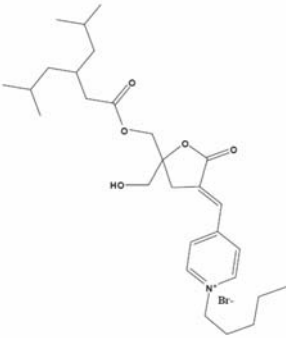
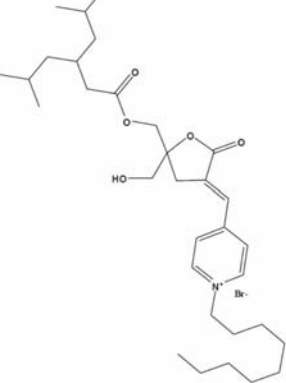
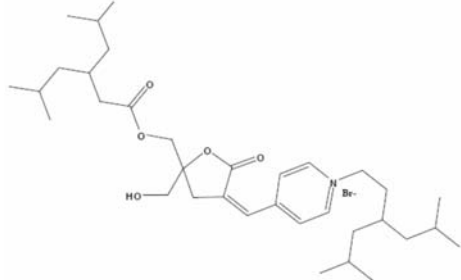
Figure VI.2. Example of combinatory libraries of DAG-lactones.

This work was carried out with specific charged compounds which were designed (153B-095, 153B-097, 153B-140 and 153B-143) (Table VI.1). They have different  $\alpha$ -(4-N-alkylpyridinium) alkylidene side chains which are derived from the parent, neutral DAG-lactone called 153C-022, by simple alkylation. In all the DAG-lactones, the most efficient branched acyl chain R1 known to enhance membrane penetration was chosen (*Marquez and Blumberg, 2003*) and, at the other end of the molecule, the  $\alpha$ -(4-N-alkylpyridinium) alkylidene side chains (position R2) were expected to interact near the surface of the C1 domain adjacent to the lipid interface.

Here, we investigate the translocation properties and PKC binding of 5 DAG-lactones: 153C-022, 153B-095, 153B-097, 153B-140 and 153B-143 (Table VI.1). These ligands are shown to induce different patterns and kinetic profiles for translocation of PKC isoforms to membranes and the lateral movement of this complex (protein-DAG lactone) along them, comparing with phorbol ester. This study aims to examine whether the pattern of membrane association might account for the biological differences.

Data point to a relationship between bilayer surface localization and disruption by the alkyl residues and binding/translocation of the PKC isoforms. Overall, the results expand our understanding on the molecular parameters affecting PKC translocation to membranes and the anchorage on them by synthetic DAG-lactones.

**Table VI.1. DAG-lactones used and its location effect in different PKC isoforms.**

DAG-lactones	DAG-lactone structure
<p><b>153C-022</b></p> <p>Localized in plasma membrane: PKC<math>\alpha</math>, PKC<math>\delta</math> and PKC<math>\epsilon</math></p>	
<p><b>153B-095</b></p> <p>No effect</p>	
<p><b>153B-097</b></p> <p>No effect</p>	
<p><b>153B-140</b></p> <p>No effect</p>	
<p><b>153B-143</b></p> <p>Localized in plasma membrane: PKC<math>\delta</math> and PKC<math>\epsilon</math></p>	

## 2. Results.

### 2.1. Translocation of EGFP-tagged PKC isoenzymes in response to DAG-lactone derivatives.

To investigate whether the DAG-lactones used in this study induced the localization of individual PKC isoenzymes in the plasma membrane and/or other membrane compartments, MCF-7 cells were transiently transfected with the fluorescent constructs PKC $\alpha$ -EGFP (representative of classical isoenzymes), PKC $\epsilon$ -EGFP or PKC $\delta$ -EGFP (representatives of novel PKCs).

After checking the effect of every DAG-lactone in different PKC isoforms localization, compounds that allowed translocation of some isoenzymes to plasma membrane were chosen in order to deeply study their effects on localization velocity ( $t_{1/2}$ ) and protein percentage anchor to membranes (Rmax) (Table VI.2).

**Table VI.2. Plasma membrane translocation parameters calculated for the different PKC isoenzymes in MCF-7 cells stimulated with DAG-lactones and PMA.**

DAG-lactone	isoenzyme	Rmax <sup>a</sup> (%)	$t_{1/2}$ <sup>b</sup> (s)
153C-022	PKC $\alpha$	0.62±0.04	62±13
	PKC $\epsilon$	0.6±0.16	3.5±1.7
	PKC $\delta$	0.56±0.12	15±4.3
153B-095	PKC $\alpha$	No effect	No effect
	PKC $\epsilon$	No effect	No effect
	PKC $\delta$	No effect	No effect
153B-097	PKC $\alpha$	No effect	No effect
	PKC $\epsilon$	No effect	No effect
	PKC $\delta$	No effect	No effect
153B-140	PKC $\alpha$	No effect	No effect
	PKC $\epsilon$	No effect	No effect
	PKC $\delta$	No effect	No effect
153B-143	PKC $\alpha$	No effect	No effect
	PKC $\epsilon$	0.77±0.1	21±5
	PKC $\delta$	0.65±0.07	24±9
PMA	PKC $\alpha$	0.64±0.08	547±192
	PKC $\epsilon$	0.68±0.08	31±18
	PKC $\delta$	0.72±0.06	47±22

<sup>a</sup>Maximal percentage of protein localized in the plasma membrane.

<sup>b</sup>Half-time of plasma membrane localization.

### **2.1.1. Effect of PMA and 153C-022 on PKC localization.**

The derivative 153C-022 (which presents only a pyridinium ring in R2 position what make it a neutral compound, that is, there is not charge) induced the plasma membrane localization of the three isoenzymes tested (Table VI.2 and Figs VI.3, VI.4 and VI.5). The percentage of protein localized in the plasma membrane (Rmax) was similar for the three isoenzymes, although the membrane distribution was heterogeneous and the three proteins concentrated in concrete areas of the plasma membrane. In addition, it was observed that this DAG-lactone induced the localization of PKC $\delta$ -ECFP in vesicles distributed through the cytosol (Fig VI.4), suggesting that the protein and/or lipid composition of these vesicles enhances the targeting effect of the DAG-lactone in the case of this novel isoenzyme.

The phorbol ester also causes the translocation to plasma membrane in three PKC isoforms used in this study in a similar way than DAG-lactone 153C-022 (heterogeneous distribution), although in PKC $\delta$ -ECFP does not localize in vesicles along cytoplasm. The percentage of protein translocated in the plasma membrane (Rmax) was similar for the three isoforms, although there is a big difference in half-time localization ( $t_{1/2}$ ) between novel and classical PKCs (Table VI.2).

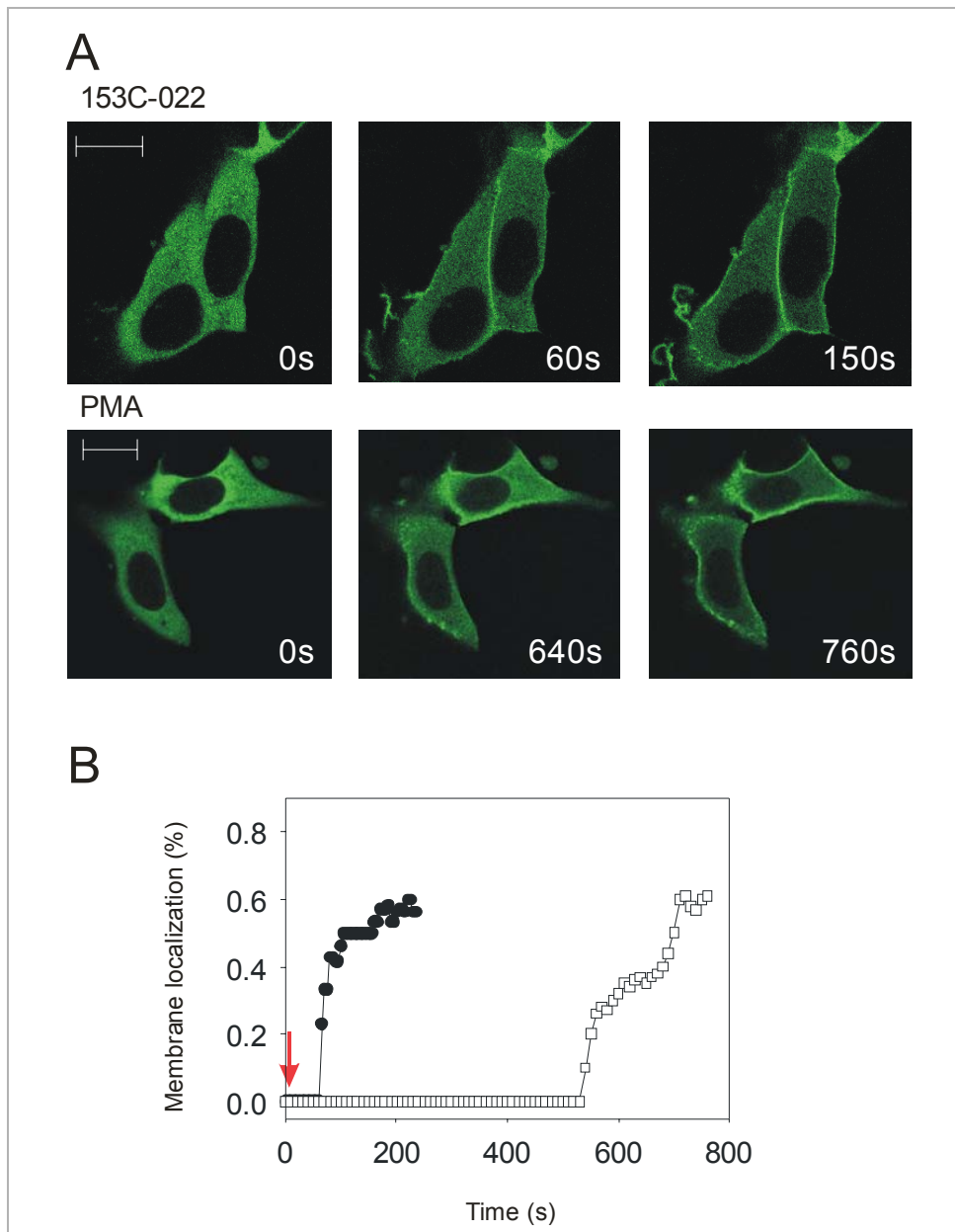


**Figure VI.3. Effect of DAG-lactone 153C-022 on the plasma membrane localization of PKC $\alpha$ .** (A) Confocal images of MCF-7 cells expressing PKC $\alpha$ -EGFP and stimulated with 40  $\mu$ M DAG-lactone 153C-022 (upper panels) or 40  $\mu$ M PMA (lower panels). Time in seconds after stimulation is indicated in each micrograph. (B) The protein localization was measured by a line profile (pixel density) traced in each frame as indicated in the materials and methods section. The resulting net change in PKC $\alpha$  plasma membrane localization upon DAG-lactone ( $\bullet$ ) and PMA ( $\square$ ) stimulations is expressed as the  $I_{mb}-I_{cyt}/I_{mb}$  ratio (%) and is represented versus time. The red arrow indicates the stimulation time;  $R_{max}$  and  $t_{1/2}$  parameters were calculated graphically (Guerrero-Valero *et al*, 2009). The profiles are representative of the results obtained in the cells analyzed ( $n=16$  for both DAG-lactone and PMA). The scale bars indicated in the micrographs correspond to 12  $\mu$ m.

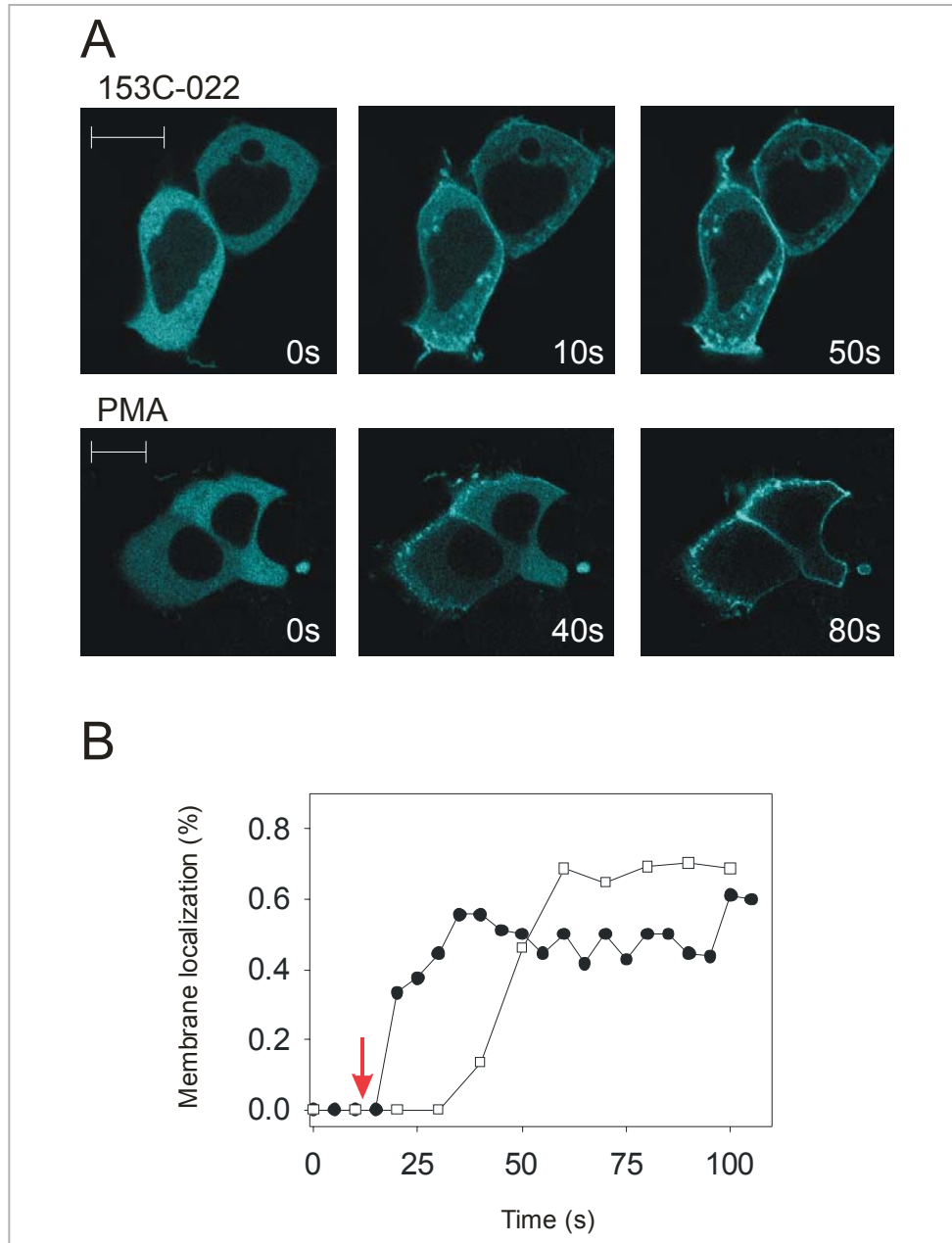


**Figure VI.4. Effect of DAG-lactone 153C-022 on the plasma membrane localization of PKC $\delta$ .** (A) Confocal images of MCF-7 cells expressing PKC $\delta$ -ECFP and stimulated with 40  $\mu$ M DAG-lactone 153C-022 (upper panels) or 40  $\mu$ M PMA (lower panels). Time in seconds after stimulation is indicated in each micrograph. (B) The protein localization was measured by a line profile (pixel density) traced in each frame as indicated in the materials and methods section. It is shown the PKC $\delta$ -ECFP localization profiles obtained after DAG-lactone (●) and PMA (□) stimulations expressed as the  $I_{mb-I_{cyt}}/I_{mb}$  ratio (%) and is represented versus time. The red arrow indicates the stimulation time;  $R_{max}$  and  $t_{1/2}$  parameters were calculated graphically (Guerrero-Valero *et al*, 2009). The profiles are representative of the results obtained in the cells analyzed (n=13 and 12 for DAG-lactone and PMA, respectively). The scale bars indicated in the micrographs correspond to 12  $\mu$ m.

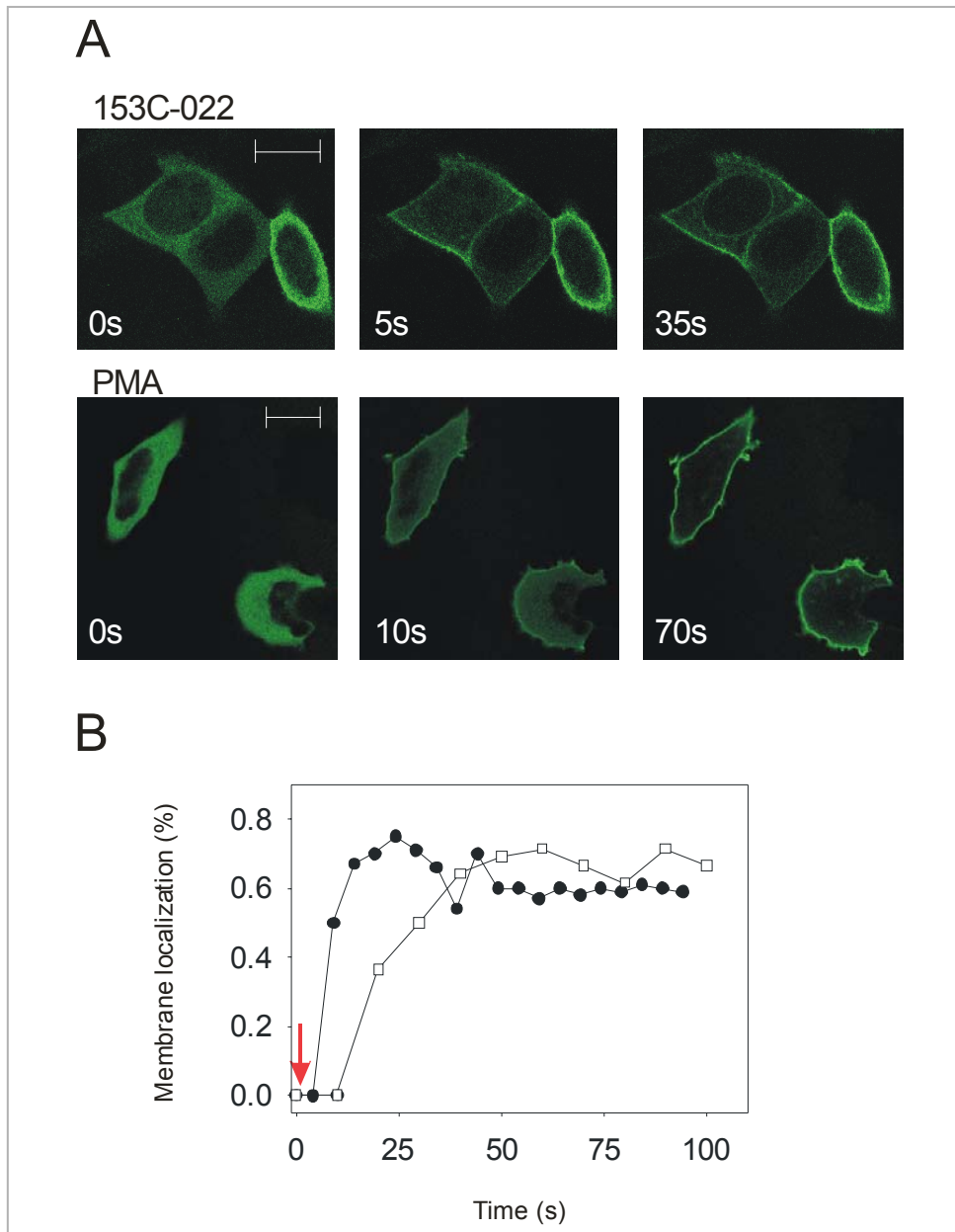


**Figure VI.5. Effect of DAG-lactone 153C-022 on the plasma membrane localization of PKC $\epsilon$ .** (A) Confocal images of MCF-7 cells expressing PKC $\epsilon$ -EGFP and stimulated with 40  $\mu$ M DAG-lactone 153C-022 (upper panels) or 40  $\mu$ M PMA (lower panels). Time in seconds after stimulation is indicated in each micrograph. (B) The protein localization was measured by a line profile (pixel density) traced in each frame as indicated in the materials and methods section. The PKC $\epsilon$ -EGFP localization profiles obtained after DAG-lactone (●) and PMA (□) stimulations is expressed as the  $I_{mb-I_{cyt}}/I_{mb}$  ratio (%) and is represented versus time. The red arrow indicates the stimulation time;  $R_{max}$  and  $t_{1/2}$  parameters were calculated graphically (Guerrero-Valero *et al.*, 2009). The profiles are representative of the results obtained in the cells analyzed ( $n=12$  and 10 for DAG-lactone and PMA, respectively). The scale bars indicated in the micrographs correspond to 12  $\mu$ m.

Comparison of the half-times of plasma membrane localization ( $t_{1/2}$ ) induced by DAG-lactone 153C-022 in transfected MCF-7 cells, indicated that PKC $\epsilon$ -EGFP translocates to the plasma membrane at significantly fewer

seconds than PKC $\delta$ -ECFP followed by PKC $\alpha$ -EGFP (Table VI.2 and Fig VI.6A), suggesting that PKC $\epsilon$ -EGFP has a higher affinity for this derivative than PKC $\delta$ -ECFP and PKC $\alpha$ -EGFP.

When the effect of PMA on protein localization was examined, significant differences in the localization velocity among isoforms were observed. The half-time of translocation of PKC $\alpha$ -EGFP was very high compared to those exhibited by PKC $\delta$ -ECFP and PKC $\epsilon$ -EGFP, while inside the novel subfamily there was no difference (Fig VI.6B and Table VI.2). This confirms the higher affinity of novel over classical PKCs to bind this phorbol ester (*Kazanietz et al, 1993; Pu et al, 2009*).

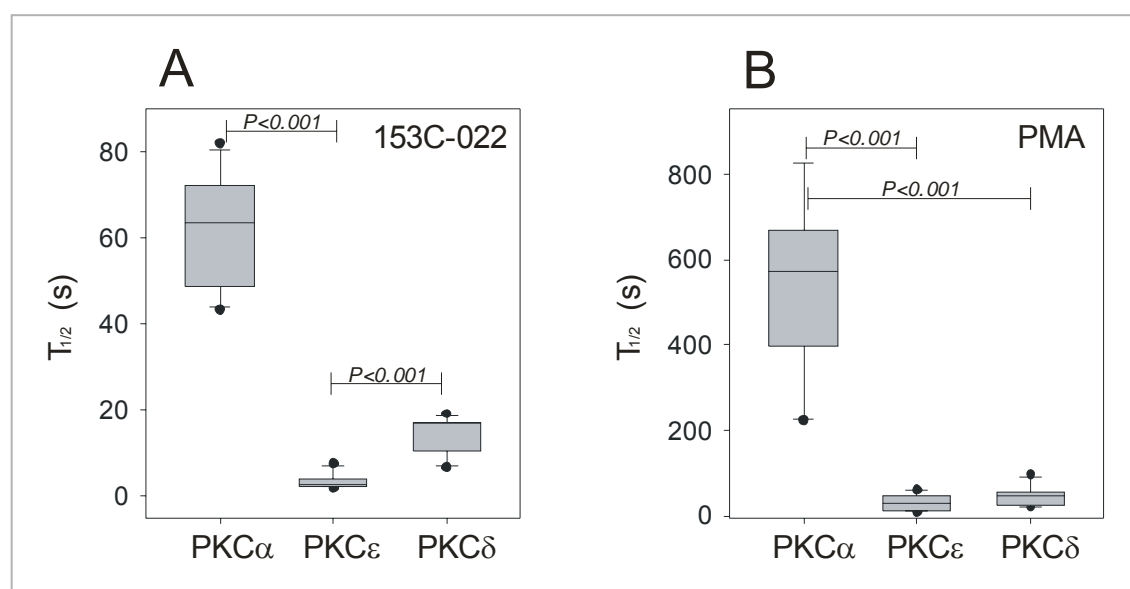


**Figure VI.6. Comparison of the effect of DAG-lactones 153C-022 and PMA on the plasma membrane translocation parameters of the different PKC isoenzymes.** The box for each condition represents the interquartile range (25-75<sup>th</sup> percentile), the black line within each box is the median value. Bottom and top bars of the whisker indicate the 10<sup>th</sup> and 90<sup>th</sup> percentiles, respectively. Outlier values are indicated (closed circles). A Mann-Whitney test was performed to determine whether a difference existed between the parameters analyzed. Comparison of the  $t_{1/2}$  parameters obtained upon stimulation of the different isoenzymes with the 153C-022 derivative (A) and PMA (B). The values obtained were considered significantly different if  $P < 0.05$ .

The additions of simple n-alkyl chains of different lengths in the R2 substituents of DAG-lactone 153C-022 rendered some derivatives. Among them, 153B-095, 153B-097 and 153B-140 were not able to induce membrane localization when they were added to MCF-7 cells transfected with the different isoenzymes tested in this study (Table VI.2). However, the DAG-lactone 153B-143 containing a highly branched alkyl chain in the R2, instead of a simple n-alkyl chain, could induce the translocation of the novel PKCs tested in this study (PKC $\epsilon$ -EGFP and PKC $\delta$ -ECFP) in transfected MCF-7 cells (Table VI.2).

### 2.1.2. Effect of 153B-143 on PKC localization.

The highly branched alkyl chain in the R2 position of 153B-143 endowed the DAG-lactone with the capacity to induce the translocation, specifically, of novel PKCs (PKC $\epsilon$ -EGFP and PKC $\delta$ -EGFP) from the cytosol to the plasma membrane at very similar rate, although the percentage of PKC $\epsilon$ -EGFP localized at the plasma membrane was slightly higher than that of PKC $\delta$ -EGFP (Table VI.2 and Fig VI.7).

This DAG-lactone derivative, like the parental one (153C-022), also induced the localization of PKC $\delta$ -EGFP in vesicles distributed through the cytosol (Fig VI.7B). This effect was not observed when the cells were stimulated with PMA, suggesting that the localization of the enzyme in vesicles is dependent on DAG-lactones stimulation.

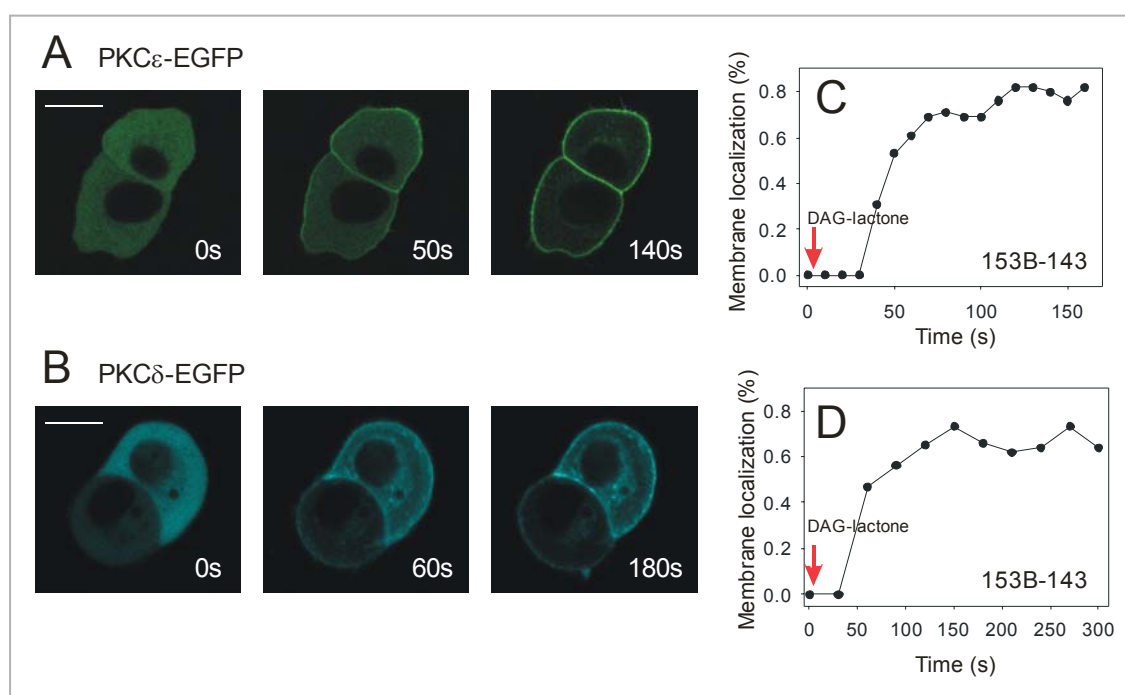


**Figure VI.7. Effect of DAG-lactone 153B-143 on the plasma membrane localization of PKC isoenzymes.** Confocal images of MCF-7 cells expressing PKC $\epsilon$ -EGFP (A) or PKC $\delta$ -EGFP (B) stimulated with 40  $\mu$ M DAG-lactone 153B-143. Time in seconds after stimulation is indicated in each micrograph. The scale bars indicated correspond to 12  $\mu$ m. (C, D) The percentage of protein localization was measured by a line profile (pixel density) traced in each frame as indicated in the materials and methods section. The resulting net change in PKC $\epsilon$  or PKC $\delta$  plasma membrane localization upon DAG-lactone ( $\bullet$ ) stimulation is expressed as the  $I_{mb} - I_{cyt} / I_{mb}$  ratio (%) and is represented versus time. The red arrow indicates the stimulation time;  $R_{max}$  and  $t_{1/2}$  parameters were calculated graphically. The profiles are representative of the results obtained in the cells analyzed ( $n=12$  and  $10$  for PKC $\epsilon$  or PKC $\delta$ , respectively).

When the translocation parameters ( $R_{max}$  and  $T_{1/2}$ ) of PKC $\epsilon$ -EGFP and PKC $\delta$ -ECFP were compared in MCF-7 cells stimulated with different compounds (PMA and several DAG-lactones), it was observed that there were slightly differences between them (Table VI.2). This confirms the similar affinity of both novel isoforms to bind several phorbol ester and DAG-lactones, with the exception of 153C-022, where significant differences were observed (Fig VI.6).

However, important differences appeared when paying attention to the half-times of plasma membrane localization ( $t_{1/2}$ ) produced by the different compounds in one isoenzyme separately (Fig VI.8 and Table VI.2). In that way, it was observed that PMA induced a slower localization of PKC $\delta$ -ECFP than DAG-lactone 153B-143, followed by 153C-022 (Fig VI.8A and Table VI.2). This suggests that this novel PKC has a higher affinity for DAG-lactones, especially for 153C-022, than PMA.

In the case of PKC $\epsilon$ -EGFP, something similar happened, although the different affinity between DAG-lactones is even higher than in PKC $\delta$ -ECFP, but it is still higher than phorbol ester (Fig VI.8B and Table VI.2).

Moreover, when  $t_{1/2}$  obtained for any of three tested isoenzymes upon PMA or DAG-lactones were compared, it was observed that the synthetic compounds induced a faster translocation to plasma membrane than PMA in all cases (Table VI.2 and Figs VI.6 and VI.8), suggesting that these isoenzymes show a bigger affinity for this derivatives than PMA.

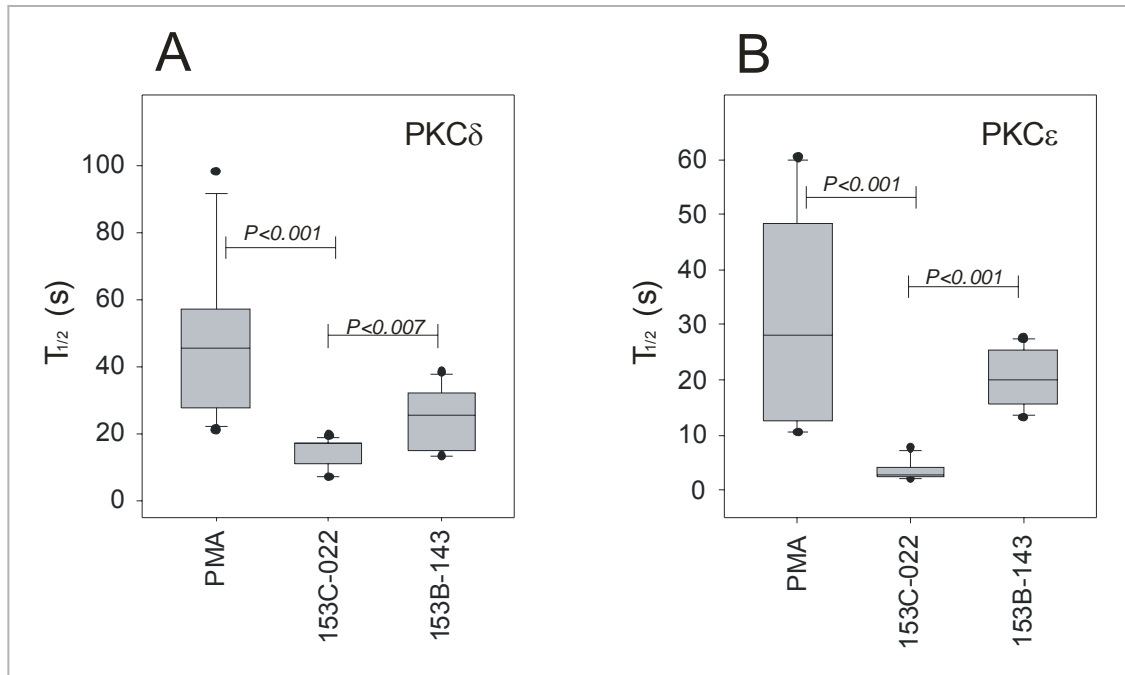


**Figure VI.8. Comparison of the effect of DAG-lactones derivatives on the plasma membrane translocation parameters of the novel PKC isoenzymes.** The box for each condition represents the interquartile range (25-75<sup>th</sup> percentile), the black line within each box is the median value. Bottom and top bars of the whisker indicate the 10<sup>th</sup> and 90<sup>th</sup> percentiles, respectively. Outlier values are indicated (closed circles). A Mann-Whitney test was performed to determine whether a difference existed between the parameters analyzed. Comparison of the  $t_{1/2}$  parameters obtained for PKC $\delta$ -ECFP (A) and PKC $\epsilon$ -EGFP (B) when they were stimulated with PMA, 153C-022 and 153B-143 derivatives. The values obtained were considered significantly different if  $P < 0.05$ .

## 2.2. Tightness of the plasma membrane binding interactions measured by FRAP.

We also studied the tightness of the protein-membrane interaction by FRAP (Fluorescence Recovery After Photobleaching) measurements.

When PKC isoforms reached a stable localization after stimulate transfected MCF-7 cells with PMA or different DAG-lactones, FRAP measurements were carried out as indicate in the materials and methods section (Chapter II). The analysis of this assays allowed us to calculate the lateral diffusion coefficient (D) and mobile fraction (Mf) in the plasma membrane of every isoform (Table VI.3).

**Table VI.3. FRAP parameters calculated for the different PKC isoenzymes in MCF-7 cells stimulated with DAG-lactones and PMA.**

DAG-lactone	isoenzyme	D ( $\mu\text{m}^2/\text{s}$ ) <sup>a</sup>	Mf <sup>b</sup> (%)
153C-022	PKC $\alpha$	1.6 $\pm$ 0.48	79 $\pm$ 15
	PKC $\epsilon$	0.76 $\pm$ 0.2	73 $\pm$ 10
	PKC $\delta$	N.D. <sup>c</sup>	N.D.
153B-143	PKC $\epsilon$	0.68 $\pm$ 0.27	81 $\pm$ 15
	PKC $\delta$	N.D.	N.D.
PMA	PKC $\alpha$	0.74 $\pm$ 0.25	53 $\pm$ 16
	PKC $\epsilon$	0.76 $\pm$ 0.3	71 $\pm$ 13
	PKC $\delta$	0.46 $\pm$ 0.2	52 $\pm$ 11

<sup>a</sup>Lateral diffusion coefficient in the plasma membrane.

<sup>b</sup>Mobile fraction in the plasma membrane.

<sup>c</sup>N.D. Not determined, PKC $\delta$  dissociates from the plasma membrane in a short time and this was incompatible with the FRAP measurements.

### 2.2.1. Effect of PMA and 153C-022 on fluorescence recovery after photobleach PKC $\alpha$ .

When the cells were stimulated with the DAG-lactone 153C-022 the diffusion coefficient of membrane-associated PKC $\alpha$ -EGFP was significantly higher ( $P < 0.001$ ) than when they were stimulated with PMA (Fig VI.9A and Table VI.3), suggesting that the interactions established between PKC $\alpha$ -EGFP and this DAG-lactone derivative allow the protein to diffuse more rapidly in the membrane than in the case of PMA.

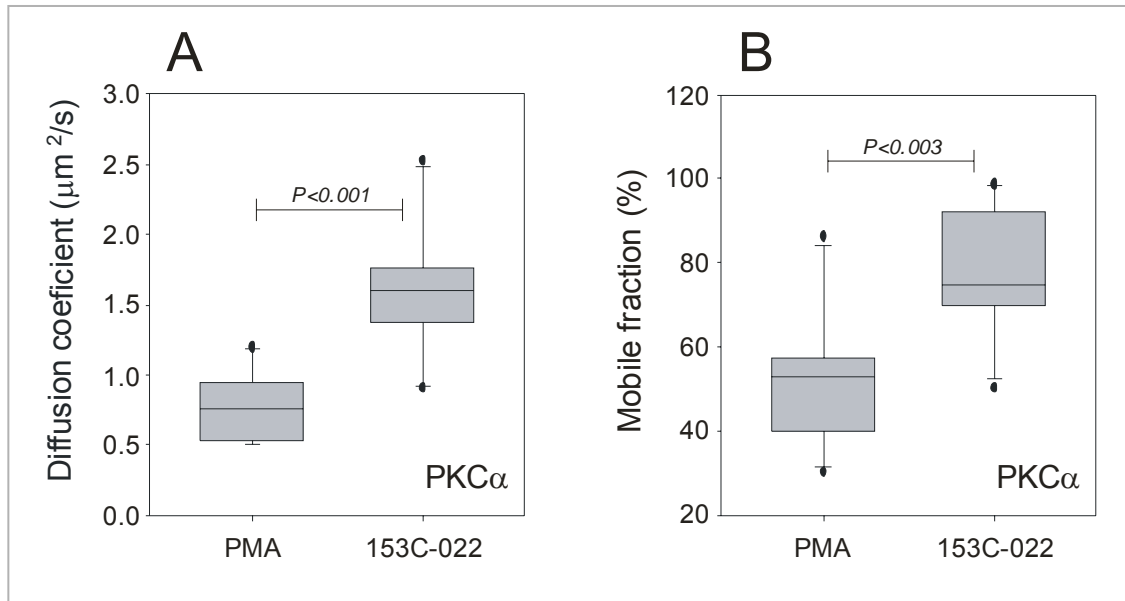


**Figure VI.9. Comparison of the effect of PMA and 153C-022 on the lateral diffusion coefficient and mobile fraction of PKC $\alpha$ .** The box for each condition represents the interquartile range (25-75<sup>th</sup> percentile), the black line within each box is the median value. Bottom and top bars of the whisker indicate the 10<sup>th</sup> and 90<sup>th</sup> percentiles, respectively. Outlier values are indicated (closed circles). A Mann-Whitney test was performed to determine whether a difference existed between the parameters analyzed. Comparison of the diffusion coefficient (A) and mobile fraction (B) parameters obtained for PKC $\alpha$ -EGFP when they were stimulated with PMA and 153C-022 derivative. The values obtained were considered significantly different if  $P < 0.05$ .

In addition, stimulation with PMA rendered a 47% of PKC $\alpha$ -EGFP immobile fraction while the 153C-022 derivative produced only a 21% (Table VI.3 and Fig VI.9B), indicating again that the interactions that PKC $\alpha$ -EGFP establishes with the DAG-lactone are less tight than those established with PMA.

### 2.2.2. Effect of PMA, 153C-022 and 153B-143 on fluorescence recovery after photobleach PKC $\epsilon$ .

In the case of PKC $\epsilon$ -EGFP, no significant differences in both diffusion coefficient and mobile fraction were observed when comparing stimulations with PMA or the DAG-lactone derivatives (153C-022 and 153B-143). However, the diffusion coefficient of PKC $\epsilon$ -EGFP in the cells stimulated with the 153C-022 derivative was significantly lower ( $P < 0.001$ ) than that of PKC $\alpha$ -EGFP (Fig VI.10 and Table VI.3), indicating that PKC $\epsilon$ -EGFP diffuses slower than PKC $\alpha$ -EGFP upon 153C-022 stimulation.

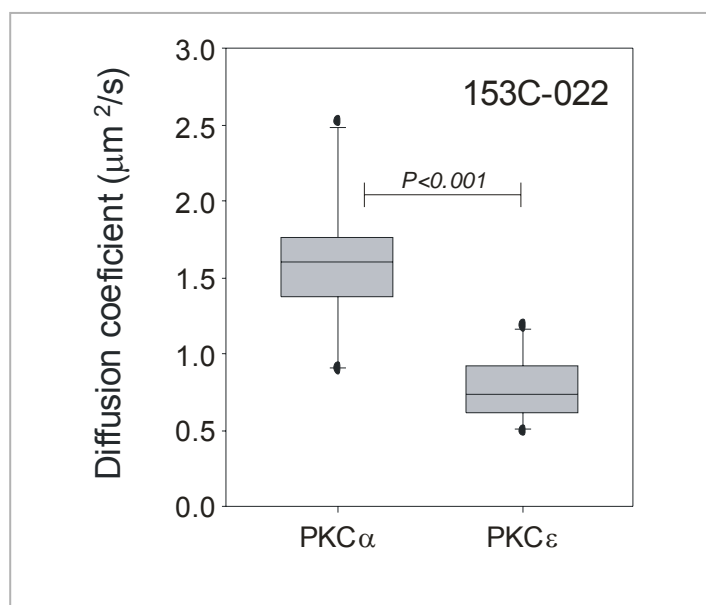


**Figure VI.10. Comparison of the effect of DAG-lactones 153C-022 on the diffusion coefficient parameter of PKC $\alpha$  and PKC $\epsilon$ .** The box for each condition represents the interquartile range (25-75<sup>th</sup> percentile), the black line within each box is the median value. Bottom and top bars of the whisker indicate the 10<sup>th</sup> and 90<sup>th</sup> percentiles, respectively. Outlier values are indicated (closed circles). A Mann-Whitney test was performed to determine whether a difference existed between the parameter analyzed upon stimulation of the different isoenzymes with the 153C-022 derivative. The values obtained were considered significantly different if  $P < 0.05$ .

### 2.2.3. Effect of PMA, 153C-022 and 153B-143 on fluorescence recovery after photobleach PKC $\delta$ .

PKC $\delta$ -ECFP has transient plasma membrane localization upon DAG-lactones stimulations and this was incompatible with the FRAP measurements.

It was only possible to calculate lateral diffusion coefficient and mobile fraction when transfected MCF-7 cells were stimulated with PMA, since PKC $\delta$ -ECFP had stable plasma membrane localization (Table VI.3). These results show that the interactions established between this novel isoform and phorbol ester allow the protein to diffuse more slowly along the membrane than other PKC isoforms, being this diffusion rate the smallest one found in this work (Fig VI.11A).

Regarding mobile fraction, the results rendered a 48% PKC $\delta$ -ECFP immobile fraction, similar to PKC $\alpha$ -EGFP, while PKC $\epsilon$ -EGFP showed only a 29% (Table VI.3 and Fig VI.11B), suggesting that the interactions of PKC $\alpha$  and PKC $\delta$  established with PMA are tighter than those established by PKC $\epsilon$  with the phorbol ester.

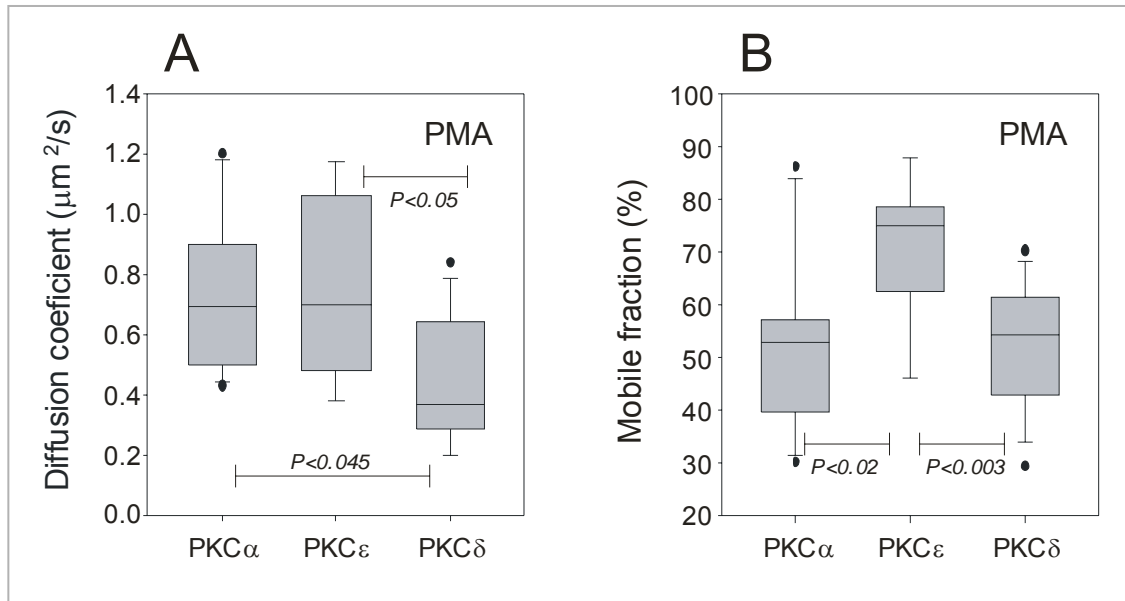


**Figure VI.11. Comparison of the effect of PMA on the diffusion coefficient and mobile fraction parameters of the different PKC isoenzymes.** The box for each condition represents the interquartile range (25-75<sup>th</sup> percentile), the black line within each box is the median value. Bottom and top bars of the whisker indicate the 10<sup>th</sup> and 90<sup>th</sup> percentiles, respectively. Outlier values are indicated (closed circles). A Mann-Whitney test was performed to determine whether a difference existed between the parameters analyzed. Comparison of the diffusion coefficient (A) and mobile fraction (B) upon stimulation of the different isoenzymes with PMA. The values obtained were considered significantly different if  $P < 0.05$ .

## CHAPTER VII

# GENE EXPRESSION PROFILE OF BREAST CANCER CELLS IN ABSENCE OF PKC $\alpha$



## 1. Introduction.

Starting in the 1990s, a genomic revolution, propelled by major technological advances, has enabled scientists to obtain the full sequences of a variety of organisms, including viruses, bacteria and invertebrates, culminating in the full draft sequence of the human genome (*Lander et al., 2001*). In the wake of this flood of sequence information, scientists are currently faced with the daunting task of translating genomic sequence information into functional biological mechanisms that will allow a better understanding of life and its disease states and hopefully offer better diagnostics and novel therapeutic interventions. High-density microarrays are uniquely qualified to tackle this daunting task and have therefore become an essential tool in life sciences research (*Sherlock, 2000; Schulze and Downward, 2001*).

In the last decade, there has been an immense growth in the use of high-throughput microarray technology for three major genetic explorations: the genome-wide analysis of gene expression, SNP genotyping, and resequencing (*Harrington et al., 2000; van Hal et al., 2000*). New applications are rapidly emerging, such as the discovery of novel transcripts (from coding and non-coding regions), the identification of novel regulatory sequences, and the characterization of functional domains in the RNA transcript. Integrating all of the information emanating from whole-genome studies will undoubtedly allow a more global understanding of the genome and the regulatory circuits that govern its activity.

The comparison of genome-wide expression patterns provides researchers with an objective and hypothesis-free method to better understand the dynamic relationship between mRNA content and biological function. This method has enabled scientists to discover, for example, the genetic pathways that are changed and disrupted in a wide range of diseases like cancer (*Armstrong et al., 2002; Yeoh et al., 2002; Huang et al., 2004*). Across multiple disciplines, whole-genome expression analysis is helping scientists to stratify disease states, predict patient outcome, and make better therapeutic choices.

In general, the classical PKC isoform, PKC $\alpha$ , is over-expressed in breast cancer cells and it has been associated with malignant transformation, increasing the motility and invasiveness of cancer cells (*Masur et al., 2001*), tumour cell proliferation, multi-drug resistance (MDR) (*Tonetti et al., 2002*), alteration of ER status (*Li et al., 2003*) and apoptosis (*Le et al., 2001*), among others. Many of these findings are based on studies with breast cancer cell lines like MCF-7 (ER+) and MDA-MB-231 (ER-).

In our laboratory it has also been demonstrated that the inhibition of PKC $\alpha$  expression in breast cancer cell lines reduces the proliferation, migration and invasion percentage, as well as, increases apoptosis (see chapter IV).

Taking into account all these studies directly relating PKC $\alpha$  and tumour progression, and the appearance of novel technologies, the next step in our investigation was to compare the gene expression profiles of control breast cancer cell lines and those where PKC $\alpha$  expression had been down-regulated.

## 2. Results.

### 2.1. Inhibition of PKC $\alpha$ expression in MCF-7 cells.

To shed light on the function of this classical PKC isoform in breast cancer cell lines, its expression was down-regulated in two cell lines: MCF-7 and MDA-MB-231 by using siRNA interference.

After scanning the chips (three control and three mutant ( $\Delta$ PKC $\alpha$ )), the raw data were processed with the statistical programming language R version 2.7.1, and Bioconductor packages. Firstly, gene expression was normalized with the robust multi-array (RMA) method, as implemented in the Bioconductor package “affy”. Genes showing significantly differential expression between PRKCA knockout and control were identified using the empirical Bayes (eBayes) moderated t-test, as implemented in the Bioconductor package “limma”. Finally, we obtained a list of these genes, which were classified into two groups: down- and up-regulated. Note that gene expressions were considered statistically significant when the p-value was smaller than 0.01.

These lists of genes, which were expressed in a significantly different manner between control and mutant ( $\Delta$ PKC $\alpha$ ) cells, were independently introduced in the GeneCodis database, (*Carmona-Saez et al., 2007; Nogales-Cadenas et al., 2009*), where they were classified following the three different categories of Gene Ontology (Gene Ontology Consortium, <http://www.geneontology.org>) (Biological Process, Cellular Component and Molecular Function) at level four of specificity and KEGG pathways (<http://www.genome.jp/kegg/>), which was the most interesting classification since it informs us about pathways where these proteins are involved.

GeneCodis (<http://genecodis.dacya.ucm.es/>) is a web-based tool that integrates different sources of biological information to search for biological features (annotations) that frequently co-occur in a set of genes and rank them by statistical significance. It can be used to determine biological annotations

or combinations of annotations that are significantly associated to a list of genes under study with respect to a reference list.

We used this tool because, to date, most of the currently available tools are designed to evaluate single annotations and they provide a list of annotations with their corresponding p-values without taking into account the potential relationships among them. Finding relationships among annotations based on co-occurrence patterns, which is implemented in GeneCodis, will extend our understanding of the biological events associated to a given experimental system.

Basically, the GeneCodis program determines annotations that are over-represented in a group of genes with respect to a reference set of genes. Two different statistical tests can be used separately, hypergeometric distribution or chi-square test, or both. In addition, a method is used to correct p-values for multiple hypothesis testing: the FDR correction or simulation correction. In this work, chi-square test and FDR correction were used.

It is important to note that only results with p-values lower than 0.05 will be shown, since GeneCodis considers that other results are not significant enough to be taken into account.

### **2.1.1. Genes down-regulated after PKC $\alpha$ inhibition.**

From the whole list of genes differently expressed between control and mutant cells (306 genes), approximately 60% (177 genes) were down-regulated, while only 129 genes were up-regulated.

After classifying down-regulated genes according to KEGG pathways, the largest group of genes was related with *pathways in cancer*. Other important groups identified were *MAPK*, *ErbB* and *p53 signalling pathways* (Fig VII.1). Another striking result is that four down-regulated genes were classified in the *Calcium signalling pathway*, suggesting that inhibition of PKC $\alpha$  synthesis also affects the transcription of other calcium-binding proteins.

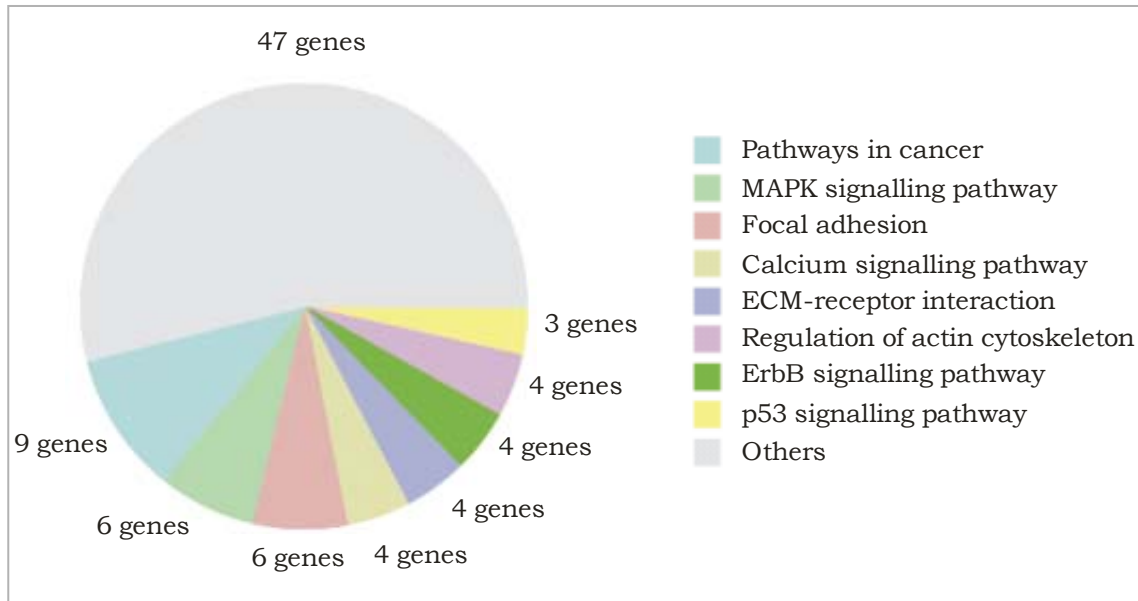


**Figure VII.1. MCF-7 down-regulated genes, after inhibition of PKC $\alpha$  expression, classified upon KEGG pathway.** The pie graph shows the number of genes per singular annotations found by GeneCodis.

Table VII.1 shows the number of genes classified into each group, the short name of these genes and the statistical value that indicates the significant level for this classification. Most groups showed a high significance level, since the corrected chi-square p-value was practically zero.

The presence of PKC $\alpha$  gene (PRKCA) in the list of down-regulated ones demonstrates that the use of specific siRNA to inhibit its expression worked correctly. In addition, the fold change in the expression of this gene is one of the most important (see annex I).

Note that some genes are included in several groups, which highlights the importance of PKC $\alpha$  in MCF-7 cells. When PKC $\alpha$  is down-regulated, other important genes, whose expression produces central proteins in some signalling pathways, are also down-regulated (for example EGFR among others).

**Table VII.1. MCF-7 down-regulated genes classified in KEGG pathways.**

<b>PATHWAYS</b>	<b>N° GENES</b>	<b>GENES</b>	<b>CHI<sup>a</sup></b>
Pathways in cancer	9	EPAS1, ITGA2, RUNX1, STAT1, PPARG, EVI1, PRKCA, CASP3, EGFR	1.92 E-08
MAPK signalling pathway	6	COL4A6, EVI1, PRKCA, CASP3, EGFR, DUSP6	9.61 E-05
Focal adhesion	6	ITGA2, CAV1, COL5A1, PRKCA, EGFR, ITGB6	7.71 E-07
Calcium signalling pathway	4	PRKCA, EGFR, ATP2B1, IL8	0.00217
ECM-receptor interaction	4	ITGA2, CD36, COL5A1, ITGB6	9.17 E-08
Regulation of actin cytoskeleton	4	ITGA2, EGFR, ITGB6, IL8	0.00673
ErbB signalling pathway	4	EREG, PRKCA, EGFR, BTC	1.57 E-07
p53 signalling pathway	3	SERPINB5, CASP3, IGFBP3	1.70 E-05

<sup>a</sup> Corrected chi square p-Value

### 2.1.2. Genes up-regulated after PKC $\alpha$ inhibition.

Only 40% of genes (129 genes from a total of 306) were up-regulated after inhibiting PKC $\alpha$  expression.

These genes were classified according KEGG pathways and some important groups were highlighted, for example *inositol phosphate metabolism* and *phosphatidylinositol signalling system*. It has been demonstrated in our laboratory that phosphoinositols, mainly PtdIns(4,5)P<sub>2</sub>, can activate PKC $\alpha$  with a higher affinity than classical cofactors (*Guerrero-Valero et al., 2007; Marín-Vicente et al., 2008*).

This fact reinforces our hypothesis and suggests that in the absence of PKC $\alpha$ , other signalling proteins (like Phospholipase C beta 4), which interact with phosphoinositols, acquire an important role in the cellular signalling driven by these compounds.

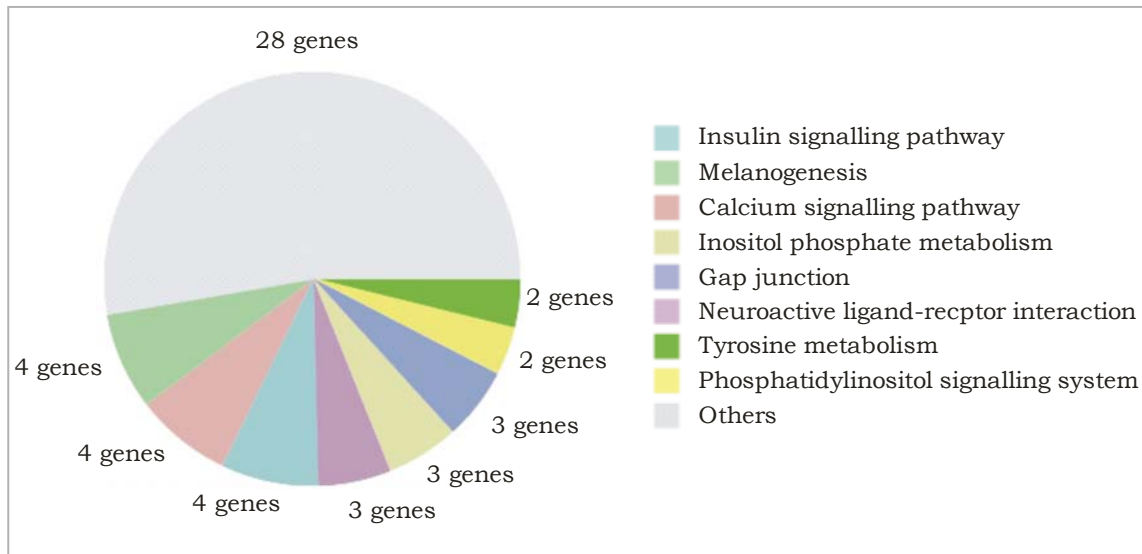


**Figure VII.2. MCF-7 up-regulated genes, after inhibition of PKC $\alpha$  expression, classified upon KEGG pathway.** The pie graph shows the number of genes per singular annotations found by GeneCodis.

The number of genes classified in each group can be observed in Table VII.2, where the short name of these genes and the statistical value that show a significant level for this classification are given. The majority of groups show a high level of significance, since the corrected chi-square p-value is practically zero.

**Table VII.2. MCF-7 up-regulated genes classified in KEGG pathways.**

PATHWAYS	N° GENES	GENES	CHI <sup>a</sup>
Insulin signalling pathway	4	PPP1R3C, PRKAR2B, PRKAB2, SOCS2	7.36 E-07
Melanogenesis	4	PLCB4, ADCY1, TCF7L2, TYRP1	1.77 E-09
Calcium signalling pathway	4	PLCB4, ERBB4, ADCY1, GNA14	3.64 E-05
Inositol phosphate metabolism	3	PLCB4, SYNJ2, ALDH6A1	1.86E-10
Gap junction	3	PLCB4, ADCY1, PDGFA	7.28E-06
Neuroactive ligand-receptor interaction	3	NPY5R, NPY1R, PTGER4	0.0296819
Tyrosine metabolism	2	AOX1, TYRP1	1.14E-05
Phosphatidylinositol signalling system	2	PLCB4, SYNJ2	0.00124674

<sup>a</sup> Corrected chi square p-Value

### 2.1.3. Validation of arrays data.

After observing the results obtained, our hypothesis was that over-expression of certain genes when PKC $\alpha$  expression is suppressed, compensates the absence of this enzyme in order to continue growing, migrating, etc. For this reason, we designed migration and apoptosis assays in which some of these over-expressed proteins were inhibited with specific drugs in order to investigate the effect of both specific inhibitors and PKC $\alpha$  suppression on migration capacity and apoptosis in MCF-7 cells.

Specific commercially available inhibitors were screened for some of the proteins whose genetic expression was up-regulated after PKC $\alpha$  inhibition. We decided to inhibit four proteins which act at the beginning of different signalling cascades, using the following compounds:

- U73122 to specifically inhibit Phospholipase C (PLC).
- KT 5720 to specifically inhibit Protein Kinase A (PKA).
- BMS-599626 to specifically inhibit Human epidermal growth factor receptor (HER or Erb B).
- Imatinib to specifically inhibit Platelet-derived growth factor receptor (PDGF).

The compounds were added separately to the growth medium in order to study the effect of each compound on migration capacity and apoptosis in the presence and in the absence of PKC $\alpha$ .

Every compound was tested at two different concentrations and, in general, at least one of them produced a significant decrease in the migration capacity of MCF-7 cells. In cells without PKC $\alpha$ , the effect of the inhibitors on the migration capacity was even higher, migration falling to the basal level.

In a deeper study of each compound, we observed that the specific inhibitor of PLC (U73122) significantly decreased the migration capacity of MCF-7 cells when they were treated with 10  $\mu$ M of the mentioned compound, while 1  $\mu$ M produced a slight effect. When MCF-7 cells expressed a residual level of PKC $\alpha$ , the effect of U73122 in migration was enhanced, the migration percentage remaining at 10% when cells were treated with 10  $\mu$ M of the drug (Fig VII.3B).

From the micrographs, it can be observed that when 10  $\mu$ M U73122 was added to the growth medium of MCF-7 cells without PKC $\alpha$ , they were unable to migrate (Fig VII.3A). In addition, 72 hours after treating with 10  $\mu$ M, these mutant cells showed small zones without cells in the monolayer and also some round and black cells floating in the medium.

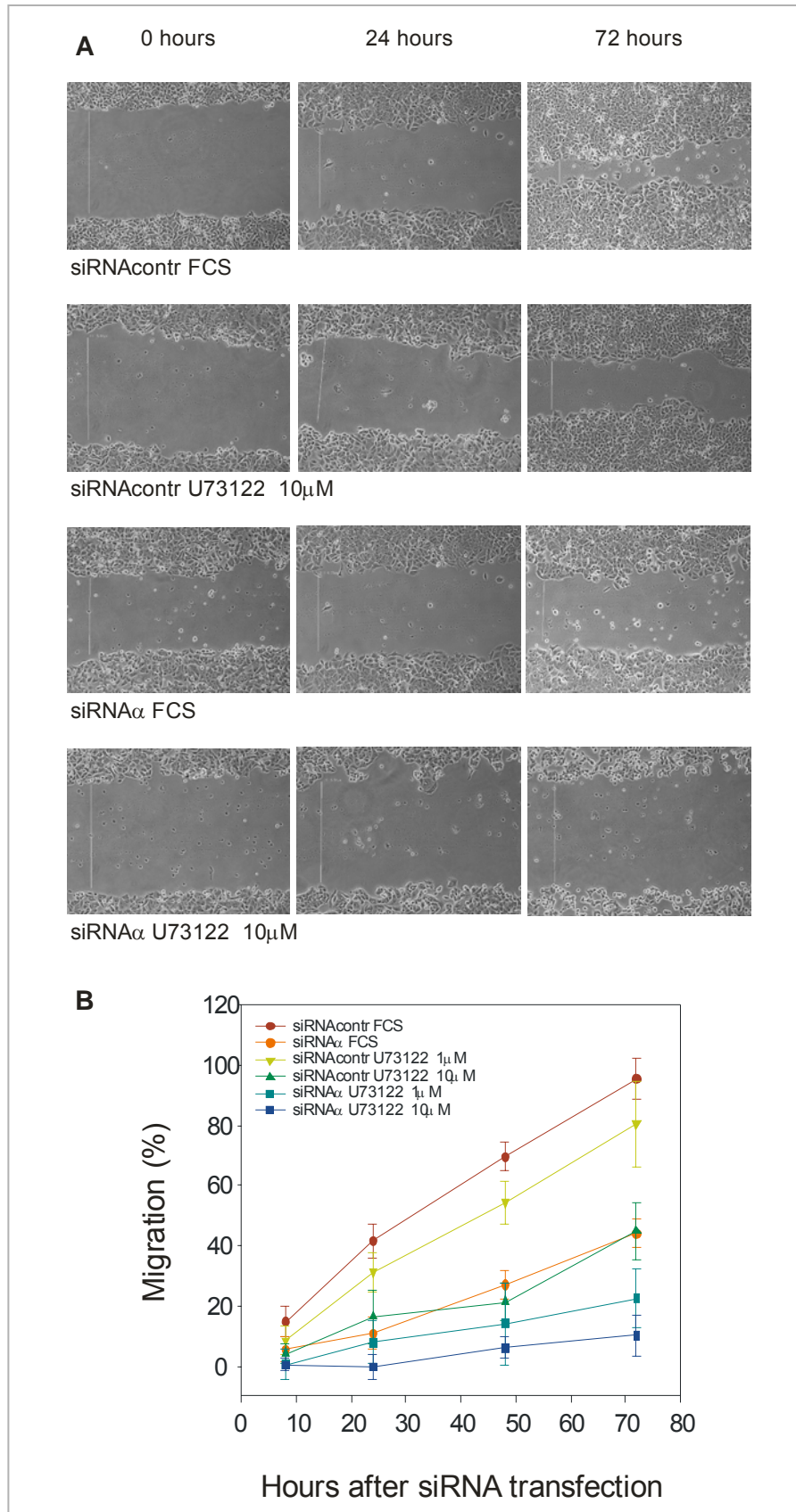


**Figure VII.3. Migration of MCF-7 cells stimulated with U73122.** A) Shows micrographs of cells with and without PKC $\alpha$  expression and treated, or not, with U73122 10  $\mu$ M at three different times (when the scratch is done, 24 and 72 hours later). In B) is represented the analysis of wound healing assays for each of the conditions tested along 72 hours. It is represented the mean and standard deviation of three independent experiments.

In the case of PKA specific inhibitor (KT5720), the results showed that the effect on migration capacity is dose-dependent in MCF-7 control cells. They lost approximately 40% of their migration capacity when they were treated with 0.1  $\mu$ M of KT5720, while, surprisingly, 1  $\mu$ M of the compound had no effect on migration (Fig VII.4).

In cells where the level of PKC $\alpha$  is reduced, KT5720 almost completely abolished cell migration in a dose-independent manner. When treated with 0.1 or 1  $\mu$ M of the drug, these mutant cells only migrated 10% compared with control cells after 72 hours (Fig VII.4).

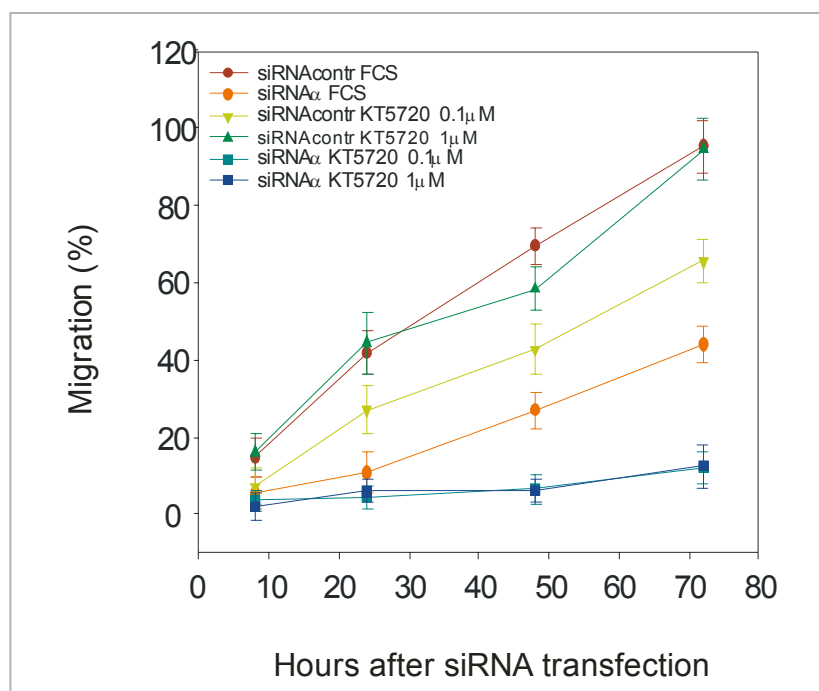


**Figure VII.4. Migration of MCF-7 cells stimulated with KT5720.** It is represented the migration profiles of MCF-7 cells upon different stimulations along 72 hours. The migration profiles consist of measuring the width of scratch wound at every time, and the migration percentage was calculated regards to initial size of scratch. Results are representative of three independent experiments.

The results obtained with these two compounds (U73122 and KT5720) showed synergy with PKC $\alpha$  inhibition, since when both treatments (siRNA $\alpha$  and specific drug) were applied, the migration capacity of MCF-7 cells almost disappeared (Fig VII.3B and Fig VII.4).

Another specific inhibitor tested was BMS-599626, which specifically inhibits HER or ErbB. This compound inhibits migration by approximately 35% at both concentrations tested in control MCF-7 cells, while in PKC $\alpha$

knockout cells the inhibition reached 80%, also independently of the concentration tested (Fig VII.5B).

In micrographs (Fig VII.5A) it can be observed that this compound inhibits the migration capacity of both control and mutant MCF-7 cells, even at the lowest concentration tested (0.1  $\mu\text{M}$ ). As in the case of U73122, when the expression of PKC $\alpha$  was suppressed in MCF-7 cells and 0.1  $\mu\text{M}$  of BMS-599626 was added to the growth medium, cells did not migrate and some clear zones appeared inside the cell monolayer (Fig VII.5A).

This substance also shows synergy with the inhibition of PKC $\alpha$  expression, although not to the same extent as the two previous compounds. In this case, mutant cells treated with BMS-599626 can migrate 20% after 72 hours.

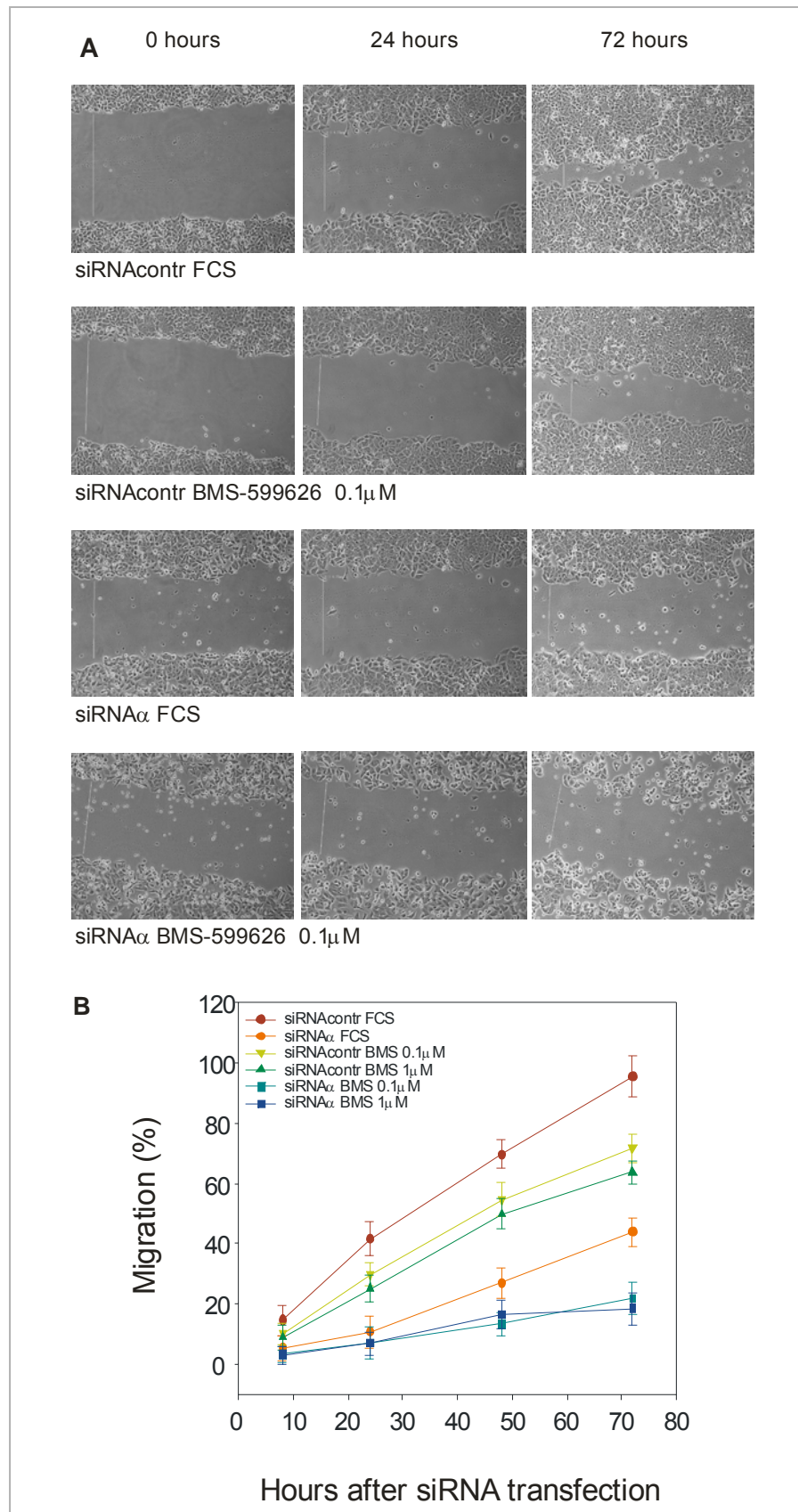


**Figure VII.5. Migration of MCF-7 cells stimulated with BMS-599626.** A) Shows micrographs of cells with and without expressing PKC $\alpha$  and treated, or not, with BMS-599626 0.1  $\mu$ M at three different moments (when the scratch is done, 24 and 72 hours later). In B) is represented the analysis of wound healing assays of every condition tested along 72 hours. It is represented the mean and standard deviation of three independent experiments.

The last compound tested was imatinib, a specific inhibitor of PDGF. The results demonstrate that this drug does not affect MCF-7 migration capacity, although the highest concentration tested seemed to inhibit this characteristic slightly in control and mutant cells after 72 hours of treatment (Fig VII.6).

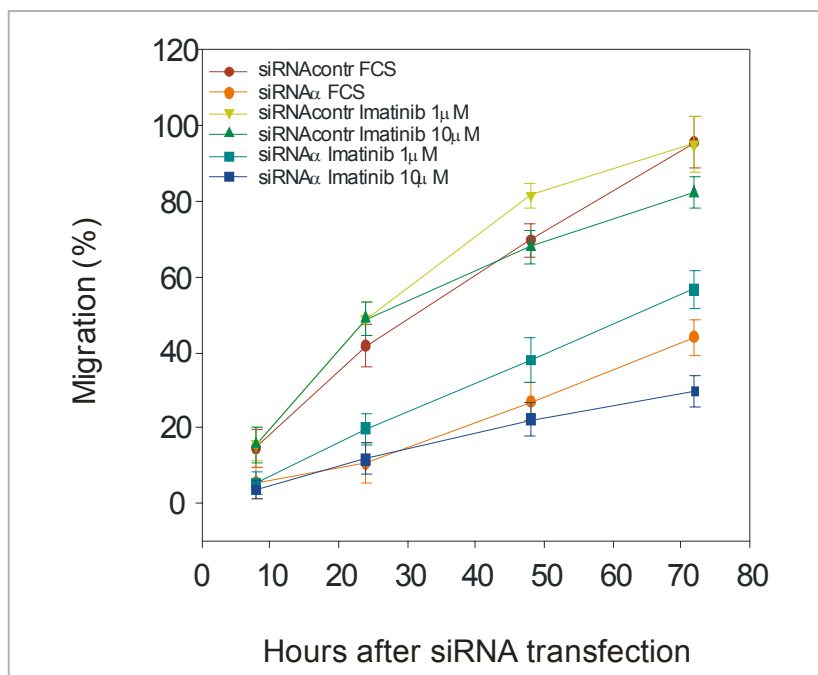


**Figure VII.6. Migration of MCF-7 cells stimulated with Imatinib.** It is represented the migration profiles of MCF-7 cells upon different stimulations along 72 hours. The migration profiles consist of measuring the width of scratch wound at every time, and the migration percentage was calculated regards to initial size of scratch. Results are representative of three independent experiments.

These results concerning migration capacity of MCF-7 cells corroborate those obtained in the microarray, since the effect of specific inhibitors is enhanced when PKC $\alpha$  expression is inhibited. MCF-7 cells over-express some genes to compensate for the absence of PKC $\alpha$ , and if some of these proteins are inhibited too, these breast cancer cells are unable to migrate.

The result obtained show that in some treatments, cells were unable to migrate, and clear zones appeared next to the cell clumps (Figs VII.3A and VII.5A). In light of this, we decided to run some experiments to measure the apoptosis of MCF-7 cells treated with the same specific inhibitors in the presence or absence of PKC $\alpha$ .

Apoptosis was also measured in order to validate the results obtained in the microarrays and, as in the migration assays, two concentrations of each compound were tested.

In general, in programmed cell death there is no synergy between specific inhibitors and the absence of PKC $\alpha$ , since the increase in apoptosis of MCF-7 is the same in the presence and in the absence of this enzyme, that is, these compounds induce a slight or moderate increase in the percentage of apoptosis independently of PKC $\alpha$  in MCF-7 cells.

Table VII.3 shows the great variety of results obtained. Both in control and mutant cells, KT5720 did not induce apoptosis while BMS-599626 hardly increased it. Two others compounds, imatinib and U73122, had a greater effect on programmed cell death, especially the highest concentration tested, duplicating or trebling the values, respectively, when the PKC $\alpha$  level was residual or normal.

In the case of U73122, the apoptosis results corroborated those obtained for migration, and some floating and black cells appeared after inhibiting PKC $\alpha$  expression and treating MCF-7 with 10  $\mu$ M of the drug for 72 hours (Fig VII.3A).

**Table VII.3. Apoptosis of MCF-7 under different treatments.**

<b>MCF-7 CONDITIONS</b>	<b>% APOPTOSIS</b>
siRNAcontrol	7.0 $\pm$ 1.8
siRNAcontrol + BMS-599626 0.1 $\mu$ M	10.3 $\pm$ 1.3
siRNAcontrol + BMS-599626 1 $\mu$ M	12.1 $\pm$ 1.5
siRNAcontrol + Imatinib 1 $\mu$ M	18.5 $\pm$ 5.9
siRNAcontrol + Imatinib 10 $\mu$ M	28.9 $\pm$ 5.7
siRNAcontrol + KT 5720 0.1 $\mu$ M	7.8 $\pm$ 1.6
siRNAcontrol + KT 5720 1 $\mu$ M	7.5 $\pm$ 1.9
siRNAcontrol + U 73122 1 $\mu$ M	12.4 $\pm$ 5.3
siRNAcontrol + U 73122 10 $\mu$ M	26.1 $\pm$ 4.5
siRNA $\alpha$	13.7 $\pm$ 2.8
siRNA $\alpha$ + BMS-599626 0.1 $\mu$ M	13.1 $\pm$ 0.3
siRNA $\alpha$ + BMS-599626 1 $\mu$ M	14.4 $\pm$ 0.7
siRNA $\alpha$ + Imatinib 1 $\mu$ M	18.3 $\pm$ 3.0
siRNA $\alpha$ + Imatinib 10 $\mu$ M	24.1 $\pm$ 2.3
siRNA $\alpha$ + KT 5720 0.1 $\mu$ M	10.0 $\pm$ 2.2
siRNA $\alpha$ + KT 5720 1 $\mu$ M	8.6 $\pm$ 1.6
siRNA $\alpha$ + U 73122 1 $\mu$ M	13.2 $\pm$ 4.0
siRNA $\alpha$ + U 73122 10 $\mu$ M	22.5 $\pm$ 6.4

The effect obtained for migration and apoptosis support the results obtained in the microarrays. All of the drugs tested decreased migration, induced apoptosis or both when PKC $\alpha$  expression was suppressed.

Imatinib hardly affected the migration capacity but increased the apoptosis of control and PKC $\alpha$  knockout MCF-7 cells. In contrast, KT 5720 and BMS-599626 had no effect on apoptosis but almost abolished the migration of MCF-7 cells without PKC $\alpha$ . The specific PLC inhibitor, U-73122, significantly increased the percentage of apoptosis and decreased the migration capacity of control and PKC $\alpha$  knockout MCF-7 cells.

## **2.2. Inhibition of PKC $\alpha$ expression in MDA-MB-231 cells.**

To shed light on the role of PKC $\alpha$  in MDA-MB-231 cells, protein expression was inhibited in the same way as explained above for MCF-7 cells and their mRNAs were extracted and submitted to differential expression by microarray analysis.

Despite the high level of PKC $\alpha$  in MDA-MB-231 cells, when its expression was down-regulated by means of specific siRNA, the expression profiles of a small number of genes (130) appeared significantly modified.

### **2.2.1. Genes down-regulated after PKC $\alpha$ inhibition.**

In MDA-MB-231, most of the genes differently expressed between control and mutant cells were down-regulated (90 genes), while only 30% were up-regulated. These results highlight the very important role of PKC $\alpha$  in MDA-MB-231, since its downregulation involves the down-regulation of many other genes.

In this cell line, after using siRNA $\alpha$ , the PRKCA expression was the lowest in down-regulated genes, reaching a value of -2.94, which is much lower than next gene (COL1A2) whose fold change was -1.31 (see annex II). This also demonstrates that transfection and interfering RNA oligonucleotides worked correctly.

After KEGG pathways classification, *pathways in cancer* was the group which included the largest number of genes (Fig VII.7). Other important annotations are *small cell lung cancer* and *cytokine-cytokine receptor interactions*, among others.

At this point it is important to mention that some of these groups are similar to those found downregulated in MCF-7 cells, for example *focal adhesion* and *ECM-receptor interactions*. This indicates that, although the genes involved in each group differ between both cell lines, some of the cascades or functions affected after inhibiting PKC $\alpha$  are similar.

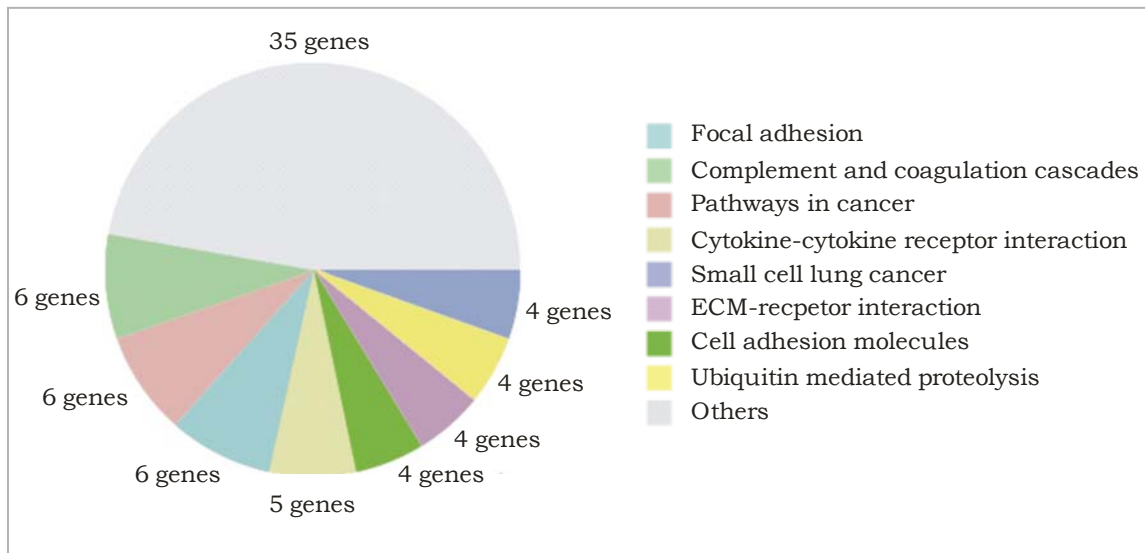


**Figure VII.7. MDA-MB-231 down-regulated genes, after inhibition of PKC $\alpha$  expression, classified upon KEGG pathway.** The pie graph shows the number of genes per singular annotations found by GeneCodis.

Table VII.4 shows the number of genes classified into each group, the short name of these genes and the statistical value that shows the significance level for this classification. All annotations show a statistical value of approximately zero, which indicates the very high significance level of this classification.

In general, all of these genes present in Table VII.4 coincide with the next hypothesis: when *prkca* expression is inhibited, the expression of other genes involved in proliferation, apoptosis arrest and cell cycle stimulation is also inhibited, for example *skp2* (Meng et al., 2010) and *birc3* (Frasor et al., 2009), respectively.

**Table VII.4. MDA-MB-231 down-regulated genes classified in KEGG pathways.**

<b>PATHWAYS</b>	<b>N° GENES</b>	<b>GENES</b>	<b>CHI<sup>a</sup></b>
Focal adhesion	6	TNC, LAMC2, BIRC3, PRKCA, COL1A2, COL6A3	1.32 E-16
Complement and coagulation cascades	6	SERPINA5, CFI, SERPINA1, C1S, C3, IL8	<1.22 E-19
Pathways in cancer	6	LAMC2, CCNE2, BIRC3, PRKCA, FZD1, SKP2	3.42 E-09
Cytokine-cytokine receptor interaction	5	TNFRSF9, CXCL3, CXCL1, CXCL2, IL6ST	2.36 E-08
Small cell lung cancer	4	LAMC2, CCNE2, BIRC3, SKP2	1.24 E-16
ECM-receptor interaction	4	TNC, LAMC2, COL1A2, COL6A3	1.54 E-16
Cell adhesion molecules (CAMs)	4	VCAM1, HLA-DRB5, CD58, HLA-DPB1	1.28 E-10
Ubiquitin mediated proteolysis	4	BRCA1, BIRC3, SKP2, MID1	9.63 E-11

<sup>a</sup> Corrected chi square p-Value

Similarly as in the case of MCF-7, some genes in MDA-MB-231 cells are included in several annotations, since proteins which are codified by these down-regulated genes are involved in several important cellular functions.

### **2.2.2. Genes up-regulated after PKC $\alpha$ inhibition.**

As mentioned above, in PRKCA knockout cells than in control cells only 40 genes showed significantly higher expression levels.

When we analyzed the up-regulated genes in PKC $\alpha$  knockout cells, other oncogenes were over-expressed and most of the groups classified by KEGG pathways involved many cancer signalling cascades, emphasizing *pathways in cancer* (Fig VII.8).

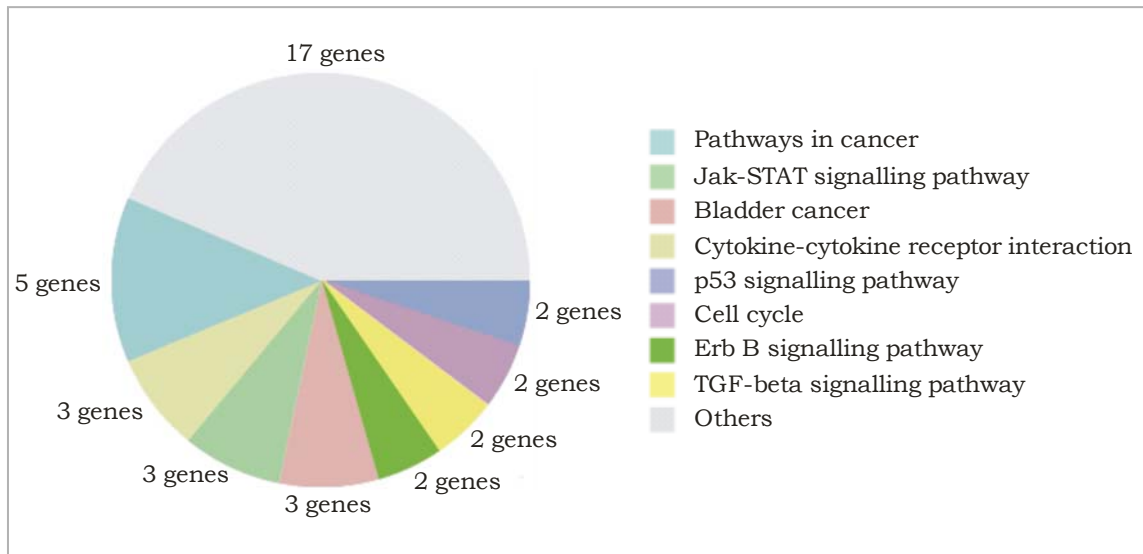


**Figure VII.8. MDA-MB-231 up-regulated genes, after inhibition of PKC $\alpha$  expression, classified upon KEGG pathway.** The pie graph shows the number of genes per singular annotations found by GeneCodis.

Table VII.5 shows the genes included in every group, and the statistical value that shows the significance level for this classification. As expected, there were just a few genes in each group, although all annotations showed a statistical value of approximately zero, which, once again, indicates the very high significance level of this classification.

The genes which appear in this table possess a malignant function, mainly Ras-related GTPase, for example *ralA* (Balasubramanian *et al.*, 2010) and *rrad* (Suzuki *et al.*, 2007) among others. On the contrary, there are also other up-regulated genes whose proteins are involved in cell cycle arrest and decreasing proliferation, for example *bmp2* (Dumont and Arteaga, 2003) and *cdkn1a* (Privat *et al.*, 2010), respectively.

**Table VII.5. MDA-MB-231 up-regulated genes classified in KEGG pathways.**

<b>PATHWAYS</b>	<b>N° GENES</b>	<b>GENES</b>	<b>CHI<sup>a</sup></b>
Pathways in cancer	5	MMP1, RALA, CDKN1A, BMP2, RRAD	9.02 E-15
Jak-STAT signalling pathway	3	IL11, SOCS2, IL24	5.39 E-12
Bladder cancer	3	MMP1, CDKN1A, THBS1	<1.22 E-19
Cytokine-cytokine receptor interaction	3	IL11, BMP2, IL24	1.97 E-07
p53 signalling pathway	2	CDKN1A, THBS1	4.90 E-12
Cell cycle	2	CDKN1A, RRAD	5.00 E-08
Erb B signalling pathway	2	CDKN1A, RRAD	7.02 E-10
TGF-beta signalling pathway	2	BMP2, THBS1	4.58 E-10

<sup>a</sup> Corrected chi square p-Value

### 2.2.3. Validation of arrays data.

Previous results obtained in our laboratory for PKC $\alpha$  knockout MDA-MB-231 cells indicated that after deleting this enzyme, cells adopt a less aggressive phenotype, since they show slower proliferation and a lower invasion capacity (Chapter IV of this Doctoral Thesis). This fact reinforces the results obtained in the microarray, where genes involved in tumour promoting are down-regulated, while genes which arrest cell cycle or induce apoptosis are up-regulated.

Apart from this validation, we designed some migration, invasion and apoptosis experiments in which we tested two concentrations of specific protein inhibitors whose genes were up-regulated in the MDA-MB-231 arrays. Specifically, we used the following compounds:

- GGTI-2133 to specifically inhibit geranylgeranyltransferase I (GGTase I) with a 140-fold selectivity over FTase.
- FTI-277 to specifically inhibit farnesyltransferase (FTase), since, even at 10  $\mu$ M, it does not inhibit GGTase.
- GM 1489 to specifically inhibit metalloproteases (MMP).

They were added separately to the growth medium in order to study the effect of each compound on migration, invasion and apoptosis in cells expressing or not PKC $\alpha$ .

As regards the migration assays, it is important to mention that in general, the concentrations tested did not have a clear effect on this cellular aspect, although some of them inhibited it slightly.

More specifically, control MDA-MB-231 cells showed a slight inhibition of their migration capacity (approximately 20%) when they were incubated with the specific inhibitor GGTI-2133 for 24 hours, independently of the concentration tested (Fig VII.9B). In the case of PKC $\alpha$  knockout cells, the effect of this compound was greater, reaching 30% inhibition, but only at 500 nM. This demonstrates the synergy between the inhibition of PKC $\alpha$  expression using siRNA and the inhibition of GGTase by means of GGTI-2133.

In the micrographs (Fig VII.9A), the fibroblast-like morphology and high number of round live cells can be observed, which is typical of MDA-MB-231. These two populations of cells were similar in both control and mutant cells, as well as in cells treated with GGTI-2133 500 nM for 24 hours.

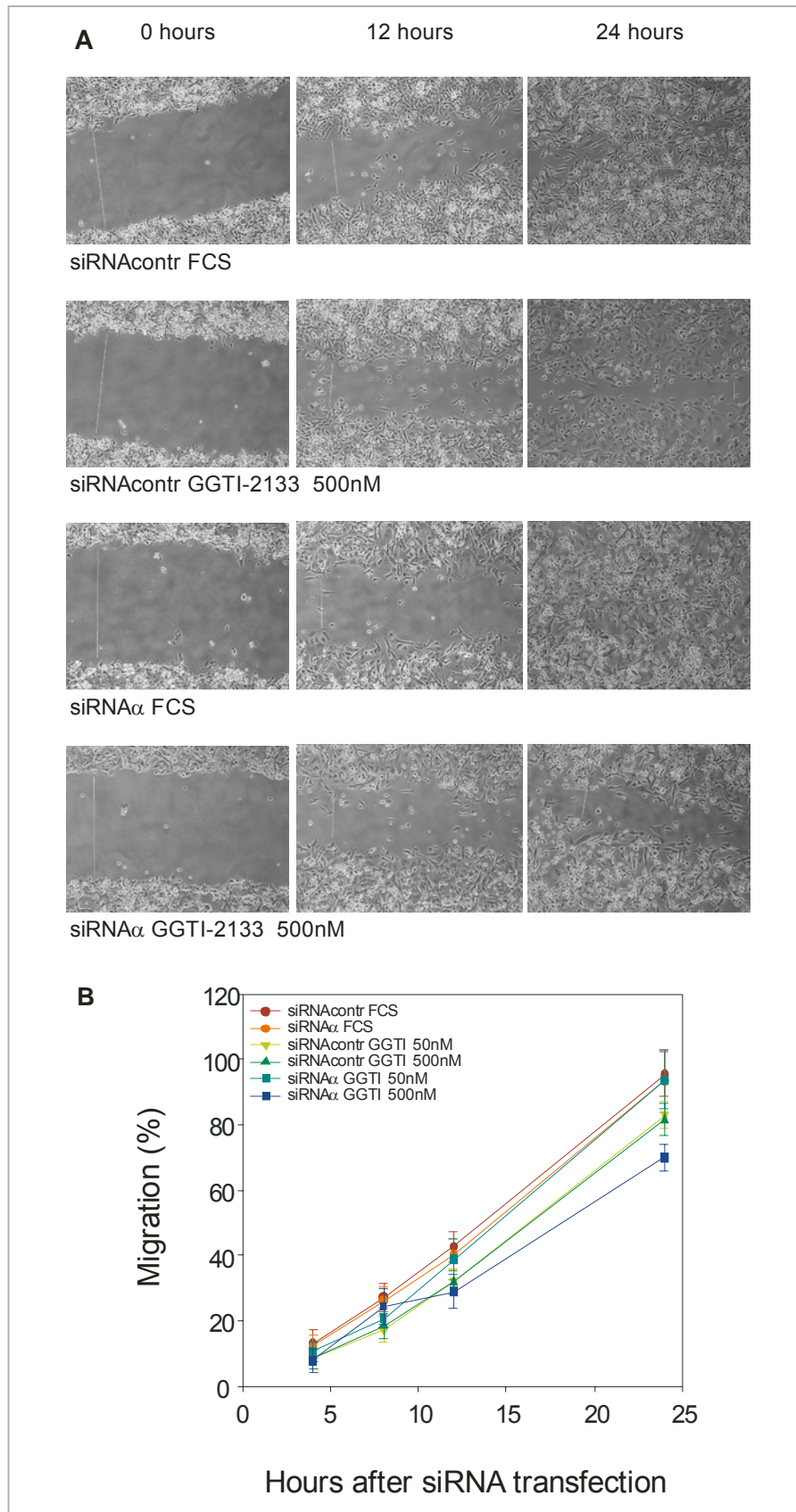


**Figure VII.9. Migration of MDA-MB-231 cells stimulated with GGTI-2133.** A) shows micrographs of cells with and without expressing PKC $\alpha$  and treated, or not, with GGTI-2133 500 nM at three different moments (0, 12 and 24 hours later). In B) is represented the analysis of wound healing assays of every condition tested along 24 hours. It is represented the mean and standard deviation of three independent experiment.

When we used compounds FTI-277 and GM 1489, no clear results were obtained in the migration assays (Fig VII.10). In the case of FTase inhibitor, no effect was observed (Fig VII.10A), but in cells treated with MMP inhibitor a striking result was obtained; only control cells incubated with 0.1  $\mu$ M of GM 1489 for 24 hours showed a lower migration percentage (approximately 70%) than the control. A higher concentration in control cells or PKC $\alpha$  knockout cells treated with this compound, had no effect on the migration capacity (Fig VII.10B).

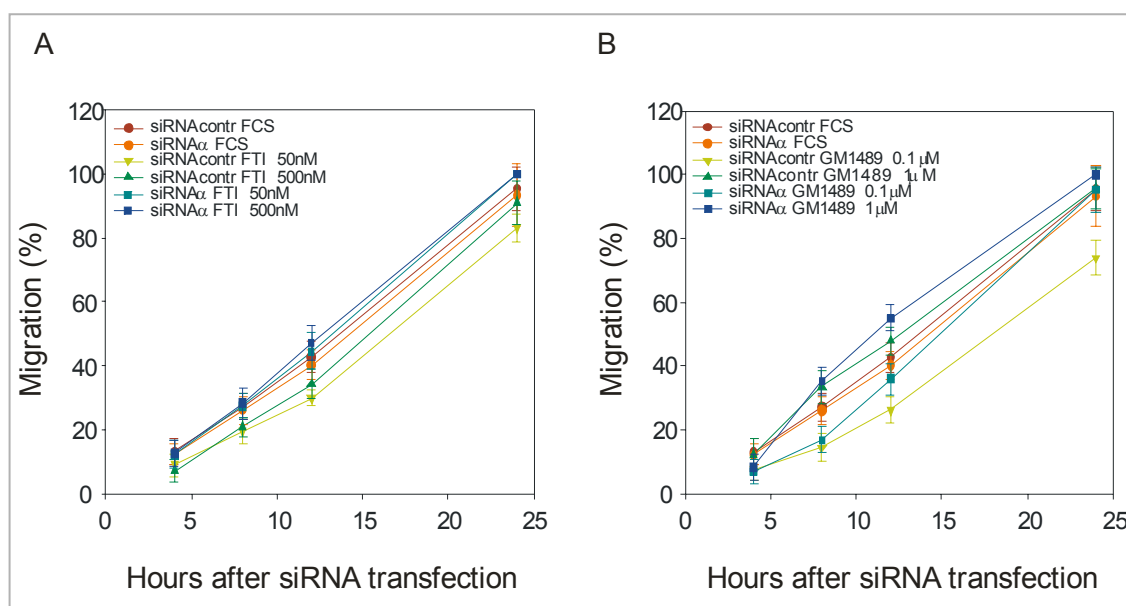


**Figure VII.10. Migration of MDA-MB-231 cells stimulated with FTI-277 (A) and GM 1489 (B).** It is represented the migration profiles of MDA-MB-231 cells upon different stimulations along 24 hours. The migration profiles consist of measuring the width of a scratch wound at the times indicated, and the migration percentage was calculated regards to initial size of the scratch. Results are representative of three independent experiments.

In general, the compounds and concentration tested had no clear effect on the migration capacity of MDA-MB-231, and higher concentrations of the different compounds should be tested.

When we measured the effect of these drugs on apoptosis no effect was found for any of them. The only increase in programmed cell death occurred when PKC $\alpha$  expression was inhibited.

**Table VII.6. Apoptosis of MDA-MB-231 under different treatments.**

<b>MDA-MB-231 CONDITIONS</b>	<b>% APOPTOSIS</b>
siRNAcontrol	2.5 ± 0.7
siRNAcontrol + GGTI-2133 50nM	2.1 ± 0.5
siRNAcontrol + GGTI-2133 500nM	2.8 ± 0.4
siRNAcontrol + FTI-277 50nM	2.3 ± 0.7
siRNAcontrol + FTI-277 500nM	2.5 ± 0.4
siRNAcontrol + GM 1489 0.1µM	2.7 ± 0.6
siRNAcontrol + GM 1489 1µM	2.5 ± 0.6
siRNA $\alpha$	4.5 ± 1.7
siRNA $\alpha$ + GGTI-2133 50nM	3.5 ± 0.4
siRNA $\alpha$ + GGTI-2133 500nM	4.4 ± 0.7
siRNA $\alpha$ + FTI-277 50nM	4.0 ± 0.9
siRNA $\alpha$ + FTI-277 500nM	3.4 ± 0.6
siRNA $\alpha$ + GM 1489 0.1µM	4.3 ± 0.9
siRNA $\alpha$ + GM 1489 1µM	3.7 ± 1.2

We also measured the effect of these specific inhibitors on extracellular matrix invasion. As we can observe in figure VII.11, none of the compounds affected the invasion process. The only significant difference was obtained when we compared the invasion of control and mutant cells grown without any compounds.

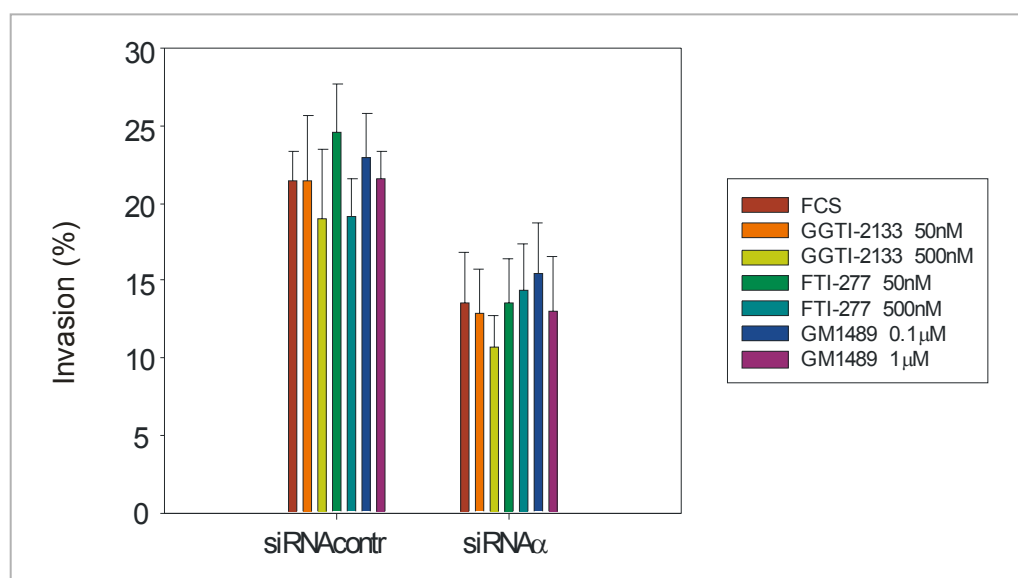


**Figure VII.11. Invasion of MDA-MB-231 cells.** It is represented the invasion percentages of MDA-MB-231 cells upon different treatments after 48 hours.

It might be thought that MMP-1 inhibitor (GM 1489) would inhibit the invasion of MDA-MB-231 cells, but no effect was observed after treating cells with two different concentrations. This may seem contradictory, but the current literature demonstrates that the balance of MMP-1/MMP-9 is extremely important as regards invasion, rather than the level of one particular metalloprotease (*Baker et al., 2006; Duerr et al., 2008*).

In general, we can conclude that the drug concentrations tested in this study do not affect the migration, invasion and apoptosis of MDA-MB-231 breast cancer cells, and so no specific conclusions can be proposed. However, experiments carried out in our laboratory demonstrate that MDA-MB-231 cells possess a less aggressive phenotype when they are transfected with siRNA $\alpha$  and it is to be expected that when the function of onco-proteins (like Ras-related GTPase) whose genes are up-regulated in these conditions, is inhibited this decrease in aggressiveness should be enhanced. Besides, it seems that higher concentrations of the specific inhibitor GGTI-2133 might inhibit migration, since 500 nM had a slight effect.



## CHAPTER VIII

# CHARACTERIZATION OF SALINOMYCIN EFFECT ON BREAST CANCER CELLS THROUGH PKC $\alpha$



## 1. Introduction.

Salinomycin is a monocarboxylic polyether antibiotic isolated from *Streptomyces albus* that exhibits a unique tricyclic spiroketal ring system and an unsaturated six-member ring in the molecule (Miyazaki *et al.*, 1974) (Fig VIII.1). This antibiotic exhibits antimicrobial activity against gram-positive bacteria, including mycobacteria, some filamentous fungi, *Plasmodium falciparum* and *Eimeria spp.*, the parasite responsible for the poultry disease called coccidiosis (Danforth *et al.*, 1997). Therefore, salinomycin has been used as an anticoccidial drug in poultry and is also fed to ruminants to improve nutrient absorption and feed efficiency (Callaway *et al.*, 2003).

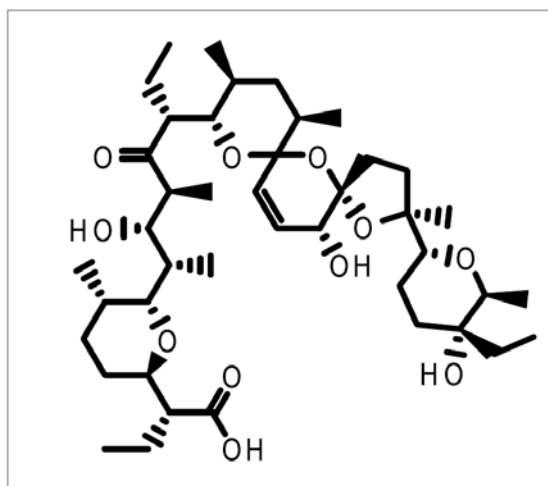


Figure VIII.1. Chemical structure of salinomycin.

Salinomycin acts in different biological membranes, including cytoplasmic and mitochondrial membranes, as an ionophore with strict selectivity for alkali ions and a great preference for potassium (Mitani *et al.*, 1975).

This compound has been identified by high-throughput screening as a selective inhibitor of cancer stem cells (CSCs) (Grupta *et al.*, 2009). These cells comprise a unique subpopulation of tumour cells that possess tumour initiation and self-renewal capacity and the ability to give rise to the heterogeneous lineages of cancer cells that make up the bulk of the tumour (Ward and Dirks, 2007). CSCs have been identified in a variety of human neoplasias, including cancers of the blood, breast, ovary, prostate and liver among others (Ailles and Weissman, 2007).

The problem with this type of cell is that they display numerous mechanisms of resistance to chemotherapeutic drugs and irradiation therapy, allowing them to survive current cancer treatments and to initiate relapse, long-term tumour recurrence and metastasis (*Dean et al., 2005*).

One of the most important mechanisms of drug resistance in CSCs is the expression of ATP-binding cassette (ABC) transporters which belong to a highly conserved superfamily of transmembrane proteins capable of exporting a wide variety of molecules and structurally unrelated chemotherapeutic drugs from the cytosol (such as paclitaxel, doxorubicin and vinblastine), thereby conferring multi-drug resistance to the cells (*Dean, 2009; Eckford and Sharom, 2009*).

In recent studies salinomycin has been used as a potent inhibitor of one of these drug transporters, specifically the P-glycoprotein (*Chen et al., 1997; Riccioni et al., 2010*). In these studies MDR cell lines were treated with salinomycin, which restored normal drug sensitivity to these cells.

It has also been demonstrated recently that salinomycin induces apoptosis in human cancer cells of different origin which display multiple mechanisms of drug and apoptosis resistance (*Fuchs et al., 2009*).

Despite the well-known activity of salinomycin against bacteria and parasites, the mechanisms by which this antibiotic act in human cancer cells to impair their viability, decrease proliferation and induce apoptosis are still unknown.

Salinomycin activates a distinct apoptotic pathway in cancer cells that is not accompanied by cell cycle arrest and which is independent of p53, caspase activation, the CD95/CD95L system and the 26S proteasome (*Nencioni et al., 2005; Fuchs et al., 2008*). In this study we try to shed light on the effect of salinomycin through PKC $\alpha$  signalling pathways, since previous research in our laboratory demonstrated that in the absence of this kinase, several breast cancer cell lines were driven to apoptosis (Chapter IV of this Doctoral Thesis).

## **2. Results.**

### **2.1. Effect of salinomycin on the migration and invasion capacities of breast cancer cell lines with down-regulated PKC $\alpha$ .**

We have studied the effect of salinomycin treatment on both migration and invasion capacities of two characteristics of malignant cancer cells. The cell lines chosen were MCF-7 and MDA-MB-231.

Migration assays were performed using the wound healing assay (see Material and Methods). As was demonstrated in a previous chapter of this Doctoral Thesis, these two cell lines showed big differences in migration capacity; while MCF-7 control cells needed approximately 72 hours to seal the scratch wound, MDA-MB-231 control cells formed the monolayer in 24 hours (Figs VIII.2 and VIII.3).

In the micrographs of MCF-7 shown in Figure VIII.2, we can observe that the migration capacity of the cells transfected with siRNAcontrol and incubated with 1  $\mu$ M salinomycin was reduced. After 72 hours of treatment, some gaps inside cell monolayer appeared, as well as round black cells floating in the medium. These effects were more evident when cells were transfected with siRNA $\alpha$ .

MCF-7 control cells had migrated approximately 95% after 72 hours, while in the presence of 1  $\mu$ M or 10  $\mu$ M salinomycin this capacity was decreased to 41% or 21%, respectively. This inhibition was more obvious when salinomycin was added to MCF-7 with down-regulated PKC $\alpha$ , in which case it completely abolish the migration capacity of the cell line, regardless of its concentration (Fig VIII.2B). These results suggest that PKC $\alpha$  and salinomycin might be involved in the migration of MCF-7 cells through the same signalling pathways, since they show synergism in the inhibition of this process.

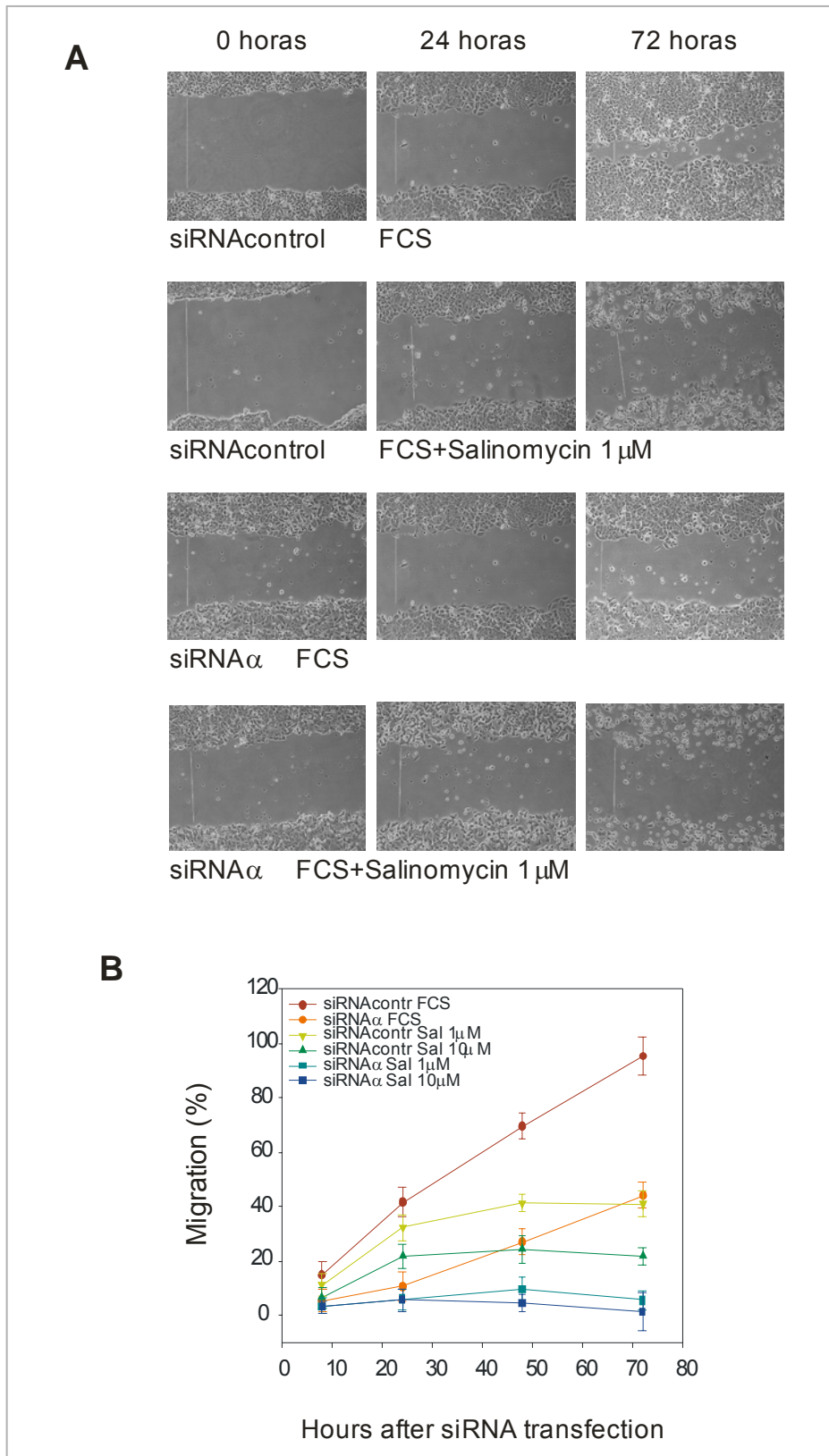


**Figure VIII.2. Migration assays of MCF-7 cells stimulate with salinomycin.** A) Shows micrographs of MCF-7 cells at time 0, 24 and 72 hours of migration. Two top rows represent cells transfected with siRNAcontrol and stimulated or not with 1 μM salinomycin, while two bottom rows are the same but transfected with siRNAα. At the bottom it is shown the migration profiles of MCF-7 cells treated with different concentrations of salinomycin (B). The migration profiles consist of measuring the width of the scratch wound at every time, and the migration percentage was calculated regards to the initial size of the scratch. Results are representative of three independent experiments.

Salinomycin also inhibited migration in MDA-MB-231 cells (Figure VIII.3A). After 24 hours of treatment with 10  $\mu$ M salinomycin some gaps in the cell monolayer appeared, as well as round and black floating cells, particularly in the PKC $\alpha$  depleted cells.

This decrease in migration percentage was mainly dependent on the salinomycin concentration, so that migration percentages of 50 and 25% were obtained with 1  $\mu$ M and 10  $\mu$ M salinomycin, respectively (Fig VIII.3B).

These results suggest that salinomycin, but not PKC $\alpha$ , is involved in the migration of MDA-MB-231 cells, and that it works rapidly, since after 8 hours of treatment, cells showed significantly lower migration capacity compared with control cells.

As was mentioned in the Material and Methods section, MDA-MB-231 cells are the only cell line tested that possess invasion capacity in BME (basement membrane extract) (Fig VIII.4A). When control cells were transfected with siRNAcontrol and incubated in growth medium for 48 hours, they exhibited an invasion capacity of 21.4%  $\pm$  1.9 (Fig VIII.4). When these cells were incubated in the presence of salinomycin, their invasiveness decreased depending on the concentration: decreasing slightly to 18% at 1  $\mu$ M; while at 10  $\mu$ M the invasion capacity decreased significantly to 7.8%.

When we studied the effect of this compound during 48 hours in MDA-MB-231 cells in the absence of PKC $\alpha$ , a similar pattern of invasion was found to that observed in control cells, that is, a slight decrease of invasiveness when 1  $\mu$ M salinomycin was tested, and a significant reduction at 10  $\mu$ M, only 6% of cells still being able to invade at this concentration (Fig VIII.4).

It should also be noted that after the simple event of depleting PKC $\alpha$  expression in cells, the invasion percentage falls to 13.6%; and the combination of PKC $\alpha$  inhibition and 1  $\mu$ M salinomycin treatment significantly reduces the invasion capacity of cells, the invasion percentage falling to 11%, so that no higher concentrations of this antibiotic are needed to obtain successful results in invasion of MDA-MB-231 cells (Fig VIII.4).

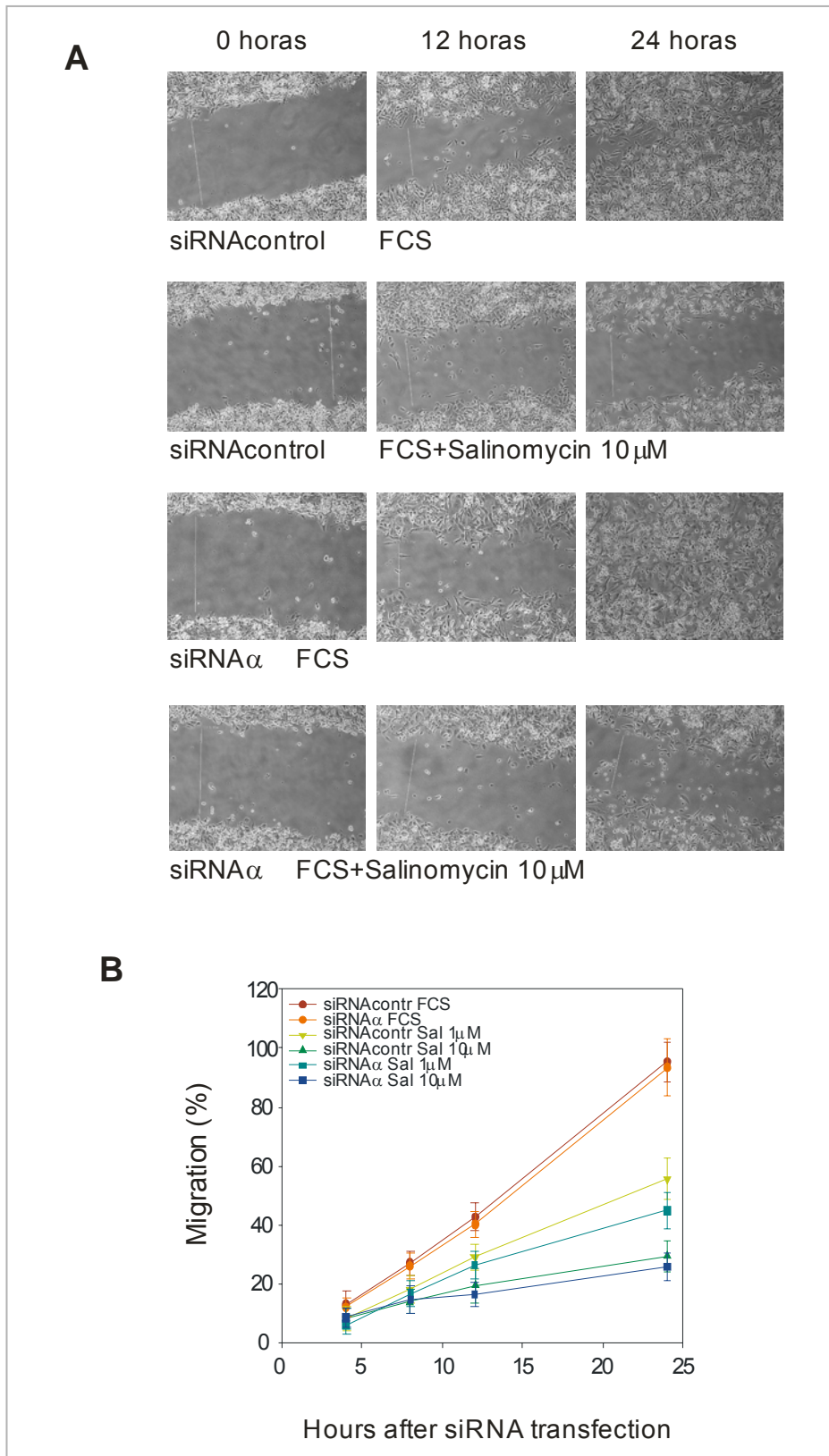


**Figure VIII.3. Migration assays of MDA-MB-231 cells stimulate with salinomycin.** A) Shows micrographs of MDA-MB-231 cells at time 0, 12 and 24 hours of migration. Two top rows represent cells transfected with siRNAcontrol and stimulated or not with 10  $\mu$ M salinomycin, while two bottom rows are the same but transfected with siRNA $\alpha$ . At the bottom it is shown the migration profiles of cells treated with different concentrations of salinomycin (B). The migration profiles consist of measuring the width of the scratch wound at every time, and the migration percentage was calculated regards to the initial size of the scratch. Results are representative of three independent experiments.

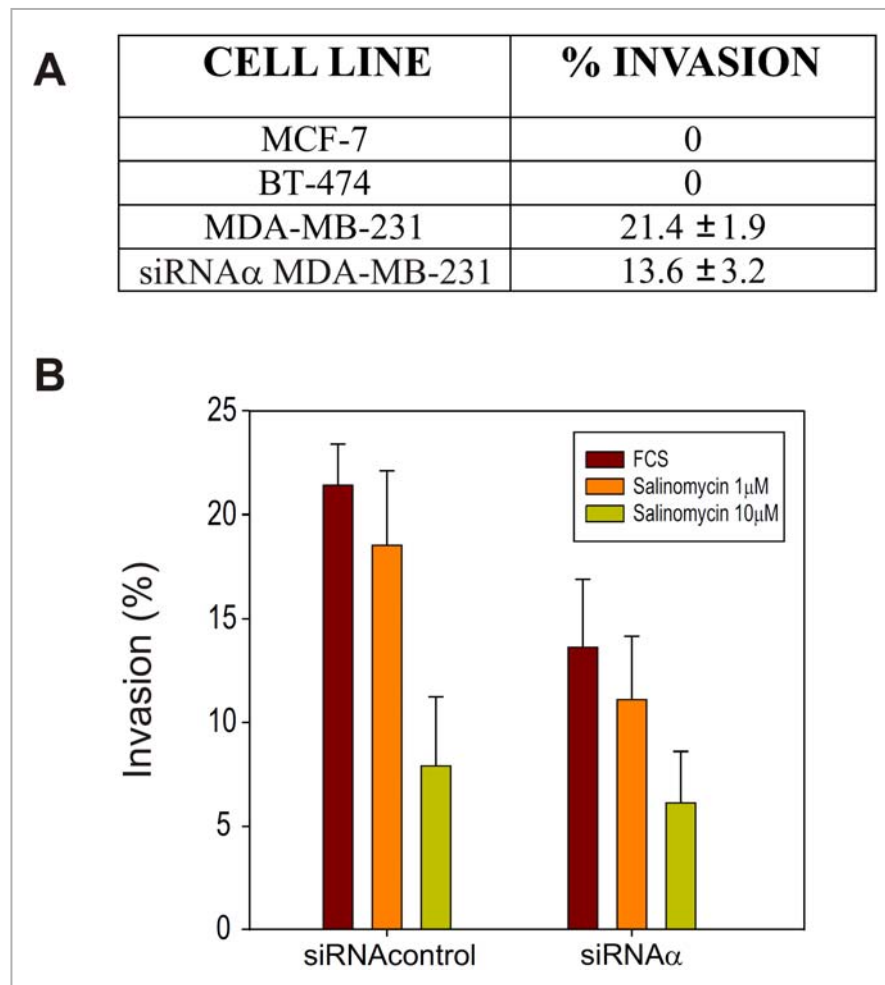


**Figure VIII.4. Invasion capacity of MDA-MB-231.** A) Shows the invasion percentage in 0.5X BME of three breast cancer cell lines tested. B) Represents the percentage of invasion of MDA-MB-231 cells transfected with siRNAcontrol or siRNA $\alpha$  and stimulated with two different concentrations of salinomycin. Results are representative of three independent experiments.

## 2.2. Salinomycin induces apoptosis in breast cancer cell lines with down-regulated PKC $\alpha$ .

Another aspect studied in MCF-7 and MDA-MB-231 cells stimulated with different concentrations of salinomycin was programmed cell death. For this, we used annexin V-Alexa Fluor<sup>®</sup> 488, since it allows early and late apoptosis to be distinguished. The percentages of apoptosis in MCF-7 and MDA-MB-231 cells in several conditions are shown in Table VIII.1.

MCF-7 cells transfected with siRNAcontrol showed a basal apoptosis of 7%, which increased 3.5- or 5-fold when they were incubated for four days in the presence of 1  $\mu$ M or 10  $\mu$ M salinomycin, respectively. When PKC $\alpha$  expression was inhibited in this cell line, the apoptosis percentage was almost doubled, reaching a value of 13.7%. Moreover, if salinomycin was added (both concentrations tested) to these mutant cells, the apoptosis increased up to 26-

27% approximately, which suggests that PKC $\alpha$  and the antibiotic are involved in apoptosis through different signalling pathways and that they do not show synergy in programmed cell death in MCF-7 cells.

In the case of MDA-MB-231 cells, the basal level of apoptosis was even lower than in MCF-7, reaching only 2.5%. After incubating MDA-MB-231 cells with salinomycin (both concentrations tested), the apoptosis percentages reached were similar to those obtained in MCF-7, meaning that the increase in this cell line is approximately 10-fold higher. In MDA-MB-231 cells with down-regulated PKC $\alpha$ , treatment with 1  $\mu$ M or 10  $\mu$ M salinomycin increased the percentage of apoptotic cells to 40% and 59%, respectively. These results highlight the cooperation between the absence of PKC $\alpha$  and salinomycin, since the effect of this compound in apoptosis is increased when PKC $\alpha$  is also depleted.

CELL LINE	CONDITIONS	% APOPTOSIS
	siRNAcontrol	7.0 $\pm$ 1.8
	siRNAcontrol + Salinomycin 1 $\mu$ M	25.3 $\pm$ 0.6
MCF-7	siRNAcontrol + Salinomycin 10 $\mu$ M	35.8 $\pm$ 6.8
	siRNA $\alpha$	13.7 $\pm$ 2.8
	siRNA $\alpha$ + Salinomycin 1 $\mu$ M	27.9 $\pm$ 8.1
	siRNA $\alpha$ + Salinomycin 10 $\mu$ M	26.1 $\pm$ 3.7
	siRNAcontrol	2.5 $\pm$ 0.7
	siRNAcontrol + Salinomycin 1 $\mu$ M	26.1 $\pm$ 6.0
MDA-MB-231	siRNAcontrol + Salinomycin 10 $\mu$ M	30.8 $\pm$ 5.8
	siRNA $\alpha$	4.5 $\pm$ 1.7
	siRNA $\alpha$ + Salinomycin 1 $\mu$ M	39.9 $\pm$ 6.4
	siRNA $\alpha$ + Salinomycin 10 $\mu$ M	59.5 $\pm$ 7.0

**Table VIII.1. Apoptosis percentage of MCF-7 and MDA-MB-231 cells stimulated with salinomycin and transfected with siRNAcontrol and siRNA $\alpha$ .** Data show the mean  $\pm$  standard deviation of 3-8 independent experiments.

The use of annexin V-Alexa Fluor® 488 to measure apoptotic cells allows us to distinguish between early and late apoptosis (Figs VIII.5 and VIII.6). In the following figures, Dot Blot graphs which group cells into four populations, depending on their physiological state, can be observed:

- Upper-left quadrant: cells stained with propidium iodide (PI), indicating dead cells.

- Lower-left quadrant: double negative cells, that is, cells not stained by PI or annexin V-Alexa Fluor® 488.
- Lower-right quadrant: cells only stained with annexin V-Alexa Fluor® 488, that is, cells in early apoptosis and not yet dead.
- Upper-right quadrant: double positive cells, that is, cells stained with annexin V-Alexa Fluor® 488 and PI, which indicates late apoptosis (apoptotic cells which have already died).

As shown in Figure VIII.5, incubation of MCF-7 cells with salinomycin for 4 days induced an increase in the apoptotic level, basically late apoptosis, indicating that this compound acts in a short period of time after it is added to a cell culture. It is also worth noting that this antibiotic induced cell death without apoptosis, increasing the percentage from 1.6% (in control cells) to 38.3% or 19.4% when 1  $\mu$ M or 10  $\mu$ M salinomycin was added to cells, respectively.

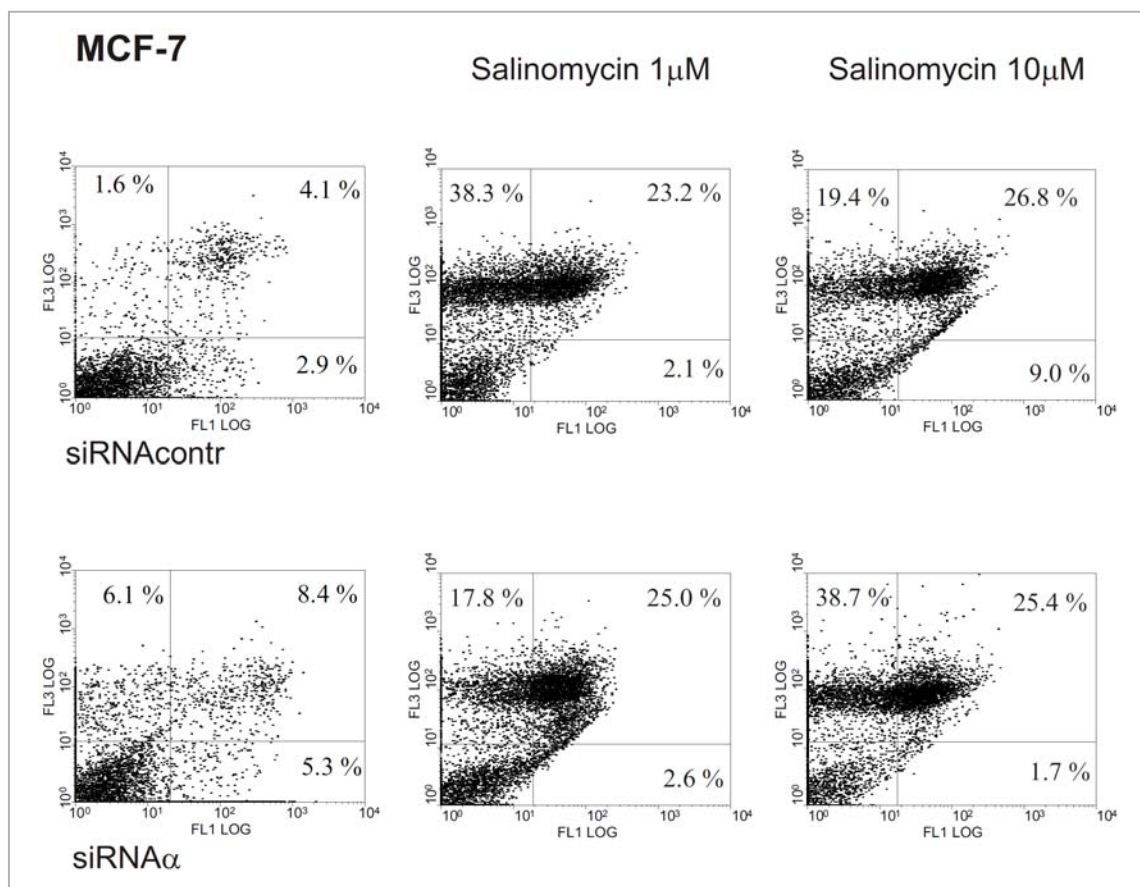


**Figure VIII.5. Apoptosis of MCF-7 cells induced by salinomycin.** Cells were stained with annexin V-Alexa Fluor 488 and PI, and detected by flow cytometry. The lower right quadrant (annexin-V<sup>+</sup> PI<sup>-</sup>) represents early apoptosis, whereas upper right quadrant (annexin-V<sup>+</sup> PI<sup>+</sup>) represents late apoptosis. All results are representative of three-eight independent experiment.

MDA-MB-231 cells possessed a very low apoptotic level in resting condition, but when salinomycin was added to the growth medium, cells were rapidly driven to apoptosis, since after 5 days of stimulation, apoptosis, particularly late apoptosis, reached 18.2% or 22.7% at 1  $\mu$ M or 10  $\mu$ M salinomycin, respectively (Fig VIII.6).

When PKC $\alpha$  was down-regulated in this cell line, the early apoptosis level increased slightly (from 1.6% to 3.6%). The most important effects were induced by salinomycin stimulation, which increased apoptotic levels, mainly late apoptosis. The percentages rising from 0.9% to 35.6% or 54.1% when cells were incubated with 1  $\mu$ M or 10  $\mu$ M salinomycin, respectively, which indicates that the effect of this antibiotic was concentration-dependent in these mutant cells (Fig VIII.6).

In MDA-MB-231 cells, the populations are better differentiated than in MCF-7 cells, especially the cells in late apoptosis.

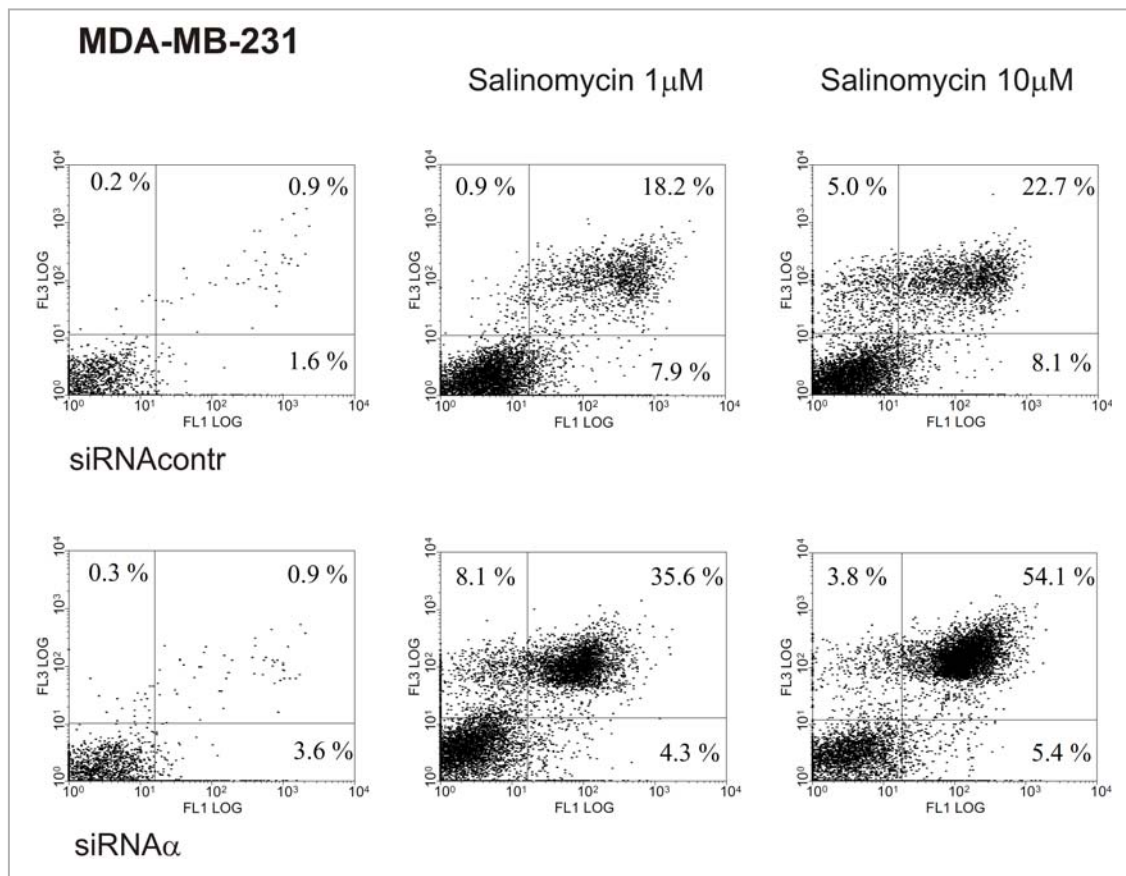


**Figure VIII.6. Apoptosis of MDA-MB-231 cells induced by salinomycin.** Cells were stained with annexin V-Alexa Fluor 488 and PI, and detected by flow cytometry. The lower right quadrant (annexin-V<sup>+</sup> PI<sup>-</sup>) represents early apoptosis, whereas upper right quadrant (annexin-V<sup>+</sup> PI<sup>+</sup>) represents late apoptosis. All results are representative of three-eight independent experiment.

## CHAPTER IX

### DISCUSSION AND CONCLUSIONS



## 1. DISCUSSION.

It is known that practically all PKC isoforms are expressed in a large variety of tissues and cells. In cancer they are deregulated, being over- or under-expressed, depending on the isoenzyme and type of cancer (*Koivunen et al., 2006*). Although every cancer must be studied independently, in general PKC $\epsilon$  and PKC $\alpha$  are commonly over-expressed in human cancer (*Cacae et al., 1996; Yuen et al., 1999; Masur et al., 2001; Pan et al., 2006*), while PKC $\delta$  is down-expressed (*Lu et al., 1997; Jackson and Foster, 2004*).

Taking the complexity of the PKC family into account, several strategies have been developed to better understand the role of each single isoform in different types of cancer so that they can be used as targets in specific treatments.

In this Doctoral Thesis the role of PKC $\alpha$  in breast cancer has been studied, using several cell lines as a model (MCF-7, BT-474 and MDA-MB-231). We have tried to shed light on the localization and activation mechanisms of this classical isoenzyme when breast cancer cell lines are stimulated with some possible substances used to treat this type of tumour. We have tested natural compounds such as fatty acids (arachidonic acid, oleic acid and omega-3 fatty acids) and synthetic substances as DAG-lactones, among others.

### 1.1. Role of the C2 domain in the arachidonic acid-dependent localization and activation of PKC $\alpha$ .

The results obtained in this study reveal clearly that the interaction of AA with PKC $\alpha$  is a process mediated by Ca<sup>2+</sup>, mainly through the *Calcium binding region*, located in the top of the C2 domain. The Ca<sup>2+</sup>-dependence of this event has been suggested for the fatty acid-induced translocation to the plasma membrane of PKC $\gamma$  in several studies, although the precise role of the C2 domain was not studied in any case (*Shirai et al., 1998; Yagi et al., 2004*).

Pioneer studies pointed to a synergistic effect exerted by AA and DAG in the localization and activation of classical and novel PKCs (*Murakami and Routtenber, 1985; Shinomura et al., 1991*). This function was attributed originally to the ability of the C1 domain to interact with AA, but these results could be re-interpreted with our new knowledge concerning the function of the C2 domain in the full activation of classical PKCs (*Bolsover et al., 2003; Guerrero-Valero et al., 2007*). This model implies that the protein initially binds to the membrane surface via the Ca<sup>2+</sup>-dependent phosphatidylserine binding of the C2 domain and, once bound, the protein undergoes conformational

changes that include the insertion of the C1 domain into the membrane and the release of the pseudosubstrate region from the active site (*Cho and Stahelin, 2005*). Due to the double nature of this sequential membrane anchorage mechanism involving the C2 and C1 domains, a synergistic effect between AA and diacylglycerol seems probable if AA also binds to the C2 domain, as has been demonstrated in our work.

The results shown here in Figures III.1, III.3 and III.5 suggest that PKC $\alpha$  interacts with AA at the plasma membrane through its C2 domain in a Ca $^{2+}$ -dependent manner. The need of a direct interaction between the C2 domain and AA was further confirmed, since the addition of AA after the cells were stimulated with ionomycin induced a very slow AA-dependent translocation of the enzyme at [Ca $^{2+}$ ]<sub>i</sub> that was not able to induce the protein localization in the membrane by itself (compare Figs III.2b and III.4b).

In addition, the data exhibited in Figure III.6 demonstrate directly that the C2 domain of PKC $\alpha$  interacts with lipid vesicles containing AA in a concentration-dependent manner and, furthermore confirm the Ca $^{2+}$ -dependence of the process. The 3D structure of the C2 domain complex with Ca $^{2+}$  and AA has not been resolved, although the molecular structure of the PKC $\alpha$ -C2 domain bound to Ca $^{2+}$  and all-*trans*-retinoic acid has been demonstrated recently, and it has been shown to activate PKC $\alpha$  by binding through the C2 domain (*Ochoa et al., 2003; López-Andreo et al., 2005*). Although AA and all-*trans*-retinoic acid have different molecular structures, both of them contain a carboxylate group at one end of the molecule. In the case of all-*trans*-retinoic acid, this acid group seems to complete the coordination sphere of Ca1, the electrostatic interactions being the predominant character of this binding process, in a way that is very similar to that described for other anionic phospholipids (*Verdaguer et al., 1999; Ochoa et al., 2002*). Thus, it is extremely possible that the carboxylate group of the AA molecule fits in the Ca $^{2+}$ -binding pocket of the C2 domain, thus completing the coordination of Ca1.

Another important observation made in this work is the evidence that AA cooperates with ionomycin to increase the [Ca $^{2+}$ ]<sub>i</sub>. This facilitates the plasma membrane localization of PKC $\alpha$  in two ways: the first by increasing the Ca $^{2+}$  influx, which increases the translocation rate, and the other through direct interaction with the *calcium binding region* of the C2 domain. Several studies have shown that AA itself influences the activities of most ion channels, including those specific for Ca $^{2+}$  (*Mignen and Shuttleworth, 2000; Soldati et al., 2002*), and it is possible that pre-incubation with AA, although not sufficient to open these channels directly, might influence them to respond quickly after the initial Ca $^{2+}$  influx is generated by ionomycin. Another possibility is that AA itself induces ion transport by affecting the biophysical

properties of the lipid membrane. Further work needs to be carried out to clarify these hypotheses.

## **1.2. Role of the C1 domain in the arachidonic acid-dependent localization and activation of PKC $\alpha$ .**

To determine whether the C1 domain is also responsible for the AA-dependent localization and activation of PKC $\alpha$ , we studied the differences in membrane association and activation between PKC $\alpha$  wild-type and C1A and C1B subdomain mutants. As it can be observed in Figure III.7, direct evidence was obtained that the C1A domain mediates the role of AA in membrane targeting and activation of the enzyme. There is growing evidence indicating that the two C1 subdomains of classical and novel PKCs exhibit different ligand affinities and distinct functional roles. In the case of PKC $\alpha$ , this has been demonstrated to contain two distinct binding sites with low and high affinity for phorbol esters, while diacylglycerol and phorbol esters bind to the two discrete sites with opposite affinities. Thus, the C1A domain has a higher affinity for DAG and the C1B domain has a higher affinity for phorbol ester (Slater *et al.*, 1998; Ananthanarayanan *et al.*, 2003). Furthermore, other studies have shown that the hydrophobic residues at the top of the C1A domain are essential for the membrane penetration and activation of PKC $\alpha$ , whereas those in the C1B domain are not involved directly in these processes (Medkova and Cho, 1999). The present study revealed that the membrane retention time of the C1A mutants of PKC $\alpha$  decreased significantly. However, no effect was observed in the case of the C1B mutants, indicating that the C1A domain, in addition to the C2 domain, plays an important role in membrane anchorage and further activation of PKC $\alpha$  by means of AA, whereas the C1B domain does not seem to be involved in this process.

It is important to note that the inhibition effect observed in the localization of the C1A domain mutants of PKC $\alpha$  was obtained in experiments performed in the absence of DAG, suggesting that AA can also mediate the membrane anchorage of the enzyme by itself, and that Trp58 and Phe60 play an important role in this process. These results imply that diacylglycerol and acidic lipids are needed for the membrane binding of the C1 domain, and that hydrophobic amino acid residues located in the rim of the binding cleft are involved in the localization process. Several reports in the literature support this notion; for example, mutations of Trp58 and Phe60 to Gly decreased the membrane penetration and activation of PKC $\alpha$  even in the case of lipid vesicles containing high concentration of PtdSer, indicating that non-specific electrostatic interactions are essential for the C1 domain membrane binding (Medkova and Cho, 1999). Moreover, it has been demonstrated that mutations in homologous residues of the C1 domain of PKC $\delta$  also affect the phorbol ester/ PtdSer-dependent binding of this enzyme (Wang *et al.*, 2001).

It is worthy of note that the maximum inhibitory effect obtained in the translocation capacity of the C1A domain mutant proteins was 50%. This suggests that the function of the C2 domain is essential for initiating the localization and activation process and, afterwards, the C1A stabilizes the anchoring and permits full activation of the enzyme. Furthermore, we cannot discard the possibility that other residues in the C1A domain might interact with AA. In fact, it has been shown that cationic residues located in the C1A domain (mainly Arg77), near the binding cleft, provide non-specific electrostatic interaction sites for anionic phospholipids that are important for the membrane binding, penetration and activation of PKC $\alpha$  (Bittova *et al.*, 2001).

In this work it has been demonstrated that, inside C1A domain, the substitution of Trp58 by Gly induced a more drastic effect on the plasma membrane localization of the enzyme than Phe60, suggesting that this residue is involved mainly in the anchorage of the C1A domain at the plasma membrane through AA. However, in other experiment where catalytic activity was measured for both mutants, the protein containing the substitution of Phe60 by Gly exhibited a higher degree of inhibition than the one containing the Trp58Gly (López-Nicolás *et al.*, 2006). These results indicate the possibility of a very fine-tuning in the mechanisms of localization and activation of PKC $\alpha$  through its C1A domain in an AA-dependent manner.

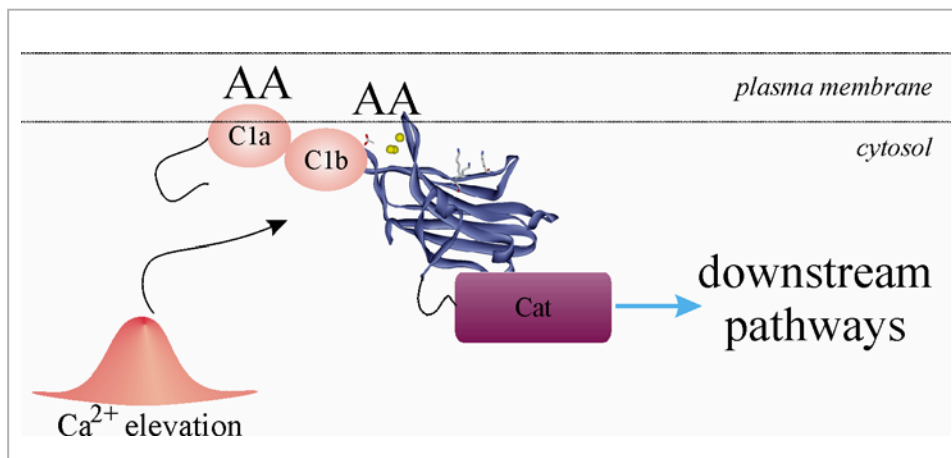


**Figure IX.1. Schematic representation of localization and further activation of PKC $\alpha$  induced by arachidonic acid.** The overall structure of the C2 domain of PKC $\alpha$  is represented as a cartoon model in purple. The four Lys residues located in the *polybasic cluster* are represented by a stick model. In the translocation model, Ca<sup>2+</sup> (represented by yellow balls) is the driving force inducing localization of the C2 domain in the membrane by binding to the *Ca<sup>2+</sup>-binding region*. There, Ca<sup>2+</sup> acts as a bridge between C2 domain and AA. After this first approach to membrane, C1A subdomain (represented as pink sphere) could establish a more stable anchorage of PKC $\alpha$  in the plasma membrane by interacting with the AA molecules available, allowing its activation and further triggering of different signalling pathways.

### **1.3. Role of C1 and C2 domains in the localization and activation of PKC $\alpha$ induced by oleic acid.**

Previous studies revealed that OA is able to localize and activate different PKC isoforms in some specific cell lines (*Chen et al., 2002; Park et al., 2003*), but the precise role of each regulatory domain was not studied. In this study, we tested the ability of OA to induce the localization of PKC $\alpha$  in the plasma membrane in three breast cancer cell lines.

According to the immunofluorescence results, OA induced the translocation of PKC $\alpha$  from the cytosol to the plasma membrane in different proportions, depending on the cell line. More specifically, 73, 58 and 28% of MCF-7, BT-474 and MDA-MB-231 cells, respectively, showed PKC $\alpha$  located in the plasma membrane. This difference could be due to the membrane properties of each cell line, which could prevent or promote the delivery of OA to the inner membrane leaflet, favouring the interaction between PKC $\alpha$  and the fatty acid. This effect reveals the importance of studying each breast cancer type independently in order to predict the best treatment for each type.

Another aspect studied in immunofluorescence was actin polymerization, for which differences between the cell lines tested were also found. While MCF-7 and BT-474 were not affected by OA, MDA-MB-231 cells reduced their actin fibre production. This reinforces the idea that every treatment acts in a different way in each type of breast cancer cell and therefore every tumour should be studied independently to find out the best possible treatment for it.

Once the ability of OA to localize PKC $\alpha$  in the plasma membrane in breast cancer cells had been checked, we looked at the role that each regulatory domain plays in the plasma membrane localization mechanism. For this, BT-474 cells were transfected with different PKC $\alpha$  mutants affected in their C1 or C2 regulatory domains.

The results obtained clearly revealed that the interaction of OA with PKC $\alpha$  is mediated by Ca<sup>2+</sup>, mainly through the *Calcium binding region* located in the top of the C2 domain. The Ca<sup>2+</sup>-dependence of this event has also been suggested for other fatty acids; for example AA-induced translocation of PKC $\gamma$  or PKC $\alpha$  to the plasma membrane, suggesting that the C2 domain plays an important role in the membrane localization of the enzyme (*Yagi et al., 2004; López-Nicolás et al., 2006*).

After demonstrating that the localization process was Ca<sup>2+</sup>-dependent, we decided to study the calcium influx into the cytoplasm after stimulation with OA and ionomycin. Previous studies revealed the modulation of some

calcium channels by OA (*Fujiwara et al., 2005; Tian et al., 2008*), favouring an increase in  $[Ca^{2+}]_i$ , which reinforces the results obtained in this study where stimulation with OA increased  $[Ca^{2+}]_i$  in BT-474 cells. Another important observation made in this work is that OA only increased the level of cytosolic calcium in tumour breast cancer cells, such as BT-474 and MCF-7, while in non-transformed cells, like MCF-10A, no effect was shown.

Although OA stimulation produces an increase in  $[Ca^{2+}]_i$  similar to that obtained with ionomycin, PKC $\alpha$  does not translocate from the cytosol to the plasma membrane; suggesting that this initial  $[Ca^{2+}]_i$  increase is not sufficient to translocate PKC $\alpha$  to the plasma membrane, perhaps because the fatty acid has not reached the inner leaflet of the plasma membrane and needs a longer incubation time.

To determine whether the C1 domain was partly responsible for the OA-dependent localization and activation of PKC $\alpha$ , we studied the differences in membrane association and activation between PKC $\alpha$  wild-type and a C1A subdomain mutant. Pioneer studies pointed to a synergistic effect exerted by some fatty acids, OA among them, and DAG in the localization and activation of PKC (*Goldberg and Zidovetzki, 1998*). This synergistic effect is easily understandable since OA binds to C2 domain, as has been demonstrated in this work.

We have focused on the C1A subdomain, since there are several reports that highlight the presence of some hydrophobic residues at the top of the C1A subdomain as being essential for the membrane penetration and activation of PKC $\alpha$ , while those in the C1B subdomain do not seem to be involved in these processes (*Medkova and Cho, 1999*). Furthermore, it has been described that in the translocation and further activation of PKC $\alpha$  by other fatty acids like AA, the C1A is the really important subdomain, and not the C1B (*López-Nicolás et al., 2006*).

The present study revealed that the membrane retention time and activation of the C1A mutant of PKC $\alpha$  decreased significantly compared with the wild type. It should be noted that the inhibition effect observed in the localization and activation of the mutant of C1A domain of PKC $\alpha$  was obtained in experiments performed in the absence of DAG, suggesting that OA can also mediate the membrane anchorage and activation of the enzyme by itself, and that Trp58 plays an important role in this process. These results imply that DAG and acidic lipids are needed for the membrane binding of C1 domain, and that hydrophobic amino acid residues located in the rim of the binding cleft are involved in the location and activation processes. Several reports in the literature support this notion; for example, mutations of Trp58 and Phe60 to Gly decreased the membrane penetration and activation of PKC $\alpha$  even when

lipid vesicles contained a high concentration of phosphatidylserine, indicating that non-specific electrostatic interactions are essential for C1 domain membrane binding (*Medkova and Cho, 1999*).

It is important to note that the maximum inhibitory effect obtained in the binding and activation capacities of the C1A domain mutant protein was 30% in both processes. This suggests that the function of the C2 domain is essential for initiating the localization and activation processes subsequently, the C1A could stabilize the anchoring and permit full activation of the enzyme. Furthermore, there are other residues in the C1A domain that might interact with OA. In fact, it has been shown that cationic residues located in the C1A domain (mainly Arg77), near the binding cleft, provide non-specific electrostatic interaction sites for anionic phospholipids that are important for the membrane binding, penetration and activation of PKC $\alpha$  (*Bittova et al., 2001*).

Similar results were obtained in the kinase activity assays, suggesting that the C2 domain, basically the *Ca<sup>2+</sup> binding region*, is essential in these processes, whereas the *lysine rich cluster* and C1 domain do not play such important roles in the localization and activation of PKC $\alpha$  induced by OA.

In general, from the results obtained in this work, a localization mechanism of PKC $\alpha$  to the plasma membrane induced by OA can be proposed. The first, and essential, interaction between kinase and the plasma membrane occurs through the C2 domain, mainly the *calcium binding region*. Once bound, the protein undergoes conformational changes that include the insertion of the C1 domain into the membrane, which stabilizes the anchoring and leads to the release of the pseudosubstrate region from the active site, triggering a full activation of the enzyme (*Cho and Stahelin, 2005; López-Nicolás et al., 2006*).

#### **1.4. Effect of PKC $\alpha$ depletion and oleic acid on breast cancer cell lines.**

Olive oil (composed of OA and some other minority components) has been considered as a leading promoter of health, especially as regards prevention rather than treatment (*Assman et al., 1997; Lipworth et al., 1997*). Some recent reports have demonstrated that oleic acid cooperates with some standard drugs used in cancer treatment, promoting their anti-proliferative and/or pro-apoptotic effects (*Menendez et al., 2005*).

In view of this application of OA in treatment, we decided to test the effects of this fatty acid alone or in combination with PKC $\alpha$  depletion on the proliferation, migration, invasion and apoptosis of breast cancer cell lines.

As regards proliferation, OA produced slight inhibition in the three cell lines tested, especially at long times, although this results can not be considered conclusive. This coincides with reports published in the past, in which the beneficial effects of OA in the prevention and treatment of some cardiovascular diseases and some types of cancer were claimed (*Zusman et al., 1997; Bartsch et al., 1999*). However, it has also been demonstrated in the recent past, that OA induces proliferation in breast cancer (*Hardy et al., 2005; Soto-Guzman et al., 2008*). These different conclusions indicate the need to clarify the effects and the action mechanism by which OA acts on breast cancer.

The most important effect of OA on inhibiting proliferation in breast cancer cells was found when PKC $\alpha$  expression was inhibited, which reinforces the notion that this isoenzyme is involved in cancer development and progression (*Tan et al., 2006*). Curiously, the level of PKC $\alpha$  did not recover with time, while the inhibition of proliferation decreased, mainly because control cells use up all the nutrients and space, while mutant cells keep growing, reaching a similar number of cells after nine days. Moreover, when OA was added to cells without PKC $\alpha$ , there was a degree of synergy between both treatments, which inhibited cell proliferation.

Striking results were obtained in migration and invasion assays, in agreement with the observation that the actin polymerization and these two typical aspects of aggressive breast cancer cells have been related (*Wang et al., 2008; Taiyab and Rao, 2010*). In MCF-7 cells, OA had no effect on actin polymerization and, as was expected, the fatty acid had no effect on the migration of these cells either. However, in MDA-MB-231 cells, the OA inhibits the production of actin fibres, but the migration and invasion capacities of these cells were not affected. In addition, it has been demonstrated that OA induces MMP-9 secretion in MDA-MB-231 cells (*Soto-Guzman et al., 2010*), although the really important fact in invasion is the balance of MMP-1/MMP-9, rather than the level of one single metalloprotease (*Baker et al., 2006; Duerr et al., 2008*).

In general, it might be expected that invasiveness will increase following OA stimulation (*Soto-Guzman et al., 2010*), since this monounsaturated fatty acid increases  $[Ca^{2+}]_i$ , thus triggering several signalling pathways by activating PKC $\alpha$ . However, we observed that OA did not induce invasion, mainly because PKC $\alpha$  requires other cofactors to be completely activated. In addition, PKC $\alpha$  is involved in a huge number of signalling pathways of opposing physiological functions, ranging from the induction of apoptosis to cellular proliferation stimulation. Once again, the complexity of the PKC family is highlighted, as is the fine-tuning of the activation mechanism of enzymes.

Traditionally, it has been reported that olive oil has beneficial effects on health (Zusman *et al.*, 1997; Bartsch *et al.*, 1999). However, nowadays it is known that OA even stimulates the migration and invasion of some breast cancer cell lines (Byon *et al.*, 2009; Soto-Guzman *et al.*, 2010; Navarro-Tito *et al.*, 2010). These conflicting results may be explained in part by the fact that in the past, individual OA was not administered, but formed part of olive oil. It is known that this vegetable oil is composed of OA and some variable amounts of secondary compounds like squalene and phenolic constituents, which contribute to its antioxidant effects, but they differ among the types and varieties of olives used to manufacture the oil (Hardy *et al.*, 1997; Martin-Moreno, 2000).

As regards the effects of OA in programmed cell death, it is important to mention the controversy existing concerning the results obtained. In this work it has been shown that there was a slight increase in apoptosis in breast cancer cells induced by OA, whereas other studies revealed the role of this fatty acid as an enhancer of cell survival and an inhibitor of apoptosis (Hardy *et al.*, 2000). As for PKC $\alpha$  and apoptosis, there is unanimity in its role, since all results indicate that PKC $\alpha$  is involved in cellular proliferation and survival (Persson *et al.*, 2007; Cameron *et al.*, 2008; Tian *et al.*, 2009), and, when it was inhibited or depleted, apoptosis increased, as has also been demonstrated in this work.

In general, there are discrepancies in the results obtained over the years and further work must be carried out to clarify the effects of OA on breast cancer.

### **1.5. Localization and activation mechanism of PKC $\alpha$ induced by omega-3 fatty acids.**

Pioneering studies revealed the ability of polyunsaturated fatty acids (PUFAs) to localize some classical and novel PKC isoforms (Huang *et al.*, 1997), so we decided to test PKC $\alpha$  localization in two breast cancer cell lines, specially MCF-7 and MDA-MB-231, after stimulation with DHA or EPA.

In MCF-7 cells both omega-3 fatty acids induced PKC $\alpha$  localization in the plasma membrane: 42% of cells in the presence of DHA and in 64% of cells after EPA stimulation. In addition, PKC $\alpha$  co-localized with F-actin filaments at the edge of the cells, without varying the natural cell morphology. In the case of MDA-MB-231 cells, only DHA was tested and it was seen to induce the localization of PKC $\alpha$  in the plasma membrane in 53% of cells. Unlike in MCF-7 cells, DHA provoked a change in morphology, leading to the total disorganization of F-actin polymerization.

Furthermore, we also studied the role of PKC $\alpha$  in these cell lines by inhibiting its expression using siRNA. In MCF-7 cells without this kinase, the morphology and size were modified (these mutant cells became bigger and more spread out). The phosphorylation of some cytoskeleton proteins by PKC $\alpha$  has been recently reported; for example, phosphorylation of  $\alpha$ 6-tubulin (Abeyweera *et al.*, 2009) or fascin (Anilkumar *et al.*, 2003) among others. It was therefore expected that in the absence of PKC $\alpha$ , these cytoskeleton proteins would be disorganized and the cell morphology changed.

In MDA-MB-231 cells with inhibited PKC $\alpha$  expression, a much more dramatic effect on morphology was observed. These mutant cells were round flattened and larger in size; besides, the nuclei were fragmented, suggesting an apoptotic process. The activation of PKC $\alpha$  is related to apoptosis inhibition (Tian *et al.*, 2009), which was corroborated in this work. Moreover, when DHA was added to these mutant cells, the residual PKC $\alpha$  reached the nuclei, where it might stimulate the apoptosis pathways in which this kinase is involved.

Previous studies showed that some PKC isoforms can localize in membranes after PUFA stimulation (Huang *et al.*, 1997), but no downstream pathways were studied. Therefore, after demonstrating the localization of PKC $\alpha$  in breast cancer cells induced by EPA and DHA, the second step consisted of running kinase assays to clarify the activation mechanism of PKC $\alpha$  upon EPA and DHA stimulation.

Surprisingly, the results obtained were not along the same line as the localization results, since DHA activated PKC $\alpha$  and also induced localization of this classical isoform in the plasma membrane in 42% of MCF-7 and 53% of MDA-MB-231 cells. In the activation mechanism of PKC $\alpha$  induced by DHA, both important regions of the C2 domain (*calcium binding region* and *lysine rich cluster*) are the essential ones, while the C1 domain plays a less crucial role than the C2 domain. This contrasts with studies carried with other fatty acids like arachidonic acid, where the C2 domain (mainly the *calcium binding region*) was also the one mainly involved in the localization and activation mechanism of PKC $\alpha$ , although the C1 domain also played an important function (López-Nicolás *et al.*, 2006).

However, EPA translocated PKC $\alpha$  from the cytoplasm to the plasma membrane in 64% of MCF-7 cells but it was not able to activate it. Further studies are needed to clarify the reasons why EPA is not able to activate PKC $\alpha$ , and to clarify whether this is due to an insufficient interaction between EPA and PKC $\alpha$  to release the pseudosubstrate domain from the catalytic centre of the enzyme.

## 1.6. Omega-3 fatty acids reduce the malignancy of breast cancer cell lines through PKC $\alpha$ .

Some typical physiological aspects of tumour cells, such as migration, invasion and apoptosis, were studied and promising results were obtained after stimulating breast cancer cell lines with omega-3 fatty acids and when PKC $\alpha$  was depleted in these cells.

Striking results for the migration capacity of MCF-7 were found when both omega-3 fatty acids were used. On the one hand, DHA inhibited the motility of these cells, as did PKC $\alpha$  depletion, and the effect was additive when both treatments were applied together. On the other hand, EPA did not alter the migration of MCF-7 cells. PKC $\alpha$  has been related to motility in breast cancer cells (Ng *et al.*, 2001) and the synergy observed between its depletion and DHA reveals that this fatty acid acts in the same signalling pathway as PKC $\alpha$  as regards cell migration.

In the case of MDA-MB-231 cell migration, it was inhibited by both omega-3 fatty acids in a PKC $\alpha$ -independent way, having DHA a greater effect than EPA, which coincides with the results obtained by Germain and co-workers (1998), who described the positive relation between the number of unsaturated bonds of fatty acids and beneficial effects. This more pronounced effect of DHA on the inhibition of migration can be explained by the fact that this fatty acid alters factors that are important for migration, such as actin fibre polymerization (Abeyweera *et al.*, 2009) and the voltage-gate Na<sup>+</sup> channel (Isbilen *et al.*, 2006).

PKC $\alpha$  has been positively related with invasion (Tan *et al.*, 2006; Syed *et al.*, 2008), that is, higher PKC $\alpha$  activity should mean greater cell invasion. This agrees with the results obtained in this work, where the inhibition of PKC $\alpha$  expression reduced the invasiveness of MDA-MB-231. This effect was more pronounced when EPA and specifically, DHA were added to cells without PKC $\alpha$ . The synergy between DHA and PKC $\alpha$  depletion can be easily explained if we take into account that this fatty acid decreases MMP9 expression (Harris *et al.*, 2001) and that the absence of PKC $\alpha$  decreases cellular invasiveness (Tan *et al.*, 2006; Syed *et al.*, 2008).

Another important factor studied in breast cancer cell lines after DHA and EPA stimulation was apoptosis. Both fatty acids increased programmed cell death in both breast cancer cell lines tested, DHA being more effective than EPA. This difference could be due to the capacity of these fatty acids to induce reactive oxygen species (ROS) production, followed by caspase-3 activation (Aires *et al.*, 2007). It has been shown that the cytotoxic effect for

tumour cells is increased in a positive relation with the unsaturation degree of fatty acids (*Germain et al., 1998*).

The effect of omega-3 fatty acids on apoptosis involves different signalling pathways, depending on the cell line: in MCF-7 apoptosis is PKC $\alpha$ -independent, while in MDA-MB-231 cells it is PKC $\alpha$ -dependent, since the addition of DHA to these last cells, when PKC $\alpha$  has been depleted, dramatically increased the percentage of apoptotic cells.

Several hypotheses have been proposed to explain the action mechanism of this polyunsaturated fatty acids: one hypothesis is that they produce an oxidative stress (tumour cells possess reduced antioxidant defenses (*Oberley et al., 2002; Fite et al., 2007*)); another hypothesis argues that the incorporation of these fatty acids to cell membranes modifies its structure and permeability, altering lipid rafts and associated signal transductions (*Schley et al., 2007*); and another that ion channels and calcium homeostasis are deregulated (*Judé et al., 2006*). Others hypothesis exist, but more studies should be carried out to clarify these possibilities.

Taking everything into account, it is clear that it is necessary to study each type of breast cancer independently, since every cell type shows different characteristics and different responses to the addition of these fatty acids.

In general, omega-3 fatty acids are used as a complement to classical treatments to improve them. The results obtained in this work corroborate that these fatty acids may be used in this way, either as a single treatment or together with PKC $\alpha$  depletion. Nevertheless more studies are necessary to improve these treatments.

### **1.7. Synthetic charged DAG-lactones induce localization of several PKC isoform to the plasma membrane.**

The biophysical properties of some DAG-lactones have been recently demonstrated (*Philosof-Mazor et al., 2008; Raifman et al., 2010a*). In this work we try to shed light on the relationships between membrane anchoring of synthetic DAG-lactones and the cellular activities of these ligands.

The data presented in a part of this Doctoral Thesis indicate that the biological properties of DAG-lactones tested (153C-022, 153B-095, 153B-097, 153B-140 and 153B-143) are indeed closely dependent on their modes of membrane anchoring, particularly the extent of their binding and localization at the lipid bilayer.

The parent DAG-lactone (153C-022), which does not carry a positive charge, induce translocation of three PKC isoforms tested ( $\alpha$ ,  $\delta$  and  $\epsilon$ ) to the plasma membrane (Table VI.2). That happens, most likely due to the insertion of this DAG-lactone into the hydrophobic core of the lipid bilayer rather than to its accumulation at the membrane surface (*Raifman et al., 2010b*).

Three other DAG-lactones derivatives, specifically 153B-095, 153B-097 and 153B-140, were not able to localize any PKC isoenzyme to membranes (Table VI.2), mainly because these compounds have extended *n*-alkyl side-residues, which do not shield the positive amine, thereby retaining their electrostatic attraction to the phosphate moieties of the phospholipid headgroups, accumulating in the lipid bilayer surface (*Raifman et al., 2010b*). These results fit with the determination of ligand binding affinities for PKC. Since the role of ligand binding to the C1 domain of PKC is to facilitate the insertion of this domain into the lipid bilayer, driving translocation, those ligands which themselves do not insert into and disrupt the bilayer structure would be less effective at promoting this insertion, although other factors will also play a role.

The branched alkyl chain DAG-lactone (153B-143) was shown to induce translocation of PKC $\delta$  and PKC $\epsilon$ , but not of PKC $\alpha$  (Table VI.2). This observation might be related to the intermediate status of lipid bilayer interactions of this ligand compared with the parental and other DAG-lactones derivatives, since its branched chain could mask the positive charge, thus facilitating the biological functionality of the ligand.

A possible explanation for the differential effect on plasma membrane translocation among the different PKC isoenzymes could be the small variations in the surface charges exhibited by the C1 domains at the rim of the DAG-lactone binding cleft. Figure IX.2 depicts an example in which solvent-accessible surfaces have been modelled into the three-dimensional structures of the C1B domains of PKC $\alpha$  and PKC $\delta$ , respectively. It is apparent in the model shown in Figure IX.2 that the surface of the top region of the PKC $\alpha$  molecule, which includes the DAG-lactone interacting site, is more hydrophobic than PKC $\delta$ . In addition, the C1B domain of PKC $\delta$  exhibits a positive charge corresponding to Lys256 which is conserved in PKC $\epsilon$  (Arg267) but not in the C1B domain of PKC $\alpha$  (His128). Taking into account that these positively-charged residues promote the interaction of the C1 domain with negatively charged phospholipids within the plasma membrane, it is highly probable that the absence of this residue in the C1B domain of PKC $\alpha$  impedes the accessibility of the protein to the DAG-lactone 153B-143 that is located in a deeper area of the membrane interface.

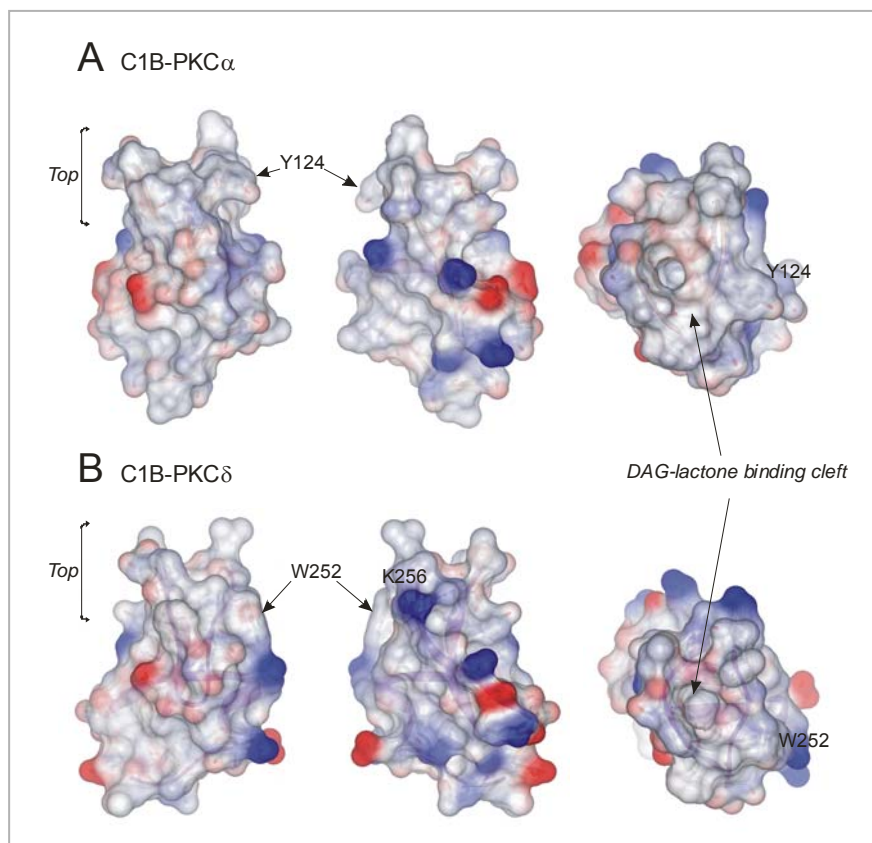


**Figure IX.2. Solvent accessible surface of the C1B domain of PKC $\alpha$  (A) and PKC $\delta$  (B) in the absence of ligands.** They were calculated by using DSVisualizer 2.0 using a probe radius of 1.4 Å. Positively and negatively charged regions are shown in blue and red respectively, while the hydrophobic surface is represented in grey. Amino acidic residues of reference have been labeled to help orientate the molecules. The molecules on the left correspond to a front view with critical Trp or Tyr residues labeled. The molecules on the centre correspond to the back view and those in the right correspond to a top view showing the DAG-lactone binding cleft (Taken from Raifman *et al* 2010).

The divergent behaviour of the five DAG-lactones studies in our work is particularly intriguing. Combinatorial libraries of DAG-lactones indicated that marked differences in biological response could be generated from modest structural variations in the hydrophobic domains of the DAG-lactones (Kang *et al.*, 2006). The probable interpretation of those observations was that the differential effects reflected changes in the pattern of association of the various PKC isoforms and other C1 domains containing effector proteins with membrane micro-domains. The present findings indicate that the combination of positive charge, which should be selective for negatively charged membrane regions, together with appropriate variation in the hydrophobic moieties incorporated into the structure, can likewise have profound effects on the pattern of interaction with membranes. It thus should provide a fruitful future strategy for generation of diversity.

### **1.8. DAG-lactones anchor PKC isoforms to the plasma membrane in a more subtle manner than phorbol ester.**

FRAP studies allow us to measure the tightness of the interaction between PKC and ligands in membranes, calculating mobile fraction and lateral diffusion coefficient of the enzyme in membranes (*Chen et al., 2006; Wang et al., 2008*).

Data obtained along this work show that DAG-lactone 153C-022 increased mobile fraction of PKC $\alpha$  in the plasma membrane. This suggests that the compound is able to mobilize a higher concentration of this classical isoform in the plasma membrane than PMA. In the case of novel PKCs, specifically PKC $\delta$  and PKC $\epsilon$ , no DAG-lactone tested modify significantly their mobile fraction when it is compared with data obtained using PMA. The effect of the variation of the mobile fraction on signalling pathways could be explained after two alternative possibilities. On the one hand, the movement of a protein along the plasma membrane could help the contact between PKCs and many molecular targets, what could involve a transient activation of several pathways. On the other hand, the protein immobilization in a specific zone of the plasma membrane entails interaction with few targets, but for a longer time, triggering this specific signalling pathway more efficiently.

Regarding lateral diffusion coefficient, the results obtained vary depending on the DAG-lactone and the PKC isoform studied. In the case of PKC $\alpha$ , the ligand 153C-022, approximately duplicates the diffusion coefficient when it is compared to PMA, indicating a faster movement of PKC $\alpha$  linked to this DAG-lactone along the plasma membrane. When PKC $\epsilon$  was studied, we observed no effect of parental DAG-lactone on lateral diffusion coefficient, although the other ligand tested (153B-143) reduced slightly this parameter compared to PMA. Again in this case, it is unknown if a faster lateral diffusion velocity is better than a slower one or viceversa for cellular responses.

Summarizing, DAG-lactone 153C-022 allows to PKC $\alpha$  moving faster and in higher proportions along the plasma membrane than PMA. In the case of PKC $\epsilon$ , this ligand affects neither lateral diffusion coefficient nor mobile fraction; whereas compound 153B-143 reduces the velocity of movements and increases slightly the mobile fraction of this novel PKC isoenzyme with respect to PMA. The effect of these variations on cellular biology is still unknown and more studies about them must be carried out.

### **1.9. Studies on gene expression arrays reveal that PKC $\alpha$ depletion decreases the malignancy of MCF-7 and MDA-MB-231 breast cancer cells.**

In MCF-7 cells, most of the genes with a significant expression were down-regulated, which suggests that PKC $\alpha$  plays an important role in these breast cancer cells by regulating the expression of many other genes. When these down-regulated genes were classified according to the KEGG pathways, we found general annotations like *pathways in cancer* and other more specific annotations like *MAPK*, *ErbB* and *p53 signalling pathways*, all of them involved in proliferation and cell cycle stimulation (Cubas *et al.*, 2010; Caiazza *et al.*, 2010). These results agree with those obtained in our laboratory, where cellular proliferation was reduced after inhibiting PKC $\alpha$  expression, perhaps because further inhibition of ERK/MAPK phosphorylation produced inhibition of Rb phosphorylation, leading to G(1) arrest (Fujii *et al.*, 2008).

MCF-7 cells with residual level of PKC $\alpha$  also over-expressed some genes which were classified into several groups according to the KEGG pathways. Some annotation like *calcium signalling pathways*, *inositol phosphate metabolism* and *phosphatidylinositol signalling system* were interesting, since PKC $\alpha$  is a Ca<sup>2+</sup>-dependent kinase and it is able to interact with PtdIns(4,5)P<sub>2</sub>, among other phosphatidylinositols (Corbalán-García *et al.*, 2007). This demonstrates that in the absence of an important signalling enzyme which uses calcium and phosphatidylinositols, other genes which codify proteins that also use these cofactors are over-expressed in order to compensate the lack of PKC $\alpha$ . Another possible explanation could be that, without PKC $\alpha$ , the concentration of these cofactors in the cell is increased, so genes involved in regulating their levels are over expressed. More studies should be carried out to clarify the role of these over-expressed genes in MCF-7 cells expressing a low level of PKC $\alpha$ .

Our hypothesis was as follows: when PKC $\alpha$ , a protein related directly with cancer development (Frankel *et al.*, 2007; Cameron *et al.*, 2008) is depleted from some cells, other oncogenes (regulated by this classical PKC isoform) will also be down-regulated. In addition, these mutant cells over-express other genes in order to maintain growth.

This hypothesis was tested by jointly using siRNA $\alpha$  treatment and some specific inhibitors of proteins whose genes are over-expressed, specifically inhibitors of PLC, PKA, HER and PDGF. The results obtained in migration and apoptosis assays confirmed the hypothesis, since PKC $\alpha$  depletion and specific inhibitors had a synergistic effect on decreasing migration, or increasing apoptosis, or both.

In the case of MDA-MB-231 cells, the role of PKC $\alpha$  seems to be more important than in MCF-7 cells, since this isoenzyme is more abundant in them (Lonne *et al.*, 2010) and when it is down-regulated by siRNA $\alpha$ , approximately 70% of genes significant differently expressed are down-regulated (10% more than MCF-7). If we compare the KEGG pathways-based classification of down-regulated genes in MCF-7 and MDA-MB-231 cells, we observe similar annotations, for instance *focal adhesion*, *ECM-receptor interactions* and *pathways in cancer*. This indicates that the cellular functions that are affected in both cell lines after PKC $\alpha$  inhibition are similar, although the genes involved are different in both cases.

Striking results were obtained in the case of up-regulated genes, since genes with a malignant function appeared in the list, mainly Ras-related GTPases, for example *ralA* (Balasubramanian *et al.*, 2010) and *rrad* (Suzuki *et al.*, 2007), among others. In contrast, the list also included up-regulated genes whose proteins are involved in cell cycle arrest and decreasing proliferation, for example *bmp2* (Dumont and Arteaga, 2003) and *cdkn1a* (Privat *et al.*, 2010), respectively.

In MDA-MB-231 cells, the hypothesis was similar to that postulated for MCF-7, since the vast majority of down-regulated genes are involved in proliferation, apoptosis arrest and cell cycle stimulation, for example *skp2* (Meng *et al.*, 2010) and *birc3* (Frasor *et al.*, 2009). Among over-expressed genes in MDA-MB-231, we found some oncogenes which we tried to inhibit by means of specific compounds, although no clear conclusion could be reached, since the concentrations tested was insufficient to have any effect on the cellular functions studied (migration, invasion and apoptosis).

### **1.10. The effects of salinomycin on breast cancer cells are enhanced by PKC $\alpha$ depletion.**

Salinomycin has recently emerged as a possible cancer treatment, but knowledge of its action mechanism is still scant.

We observed that salinomycin affects some important processes, such as migration, invasion and apoptosis, in two breast cancer cell lines. Moreover, these effects seem to be related with PKC $\alpha$  in some of these processes.

In MCF-7 cells, salinomycin decreased migration significantly, and when added to cells which do not express PKC $\alpha$ , the migration capacity was completely abolished. This observation suggests that salinomycin inhibits migration of MCF-7 cells through a signalling pathway where PKC $\alpha$  is also involved. In the case of the other breast cancer cell line studied, MDA-MB-231,

salinomycin also inhibited migration, although independently of PKC $\alpha$ , which indicates that different mechanisms are used in different cell lines.

MDA-MB-231 cells were also used to study invasion, which was found to be reduced after salinomycin stimulation, although the greatest inhibition was obtained when MDA-MB-231 cells with down-regulated PKC $\alpha$  were incubated with salinomycin, suggesting that the combination of treatments would be the best therapy.

To date, no explanation of these effects exists, although a genetic action of salinomycin has been proposed as a possible basis for its biological effects. Cancer stem cells over-express some genes related with the aggressiveness of some tumours, and salinomycin can decrease the activity of these genes (*Grupta et al., 2009; Lander et al., 2009*).

We also found that salinomycin rapidly induces apoptosis in both cell lines studied, since in MCF-7 and MDA-MB-231 cells the most important increase was in late apoptosis, that is, when most apoptotic cells were dead. The apoptosis signalling pathways activated by salinomycin are not the same in both cell lines, since the programmed cell death is PKC $\alpha$ -independent in MCF-7, whereas in MDA-MB-231 the effect of salinomycin is enhanced when PKC $\alpha$  expression is inhibited.

Because of the novelty of salinomycin, the exact mechanism of the antibiotic-induced apoptosis is still unclear and needs further investigations, although a distinct apoptotic pathway in cancer cells, which is not accompanied by cell cycle arrest and independent of p53, caspase activation, the CD95/CD95L system and the 26S proteasome, has been proposed (*Fuchs et al., 2009*).

In this study, we suggest that PKC $\alpha$  is related with the effect of salinomycin on decreasing migration in MCF-7 and inducing apoptosis in MDA-MB-231 cells, although the underlying mechanism of action or the target within the cells have not been revealed. For this reason, additional research is needed to determine exactly how salinomycin acts to kill cancer stem cells and to assess whether it can produce the same tumour-reducing power in humans as it does in mice and cell cultures.

## 2. CONCLUSIONS.

The study performed with several fatty acids and other bioactive compounds (DAG-lactones and salinomycin) contributes to our knowledge of the molecular mechanism that controls the localization and activation of PKC $\alpha$  induced by these molecules in breast cancer cell lines. Furthermore, the use of siRNA $\alpha$  to inhibit the expression of PKC $\alpha$  revealed the role of this enzyme in several aspects of breast cancer cells, including proliferation, migration, invasion and apoptosis. Therefore, we can conclude the following:

- 1) The localization of PKC $\alpha$  in the plasma membrane of MCF-7 cells stimulated with arachidonic acid is a Ca<sup>2+</sup>-dependent process.
- 2) The initial interaction between PKC $\alpha$  and arachidonic acid embedded in the plasma membrane is through the C2 domain, more specifically the *calcium binding region*, using Ca<sup>2+</sup> as a bridge. After that, the C1A subdomain plays an important role, establishing a more stable anchorage of the enzyme in the membrane by interacting with available arachidonic acid molecules. The *lysine rich cluster* motif of the C2 domain and the C1B subdomain do not play important roles in the localization mechanism induced by arachidonic acid in MCF-7 cells.
- 3) Oleic acid is responsible for increasing intracytosolic calcium in transformed breast cancer cells like MCF-7 and BT-474, but not in non-transformed cells like MCF-10A. Furthermore, this increase is due to extracellular Ca<sup>2+</sup> influx and not so to release from intracellular reservoirs.
- 4) In the localization and activation mechanism of PKC $\alpha$  induced by oleic acid, the *calcium binding region* plays an essential role, while the *lysine rich cluster* motif and the C1 domain play less relevant roles in these processes.
- 5) PKC $\alpha$  depletion by means of siRNA reduces the malignant phenotype of breast cancer cell lines, decreasing their proliferation rates, migration and invasion capacities and increasing apoptosis.
- 6) Oleic acid does not affect the migration capacity of breast cancer cells, but it slightly reduces the proliferation rate of MCF-7 and BT-474 cells and the invasion of MDA-MB-231, while it increases the apoptosis percentage of MCF-7 and MDA-MB-231 cells, and shows slight synergy with PKC $\alpha$  depletion in both cell lines.
- 7) Eicosapentaenoic and docosahexaenoic acids can localize PKC $\alpha$  in the plasma membrane in breast cancer cells, but only the latter acid is able to activate this enzyme. In this process, C2 domain is essential through the intervention of the *calcium binding region* and *lysine rich cluster*, while

C1 domain plays a less relevant role in this activation mechanism of PKC $\alpha$ .

- 8) Both omega-3 fatty acids inhibit the migration of MDA-MB-231 cells independently of PKC $\alpha$  (the effect of docosahexaenoic acid being more pronounced); while in MCF-7 cells only docosahexaenoic acid reduces the migration in a PKC $\alpha$ -dependent manner. Furthermore, the invasion of MDA-MB-231 cells is reduced by both polyunsaturated fatty acids, which show slight synergy with PKC $\alpha$  depletion.
- 9) Both omega-3 fatty acids also induce apoptosis in MCF-7 cells to a similar degree and independently of PKC $\alpha$  depletion, while in MDA-MB-231 cells the increase of apoptosis is synergistic with PKC $\alpha$  depletion and docosahexaenoic acid is more effective than eicosapentaenoic acid.
- 10) The extent of bilayer insertion of the non-branched, *N*-(*n*-alkylpyridinium) chains of the positively-charged DAG-lactones significantly affects the translocation capabilities of the different PKC isoforms, especially PKC $\alpha$ , PKC $\epsilon$  and PKC $\delta$ .
- 11) PKC recognizes essentially biomimetic DAG-lactone ligands deeply inserted in the plasma membrane. In contrast, anchoring of the DAG-lactones displaying positively charged *N*-(*n*-alkylpyridinium) linear chains on the membrane surface interferes with the accessibility and recognition by PKC enzymes, suppressing translocation.
- 12) DAG-lactone 153B-143 interacts specifically with novel PKC isoforms and not with PKC $\alpha$ , suggesting that this ligand possesses specificity for this group of isoenzymes; therefore this compound could be used to regulate the functions of these isoenzymes in future treatments.
- 13) PMA induces the slower localization of PKC $\delta$ -ECFP than DAG-lactone 153B-143 and 153C-022. This suggests that this novel PKC has a higher affinity for DAG-lactones than for PMA, especially for 153C-022. In the case of PKC $\epsilon$ -EGFP, something similar occurs, although the different affinity for both DAG-lactones is even higher than when PKC $\delta$ -ECFP is considered. The three isoenzymes tested show a higher affinity to some DAG-lactones than PMA.
- 14) PMA induced translocation of PKC isoforms from cytoplasm to the plasma membrane follow the order PKC $\epsilon$  > PKC $\delta$  > PKC $\alpha$ , suggesting that novel PKC isoforms possess a higher affinity for phorbol ester than classical ones, especially PKC $\epsilon$ . Besides, this higher affinity of novel PKC isoforms than of classical ones was also observed in the case of the DAG-lactones tested.
- 15) PKC $\alpha$  shows faster lateral diffusion along the plasma membrane in the presence of DAG-lactone 153C-022 than in the presence of PMA. Moreover, the mobile fraction of this isoenzyme in the plasma membrane

upon stimulation with this DAG-lactone is also larger than that provoked by phorbol ester.

- 16) PKC $\epsilon$  does not show significant differences in lateral diffusion nor mobile fraction comparing stimulations with PMA and DAG-lactones. However, the diffusion coefficient of this novel isoform is significantly smaller than that of PKC $\alpha$  after 153C-022 DAG-lactone stimulation, indicating that PKC $\epsilon$  is anchored to the plasma membrane more tightly than PKC $\alpha$  in the presence of this DAG-lactone.
- 17) Among all PKC isoforms studied, PKC $\delta$  possesses the smallest diffusion coefficient after PMA stimulation, while the mobile fraction upon phorbol ester stimulation is similar to that observed for PKC $\alpha$  and significantly smaller than observed in the other novel PKC isoform studied (PKC $\epsilon$ ).
- 18) MCF-7 and MDA-MB-231 breast cancer cell lines, in which PKC $\alpha$  has been down-regulated by means of siRNA $\alpha$ , show a deregulated gene expression profile, most of the genes affected being down-regulated. In addition, these genes are involved in pro-tumour signalling pathways like *MAPK*, *ErbB* or *p53*. In contrast, up-regulated genes are involved in cell cycle arrest and decreasing proliferation, which indicates that by inhibiting PKC $\alpha$  expression in breast cancer cells, cellular malignancy is reduced.
- 19) The depletion of PKC $\alpha$  and the inhibition of some proteins whose genes are up-regulated (specifically, Phospholipase C, Protein kinase A and Erb B) in MCF-7 cells, abolished the migration of these breast cancer cells. Apoptosis also increased significantly when MCF-7 cells, in the absence of PKC $\alpha$ , were treated with a specific PDGF inhibitor.
- 20) Salinomycin inhibited migration in MCF-7 cells and abolished it when the cells did not express PKC $\alpha$ . In addition, this antibiotic was able to induce apoptosis in a PKC $\alpha$ -independent way.
- 21) In MDA-MB-231 breast cancer cells, salinomycin affected migration and invasion, which was reduced independently of PKC $\alpha$ , whereas the increase in apoptosis induced by this compound was enhanced when PKC $\alpha$  expression was inhibited.



ANNEX I

MCF-7 DEREGULATED GENES



<b>Gene</b>	<b>Fold change</b>	<b>chrom</b>	<b>adj.P.Val</b>
KRT20	-3.64651439	17	2.29E-05
S100A8	-2.65879406	1	0.00021707
COL4A6	-2.65024516	23	2.13E-05
CYP24A1	-2.47994933	20	2.13E-05
AKR1B10	-2.31857403	7	0.00028844
CD36	-2.23301461	7	2.13E-05
COL4A5	-2.02849296	23	3.53E-05
S100A9	-1.94340611	1	9.74E-05
ITGB6	-1.92314009	2	0.00041231
SPRR1A	-1.90945948	1	0.00014427
PRKCA	-1.81362921	17	9.22E-05
SPRR1B	-1.79747134	1	0.00014131
TMEM45A	-1.76911017	3	2.13E-05
KRT23	-1.75188952	17	0.00037956
IFI44L	-1.74681723	1	0.00123718
IFIT3	-1.71541697	10	0.00014131
MALL	-1.60147076	2	2.13E-05
GPX2	-1.55178661	14	0.00014131
EIF4B	-1.54690645	12	0.00021707
SLC7A11	-1.51470856	4	0.00049341
GBP1	-1.46517108	1	7.87E-05
PSMB9	-1.40179169	6	0.00095834
DIO2	-1.39255157	14	0.00224248
ALDH1A3	-1.38208253	15	0.00246247
SULF1	-1.37420862	8	0.00073722
S100A2	-1.34168634	1	2.18E-05
SCGB1A1	-1.32880286	11	0.00018279
EPAS1	-1.32605548	2	0.00030992
PSMB8	-1.3079589	6	0.0003679
ELK3	-1.29413548	12	0.00118571
OAS2	-1.28896349	12	0.00879934
MX2	-1.2688498	21	0.00039071
SERPINB5	-1.26249866	18	0.00031311
KRT4	-1.24137715	12	0.00013334
RNF128	-1.23422153	23	0.00014131
TRIM2	-1.22255969	4	0.00228676
LAMP3	-1.21747918	3	0.00021094
TP63	-1.21702223	3	4.86E-05
UGT1A6	-1.19429707	2	0.00090602
DUSP6	-1.18951198	12	0.00395966
LIMCH1	-1.17662913	4	0.00014131
UGT1A3	-1.16447841	2	0.00021707
KLF5	-1.1519894	13	0.00331744
IL8	-1.14158152	4	0.00123735
S100A7	-1.12894456	1	0.00302593
TNS3	-1.12821522	7	0.00257854
TRIB2	-1.12168829	2	0.00074635
LYPD1	-1.11560484	2	0.0019012

ABLIM1	-1.10128266	10	0.00039278
EGFR	-1.09914123	7	0.00661713
AQP3	-1.09631645	9	0.00118571
WISP2	-1.09260965	20	0.00128422
TNFSF10	-1.09239329	3	0.00091977
RSAD2	-1.08112772	2	0.00115249
HERC5	-1.06007573	4	0.00294119
C10orf116	-1.03608958	10	0.00340953
XAF1	-1.01601272	17	0.0044067
CAV1	-1.00598728	7	0.00103891
FLJ11286	-0.97872601	19	0.00434613
EMP1	-0.95987951	12	0.0009322
SNAI2	-0.95675997	8	0.00065227
UGT1A9	-0.9531239	2	0.00031311
BTC	-0.95115187	4	0.00016693
OAS1	-0.94441384	12	0.00089183
COL5A1	-0.94181237	9	0.00585505
PSPH	-0.94080215	7	0.00331744
BCL6	-0.93967702	3	0.00038054
UGT1A1	-0.9378705	2	0.00075804
LGALS7	-0.93332396	19	0.00652306
DHRS3	-0.93206234	1	0.0025095
PARP12	-0.92871881	7	0.00138847
BTN3A3	-0.92141657	6	0.00664637
GABBR2	-0.89425559	9	0.00019264
DNM3	-0.88981987	1	0.00115249
UPK3B	-0.88077709	7	0.0013
IFI35	-0.87760941	17	0.00433141
ZFP36L1	-0.87693046	14	0.0027211
SLPI	-0.87608732	20	0.0025095
TMPRSS4	-0.87303664	11	0.0008162
ERLIN2	-0.87185062	8	0.00100198
PITX1	-0.86105218	5	0.00030992
ANXA8L2	-0.8599917	10	0.00151953
SGCE	-0.85576918	7	0.00078968
CADPS2	-0.8496243	7	0.00236171
HCP5	-0.84516339	6	0.001209
SLC7A5	-0.8385282	16	0.00097239
LOXL1	-0.83526576	15	0.0020135
ABCC3	-0.83334413	17	0.00643126
HLA-B	-0.81597107	6	0.00057177
IGFBP3	-0.81316009	7	0.00119536
SGCG	-0.81192839	13	0.00434613
GRB10	-0.80245802	7	0.00556911
ZFP36L2	-0.79727507	2	0.00349273
EVI1	-0.7970973	3	0.00606439
SIX2	-0.79439463	2	0.00322266
GABRP	-0.79266415	5	0.00373718
USP18	-0.78907134	22	0.00056032
NMI	-0.78411746	2	0.00371609
MX1	-0.78328144	21	0.00879934
MDK	-0.78322286	11	0.00106869

IFITM1	-0.77679956	11	0.00536165
SMARCA1	-0.76644663	23	0.00719241
LGALS3BP	-0.75830236	17	0.00066407
OASL	-0.75416037	12	0.00123735
ACP6	-0.74607583	1	0.00233271
HIST1H2BJ	-0.74594072	6	0.00224248
EREG	-0.74308485	4	0.00135896
TOX3	-0.74105209	16	0.00603103
STCH	-0.73607603	21	0.00244995
SEMA3E	-0.7262731	7	0.00163699
PPARG	-0.72305642	3	0.00228676
RARRES3	-0.71697424	11	0.00556911
THADA	-0.7080647	2	0.00089975
CENPF	-0.7072182	1	0.00664637
TMEPAI	-0.7029672	20	0.00217913
TGM2	-0.69717741	20	0.00119463
TGOLN2	-0.69685445	2	0.00708172
TRIM5	-0.69579013	11	0.00316556
ITGA2	-0.69553906	5	0.00184415
PPFIA1	-0.6824947	11	0.00541174
HOMER3	-0.67083196	19	0.00798735
ZEB1	-0.66631584	10	0.00243166
SLC5A3	-0.66553306	21	0.0084647
STAT1	-0.66007148	2	0.00217913
SORL1	-0.65433008	11	0.00399583
LOC644450	-0.64508237	NA	0.00565619
RIPK4	-0.63967637	21	0.00081328
DOCK4	-0.63871437	7	0.00660322
PTGES	-0.63670112	9	0.00162425
SEMA5A	-0.62017338	5	0.00761775
GAL	-0.6152471	11	0.00660322
TAP1	-0.60491507	6	0.0086376
TNFAIP8	-0.59042984	5	0.00434613
PPP2R1B	-0.58847263	11	0.00458458
HLA-A	-0.58227999	6	0.00191768
PPAP2A	-0.57044717	5	0.00270881
MTSS1	-0.56894155	8	0.00974769
HLA-F	-0.56502175	6	0.00217913
PDE4D	-0.55933512	5	0.00353578
PALLD	-0.55771977	4	0.00702752
UPF1	-0.55496601	19	0.00702752
MT1H	-0.55150491	16	0.00968195
NFIL3	-0.54549945	9	0.00229168
CLIP2	-0.54006327	7	0.00968195
UPF3B	-0.53975686	23	0.00475943
FRMD4B	-0.53969248	3	0.00617473
DONSON	-0.53519832	21	0.00563743
PCTP	-0.52865636	17	0.0025095
HLA-C	-0.52578547	6	0.00434613
FLJ13236	-0.52070568	12	0.00660322
HLA-G	-0.50993374	6	0.00337393
ZC3HAV1	-0.50329991	7	0.00891792

MATN2	-0.50179671	8	0.00630818
PDXK	-0.49415877	21	0.00533242
IFITM2	-0.49279564	11	0.00861937
APOL3	-0.4914781	22	0.00729035
WHSC1	-0.4908037	4	0.00817466
ATG2A	-0.48945602	11	0.00509357
HIRA	-0.48460028	22	0.00630818
IFITM3	-0.48277198	11	0.00946756
DPYD	-0.48033232	1	0.00617473
FERMT1	-0.47961283	20	0.00708172
ZNF302	-0.47727834	19	0.00906611
ZNF813	-0.47136132	19	0.00976637
IRF1	-0.46686515	5	0.00968195
CASP3	-0.46661377	4	0.00661713
PLEKHA4	-0.46019245	19	0.00861223
MAGED4B	-0.45533194	23	0.00624152
RUNX1	-0.44581379	21	0.00868928
LRRC6	-0.44323358	8	0.00915064
PRSS23	-0.44132783	11	0.00584686
GALNT6	-0.44115178	12	0.00592919
ARHGEF18	-0.43669355	19	0.00879934
SLC25A12	-0.43102134	2	0.00867402
LOC26010	-0.41801473	2	0.00857207
ATP2B1	-0.41751611	12	0.00746612
TLE4	-0.39980315	9	0.00816647
FAM152A	0.41400775	1	0.00868928
CCDC121	0.41965758	2	0.00989468
RWDD2A	0.42542438	6	0.00708172
TCEAL1	0.43489398	23	0.00968195
C10orf97	0.44166429	10	0.00847671
TERF1	0.44968719	8	0.00630818
NDUFS2	0.45167478	1	0.00567529
ARL1	0.45891387	12	0.00934835
PGM3	0.4600804	6	0.00582655
PDCD4	0.46301582	10	0.00533242
NAP1L2	0.46805268	23	0.00984454
C1orf34	0.47379553	1	0.00591191
DKFZp667G2110	0.47646834	3	0.00434613
FDFT1	0.47915442	8	0.00737839
CCNI	0.48026149	4	0.00458083
PEX11A	0.48134618	15	0.00661713
ACO1	0.48243425	9	0.00741578
RNF13	0.48432651	3	0.00791136
TMEM106B	0.4855609	7	0.00560269
PPP2R2A	0.4880044	8	0.00455747
C5orf4	0.49276639	5	0.00664637
TCF25	0.49398981	16	0.00989468
PRCP	0.49978251	11	0.00433141
PTK6	0.50549231	20	0.00524437
SELENBP1	0.5082262	1	0.00617473
MANEA	0.50898327	6	0.00763893
ABHD2	0.51027307	15	0.00434613

LASS2	0.51118188	1	0.00372958
SYNJ2	0.5157682	6	0.00738157
PLEKHB2	0.51631052	2	0.00798735
KIAA1467	0.52451974	12	0.00664637
SGMS1	0.52801057	10	0.0084751
ABI1	0.52874643	10	0.00433141
TCF7L2	0.52938563	10	0.00738157
SNX10	0.53437809	7	0.0047343
SNX7	0.53736423	1	0.00894234
DBNDD1	0.5435121	16	0.00455747
DNAJB9	0.552971	7	0.00737839
SDCBP	0.55809117	8	0.00331744
PRKAB2	0.5708068	1	0.00434613
TPK1	0.57112481	7	0.00785792
ACADSB	0.57420818	10	0.00598291
ZNF415	0.5763626	19	0.00340953
SLC16A4	0.58040021	1	0.00259571
CLU	0.58243775	8	0.00983955
STK3	0.58341355	8	0.00652306
TXNIP	0.5842432	1	0.00565619
ALDH6A1	0.58836175	14	0.00322266
PNRC1	0.59231628	6	0.00137547
HEY2	0.59455282	6	0.00805971
NPY1R	0.59976359	4	0.00488784
UBXD6	0.60251496	8	0.00224248
STBD1	0.60325557	4	0.00395966
MICB	0.6060121	6	0.00968195
FAM134B	0.62061628	5	0.00270939
DEPDC6	0.62269809	8	0.00302593
CD55	0.62297081	1	0.00664637
GDPD3	0.62677692	16	0.00448705
SPDEF	0.62825124	6	0.00263443
WWP1	0.6298649	8	0.00556911
PPP1R3C	0.63206563	10	0.00302593
ENPP4	0.64350772	6	0.00934448
GLUD2	0.64817687	23	0.00123718
TYRP1	0.66165354	9	0.00137547
GFRA1	0.66719866	10	0.00810964
PPP1R3D	0.66746642	20	0.00763893
ADCY1	0.66773499	7	0.00162023
MUC1	0.66818439	1	0.00713851
SGK1	0.66983715	6	0.00524437
STC1	0.67285662	8	0.00488784
PRKAR2B	0.67309342	7	0.00302593
PGM1	0.67614902	1	0.00246247
TSPAN12	0.67721777	7	0.00805971
SLC7A2	0.67801139	8	0.00828594
ERBB4	0.68597965	2	0.00664637
RFTN1	0.68997327	3	0.00226771
RUNX1T1	0.69105161	8	0.00244995
KIAA1324	0.69422647	1	0.00741578
PVRL3	0.70019391	3	0.00696701

APOD	0.70154863	3	0.00333276
LCP1	0.70380749	13	0.0027211
LGR4	0.70866684	11	0.00433141
RAB31	0.71000162	18	0.00191768
FILIP1L	0.71205448	3	0.00062378
KIF5C	0.72255128	2	0.00455966
NPY5R	0.74498004	4	0.00434613
GPR37	0.7456384	7	0.00115249
KCNJ3	0.75256864	2	0.00434613
PCDH7	0.75394973	4	0.00861223
MGAT4A	0.76514769	2	0.00674824
LYPLA1	0.78961098	8	0.00524437
PDGFA	0.80583136	7	0.0017646
GOLSYN	0.80988026	8	0.00106869
GLUL	0.81271405	1	0.0054678
SIGLEC15	0.83997712	18	0.00065347
GNA14	0.84559915	9	0.00066407
HS3ST3A1	0.85138537	17	0.00664637
AGR2	0.85229737	7	0.00089183
CYP26B1	0.8568481	2	0.00081328
SCUBE2	0.90014047	11	0.00039071
DIRAS2	0.93637465	9	0.00463009
RHOB	0.93935853	2	0.00014131
B3GALNT1	0.94579592	3	0.00077756
CPE	0.94848354	4	0.00013334
GPNUMB	0.9532871	7	0.00226771
PLCB4	0.95670017	20	0.00100198
MPPED2	0.95686634	11	0.00783218
KCNJ8	0.98437709	12	0.00891792
IGFBP5	0.99676329	2	9.84E-05
MLSTD1	0.99841048	12	0.00457731
SOCS2	1.02203823	12	0.00311366
NUCB2	1.08446728	11	0.0009251
DIO1	1.14173345	1	0.00142014
SEPP1	1.14471912	5	0.00434613
MAGEA11	1.15254093	23	0.0003679
UGT2B15	1.19981873	4	0.00816647
UGCG	1.23351589	9	0.00556911
CRISP3	1.24779516	6	0.00095834
COL21A1	1.26813005	6	0.0008162
FHL1	1.28211293	23	9.22E-05
SERPINA1	1.30259376	14	0.00021707
AOX1	1.30447647	2	4.49E-05
ID4	1.3220837	6	3.53E-05
ALCAM	1.33639975	3	0.00454852
ATRNL1	1.34272223	10	0.00013055
CA2	1.35230031	8	0.00014131
PTGER4	1.36111158	5	3.62E-05
CSTA	1.74271852	3	0.00039071
MSMB	2.24704815	10	9.22E-05

ANNEX II

MDA-MB-231 DEREGULATED GENES



<b>Gene</b>	<b>Fold change</b>	<b>chrom</b>	<b>adj.P.Val</b>
PRKCA	-2.93804901	17	1.66E-05
COL1A2	-1.30579456	7	0.00042855
CFB	-1.257127	6	0.00203207
CCNE2	-1.14583648	8	0.00031127
SLC6A14	-1.13845879	23	0.00612802
IL8	-1.13705489	4	0.00166525
TSPAN8	-1.11217306	12	0.0004395
RARRES1	-1.1061298	3	0.0004395
HLA-DRA	-1.09843327	6	0.00038118
CHI3L2	-1.08706865	1	0.00137555
CXCL1	-1.0754295	4	0.00112859
ANGPT1	-1.05573588	8	0.00144155
CXCL2	-1.04588123	4	0.0006181
SERPINA3	-1.035851	14	0.00144155
ZNF91	-0.97951979	19	0.00351278
C3	-0.97297068	19	0.00427036
MCM10	-0.93745355	10	0.0007442
KLRC3	-0.8998315	12	0.00038118
HLA-DRB1	-0.88883129	6	0.00166525
IL6ST	-0.8808793	5	0.00427036
CFI	-0.87341872	4	0.00255576
SEPT4	-0.858056	17	0.00554946
PDZK1IP1	-0.85275894	1	0.00166525
HLA-DPA1	-0.80736826	6	0.00266805
SLC38A4	-0.78440696	12	0.0032009
SERPINA5	-0.78428579	14	0.00390426
HS2ST1	-0.7797171	1	0.00144155
SERPINA1	-0.76933811	14	0.00495942
AQP1	-0.75394225	7	0.00381157
VCAM1	-0.74973556	1	0.00468453
ADAM28	-0.74942658	8	0.00759164
KLRC2	-0.74884107	12	0.0090277
TNC	-0.74792876	9	0.00381157
TNFRSF9	-0.73406931	1	0.00530105
MDM1	-0.73034316	12	0.00915281
COL6A3	-0.72746001	2	0.0039779
FZD1	-0.72134273	7	0.00261294
LIPG	-0.71501297	18	0.00427036
MKI67	-0.70895197	10	0.00203207
NOX5	-0.70874384	15	0.00166525
HLA-DPB1	-0.70716143	6	0.00396165
ICK	-0.70632654	6	0.00666409
C1S	-0.70495765	12	0.0075095
METTL7A	-0.70467551	12	0.00254224
RABGAP1L	-0.69657526	1	0.00188357
HLA-DRB4	-0.69035494	NA	0.00381157
HPGD	-0.68633676	4	0.00358446
SOX4	-0.68207545	6	0.00787054

CXCL3	-0.67458492	4	0.00427036
HLA-DRB5	-0.67337707	6	0.00345293
CD24	-0.66500833	24	0.00468453
ATP2B2	-0.66481182	3	0.00858621
EFEMP1	-0.66256082	2	0.00447166
OPTN	-0.65544184	10	0.00261294
MID1	-0.65111038	NA	0.00754329
CD58	-0.64317863	1	0.00265103
EZH2	-0.64086491	7	0.00396165
MDFIC	-0.64062846	7	0.0039779
LOC100133484	-0.63920045	6	0.00358446
HNRNPA3	-0.63585231	2	0.00759164
NT5E	-0.6327477	6	0.00501414
E2F8	-0.62584674	11	0.00759164
NSBP1	-0.61690929	23	0.00759164
ZNF43	-0.61200614	19	0.00447166
RANBP6	-0.61115432	9	0.00759164
FRK	-0.60788684	6	0.00759164
SLC2A6	-0.60769684	9	0.00811268
KAL1	-0.60764523	23	0.00722266
BIRC3	-0.60463231	11	0.00530138
ZNF268	-0.60445843	12	0.00427036
SKP2	-0.60421158	5	0.00758066
MKL2	-0.59975383	16	0.00787054
EIF3J	-0.59122971	15	0.0039779
USP48	-0.58851032	1	0.00554946
ZNF573	-0.58099205	19	0.00759164
ZC3H12A	-0.57502811	1	0.00351278
BRCA1	-0.5606799	17	0.00844916
TRIM22	-0.54708446	11	0.00542257
IVNS1ABP	-0.54371848	1	0.00908548
SORL1	-0.54203548	11	0.00468453
LAMC2	-0.53798943	1	0.00714886
WHSC1	-0.52511099	4	0.00977543
CYP26B1	-0.52391296	2	0.00811268
MCM4	-0.51810763	8	0.00666409
PRRG4	-0.51695381	11	0.00666409
FLJ21075	-0.5144409	7	0.00671932
BAZ1B	-0.50835955	7	0.00915281
ZNF37B	-0.48942636	NA	0.00758066
PER2	-0.4817248	2	0.00666409
RNF144A	-0.48005349	2	0.00969884
IDS	0.44083826	23	0.00993449
CDKN1A	0.51481379	6	0.00468453
RALA	0.51801951	7	0.00936657
CITED2	0.51826118	6	0.00542257
BMP2	0.52652646	20	0.00491807
ADFP	0.53130939	9	0.00759164
DUSP13	0.5478814	10	0.00671932
NPC1	0.5560661	18	0.00775227
FA2H	0.58061733	16	0.00468453
ZEB1	0.60106546	10	0.00797726

SOCS2	0.61341657	12	0.00722266
NMT2	0.61350844	10	0.00977543
SYNGR3	0.61808914	16	0.00468453
ADM	0.62571423	11	0.00468453
ARMC9	0.6259654	2	0.00427036
SQSTM1	0.64162977	5	0.00358446
FKBP1A	0.64296699	20	0.0043683
C17orf39	0.67687231	17	0.00650947
SCD	0.67835559	10	0.00381157
PSG2	0.6819959	19	0.00326782
G0S2	0.68540339	1	0.00351278
DUSP1	0.69700704	5	0.00722266
CPA4	0.69880513	7	0.00468453
GAD1	0.76080862	2	0.00468453
RRAD	0.77630671	16	0.00326782
PSG4	0.79312102	19	0.00390426
THBS1	0.8144769	15	0.00266805
MMP1	0.85172437	11	0.00427036
IL11	0.85482295	19	0.00491807
ABCG2	0.85490975	4	0.0032009
GDF15	0.91836729	19	0.00137555
PSG9	0.9278479	19	0.00229586
MBL2	1.00391924	10	0.00427036
PSG6	1.00757022	19	0.00137555
PSG7	1.06503358	19	0.0006181
PSG3	1.08920126	19	0.00554946
PSG1	1.10915781	19	0.00020516
PSG5	1.20141468	19	0.00166525
SCG5	1.26577532	15	0.00242602
IL24	1.5548423	1	0.00533577



## BIBLIOGRAPHY



- Abbas T, White D, Hui L, Yoshida K, Foster DA and Bargonetti J. (2004) Inhibition of human p53 basal transcription by down-regulation of protein kinase C $\delta$ . *J. Biol. Chem.* 279: 9970–9977.
- Abeyweera TP, Chen X and Rotenberg SA. (2009) Phosphorylation of  $\alpha$ 6-tubulin by protein kinase C $\alpha$  activates motility of human breast cells. *J Biol Chem.*; 284: 17648-56.
- Abulrob AN, Mason M, Bryce R and Gumbleton M. (2000) The effect of fatty acids and analogues upon intracellular levels of doxorubicin in cells displaying Pglycoprotein mediated multidrug resistance. *J Drug Target.* 8: 247–56.
- Affymetrix Technical Note (2005). Guide to Probe Logarithmic Intensity Error (PLIER) Estimation. <http://www.affymetrix.com>.
- Affymetrix. Genechip expression analysis (data analysis fundamentals), 2002.
- Aggarwal, B.B.; Sundaram, C.; Malani, N. and Ichikawa, H. (2007) Curcumin: the Indian solid gold. *Adv. Exp. Med. Biol.*, 595: 1-75.
- Ahmed, S., Kozma, R., Lee, J., Monfries, C., Harden, N. y Lim. L. (1991) The cysteine-rich domain of human proteins, neuronal chimaerin, protein kinase C and diacylglycerol kinase binds zinc. Evidence for the involvement of a zinc-dependent structure in phorbol ester binding. *Biochem. J.*, 280: 233–241.
- Ailles L.E. and Weissman I.L. (2007) Cancer stem cells in solid tumors. *Curr. Opin. Biotechnol.* 18: 460–466.
- Aires V, Hichami A, Filomenko R, Plé A, Rébé C, Bettaieb A, Khan NA. (2007) Docosahexaenoic acid induces increases in [Ca<sup>2+</sup>]<sub>i</sub> via inositol 1,4,5-triphosphate production and activates protein kinase C  $\gamma$  and  $\delta$  via phosphatidylserine binding site: implication in apoptosis in U937 cells. *Mol Pharmacol.* 72: 1545-56.
- Akers, R.F., Lovinger, D.M., Colley, P.A., Linden, D.J. y Routtenberg, A. (1986) Translocation of protein kinase C activity may mediate hippocampal long-term potentiation. *Science*, 231: 587-589.
- Akiba, S., Mizunaga, S., Kume, K., Hayama, M. y Sato, T. (1999). Involvement of group VI Ca<sup>2+</sup>-independent phospholipase A<sub>2</sub> in protein kinase C-dependent arachidonic liberation in zymosan-stimulated macrophage-like P388D<sub>1</sub> cells. *J. Biol. Chem.* 274, 19906-19912.
- Akiba, S., Ohno, S., Chiba, M., Kume, K., Hayama, H. y Sato, T. (2002). Protein kinase C $\alpha$ -dependent increase in Ca<sup>2+</sup>-independent phospholipase A<sub>2</sub> in membranes and arachidonic acid liberation in zymosan-stimulated macrophage-like P388D<sub>1</sub> cells. *Biochem. Pharmacol.* 63, 1969-1977.
- Akimoto, K., Mizuno, K., Osada, S.I., Hirai, S.L., Tanuma, S.I., Suzuki, K. y Ohno, S. (1994) A new member of the third class in the protein kinase C family, PKC $\lambda$ , expressed dominantly in an undifferentiated mouse embryonal carcinoma cell line and also in many tissues and cells. *J. Biol. Chem.*, 269: 12677-12683.
- Akimoto, K., R. Takahashi, S. Moriya, N. Nishioka, J. Takayanagi, K. Kimura, Y. Fukui, S. Osada, K. Mizuno, S. Hirai, A. Kazlauskas and S. Ohno. (1996) EGF of PDGF receptors activate atypical PKC-lambda through phosphatidylinositol 3-kinase. *EMBO J*, 15, 788-798.
- Alcón, S., Morales, S., Camello, P. y Pozo, M. (2002) Contribution of different phospholipases and arachidonic acid metabolites in the response of gallbladder smooth muscle to cholecystokinin. *Biochem. Pharmacol.*, 64: 1157-1167.
- Alessi, D.R., James, S.R., Downes, C.P., Holmes, A.B., Gaffney, P.R., Reese, C.B. y Cohen, P. (1997). Characterization of a 3-phosphoinositide-dependent protein kinase which phosphorylates and activates protein kinase C  $\alpha$ . *Curr. Biol.* 7, 261-269.

- Almholt K, Arkhammar PO, Thastrup O, Tullin S. (1999). Simultaneous visualization of the translocation of protein kinase Calpha-green fluorescent protein hybrids and intracellular calcium concentrations. *Biochem J.* Jan 15;337 ( Pt 2):211-8.
- Al-Shahrour, F., Minguez, P., Tárraga, J., Montaner, D., Alloza, E., Vaquerizas, J., Conde, L., Blaschke, C., Vera, J. and Dopazo, J. (2006) BABELOMICS: A systems biology perspective in the functional annotation of genome-scale experiments. *Nucleic Acids Research.*, 346: 460-464.
- Amaral P, Miguel R, Mehdad A, Cruz C, Monteiro Grillo I, Camilo M and Ravasco P. (2010) Body fat and poor diet in breast cancer women. *Nutr Hosp.* 25: 456-61.
- Anand, P.; Kunnumakkara, A.B.; Newman, R.A. and Aggarwal, B.B. (2007) Bioavailability of curcumin: problems and promises. *Mol. Pharm.*, 6: 807-18.
- Anand, P.; Sundaram, C.; Jhurani, S.; Kunnumakkara, A.B. and Aggarwal, B.B. (2008) Curcumin and cancer: an “old-age” disease with an “age-old” solution. *Cancer Lett.*, 267: 133-64.
- Ananthanarayanan, B., Stahelin, R.V., Digman, M.A. y Cho, W. (2003) Activation mechanisms of conventional protein kinase C isoforms are determined by the ligand affinity and conformational flexibility of their C1 domains. *J. Biol. Chem.*, 278: 46886–46894.
- Anderson, K.E., Coadwell, J., Stephens, L.R., y Hawkins, PT. (1998) Translocation of PDK-1 to the plasma membrane is important in allowing PDK-1 to activate protein kinase B. *Curr Biol.*, 8(12): 684-91.
- Anilkumar, N., Parsons, M., Monk, R., Ng, T. y Adams, J. (2003) Interaction of fascin and protein kinase Ca: A novel intersection in cell adhesion and motility. *EMBO J.*, 22: 5390-5402.
- Apidianakis, Y., Mindrinos, M. N., Xiao, W., Lau, G. W., Baldini, R. L., Davis, R. W., and Rahme, L. G. (2005). Profiling early infection responses: *Pseudomonas aeruginosa* eludes host defenses by suppressing antimicrobial peptide gene expression. *Proc. Natl. Acad. Sci.*: 102: 2573–2578.
- Armstrong, S. A., Staunton, J. E., Silverman, L. B., Pieters, R., den Boer, M. L., Minden, M. D., Sallan, S. E., Lander, E. S., Golub, T. R., and Korsmeyer, S. J. (2002). MLL translocations specify a distinct gene expression profile that distinguishes a unique leukemia. *Nat. Genet.* 30, 41–47.
- Aroca, J.D., Sánchez-Piñera, P., Corbalán-García, S., Conesa-Zamora, P., de Godos, A. y Gómez-Fernández, J.C. (2001). Correlation between the effect of the anti-neoplastic ether lipid 1-O-octadecyl-2-O-methyl-glycero-3-phosphocholine on the membrane and the activity of protein kinase Ca. *Eur. J. Biochem.* 268, 6369-6378.
- Arribas S.M., Daly C.J., González M.C. y McGrath J.C. (2007) Imaging the vascular wall using confocal microscopy. *J Physiol.*, 584:5-9.
- Asaoka, Y., Yoshida, K., Oka, M., Shinomura, T., Mishima, H., Matsushima, S. y Nishizuka, Y. (1992). The signal-induced phospholipid degradation cascade and protein kinase C activation. *Ciba Found Symp.*, 164: 50-65.
- Assender JW, Gee JM, Lewis I, Ellis IO, Robertson JF, Nicholson RI. (2007) Protein kinase C isoform expression as a predictor of disease outcome on endocrine therapy in breast cancer. *J Clin Pathol*; 60:1216–21.
- Assman G, De Backer G, Bagnara S et al. (1997) International consensus statement of olive oil and the Mediterranean diet: implications for health in Europe. *Eur J Cancer Prev*; 6: 418–421.
- Axelrod, D., Koppel, D., Schelessinger, J., Elson, E. and Webb, W. (1976) Mobility measurements by analysis of fluorescence photobleaching recovery kinetics. *Biophys. J.*, 16, 1055-1069.

- Axelrod, J. (1990) Receptor-mediated activation of phospholipase A<sub>2</sub> and arachidonic acid release in signal transduction. *Biochem. Soc. Trans.*, 18: 503-507.
- Aziz, M. H., H. T. Manoharan, D. R. Church, N. E. Dreckschmidt, W. Zhong, T. D. Oberley, G. Wilding and A. K. Verma. (2007) Protein kinase C epsilon interacts with signaltransducers and activators of transcription 3 (Stat3), phosphorylates Stat3 Ser727, and regulates its constitutive activation in prostate cancer. *Cancer Res*, 67, 8828-8838.
- Baeuerle, P.A., Lenardo, M., Pierce, J.W. y Baltimore, D. (1988) Phorbol-ester-induced activation of the NF-kappa  $\beta$  transcription factor involves dissociation of an apparently cytoplasmic NF-kappa  $\beta$ /inhibitor complex. *Cold Spring Harb. Symp. Quant. Biol.*, 53: 789-798.
- Bai, J., Tucker, W. C. y Chapman, E. R. (2004) PtdIns(4,5)P<sub>2</sub> increases the speed of response of synaptotagmin and steers its membrane-penetration activity toward the plasma membrane. *Nat Struct Mol Biol.*, 11: 36-44.
- Baier Bitterlich, G., Uberall, F., Bauer, B., Fresser, F., Wachter, H., Grunicke, H., Utermann, G., Altman, A. y Baier, G. (1996) Protein kinase C-theta isoenzyme selective stimulation of the transcription factor complex AP-1 in T lymphocytes. *Mol Cell Biol.*, 16(4):1842-50.
- Baker EA, Leaper DJ, Hayter JP and Dickenson AJ. (2006) The matrix metalloproteinase system in oral squamous cell carcinoma. *Br J Oral Maxillofac Surg.* 44: 482-6.
- Balasubramanian N, Meier JA, Scott DW, Norambuena A, White MA, and Schwartz MA. (2010) RalA-exocyst complex regulates integrin-dependent membrane raft exocytosis and growth signaling. *Curr Biol.* 20(1):75-9.
- Balendran, A., Biondi, R.M., Cheung, P.C., Casamayor, A., Deak, M. y Alessi, D.R. (2000) A 3-phosphoinositide-dependent protein kinase-1 (PDK1) docking site is required for the phosphorylation of protein kinase C zeta (PKC zeta ) and PKC-related kinase 2 by PDK1. *J Biol Chem.*, 275(27): 20806-13.
- Balsinde, J. y Balboa, M.A. (2005). Cellular regulation and proposed biological functions of group VIA calcium-independent phospholipase A<sub>2</sub> in activated cells. *Cell Signal* 17, 1052-1062.
- Banaszynski, L.A., Chen, L.C., Maynard Smith L.A., Ooi A.G. y Wandless TJ. (2006) A rapid, reversible, and tunable method to regulate protein function in living cells using synthetic small molecules. *Cell.* 126(5): 995-1004.
- Banci, L., Cavallaro, G., Kheifets, V. y Mochly Rosen, D. (2002) Molecular dynamics characterization of the C2 domain of protein kinase C $\beta$ . *J.Biol. Chem.*, 277:12988–12997.
- Barr, L. F. *et al.*(1991) *c-Myc* gene-induced alterations in protein-kinase-C expression — a possible mechanism facilitating *Myc-Ras* gene complementation. *Cancer Res.* 51, 5514–5519.
- Barry, O.P., Kazanietz, M.G., Patricó, D. y Fitzgerald, G.A. (1999). Arachidonic acid in platelet microparticles up-regulates cyclooxygenase-2-dependent prostaglandin formation via a protein kinase C/ mitogen-activated protein kinase- dependent pathway. *J. Biol. Chem.* 11, 7547-7556.
- Bartsch, H., Nair, J. and Owen, R. W. (1999) Dietary polyunsaturated fatty acids and cancers of the breast and colorectum: emerging evidence for their role as risk modifiers. *Carcinogenesis*, 20: 2209 –218.
- Bartoli, R., Fernandez-Ba\_ares, F., Navarro, E., Castella, E. et al. (2000) Effect of olive oil on early and late events of colon carcinogenesis in rats: modulation of arachidonic acid metabolism and local prostaglandin E(2) synthesis. *Gut*, 46, 191–199.
- Basu A, Woolard MD and Johnson CL. (2001) Involvement of protein kinase C-delta in DNA damage-induced apoptosis. *Cell Death Differ.* 8, 899–908.

- Bazzi, M.D., y Nelsestuen, G.L. (1987) Association of protein kinase C with phospholipid vesicles, *Biochemistry*, 26: 115–122.
- Bazzi, M.D., y Nelsestuen, G.L. (1989) Properties of the protein kinase C-phorbol ester interaction. *Biochemistry*, 28: 3577–3585.
- Becker, K.P., y Hannun, Y.A. (2003) PKC-dependent sequestration of membrane are cycling components in a subset of recycling endosomes, *J. Biol. Chem.*, 278: 52747–52754.
- Behn Krappa, A. y Newton, A.C. (1999). The hidrophobic phosphorylation motif of conventional protein kinase C is regulated by autophosphorylation. *Curr. Biol.*, 9: 728-737.
- Bell, R.M. (1986). Protein kinase C activation by diacylglycerol second messengers. *Cell* 45, 631-632.
- Bell, R. y Burns, D. (1991) Lipid activation of protein kinase C. *J. Biol. Chem.*, 266, 4661–4664.
- Bell, R.M., Hannun, Y.A., y Loomis, C.R. (1986) Mechanism of regulation of protein kinase C by lipid second messengers. *Symp Fundam Cancer Res.*, 39:145-56.
- Benes, C.H., Wu, N., Elia, A.E.H., Dharia, T. Cantley, L.C. Soltoff, S.P. (2005) The C2 domain of PKC  $\delta$  is a phosphotyrosine binding domain, *Cell*, 121: 271–280.
- Besson, A. and Yong V.W. (2000) Involvement of p21 waf1/Cip1 in protein kinase-alpha induced cell cycle progression. *Mol Cell Biol*, 20, 4580-4590.
- Besson, A. Wilson, T.L. and Yong, V.W. (2002) The anchoring protein RACK1 links Protein Kinase C  $\epsilon$  to integrin beta chains. Requirements for adhesion and motility. *J. Biol. Chem.*, 277: 22073–22084.
- Biondo PD, Brindley DN, Sawyer MB and Field CJ. (2008) The potential for treatment with dietary long-chain polyunsaturated n-3 fatty acids during chemotherapy. *J Nutr Biochem*. 19:787–96.
- Bittova, L., Stahelin, R.V. y Cho, W. (2001) Roles of ionic residues of the C1 domain in protein kinase  $C\alpha$  activation and the origin of phosphatidylserine specificity. *J. Biol. Chem.*, 276: 4218–4226.
- Black, J.D. (2000). Protein kinase C-mediated regulation of the cell cicle. *Front. Biosci*. 5, D406-D423.
- Blobe GC, Obeid LM and Hannun YA. (1994) Regulation of protein kinase C and role in cancer biology. *Cancer Metastasis Reviews* 13 724–730.
- Blobe, G.C., Stribling, D.S., Fabbro, D., Stabel, S. y Hannun, Y.A. (1996) Protein kinase C  $\beta$ II specifically binds to and is activated by F-actin. *J. Biol. Chem*. 271: 15823-15830.
- Blumberg, P.M. (1988). Protein kinase C as the receptor for the phorbol esters tumor promoters: sixth Rhodes memorial award lecture. *Cancer Res*. 48, 1-8.
- Boerma, M., van der Wees, C. G., Vrieling, H., Svensson, J. P., Wondergem, J., van der Laarse, A., Mullenders, L. H., and van Zeeland, A. A. (2005). Microarray analysis of gene expression profiles of cardiac myocytes and fibroblasts after mechanical stress, ionizing or ultraviolet radiation. *BMC Genom*. 6, 6.
- Bolsover, S., Ibrahim, O., O'Luanagh, N., Williams, H. y Cockroft, S. (2001). Use of fluorescent  $Ca^{2+}$  dyes with green fluorescent protein and its variants: problems and solutions. *Biochem. J*. 356, 345-352.
- Bolsover, S., Gomez Fernandez, J. and Corbalan-Garcia, S. (2003) Role of the  $Ca^{2+}$ /PtdSer binding region of the C2 domain in the translocation of PKC $\alpha$  to the plasma membrane. *J Biol Chem.*, 278: 10282-10290.
- Boni, L.T., Rando, R.R. (1985) The nature of protein kinase C activation by physically defined phospholipid vesicles and diacylglycerols. *J. Biol.Chem*. 260: 10819–10825.

- Bordin, L., Priante, G., Musacchio, E., Giunco, S., Tibaldi, E., Clari, G. y Baggio, B. (2003). Arachidonic acid-induced Il-6 expression is mediated by PKC $\alpha$  activation in osteoblastic cells. *Biochemistry* 42, 4485-4491.
- Bornancin, F. y Parker, P.J. (1996) Phosphorylation of Thr 638 critically controls the dephosphorylation and inactivation of protein kinase Ca. *Curr. Biol.* 6: 1114-1123.
- Bornancin, F. y Parker, P.J. (1997). Phosphorylation of protein kinase Ca on Ser 657 controls the accumulation of active enzyme and contributes to its phosphatase-resistant state. *J. Biol. Chem.* 272: 3544-3549.
- Bos PD, Nguyen DX and Massagué J. (2010) Modeling metastasis in the mouse. *Curr Opin Pharmacol.* 10: 571-7.
- Boskovic, G., Desai, D. y Niles, R.M. (2002). Regulation of retinoic acid receptor  $\alpha$  by protein kinase C in B16 mouse melanoma cells. *J. Biol. Chem.* 277, 26113-26119.
- Bougnoux P, Koscielny S, Chajès V, Descamps P, Couet C and Calais C. (1994) Alpha-linolenic acid content of adipose tissue: a host determinant of the risk of early metastasis in breast cancer patients. *Br J Cancer* 70: 330-4.
- Bougnoux P, Germain E, Chajès V, Hubert B, Lhuillery C, Body G, et al. (1999) Cytotoxic drug efficacy and docosahexaenoic acid level in adipose tissue of patients with locally advanced breast carcinoma. *Br J Cancer* 79: 1765-9.
- Bougnoux P., Maillard V. and Chajes V. (2005). Omega-6/omega-3 polyunsaturated fatty acids ratio and breast cancer. *World Rev. Nutr. Diet* 94, 158-165.
- Bougnoux P, Hajjaji N, Maheo K, Couet C and Chevalier S. (2010) Fatty acids and breast cancer: sensitization to treatments and prevention of metastatic re-growth. *Prog Lipid Res.* 49: 76-86.
- Boyde A., Petran M., y Hadravsky M. (1983) Tandem scanning reflected light microscopy of internal features in whole bone and tooth samples. *J Microsc.*, 132(Pt 1):1-7.
- Brandlin, I., Hubner, S., Eiseler, T., Martinez-Moya, M., Horschinek, A., Hausser, A., Link, S., Rupp, P., Storz, K., Pfizenmaier, y Johannes. F.J.(2002) Protein kinase C (PKC) mediated PKC activation modulates ERK and JNK signal pathways. *J. Biol. Chem.* 277:6490-6496.
- Britton, S., Freeman, T., Vafiadaki, E., Keers, S., Harrison, R., Bushby, K. y Bashir, R. (2000) The third human FER-1-like protein is highly similar to dysferlin, *Genomics* 68 313-321.
- Brodie, C. y Blumberg, P.M. (2003) Regulation of cell apoptosis by protein kinase C $\delta$ . *Apoptosis*, 8: 19-27.
- Brose, N., Hofmann, K., Hata, Y. y Südhof, T.C. (1995). Mammalian homologues of *Caenorhabditis elegans* unc-13 gene define novel family of C2-domain proteins. *J. Biol. Chem.* 270, 25273-25280.
- Brown AJ, Pang E, Roberts DC. (1991) Persistent changes in the fatty acid composition of erythrocyte membranes after moderate intake of n-3 polyunsaturated fatty acids: study design implications. *Am J Clin Nutr*, 54: 668-73.
- Bunney, T.D, Katan M. (2006) Phospholipase C $\epsilon$ : linking second messengers and small GTPases. *Trends Cell Biol.* 16(12):640-8.
- Burns, D.J. y Bell, R.M. (1991) Protein kinase C contains two phorbol ester binding domains, *J. Biol. Chem.* 266: 18330-18338.
- Byon CH, Hardy RW, Ren C, Ponnazhagan S, Welch DR, McDonald JM and Chen Y. (2009) Free fatty acids enhance breast cancer cell migration through plasminogen activator inhibitor-1 and SMAD4. *Lab Invest.*; 89: 1221-8.

- Cacace, A. M. *et al.* (1996) PKC $\epsilon$  functions as an oncogene by enhancing activation of the Raf kinase. *Oncogene* 13, 2517–2526.
- Cai, H., Smola, U., Wixler, V., Eisenmann-Tappe, I., Díaz-Meco, M.T., Moscat, J., Rapp, U. y Cooper, G.M. (1997) Role of diacylglycerol-regulated protein kinase C isoforms in growth factor activation of the Raf-1 protein kinase. *Mol. Cell Biol.* 17, 732–741.
- Caiazza F, Harvey BJ and Thomas W. (2010) Cytosolic phospholipase A2 activation correlates with HER2 overexpression and mediates estrogen-dependent breast cancer cell growth. *Mol Endocrinol.* 24: 953-68.
- Callaway T.R., Edrington T.S., Rychlik J.L., Genovese K.J., Poole T.L., Jung Y.S., Bischoff K.M., Anderson R.C. and Nisbet D.J. (2003) Ionophores: their use as ruminant growth promotants and impact on food safety. *Curr. Issues Intest. Microbiol.* 4: 43–51.
- Calviello G, Serini S, Piccioni E, Pessina G. (2009) Antineoplastic effects of n-3 polyunsaturated fatty acids in combination with drugs and radiotherapy: preventive and therapeutic strategies. *Nutr Cancer*, 61: 287–301.
- Cameron AJ, Procyk KJ, Leitges M and Parker PJ. (2008) PKC alpha protein but not kinase activity is critical for glioma cell proliferation and survival. *Int J Cancer*; 123: 769-79.
- Canagarajah, B., Leskow, F.C. Ho, J.Y.S. Mischak, H. Saidi, L.F. Kazanietz, M.G. Hurley, J.H. (2004) Structural mechanism for lipid activation of the Rac-specific GAP, beta 2-chimaerin, *Cell*, 119: 407–418.
- Cantley, LC, Neel BG. (1999) New insights into tumor suppression: PTEN suppresses tumor formation by restraining the phosphoinositide 3-kinase/AKT pathway. *Proc Natl Acad Sci U S A.* 96(8):4240-5.
- Carducci, M.A.; Musib, L.; Kies, M.S.; Pili, R.; Truong, M.; Brahmer, J.R.; Cole, P.; Sullivan, R.; Riddle, J.; Schmidt, J.; Enas, N.; Sinha, V.; Thornton, D.E.; Herbst, R.S. (2006) Phase I dose escalation and pharmacokinetic study of enzastaurin, an oral protein kinase C-beta inhibitor, in patients with advanced cancer. *J. Clin. Oncol.*, 24: 4092-9.
- Carmona-Saez P, Chagoyen M, Tirado F, Carazo JM, Pascual-Montano A. (2007) GENECODIS: A web-based tool for finding significant concurrent annotations in gene lists. *Genome Biology*; 8 (1): R3.
- Carrasco, S. Mérida, I. (2004) Diacylglycerol-dependent binding recruits PKC theta and RasGRP1 C1 domains to specific subcellular localizations in living T lymphocytes. *Mol. Biol. Cell.*, 15: 2932–2942.
- Carroll K.K. (1991). Dietary fats and cancer. *Am. J. Clin. Nutr.* 53, 1064S-1067S.
- Carter, C.A.; Parham, G.P. and Chambers, T. (1998) Cytoskeletal reorganization induced by retinoic acid treatment of human endometrial adenocarcinoma (RL95-2) cells is correlated with alterations in protein kinase C-alpha. *Pathobiology*, 66: 284-292.
- Casamayor, A, Torrance PD, Kobayashi T, Thorner J, Alessi DR. (1999) Functional counterparts of mammalian protein kinases PDK1 and SGK in budding yeast.. *Curr Biol.* 9(4):186-97.
- Cases-Langhoff, C., Voss, B., Garner, A.M., Appeltauer, U., Takei, K., Kindler, S., Veh, R.W., De C., Gundelfinger, E.D. y Garner, C.C. (1996). A novel 420 kDa protein associated with the presynaptic cytomatrix, *Eur. J. Cell Biol.* 69 214–223.
- Cave, W. T. (1996). Dietary omega-3 polyunsaturated fats and breast cancer. *Nutrition*, 12, S39–S42.
- Cazaubon, S., Bornancin, F. y Parker, P.J. (1994) Thr 497 is a critical site for permissive activation of protein kinase Ca. *Biochem. J.* 30; 443–448.
- Cenni, V., Doppler, H., Sonnenburg, E.D., Maraldi, N., Newton, A.C. y Toker, A. (2002) Regulation of novel protein kinase C $\epsilon$  by phosphorylation. *Biochem. J.* 363: 537–545.

- Chakraborti, S. (2003). Phospholipase A2 isoforms: a perspective. *Cell Signal*. 15, 637-665.
- Chakraborti, S., Michael, J.R. y Chakraborti, T. (2004). Role of an aprotinin-sensitive protease in protein kinase C $\alpha$ -mediated activation of cytosolic phospholipase A<sub>2</sub> by calcium ionophore (A23187) in pulmonary endothelium. *Cell Signal*. 16, 751-762.
- Chapline, C., Mousseau, B., Ramsay, K., Duddy, S., Li, Y., Kiley, S.C. y Jaken, S. (1996). Identification of a major protein kinase C-binding protein and substrate in rat embryo fibroblasts. Decreased expression in transformed cells. *J. Biol. Chem.* 271: 6417-6422.
- Chapline, C., Cottom, J., Tobin, H., Hulmes, J., Crabb, J. y Jaken, S. (1998) A major transformation-sensitive PKC binding protein is also a PKC substrate involved in cytoskeletal remodeling. *J. Biol. Chem.* 273: 19482-19489.
- Chen G., Duran G.E., Steger K.A., Lacayo N.J., Jaffrezou J.P., Dumontet C. and Sikic B.I. (1997) Multidrug-resistant human sarcoma cells with a mutant P-glycoprotein, altered phenotype and resistance to cyclosporins, *J. Biol. Chem.* 272: 5974-5982.
- Chen JS, Greenberg AS and Wang SM. (2002) Oleic acid-induced PKC isozyme translocation in RAW 264.7 macrophages. *J Cell Biochem.*; 86: 784-91.
- Chen, J.S, and Exton J.H. (2004) Regulation of phospholipase D2 activity by protein kinase C  $\alpha$ . *J Biol Chem.*, 279(21):22076-83.
- Chen Y, Lagerholm BC, Yang B, Jacobson K. (2006) Methods to measure the lateral diffusion of membrane lipids and proteins. *Methods*.39: 147-53.
- Chen, Y.B. and LaCasce, A.S. (2008) Enzastaurin. *Exp. Opin. Investig. Drugs*, 17: 939-44.
- Cho, W. y Stahelin, R.V. (2005) Membrane-protein interactions in cell signaling and membrane trafficking. *Annu Rev Biophys Biomol Struct.*, 34: 119-151.
- Choi, S. H., Hyman, T. and Blumberg, P. M. (2006) Differential effect of bryostatin 1 and phorbol 12-myristate 13-acetate on HOP-92 cell proliferation is mediated by down-regulation of protein kinase Cdelta. *Cancer research*. 66, 7261-7269.
- Chou, M.M., Hou, W., Johnson, J., Graham, L.K., Lee, M.H., Chen, C.S., Newton, A.C., Schaffhausen, B.S. y Toker, A. (1998). Regulation of protein kinase C  $\zeta$  by PI 3-kinase and PDK-1. *Curr. Biol.* 6: 1069-1077.
- Coffey, E.T., Herrero, I., Sihra, T.S., Sánchez-Prieto, J. y Nicholls, D.G. (1994). Glutamate exocytosis and MARCKS phosphorylation are enhanced by a metabotropic glutamate receptor coupled to a protein kinase C synergistically activated by diacylglycerol and arachidonic acid. *J. Neurochem.* 63, 1303-1310.
- Coleman E.S, Wooten M.W. (1994) Nerve growth factor-induced differentiation of PC12 cells employs the PMA-insensitive protein kinase C-zeta isoform. *J.Mol.Neurosci.*, 5(1):39-57.
- Colon-Gonzalez, F. and Kazanietz MG. (2006) C1 domains exposed: from diacylglycerol binding to protein-protein interactions. *Biochim Biophys Acta*, 1761: 827-37.
- Conesa Zamora, P., Gómez Fernández, J. y Corbalán García, S. (2000) The C2 domain of PKC $\alpha$  is directly involved in the DAG-dependent binding of the C1 domain to the membrane. *Biochim Biophys Acta.*, 1487: 246-254.
- Conesa Zamora, P., López Andreo, M.J., Gómez-Fernández, J. C. y Corbalán-García, S. (2001) Identification of the PtdSer binding site in the C2 domain that is important for PKC $\alpha$  activation and *in vivo* cell localization. *Biochemistry*, 40: 13898-13905.
- Conrad, S., Genth, H., Hofmann, F., Just, I. and Skutella, T. (2007) Neogenin-RGMA signaling at the growth cone is bone morphogenetic protein-independent and involves RhoA, ROCK, and PKC. *J. Biol. Chem.*, 282: 16423-33.

- Corbalán-García, S., Teruel, J.A., Villalain, J. y Gómez-Fernández, J.C. (1994). Extensive proteolytic digestion of the (Ca<sup>2+</sup> + Mg<sup>2+</sup>)-ATPase from sarcoplasmic reticulum leads to a highly hydrophobic proteinaceous residue with a mainly alpha-helical structure. *Biochemistry* 33, 8247-8254.
- Corbalán-García, S. Rodríguez-Alfaro, Gómez-Fernández, J.C. (1999) Determination of the calcium-binding sites of the C2 domain of protein kinase C  $\alpha$  that are critical for its translocation to the plasma membrane, *Biochem. J.* 337: 387-395.
- Corbalán-García, S., García-García, J., Rodríguez-Alfaro, J. y Gómez-Fernández, J.C. (2003) A new PtdIns(4,5)P<sub>2</sub>-binding site located in the C2 domain of PKC $\alpha$ . *J. Biol. Chem.*, 278: 4972-4980.
- Corbalán-García S, Gómez-Fernández J.C. (2006) Protein kinase C regulatory domains: The art of decoding many different signals in membranes. *Biochim Biophys Acta.*, 1761 (7): 633-54.
- Corbalán-García S, Guerrero-Valero M, Marín-Vicente C and Gómez-Fernández J.C. (2007) The C2 domains of classical/conventional PKCs are specific PtdIns(4,5)P(2)-sensing domains. *Biochem Soc Trans.* 2007 Nov;35(Pt 5):1046-8.
- Corbin, J.A., Evans, J.H., Landgraf, K.E. y Falke, J.J. (2007) Mechanism of specific membrane targeting by C2 domains: Localized pools of target lipids enhance Ca<sup>2+</sup> affinity. *Biochemistry*, 46: 4322-4336.
- Cormack, B.P., Valdivia R.H., Falkow, S. (1996) FACS-optimized mutants of the green fluorescent protein (GFP). *Gene* 173: 33-8.
- Coudronniere, N., Villalba, M., Englund, N., Altman, A. (2000) NF-kappa B activation induced by T cell receptor/CD28 co-stimulation is mediated by protein kinase C-theta. *Proc Natl Acad Sci U S A.* 97(7):3394-9.
- Coussens, L. Parker, P.J. Rhee, L. Yang-Feng, T.L. Chen, E. Waterfield, M.D. Francke, U. Ullrich, A. (1986) Multiple, distinct forms of bovine and human protein kinase C suggest diversity in cellular signaling pathways. *Science* 233: 859-866.
- Cskuai, M., y Mochly Rosen, D. (1999) Pharmacologic modulation of protein kinase C isozymes: the role of RACKs and subcellular localisation. *Pharmacol Res.* 39(4):253-9.
- Csukai, M., Chen, C.H., De Matteis, M.A. y Mochly Rosen, D. (1997) The coatomer protein  $\beta$ -COP, a selective binding protein (RACK) for protein kinase C $\epsilon$ . *J. Biol. Chem.* 272: 29200-29206.
- Cubas R, Zhang S, Li M, Chen C, Yao Q. (2010) Trop2 expression contributes to tumor pathogenesis by activating the ERK MAPK pathway. *Mol Cancer.* 9: 253.
- Cubitt, A.B., Heim, R., Adams, S.R., Boyd, A.E., Gross, L.A. y Tsien, R.Y. (1995) *Trends Biochem. Sci.* 20, 448-455.
- D'Costa, A. M. *et al.* (2006) The proapoptotic tumor suppressor protein kinase C- $\delta$  is lost in human squamous cell carcinomas. *Oncogene* 25, 378-386.
- Dalma-Weiszhausz, Dennise D., Warrington Janet, Tanimoto Eugene Y. and Miyada C. Garret. (2006) The Affymetrix GeneChip® Platform: An Overview. *METHODS IN ENZYMOLOGY*, 410: 3-28.
- Danforth H.D., Ruff M.D., Reid W.M. and Miller R.L. (1977) Anticoccidial activity of salinomycin in battery raised broiler chickens, *Poult. Sci.* 56: 926-932.
- Daniel, L.W., Civoli, F., Rogers, M.A., Smitherman, P.K., Raju, P.A. y Roederer, M. (1995). ET-18-OCH<sub>3</sub> inhibits nuclear factor-kappa  $\beta$  activation by 12-O-tetradecanoylphorbol-13-acetate but not by tumor necrosis factor- $\alpha$  or interleukin 1  $\alpha$ . *Cancer Res.* 55, 4844-4849.

- Das Evcimen N and King GL. (2007) The role of protein kinase C activation and the vascular complications of diabetes. *Pharmacol Res*, 55:498-510.
- Datta, R., H. Kojima, K. Yoshida and D. Kufe. (1997) Caspase-3-mediated cleavage of protein kinase C-theta in induction of apoptosis. *J Biol Chem*, 272, 20317-20.
- Dean M., Fojo T. and Bates S. (2005) Tumor stem cells and drug resistance. *Nat. Rev. Cancer* 5: 275-284.
- Dean M. (2009) ABC transporters, drug resistance, and cancer stem cells. *J. Mammary Gland Biol. Neoplasia* 14: 3-9.
- Dekker, L.V. y Parker, P.J. (1994) Protein kinase C-a question of specificity. *Trends Biochem Sci*. 19(2):73-7.
- Dekker, L.V., McIntyre, P. y Parker, P.J. (1993) Mutagenesis of the regulatory domain of rat protein kinase C $\eta$ . A molecular basis for restricted histone kinase activity. *J. Biol. Chem.* 268: 19498-19504.
- Dekker, L.V. y Parker, P.J. (1997). Regulated binding of the protein kinase C substrate GAP-43 to the V0/C2 region of protein kinase C $\delta$ . *J. Biol. Chem.* 272: 12747-12753.
- Dempsey, E.C., Newton, A.C., MochlyRosen, D., Fields, A.P., Reyland, M.E., Insel, P.A. y Messing, R.O. (2000) Protein kinase C isozymes and the regulation of diverse cell responses. *Am. J. Physiol. Lung Cell Mol. Physiol.* 279: L429:L438.
- Denning, M.F., Wang, Y., Tibudan, S., Alkan, S., Nickoloff, B.J. y Qin, J.Z. (2002) Caspase activation and disruption of mitochondrial membrane potential during UV radiation-induced apoptosis of human keratinocytes requires activation of protein kinase C. *Cell Death Differ.* 9(1):40-52.
- DeVries, T. A., R. L. Kalkofen, A. A. Matassa and M.E. Reyland. (2004) Protein kinase C-delta regulates apoptosis via activation of STAT1. *J Biol Chem*, 279, 45603-45612.
- DeVries-Seimon, T. A., A. M. Ohm, M. J. Humphries and M. E. Reyland. (2007) Induction of apoptosis is driven by nuclear retention of PKCdelta. *J Biol Chem*, 282, 22307-14.
- Ding, L., H. Wang, W. Lang and L. Xiao. (2002) Protein Kinase C-epsilon Promotes Survival of Lung cancer cells by suppressing apoptosis through dysregulation of the mitochondrial caspase pathway. *J Biol Chem*, 277, 35305-35313.
- Díaz-Guerra, M.J.M., Junco, M. y Boscá, L. (1991). Oleic acid promotes changes in the subcellular distribution of protein kinase C in isolated hepatocytes. *J.Biol. Chem.* 266, 23568-23576.
- Díaz-Meco, M.T., Municio, M.M., Frutos, S., Sánchez, P., Lozano, J., y Sanz, L. Moscat, J. (1996) The product of par-4, a gene induced during apoptosis interacts selectively with the atypical isoforms of protein kinase C. *Cell*, 86: 777-786.
- Díaz-Meco, M.T. Municio, M.M. Sánchez, P. Lozano, J. Moscat, J. (1996) Lambda-interacting protein, a novel protein that specifically interacts with the zinc finger domain of the atypical protein kinase C isotype lambda/iota and stimulates its kinase activity in vitro and in vivo. *Mol.Cell. Biol.* 16: 105-114.
- Díaz-Meco, M. Moscat, J. (2001) MEK5, a new target of the atypical protein kinase C isoforms in mitogenic signalling, *Mol. Cell. Biol.* 4: 1218-1227.
- Disatnik, M.H., Buraggi G., Mochly Rosen D. (1994) Localization of protein kinase C isozymes in cardiac myocytes. *Exp Cell Res.* 210(2):287-97.
- Dogne, J.M., Delarge, J., David, J.L. y Masereel, B. (2000). New trends in tromboxane and prostacyclin modulators. *Curr. Med. Chem.* 7, 609-628.

- Duan D., Lewin NE., Sigano DM., Blumberg PM. And Marquez VE. (2004) Conformationally constrained analogues of diacylglycerol. 21. A solid-phase method of synthesis of diacylglycerol lactones as a prelude to a combinatorial approach for the synthesis of protein kinase C isoenzyme-specific ligands. *J Med Chem*, 47: 3248-54.
- Duan D., Sigano DM., Kelley JA., Lai CC., Lewin NE., Kedei N., Peach ML., Lee J., Abeyweera TP., Rotenberg SA., Kim H., Kim YH., El Lazzouli S., Chung JU., Young HA., Young MR., Baker A., Colburn NH., Haimovitz-Friedman A., Truman JP., Parrish DA., Deschamps JR., Perry NA., Surawski RJ., Blumberg PM. And Marquez VE. (2008) Conformationally constrained analogues of diacylglycerol. 29. Cells sort diacylglycerol-lactone chemical zip codes to produce diverse and selective biological activities. *J Med Chem*, 51: 5198-220.
- Duerr S, Wendler O, Aigner T, Karosi S and Schick B (2008) Metalloproteinases in juvenile angiofibroma—a collagen rich tumor. *Hum Pathol*. 39: 259-68.
- Dumont N, and Arteaga CL. (2003) A kinase-inactive type II TGFbeta receptor impairs BMP signaling in human breast cancer cells. *Biochem Biophys Res Commun*. 301(1):108-12.
- Dutil, E.M. and Newton, A.C. (2000). Dual role of pseudosubstrate in the coordinated regulation of protein kinase C by phosphorylation and diacylglycerol. *J. Biol. Chem*. 275: 10697-10701.
- Dutil, E.M., Toker, A. y Newton, A.C. (1998). Regulation of conventional protein kinase C isozymes by phosphoinositide-dependent kinase 1 (PDK-1). *Curr. Biol*. 8: 1366–1375.
- Eckford P.D. and Sharom F.J. (2009) ABC efflux pump-based resistance to chemotherapy drugs. *Chem. Rev*. 109: 2989–3011.
- Edwards, A.S. y Newton, A.C. (1997) Regulation of protein kinase C  $\beta$ II by its C2 domain, *Biochemistry*, 36:15615–15623.
- Edwards, A.S. y Newton, A.C. (1997b). Phosphorylation at conserved carboxyl-terminal hydrophobic motif regulates the catalytic and regulatory domains of protein kinase C. *J. Biol. Chem*. 272: 18382-18390.
- Edwards, A.S., Faux, M.C., Scott, J.D. y Newton, A.C. (1999) Carboxyl-terminal phosphorylation regulates the function and subcellular localization of protein kinase C- $\beta$ II. *J. Biol. Chem*. 274: 6461–6468.
- Efron B., Storey J.D. and Tibshirani R. (2001) Empirical bayes analysis of a microarray experiment. *Journal of the American Statistical Association*, 96: 1151–1160.
- England, K., Watson, J., Beale, G., Warner, M., Cross, J. y Rumsby, M. (2001) Signalling pathways regulating the dephosphorylation of Ser729 in the hydrophobic domain of protein kinase C $\epsilon$  upon cell passage. *J. Biol. Chem*. 276: 10437–10442.
- Escrich E., Moral R., Grau L., Costa I. and Solanas M. (2007). Molecular mechanisms of the effects of olive oil and other dietary lipids on cancer. *Mol. Nutr. Food Res*. 51, 1279-1292.
- Essen, L.O., Perisic, O., Cheung, R., Katan, M., y Williams, R.L. (1996) Crystal structure of a mammalian phosphoinositide-specific phospholipase C  $\delta$ . *Nature*. 380(6575):595-602.
- Evans, J. H., Murray, D., Leslie, C. C. y Falke, J. J. (2006) Specific translocation of PKC $\alpha$  to the plasma membrane requires both Ca<sup>2+</sup> and PtdIns(4,5)P<sub>2</sub> recognition by its C2 domain. *Mol Biol Cell*, 17(1): 56-66.
- Fabbro D, Ruetz S, Bodis S, Pruschy M, Csermak K and Man A. (2000) PKC412—a protein kinase inhibitor with a broad therapeutic potential. *Anticancer Drug Des*. 15: 17–28.
- Facchinetti V, Ouyang W, Wei H, Soto N, Lazorchak A, Gould C, Lowry C, Newton AC, Mao Y, Miao RQ, Sessa WC, Qin J, Zhang P, Su B and Jacinto E. (2008) The mammalian target of rapamycin complex 2 controls folding and stability of Akt and protein kinase C. *EMBO J* 27: 1932–1943.

- Ferlay J, Bray P, Pisani P and Parkin DM. (2001) Cancer Incidence, Mortality and Prevalence Worldwide, version 1 ed. IARC CancerBase No 5. Lyon, IARC Press, 2001.
- Ferrante, A., Huang, Z.H., Nandoskar, M., Hii, C.S., Robinson, B.S., Rathjen, D.A., Poulos, A., Morris, C.P. y Ferrante, A. (1997). Altered responses of human macrophages, to lipopolysaccharide by hydroperoxy eicosatetraenoic acid, hydroxy eicosatetraenoic acid and arachidonic acid: inhibition of TNF production. *J. Clin. Invest.* 99, 1445-1452.
- Fields A. P. and R. P. Regala. (2007) Protein kinase C $\alpha$ : Human oncogene, prognostic marker and therapeutic target: *Pharmacol Res*, 55, 487-497.
- Fite A, Goua M, Wahle KW, Schofield AC, Hutcheon AW and Heys SD. (2007) Potentiation of the anti-tumour effect of docetaxel by conjugated linoleic acids (CLAs) in breast cancer cells in vitro. *Prostaglandins Leukot Essent Fatty Acids.* 77:87-96.
- Flint, A.J., Paladini, R.D. y Koshland, D.E. (1990). Autophosphorylation of protein kinase C at three separated regions of its primary sequence. *Science* 249, 408-411.
- Förster, T. (1966) *Modern Quantum Chemistry*, Ed. O. Sinanglu, Sección II-B, 93-137, New York Academic Press.
- Fowler, L., Dong, L.Q., Van der Water, B., Bowes, R., Stevens, J.L. y Jaken, S. (1998a). Transformation-sensitive changes in expression, localization, and phosphorylation of adducins in renal proximal tubule epithelial cells. *Cell Growth Diff.* 9:177-184.
- Fowler, L., Everitt, J.L., Stevens, J.L. y Jaken, S. (1998b). Redistribution and enhanced protein kinase C-mediated phosphorylation of  $\alpha$ - and  $\gamma$ -adducin during renal tumor progression. *Cell Growth Diff.* 9: 405-413.
- Frankel LB, Lykkesfeldt AE, Hansen JB, Stenvang J. (2007) Protein Kinase C  $\alpha$  is a marker for antiestrogen resistance and is involved in the growth of tamoxifen resistant human breast cancer cells. *Breast Cancer Res Treat.*;104: 165-79.
- Frasor J, Weaver A, Pradhan M, Dai Y, Miller LD, Lin CY, Stanculescu A. (2009) Positive cross-talk between estrogen receptor and NF- $\kappa$ B in breast cancer. *Cancer Res* 69 (23): 8918-25.
- Fuchs D., Berges C., Opelz G., Daniel V. and Naujokat C. (2008) Increased expression and altered subunit composition of proteasomes induced by continuous proteasome inhibition establish apoptosis resistance and hyperproliferation of Burkitt lymphoma cells. *J. Cell. Biochem.* 103: 270-283.
- Fuchs D., Heinold A., Opelz G., Daniel V. and Naujokat C. (2009) Salinomycin induces apoptosis and overcomes apoptosis resistance in human cancer cells. *Biochem. Biophys. Res. Commun.* 390: 743-749.
- Fuchs D, Daniel V, Sadeghi M, Opelz G and Naujokat C. (2010) Salinomycin overcomes ABC transporter-mediated multidrug and apoptosis resistance in human leukemia stem cell-like KG-1a cells. *Biochem Biophys Res Commun.* 394:1098-104.
- Fujii T, Yokoyama G, Takahashi H, Namoto R, Nakagawa S, Toh U, Kage M, Shirouzu K and Kuwano M. (2008) Preclinical studies of molecular-targeting diagnostic and therapeutic strategies against breast cancer. *Breast Cancer.* 15: 73-8.
- Galderisi U, Cascino A and Giordano A. (1999) Antisense oligonucleotides as therapeutic agents. *J Cell Physiol*; 181:251-7.
- Gao, T., Toker, A. y Newton, A.C. (2001) The carboxyl terminus of protein kinase C provides a switch to regulate its interaction with the phosphoinositide-dependent kinase, PDK-1. *J. Biol. Chem.* 276: 19588-19596.
- Gao, T. y Newton, A.C. (2002). The turn motif is a phosphorylation switch that regulates the binding of Hsp70 to protein kinase C. *J. Biol. Chem.* 277, 31585-31592.

- García Fernández, L.F., Losada, A., Alcaide, V., Alvarez, A.M., Cuadrado, A., González, L., Nakayama, K., Nakayama, K.I., Fernández Sousa, J.M., Muñoz, A. y Sánchez Puelles, J.M. (2002) Aplidin induces the mitochondrial apoptotic pathway via oxidative stress-mediated JNK and p38 activation and protein kinase C  $\delta$ . *Oncogene*, 21(49):7533-44.
- García-García, J., Corbalán García, S. y Gómez Fernández, J. (1999) Effect of calcium and phosphatidic acid binding on the C2 domain of PKC alpha as studied by Fourier transform infrared spectroscopy. *Biochemistry*, 38: 9667-9675.
- García-García, J., Gómez Fernández, J. y Corbalán García, S. (2001) Structural characterization of the C2 domain of novel protein kinase C  $\epsilon$ . *Eur.J. Biochem.* 268: 1107-1117.
- García-Rocha, M., Avil, J. y Lozano, J. (1997) The zeta isozyme of protein kinase C binds to tubulin through the pseudosubstrate domain. *Exp Cell Res.* 230(1):1-8.
- Geiger T, Muller M, Dean NM and Fabbro D. (1998) Antitumor activity of a PKC-alpha antisense oligonucleotide in combination with standard chemotherapeutic agents against various human tumors transplanted into nude mice. *Anticancer Drug Des.* 13: 35-45.
- Germain E, Chajes V, Cognault S, Lhuillery C and Bougnoux P. (1998) Enhancement of doxorubicin cytotoxicity by polyunsaturated fatty acids in the human breast tumor cell line MDA-MB-231: relationship to lipid peroxidation. *Int J Cancer.* 75: 578-83.
- Germain E, Bonnet P, Aubourg L, Grangepon MC, Chajes V and Bougnoux P. (2003) Anthracycline-induced cardiac toxicity is not increased by dietary omega-3 fatty acids. *Pharmacol Res.* 47:111-7.
- Ghosh, S. y Baltimore, D. (1990) Activation in vitro of NF-kappa  $\beta$  by phosphorylation of its inhibitor I kappa  $\beta$ . *Nature* 344: 678-682.
- Gil, C., Molina, E., Plana, M., Carabaz, A., Cabre, F., Mauleon, D., Carganico, G. e Itarte, E. (1996). Differential effect of alkyl chain-modified ether lipids on protein kinase C autophosphorylation and histone phosphorylation. *Biochem. Pharmacol.* 52, 1843-1847.
- Gill, C. I., Boyd, A., McDermott, E., McCann, M., et al. (2005) Potential anti-cancer effects of virgin olive oil phenols on colorectal carcinogenesis models in vitro. *Int. J. Cancer*, 117, 1-7.
- Gill PK, Gescher A and Gant TW. (2001) Regulation of MDR1 promoter activity in human breast carcinoma cells by protein kinase C isozymes alpha and theta, *Eur. J. Biochem.* 268 4151-4157.
- Giorgione, J.R. Lin, J.H., McCammon, J.A. y Newton, A.C. (2006) Increased membrane affinity of the C1 domain of protein kinase C $\delta$  compensates for the lack of involvement of its C2 domain in membranerecruitment, *J. Biol. Chem.* 281:1660-1669.
- Gjörloff Wingren, A., Saxena, M., Han, S., Wang, X., Alonso, A., Renedo, M., Oh, P., Williams, S., Schnitzer, J., Mustelin, T. (2000) Subcellular localization of intracellular protein tyrosine phosphatases in T cells. *Eur J Immunol.* 30(8):2412-21.
- Goldberg, E.M. and Zidovetzki, R. (1997). Effect of dipalmitoylglycerol and fatty acids on membrane structure and protein kinase C activity. *Biophys J*, 73: 2603-14.
- Goldberg, E.M. and Zidovetzki, R. (1998). Synergistic effects of dyacylglycerol and fatty acids on membrane structure and protein kinase C activity. *Biochemistry* 37, 5623-5632.
- Golub, T., Wacha, S. y Caroni, P. (2004) Spatial and temporal control of signaling through lipid rafts. *Curr Opin Neurobiol.*, 14: 542-550.
- Gómez Fernández, J.C y Corbalán García S. (2007) Diacylglycerols, multivalent membrane modulators. *Chem Phys Lipids.* 148(1):1-25.
- Gonzalez, C. A. (2006) The European Prospective Investigation into Cancer and Nutrition (EPIC). *Public Health Nutr.*, 9, 124 -126.

- Gonzalez-Guerrico AM. and Kazanietz MG. (2005) Phorbol ester-induce apoptosis in prostate cancer cells via autocrine activation of the extrinsic apoptotic cascade: a key role for protein kinase C delta. *J Biol Chem*, 280: 38982-91.
- Goodnight, J.A., H. Mischak, W. Kolch, y J.F. Mushinski. (1995) Immunocytochemical localization of eight protein kinase C isozymes overexpressed in NIH 3T3 fibroblasts. *J. Biol. Chem.* 270:9991-10001.
- Gordge, P.C.; Hulme, M.J.; Clegg, R.A. and Miller, W.R. (1996) Elevation of protein kinase A and protein kinase C activities in malignant as compared with normal human breast tissue. *Eur. J. Cancer*, 32A: 2120-2126.
- Gould CM, Kannan N, Taylor SS and Newton AC. (2008) The chaperones Hsp90 and Cdc37 mediate the maturation and stabilization of protein kinase C through a conserved PXXP motif in the C-terminal tail. *J Biol Chem* 284: 4921-4935.
- Graff JR, McNulty AM, Hanna KR, Konicek BW, Lynch RL, Bailey SN, et al. (2005) The protein kinase C beta-selective inhibitor, Enzastaurin (LY317615.HCl), suppresses signaling through the AKT pathway, induces apoptosis, and suppresses growth of human colon cancer and glioblastoma xenografts. *Cancer Res*; 65:7462-9.
- Griner, E.M, Kazanietz M.G. (2007) Protein kinase C and other diacylglycerol effectors in cancer. *Nat Rev Cancer*. 7(4):281-94.
- Grodsky, N., Li, Y., Bouzida, D., Love, R., Jensen, J., Nodes, B., Nonomiya, J. y Grant, S. (2006). Structure of the catalytic domain of human protein kinase C-βII complexed with a bisindolylmaleimide inhibitor. *Biochemistry* 45: 13970-13981.
- Grossoni VC, Todaro LB, Kazanietz MG, de Kier Joffé ED and Urtreger AJ. (2009) Opposite effects of protein kinase C beta1 (PKCbeta1) and PKCepsilon in the metastatic potential of a breast cancer murine model. *Breast Cancer Res Treat.*; 118: 469-80.
- Guertin DA, Stevens DM, Thoreen CC, Burds AA, Kalaany NY, Moffat J, Brown M, Fitzgerald KJ and Sabatini DM. (2006) Ablation in mice of the mTORC components raptor, rictor, or mLST8 reveals that mTORC2 is required for signaling to Akt-FOXO and PKCalpha, but not S6K1. *Dev Cell* 11: 859-871.
- Gupta P.B., Onder T.T., Jiang G., Tao K., Kuperwasser C., Weinberg R.A. and Lander E.S. (2009) Identification of selective inhibitors of cancer stem cells by highthroughput screening, *Cell* 138: 645-659.
- Gschwendt M. (1999) Protein kinase C delta. *Eur J Biochem.* 259(3):555-64.
- Guerrero Valero, M., Marín Vicente, C., Gómez Fernández, J. and Corbalán García, S. (2007) The C2 domains of classical PKC are specific PtdIns(4,5)P<sub>2</sub>-sensing domains with different affinities for membrane binding. *J. Mol. Biol.*, 371: 608-621.
- Guerrero Valero, M., Ferrer Orta, C., Querol Audí, J., Marín Vicente, C., Fita, I., Gómez Fernández, J.C., Verdaguer, N. and Corbalán García, S. (2009) Structural and mechanistic insights into the association of PKCalpha-C2 domain to PtdIns(4,5)P<sub>2</sub>. *Proc Natl Acad Sci USA*, 106 (16): 6603-7.
- Gupta, K.P.; Ward, N.E.; Gravitt, K.R.; Bergman, P.J. and O'Brian, C.A. (1996) Partial reversal of multidrug resistance in human breast cancer cells by an N-myristoylated protein kinase C-alpha pseudosubstrate peptide. *J. Biol. Chem.*, 271: 2102-2111.
- Gysin, S., e Imber, R. (1997) Phorbol-ester-activated protein kinase C-alpha lacking phosphorylation at Ser657 is down-regulated by a mechanism involving dephosphorylation. *Eur J Biochem.* 249(1):156-60.
- Han, E. K. H., Cacace, A. M., Sgambato, A. and Weinstein, I. B. (1995) Altered expression of cyclins and c-Fos in R6 cells that overproduce Pkc-ε. *Carcinogenesis* 16, 2423-2428.
- Hanks, S.K., Quinn, A.M. y Hunter, T. (1988). The protein kinase family: conserved features and deduced phylogeny of the catalytic domains. *Science* 241, 42-52.

- Hannun, Y.A. Loomis, C.R. y Bell, R.M. (1985) Activation of protein kinase C by triton X-100 mixed micelles containing diacylglycerol and phosphatidylserine. *J. Biol. Chem.* 260: 10039–10043.
- Hannun, Y.A. y Bell, R.M. (1986) Phorbol ester binding and activation of protein kinase C on triton X-100 mixed micelles containing phosphatidylserine. *J. Biol. Chem.* 261: 9341–9347.
- Hansra, G., García Paramio, P., Prevostel, C., Whelan, R.D., Bornancin, F., Parker, P.J. (1999) Multisite dephosphorylation and desensitization of conventional protein kinase C isotopes. *Biochem J.* 342 ( Pt 2):337-44.
- Hardy RW, Wickramasinghe NS, Ke SC and Wells A. (1997) Fatty acids and breast cancer cell proliferation. *Adv Exp Med Biol*; 422: 57–69.
- Hardy S, Langelier Y and Prentki M. (2000) Oleate activates phosphatidylinositol 3-kinase and promotes proliferation and reduces apoptosis of MDA-MB-231 breast cancer cells, whereas palmitate has opposite effects. *Cancer Res.*; 60: 6353-8.
- Hardy S, St-Onge GG, Joly E, Langelier Y and Prentki M. (2005) Oleate promotes the proliferation of breast cancer cells via the G protein-coupled receptor GPR40. *J Biol Chem.*; 280: 13285-91.
- Harrington C. A., Rosenow C., and Retief J.. (2000) Monitoring gene expression using DNA microarrays. *Curr Opin Microbiol*, 3: 285–91.
- Hartwig, J.H., Thelen, M., Rosen, A., Janmey, P.A., Nairn, A.C. y Aderem, A. (1992). MARCKS is an actin filament crosslinking protein regulated by protein kinase C and calcium-calmodulin. *Nature*, 356: 618-622.
- Hauge C, Antal TL, Hirschberg D, Doehn U, Thorup K, Idrissova L, Hansen K, Jensen ON, Jorgensen TJ, Biondi RM and Frodin M. (2007) Mechanism for activation of the growth factor-activated AGC kinases by turn motif phosphorylation. *EMBO J* 26: 2251–2261.
- Heit, I. *et al.* (2001) Involvement of protein kinase C  $\delta$  in contact-dependent inhibition of growth in human and murine fibroblasts. *Oncogene* 20, 5143–5154.
- Hirano, Y. Yoshinaga, S. Ogura, K. Yokochi, M. Noda, Y. Sumimoto, H. y Inagaki, F. (2004) Solution structure of atypical protein kinase C PB1 domain and its mode of interaction with ZIP/P62 and MEK5, *J. Biol. Chem.* 279: 31883–31890.
- Hizli, A. A., A. R. Black, M. A. Pysz and J. D. Black. (2006) Protein kinase C- $\alpha$  signaling inhibits cyclin D1 translation in intestinal epithelial cells. *J Biol Chem*, 281, 14596-14603.
- Hocevar, B., Burns, D. y Fields, A. (1993) Identification of protein kinase C (PKC) phosphorylation sites on human lamin B. Potential role of PKC in nuclear lamina structural dynamics. *J. Biol. Chem.*, 268: 7545-7552.
- Hofmann, J. (1997). The potential for isozyme-selective modulation of protein kinase C. *FASEB J.* 11, 649-669.
- Holmes MD, Hunter DJ, Colditz GA et al. (1999) Association of dietary intake of fat and fatty acids with risk of breast cancer. *J Am Med Assoc*; 281: 914–920.
- Hommel, U. Zurini, M. Luyten, M. Solution structure of a cysteine richdomain of rat protein kinase C, *Nat. Struct. Biol.* 1 (1994) 383–387.
- Hou, Y., Lascola, J., Dulin, N.O., ye, R.D. y Browning, D.D. (2003). Activation of cGMP-dependent protein kinase by protein kinase C. *J. Biol. Chem.* 278, 16706-16712.
- House, C. y Kemp, B.E. (1987) Protein kinase C contains a pseudosubstrate prototope in its regulatory domain, *Science*, 238: 1726–1728.

- House, C. y Kemp, B.E. (1990). Protein kinase C pseudosubstrate prototipe: structure-function relationships. *Cell Signalling* 2, 187-190.
- Hovius, R., Valloton, P., Wohland, T. y Vogel, H. (2000) *Trends Pharmac. Sci.* 27, 266-273.
- Hsiao, W. L. W., Housey, G. M., Johnson, M. D. and Weinstein, I. B. (1989). Cells that overproduce protein kinase-C are more susceptible to transformation by an activated *H-Ras* oncogene. *Mol. Cell. Biol.* 9, 2641-2647.
- Huang, J., Wei, W., Zhang, J., Liu, G., Bignell, G. R., Stratton, M. R., Futreal, P. A., Wooster, R., Jones, K. W., and Shaper, M. H. (2004). Whole genome DNA copy number changes identified by high density oligonucleotide arrays. *Hum. Genom.* 1, 287-299.
- Huang, K.P. Huang, F.L. Nakabayashi, H. Yoshida, Y. (1989) Expression and function of protein kinase C isozymes. *Acta Endocrinol. (Copenh)* 121: 307-316.
- Huang, X.P., Pi, Y., Lokuta, A.J., Greaser, M.L. y Walker, J.W. (1997). Arachidonic acid stimulates protein kinase C- $\epsilon$  redistribution in heart cells. *J. Cell Sci.* 110, 1625-1634.
- Huang ZH, Hii CS, Rathjen DA, Poulos A, Murray AW, Ferrante A. (1997) N-6 and n-3 polyunsaturated fatty acids stimulate translocation of protein kinase Calpha, -betaI, -betaII and -epsilon and enhance agonist-induced NADPH oxidase in macrophages. *Biochem J.* 15; 325 ( Pt 2):553-7.
- Hubbard, S.R., Bishop, W.R., Kirschmeier, P., George, S.J., Cramer, S.P. y Hendrickson, W.A. (1991). Identification and characterization of zinc binding sites in protein kinase C. *Science* 254, 1776-1779.
- Huber, R. Schneider, M. Mayr, I. Romisch, J. Paques, E.P. (1990) The calcium binding sites in human annexin V by crystal structure analysis at 2.0 Å resolution. Implications for membrane binding and calcium channel activity, *FEBS Lett.* 275: 15-21.
- Hulbert, A. J., Turner, N., Storlien, L. H., Else, P. L. (2005) Dietary fats and membrane function: implications for metabolism and disease. *Biol. Rev. Camb. Philos. Soc.*, 80, 155-169.
- Humphries, M. J., K. H. Limesand, J. C. Schneider, K. I. Nakayama, S. M. Anderson and M. E. Reyland. (2006) Suppression of apoptosis in the protein kinase C-delta null mouse *in vivo*. *J Biol Chem*, 281, 9728-9737.
- Hurley, J.H., Newton, A.C., Parker, P.J., Blumberg, P.M. and Nishizuka, Y. (1997) Taxonomy and function of C1 protein kinase C homology domains. *Protein Sci.* 6: 477-480.
- Hurley, J.H. and Meyer, T. (2001) Subcellular targeting by membrane lipids. *Curr.Opin. Cell Biol.* 13: 146-152.
- Ichikawa, S. Hatanaka, H. Takeuchi, Y. Ohno, S. and Inagaki, F. (1995) Solution structure of cysteine-rich domain of protein kinase C alpha, *J. Biochem. (Tokyo)* 117: 566-574.
- Ikenoue T, Inoki K, Yang Q, Zhou X and Guan KL. (2008) Essential function of TORC2 in PKC and Akt turn motif phosphorylation, maturation and signalling. *EMBO J* 27: 1919-1931.
- Inoue, M. Kishimoto, A. Takai, W. Nishizuka, Y. (1977) Studies on a cyclicnucleotide-independent protein kinase and its proenzyme in mammalian tissues II. *J. Biol. Chem.* 252: 7610-7916.
- Inoue, T., Heo, W. D., Grimley, J. S., Wandless, T. J. and Meyer, T. (2005) An inducible translocation strategy to rapidly activate and inhibit small GTPase signaling pathways. *Nat Methods.*, 2: 415-418.
- Ip, C. (1997) Review of the effects of trans fatty acids, oleic acid, n-3 polyunsaturated fatty acid, and conjugated linoleic acid on mammary carcinogenesis in animals. *Am. J. Clin. Nutr.*, 66: 1523S-1529S.

- Irie, K. Yanai, Y. Oie, K. Ishizawa, J. Nakagawa, Y. Ohigashi, H. Wender, P.A. Kikkawa, U. (1997) Comparison of chemical characteristics of the first and the second cysteine-rich domains of protein kinase C gamma. *Bioorg.Med. Chem.* 5, 1725-1737.
- Irie, K., Oie, K., Nakahara, A., Yanai, Y., Ohigashi, H., Wender, P.A., Fukuda, H., Konishi, H. y Kikkawa, U. (1998). Molecular basis of protein kinase C isozyme-selective binding: the synthesis, folding, and forbol ester binding of cysteine-rich domains of all protein kinase C isozymes. *J. Am. Chem. Soc.* 120, 9159-9167.
- Irie, K. Nakahara, A. Nakagawa, Y. Ohigashi, H. Shindo, M. Fukuda, H. Konishi, H. Kikkawa, U. Kashiwagi, K. Saito, N. (2002) Establishment of a binding assay for protein kinase C isozymes using synthetic C1 peptides and development of new medicinal leads with protein kinase C isozyme and C1 domain selectivity. *Pharmacol. Ther.* 93: 271-281.
- Irizarry, R. A., Bolstad, B. M., Collin, F., Cope, L. M., Hobbs, B., and Speed, T. P. (2003). Summaries of Affymetrix GeneChip probe level data. *Nucleic Acids Res.* 31, e15.
- Isbilen B, Fraser SP and Djamgoz MB. (2006) Docosahexaenoic acid (omega-3) blocks voltage-gated sodium channel activity and migration of MDA-MB-231 human breast cancer cells. *Int J Biochem Cell Biol.*; 38: 2173-82.
- Izumi, Y., Hirose, T., Tamai, Y., Hirai, S., Nagashima, Y., Fujimoto, T., Tabuse, Y., Kempfues, K.J. and Ohno, S. (1998). An atypical PKC directly associates and colocalizes at the epithelial tight junction with ASIP, a mammalian homologue of *Caenorhabditis elegans* polarity protein PAR-3. *J. Cell. Biol.* 143, 95-106.
- Jackson, D. N. and D. A. Foster. (2004) The enigmatic protein kinase C-delta: complex roles in cell proliferation and survival. *FASEB J*, 18, 627-636.
- Jackson, D., Y. Zheng, D. Lyo, Y. Shen, K. Nakayama, K. Nakayama, M. Humphries, M. Reyland and F. DA. (2005) Suppression of cell migration by protein kinase C-delta. *Oncogene*, 24, 3067-3072.
- Jacobson, K., Mouritsen, O. and Anderson, R. (2007) Lipid rafts: At a crossroad between cell biology and physics. *Nature Cell Biol.*, 9: 7-14.
- Jaken S. (1996) Protein kinase C isozymes and substrates. *Curr Opin Cell Biol.* 8(2):168-73.
- Jaken, S. and Parker, P.J. (2000) Protein kinase C binding partners. *BioEssays* 22: 245-254.
- Jamieson, L., L. Carpenter, T. J. Biden & A. P. Fields (1999) Protein Kinase C-iota activity is necessary for Bcr-Abl-mediated resistance to drug-induced apoptosis. *J Biol Chem*, 274, 3927-3930.
- Jimenez, J.L. Smith, G.R. Contreras Moreira, B. Sgouros, J.G. Meunier, F.A. Bates, P.A. Schiavo, G. (2003) Functional recycling of C2 domains through out evolution: a comparative study of synaptotagmin, protein kinase C and phospholipase C by sequence, structural and modeling approaches, *J. Mol. Biol.* 333: 621-639.
- Johannes, F.J., Prestle, J., Eis, S., Oberhagermann, P. y Pfizenmaier, K. (1994). PKC $\mu$  is a novel, atypical member of the protein kinase C family. *J. Biol. Chem.* 269, 6140-6148.
- Johnson, L., Gray, M., Chen, C.H. y Mochly-Rosen, D. (1996) A protein kinase C translocation inhibitor as an isozyme-selective antagonist of cardiac function. *J. Biol. Chem.* 271: 24962-24966.
- Johnson, J.E. Giorgione, J. y Newton, A.C. (2000) The C1 and C2 domains of protein kinase C are independent membrane targeting modules, with specificity for phosphatidylserine conferred by the C1 domain. *Biochemistry* 39: 11360-11369.
- Johnson, L.N. y Lewis, R.J. (2001) Structural basis for control by phosphorylation. *Chem. Rev.* 101: 2209-2242.

- Joseloff, E., Cataisson, C., Aamodt, H., Ocheni, H., Blumberg, P., Kraker, A.J. y Yuspa, S.H. (2002). Src family kinases phosphorylate protein kinase C- $\delta$  on tyrosine residues and modify the neoplastic phenotype of skin keratinocytes. *J. Biol. Chem.* 277, 12318-12323.
- Joyce JA and Pollard JW. (2009) Microenvironmental regulation of metastasis. *Nat Rev Cancer.* 9:239-52.
- Judé S, Roger S, Martel E, Besson P, Richard S, Bougnoux P, Champeroux P, Le Guennec JY. (2006) Dietary long-chain omega-3 fatty acids of marine origin: a comparison of their protective effects on coronary heart disease and breast cancers. *Prog Biophys Mol Biol.* 90: 299-325.
- Kang, J. H., Benzaria, S., Sigano, D. M., Lewin, N. E., Pu, Y., Peach, M. L., Blumberg, P. M. and Marquez, V. E. (2006) Conformationally constrained analogues of diacylglycerol. 26. Exploring the chemical space surrounding the C1 domain of protein kinase C with DAG-lactones containing aryl groups at the sn-1 and sn-2 positions. *Journal of medicinal chemistry.* 49: 3185-3203
- Kanoh, H., Yamada, K. y Sakane, F. (2002). Diacylglycerol kinases: emerging downstream regulators in cell signaling systems. *J. Biochem.* 131, 629-633.
- Kashiwagi, K., Shirai, Y., Kuriyama, M., Sakai, N. y Saito, N. (2002). Importance of C1B domain for lipid messenger-induced targeting of protein kinase C. *J. Biol. Chem.* 277, 18037-18045.
- Katan, M. y Allen, V.L. (1999). Modular PH and C2 domains in membrane attachment and other functions. *FEBS Lett.* 452, 36-40.
- Katan M. (2005) New insights into the families of PLC enzymes: looking back and going forward. *Biochem J.* 391(Pt 3): 7-9.
- Kato T, Hancock RL, Mohammadpour H, McGregor B, Manalo P, Khaiboullina S, et al. (2002) Influence of omega-3 fatty acids on the growth of human colon carcinoma in nude mice. *Cancer Lett.* 187:169-77.
- Kawakami Y, Kitaura J, Hartman SE, Lowell CA, Siraganian RP, Kawakami T. (2000) Regulation of protein kinase C beta I by two protein-tyrosine kinases, Btk and Syk. *Proc Natl Acad Sci U S A.* 97(13): 7423-8.
- Kazanietz MG. (2002) Novel "nonkinase" phorbol ester receptors: the C1 domain connection. *Mol Pharmacol.* 61(4):759-67.
- Kazanietz MG. (2005) Targeting protein kinase C and non-kinase phorbol ester receptor: emerging concepts and therapeutic implications. *Biochim Biophys Acta,* 1754: 296-304.
- Kazanietz, M.G. Krausz, K.W. Blumberg, P.M. (1992) Differential irreversible insertion of protein kinase C into phospholipid vesicles by phorbol esters and related activators. *J. Biol. Chem.* 267: 20878-20886.
- Kazanietz, M. G., Areces, L. B., Bahador, A., Mischak, H., Goodnight, J., Mushinski, J. F. and Blumberg, P. M. (1993) Characterization of ligand and substrate specificity for the calcium-dependent and calcium-independent protein kinase C isozymes. *Mol Pharmacol,* 44(2), August, 298-307.
- Kazanietz, M.G., Lewin, N.E., Gao, F., Pettit, G.R. y Blumberg, P.M. (1994) Binding of [26-3H]bryostatin 1 and analogs to calcium-dependent and calcium-independent protein kinase C isozymes. *Mol. Pharmacol.* 46: 374-379.
- Kelley GG, Reks SE, Ondrako JM, Smrcka AV. (2001) Phospholipase C(epsilon): a novel Ras effector. *EMBO J.* 20(4): 743-54.
- Kemp, B.E. and Pearson, R.B. (1990) Protein kinase recognition sequence motifs. *Trends Biochem. Sci.* 15: 342-346.

- Keranen, L.M., Dutil, E.M. and Newton, A.C. (1995) Protein kinase C is regulated in vivo by three functionally distinct phosphorylations. *Curr. Biol.* 5: 1394-1403.
- Keranen, L.M. and Newton A.C. (1997). Ca<sup>2+</sup> differentially regulates conventional protein kinase C's membrane interaction and activation. *J. Biol. Chem.* 272, 25959-25967.
- Khan, W.A., El Touny, S. and Hannun, Y.A. (1991). Arachidonic and *cis*-unsaturated fatty acids induce selective platelet substrate phosphorylation through activation of cytosolic protein kinase C. *FEBS Lett.* 292, 98-102.
- Khan, W. A., Blobe, G.C. and Hannun, Y.A. (1995). Arachidonic acid and free fatty acids stimulates protein kinase C-epsilon redistribution in heart cells. *J. Cell. Sci.* 7, 171-184.
- Kohlmeier L and Kohlmeier M. (1995) Adipose tissue as a medium for epidemiologic exposure assessment. *Environ-Health-Perspect.* 103(Suppl.):99-106.
- Kikkawa, U., Takai, Y., Tanaka, Y., Miyake, R. & Nishizuka, Y. (1983). Protein kinase-C as a possible receptor protein of tumor-promoting phorbol esters. *J. Biol.Chem.* 258, 1442-1445.
- Kiley, S. y Parker, P.J. (1995). Differential localization of protein kinase C isozymes in U937 cells: evidence for distinct isozyme functions during monocyte differentiation. *J. Cell Sci.* 108, 1003-1016.
- Kilpatrick LE, Lee JY, Haines KM, Campbell DE, Sullivan KE, Korchak HM. (2002) A role for PKC-delta and PI 3-kinase in TNF-alpha-mediated antiapoptotic signaling in the human neutrophil. *Am J Physiol Cell Physiol* 283(1): C48-57.
- Kim, H.H.; Ahn, K.S.; Han, H.; Choung, S.Y.; Choi, S.Y. and Kim, I.H. (2005) Decursin and PDBu: two PKC activators distinctively acting in the megakaryocytic differentiation of K562 human erythroleukemia cells. *Leuk. Res.*, 29: 1407-13.
- Kim, J.-S., Z.-Y. Park, Y.-J. Yoo, S.-S. Yu & J.-S. Chun. (2005) p38 kinase mediates nitric oxide-induced apoptosis of chondrocytes through the inhibition of protein kinase Czeta by blocking autophosphorylation. *J Biol Chem*, 12, 201-212.
- Kirwan, A.F., Bibby, A. C., Mvilongo, T., Riedel, H., Burke, T., Millis, S.Z. y Parissenti, A.M. (2003). Inhibition of protein kinase C catalytic activity by additional regions within the human protein kinase Ca regulatory domain lying outside of the pseudosubstrate sequence. *Biochem. J.* 373, 571-581.
- Kitagawa, Y., Matsuo, Y., Minowada, J. y Nishizuka, Y. (1991). Protein kinase C of a human megakaryoblastic leukemic cell line (MEG-01). Analysis of subspecies and activation by diacylglycerol and free fatty acids. *FEBS Lett.* 288, 37-40.
- Klauck TM, Faux MC, Labudda K, Langeberg LK, Jaken S, Scott JD. (1996) Coordination of three signaling enzymes by AKAP79, a mammalian scaffold protein. *Science*, 271(5255): 1589-92.
- Knighton, D.R., Zheng, J.H., Ten Eyck, L.F., Ashford, V.A., Xuong, N.H., Taylor, S.S. y Sowadski, J.M. (1991). Crystal structure of the catalytic subunit of cyclic adenosine monophosphate-dependent protein kinase. *Science* 253, 407-414.
- Knopf, J.L. Lee, M.H. Sultzman, L.A. Kriz, R.W. Loomis, C.R. Hewick, R.M. Bell, R.M. (1986) Cloning and expression of multiple protein kinase CCDNAs. *Cell* 46: 491-502.
- Kobayashi N, Barnard RJ, Henning SM, Elashoff D, Reddy ST, Cohen P, et al. (2006) Effect of altering dietary omega-6/omega-3 fatty acid ratios on prostate cancer membrane composition, cyclooxygenase-2, and prostaglandin E2. *Clin Cancer Res*; 12: 4662-70.
- Kohn EA, Yoo CJ and Eastman A. (2003) The protein kinase C inhibitor Go6976 is a potent inhibitor of DNA damageinduced S and G2 cell cycle checkpoints. *Cancer Res.* 63: 31-35.

- Kohout, S. Corbalán García, S. Torrecillas, A. Gómez Fernández, J. Falke, J. (2002) C2 domains of protein kinase C isoforms alpha, beta, and gamma: activation parameters and calcium stoichiometries of the membrane bound state. *Biochemistry* 41: 11411–11424.
- Kohout SC, Corbalán García S, Gómez Fernández JC, Falke JJ. (2003) C2 domain of protein kinase C alpha: elucidation of the membrane docking surface by site-directed fluorescence and spin labeling. *Biochemistry*, 42: 1254-65.
- Koivunen J, Aaltonen V, Koskela S, Lehenkari P, Laato M and Peltonen J. (2004) Protein kinase C alpha/beta inhibitor Go6976 promotes formation of cell junctions and inhibits invasion of urinary bladder carcinoma cells. *Cancer Res*, 64: 5693–5701.
- Koivunen J, Aaltonen V, and Peltonen J. (2006) Protein kinase C (PKC) family in cancer progression. *Cancer Letters*, 235: 1-10.
- Kolkova, K., Stensman, H., Berezin, V., Bock, E. and Larsson, C. (2005) Distinct roles of PKC isoforms in NCAM-mediated neurite outgrowth. *J Neurochem*, 92(4): 886-894.
- Konishi H, Tanaka M, Takemura Y, Matsuzaki H, Ono Y, Kikkawa U, Nishizuka Y. (1997) Activation of protein kinase C by tyrosine phosphorylation in response to H<sub>2</sub>O<sub>2</sub>. *Proc Natl Acad Sci U S A*. 94(21):11233-7.
- Kuroda, S., Tokunaga, C., Kiyohara, Y., Higuchi, O., Konishi, H., Mizuno, K., Gill, G.N. y Kikkawa, U. (1996). Protein-protein interaction of zinc finger LIM domains with protein kinase C. *J. Biol. Chem.* 271, 31029-31032.
- Kushi L. and Giovannucci E. (2002). Dietary fat and cancer. *Am. J. Med.* 113, 63S-70S.
- Kwon, O.J., Gainer, H., Wray, S. y Chin, H. (1996). Identification of a novel protein containing two C2 domains selectively expressed in the rat brain and kidney. *FEBS Lett.* 378, 135-139.
- La Porta CA, Tessitore L and Comolli R. (1997) Changes in protein kinase C alpha, delta and in nuclear beta isoform expression in tumour and lung metastatic nodules induced by diethylnitrosamine in the rat. *Carcinogenesis*, 18: 715–719.
- Lacal, J. C., Fleming, T. P., Warren, B. S., Blumberg, P. M. and Aaronson, S. A. (1987). Involvement of functional protein-kinase-C in the mitogenic response to the *HRas* oncogene product. *Mol. Cell. Biol.* 7, 4146–4149.
- Laemmli UK. (1970) Cleavage of structural proteins during the assembly of the head of bacteriophage T4. *Nature*. 227(5259): 680-5.
- Lahn M, Köhler G, Sundell K, Su C, Li S, Paterson BM and Bumol TF. (2004) Protein kinase C alpha expression in breast and ovarian cancer. *Oncology*.; 67: 1-10.
- Lakowicz, J.R. (1983) *“Principles of Fluorescence Spectroscopy”* Plenum Publishing Corporation, New York.
- Lal, M.A., Proulx, P.R. y Hébert, R.L. (1998). A role for PKC and MAP kinase in bradykinin-induced arachidonic acid release in rabbit CCD cells. *Am. J. Physiol. (Renal Physiol.)* 43, F728-F735.
- Lander, E. S., Linton, L. M., Birren, B., Nusbaum, C., Zody, M. C., Baldwin, J., Devon, K., Dewar, K., Doyle, M., FitzHugh, W., Funke, R., Gage, D., Harris, K., Heaford, A., Howland, J., Kann, L., Lehoczky, J., LeVine, R., McEwan, P., McKernan, K., Meldrum, J., Mesirov, J. P., Miranda, C., Morris, W., Naylor, J., Raymond, C., Rosetti, M., Santos, R., Sheridan, A., Sougnez, C., Stange-Thomann, N., Stojanovic, N., Subramanian, A., Wyman, D., Rogers, J., Sulston, J., Ainscough, R., Beck, S., Bentley, D., Burton, J., Clee, C., Carter, N., Coulson, A., Deadman, R., Deloukas, P., Dunham, A., Dunham, I., Durbin, R., French, L., Grafham, D., Gregory, S., Hubbard, T., Humphray, S., Hunt, A., Jones, M., Lloyd, C., McMurray, A., Matthews, L., Mercer, S., Milne, S., Mullikin, J. C., Mungall, A., Plumb, R., Ross, M., Shownkeen, R., Sims, S., Waterston, R. H., Wilson, R. K., Hillier, L. W., McPherson, J. D., Marra, M. A., Mardis, E. R., Fulton, L. A.,

- Chinwalla, A. T., Pepin, K. H., Gish, W. R., Chissoe, S. L., Wendl, M. C., Delehaunty, K. D., Miner, T. L., Delehaunty, A., Kramer, J. B., Cook, L. L., Fulton, R. S., Johnson, D. L., Minx, P. J., Clifton, S. W., Hawkins, T., Branscomb, E., Predki, P., Richardson, P., Wenning, S., Slezak, T., Doggett, N., Cheng, J. F., Olsen, A., Lucas, S., Elkin, C., Uberbacher, E., Frazier, M., et al. (2001). Initial sequencing and analysis of the human genome. *Nature* 409, 860–921.
- Lander E, Jiang G and Tao K. (2009) Taking aim at aggressive cancer cells. *Cancer Biol Ther.*; 8 (16):ii.
- Landgraf KE, Malmberg NJ and Falke JJ. (2008) Effect of PIP2 binding on the membrane docking geometry of PKC alpha C2 domain: an EPR site-directed spin-labeling and relaxation study. *Biochemistry*. 2008 Aug 12;47(32):8301-16. Epub 2008 Jul 9.
- Larsson, S. C., Kunlin, M., Ingelman-Sundberg, M. and Wolk, A. (2004). Dietary long-chain n-3 fatty acids for the prevention of cancer: a review of potential mechanisms. *Am. J. Clin. Nutr.* 79, 935–945.
- Lasfargues EY et al. (1978) Isolation of two human tumor epithelial cell lines from solid breast carcinomas. *J. Natl. Cancer Inst.* 61: 967-978.
- Lasfargues EY et al. (1979) A human breast tumor cell line (BT-474) that supports mouse mammary tumor virus replication. *In Vitro* 15: 723-729.
- Lavie Y, Zhang ZC, Cao HT, Han TY, Jones RC, Liu YY, Jarman M, Hardcastle IR, Giuliano AE and Cabot MC. (1998) Tamoxifen induces selective membrane association of protein kinase C epsilon in MCF-7 human breast cancer cells. *Int J Cancer.*; 77: 928-32.
- Leach, K. L., James, M. L. & Blumberg, P. M. (1983). Characterization of a specific phorbol ester aporeceptor in mouse-brain cytosol. *Proc. Natl Acad. Sci. USA* 80, 4208–4212.
- Le Good, J.A., Ziegler, W.H., Parekh, D.B., Alessi, D.R., Cohen, P. y Parker, P.J. (1998). Protein kinase C isotypes controlled by phosphoinositide 3-kinase through the protein kinase PDK1. *Science* 281: 2042-2045.
- Le XF, Marcelli M, McWatters A, Nan B, Mills GB, O'Brian CA and Bast RC Jr (2001) Heregulin-induced apoptosis is mediated by down-regulation of Bcl-2 and activation of caspase-7 and is potentiated by impairment of protein kinase C alpha activity. *Oncogene*; 20:8258–8269.
- Lee H-W, Smith L, Pettit GR, Vinitzky A and Smith JB. (1996) Ubiquitination of protein kinase C  $\alpha$  and degradation by the proteasome. *Journal of Biological Chemistry* 271: 20973–20976.
- Lee, M.H. y Bell, R.M. (1991). Mechanism of protein kinase C activation by phosphatidylinositol 4,5-bisphosphate. *Biochemistry* 30, 1041-1049.
- Lee MM and Lin SS. (2000) Dietary fat and breast cancer. *Annu Rev Nutr*; 20: 221–248.
- Lehel, C., Z. Olah, G. Jakab, and W.B. Anderson. (1995). Protein kinase C is localized to the Golgi via its zinc-finger domain and modulates Golgi function. *Proc. Natl. Acad. Sci. USA*. 92: 1406–1410.
- Leitges, M., L. Sanz, P. Martin, A. Duran, U. Braun, J. F. Garcia, F. Camacho, M. T. Diaz-Meco, P. D. Rennert and J. Moscat. (2001) Targeted disruption of the zeta PKC gene results in the impairment of the NF-kappaB pathway. *Mol Cell*, 8, 771-780.
- Lenardo, M.J. y Baltimore, D. (1989) NF- $\kappa$ B: a pleiotropic mediator of inducible tissue-specific gene control. *Cell* 58: 227-229.
- Leroy, I., A. de Thonel, G. Laurent and A. Quillet-Mary. (2005) Protein kinase C zeta associates with death inducing signaling complex and regulates Fas ligand-induced apoptosis. *Cell Signal*, 17, 1149-1157.

- Lester, D.V., Collin, C., Etcheberrigaray, R y Alkion, D.L. (1991). Arachidonic acid and diacylglycerol act synergistically to activate protein kinase C *in vitro* and *in vivo*. *Biochim. Biophys. Res. Commun.* 179, 1522-1528.
- Li CI, Daling JR and Malone KE. (2003) Incidence of invasive breast cancer by hormone receptor status from 1992 to 1998. *J Clin Oncol*; 21/1:28-34.
- Li H, Zhao L, Yang Z, Funder JW and Liu JP. (1998) Telomerase is controlled by protein kinase C alpha in human breast cancer cells. *J Biol Chem*; 273:33436-33442.
- Li W, Zhang J, Bottaro DP, Pierce JH. (1997) Identification of serine 643 of protein kinase C-delta as an important autophosphorylation site for its enzymatic activity. *J Biol Chem.* 272(39): 24550-5.
- Li Z, Wen Z, Han J. (1999) The effect of thrombin on tissue factor activity in cultured bovine aortic endothelial cells and its correlation with PKC pathway. *Zhonghua Xue Ye Xue Za Zhi.* 20(3):130-3.
- Liedtke, C.M. Yun, C.H.C., Kyle, N. Wang,D. (2002) Protein kinase C epsilon dependent regulation of cystic fibrosis transmembrane regulator involves binding to a receptor for activated C kinase (RACK1) and RACK1 binding to Na<sup>+</sup>/H<sup>+</sup> exchange regulatory factor, *J. Biol. Chem.* 277: 22925-22933.
- Liedtke CM, Hubbard M, Wang X. (2003) Stability of actin cytoskeleton and PKC-delta binding to actin regulate NKCC1 function in airway epithelial cells. *Am J Physiol Cell Physiol.* 284(2): C487-96.
- Lincz LF. (1998) Deciphering the apoptotic pathway: all roads lead to death. *Immunol Cell Biol.*; 76(1): 1-19.
- Lippman SM and Hong WK. (2002) The biology behind cancer prevention by delay. *Clin Cancer Res.* 8:305-13.
- Lipworth L, Martinez ME, Angell J et al. (1997) Olive oil and human cancer: an assessment of the evidence. *Prev Med*; 26: 181-190.
- Liron T, Chen LE, Khaner H, Vallentin A, Mochly-Rosen D. (2007) Rational design of a selective antagonist of epsilon protein kinase C derived from the selective allosteric agonist, pseudo-RACK peptide. *J Mol Cell Cardiol.* 42(4): 835-41.
- Liu, J. F., Crepin, M., Liu, J. M., Barritault, D. and Ledoux, D. (2002) FGF-2 and TPA induce matrix metalloproteinase-9 secretion in MCF-7 cells through PKC activation of the Ras/ERK pathway. *Biochem. Biophys. Res. Commun.* 293, 1174-1182.
- Liu, L. Song, X. He, D. Komma, C. Kita, A. Virbasius, J. Huang, G. Bellamy, H. Miki, K. Czech, M. Zhou, G. (2006) Crystal structure of the C2 domain of class II phosphatidylinositide 3-kinase C2 alpha. *J. Biol. Chem.* 281: 4254-4260.
- Liu, Y., Liu, D., Heath, L., Meyers, D.M., Krafte, D.S., Wagoner, P.K., Silvia, C.P., Yu, W. y Curran, M.E. (2001). Direct activation of an inwardly rectifying potassium channel by arachidonic acid. *Mol. Pharmacol.* 59, 1061-1068.
- Lønne GK, Cornmark L, Zahirovic IO, Landberg G, Jirström K, Larsson C. (2010) PKCalpha expression is a marker for breast cancer aggressiveness. *Mol Cancer*; 9: 76.
- López-Andreo, M. Gómez Fernández, J. Corbalán García, S. (2003) The simultaneous production of phosphatidic acid and diacylglycerol is essential for the translocation of protein kinase C epsilon to the plasma membrane in RBL-2H3 cells, *Mol. Biol. Cell.* 14: 4885-4895.
- López-Andreo, M., Torrecillas, A., Conesa Zamora, P., Corbalán García, S. y Gómez-Fernández, J. (2005) Retinoic acid as a modulator of the activity of protein kinase C alpha. *Biochemistry.* 44: 11353-11360.

- López I, Mak EC, Ding J, Hamm HE, Lomasney JW. (2001) A novel bifunctional phospholipase c that is regulated by G alpha 12 and stimulates the Ras/mitogen-activated protein kinase pathway. *J Biol Chem.* 276(4): 2758-65.
- López-Nicolás, R., López Andreo, M. J., Marín Vicente, C., Gómez Fernández, J. C. and Corbalán-García, S. (2006) Molecular mechanisms of protein kinase C alpha localization and activation by arachidonic acid. The C2 domain also plays a role. *J. Mol. Biol.*, 357: 1105-1120.
- Lu, Z., A. Hornia, Y.-W. Jiang, Q. Zang, S. Ohno and D. Foster (1997) Tumor promotion by depleting cells of protein kinase C-delta. *Mol Cell Biol*, 17, 3418-3428.
- Lu, D., J. Huang and A. Basu. (2006) Protein kinase C epsilon activates protein kinase B/Akt via DNA-PK to protect against tumor necrosis factor-alpha-induced cell death. *J Biol Chem*, 281, 22799-22807.
- Luo B, Prescott SM, Topham MK. (2003) Association of diacylglycerol kinase zeta with protein kinase C alpha: spatial regulation of diacylglycerol signaling. *J Cell Biol.* 160(6):929-37.
- Luria A, Tennenbaum T, Sun QY, Rubinstein S, Breitbart H. (2000) Differential localization of conventional protein kinase C isoforms during mouse oocyte development. *Biol Reprod.* 62(6):1564-70.
- Ma, Z., Ramanadham, S., Wothmann, M., Bohrer, A., Hsu, F.F. y Turk, J. (2001). Studies of insulin secretory responses and of arachidonic incorporation into phospholipids of stably transfected insulinom cells that overexpress group VIA phospholipase A<sub>2</sub> (iPLA<sub>2</sub>β) indicate a signalling rather than a housekeeping role for iPLA<sub>2</sub>β. *J. Biol. Chem.* 276, 3103-3115.
- Maasch C, Wagner S, Lindschau C, Alexander G, Buchner K, Gollasch M, Luft FC, Haller H. (2000) Protein kinase c alpha targeting is regulated by temporal and spatial changes in intracellular free calcium concentration [Ca(2+)](i). *FASEB J.* 14(11):1653-63.
- Mackay, K. and Mochly-Rosen, D. (2001). Arachidonic acid protects neonatal rat cardiac myocytes from ischaemic injury through ε protein kinase C. *Cardiovasc. Res.* 50, 65-74.
- Mackay HJ and Twelves CJ. (2003) Protein Kinase C: a target for anticancer drugs? *Endocrine-Related Cancer*, 10: 389-396.
- Mackay, H. J. and Twelves, C. J. (2007) Targeting the protein kinase C family: are we there yet? *Nature reviews.* 7, 554-562
- Madamanchi, N.R., Bukoski, R.D., Runge, M.S. y Rao, G.N. (1998). Arachidonic acid activates Jun N-terminal kinase in vascular smooth muscle cells. *Oncogene* 1998 16, 417-422.
- Maheo K, Vibet S, Steghens JP, Dartigeas C, Lehman M, Bougnoux P, et al. (2005) Differential sensitization of cancer cells to doxorubicin by DHA: a role for lipoperoxidation. *Free Radic Biol Med.* 39:742-51.
- Mahmmoud, Y.A. (2007) Modulation of protein kinase C by curcumin: inhibition and activation switched by calcium ions. *Br. J. Pharmacol.*, 150: 200-8.
- Maillard V., Bougnoux P., Ferrari P., Jourdan M.L., Pinault M., Lavillonnière F., Body G., Le Floch O. and Chajès V. (2002). N-3 and N-6 fatty acids in breast adipose tissue and relative risk of breast cancer in a case-control study in Tours, France. *Int. J. Cancer* 98, 78-83.
- Majumder PK, Pandey P, Sun X, Cheng K, Datta R, Saxena S, Kharbanda S, Kufe D. (2000) Mitochondrial translocation of protein kinase C delta in phorbol ester-induced cytochrome c release and apoptosis. *J Biol Chem.* 275(29): 21793-6.
- Majumder, P., N. Mishra, X. Sun, A. Bharti, S. Kharbanda, S. Saxena and D. Kufe. (2001) Targeting of protein kinase C-delta to mitochondria in the oxidative stress response. *Cell Death Differ*, 12, 465-470.

- Makowske, M. y Rosen, O.M. (1989) Complete activation of protein kinase C by an antipeptide antibody directed against the pseudosubstrate prototope. *J. Biol. Chem.* 264: 16155-16159.
- Mandil, R. et al. (2001) Protein kinase Ca and protein kinase Cδ play opposite roles in the proliferation and apoptosis of glioma cells. *Cancer Res.* 61, 4612-4619.
- Mangoura, D., Sogos, V., Dawson, D. (1995) Phorbol esters and PKC signaling regulate proliferation, vimentin cytoskeleton assembly and glutamine synthetase activity of chick embryo cerebrum astrocytes in culture. *Brain Res Dev Brain Res.* 87(1):1-11.
- Marais, R. y Marshall, C.J. (1996) Control of the ERK MAP kinase cascade by Ras and Raf. *Cancer Surv.* 27: 101-125.
- Marin-Vicente, C., Gómez Fernández, J. and Corbalán García, S. (2005) The ATP-dependent membrane localization of PKCα is regulated by Ca<sup>2+</sup> influx and PtdIns(4,5)P<sub>2</sub> in differentiated PC12 cells. *Mol. Biol. Cell.*, 16: 2848-2861.
- Marin-Vicente, C., Nicolás Molina F., Gómez Fernández, J. and Corbalán García, S. (2008) The PtdIns(4,5)P<sub>2</sub> ligand itself influences the localization of PKCα in the plasma membrane of intact living cells. *J. Mol. Biol.* 377(4):1038-52.
- Mariny-Baron G. and Fabbro D. (2007) Classical PKC isoforms in cancer. *Pharmacological research*, 55: 477-486.
- Marmor, MD., Skaria, KB and Yarden Y. (2004). Signal transduction and oncogenesis by Erb/HER receptors. *Int J Radian Oncol Biol Phys* 58:903-913.
- Marquez VE, Nacro K, Benzaria S, Lee J, Sharma R, Teng K, Milne GW, Bienfait B, Wang S, Lewin NE and Blumberg PM. (1999) The transition from a pharmacophore-guided approach to a receptor-guided approach in the design of potent protein kinase C ligands. *Pharmacol Ther.*; 82: 251-61.
- Marquez, V. E. and Blumberg, P. M. (2003) Synthetic diacylglycerols (DAG) and DAG-lactones as activators of protein kinase C (PK-C). *Accounts of chemical research.* 36, 434-443
- Martelli AM, Bortul R, Tabellini G, Faenza I, Cappellini A, Bareggi R, Manzoli L, Cocco L. (2002) Molecular characterization of protein kinase C-α binding to lamin A. *J Cell Biochem.*;86(2): 320-30.
- Martin-Moreno JM. (2000) The role of olive oil in lowering cancer risk: in this real gold or simply pinchbeck? *J Epidemiol Community Health*; 54: 726-727.
- Masur K, Lang K, Niggemann B, Zanker KS, Entschladen F. (2001) High PKC alpha and low E-cadherin expression contribute to high migratory activity of colon carcinoma cells. *Mol. Biol. Cell* 12: 1973-1982.
- Matassa, A., L. Carpenter, T. Biden, M. Humphries and M. Reyland. (2001) PKC-delta is required for mitochondrial dependent apoptosis in salivary epithelial cells. *J Biol Chem*, 276, 29719-29728.
- Mayer, R.J. y Marshall, L.A. (1993). New insights on mammalian phospholipase A<sub>2</sub>(s); comparison of arachidonyl-selective and -nonselective enzymes. *FASEB J.* 7, 339-348.
- McCarty, M.F. (1996) Up-regulation of intracellular signalling pathways may play a central pathogenic role in hypertension, atherogenesis, insulin resistance, and cancer promotion--the 'PKC syndrome'. *Med. Hypothesis*, 46: 191-221.
- McLaughlin, S., Wang, J., Gambhir, A. y Murray, D. (2002) PtdIns(4,5)P<sub>2</sub> and proteins: Interactions, organization, and information flow. *Annu Rev Biophys Biomol Struct.*, 31: 151-175.
- McPhail, L. C., Clayton, C. C. and Snyderman, R. (1984). A potential second messenger role for unsaturated fatty acids: activation of Ca<sup>2+</sup>-dependent protein kinase. *Science*, 224, 622-625.

- Medkova, M. y Cho, W. (1998) Differential membrane-binding and activation mechanisms of protein kinase C-alpha and -epsilon, *Biochemistry* 37: 4892-4900.
- Medkova M, Cho W. (1999) Interplay of C1 and C2 domains of protein kinase C-alpha in its membrane binding and activation. *J Biol Chem.*, 274: 19852-61.
- Meyer T, Regenass U, Fabbro D, Alteri E, Rosel J, Muller M, Caravatti G and Matter A (1989) A derivative of staurosporine (CGP 41251) shows selectivity for protein kinase C inhibition and in vitro anti-proliferative as well as in vivo anti-tumor activity. *Int J Cancer*, 43: 851-856.
- Mellor, H. y Parker, P.J. (1998) The extended PKC superfamily. *Biochem. J.*, 332: 281-292.
- Menendez, J. A., Vellon, L., Colomer, R., Lupu, R. (2005) Oleic acid, the main monounsaturated fatty acid of olive oil, suppresses Her-2/neu (erbB-2) expression and synergistically enhances the growth inhibitory effects of trastuzumab (Herceptin™) in breast cancer cells with Her-2/neu oncogenes amplification. *Ann. Oncol.*, 16, 359-371.
- Meng J, Ding Y, Shen A, Yan M, He F, Ji H, Zou L, Liu Y, Wang Y, Lu X and Wang H. (2010) Overexpression of PPARgamma can down-regulate Skp2 expression in MDA-MB-231 breast tumor cells. *Mol Cell Biochem* DOI 10.1007/s11010-010-0570-y.
- Messerschmidt, A. Macieira, S. Velarde, M. Badeker, M. Benda, C. Jestel, A. Brandstetter, H. Neufeind, T. Blaesse, M. (2005) Crystal structure of the catalytic domain of human atypical protein kinase C-iota reveals interaction mode of phosphorylation site in turn motif, *J. Mol. Biol.* 352: 918-931.
- Meves, H. (1994). Modulation of ion channels by arachidonic acid. *Prog. Neurobiol.* 43, 175-186.
- Meyer T. y Oancea E. (2000) Studies of signal transduction events using chimeras to green fluorescent protein. *Methods Enzymol.*, 327: 500-13.
- Mignen, O. y Shuttleworth, T. J. (2000) IARC, a novel arachidonate-regulated, noncapacitative Ca<sup>2+</sup> entry channel. *J. Biol. Chem.* 275: 9114-9119.
- Miles, E. A., Zoubouli, P., Calder, P. C. (2005) Differential anti-inflammatory effects of phenolic compounds from extra virgin olive oil identified in human whole blood cultures. *Nutrition*, 21, 389-394.
- Mineo C, Ying YS, Chapline C, Jaken S, Anderson RG. (1998) Targeting of protein kinase C alpha to caveolae. *J Cell Biol.* 141(3):601-10.
- Mischak, H., Goodnight, J.A., Kölch, W., Martiny-Baron, G., Schächtele, C., Kazanietz, M.G., Blumberg, P.M., Pierce, J.H. y Mushinski, J.F. (1993). Overexpression of protein kinase C-δ and -ε in the NIH 3T3 cells induces opposite effects on growth, morphology, anchorage dependence, and tumorigenicity. *J. Biol. Chem.* 268, 6090-6096.
- Mitani M., Yamanishi T. and Miyazaki Y. (1975) Salinomycin: a new monovalent cation ionophore. *Biochem. Biophys. Res. Commun.* 27: 1231-1236.
- Miyazaki Y., Shibuya M., Sugawara H., Kawaguchi O. and Hirsoe C. (1974) Salinomycin, a new polyether antibiotic. *J. Antibiot.* 27: 814-821.
- Mochly-Rosen D, Khaner H, Lopez J, Smith BL. (1991) Intracellular receptors for activated protein kinase C. Identification of a binding site for the enzyme. *J Biol Chem.* 266(23):14866-8.
- Mochly-Rosen, D. Miller, K.G. Scheller, R.H. Khaner, H. Lopez, J. Smith, B.L. (1992) P65 fragments, homologous to the C2 region of protein kinase C, bind to the intracellular receptors for protein kinase C. *Biochemistry* 31: 8120-8124.
- Mochly-Rosen D. (1995) Localization of protein kinases by anchoring proteins: a theme in signal transduction. *Science.* 268(5208):247-51.

- Mochly Rosen D, Gordon AS. (1998) Anchoring proteins for protein kinase C: a means for isozyme selectivity. *FASEB J.* 12(1):35-42.
- Mogami, H., Zhang, H., Suzuki, Y., Urano, T., Saito, N., Kojima, I. y Petersen, O.H. (2003) Decoding of short-lived  $\text{Ca}^{2+}$  influx signals into long term substrate phosphorylation through activation of two distinct classes of PKC. *J Biol Chem.* 278: 9896-9904.
- Moghaddami, N., Costabile, M., Grover, P.K., Jersmann, H.P.A., Huang, Z.H., Hii, C.S.T. y Ferrante, A. (2003). Unique effect of arachidonic acid on human neutrophil TNF receptor expression: Up-regulation involving protein kinase C, extracellular signal-regulated kinase, and phospholipase  $\text{A}_2$ . *J. Immunol.* 171, 2616-2624.
- Moral, R., Solanas, M., Garc\_a, G., Colomer, R., Escrich, E. (2003) Modulation of EGFR and neu expression by n-6 and n-9 high-fat diets in experimental mammary adenocarcinomas. *Oncol. Rep.*, 10, 1417-1424.
- Moscat J. and Díaz Meco M. (2000) The atypical PKC. Functional specificity mediated by specific protein adapters. *EMBO Rep.* 1: 399-403.
- Moscat J., Rennert P. and Díaz Meco M. (2006) PKC $\zeta$  at the crossroad of NF-KB and Jak1/Stat6 signaling pathways. *Cell Death Differ.* 13: 702-711.
- Mosior M, McLaughlin S. (1991) Peptides that mimic the pseudosubstrate region of protein kinase C bind to acidic lipids in membranes. *Biophys J.* 60(1):149-59.
- Mosior, M. y Newton, A.C. (1996). Calcium-independent binding to interfacial phorbol esters causes protein kinase C to associate with membranes in the absence of acidic lipids. *Biochemistry* 35: 1612-1623.
- Mukai, H. y Ono, Y. (1994). A novel protein kinase with leucine zipper-like sequences: its catalytic domain is highly homologous to that of protein kinase C. *Biochem. Biophys. Res. Commun.* 199, 897-904.
- Murakami, K. and Routtenberg, A. (1985). Direct activation of protein kinase C by unsaturated fatty acids (oleate and arachidonate) in the absence of phospholipids and  $\text{Ca}^{2+}$ . *FEBS Letters*, 192, 189-193.
- Murakami, K., Chan, S.Y. y Routtenberg, A. (1986). Protein kinase C activation by *cis*-fatty acids in the absence of  $\text{Ca}^{2+}$  and phospholipids. *J. Biol. Chem.* 261, 15424-15429.
- Murriel, C. L., E. Churchill, K. Inagaki, L. I. Szweda and D. Mochly-Rosen. (2004) Protein kinase Cdelta activation induces apoptosis in response to cardiac ischemia and reperfusion damage: A mechanism involving BAD and the mitochondria. *J Biol Chem*, 279, 47985-47991.
- Myat, M.M., Anderson, S., Allen, L.A. y Aderem, A. (1997) MARCKS regulates membrane ruffling and cell spreading. *Curr. Biol.* 7: 611-614.
- Nabha SM, Glaros S, Hong M, et al. (2005) Upregulation of PKC-delta contributes to antiestrogen resistance in mammary tumor cells. *Oncogene* ;24:3166-76.
- Nacro K., Bienfait B., Lee J., Han KC., Kang JH., Benzaria S., Lewin NE., Bhattacharyya DK., Blumberg PM., and Marquez VE. (2000) Conformationally constrained analogues of diacylglycerol (DAG). 16. How much structural complexity is necessary for recognition and high binding affinity to protein kinase C? *J Med Chem*, 43: 921-44.
- Nakhost A, Dyer JR, Pepio AM, Fan X, Sossin WS. (1999) Protein kinase C phosphorylated at a conserved Thr is retained in the cytoplasm. *J Biol Chem.* 274(41):28944-9.
- Nalefski, E.A. Falke, J.J. (1996) The C2 domain calcium-binding motif: structural and functional diversity, *Protein Sci.* 5: 2375-2390.
- Nalefski, E.A. Slazas, M.M. Falke, J.J. (1997)  $\text{Ca}^{2+}$ -signaling cycle of a membrane-docking C2 domain. *Biochemistry* 36: 12011-12018.

- Nalefski, E.A. Newton, A.C. (2001) Membrane binding kinetics of protein kinase C beta II mediated by the C2 domain. *Biochemistry* 40: 13216–13229.
- Nalefski, E.A. Wisner, M.A. Chen, J.Z. Sprang, S.R. Fukuda, M. Mikoshiba, K Falke, J.J. (2001) C2 domains from different Ca<sup>2+</sup> signaling pathways display functional and mechanistic diversity, *Biochemistry* 40: 3089–3100.
- Nauert JB, Klauck TM, Langeberg LK, Scott JD. (1997) Gravin, an autoantigen recognized by serum from myasthenia gravis patients, is a kinase scaffold protein. *Curr Biol.* 7(1):52-62.
- Navarro-Tito N, Soto-Guzman A, Castro-Sanchez L, Martinez-Orozco R and Salazar EP. (2010) Oleic acid promotes migration on MDA-MB-231 breast cancer cells through an arachidonic acid-dependent pathway. *Int J Biochem Cell Biol.* 42: 306-17.
- Negri, E.; Vacchia, C.L.; Franceschi, S.; Levi, F. And Parazzini, F. (1996) Intake of selected micronutrients and the risk of endometrial carcinoma. *Cancer*, 77: 917-923.
- Nencioni A., Wille L., Dal Bello G., Boy D., Cirmena G., Wesselborg S., Belka C., Brossart P., Patrone F. and Ballestrero A. (2005) Cooperative cytotoxicity of proteasome inhibitors and tumor necrosis factor-related apoptosis-inducing ligand in chemoresistant Bcl-2-overexpressing cells. *Clin. Cancer Res.* 11: 4259–4265.
- Neri, A.; Marmiroli, S.; Tassone, P.; Lombardi, L.; Nobili, L.; Verdelli, D.; Civallero, M.; Cosenza, M.; Bertacchini, J.; Federico, M.; De Pol, A.; Deliliers, G.L.; Sacchi, S. (2008) The oral PKC-beta inhibitor enzastaurin (LY317615) suppresses signalling through the AKT pathway, inhibits proliferation and induces apoptosis in multiple myeloma cell lines. *Leuk. Lymphoma*, 49: 1374-83.
- Neri, L.M., Borgatti, P., Capitani, S. y Martelli, A.M. (2002). Protein kinase C isoforms and lipid second messengers: a critical partnership?. *Histol. Histopathol.* 17, 1311-1316.
- Neuhoff V, Arold N, Taube D, Ehrhardt W. (1988) Improved staining of proteins in polyacrylamide gels including isoelectric focusing gels with clear background at nanogram sensitivity using Coomassie Brilliant Blue G-250 and R-250. *Electrophoresis*, 9(6): 255-62.
- Newton, A.C. (1993). Interaction of proteins with lipid headgroups: lessons from protein kinase C. *Annu. Rev. Biophys. Biomol. Struct.* 22, 21-25.
- Newton, A.C. (1995). Protein kinase C: structure, function, and regulation. *J. Biol. Chem.* 270: 28495-28498.
- Newton, A.C. (1997). Regulation of protein kinase C. *Curr. Opin. Cell. Biol.* 9: 161-167.
- Newton, A. C. y Johnson, J. E. (1998) Protein kinase C: A paradigm for regulation of protein function by two membrane-targeting modules. *Biochim Biophys Acta.*, 1376: 155-172.
- Newton, A. C. (2001) Protein kinase C: Structural and spatial regulation by phosphorylation, cofactors, and macromolecular interactions. *Chem Rev.*, 101: 2353-2364.
- Newton, A.C. (2003) Regulation of the ABC kinases by phosphorylation: Protein kinase C as a paradigm, *Biochem. J.* 370: 361–371.
- Newton, A.C. (2010) Protein Kinase C: poised to signal. *Am J Physiol Endocrinol Metab* 298: E395–E402.
- Ng T, Parsons M, Hughes WE, Monypenny J, Zicha D, Gautreau A, Arpin M, Gschmeissner S, Verveer PJ, Bastiaens PI, Parker PJ. (2001) Ezrin is a downstream effector of trafficking PKC-integrin complexes involved in the control of cell motility. *EMBO J.*; 20: 2723-41.
- Nishikawa, K., Toker, A., Johannes, F.J., Songyang, Z. y Cantley, L.C. (1997) Determination of the specific substrate sequence motifs of protein kinase C isozymes. *J. Biol. Chem.* 272: 952-960.

- Nishizuka Y. (1986) Perspectives on the role of protein kinase C in stimulus-response coupling. *J Natl Cancer Inst.* 76(3): 363-70.
- Nishizuka, Y. (1992) Intracellular signaling by hydrolysis of phospholipids and activation of protein kinase C. *Science*, 258: 607-614.
- Nishizuka, Y. (1995) Protein kinase C and lipid signaling for sustained cellular responses. *FASEB J.*, 9: 484-496.
- Nogales-Cadenas R, Carmona-Saez P, Vazquez M, Vicente C, Yang X, Tirado F, Carazo JM, Pascual-Montano A. (2009) GeneCodis: interpreting gene lists through enrichment analysis and integration of diverse biological information. *Nucleic Acids Research*; doi: 10.1093/nar/gkp416.
- Nomura, H. Ase, K. Sekiguchi, K. Kikkawa, U. Nishizuka, Y. Nakano, Y. Satoh, T. (1986) Stereospecificity of diacylglycerol for stimulus-response coupling in platelets. *Biochem. Biophys. Res. Commun.* 140 1143-1151.
- Novak EJ, Rabinovitch PS. (1994) Improved sensitivity in flow cytometric intracellular ionized calcium measurement using fluo-3/Fura Red fluorescence ratios. *Cytometry.* 17(2):135-41.
- Nyby MD, Hori MT, Ormsby B, Gabrielian A and Tuck ML. (2003) Eicosapentaenoic acid inhibits Ca<sup>2+</sup> mobilization and PKC activity in vascular smooth muscle cells. *Am J Hypertens.*; 16: 708-14.
- O'Brian CA, Chu F, Bornmann WG and Maxwell DS. (2006) Protein kinase Calpha and epsilon small-molecule targeted therapeutics: a new roadmap to two Holy Grails in drug discovery? *Expert Rev Anticancer Ther.*; 6: 175-86.
- O'Flaherty, J.T., Chadwell, B.A., Kearns, M.W., Sergeant, S. y Daniel, L.W. (2001) Protein kinases C translocation responses to low concentrations of arachidonic acid. *J. Biol. Chem.* 276: 24743-24750.
- Oancea, E. y Meyer, T. (1998) Protein kinase C as a molecular machine for decoding Ca<sup>2+</sup> and DAG signals. *Cell*, 95: 307-318.
- Oancea, E., Teruel, M. N., Quest, A. F. y Meyer, T. (1998) Green fluorescent protein (GFP)-tagged cysteine-rich domains from PKC as fluorescent indicators for DAG signaling in living cells. *J Cell Biol.*, 140: 485-498.
- Oberley TD. (2002) Oxidative damage and cancer. *Am J Pathol.* 160:403-8.
- Ochoa, W. García García, J. Fita, I. Corbalán García, S. Verdaguer, N. Gómez Fernández, J. (2001) Structure of the C2 domain from novel protein kinase C epsilon. A membrane binding model for Ca<sup>2+</sup>-independent C2 domains, *J. Mol. Biol.* 311: 837-849.
- Ochoa, W., Corbalán García, S., Eritja, R., Rodríguez Alfaro, J., Gómez Fernández, J., Fita, I. and Verdaguer, N. (2002) Additional binding sites for anionic phospholipids and calcium ions in the crystal structures of complexes of the C2 domain of protein kinase c alpha. *J. Mol. Biol.*, 320: 277-291.
- Ochoa, W. Torrecillas, A. Fita, I. Verdaguer, N. Corbalán García, S. Gómez Fernández, J.C. (2003) Retinoic acid binds to the C2-domain of protein kinase C (Alpha), *Biochemistry* 42: 8774-8779.
- Ohno, S., Konno, Y., Akita, Y., Yano, A. y Suzuki, K. (1990) A point mutation at the putative ATP-binding site of protein kinase C- $\alpha$  abolishes the kinase activity and renders it down-regulation-insensitive. A molecular link between autophosphorylation and down-regulation. *J. Biol. Chem.* 265: 6296-6300.
- Ohno, S. Nishizuka, Y. (2002) Protein kinase C isotypes and their specific functions: prologue, *J. Biochem. (Tokyo)* 132: 509-511.

- Oka M, Okada T, Nakamura S, Ohba M, Kuroki T, Kikkawa U, Nagai H, Ichihashi M, Nishigori C. (2003) PKC delta inhibits PKC alpha-mediated activation of phospholipase D1 in a manner independent of its protein kinase activity. *FEBS Lett.* 554(1-2): 179-83.
- Olivier, A.R. y Parker, P.J. (1991) Expression and characterization of protein kinase C- $\delta$ . *Eur. J. Biochem.* 200: 805-810.
- Ono, Y. T. Kurokawa, K. Kawahara, O. Nishimura, R. Marumoto, K. Igarashi, Y. Sugino, U. Kikkawa, K. Ogita, Y. Nishizuka. (1986) Cloning of rat brain protein kinase C complementary DNA. *FEBS Lett.* 203: 111-115.
- Ono, Y., Fujii, T., Ogita, K., Kikkawa, U., Igarashi, K. y Nishizuka, Y. (1987a) Identification of three additional members of rat protein kinase C family:  $\delta$ -,  $\epsilon$ - and  $\zeta$ -subspecies. *FEBS Lett.* 226: 125-128.
- Ono, Y., Fujii, T., Ogita, K., Kikkawa, U., Igarashi, K. y Nishizuka, Y. (1988b) The structure, expression, and properties of additional members of the protein kinase C family. *J. Biol. Chem.* 263: 6927-6932.
- Ono, Y., Fujii, T., Igarashi, K., Kino, C., Tanaka, U., Kikkawa, U. y Nishizuka, Y. (1989a) Phorbol ester binding to protein kinase C requires a cysteine-rich zinc-finger-like sequence. *Proc. Natl. Acad. Sci. U.S.A.* 86: 4868-4871.
- Ono, Y., Fujii, T., Ogita, K., Kikkawa, U., Igarashi, K. y Nishizuka, Y. (1989b) Protein kinase C- $\zeta$  subspecies from rat brain: its structure, expression, and properties. *Proc. Natl. Acad. Sci. U.S.A.* 86: 3099-3103.
- Orita, S., Sasaki, T., Naito, A., Komuro, R., Ohtsuka, T., Maeda, M., Suzuki, H., Igarashi, H. y Takai, Y. (1995) Doc2: a novel brain protein having two repeated C2-like domains, *Biochem. Biophys. Res. Commun.* 206 439-448.
- Orr, J.W. L.M. Keranen, A.C. Newton. (1992) Reversible exposure of the pseudosubstrate domain of protein kinase C by phosphatidylserine and diacylglycerol, *J. Biol. Chem.* 267: 15263-15266.
- Orr, J.W. y Newton, A.C. (1994a) Intrapeptide regulation of protein kinase C. *J. Biol. Chem.* 269: 8383-8387.
- Orr, J.W. y Newton, A.C. (1994b) Requirement for negative charge on "activation loop" of protein kinase C. *J. Biol. Chem.* 269: 27715-27718.
- Osada S, Mizuno K, Saido TC, Suzuki K, Kuroki T, Ohno S. (1992) A new member of the protein kinase C family, nPKC theta, predominantly expressed in skeletal muscle. *Mol Cell Biol.* 12(9):3930-8.
- Osada, S., Mizuno, K., Saido, T.C., Akita, Y., Suzuki, K., Kuroki, T. y Ohno, S. (1990) A phorbol ester receptor/protein kinase, nPKC $\eta$ , a new member of the protein kinase C family predominantly expressed in lung and skin. *J. Biol. Chem.* 265: 22434-22440.
- Owen, R.W., Haubner, R., Wurtele, G., Hull, E., et al. (2005) Olives and olive oil in cancer prevention. *Eur. J. Cancer Prev.*, 13, 319-326.
- Pak, Y. I.J. Enyedy, J. Varady, J.W. Kung, P.S. Lorenzo, P.M. Blumberg, S. Wang. (2001) Structural basis of binding of high-affinity ligands to protein kinase C: prediction of the binding modes through a new molecular dynamics method and evaluation by site-directed mutagenesis, *J. Med. Chem.* 44: 1690-1701.
- Palmer, R.H., Ridden, J. y Parker, P.J. (1994). Identification of multiple, novel, protein kinase C-related gene products. *FEBS Lett.* 356, 5-8.
- Pan, Q. et al. (2005) Protein kinase C  $\epsilon$  is a predictive biomarker of aggressive breast cancer and a validated target for RNA interference anticancer therapy. *Cancer Res.* 65, 8366-8371.

- Pan, Q., Bao, L. W., Teknos, T. N. & Merajver, S. D. (2006) Targeted disruption of protein kinase C  $\epsilon$  reduces cell invasion and motility through inactivation of RhoA and RhoC GTPases in head and neck squamous cell carcinoma. *Cancer Res.* 66, 9379–9384.
- Pappa, H. J. Murray-Rust, L.V. Dekker, P.J. Parker, N.Q. McDonald. (1998) Crystal structure of the C2 domain from protein kinase C-delta, *Structure* 6: 885–894.
- Pardini RS. (2006) Nutritional intervention with omega-3 fatty acids enhances tumor response to anti-neoplastic agents. *Chem Biol Interact*; 162: 89–105.
- Parekh, D.B., Wolfgang, Z. and Parker, P.J. (2000) Multiple pathways control protein kinase C phosphorylation. *EMBO J.* 19: 496-503.
- Parekh, D.B., Katso, R.M., Leslie, N.R., Downes, C.P., Procyk, K.J., Waterfield, M.D. and Parker, P.J. (2000). Beta 1-integrin and PTEN control the phosphorylation of protein kinase C. *Biochem. J.* 352, 425-433.
- Pariza MW. (1997) Dietary fat, calorie restriction, ad libitum feeding, and cancer risk. *Nutr Rev*; 45: 1–7.
- Park JY, Kim YM, Song HS, Park KY, Kim YM, Kim MS, Pak YK, Lee IK, Lee JD, Park SJ and Lee KU. (2003) Oleic acid induces endothelin-1 expression through activation of protein kinase C and NF-kappa B. *Biochem Biophys Res Commun.*; 303: 891-5.
- Parker PJ and Parkinson SJ. (2001) AGC protein kinase phosphorylation and protein kinase C. *Biochem Soc Trans* 29: 860–863.
- Parkin DM, Bray FI, Devesa SS. (2001) Cancer burden in the year 2000. The global picture. *Eur J Cancer.* 37:S4–66.
- Patiño R, Yoshizaki G, Bolamba D, Thomas P. (2003). Role of arachidonic acid and protein kinase C during maturation-inducing hormone-dependent meiotic resumption and ovulation in ovarian follicles of Atlantic croaker. *Biol Reprod.* Feb;68(2):516-23.
- Paul D. Thomas, Anish Kejariwal, Nan Guo, Huaiyu Mi, Michael J. Campbell, Anushya Muruganujan, and Betty Lazareva-Ulitsky. (2006) Applications for protein sequence-function evolution data: mRNA/protein expression analysis and coding SNP scoring tools. *Nucl. Acids Res.* 34: W645-W650.
- Pears, C.J., Kour, G., House, C., Kemp, B.E. y Parker, P.J. (1990) Mutagenesis of the pseudosubstrate site of protein kinase C leads to activation. *Eur. J. Biochem.* 194: 89-94.
- Pears, C.J., Schaap, D. y Parker, P.J. (1991) The regulatory domain of protein kinase C- $\epsilon$  restricts the catalytic-domain-specificity. *Biochem. J.* 276: 257-260.
- Peng, C.H.; Tseng, T.H.; Liu, J.Y.; Hsieh, Y.H.; Huang, C.N.; Hsu, S.P. and Wang, C.J. (2004) Penta-acetyl geniposide-induced C6 glioma cell apoptosis was associated with the activation of protein kinase Cdelta. *Chem. Biol. Interact.*, 147: 287-96.
- Perletti, G. P., Marras, E., Concari, P., Piccinini, F. And Tashjian, A. H. (1999) PKC $\delta$  acts as a growth and tumor suppressor in rat colonic epithelial cells. *Oncogene* 18, 1251–1256.
- Persson T, Yde CW, Rasmussen JE, Rasmussen TL, Guerra B, Issinger OG and Nielsen J. (2007) Pyrazole carboxamides and carboxylic acids as protein kinase inhibitors in aberrant eukaryotic signal transduction: induction of growth arrest in MCF-7 cancer cells. *Org Biomol Chem.*; 5: 3963-70.
- Petran M, Hadravsky M, Benes J, Boyde A. (1986) In vivo microscopy using the tandem scanning microscope. *Ann N Y Acad Sci.* 483: 440-7.
- Philosof-Mazor, L., Volinsky, R., Comin, M. J., Lewin, N. E., Kedei, N., Blumberg, P. M., Marquez, V. E. and Jelinek, R. (2008) Self-assembly and lipid interactions of diacylglycerol lactone derivatives studied at the air/water interface. *Langmuir.* 24: 11043-11052.

- Pinton, P., Tsuboi, T., Ainscow, E.K., Pozzan, T., Rizzuto, R. and Rutter, G.A. (2002) Dynamics of glucose-induced membrane recruitment of PKC betaII in living pancreatic islet beta-cells. *J. Biol. Chem.*, 277: 37702-37710.
- Playle LC, Hicks DJ, Qualtrough D and Paraskeva C. (2002) Abrogation of the radiation-induced G2 checkpoint by the staurosporine derivative UCN-01 is associated with radiosensitisation in a subset of colorectal tumour cell lines. *Br. J. Cancer* 87: 352-358.
- Plo, I., H. Hernandez, G. Kohlhagen, D. Lautier, Y. Pommier & G. Laurent. (2002) Overexpression of the atypical protein kinase C zeta reduces topoisomerase II catalytic activity, cleavable complexes formation, and drug-induced cytotoxicity in monocytic U937 leukemia cells. *J Biol Chem*, 277, 31407-31415.
- Podar K, Raab MS, Zhang J, McMillin D, Breitzkreutz I, Tai YT, et al.. (2006) Targeting PKC in multiple myeloma: in vitro and in vivo effects of the novel, orally available small-molecule inhibitor Enzastaurin (LY317615.HCl). *Blood*.
- Polyak K and Weinberg RA. (2009) Transitions between epithelial and mesenchymal states: acquisition of malignant and stem cell traits. *Nat Rev Cancer* 9 :265-73.
- Ponting, C. T. Ito, J. Moscat, M. Díaz Meco, F. Inagaki, H. Sumimoto. (2002) OPR, PC and AID: all in the PB1 family. *Trends Biochem. Sci.* 278: 10.
- Prasad N, Topping RS, Zhou D, Decker SJ. (2000) Oxidative stress and vanadate induce tyrosine phosphorylation of phosphoinositide-dependent kinase 1 (PKK1). *Biochemistry*. 39(23): 6929-35.
- Prendiville J., Crowther D., Thatcher N., Woll PJ., Fox BW., McGown A., Testa N., Stern P., McDermott R., Potter M. et al (1993) A phase I study of intravenous bryostatin 1 in patients with advanced cancer. *Br J Cancer*, 68: 428-24.
- Prekeris, R., Mayhew, M.W., Cooper, J.B. y Terrian, D.M. (1996) Identification and localization of an actin-binding motif that is unique to the  $\epsilon$  isoform of protein kinase C and participates in the regulation of synaptic function. *J. Cell. Biol.* 132: 77-90.
- Prekeris, R., Hernández, R.M., Mayhew, M.W., White, M.K. y Terrian, D.M. (1998) Molecular analysis of the interactions between protein kinase C- $\epsilon$  and filamentous actin. *J. Biol. Chem.* 273: 26790-26798.
- Priante, G., Bordin, L., Masacchio, E., Clari, G. y Baggio, B. (2002). Fatty acids and cytokine mRNA expression in human osteoblastic cells. A specific effect of arachidonic acid. *Clin. Sci.* 102, 403-409.
- Privat M, Aubel C, Arnould S, Communal Y, Ferrara M, and Bignon YJ. (2010) AKT and p21 WAF1/CIP1 as potential genistein targets in BRCA1-mutant human breast cancer cell lines. *Anticancer Res.* 30(6):2049-54.
- Propper DJ, McDonald AC, Man A, Thavasu P, Balkwill F, Braybrooke JP, et al. (2001) Phase I and pharmacokinetic study of PKC412, an inhibitor of protein kinase C, *J. Clin. Oncol.* 19: 1485-1492.
- Pu Y., Perry NA., Yang D., Lewin NE., Kedei N., Braun DC., Choi SH., Blumberg PM., Garfield SH., Stone JC., Duan D. and Marquez VE. (2005) A novel diacylglycerol-lactone shows marked selectivity in vitro among C1 domains of protein kinase C (PKC) isoforms alpha and delta as well as selectivity for RasGRP compared with PKCalpha. *J Biol Chem*, 280: 27329-38.
- Pu Y, Garfield SH, Kedei N and Blumberg PM. (2009) Characterization of the differential roles of the twin C1a and C1b domains of protein kinase C-delta. *J. Biol. Chem.*, 284, 1302-1312.
- Quest AF, Bardes ES, Bell RM. (1994) A phorbol ester binding domain of protein kinase C gamma. Deletion analysis of the Cys2 domain defines a minimal 43-amino acid peptide. *J Biol Chem.* 269(4): 2961-70.

- Quest, A.F. J. Bloomenthal, E.S. Bardes, R.M. Bell. (1992) The regulatory domain of protein kinase C coordinates four atoms of zinc, *J. Biol. Chem.* 267: 10193–10197.
- Quest, A.F. y Bell, R.M. (1994) The regulatory region of protein kinase C- $\gamma$ . Studies of phorbol ester binding to individual and combined functional segments expressed as glutathione S-transferase fusion proteins indicate a complex mechanism of regulation by phospholipids, phorbol esters, and divalent cations. *J. Biol. Chem.* 269: 20000-20012.
- Rabinovitz I, Tsomo L and Mercurio AM. (2004) Protein kinase Calpha phosphorylation of specific serines in the connecting segment of the beta 4 integrin regulates the dynamics of type II hemidesmosomes. *Mol. Cell Biol.* 24: 4351–4360.
- Radomska-Pandya, A., Chen, G., Czernik, P.J., Little, J.M., Samokyszyn, V.M., Carter, C.A. y Nowak, G. (2000). Direct interaction of all-trans-retinoic acid with protein kinase C (PKC). Implications for PKC signaling and cancer therapy. *J. Biol. Chem.* 275, 22324-22330.
- Raifman, O., Kolusheva, S., Comin, M. J., Kedei, N., Lewin, N. E., Blumberg, P. M., Marquez, V. E. and Jelinek, R. (2010a) Membrane anchoring of diacylglycerol lactones substituted with rigid hydrophobic acyl domains correlates with biological activities. *The FEBS journal.* 277: 233-243.
- Raifman O, Kolusheva S, El Kazzouli S, Sigano DM, Kedei N, Lewin NE, Lopez-Nicolas R, Ortiz-Espin A, Gomez-Fernandez JC, Blumberg PM, Marquez VE, Corbalan-Garcia S and Jelinek R. (2010b) Membrane-surface anchoring of charged diacylglycerol-lactones correlates with biological activities. *ChemBiochem.* 11: 2003-9.
- Rando RR, y Young N. (1984) The stereospecific activation of protein kinase C. *Biochem Biophys Res Commun.* 122(2):818-23.
- Rasband, W.S. (1997–2009) ImageJ, U. S. National Institutes of Health, Bethesda, MD, USA.
- Rebecchi, M. J. y Pentylala, S. N. (2000) Structure, function, and control of phosphoinositide-specific phospholipase C. *Physiol Rev.*, 80: 1291-1335.
- Reither, G., Schaefer, M. and Lipp, P. (2006) PKC $\alpha$ : A versatile key for decoding the cellular calcium toolkit. *J. Cell Biol.*, 174: 521-533.
- Reno, E. M., J. M. Haughian, I. K. Dimitrova, T. A. Jackson, K. R. Shroyer and A. P. Bradford. (2008) Analysis of protein kinase C delta expression in endometrial tumors. *Human Pathology*, 39, 21-29.
- Rey, O., J.R. Reeve Jr., E. Zhukova, J. Sinnet-Smith, and E.G. Rozengurt. (2004). G protein-coupled receptor-mediated phosphorylation of the activation loop of protein kinase D: dependence on plasma membrane translocation and protein kinase C. *J. Biol. Chem.* 279: 34361–34372.
- Reyland, M. E. (2007) PKC and Apoptosis. In: *Apoptosis, Cell Signaling, and Human Disease: Molecular Mechanisms*. Ed: R. Srivastava. Humana Press Inc, Totowa, N.J.
- Reyland ME. (2009) Protein kinase C isoforms: Multi-functional regulators of cell life and death. *Frontiers in Bioscience* 14, 2386-2399.
- Riccioni R, Dupuis ML, Bernabei M, Petrucci E, Pasquini L, Mariani G, Cianfriglia M and Testa U. (2010) The cancer stem cell selective inhibitor salinomycin is a p-glycoprotein inhibitor. *Blood Cells Mol Dis.* 45: 86-92.
- Ritch P, Rudin CM, Bitran JD, Edelman MJ, Makalinao A, Irwin D, et al. (2006) Phase II study of PKC-alpha antisense oligonucleotide aprinocarsen in combination with gemcitabine and carboplatin in patients with advanced non-small cell lung cancer. *Lung Cancer* 52:173–80.
- Rizo, J. T.C. Südhof. (1998) C2-domains, structure and function of a universal Ca<sup>2+</sup>-binding domain, *J. Biol. Chem.* 273: 15879–15882.

- Rock CL and Demark-Wahnefried W. (2002) Nutrition and survival after the diagnosis of breast cancer: a review of the evidence. *J Clin Oncol.* 20:3302–16.
- Rodríguez-Alfaro, J., Gómez-Fernández, J. y Corbalán-García, S. (2004) Role of the lysine-rich cluster of the C2 domain in the PtdSer-dependent activation of PKC $\alpha$ . *J Mol Biol.*, 335: 1117-1129.
- Roffey J, Rosse C, Linch M, Hibbert A, McDonald NQ and Parker PJ. (2009) Protein Kinase C- the state of play. *Current Opinion in Cell Biology*, 21: 268-279.
- Ron, D. D. and Mochly-Rosen. (1995) An autoregulatory region in protein kinase C: the pseudoanchoring site. *Proc. Natl. Acad. Sci. U. S. A.* 92: 492–496.
- Ron, D. Luo, J. Mochly-Rosen, D. (1995) C2 region-derived peptides inhibit translocation and function of beta protein kinase C *in vivo*, *J. Biol. Chem.* 270: 24180–24187.
- Ron, D. y Kazanietz, M.G. (1999) New insights into the regulation of PKC and novel phorbol ester receptors, *FASEB J.*, 13: 1658–1676.
- Rose, D. P. (1997) Effects of dietary fatty acids on breast and prostate cancers: evidence from *in vitro* experiments and animal studies. *Am. J. Clin. Nutr.*, 66, 1513S–1522S.
- Rose, D. P. and Conolly, J.M. (1999). Omega-3 fatty acids as cancer chemopreventive agents. *Pharmacol. Ther.* 83, 217–244.
- Rose DP and Connolly JM. (2000) Regulation of tumor angiogenesis by dietary fatty acids and eicosanoids. *Nutr Cancer.*; 37: 119-27.
- Saijo, K. Mecklenbräuker, I., Santana, A., Leitger, M., Schmedt C. and Tarakhovsky A. (2002) Protein Kinase C  $\beta$  Controls Nuclear Factor  $\kappa$ B Activation in B Cells Through Selective Regulation of the I $\kappa$ B Kinase  $\alpha$  *J. Exp. Med.* 195: 1647–1652.
- Sánchez Bautista S, Kazaks A, Beaulande M, Torrecillas A, Corbalán García S and Gómez Fernández JC. (2006) Structural study of the catalytic domain of PKC $\zeta$  using infrared spectroscopy and two-dimensional infrared correlation spectroscopy. *FEBS J.* 273(14):3273-86.
- Sánchez Bautista, S., Marín Vicente, C., Gómez Fernández, J. C. and Corbalán García, S. (2006) The C2 domain of PKC $\alpha$  is a Ca<sup>2+</sup>-dependent PtdIns(4,5)P<sub>2</sub> sensing domain: A new insight into an old pathway. *J Mol Biol.*, 362: 901-914.
- Sánchez Bautista S, Corbalán García S, Pérez Lara A and Gómez Fernández JC. (2009) A comparison of the membrane bindings properties of C1B domains of PKC $\gamma$ , PKC $\delta$  and PKC $\epsilon$ . *Biophysics J.*, 96: 3638-47.
- Sánchez Piñera, P. V. Micol, S. Corbalán García, J.C. Gómez Fernández. (1999) A comparative study of the activation of protein kinase C alpha by different diacylglycerol isomers. *Biochem. J.* 337: 387–395.
- Santiago-Walker, A. E., A. J. Fikaris, G. D. Kao, E. J. Brown, M. G. Kazanietz and J. L. Meinkoth. (2005) Protein kinase C-delta stimulates apoptosis by initiating G1 phase cell cycle progression and S phase arrest. *J Biol Chem*, 280, 32107-32114.
- Sarbassov DD, Ali SM, Kim DH, Guertin DA, Latek RR, Erdjument-Bromage H, Tempst P and Sabatini DM. (2004) Rictor, a novel binding partner of mTOR, defines a rapamycin-insensitive and raptor-independent pathway that regulates the cytoskeleton. *Curr Biol* 14: 1296–1302.
- Saunders CM, Swann K, Lai FA. (2007) PLC $\zeta$ , a sperm-specific PLC and its potential role in fertilization. *Biochem Soc Symp.*(74): 23-36.
- Schaap, D. and Parker, P.J. (1990) Expression, purification, and characterization of protein kinase C- $\epsilon$ . *J. Biol. Chem.* 265: 7301-7307.

- Schaap, D., Hsuan, J., Totty, N. y Parker, P.J. (1990). Proteolytic activation of protein kinase C- $\epsilon$ . *Eur. J. Biochem.* 191, 431-435.
- Schachter, J.B., Lester, D.S. y Alkon, D.L. (1996). Synergistic activation of protein kinase C by arachidonic and diacylglycerols in vitro: generation of a stable membrane-bound, cofactor-independent state of protein kinase C activity. *Biochim. Biophys. Acta* 1291, 167-176.
- Schadt, E. E., Edwards, S.W., GuhaThakurta, D., Holder, D., Ying, L., Svetnik, V., Leonardson, A., Hart, K. W., Russell, A., Li, G., Cavet, G., Castle, J., McDonagh, P., Kan, Z., Chen, R., Kasarskis, A., Margarint, M., Caceres, R.M., Johnson, J.M., Armour, C.D., Garrett-Engle, P.W., Tsinoremas, N. F., and Shoemaker, D. D. (2004). A comprehensive transcript index of the humangenome generated using microarrays and computational approaches. *Genome Biol.* 5, R73.
- Schechtman, D. and D. Mochly-Rosen. (2002) Isozymespecific inhibitors and activators of protein kinase C. *Methods Enzymol*, 345, 470-489.
- Schechtman D, Craske ML, Kheifets V, Meyer T, Schechtman J, Mochly-Rosen D. (2004) A critical intramolecular interaction for protein kinase C $\epsilon$  translocation. *J Biol Chem.* 279(16):15831-40.
- Schley PD, Brindley DN and Field CJ. (2007) (n-3) PUFA alter raft lipid composition and decrease epidermal growth factor receptor levels in lipid rafts of human breast cancer cells. *J Nutr.* 137: 548-53.
- Schonwasser, D.C., Marais, R.M., Marshall, C.J. y Parker, P.J. (1998) Activation of the mitogen-activated protein kinase/extracellular signal-regulated kinase pathway by conventional, novel, and atypical protein kinase C isoforms. *Mol. Cell Biol.* 18: 790-798.
- Schultz, A., Jonsson, J.I. and Larsson, C. (2003). The regulatory domain of protein kinase C $\theta$  localizes to the Golgi complex and induces apoptosis in neuroblastoma and Jurkat cells. *Cell Death Differ.* 10, 662-675
- Schultz, A. Ling, M. and Larsson. C. (2004) Identification of an amino acid residue in the protein kinase C C1b domain crucial for its localization to the Golgi network, *J. Biol. Chem.* 279: 31750-31760.
- Schulze A. and Downward J. (2001) Navigating gene expression using microarrays—a technology review. *Nat Cell Biol*, 3: E190-5.
- Schwartz, Z., Sylvia, V.L., Curry, D., Luna, M.H., Dean, D.D. y Boyan, B.D. (1999). Arachidonic acid directly mediates the rapid effects of 24-25-dihydroxyvitamin D<sub>3</sub> via protein kinase C and indirectly through prostaglandin production in resting zone chondrocytes. *Endocrinology* 140, 2991-3002.
- Selbie, L.A., Schmitz-Peiffer, C., Sheng, Y. y Biden, T.J. (1993) Molecular cloning and characterization of PKC $\zeta$ , an atypical isoform of protein kinase C derived from insulin-secreting cells. *J. Biol. Chem.* 15: 24296-24302.
- Senkal M, Haaker R, Linseisen J, Wolfram G, Homann HH, Stehle P. (2005) Preoperative oral supplementation with long-chain Omega-3 fatty acids beneficially alters phospholipid fatty acid patterns in liver, gut mucosa, and tumor tissue. *J Parenter Enteral Nutr*, 29: 236-40.
- Serova M., Ghoul A., Benhadji KA., Cvitkovic E., Faivre S., Calvo F., Lokiec F. and Raymond E. (2006) Preclinical and clinical development of novel agents that target the protein kinase C family. *Semin Oncol*, 33: 466-78.
- Shanmugam M, Krett NL, Maizels ET, Murad FM, Rosen ST and Hunzicker-Dunn M. (2001) A role for protein kinase C delta in the differential sensitivity of MCF7 and MDA-MB 231 human breast cancer cells to phorbol ester-induced growth arrest and p21(WAF1) CIP1 induction. *Cancer Letters* 172 43-53.

- Shao, X. Davletov, B.A. Sutton, R.B. Südhof, T.C. Rizo, J. (1996) Bipartite Ca<sup>2+</sup>-binding motif in C2 domains of synaptotagmin and protein kinase C. *Science*, 273: 248–251.
- Shen, N. Guryev, O. Rizo, J. (2005) Intramolecular occlusion of the diacylglycerol binding site in the C1 domain of munc13-1. *Biochemistry* 44: 1089–1096.
- Sherlock G. (2000) Analysis of large-scale gene expression data. *Curr Opin Immunol*, 12: 201–5.
- Shibatohge M, Kariya K, Liao Y, Hu CD, Watari Y, Goshima M, Shima F, Kataoka T. (1998) Identification of PLC210, a *Caenorhabditis elegans* phospholipase C, as a putative effector of Ras. *J Biol Chem*. 273(11): 6218–22.
- Shin, O.H., Han, W., Wang, Y. y Südhof, T.C. (2005). Evolutionarily conserved multiple C2 domain proteins with two transmembrane regions (MCTPs) and unusual Ca<sup>2+</sup> binding properties. *J. Biol. Chem.*, 280, 1641–1651.
- Shinomura, T., Asaoka, Y., Oka, K., Yoshida, K. and Nishizuka, Y. (1991). Synergistic action of diacylglycerol and unsaturated fatty acids for protein kinase C activation: its possible implications. *Proc. Natl Acad. Sci. USA*, 88, 5149–5153.
- Shirai, Y. K. Kashiwagi, K. Yagi, N. Sakai, N. Saito. (1998) Distinct effects of fatty acids on translocation of gamma- and epsilon-subspecies of protein kinase C. *J. Cell Biol*. 143: 511–521.
- Shirataki, H., Kaibuchi, K., Sakoda, T., Kishida, S., Yamaguchi, T., Wada, K., Miyazaki, M. y Takai, Y. (1993). Rabphilin-3A, a putative target protein for smg p25A/rab3A p25 small GTP-binding protein related to synaptotagmin. *Mol. Cell. Biol*. 13, 2061–2068.
- Silinsky EM, Searl TJ. (2003) Phorbol esters and neurotransmitter release: more than just protein kinase C? *Br J Pharmacol*. 138(7):1191–201.
- Singleton, S.F. y Xiao, J. (2002). The stretched DNA geometry of recombination and repair nucleoprotein filaments. *Biopolymers* 61, 145–158.
- Sitailo, L. A., S. S. Tibudan and M. F. Denning. (2006) The protein kinase C-delta catalytic fragment targets Mcl-1 for degradation to trigger apoptosis. *J Biol Chem*, 281, 29703–29710.
- Sivaprasad, U., E. Shankar and A. Basu. (2006) Downregulation of Bid is associated with PKC-epsilon mediated TRAIL resistance. *Cell Death Differ*, 14, 851–860.
- Six, D.A. y Dennis, E.A. (2000). The expanding superfamily of phospholipase A<sub>2</sub> enzymes: classification and characterization. *Biochim. Biophys. Acta* 1488, 1–19.
- Slater, S.J., Taddeo, F.J., Mazurek, A., Stagliano, B.A., Milano, S.K., Kelly, M.B., Ho, C. y Stubbs, C.D. (1998). Inhibition of membrane lipid-independent protein kinase C $\alpha$  activity by phorbol esters, diacylglycerols, and bryostatin-1. *J. Biol. Chem*. 273, 23160–23168.
- Sliva, D., English, D., Lyons, D. and Lloyd, F. P. (2002) Protein kinase C induces motility of breast cancers by upregulating secretion of urokinase-type plasminogen activator through activation of AP-1 and NF- $\kappa$ B. *Biochem. Biophys. Res. Commun*. 290, 552–557.
- Smallridge RC, Kiang JG, Gist ID, Fein HG, Galloway RJ. (1992) U-73122, an aminosteroid phospholipase C antagonist, non competitively inhibits thyrotropin-releasing hormone effects in GH3 rat pituitary cells. *Endocrinology*, 131: 1883–8.
- Soderling, T.R. (1990). Protein kinases. Regulation by autoinhibitory domains. *J. Biol. Chem*. 265, 1823–1826.
- Soh, J.-W. and I. B. Weinstein. (2003) Roles of specific isoforms of protein kinase C in the transcriptional control of cyclin D1 and related genes. *J Biol Chem*, 278, 34709–34716.

- Solanas, M., Hurtado, A., Costa, I., Moral, R., et al. (2002) Effects of a high olive oil diet on the clinical behavior and histopathological features of rat DMBA-induced mammary tumors compared with a high corn oil diet. *Int. J. Oncol.*, 21, 745–753.
- Soldati, L., Lombardi, C., Adamo, D., Terranegra, A., Bianchin, C., Bianchi, G. and Vezzoli, G. (2002). Arachidonic acid increases intracellular calcium in erythrocytes. *Biochem. Biophys. Res. Commun.* 293, 974–978.
- Songyang, Z. y Cantley, L.C. (1995). Recognition and specificity in protein tyrosine kinase-mediated signalling. *Trends Biochem. Sci.* 20, 470-475.
- Sonnenburg, E.D., Gao, T. y Newton, A.C. (2001). The phosphoinositide-dependent kinase, PDK-1, phosphorylates conventional protein kinase C isozymes by a mechanism that is independent of phosphoinositide 3-kinase. *J. Biol. Chem.* 276, 45289–45297.
- Sossin, W.S. y Schwartz, J.H. (1993). Ca<sup>2+</sup>-independent protein kinase Cs contain an amino-terminal domain similar to the C2 consensus sequence. *Trends Biochem. Sci.* 18, 207-208.
- Soto-Guzman A, Robledo T, Lopez-Perez M and Salazar EP. (2008) Oleic acid induces ERK1/2 activation and AP-1 DNA binding activity through a mechanism involving Src kinase and EGFR transactivation in breast cancer cells. *Mol Cell Endocrinol.*; 294: 81-91.
- Soto-Guzman A, Navarro-Tito N, Castro-Sanchez L, Martinez-Orozco R and Salazar EP. (2010) Oleic acid promotes MMP-9 secretion and invasion in breast cancer cells. *Clin Exp Metastasis.*; 27: 505-15.
- Souroujon MC, Mochly-Rosen D. (1998) Peptide modulators of protein-protein interactions in intracellular signaling. *Nat Biotechnol.* 16(10):919-24.
- Stahelin, R.V. Digman, M.A. Medkova, M. Ananthanarayanan, B. Rafter, J.D. Melowic, H.R. Cho, W. (2004) Mechanism of diacylglycerol-induced membrane targeting and activation of protein kinase C delta, *J. Biol.Chem.* 279: 29501–29512.
- Stahelin, R.V. Digman, M.A. Medkova, M. Ananthanarayanan, B. Melowic, H.R. Rafter, J.D. Cho. W. (2005) Diacylglycerol-induced membranetargeting and activation of protein kinase cepsilon: mechanistic differences between protein kinases C delta and cepsilon. *J. Biol. Chem.* 280: 19784–19793.
- Stark, A. H., Madar, Z. (2002) Olive oil as a functional food: Epidemiology and nutritional approaches. *Nutr. Rev.*, 60, 170–176.
- Stebbins, E.G. Mochly-Rosen, D. (2001) Binding specificity for RACK1 resides in the V5 region of beta II protein kinase C. *J. Biol. Chem.* 276: 29644–29650.
- Steck, P.A., Pershouse, M.A., Jasser, S.A., Yung, W.K., Lin, H., Ligon, A.H., Langford, L.A., Baumgard, M.L., Hattier, T., Davis, T., Frye, C., Hu, R., Swedlund, B., Teng, D.H y Tavtigian, S.W. (1997) Identification of a candidate tumour suppressor gene, MMAC1, at chromosome 10q23.3 that is mutated in multiple advanced cancers, *Nat. Genet.* 15 356–362.
- Steinberg, R., O. A. Harari, E. A. Lidington, J. J. Boyle, M. Nohadani, A. M. Samarel, M. Ohba, D. O. Haskard and J. C. Mason. (2007) A protein kinase Cepsilon-anti-apoptotic kinase signaling complex protects human vascular endothelial cells against apoptosis through induction of Bcl-2. *J Biol Chem*, 282, 32288-32297.
- Stempka L, Girod A, Müller HJ, Rincke G, Marks F, Gschwendt M, Bossemeyer D. (1997) Phosphorylation of protein kinase C delta (PKCdelta) at Thr 505 is not a prerequisite for enzymatic activity. Expression of rat PKC delta and an Ala 505 mutant in bacteria in a functional form. *J Biol Chem.* 272(10): 6805-11.
- Stempka, L., Schnolzer, M., Radke, S., Rincke, G., Marks, F. y Gschwendt, M. (1999). Requirements of protein kinase C delta for catalytic function. Role of glutamic acid 500 and autophosphorylation on serine 643. *J. Biol. Chem.* 274, 8886-8892.

- Su, T.T. *et al.* (2002) PKC- $\beta$  controls I $\kappa$ B kinase lipid raft recruitment and activation in response to BCR signaling. *Nat. Immunol.* 3, 780–786.
- Südhof, T.C. (2002) Synaptotagmins: why so many? *J. Biol. Chem.* 277: 7629–7632.
- Sun W, Kalen AL, Smith BJ, Cullen JJ and Oberley LW. (2009) Enhancing the antitumor activity of adriamycin and ionizing radiation. *Cancer Res.* 69: 4294–300.
- Sun, X., F. Wu, R. Datta, S. Kharbanda and D. Kufe. (2000) Interaction between Protein Kinase C- $\delta$  and the c-Abl tyrosine kinase in the cellular response to oxidative stress. *J Biol Chem*, 275, 7470-7473.
- Sutton RB, Ernst JA, Brunger AT. (1999) Crystal structure of the cytosolic C2A-C2B domains of synaptotagmin III. Implications for Ca<sup>2+</sup>-independent snare complex interaction. *J Cell Biol.* 147(3):589-98.
- Sutton, R.B., Davletov, B.A Berghuis, A.M. Südhof, T.C. Sprang, S.R. (1995) Structure of the first C2 domain of synaptotagmin I: a novel Ca<sup>2+</sup>/phospholipid-binding fold. *Cell* 80: 929–938.
- Sutton, R. B. and Sprang, S. R. (1998) Structure of the PKC $\beta$  phospholipid-binding C2 domain complexed with Ca<sup>2+</sup>. *Structure*, 6: 1395-1405.
- Suzuki, A., Akimoto, K., Ohno, S. (2003) Protein Kinase C  $\{\lambda\}/\{\iota\}$  (PKC $\{\lambda\}/\{\iota\}$ ): A PKC Isozyme Essential for the Development of Multicellular Organisms. *J Biochem* 133: 9-16.
- Suzuki M, Shigematsu H, Shames DS, Sunaga N, Takahashi T, Shivapurkar N, Iizasa T, Minna JD, Fujisawa T and Gazdar AF. (2007) Methylation and gene silencing of the Ras-related GTPase gene in lung and breast cancers. *Ann Surg Oncol.* 2007 Apr;14(4):1397-404.
- Suzuma, K. *et al.* (2002) Characterization of protein kinase C $\beta$  isoform's action on retinoblastoma protein phosphorylation, vascular endothelial growth factor-induced endothelial cell proliferation, and retinal neovascularization. *Proc. Natl Acad. Sci. USA* 99, 721–726.
- Swairjo, M.A. Concha, N.O. Kaetzel, M.A. Dedman, J.R. Seaton. B.A. (1995) Ca<sup>2+</sup>-bridging mechanism and phospholipid head group recognition in the membrane-binding protein annexin V. *Nat. Struct. Biol.* 2: 968–974.
- Swannie, H.C. and Stanley, B.K. (2002). Protein kinase C inhibitors. *Curr. Oncol.* 4, 37-46.
- Syed DN, Afaq F, Sarfaraz S, Khan N, Kedlaya R, Setaluri V, Mukhtar H. (2008) Delphinidin inhibits cell proliferation and invasion via modulation of Met receptor phosphorylation. *Toxicol Appl Pharmacol.*; 231: 52-60.
- Szallasi, Z. *et al.* (1994) Bryostatins protect protein kinase C $\delta$  from down-regulation in mouse keratinocytes in parallel with its inhibition of phorbol ester-induced differentiation. *Mol. Pharmacol.* 46, 840–850.
- Szallasi, Z., Du, L., Levine, R., Lewin, N.E., Nguyen, P.N., Williams, M.D., Pettit, G.R. y Blumberg, P.M. (1996). The bryostatins inhibit growth of B16/F10 melanoma cells in vitro through a protein kinase C-independent mechanism: dissociation of activities using 26-epi-bryostatin 1. *Cancer Res.* 56, 2105-2111.
- Tabellini, G., Bortul, R., Aluigi, M., Billi, A., Bareggi, R., Grill, V., Narducci, P. y Martelli, A. (2002) Binding of elements of protein kinase C- $\alpha$  regulatory domain to lamin B1. *Cell Signal*, 14: 819-27.
- Tabuse Y, Izumi Y, Piano F, Kempfues KJ, Miwa J, Ohno S. (1998) Atypical protein kinase C cooperates with PAR-3 to establish embryonic polarity in *Caenorhabditis elegans*. *Development.* 125(18): 3607-14.
- Taiyab A and Rao CM. (2010) HSP90 modulates actin dynamics: Inhibition of HSP90 leads to decreased cell motility and impairs invasion. *Biochim Biophys Acta.*

- Takahashi I, Kobayashi E, Asano K, Yoshida M and Nakano H (1987) UCN-01, a selective inhibitor of protein kinase C from Streptomyces. *J Antibiot* (Tokyo), 40: 1782-1784.
- Takahashi M, Mukai H, Oishi K, Isagawa T, Ono Y. (2000) Association of immature hypophosphorylated protein kinase C epsilon with an anchoring protein CG-NAP. *J Biol Chem.* 275(44): 34592-6.
- Takeshita, M., Ueda, H., Shirabe, K., Higuchi, Y., Yoshida, S. (1997) Lack of promotion of colon carcinogenesis by high-oleic safflower oil. *Cancer*, 79, 1487-1493.
- Takimura, T., Kamata, K., Fukasawa, K., Ohsawa, H., Komatani, H., Yoshizumi, T., Takahashi, I., Kotani, H. and Iwasawa, Y. (2010) Structures of the PKC-iota kinase domain in its ATP-bound and apo forms reveal defined structures of residues 533-551 in the C-terminal tail and their roles in ATP binding. *Acta Crystallogr., Sect.D* **66**: 577-583.
- Tamamura H., Sigano DM., Lewin NE., Peach ML., Nicklaus MC., Blumberg PM. and Marquez VE. (2004) Conformationally constrained analogues of diacylglycerol (DAG). 23. Hydrophobic ligand-protein interactions versus ligand-lipid interactions of DAG-lactones with protein kinase C (PKC). *J Med Chem*, 47: 4858-64.
- Tan M., Li P., Sun M., Yin G. and Yu D. (2006) Upregulation and activation of PKC $\alpha$  by ERBB2 through Src promotes breast cancer cell invasion that can be blocked by combined treatment with PKC $\alpha$  and Src inhibitors. *Oncogene* 25, 3286-3295.
- Tanaka M, and Herr W. (1990) Differential transcriptional activation by Oct-1 and Oct-2: interdependent activation domains induce Oct-2 phosphorylation. *Cell*, 60 (3): 375-86.
- Tanaka Y, Gavrielides MV, Mitsuuchi Y, Fujii T, Kazanietz MG. (2003) Protein kinase C promotes apoptosis in LNCaP prostate cancer cells through activation of p38 MAPK and inhibition of the Akt survival pathway. *J Biol Chem.* 278(36):33753-62.
- Tanaka, S., Tominaga, M., Yasuda, I., Kishimoto, A. y Nishizuka, Y. (1991) Protein kinase C in rat brain synaptosomes.  $\beta$ II-subspecies as a major isoform associated with membrane-skeleton elements. *FEBS Lett.* 294: 267-270.
- Taylor, S.S., Buechler, J.A. y Yonemoto, W. (1990) cAMP-dependent protein kinase: framework for a diverse family of regulatory enzymes. *Annu. Rev. Biochem.* 59: 971-1005.
- Taylor, S.S. y Radzio-Andzelm, E. (1994) Three protein kinase structures define a common motif. *Structure* 15: 345-355.
- Thelen, M., Rosen, A., Nairn, A.C. y Aderem, A.A. (1991) Regulation by phosphorylation of reversible association of a myristoylated protein kinase C substrate with the plasma membrane. *Nature*, 351: 320-322.
- Thomas PD, Campbell MJ, Kejariwal A, Mi H, Karlak B, Daverman R, Diemer K, Muruganujan A, Narechania A. (2003) PANTHER: a library of protein families and subfamilies indexed by function. *Genome Res.* 13(9):2129-41.
- Thomas PD, Kejariwal A, Campbell MJ, Mi H, Diemer K, Guo N, Ladunga I, Ulitsky-Lazareva B, Muruganujan A, Rabkin S, Vandergriff JA, Doremieux O. (2003) PANTHER: a browsable database of gene products organized by biological function, using curated protein family and subfamily classification. *Nucleic Acids Res.*31(7): 2024.
- Tian F, Wu H, Li Z, Wang N, Huang J, Li C and Xie F. (2009) Activated PKC $\alpha$ /ERK1/2 signaling inhibits tamoxifen-induced apoptosis in C6 cells. *Cancer Invest.*; 27: 802-8.
- Tian, X.; Wang, P.P.; Liu, Y.P.; Hou, K.Z.; Jin, B.; Luo, Y. and Qu, X.J. (2007) Effect of bufalin-inducing apoptosis on Bcl-2 and PKC in HL-60 cells. *Zhongguo Shi Yan Xue Ye Xue Za Zhi*, 15: 67-71.

- Tian Y, Corkey RF, Yaney GC, Goforth PB, Satin LS and Moitoso de Vargas L. (2008) Differential modulation of L-type calcium channel subunits by oleate. *Am J Physiol Endocrinol Metab.*; 294: E1178-86.
- Toker A, y Newton AC. (2000) Cellular signaling: pivoting around PDK-1. *Cell.* 103(2):185-8.
- Tonetti DA, Chisamore MJ, Grdina W, Schurz H and Jordan VC. (2000) Stable transfection of protein kinase C alpha cDNA in hormone-dependent breast cancer cell lines. *Br J Cancer*, 83: 782-791.
- Tonetti DA, Morrow N, Kidwai A, Gupta A and Badve S. (2002) Elevated protein kinase C expression may be predictive of tamoxifen treatment failure. *Proceedings of the American Association for Cancer Research*, 21 Abstract 420.
- Torrecillas, A., Corbalán-García, S., de Godos, A y Gómez-Fernández, J.C. (2001). Activation of protein kinase C $\alpha$  by lipid mixtures containing different proportions of diacylglycerols. *Biochemistry* 40, 15038-15046.
- Torrecillas, A. S. Corbalán García, J. Gómez Fernández. (2003) Structural study of the C2 domains of the classical PKC isoenzymes using infrared spectroscopy and two-dimensional infrared correlation spectroscopy. *Biochemistry* 42: 11661-11668.
- Torrecillas, A. Laynez, J. Menéndez, M. Corbalán-García, S. Gómez-Fernández, J. (2004) Calorimetric study of the interaction of the C2 domains of classical protein kinase C isoenzymes with Ca<sup>2+</sup> and phospholipids. *Biochemistry* 43: 11727-11739.
- Treisman, R. (1996) Regulation of transcription by MAP kinase cascades. *Curr. Opin. Cell Biol.* 8: 205-215.
- Trichopoulou A., Lagiou P., Kuper H. and Trichopoulos D. (2000) Cancer and Mediterranean dietary traditions. *Cancer Epidemiol. Biomarkers Prev.* 9, 869-873.
- Tsien RW, Lipscombe D, Madison D, Bley K, Fox A. (1995) Reflections on Ca<sup>2+</sup>-channel diversity, 1988-1994. *Trends Neurosci.* 18(2): 52-4.
- Tsutakawa, S.E., Medzihradzsky, K.F., Flint, A.J., Burlingame, A.L. y Koshland, D.E. (1995). Determination of *in vivo* phosphorylation sites in protein kinase C. *J. Biol. Chem.* 270: 26807-26812.
- Tucker, W.C. E.R. Chapman, (2002) Role of synaptotagmin in Ca<sup>2+</sup>-triggered exocytosis, *Biochem. J.* 366: 1-13.
- Uberall, F., Giselbrecht, S., Hellbert, K., Fresser, F., Bauer, B., Gschwendt, M., Grunicke, H.H. y Baierm, G. (1997) Conventional PKC- $\alpha$ , novel PKC- $\epsilon$  and PKC- $\theta$ , but not atypical PKC- $\lambda$  are MARCKS kinases in intact NIH 3T3 fibroblasts. *J. Biol. Chem.* 272: 4072-4078.
- Ueda, Y., Hirai, S., Osada, S., Suzuki, A., Mizuno, K. y Ohno, S. (1996) Protein kinase C  $\delta$  activates the MEK-ERK pathway in a manner independent of Ras and dependent on Raf. *J. Biol. Chem.* 271: 23512-23519.
- Vallentin, A., Prevostel, C., Fauquier, T., Bonnefont, X., and Joubert, D. (2000). Membrane targeting and cytoplasmic sequestration in the spatio-temporal localization of human protein kinase C. *J. Biol. Chem.* 275: 6014-6021.
- Van Blitterswijk, W.J. y Houssa, B. (2000). Properties and functions of diacylglycerol kinases. *Cell signal* 12, 595-605.
- Van, B. J.Wim, D.L. Van, H. Arnold, R.J. Veldman, M. Verheij, J. Borst, (2003) Ceramide: second messenger or modulator of membrane structure and dynamics? *Biochem. J.* 369: 199-211.
- van Engeland, M; Nieland, LJW; Ramaekers, FCS, et al. (1998) Annexin V-affinity assay: A review on an apoptosis detection system based on phosphatidylserine exposure. *CYTOMETRY*; 31 (1):1-9

- Van Gelder, R. N., von Zastrow, M. E., Yool, A., Dement, W. C., Barchas, J. D., and Eberwine, J. H. (1990). Amplified RNA synthesized from limited quantities of heterogeneous cDNA. *Proc. Natl. Acad. Sci. USA* 87, 1663–1667.
- van Hal N. L., Vorst O., van Houwelingen A. M., Kok E. J., Peijnenburg A., Aharoni A., van Tunen A. J., and J. Keijer. (2000) The application of DNA microarrays in gene expression analysis. *J Biotechnol*, 78: 271–80.
- Vance JE, Steenbergen R. (2005) Metabolism and functions of phosphatidylserine. *Prog Lipid Res.* 44(4): 207–34.
- Varga, A. *et al.* (2004) Tumor grade-dependent alterations in the protein kinase C isoform pattern in urinary bladder carcinomas. *Eur. Urol.* 46, 462–465.
- Venter JC, Adams MD, Myers EW, Li PW, Mural RJ, Sutton GG, Smith HO, Yandell M, Evans CA, Holt RA, Gocayne JD, Amanatides P, Ballew RM, Huson DH, Wortman JR, *et al.* (2001) The sequence of the human genome. *Science*, 291:1304–1351.
- Verdaguer, N., Corbalán-García, S., Ochoa, W., Fita, I. y Gómez Fernández, J. (1999) Ca<sup>2+</sup> bridges the C2 membrane-binding domain of PKC $\alpha$  directly to PtdSer. *EMBO J.*, 18: 6329–6338.
- Verdaguer, N. Corbalán García, S. Ochoa, W. Gómez Fernández, J. Fita, I. (2004) Membrane binding C2-like domains, en A. Messerschmidt, W. Bode, M. Cygler (Eds.), *Handbook of Metalloproteins*, New York.
- Vergères, G., Manenti, S., Weber, T. y Stürzinger, C. (1995) The myristoyl moiety of myristoylated alanine-rich C kinase substrate (MARCKS) and MARCKS-related protein is embedded in the membrane *J. Biol. Chem.* 270: 19879–19887.
- Vibet S, Goupille C, Bougnoux P, Steghens JP, Gore J and Maheo K. (2008) Sensitization by docosahexaenoic acid (DHA) of breast cancer cells to anthracyclines through loss of glutathione peroxidase (GPx1) response. *Free Radic Biol Med* 44: 1483–91.
- Visvader JE and Lindeman GJ. (2008) Cancer stem cells in solid tumours: accumulating evidence and unresolved questions. *Nat Rev Cancer* 8: 755–68.
- Voss, O. H., S. Kim, M. D. Wewers and A. I. Doseff. (2005) Regulation of monocyte apoptosis by the protein kinase C delta-dependent phosphorylation of caspase-3. *J Biol Chem*, 280, 17371–17379.
- Wagner, J., von Matt, P., Sedrani, R., Albert, R., Cooke, N., Ehrhardt, C., Geiser, M., Rummel, G., Stark, W., Strauss, A., Cowan-Jacob, S.W., Beerli, C., Weckbecker, G., Evenou, J.P., Zenke, G. and Cottens, S. (2009) Discovery of 3-(1H-indol-3-yl)-4-[2-(4-methylpiperazin-1-yl)quinazolin-4-yl]pyrrole-2,5-dione (AEB071), a potent and selective inhibitor of protein kinase C isotypes. *J. Med. Chem.* 52: 6193–6196
- Wakelam, M.J.O., (1998) DAG, when is it an intracellular messenger? *Biochim. Biophys. Acta.*, 1436: 117–126.
- Waldron R.T. y Rozengurt, E. (2003). Protein kinase C phosphorylates protein kinase D activation loop Ser744 and Ser 748 and releases autoinhibition by the pleckstrin homology domain. *J. Biol. Chem.* 278, 154–163.
- Walker, E.H., Perisic, O., Ried, C., Stephens, L. y Williams, R.L. (1999). Structural insights into phosphoinositide 3-kinase catalysis and signalling. *Nature* 402, 313–320.
- Wang, Q.J., Fang, T.W., Fenick, D., Garfield, S., Bienfait, B., Márquez, V.E. y Blumberg, P.M. (2000). The lipophilicity of phorbol esters as a critical factor in determining the pattern of translocation of protein kinase C- $\delta$  fused to green fluorescent protein. *J. Biol. Chem.* 275, 12136–12146.
- Wang, Q.J. Fang, T.W. Nacro, K. Marquez, V.E. Wang, S. Blumberg. P.M. (2001) Role of hydrophobic residues in the C1b domain of protein kinase C delta on ligand and phospholipid interactions, *J. Biol. Chem.* 276:19580–19587.

- Wang PS, Chou FS, Porchia L, Saji M and Pinzone JJ. (2008) Troglitazone inhibits cell migration, adhesion, and spreading by modulating cytoskeletal rearrangement in human breast cancer cells. *Mol Carcinog.*; 47: 905-15.
- Wang S, Wang Z, Dent P, Grant S. (2003) Induction of tumor necrosis factor by bryostatin 1 is involved in synergistic interactions with paclitaxel in human myeloid leukemia cells. *Blood.* 101(9): 3648-57.
- Wang Y, Shyy JY, Chien S. (2008) Fluorescence proteins, live-cell imaging, and mechanobiology: seeing is believing. *Annu Rev Biomed Eng.* 10: 1-38.
- Ward R.J. and Dirks P.B. (2007) Cancer stem cells: at the headwater of tumor development, *Annu. Rev. Pathol.* 2: 175-189.
- Way KJ, Chou E and King GL. (2000) Identification of PKC-isoformspecific biological actions using pharmacological approaches. *Trends in Pharmacological Science* 21: 181-187.
- Ways, D. K. Kukoly CA, DeVente J, Hooker JL, Bryant WO, Posekany KJ, Fletcher DJ, Cook PP and Parker PJ. (1995) MCF-7 breast-cancer cells transfected with protein-kinase C- $\alpha$  exhibit altered expression of other protein-kinase-C isoforms and display a more aggressive neoplastic phenotype. *J. Clin. Invest.* 95, 1906-1915.
- Wender PA, Irie K, Miller BL. (1995) Identification, activity, and structural studies of peptides incorporating the phorbol ester-binding domain of protein kinase C. *Proc Natl Acad Sci U S A.* 92(1): 239-43.
- Wender, P.A. and Verma, V.A. (2008) The design, synthesis, and evaluation of C7 diversified bryostatin analogs reveals a hot spot for PKC affinity. *Org. Lett.*, 10: 3331-4.
- Wender, P.A., Dechristopher, B.A. and Schrier, A.J. (2008) Efficient synthetic access to a new family of highly potent bryostatin analogues *via* a Prins-driven macrocyclization strategy. *J. Am. Chem. Soc.*, 130: 6658-9.
- Wiemer EA. (2007) The role of microRNAs in cancer: no small matter. *Eur J Cancer.* 43(10):1529-44.
- Wilkinson, S.E., Parker, P.J. and Nixon, J.S. (1993) Isoenzyme specificity of bisindolylmaleimides, selective inhibitors of PKC. *Biochem. J.*, 294: 335-337.
- Williams RL, Katan M. (1996) Structural views of phosphoinositide-specific phospholipase C: signalling the way ahead. *Structure.* 4(12):1387-94.
- Wilson, M. Gill, D. Perisic, O. Quinn, M. Williams, R. (2003) PB1 domain mediated heterodimerization in NADPH oxidase and signaling complexes of atypical PKC with Par6 and P62. *Mol. Cell* 12: 39-50.
- Wing, M.R. *et al.* (2001) Activation of phospholipase C-epsilon by heterotrimeric G protein betagamma-subunits. *J. Biol. Chem.* 276: 48257-48261.
- Wing, M.R. *et al.* (2003) Direct activation of phospholipase C-epsilon by Rho. *J. Biol. Chem.* 278: 41253-41258.
- Wu D, Jiang H, Katz A, Simon MI. (1993) Identification of critical regions on phospholipase C-beta 1 required for activation by G-proteins. *J Biol Chem.* 268(5): 3704-9.
- Wu H, Goel V, Haluska FG. (2003) PTEN signaling pathways in melanoma. *Oncogene.* 22(20): 3113-22.
- Wu T., Y.-H. Hsieh, Y.-S. Hsieh and J. Liu. (2008) Reduction of PKC-alpha decreases cell proliferation, migration, and invasion of human malignant hepatocellular carcinoma. *J Cell Biochem.* 103, 9-20.
- Wynder EL, Cohen LA, Muscat JE *et al.* (1997) Breast cancer: weighing the evidence for a promoting role of dietary fat. *J Natl Cancer Inst.* 89: 766-772.

- Xia, P. *et al.* (1996) Characterization of vascular endothelial growth factor's effect on the activation of protein kinase C, its isoforms, and endothelial cell growth. *J. Clin. Invest.* 98, 2018–2026.
- Xiao B, Smerdon SJ, Jones DH, Dodson GG, Soneji Y, Aitken A, Gamblin SJ. (1995) Structure of a 14-3-3 protein and implications for coordination of multiple signalling pathways. *Nature.* 376(6536):188-91.
- Xu, J., Weng, Y.-I., Simoni, A., Krugh, B. W., Liao, Z., Weisman, G. A. and Sun, G. Y. (2002). Role of PKC and MAPK in cytosolic PLA2 phosphorylation and arachidonic acid release in primary murine astrocytes. *J. Neurochem.* 83, 259–270.
- Xu, R.X. Pawelczyk, T. Xia, T.H. Brown. S.C. (1997) NMR structure of a protein kinase C- $\gamma$  phorbol-binding domain and study of protein-lipid micelle interactions. *Biochemistry* 36: 10709–10717.
- Xu, Z.-B. Chaudhary, D. Olland, S. Wolfrom, S. Czerwinski, R. Malakian, K. Lin, L. Stahl, M.L. Joseph-McCarthy, D. Benander, C. Fitz, L Greco, R. Somers, W.S. Mosyak, L. (2004) Catalytic domain crystal structure of protein kinase C-theta (PKCtheta), *J. Biol. Chem.* 279: 50401–50409.
- Xue H, Sawyer MB, Field CJ, Dieleman LA and Baracos VE. (2007) Nutritional modulation of antitumor efficacy and diarrhea toxicity related to irinotecan chemotherapy in rats bearing the ward colon tumor. *Clin Cancer Res.* 13:7146–54.
- Yaffe, M.B., Rittinger, K., Volinia, S., Caron, P.R., Aitken, A., Leffers, H., Bamblin, S.J., Smerdon, S.J. y Cantley, L.C. (1997). The structural basis for 14-3-3:phosphopeptide binding specificity. *Cell* 91, 961-971.
- Yaffe, M.B. (2002). Phosphotyrosine-binding domains in signal transduction. *Nat. Rev. Mol. Cell Biol.* 3, 177-186.
- Yagi, K. Shirai, Y. Hirai, M. Sakai, N. Saito, N. (2004) Phospholipase A2 products retain a neuron specific gamma isoform of PKC on the plasma membrane through the C1 domain—A molecular mechanism for sustained enzyme activity. *Neurochem. Int.* 45: 39–47.
- Yakushiji, K., Sawai, H., Kawai, S., Kambara, M. y Domae, N. (2003). Characterization of C2-ceramide-resistant HL-60 subline (HL-CR): involvement of PKC $\delta$  in C2-ceramide resistance. *Exp. Cell Res.* 286, 396-402.
- Yamaki, T., Yano, T., Satoh, H., Endo, T., et al. (2002) High oleic acid oil suppresses lung tumorigenesis in mice through the modulation of extracellular signal-regulated kinase cascade. *Lipids*, 37, 783 –788.
- Yang, C-F. and Kazanietz, M.G. (2003) Divergence and complexities in DAG signalling: looking beyond PKC. *Trends in Pharmacol. Sci.*, 24: 602-608.
- Yang, Q., Alemany, R., Casas, J., Kitajka, K., et al. (2005) Influence of the membrane lipid structure on signal processing via G protein-coupled receptors. *Mol. Pharmacol.*, 68, 210 –217.
- Yao L, Suzuki H, Ozawa K, Deng J, Lehel C, Fukamachi H, Anderson WB, Kawakami Y, Kawakami T. (1997) Interactions between protein kinase C and pleckstrin homology domains. Inhibition by phosphatidylinositol 4,5-bisphosphate and phorbol 12-myristate 13-acetate. *J Biol Chem.* 272(20):13033-9.
- Yeoh, E. J., Ross, M. E., Shurtleff, S. A., Williams, W. K., Patel, D., Mahfouz, R., Behm, F. G., Raimondi, S.C., Relling, M. V., Patel, A., Cheng, C., Campana, D., Wilkins, D., Zhou, X., Li, J., Liu, H., Pui, C. H., Evans, W. E., Naeve, C., Wong, L., and Downing, J. R. (2002). Classification, subtype discovery, and prediction of outcome in pediatric acute lymphoblastic leukemia by gene expression profiling. *Cancer Cell* 1, 133–143.

- Yonemoto, W., McGlone, M.L., Grant, B. y Taylor, S.S. (1997). Autophosphorylation of the catalytic subunit of cAMP-dependent protein kinase in *Escherichia coli*. *Protein. Eng.* 10, 915-925.
- Yoshida, K., Y. Miki and D. Kufe. (2002) Activation of SAPK/JNK signaling by Protein Kinase C-delta in response to DNA damage. *J Biol Chem*, 277, 48372-48378.
- Yuen, A.R., Halsey, J., Fisher, G.A., Holmlund, J.T., Geary, R.A., Kwoh, T.J., Dorr, A., Sikic, B.I. (1999) Phase I study of an antisense oligonucleotide to PKC alpha in patients with cancer. *Clin. Cancer. Res.* 5, 3357-3363.
- Zacharias, D. A., Violin, J. D., Newton, A. C. and Tsien, R. Y. (2002) Partitioning of lipid-modified monomeric GFPs into membrane microdomains of live cells. *Science*, 296: 913-916.
- Zhang, G. Kazanietz, M.G. Blumberg, P.M. Hurley, J.H. (1995) Crystal structure of the Cys2 activator-binding domain of protein kinase C  $\delta$  in complex with phorbol ester. *Cell*, 81: 917-924.
- Zhang J, Wang L, Schwartz J, Bond RW, Bishop WR. (1994) Phosphorylation of Thr642 is an early event in the processing of newly synthesized protein kinase C  $\beta$  1 and is essential for its activation. *J Biol Chem.* 269(30):19578-84.
- Zhou, M., Horita, D.A., Waugh, D.S., Byrd, R.A. y Morrison, D.K. (2002). Solution structure and functional analysis of the cysteine-rich C1 domain of kinase suppressor of Ras (KSR). *J. Mol. Biol.* 315, 435-446.
- Zhu Z.R., Agren J., Männistö S., Pietinen P., Eskelinen M., Syrjänen K. and Uusitupa M. (1995). Fatty acid composition of breast adipose tissue in breast cancer patients and in patients with benign breast disease. *Nutr. Cancer*, 24:151-160.
- Zidovetzki, R. y Lester, D.S. (1992). The mechanism of activation of protein kinase C: a biophysical perspective. *Biochim. Biophys. Acta* 1134, 261-272.
- Ziegler, W.H., Parekh, D.B., Le Good, J.A., Whelan, R.D., Kelly, J.J., Frech, M., Hemmings, B.A. y Parker, P.J. (1999) Rapamycin-sensitive phosphorylation of PKC on a carboxy-terminal site by an atypical PKC complex. *Curr. Biol.* 9: 522-529.
- Zonder JA, Shields AF, Zalupski M, Chaplen R, Heilbrun LK, Arlauskas P and Philip P. (2001) A phase II trial of bryostatín 1 in the treatment of metastatic colorectal cancer. *Clinical Cancer Research*, 7: 38-42.
- Zusman, I., Gurevich, P., Madar, Z., Nyska, A., et al. (1997) Tumorpromoting and tumor-protective effects of high-fat diets on chemically induced mammary cancer in rats. *Anticancer Res.*, 17, 349-356.